

Springer Natural Hazards

Radu Vacareanu
Constantin Ionescu *Editors*

The 1940 Vrancea Earthquake. Issues, Insights and Lessons Learnt

Proceedings of the Symposium
Commemorating 75 Years from
November 10, 1940 Vrancea Earthquake

 Springer

Springer Natural Hazards

More information about this series at <http://www.springer.com/series/10179>

Radu Vacareanu · Constantin Ionescu
Editors

The 1940 Vrancea Earthquake. Issues, Insights and Lessons Learnt

Proceedings of the Symposium
Commemorating 75 Years from
November 10, 1940 Vrancea Earthquake

Editors

Radu Vacareanu
Seismic Risk Assessment Research Center
Technical University of Civil Engineering
of Bucharest
Bucharest
Romania

Constantin Ionescu
National Institute for Earth Physics
Măgurele
Romania

ISSN 2365-0656

Springer Natural Hazards

ISBN 978-3-319-29843-6

DOI 10.1007/978-3-319-29844-3

ISSN 2365-0664 (electronic)

ISBN 978-3-319-29844-3 (eBook)

Library of Congress Control Number: 2016931431

© Springer International Publishing Switzerland 2016

This work is subject to copyright. All rights are reserved by the Publisher, whether the whole or part of the material is concerned, specifically the rights of translation, reprinting, reuse of illustrations, recitation, broadcasting, reproduction on microfilms or in any other physical way, and transmission or information storage and retrieval, electronic adaptation, computer software, or by similar or dissimilar methodology now known or hereafter developed.

The use of general descriptive names, registered names, trademarks, service marks, etc. in this publication does not imply, even in the absence of a specific statement, that such names are exempt from the relevant protective laws and regulations and therefore free for general use.

The publisher, the authors and the editors are safe to assume that the advice and information in this book are believed to be true and accurate at the date of publication. Neither the publisher nor the authors or the editors give a warranty, express or implied, with respect to the material contained herein or for any errors or omissions that may have been made.

Printed on acid-free paper

This Springer imprint is published by SpringerNature

The registered company is Springer International Publishing AG Switzerland

Preface

The November 10, 1940 Vrancea intermediate-depth earthquake, with a moment magnitude $M_W = 7.7$, is the strongest seismic event in the past 100 years in Romania and it ranks as the largest intermediate-depth earthquake that occurred in Europe in the twentieth century. This seismic event caused a high death toll (more than 550 people) and more than 1200 casualties, as well as very heavy damage in the epicentral region and hundreds of kilometers away from the epicenter. In Bucharest, the tallest reinforced concrete structure at that time—Carlton building—completely collapsed.

The *National Symposium 75 Years from November 10th 1940 Vrancea Earthquake* took place on November 10, 2015 at the *Technical University of Civil Engineering of Bucharest (UTCB)*. The symposium aimed at sharing the lessons learnt after 1940 Vrancea earthquake and the research progresses in seismology and earthquake engineering in Romania 75 years after. The event was jointly organized by *UTCB* (through the *Seismic Risk Assessment Research Center*) and *National Institute for Earth Physics (INFP)* with the support of *Romanian Association of Civil Engineers (AICR)*.

The symposium greatly benefited from the comprehensive and professional support of the Scientific and Organizing Committees. The full list of the Committees' members is given in Appendix A.

The symposium's Scientific and Organizing Committees invited specialists from academia, researchers, and practitioners to participate and to contribute with scientific papers to this event. At the time of the symposium, a Book of Abstracts published by CONSPRESS (the publishing house of the Technical University of Civil Engineering of Bucharest) was distributed to the participants. Fifty-two abstracts were received and published. The distribution of the abstracts in between the topics was as follows:

- 11 in Topic 1—Effects and Lessons from November 10th, 1940 Vrancea Earthquake
- 20 in Topic 2—Seismicity of Romania. Seismic Hazard Assessment; Local Soil Conditions Effect

- 12 in Topic 3—Structural Design in Seismic Areas; Performance-Based Design
- 9 in Topic 4—Seismic Evaluation and Rehabilitation. Seismic Risk Assessment.

A very well-balanced distribution of contributions between seismology and earthquake engineering was achieved during the symposium. The detailed program of the symposium is presented in Appendix B.

Because of the harsh times in the fifth decade of the past century, the lessons learnt after 1940 Vrancea earthquake were not extensively and completely shared with the international scientific community and thus, this book is trying to fill a gap in the knowledge acquired after major disasters.

Most of the original relevant literature concerning the 1940 Vrancea earthquake is in Romanian, so it is not available for the international scientific community. Moreover, even though the relevant scientific information in the past 25 years is in English, each journal article considers the November 10, 1940 Vrancea earthquake as a piece in the great puzzle that represents the intermediate-depth seismicity of Vrancea. This book gathers altogether the relevant information about this destructive earthquake in one compelling piece and offers to the international scientific community the opportunity to study in depth one of the most important earthquakes in Europe in the twentieth century. To this aim, the seismic effects of 1940 Vrancea earthquake are revisited with the state-of-the-art knowledge to acquire and share the most important lessons.

The lessons learnt and the current understanding of the 1940 Vrancea earthquake are presented to the reader along with state-of-the-art information on the seismicity of Romania, seismic hazard and risk assessments and seismic evaluation and rehabilitation of buildings and structures. Moreover, a collection of genuine information from Romanian post-disaster reports and textbooks concerning the 1940 Vrancea earthquake, compiled and translated into English, accompanies the book. An English translation of the chronicle of the aftermath of November 10, 1940 disaster is presented in Appendix C.

The most valuable full papers submitted were selected by the international reviewers and members of Scientific Committee and are published in this contributed volume. The book contains the Proceedings of the Symposium Commemorating 75 years from November 10, 1940 Vrancea Earthquake and includes, inter alia, most of the available information on this major seismic event and its consequences. The proceedings are structured in four parts, namely:

1. Effects and Lessons from November 10, 1940 Vrancea Earthquake
2. Seismicity of Romania. Seismic Hazard Assessment; Local Soil Conditions Effect
3. Structural Design in Seismic Areas; Performance-Based Design
4. Seismic Evaluation and Rehabilitation. Seismic Risk Assessment.

The sharing of the 34 chapters in between the parts is as follows: eight in Part I, twelve in Part II, six in Part III, and eight in Part IV. Again, a very good balance between the chapters addressing engineering seismology (Part II) and earthquake

engineering (Parts III and IV) is achieved. Each chapter starts with an overview that provides a summary of the papers included.

Each chapter has benefitted from the professional input and hard work of the following coordinators: Alexandru Aldea and Mircea Radulian (Part I), Mihaela Popa and Florin Pavel (Part II), Viorel Popa (Part III) and Carmen Cioflan and Mihail Iancovici (Part IV). The coordinators liaised with the authors and the reviewers and ensured the scientific quality and relevance of the manuscripts. The full list of the reviewers, to whom we are deeply indebted for their excellent timely work, is given as follows:

- Alexandru Aldea (Technical University of Civil Engineering of Bucharest, Romania)
- Anastasios Anastasiadis (Aristotle University of Thessaloniki, Greece)
- Luminița Ardeleanu (National Institute for Earth Physics, Magurele, Romania)
- Andrei Bala (National Institute for Earth Physics, Magurele, Romania)
- Alex Barbat (Universitat Politècnica de Catalunya • BarcelonaTech, Spain)
- Virgil Breabăn (“Ovidius” University of Constanta, Romania)
- Mihai Budescu (Technical University “Gheorghe Asachi” of Iasi, Romania)
- John Douglas (University of Strathclyde, Glasgow, Scotland, United Kingdom)
- Emil-Sever Georgescu (National Institute for Research and Development in Constructions, Urbanism and Sustainable Land Planning URBAN-INCERC, Bucharest, Romania)
- Athanassios Ganas (Institute of Geodynamics, National Observatory of Athens, Greece)
- Daniel Grecea (Politechnica University of Timisoara, Romania)
- Marian Ivan (Faculty of Geology and Geophysics, University of Bucharest, Romania)
- Mihaela Kouteva-Guentcheva (Faculty of Structural Engineering, University of Architecture, Civil Engineering and Geodesy, Sofia, Bulgaria)
- Grzegorz Lizurek (Institute of Geophysics PAS, Warszawa, Poland)
- Eugen Lozincă (Technical University of Civil Engineering of Bucharest, Romania)
- Gheorghe Mărmureanu (National Institute for Earth Physics, Magurele, Romania)
- Öcal Necmioğlu (Department of Geophysics, Boğaziçi University, Istanbul, Turkey)
- Florin Pavel (Technical University of Civil Engineering of Bucharest, Romania)
- Mircea Petrina (Technical University of Cluj-Napoca, Romania)
- Radu Petrovici (University of Architecture and Urbanism “Ion Mincu”, Bucharest, Romania)
- Kyriazis Ptilakis (Aristotle University of Thessaloniki, Greece)
- Mihaela Popa (National Institute for Earth Physics, Magurele, Romania)
- Viorel Popa (Technical University of Civil Engineering of Bucharest, Romania)
- Mircea Radulian (National Institute for Earth Physics, Magurele, Romania)

- Peter Varga (MTA CSFK Geodetic and Geophysical Institute, Budapest, Hungary)
- Friedemann Wenzel (Karlsruhe Institute of Technology and Geophysical Institute, Karlsruhe, Germany).

Acknowledgments

The editors wish to extend their gratitude to the members of the Scientific and Organizing Committees, to the reviewers, to the chapters' coordinators and to all the contributing authors for their full involvement and cooperation in developing this book.

The professional involvement and work of the chapters' coordinators and the constructive suggestions of the reviewers greatly contributed to the quality of the manuscripts.

The editors acknowledge the dutiful and careful checking of all the manuscripts performed, before the final submission to Springer, by our colleagues from Technical University of Civil Engineering of Bucharest (UTCB) and National Institute for Earth Physics (INFP): Carmen Cioflan, Veronica Colibă, Ionuț Crăciun, Cristi Ghiță, Cristian Neagu, Florin Pavel, and Dragoș Toma-Dănilă.

A final word of gratitude is conveyed to Dörthe Mennecke-Bühler, Johanna Schwarz, Ashok Arumairaj, Sivajothi Ganesarathinam, and all the editorial staff from Springer International Publishing AG for their professional coordination and support in preparing this contributed volume.

Bucharest
December 2015

Radu Vacareanu
Constantin Ionescu

Contents

Part I Effects and Lessons from November 10th, 1940 Vrancea Earthquake	
Overview of Part I	3
Alexandru Aldea and Mircea Radulian	
The Strong Romanian Earthquakes of 10.11.1940 and 4.03.1977. Lessons Learned and Forgotten?	19
Andrei Bala and Dragos Toma-Danila	
Before and After <i>November 10th, 1940 Earthquake</i>	37
Ileana Calotescu, Cristian Neagu and Dan Lungu	
The Collapse of Carlton Building in Bucharest at November 10, 1940 Earthquake: An Analysis Based on Recovered Images	57
Emil-Sever Georgescu	
Main Characteristics of November 10, 1940 Strong Vrancea Earthquake in Seismological and Physics of Earthquake Terms	73
Gheorghe Marmureanu, Carmen Ortanza Cioflan, Alexandru Marmureanu and Elena Florinela Manea	
The 10 November 1940—The First Moment of Truth for Modern Constructions in Romania	85
Radu Petrovici	
Macroseismic Effect of the November 10, 1940 Earthquake in the Territory of Moldova, Ukraine and Russia	101
Nila Stepanenco and Vladlen Cardanet	
Causes and Effects of the November 10, 1940 Earthquake	113
Ion Vlad	

Part II Seismicity of Romania. Seismic Hazard Assessment; Local Soil Conditions Effect	
Overview of Part II: Seismicity of Romania. Seismic Hazard Assessment; Local Soil Conditions Effects.	131
Mihaela Popa and Florin Pavel	
Use of Various Discrimination Techniques to Separate Small Magnitude Events Occurred in the Northern Part of Romania	135
Felix Borleanu, Bogdan Grecu, Mihaela Popa and Mircea Radulian	
Prediction of Site Characterization Based on Field Investigations and Empirical Correlations	151
Elena-Andreea Călărășu, Cristian Arion and Cristian Neagu	
Spectral Displacement Demands for Strong Ground Motions Recorded During Vrancea Intermediate-Depth Earthquakes	169
Ionut Craciun, Radu Vacareanu and Florin Pavel	
Analysis of the Seismic Activity in the Vrancea Intermediate-Depth Source Region During the Period 2010–2015	189
Andreea Craiu, Mihail Diaconescu, Marius Craiu, Alexandru Marmureanu and Constantin Ionescu	
A Contemporary View to the Impact of the Strong Vrancea Earthquakes on Bulgaria.	205
Mihaela Kouteva-Guentcheva and Krasimir Boshnakov	
Site Dependent Seismic Hazard Assessment for Bucharest Based on Stochastic Simulations	221
Florin Pavel, Daniel Ciuiu and Radu Vacareanu	
Scaling Properties for the Vrancea Subcrustal Earthquakes: An Overview.	235
Emilia Popescu, Mircea Radulian and Anica Otilia Placinta	
The 2013 Earthquake Swarm in the Galati Area: First Results for a Seismotectonic Interpretation	253
Mihaela Popa, Eugen Oros, Corneliu Dinu, Mircea Radulian, Felix Borleanu, Maria Rogozea, Ioan Munteanu and Cristian Neagoe	
Comparison of Three Major Historical Earthquakes with Three Recent Earthquakes.	267
Maria Rogozea, Mircea Radulian, Mihaela Popa, Daniel Nistor Paulescu, Eugen Oros and Cristian Neagoe	
An Attempt to Bridge the Gap Between the Traditional Concept of Seismic Intensity and the Need of Accuracy Required by Engineering Activities.	285
Horea Sandi and Ioan Sorin Borcia	

Earthquake Precursors Assessment in Vrancea Region Through Satellite and In Situ Monitoring Data 305
 Maria Zoran, Dan Savastru and Doru Mateciuc

Part III Structural Design in Seismic Areas; Performance-Based Design

Overview of Part III: Structural Design in Seismic Areas; Performance Based Design 317
 Viorel Popa

Influence of the Infill Panels Masonry Type on the Seismic Behaviour of Reinforced Concrete Frame Structures 319
 Mircea Bârnaure, Ana Maria Ghiță and Daniel Nicolae Stoica

A Time-Domain Approach for the Performance-Based Analysis of Tall Buildings in Bucharest 333
 Mihail Iancovici and George Vezeanu

Unidirectional Cyclic Behavior of Old Masonry Walls in Romania 351
 Eugen Lozincă, Viorel Popa, Dragoș Coțofană and Alexandru Basarab Cheșcă

Viscous Damper Distribution Using Genetic Algorithms and Pattern Search Optimization 363
 Andrei Pricopie and Alin Costache

Selecting and Scaling Strong Ground Motion Records Based on Conditional Mean Spectra. Case Study for Iasi City in Romania 377
 Radu Vacareanu, Mihail Iancovici and Florin Pavel

Part IV Seismic Evaluation and Rehabilitation. Seismic Risk Assessment

Overview of Part IV: Seismic Evaluation and Rehabilitation. Seismic Risk Assessment 395
 Carmen Ortanza Cioflan and Mihail Iancovici

Estimation of Damage-Loss from Scenario Earthquake Analogous to November 10, 1940 in Republic of Moldova 399
 Vasile Alcaz, Eugen Isicico, Victoria Ghinsari and Sergiu Troian

Some Remarks Regarding Seismic Vulnerability for Orthodox Churches 411
 Mihai Budescu, Lucian Soveja and Ioana Olteanu

Seismic Loss Estimates for Scenarios of the 1940 Vrancea Earthquake 425
 Carmen Ortanza Cioflan, Dragos Toma-Danila and Elena Florinela Manea

Rapid Earthquake Early Warning (REWS) in Romania: Application in Real Time for Governmental Authority and Critical Infrastructures	441
Constantin Ionescu, Alexandru Marmureanu and Gheorghe Marmureanu	
Seismic Assessment and Rehabilitation of Existing Constructions after the 10th November 1940 and 4th March 1977 Earthquakes in Romania	451
Mircea Mironescu, Adrian Mircea Stănescu, Teodor Brotea, Radu Florin Comănescu, Daniel Dumitru Purdea and Mircea V. Stănescu	
Analytical Seismic Fragility Functions for Dual RC Structures in Bucharest	463
Paul Olteanu, Veronica Coliba, Radu Vacareanu, Florin Pavel and Daniel Ciuiu	
Conceptual Framework for the Seismic Risk Evaluation of Transportation Networks in Romania	481
Dragos Toma-Danila, Iuliana Armas and Carmen Ortanza Cioflan	
Appendix A: Members of Scientific and Organizing Committees	497
Appendix B: Program of the <i>National Symposium 75 Years from November 10th 1940 Vrancea Earthquake</i>	499
Appendix C: Testimonies on the Aftermath of November 10th 1940 Vrancea Earthquake in the Putna County	503

Part I
Effects and Lessons from November 10th,
1940 Vrancea Earthquake

Overview of Part I

Alexandru Aldea and Mircea Radulian

1 Romania's Seismicity and the November 10th, 1940 Vrancea Intermediate Depth Earthquake

The seismic activity in Romania is dominated by the earthquakes generated at intermediate depths (60–180 km) in the Vrancea region, located at the bend of the South-Eastern Carpathians. This area represents the junction of several tectonic units: East-European Plate to the North and North-East, Scythian Platform to the East, North Dobrogea orogen to the South-East, Moesian Platform to the South and South-West and Carpathian orogen and Transylvanian Basin (Intra-Alpine plate) to the West and North-West. It is a region now in a stage of post-continental collision (Ismail-Zadeh et al. 2012 and herein references).

The seismicity concentrates in a narrow high-velocity lithospheric volume embedded in the upper mantle beneath the South-Eastern Carpathians Arc bend. The rate of seismic moment per volume, $\sim 0.8 \times 10^{19}$ Nm/year, is comparable to southern California (Wenzel et al. 1998) and is in a strong contrast with the low seismicity characterizing the rest of the Carpathians orogeny system. To explain the extreme concentration of the focal volume continuously generating earthquakes in the mantle and its relative isolation (the Vrancea seismogenic zone is one of the few examples of prominent localized intermediate-depth seismicity situated far from active plate boundaries), a complex geodynamics involving manifold processes

A. Aldea (✉)
Technical University of Civil Engineering, Bucharest, Romania
e-mail: aldea@utcb.ro

M. Radulian
National Institute for Earth Physics, Magurele, Romania
e-mail: mircea@infp.ro

(roll-back, break-off, delamination, gravitational instability, dehydration, thermal shear runaway) is invoked (e.g., Fuchs et al. 1979; Oncescu 1984; Linzer 1996; Gîrbacea and Frisch 1998; Sperner et al. 2001; Gvirtzman 2002; Cloetingh et al. 2004; Ismail-Zadeh et al. 2005, 2012; Houseman and Gemmer 2007; Lorinczi and Houseman 2009).

The catalogue of Vrancea earthquakes is considered complete for magnitude M_w 6.5 for an interval of six centuries (Oncescu et al. 1999). In average five shocks with magnitude $M_w > 6.5$ are recorded per century. The maximum recorded magnitude is attributed to the event of 1802 ($M_w = 7.9$). In the last century, four shocks with magnitude above 7 were recorded, characterized by large damage over extended and dense-populated areas.

The event produced on 10th November 1940 ($M_w = 7.7$) was the largest instrumentally recorded earthquake recorded in Romania and the fourth of the largest intermediate-depth earthquakes recorded since 1900 until present day. The macroseismic effects were felt over an area of about two million km^2 , while the ground motion induced by the seismic waves was recorded at the global scale (as far as Wellington in New Zealand).

A significant increase in the background seismicity preceded by a few months the triggering of the major shock in 1940. As remarkable precursor events we mention the events of 24th June 1940 ($M_w = 5.9$), 22nd October 1940 ($M_w = 6.5$) and 8th November 1940 ($M_w = 5.9$). The aftershock activity was less extensive as compared with aftershock activity for crustal events of similar size (the largest aftershock of $M_w 5.9$ was produced on 11th November 1940) which is a typical feature for the Vrancea intermediate-depth earthquakes. However, both the pre- and post-shock activities were notably greater than those associated with the subsequent major events of March 1977 ($M_w = 7.4$) and August 1986 ($M_w = 7.1$).

The occurrence of the major earthquake of 10th November 1940 marked a turning point in the research of the seismic phenomenon in the SE Carpathians Arc bend. Through the magnitude of the effects, widely felt, and the multitude of instrumental data which at that time was a unique worldwide database, the earthquake was an event truly revealing in many ways. At the same time, it raised a lot of questions and controversies as concerns the seismological and geotectonical interpretation of the earthquake phenomenon.

2 November 10th, 1940 Earthquake: Victims and Damage

“The November 10th, 1940 earthquake sprinkled ruins all over Romania and threw mourning over the people” (Romanian Academy of Sciences 1941)

2.1 *Earthquake Victims*

The first official data concerning the victims was issued on November 11th: The Communicate of Ministerial Council indicated in Romania 267 deaths and 476 injured (as counted until the evening of November 10th).

The Romanian telegraphic information society Rador informed the world about the earthquake in the morning of November 10th, indicating an unidentified number of victims. Rador disseminated the official ministerial data from November 11th on November 12th to London, Rome, Budapest, Athens, Belgrade, Berlin, Moscow, Ankara, Sofia, Berne, Madrid, Clermont-Ferrand (Agerpres 2015).

Around the world journals, magazines and TV news were informing about the Romanian earthquake effects.

In France for example:

- on November 12th, L'Ouest-Éclair newspaper (1940) indicates over 500 deaths in Bucharest, 30 deaths and 100 injured in Galati in Romania, injured people in Sofia (Bulgaria), several dozens of deaths and hundreds of injured in Hungary and Transylvania;
- on November 14th, La Vendée Républicaine newspaper (1940) indicates 500 deaths in Bucharest, 30 deaths and 100 injured in Galati in Romania, and injured people in Sofia (Bulgaria);
- on November 30th, L'Illustration magazine (1940) gives the official Romanian data and also indicates victims details in Galati (45 deaths and 35 injured) and in Focsani (30 deaths and 60 injured) in Romania and mentions injured people in Bulgaria;
- on December 11th, l'INA (1940) TV news indicates hundreds of deaths and injured.

In United States:

- on November 23rd, in Nature journal Tillotson (1940) indicates “More than 150 are known to have been killed in Bucharest alone [...] Panciu is said to have been completely destroyed and there are 23 dead and 71 seriously injured [...] At Jassy, 4 were killed and 6 gravely injured [...] Galati [...] the casualties were reported as 36 killed and a 130 injured.” He estimates “casualties throughout the country as 400 killed and 800 severely injured”. Tillotson also mentions about 15 persons injured at Rutschuk in Bulgaria;
- on November 25th, Time magazine writes “In Bucharest 98 bodies had been taken from the stony ruins of the elegant Carlton apartments. The national toll rose to 357 dead, thousands injured.”

In Germany on November 28th, Die Deutsche Wochenschau TV news (1940) indicates almost 300 deaths and over 400 injured in Romania.

In UK on January 9th, British Pathé TV news (1941) talks about 300 deaths in the collapse of one tall building in Bucharest.

In all reports, a special attention was paid to the collapse of Carlton building in central Bucharest, a modern tall reinforced concrete frame structure that buried in its ruins over a hundred persons, Fig. 1.

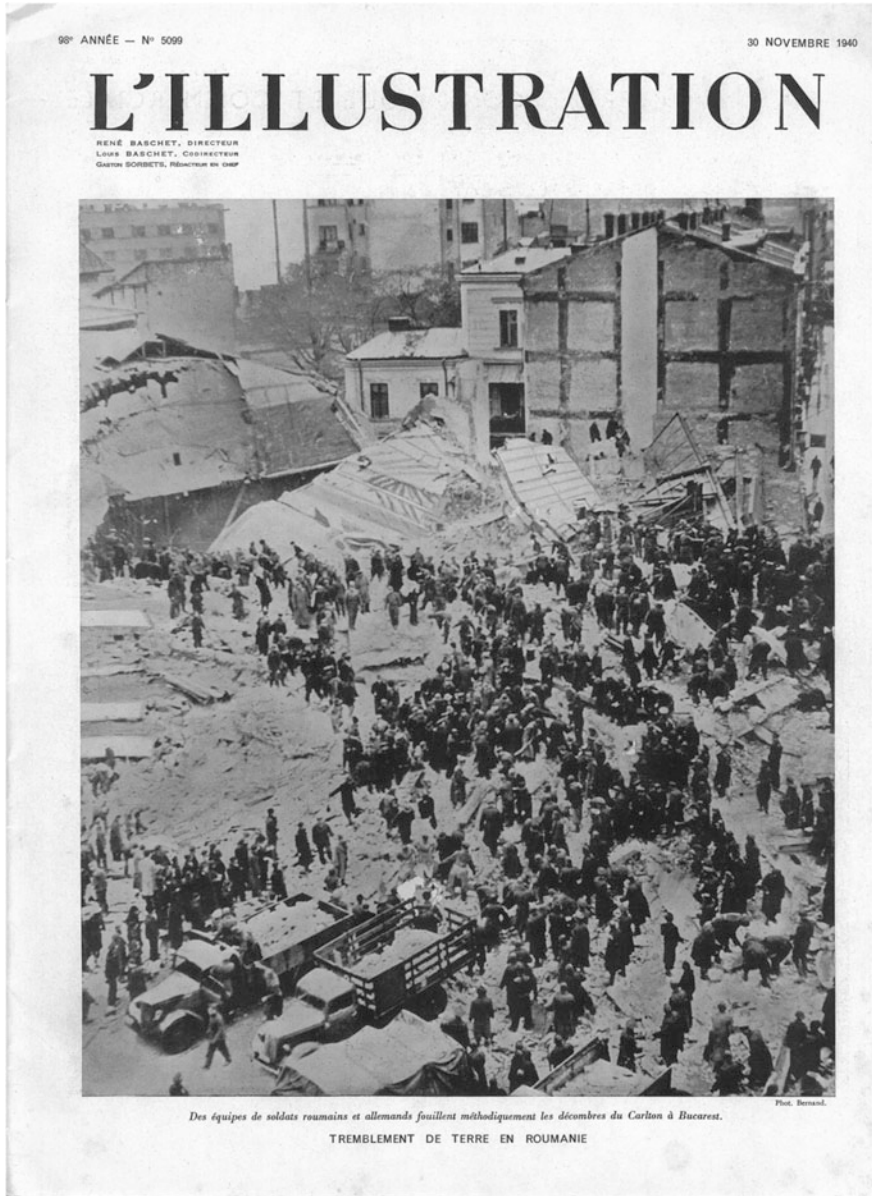


Fig. 1 Collapse of Carlton building in Bucharest—Romania during the November 10th, 1940 Vrancea earthquake (L'illustration 1940)

Carlton collapse is described in the paper of Georgescu (present Chapter). The search and rescue operation involved not only Romanian fire fighters, military and citizens, but also German soldiers and Italian volunteers, Fig. 2 (La Tribuna Illustrata 1940).



Fig. 2 Search and rescue operations after the collapse of Carlton building in Bucharest—Romania during the November 10th, 1940 Vrancea earthquake (La Tribuna Illustrata 1940)

Due to the war period, the precise number of victims of the November 10th, 1940 Vrancea earthquake was not estimated and there were no final official data. The same is valid also for the neighbouring countries Bulgaria, Hungary and Ukraine and territories Transylvania, Bessarabia and Northern Bukovina that were under Hungarian and Soviet Union occupation.

As above presented, there were injured persons in Bulgaria, deaths and injured in Hungary.

For Bessarabia (Moldavian SSR) Stepanenco and Cardanet (present Chapter) indicate that “there were 17 people killed and died of severe wounds, 66 seriously injured, 546 lightly wounded people”. However, another study indicated over 78 deaths and approximately 1000 injured (Drumea 2000).

In their study of 2012, Georgescu and Pomonis gathered data from different sources and indicate a total death toll of 593 and 1271 injured for the Romanian territories.

Other studies are indicating larger numbers of deaths: 980 (EM-DAT: The OFDA/CRED International Disaster Database), 1000 (Gutenberg and Richter 1954; Tazieff 1962, USGS), >1000 (Beles and Ifrim 1962; Coburn and Spence 1992).

With a total number of deaths over 600 and probably reaching 1000 and with over 1000 injured persons in Romania, Hungary, Moldavian SSR and Bulgaria, the November 10th, 1940 Vrancea earthquakes produced a strong public impact around the world and ranked in the top 10 of the deadliest European earthquakes of 20th century.

2.2 *Earthquake Damage*

The Communicate of Ministerial Council of November 11th, 1940 indicated substantial damage in Bucharest where 183 buildings were heavily damaged and had to be evacuated and other 402 buildings suffered lower damages. The collapse of Carlton building is also presented. The Communicate mentions heavy damage in the cities of Galati, Focsani and on Prahova river valley, and slight damage in another 19 cities.

Unfortunately, the damage proved to be much higher.

Popescu (1941) presents a map with an estimation of the macroseismic area of the earthquake, concluding that it over passed 2 million km²: “The shaking was felt toward east in all the south-western Soviet Union (Odessa, Charkow, Kiew, Moscow—where it even produced slight damages). Toward north, it reached Leningrad; toward west it was felt beyond Tissa river and toward south-west and south if was felt in Yugoslavia, all Bulgaria up to Istanbul.” Popescu also estimated the maximum seismic intensity of X (on Mercalli-Cancani-Sieberg international scale) and indicated that the region with intensities equal or higher to VIII reached 80,000 km².

Demetrescu (1941) built a seismic intensity map (shown in Bala and Toma-Danila, present Chapter) using data from Romania and Bulgaria and estimated an MSC intensity of X in at least 5 locations. The northern part of Bulgaria was in intensity VII area while almost all the rest of the country (except the far south) in V and VI.

Radulescu (1941) presented a description of the severe damage accompanied by photos in several cities from the epicentral region (Panciu, Barlad, Focsani, etc.) and in Bucharest for which he drew up a first seismic damage microzonation map indicating that building damage was spread all across the city. He also presented several examples of induced hazard (liquefaction, landslides, ground cracking in river meadows, etc.).

Several seismic intensity maps were drawn by researchers and institutions in the years after the earthquake (some of them shown in the papers from this Chapter), and data from the strong earthquake of November 10th, 1940 was the basis of the maps from the 1941 and 1945 Romanian seismic design regulations and in the national macroseismic zonation map from 1952.

In the recent years, a significant effort was made for the reevaluation of the seismic intensities.

Pantea and Constantin (2011) made a “reinterpretation of over 4500 macroseismic questionnaires, as well as the critical and serious research of the expertise reports, monographies, photos, scientific papers published both inside and outside the country”. They produce for Romania’s territory a map in terms of MSK-64 (Medvedev, Sponheur, Karnik) seismic intensities, Fig. 3.

Konrod et al. (2013) integrated transnational macroseismic data for the strongest earthquakes of Vrancea (Romania), including the 1940 event, using up-to-date procedures for producing isoseismals. The macroseismic map, Fig. 4, confirms the NE-SW directivity of the earthquake effects and a large area with seismic intensity equal and higher to IX.

Building damage was widely described in the press of the time, in Romania and abroad.

In France for example:

- on November 12th, L’Ouest-Éclair newspaper (1940) indicates that all buildings in Bucharest suffered, and that damage was reported in Bulgaria, Hungary and Transylvania;
- on November 30th, L’Illustration magazine (1940) indicates extensive damage in the cities of Bucharest, Ploiesti, Galati, Focsani, Targoviste, Mizil, Iasi, Campina, together with suggestive images (Fig. 5);
- on December 11th, l’INA TV news talk about thousands of buildings destroyed.

In UK on January 9th, British Pathé TV news (1941) indicate that about 13,000 km² of the Kingdom of Romania were transformed into ruins and that the effects were similar to those of a war.

In United States:

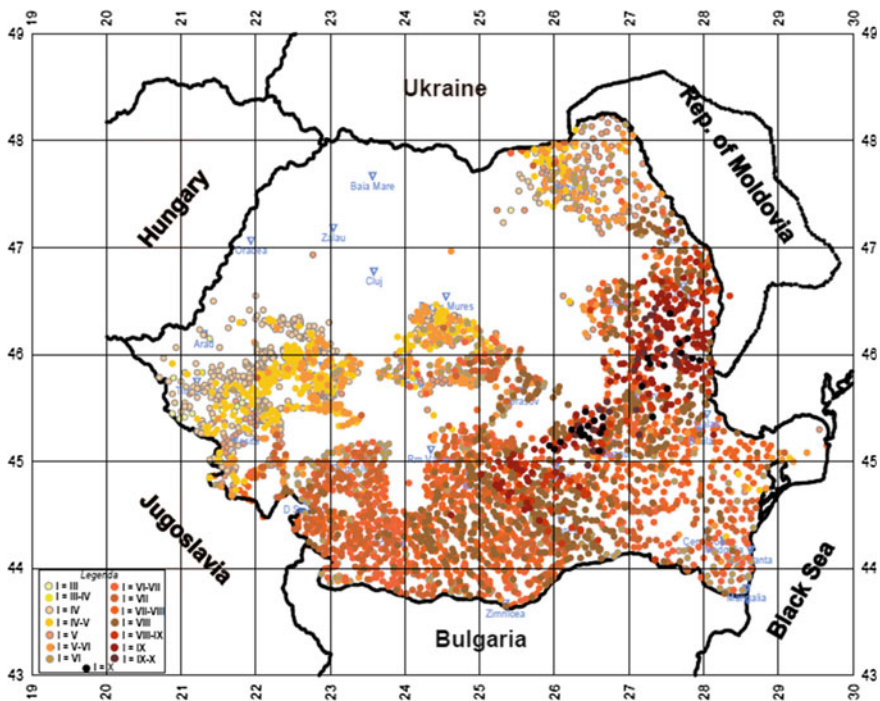


Fig. 3 Reevaluated macroseismic map of November 10, 1940 earthquake (Pantea and Constantin 2011)

- on November 13th, Eleanor Roosevelt (1940) noted: “In Romania, the earthquake seems to have accomplished in a few short hours what all the aviators of Great Britain have tried unsuccessfully to do for weeks—fires are raging, oil wells are destroyed [...]”
- on November 23rd, in Nature journal Tillotson (1940) summarises the most important damages in Bucharest and mentions that “among other buildings 200 were destroyed and 400 damaged” and “More than a 1000 badly damaged houses have had to be evacuated in Bucharest, and there is scarcely a house not affected in some way”; he also presents data concerning the damage in other cities: “At Focsani [...] 70 % of the houses in the centre of the town are said to be razed and hundreds of people rendered homeless. [...] At Giurgiu [...] 65 % of the houses are reported destroyed. [...] At Buzau [...] hundreds of buildings have been destroyed and many people killed. [...] Panciu is said to have been completely destroyed [...]. Galati [...] suffered severely. The cathedral and St. Helen’s church were destroyed, scores of houses severely damaged [...]”; he also presents information about damage in Bulgaria: “At Rutschuk, just on the Bulgarian side of the frontier, 10 houses were damaged [...]”.

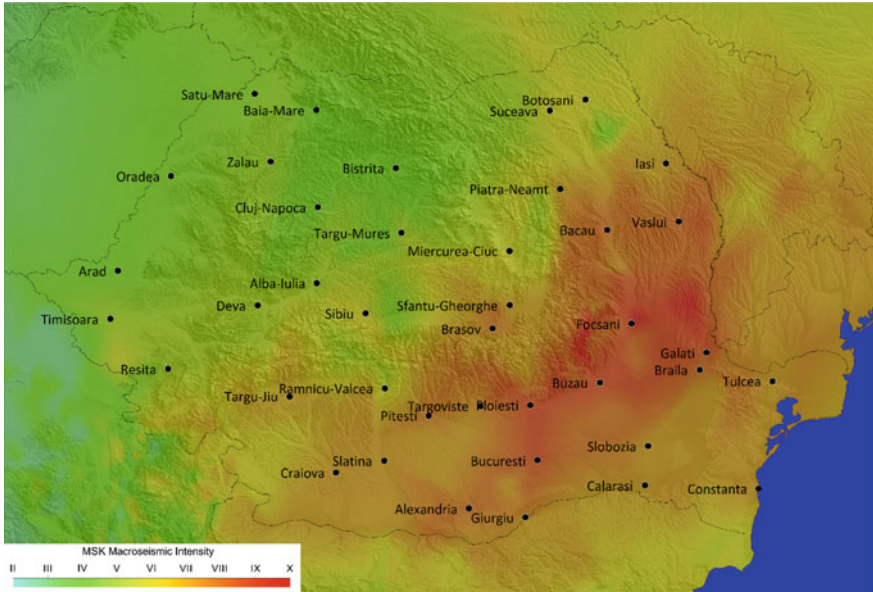


Fig. 4 Macroseismic map of November 10, 1940 earthquake (macroseismic intensities data from Konrod et al. 2013)

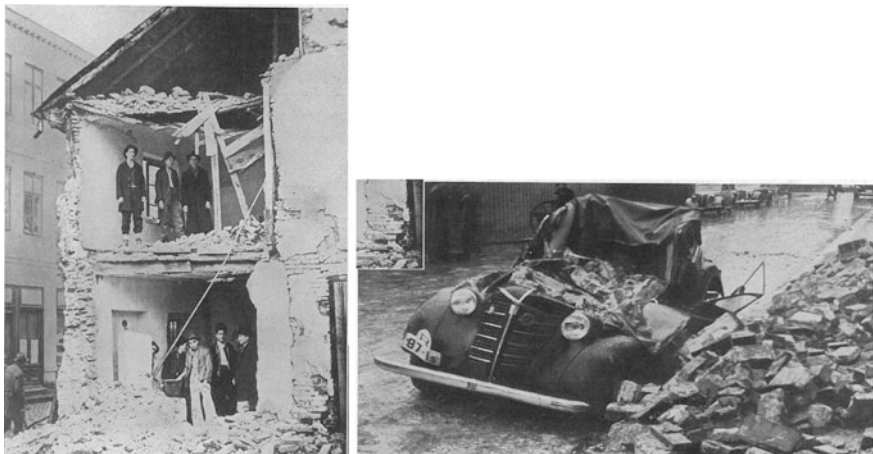


Fig. 5 1940 earthquake damage in Romania (L'Illustration 1940)

In Romania all national, regional and local papers reported about the earthquake effects for several days. Several scientific papers were published in Romania and abroad in 1940 and 1941, most of them referenced in the papers from this Chapter.

Two of the most important scientific papers, considered by many as the starting point of earthquake engineering in Romania, were published by Beles (1941a, b), one in French and one, extended, in Romanian. Beles, a professor at the Polytechnic School of Bucharest, at the Civil Engineering Faculty, described and analysed in detail the building damage and suggested repairing and retrofitting solutions. Several aspects from his impressive work are found in this Chapter's papers.

Over Romania, extensive damage occurred to most of the important buildings like city-halls, prefectures, schools, hospitals, railway stations, etc., in general masonry buildings. In Bucharest, damage also occurred to many reinforced-concrete structures that were built in between the wars. Elements concerning the building stock prior to the earthquake are given in some of the papers from this Chapter. Impressive images were published over time in different papers and there is a continuous effort of retrieving such useful historical information (for example Agerpres, 2014, website).

The paper of Calotescu et al. (present Chapter) shows severe damage in Kishinev.

Another category of damaged constructions, whose destructions had a powerful social impact included churches and monasteries. All around the country many religious buildings suffered complete collapse or severe damage. The paper Marmureanu et al. (present Chapter) covers a number of damaged churches and the seismic intensity evaluation at those locations.

Antonescu (1942) was concerned with new design solutions for new churches. He mentioned that predictions about earthquake strength were over passed and that a high destructive force was noticed in areas where nobody expected. Churches that stood up against earthquakes with little damage for many centuries were now destroyed or severely damaged. He indicates that prior to the earthquakes several churches were strengthened by inserting a reinforced concrete skeleton and that these churches had a good behaviour during the 1940 earthquake, and he recommended the reinforced concrete structures with in filled masonry as a possible solution for new churches.

A special damage case was the city of Panciu. All news, national and international attracted the public attention toward the city of Panciu, located in the epicentral area, and national and international aid was directed to support Panciu inhabitants. Images and TV news showed King Michael of Romania visiting the city soon after the earthquake. Capatana (1941), the mayor of the city at that time, presented an overwhelming picture of the disaster: "the only town in Romania that was 99 % destroyed, from 371 masonry houses only 5 stood up, together with 57 adobe or wooden houses at city borders." Capatana also mentions about 42 dead persons and 76 injured from which several died later. The almost entire ruin of the city, Fig. 6, induced a special reaction from Romanian state who issued a Law (1942) for the city reconstruction.



Fig. 6 1940 earthquake damage in Panciu, Romania (Capatana, 1941): Hotel Gatza (*upper left*), Capatana Pharmacy (*upper right*) Carol Street (northern part *lower left* and southern part *lower right*)

3 November 10th, 1940 Earthquake: Concluding Remarks

“Altogether, the shock constituted one of the great earthquakes of the world” (Tillotson 1940)

The Chapter devoted to the effects and lessons from November 10th, 1940 Vrancea earthquake groups seven papers dealing with earthquake characteristics, seismic intensities, victims and building damage, earthquake engineering and seismology and building design before and after the earthquake. In the annex of the overview a brief description of the papers is given.

The wide macroseismic area and the large destruction area of the 1940 earthquake, as well as of other strong Vrancea earthquakes (1802, 1977, 1986, 1990, 2004) are a direct effect of the intermediate depth at which these earthquakes occur.

Vrancea earthquakes are not Romanian earthquakes, but European earthquakes being felt in several countries (Romania, Bulgaria, Republic of Moldova, Ukraine, Russia, Greece, Turkey, Hungary, Yugoslavia, etc.) and producing victims and damage on a wide area beyond Romania’s borders.

The large magnitude ($M_W = 7.7$), the huge macroseismic field with seismic intensities reaching X and with a large area with intensities equal or higher to IX, the relatively large number of victims, altogether rank the November 10th, Vrancea intermediate depth earthquake as one of the major European earthquakes.

Appendix: Summary of the Papers in this Chapter

The paper by Marmureanu et al. introduces a brief presentation of the seismicity of Vrancea source before the November 10th, 1940 earthquake. An important part of the paper is devoted to the description (data selected from various sources) of the earthquake effects in Romania, focusing on several cities which experienced extensive damage (Barlad, Ploiesti, Bucharest, Targoviste, Buzau). The paper ends by presenting data on earthquake damage of a number of churches and monasteries in Romania, the authors estimating MSK seismic intensity values at the sites of damaged religious buildings.

The paper of Calotescu et al. begins with the presentation of the evolution of seismic design of buildings in Romania with emphasis on Bucharest, “Europe’s capital of earthquakes” (The Guardian, March 25th 2014, online edition). Following 1940 Vrancea earthquake, new seismic design regulations (1941, 1945) were prepared (but not enforced) and macroseismic hazard maps were documented. In the paper the most representative macroseismic maps available to the authors compared and discussed. Seismological data available before and after the Nov. 10th, 1940 event and data related to the damage produced by historic strong Vrancea earthquakes (1802, 1838, 1940) are presented and discussed.

The paper of Georgescu focuses on the complete collapse during the November 10th, 1940 earthquake of Carlton building in Bucharest. With about 45 m height, the modern Carlton building was one of the symbols of the capital city Bucharest and was a representative work of avant-garde architecture. Located in the city center, the building had a reinforced concrete frame structure with in filled masonry walls. Using an extensive bibliographic documentation (from Romania, Germany, Belgium and France), the paper describes the possible collapse mechanism and the Search and Rescue operations.

The paper of Petrovici begins with a historical overview on the seismicity and on the reinforced concrete design and construction in Romania. The paper continues with the presentation of the main aspects of architectural and structural building design in Romania prior to the 1940 earthquake and ends with a critical analysis of the main post-earthquake lessons from Beles (1941a, b), with elements concerning the 1977 earthquake effects and with a warning for the potential damage during a future strong earthquake.

The paper of Bala and Toma-Danila is structured in two main parts: one devoted to the seismological aspects of the November 10th, 1940 earthquake and its effects in Romania (with special emphasis on the paper of Beles (1941a, b), on the conclusions and recommendations that were made) and other devoted to the seismological aspects of the March 4th, 1977 earthquake and its effects in Romania. The authors underline the link between the 1977 collapses and the damages from 1940, in Bucharest and the lessons to be considered for preventing future earthquake effects.

The paper of Vlad discusses the seismic event of November 10th, 1940 in the light of “seismic islands”, situated far away from the vicinity of the located

epicentre of the earthquake. In this respect, the most representative example is that of Bucharest, located nearly 160 km from the epicentre, and where the macroseismic intensity was set to IX, according to the seismic intensity scale of G. Mercalli and processed by A. Sieberg. The paper focuses on the relevant issues regarding the design and construction practices of the building categories that were severely damaged by the destructive 1940 Vrancea earthquake.

In the paper of Stepanenco and Cardanet the available macroseismic data to the northeast of the epicentre of November 10th 1940 Vrancea earthquake are analyzed. As a result of the previously-mentioned analysis and through the generalization of macroseismic information contained in the relevant literature, a new table with intensity values for the territory of Moldova, Ukraine and Russia was developed, and the isoseismal map of this earthquake are re-drawn. The macroseismic effects for the Eastern Europe of the Vrancea earthquakes of January 23, 1838, March 4, 1977, August 30, 1986 and May 30, 1990 are compared and discussed.

References

- Agerpres (2014) <http://foto.agerpres.ro/index.php?p=1&q=cutremur%20din%201940&qt=1&qf=1&d=-1&u=1&h=1&r=1&md=1&f=0&e=0&x=0&t=0>
- Agerpres (2015) <http://www.agerpres.ro/flux-documentare/2015/11/10/documentar-75-de-ani-de-la-cutremurul-din-1940-08-07-39>
- Antonescu P (1942) New churches after the earthquake (in Romanian). Annals of Romanian academy, memoirs of history section, series III, vol XXIV, Mem. 18. National Printing House, Bucharest, 34p
- Beles A (1941a) Le tremblement de terre du 10 Novembre 1940 et les bâtiments, Comptes Rendus des Séances de l'Académie des Sciences de Roumanie, "Numéro consacré aux recherches sur le tremblement de terre du 10 Novembre 1940 en Roumanie", Tome V, Numéro 3, Mai-Juin, Ed. Cartea Romaneasca, Bucuresti, pp 270–288
- Beles A (1941b) Earthquakes and buildings (in Romanian), Bulletin of the Polytechnic Society of Romania, year LV, Nr. 10–11, pp 1045–1094 and pp 1171–1211
- Beles A, Ifrim M (1962) Engineering seismology (in Romanian). Ed. Tehnica, Bucharest, 247 p
- British Pathé, Rumanian Earthquake, 9th of January (1941). <http://www.britishpathe.com/video/rumanian-earthquake>
- Căpățînă AD (1941) The history of Panciu city and of the "Brazi" and "Sf. Ion" hermitages collapsed by November 10th 1940 earthquake (in romanian), Ed. "Cartea Românească", Bucharest
- Coburn A, Spence R (1992) Earthquake protection. Wiley, New York 355p
- Comptes Rendus des Séances de l'Académie des Sciences de Roumanie (1941) Numéro consacré aux recherches sur le tremblement de terre du 10 Novembre 1940 en Roumanie, Tome V, Numéro 3, Mai-Juin, Ed. Cartea Romaneasca, Bucuresti, pp 177–288
- Cloetingh SAPL, Burov E, Matenco L, Toussaint G, Bertotti G, Andriessen PAM, Wortel MJR, Spakman W (2004) Thermo-mechanical controls on the model of continental collision in the SE Carpathians (Romania). Earth Planet Sci Lett 218:57–76
- Demetrescu G (1941) Remarques sur le tremblement de terre de Roumanie du 10 nov. 1940, Comptes Rendus des Séances de l'Académie des Sciences de Roumanie, Numéro consacré aux recherches sur le tremblement de terre du 10 Novembre 1940 en Roumanie, Tome V, Numéro 3, Mai-Juin, Ed. Cartea Romaneasca, Bucuresti, pp 224–242

- Die Deutsche Wochenschau Nr. 534, 28th Nov. (1940) Internet archive. <https://archive.org/details/1940-11-28-Die-Deutsche-Wochenschau-Nr.534>
- Drumea A (2000) Seismic zonation of Romania and Republic of Moldova (in Romanian), Report, Academy of Sciences of Republic of Moldova, Institute of Geology and Geophysics, 55 p
- EM-DAT: the OFDA/CRED international disaster database. www.emdat.be/
- Fuchs K, Bonjer K, Bock G, Cornea I, Radu C, Enescu D, Jianu D, Nourescu A, Merkle G, Moldoveanu T, Tudorache G (1979) The Romanian earthquake of March 4, 1977. II. Aftershocks and migration of seismic activity. *Tectonophysics* 53:225–247
- Georgescu ES, Pomonis A (2012) Building damage vs. territorial casualty patterns during the Vrancea (Romania) Earthquakes of 1940 and 1977. Proceedings of the 15-th WCEE, Lisbon, 24–28 sept 2012
- Girbacea R, Frisch W (1998) Slab in the wrong place: lower lithospheric mantle delamination in the last stage of the Eastern Carpathian subduction retreat. *Geology* 26:611–614
- Gutenberg B, Richter CF (1954) Seismicity of the earth and associated phenomena, Facsimile of the Edition of 1954. Hafner Publishing Company 1965:130p
- Gvirtzman Z (2002) Partial detachment of a lithospheric root under the southeast Carpathians: toward a better definition of the detachment concept. *Geology* 30(1):51–54
- Houseman GA, Gemmer L (2007) Intra-orogenic extension driven by gravitational instability: Carpathian-Pannonian orogeny. *Geology* 35:1135–1138
- INA—Institut national de l’audiovisuel, Tremblement de terre en Roumanie, 11 Dec. (1940). <http://www.ina.fr/video/AFE85000224>
- Ismail-Zadeh A, Mueller B, Schubert G (2005) Three-dimensional modeling of present day tectonic stress beneath the earthquake-prone southeastern Carpathians based on integrated analysis of seismic, heat flow, and gravity observations. *Phys Earth Planet Inter* 149:81–98
- Ismail-Zadeh A, Mațenco L, Radulian M, Cloetingh S, Panza GF (2012) Geodynamics and intermediate-depth seismicity in Vrancea (The South-Eastern Carpathians): current state-of-the art. *Tectonophysics* 530–531:50–79
- Kronrod T, Radulian M, Panza G, Popa M, Paskaleva I, Radovanovich S, Gribovski K, Sandu I, Pekevski S (2013) Integrated transnational macroseismic data set for the strongest earthquakes of Vrancea (Romania). *Tectonophysics* 590:1–23, 1 April 2013
- La Tribuna Illustrata (1940) 24 Nov.1940, anno XLVIII – N.48
- L’Illustration (1940) No. 5099, 30 November 1940, Le tremblement de terre en Roumanie, pp 309–311
- La Vendée Républicaine (1940) No. 2951, 55^{ème} année, 14 November 1940
- Law Nr. 665, 6th of August 1942 (1942) Official Gazette of Romania, nr. 213, from 12.09.1942, p 7561
- Linzer H-G (1996) Kinematics of retreating subduction along the Carpathian arc, Romania. *Geology* 24:167–170
- Lorinczi P, Houseman GA (2009) Lithospheric gravitational instability beneath the southeast Carpathians. *Tectonophysics* 474:322–336
- Onescu MC (1984) Deep structure of the Vrancea region, Romania, inferred from simultaneous inversion for hypocentres and 3-D velocity structure. *Ann Geophys* 2:23–28
- Onescu M, Mârza V, Rizescu M, Popa M (1999) The Romanian earthquake catalogue between 1984–1997. In: Wenzel F, Lungu D, Novak O (eds) Vrancea earthquakes: tectonics, hazard and risk mitigation. Kluwer Academic Publishers, Dordrecht, pp 43–47
- Pantea A, Constantin P (2011) Reevaluated macroseismic map of Vrancea (Romania) earthquake occurred on November 10, 1940. *Rom J Phys* 56(3–4):578–589
- Popescu IG (1941) Etude comparative sur quelques tremblements de terre de Roumanie du type de celui du 10 Nov. 1940, Comptes Rendus des Séances de l’Académie des Sciences de Roumanie, Numéro consacré aux recherches sur le tremblement de terre du 10 Novembre 1940 en Roumanie, Tome V, Numéro 3, Mai-Juin, Ed. Cartea Romaneasca, Bucuresti, pp 204–223
- Radulescu NAI (1941) Considerations géographiques sur le tremblement de terre du 10 Nov. 1940, Comptes Rendus des Séances de l’Académie des Sciences de Roumanie, Numéro consacré aux

- recherches sur le tremblement de terre du 10 Novembre 1940 en Roumanie, Tome V, Numéro 3, Mai-Juin, Ed. Cartea Romaneasca, Bucuresti, pp 242–269
- Roosevelt E (1940) A comprehensive electronic edition of “my day” newspaper columns. <https://www.gwu.edu/~erpapers/myday/>
- Sperner B, Lorenz F, Bonjer K, Hettel S, Müller B, Wenzel F (2001) Slab break-off abrupt cut or gradual detachment? New insights from the Vrancea region (SE Carpathians, Romania). *Terra Nova* 13:172–179
- Tazieff H (1962) Quand la Terre tremble, Ed. Artheme Fayard, Paris, 336 p
- Tillotson E (1940) The Rumanian earthquake of November 10, *Nature*, No. 3708, Nov 23, pp 675–677
- Wenzel F, Achauer U, Enescu D, Kissling E, Mocanu V (1998) Detailed look at final stage of plate break-off is target of study in Romania. *EOS, Transac Am Geophys Union* 79(48):589–594

The Strong Romanian Earthquakes of 10.11.1940 and 4.03.1977. Lessons Learned and Forgotten?

Andrei Bala and Dragos Toma-Danila

Abstract Bucharest is among the European capitals most vulnerable to earthquakes. Although located at a relatively large epicentral distance (about 140–160 km) from Vrancea area, Bucharest has suffered much destruction and loss of life during great Vrancea earthquakes. In the last century, November 10th, 1940 earthquake ($M_w = 7.7$) caused the completely collapse of Carlton building located in the central city area, killing over 300 people, and many other high buildings were affected in capital city as in other cities closer to the epicenter. More than 1000 people were killed in a matter of minutes in all Romania during the earthquake, while city of Panciu was destroyed in 90–95 % proportion. This was the moment when the first alarm signal regarding the introducing of mandatory regulations in the seismic design of buildings came out. However, the recommendations made by the specialists were largely ignored by the authorities of the time, so that the next major earthquake of March 4, 1977 ($M_w = 7.4$) caused the biggest recorded disaster in the history of Bucharest. The earthquake of 1977 caused only in Bucharest the collapse of 32 buildings, 8–12 floors high, while about 150 old buildings, with 4–6 floors were badly damaged. Most of the collapsed buildings were built between the 1920 and 1940, they did not benefit of the anti-seismic design. In the case of Bucharest the buildings have been previously damaged in the 1940 earthquake and during the bombardments in the World War II. Over 1500 people died and about 7500 were wounded, most of them in Bucharest City. The total cost of the damage amounted to more than 2 billion dollars, two thirds being related to the capital city only. The aim of the paper is to present aspects related to the consequences of the Vrancea 1940 and 1977 earthquakes, highlighting the differences between the two catastrophic events and their consequences. Therefore everything learned from the past should not be forgotten in order to insure that the next catastrophic event will find a better prepared society.

A. Bala (✉) · D. Toma-Danila
National Institute for Earth Physics, 12 Calugareni str., 077125 Magurele, Romania
e-mail: andrei_bala@infp.ro

D. Toma-Danila
e-mail: toma@infp.ro

Keywords Strong Vrancea earthquakes · Destroyed cities · Damaged and collapsed buildings · The most seismically endangered capital city in Europe

1 Introduction

Studies and observations made after the occurrence of strong earthquakes in the Vrancea area have shown that in Bucharest higher buildings are the most exposed to destruction comparatively with the small buildings, and the destruction effects are much attenuated when moment magnitude of the Vrancea earthquake is less than 7. These two features make Bucharest a unique city in order to study the influence of local conditions upon the ground movement during an earthquake. To explain the damage caused by the strong Vrancea earthquakes ($M_W > 7$), Raileanu et al. (2007), and Bala et al. (2007), Grecu et al. (2011) consider that two factors are particularly important, namely: local conditions (thickness of sedimentary layers and physical and dynamic parameters of the sedimentary package), as well as the seismic source radiation.

In a recent paper, Bala et al. (2015) show that the earthquake mechanism and depth of the event, as well as the seismic path, which is controlled by the depth of occurrence, are responsible to the same extent as the local site effects for the intensity of the ground movement induced by a moderate Vrancea earthquake. According to the single recording of the 1977 earthquake available in Bucharest (*INCERC* station), a spectral amplification with a predominant period of 1.6–1.7 s was derived and assumed to be the key element causing major damage to high tall buildings, higher than 10 floors (Enescu et al. 1982). It was also considered as potential characteristic period for future $M_W > 7$ events. However in 1986, after an event of $M_W = 7.1$, spectral amplification peaks at periods of 0.5, 0.75 and 1.4 s were found on recordings at *INCERC* station, east of Bucharest (NS component; Aldea et al. 2004), proving that strong Vrancea earthquakes might have a larger domain of characteristic periods and by consequence, some other buildings might be at risk.

Bala et al. (2015) conclude that local PGA recorded in Bucharest during strong Vrancea earthquakes is depending not only by seismic site effects and magnitude of the seismic event, but is controlled by all characteristics of a certain event, like fault mechanism, depth of occurrence and distance.

In particular when the fundamental period of sedimentary package lies in the 0.5–2 s, which seems to be the situation in the case of Bucharest, and coincides with the predominant spectral characteristics of the major seismic event, then disaster strikes. Therefore, knowledge of the distribution of resonance period of the ground is most important for local hazard study, and in particular in Bucharest city which is considered the most endangered capital city in Europe by a strong earthquake.

2 The Great Earthquake of November 10th, 1940

Year 1940 was one with a high seismic activity in Vrancea, due not only to the earthquake on November 10th and its aftershocks, but in fact, along this year, several earthquakes have occurred with a significant magnitude from the very beginning of year (Fig. 1). These earthquakes, with moment magnitude greater than 4.5, occurred at depths of 125–160 km (ROMPLUS). They have occurred before the November strong event and after as numerous aftershocks. By contrary, in 1977 only one event precedes the strong event and after that, only one aftershock greater than magnitude 4 was recorded in the next 3 months.

On October 22nd 1940 a strong earthquake, occurred in Vrancea, at 150 km depth (Demetrescu 1941); this earthquake was strongly felt especially in Muntenia and Moldova (with intensities which on an extended area were of VII on Mercalli scale).

The great earthquake measuring $M_{GR} = 7.4$ ($M_w = 7.7$) and maximum intensity $I_0 = IX - X$ occurred at 150 km depth (Demetrescu 1941), on 10th of November 1940, at 3:39 AM (local time). The most severe consequences were noticed in south and center of Moldova (Moldavian Platform), but also in the north-east of Muntenia (Moesian Platform). The town of *Panciu* was destroyed in a proportion of 90–95 %. Towns like *Focșani*, *Galați*, *Marașesti*, *Tecuci* and *Iași* have suffered great damage. The main damage in Bucharest was the collapse of Carlton block, although other buildings were significantly damaged. The earthquake on November 10th 1940 had many aftershocks, from the very first moments, among which, 6 measured more than $M_{GR} = 5.0$. The strongest aftershock was recorded in the morning of November 11th, 1940, with a maximum intensity of VI, focal depth: 150 km; this aftershock seemed to be weakly felt in Bucharest. The series of aftershocks continued towards the beginning of December 1940, and after that they gradually disappear (Fig. 1).

The macroseismic effects were felt on a surface of over 2,000,000 km² in Eastern Europe, being reported in the north up to *St. Petersburg* (Russia) at over 1300 km distance, where seismic intensities of IV-V (MCS degrees) were estimated, in the south, up to Greece, in the east, up to the *Harkov-Moscow* line, with estimated intensities of V-VI (MCS degrees), in the west, up to Belgrade (Serbia) and Budapest (Hungary) and in the north up to Warsaw (Poland). The distribution of the

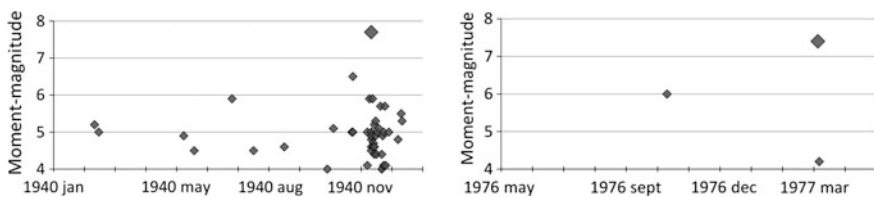


Fig. 1 Earthquakes over moment magnitude 4 produced in Romania around the major events of 1940 (left) and 1977 (right). Source ROMPLUS catalog (Onicescu et al. 1999)

macroseismic effects over such a large area is a measure of the significant energy released during the earthquake (Pantea and Constantin 2011).

The parameters of the earthquake of 10th of November 10th, 1940 could not be determined from the instrumental recordings in Romania, because the first impulse of the longitudinal wave destroyed inferior suspension of the only seismograph installed on the ground floor of the Romanian Observatory from Bucharest (Petrescu 1955). In order to determine the source parameters of the earthquake from the November 10th, 1940, the recordings from different worldwide stations operating that time were used (Demetrescu 1941). The number of the victims of the VRANCEA earthquake from the November 10th, 1940, could not be exactly established or published because of the censure imposed by the political situation and the state of war, which have begun in 1941. Some sources stated that the casualties surpassed 1000 deaths and 3000 wounded throughout Romania.

However Prof. Gh. Demetrescu tried to compute some coordinates for the earthquake in his paper (Demetrescu 1941), based on several recordings outside the country. He established a first set of coordinates at lat 45.8°N and longitude 26.6°E . All the arrival times at the seismic stations that have recorded the earthquake were put on a graphic and after some consideration the true epicentre was chosen. The depth was estimated at 100–200 km, with a great uncertainty. Demetrescu succeeded to perform a quite good location of epicentre close to the location in Romplus catalogue. It was also his merit to bring scientific arguments in favour of a Vrancea subcrustal event. Today the estimation of the coordinates from ROMPLUS catalog is almost the same: lat. 45.8°N ; long. 26.7° and depth at 150 km. As for the magnitude, most of the scientists agreed that a value $M_{\text{GR}} = 7.4$ was a good approximation, which today corresponds to a moment magnitude $M_{\text{W}} = 7.7$ (ROMPLUS).

2.1 *The Destructive Effects of the Earthquake of November 10th, 1940*

Demetrescu published in 1937–1941 several seismological notes where he presented the problems of the seismic wave interpretation and the determination of the seismic foci coordinates. He studied the Vrancea earthquakes of November 1st, 1929, July 13th, 1938, October 22nd, 1940 as well as the earthquake of November 10th, 1940. Demetrescu evidenced first the deep seismic focus in the bending zone of the Carpathians (Vrancea zone), a persistent and isolated focus comparable with the foci of the Hindukush Mts. (Afghanistan) and Bucaramanga (Columbia, South America). The extension of the Romanian seismological network happened after the Vrancea major earthquake of November 10th, 1940 ($M_{\text{GR}} = 7.4$). Demetrescu reorganized the seismological activity by improving the instrumental endowing and setting up five new stations: *Focşani* (1942), *Bacău* (1942), *Câmpulung Muscel* (1943), *Iasi* (1951) and *Vrâncioaia* (1952), all working till now (Radulescu 2009).

Regarding the strong shock of November 10th, 1940 ($M_{GR} = 7.4$), he elaborated the map of the macro-seismic intensities for the Romania and Bulgaria (Demetrescu 1941). A large zone of intensities VIII + IX appear just near the epicentral area. In a later version of the map some local maxima (of X degree) were cited in different points, superimposed on the central zone (Petrescu 1955; Atanasiu 1961). He mentioned some localities in which the intensity was at least of Xth degree: *Panciu, Targu Bujor, Focsani, Lopatari, Neculele*. For Bucharest an intensity of IX was appreciated. Macro-seismic intensities of V–VI degree appeared in Moscow area (at 1300 km distance) and V in southwestern Bulgaria (at 600 km). All the intensities cited here are given in Mercalli-Cancani-Sieberg scale (MCS).

The macroseismic scale MCS is the scale of Mercalli, improved by Cancani to 12° and revised by the German seismologist August Sieberg. The 12° scale was the idea of the Italian physicist Adolf Cancani who suggested to make “total destruction—degree 12” and then there was room for a better grading of levels of damage at intensities 9, 10 and 11. August Sieberg in 1912 write the description of damage at these different degrees (Musson 2012).

The destructive effects of the earthquake of 10.11.1940 in Bucharest were presented the best by Beleş (1941), who was a civil engineer, Professor at Politechnic University in Bucharest (1938–1948) and at Institute of Civil Engineering Bucharest (1963–1976). In recognition of his merits he was appointed correspondent member from 1955 and full member from 1963 of the Romanian Academy (Fig. 2).

In 1941 he presented an extended study, *The earthquake and constructions*, in Romanian. Beleş presented several different buildings damaged in Bucharest, as a result of November 10th, 1940 earthquake, with photos and comments, beginning with the Carlton building, which suffered a total collapse just in the beginning of the seismic movement. In Fig. 3 the distribution of these buildings on a present Bucharest map is given.

In his study, Beleş (1941) begins by presenting the earthquake characteristics and the intensity scale of Mercalli-Cancani-Sieberg of 12 grades, which is presented thoroughly. For each grade he presented not only the description of the effects upon constructions, but also the values of the horizontal acceleration of the ground motion. For a IX grade, a horizontal acceleration of 50–100 cm/s² might occur, as it was appreciated in his study the intensity of November 10th event in Bucharest.

After presenting the different damages the author insisted on the necessity of repairing all the parts and most of all the concrete frame of the buildings affected by the earthquake. Actually, in some cases which Beleş (1941) presented, this repairing process was poorly executed and by consequence appear the premises to further increase the damage in the next great earthquake.

The author mentioned that the well-known seismologist A. Sieberg, co-author of the Mercalli-Cancani-Sieberg intensity scale, have visited Romania in 1941, where he sustained a couple of conferences about the earthquake. In his conferences Sieberg “*draws attention seriously upon the lack of professionalism in which the repairs of the damaged buildings are made, preparing in this way for the next*

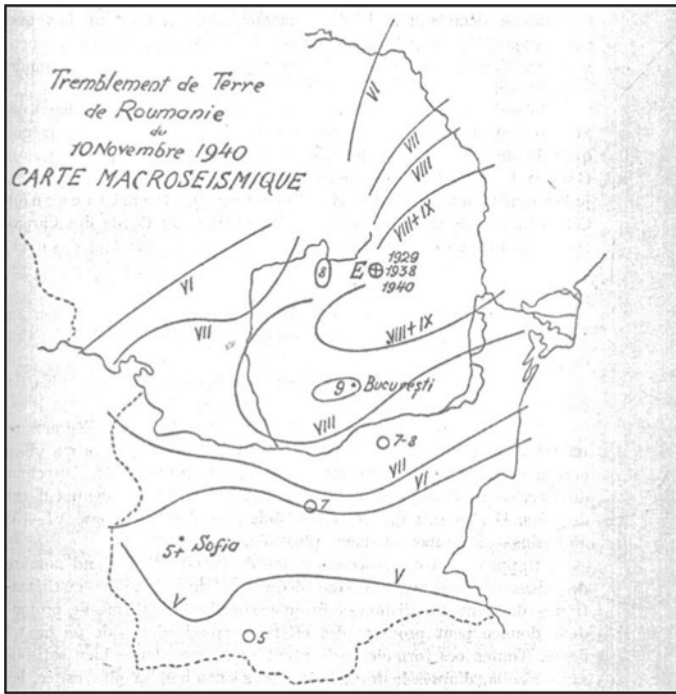


Fig. 2 The isoseismal map of the 10.11.1940 event based on macroseismic effect on MCS scale (Demetrescu 1941)

earthquake, a disaster of a greater amplitude compared with the one from the past” (Beleş 1941).

Beleş presented in his study a set of observations upon the damages suffered by buildings with reinforced concrete frame structure and he also made some recommendations for the future. The largest part of the study deals with the total collapse of the Carlton building, right in the centre of Bucharest, at the corner of Regala str. with Bratianu Blvd.

Two main flaws in design were found, discussed and blamed for the collapse: (1) A set of “non-rational” concrete columns in front of the building, having an *L* shape with non-usual dimensions of the section 20–24 cm by 120–170 cm; (2) Many discontinuities of the columns in the vertical direction. Beginning with the III-rd floor a series of concrete columns were suppressed and they were replaced by other columns placed on the beams for the next 5–6 floors. Another failure in design was placing beams with a large section on rather thin concrete columns.

The main cause for the collapse was the shear forces induced by the earthquake that far exceeded the capacity in shear of the columns at the first ground floor. These columns failed in shear and they perforated the bellow floor to the first and

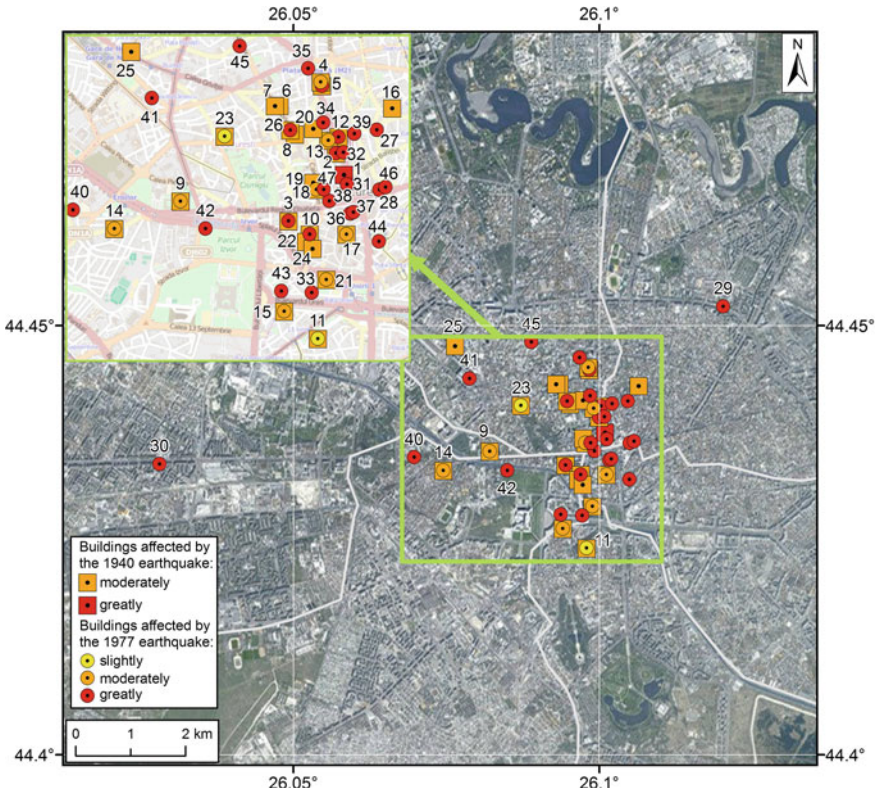


Fig. 3 Position of the buildings greatly affected by the earthquakes in 1940 and 1977 in the centre of Bucharest City. With *squares*—buildings damaged in 1940 event (data from Beleş 1941); with *circles*—buildings damaged in 1977 earthquake (data after Lupan 1982)

second underground levels. The reinforced mainframe began to collapse at the III-rd and IV-th floors, where the columns were placed on beams. This scenario is in complete agreement with the eyewitnesses that stated: “The building looks that begin to sink, then begin to bulge in the middle, and finally suffered a complete collapse” (Beleş 1941).

At that time the buildings, even the tall ones, with reinforced concrete frames, were not designed in generally to support the shear forces that occurred during an earthquake. Most of them were built following the German regulations that do not include, at that time, the necessity to withstand the horizontal forces generated by an earthquake.

All the studies and reports following the earthquake led to the conclusions that in order to support an earthquake with controlled damage a construction should stand horizontal forces that are equal to the mass of the building multiplied by the maximum acceleration given by the strong ground motion.

Other important recommendations were made by Beleş (1941):

1. *The necessity of placing the building on a solid ground, which do not amplify the effect of the earthquakes.* The weak soils of heterogeneous structure, like recent filling, the young silts along the rivers must be avoided. This recommendation prefigures and recognizes the importance of seismic site effects that might introduce important amplification of the ground during a strong earthquake. The author recognizes that in Bucharest this problem appear along the Dambovitza river, where young sediments are in place. He considers that the foundation of the building must be continuous and as deep as possible, but without touching the phreatic level, which might “amplify the seismic movements”.
2. *The necessity to reduce the building heights.* This appears only for mechanical reasons, and the link with a possible resonance with the seismic waves was not yet introduced. That recommendation was almost completely ignored by the authorities in the new constructions erected in Bucharest in the following years.
3. *The horizontal layout of the building must be rectangular in shape, close to a square in order to resist to the earthquakes.* That idea was in generally followed for the new blocks erected in communist era, but some buildings that did not respect that were badly damaged at the earthquake in 1977.
4. *The floors must have the center of mass as close as possible to the center of stiffness.* That recommendation was usually followed, but in some cases some heavy weights were put in the building after construction, also like in the case of the building of Institute for Geology.

All these important recommendations, which were made in 1941 were reintroduced when Beleş and Ifrim (1962) published the book “Elements of seismology engineering” (in Romanian), in which the bases of this important discipline are set up. Beleş treated all the important feature of the earthquake in 1940 in a manner that belongs equally to seismology and to civil engineering. He treated also the damages of the earthquake with a thorough attention, speaking of the great damages suffered by the concrete frame of important buildings in central part of Bucharest, with more than 9 floors: *Belvedere, Wilson, Lengyel, Pherekide, Broşteni, Galaşescu*. Beleş insisted that if they will be not-strengthened in a professional manner, these important buildings could be destroyed in the next great earthquake. Unfortunately, this grim prediction come true in the earthquake of 4.03.1977 for at least 4 of the cited buildings. The others have also suffered important damage even to collapse.

There were of course other buildings damaged by the earthquake in 1940, beside the important buildings having more than 9 floors, that were mentioned in the study of Beleş (1941). Important damages suffered some monumental buildings: Romanian Atheneum, National Theater, Opera House, Home Savings Bank (C.E.C.), the Post Palace (now National History Museum), Palace of Justice. Church *Popa Tatu* in Lipsani street collapsed and on Stirbei Voda str., the statue of General *Cernat* was toppled out of the statue pedestal.

3 The Strong Vrancea Earthquake of March 4th, 1977

In 4.03.1977 at the hour 19:21:56 (GMT) a destructive earthquake occurred in the Vrancea seismogenic region, having destructive effects over a large area, extending from Vrancea area to the NE, towards Moscow, and to SW, into Bulgaria. The epicentre was established first at 45.8°N and 25.8°E and the depth at 95–100 km. Almost all the information and Romanian studies about this great earthquake are gathered in the volume “The earthquake from Romania of March 4, 1977”, published in Romanian language under the coordination of Bălan, Cristescu and Cornea (eds) (1982).

The most important feature of this earthquake was the multi-shock character that was stated even in 1977 on the basis of seismological observations of Muller (1977) and Peterschmitt (1977). This particular character was described also by Mueller et al. (1978), like in Fig. 4. If one checks the position of the hipocenters of principal shocks, the conclusion is that they are like bursts of a single rupture process which affected a slab of at least 30 × 60 km. This rupture propagated with a velocity of up to 4.98 km/s and it have developed on a curve path, between 93–79 and 93–102 km depth. The direction of the shear displacement being from the NE towards SW, it appears that the slab was broken to a SW direction, from F and S1 towards S3 (Fig. 4).

The position of the principal shocks S1–S3, together with the mechanism of the initiating and propagating of the rupture are the principal factors of this directional effect recognized by Mueller et al. (1978), which explains why the maximum damage have been recorded to the SW, towards Bucharest. The magnitude of the earthquake of March 4, 1977 was adopted by many seismologists as $M_{GR} = 7.2$, as being the maximum magnitude attributed to the shock S3 (Enescu et al. 1982). Today moment magnitude is established at $M_W = 7.4$ in ROMPLUS.

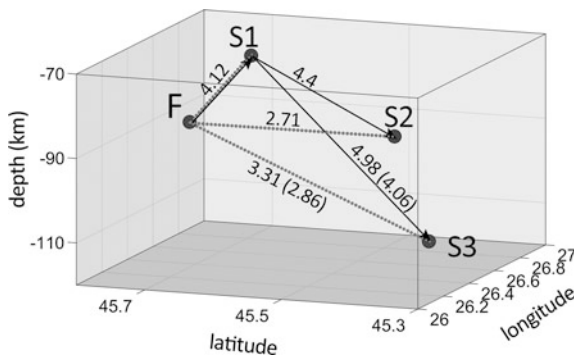


Fig. 4 Position of the foreshock and 3 principal shocks of the earthquake of 4.03.1977. Coordinates after Muller et al. (1978). The numbers are propagation velocity in (km/s) for two scenarios

The focal mechanisms of the principal shocks of the 1977 earthquake were studied by several authors as there were different solutions for the number and characteristics of the principal shocks. A study of Enescu (1980), confirmed by other authors, established that the fault plane solutions were almost the same, indicating a fault mechanism oriented NE–SW which is sinking toward NW.

The hypocenter of the earthquake of 4.03.1977 is placed at least 40 km above the hypocentre of the earthquake of 1940. After Fuchs et al. (1979) the total surface of the rupture produced in 1977 must be at least 1800 km². The energy of the 1977 earthquake was lower than that of the earthquake from 1940, due to the relative reduced time, only 37 years, that passed between the two strong seismic events. By contrast, between the earthquake of 23 January 1838 ($M_s = 7.3/M_w = 7.5$, the previous great earthquake in Romania) and 1940, more than 100 years have passed. The energy of the 1977 earthquake focused towards SW, having important effects in *Cislau, Valenii de Munte, Bucuresti, Zimnicea in Romania and Svistov in Bulgaria*.

There is no direct information about the multi-shock character of other Romanian earthquakes in the past. There are studies of historic events, as Atanasiu (1961), which suggested that some events have had symmetrical effects in Moldova and in Muntenia (events from 30.07.1897; 16.10.1900; 1.07.1914). Other seismic events have had their important effects either in Muntenia (27.12.1895; 15.10.1905) or in Moldova (4.03.1894; 25.05.1912). We should assume that the latter events could have been multi-shock events with the main rupture towards SW, like the 1977 event, or towards NE.

3.1 The Destructive Effects of the Earthquake of 4.03.1977 in Bucharest

The earthquake of 1977 was analysed from its destructive effects in detail in Bălan, Cristescu and Cornea (1982). A map of the macroseismic effects of the earthquake that was realised on the basis of 12,000 of questionnaires which existed in Romania is presented in Fig. 5. The isoseismal lines were expressed in the MSK scale.

The **Medvedev–Sponheuer–Karnik scale**, also known as the **MSK** or **MSK-64**, is a macroseismic intensity scale used to evaluate the severity of ground shaking on the basis of observed effects in an area of the earthquake occurrence. The Medvedev–Sponheuer–Karnik scale is somewhat similar to the Modified Mercalli (MM) scale used in the United States. The MSK scale has also 12 intensity degrees expressed in Roman numerals.

Although it is generally accepted that the event of 1977 had a lower energy ($M_w = 7.4$) in comparison with the earthquake of November 10th 1940 ($M_w = 7.7$), the former have inflicted more damages throughout Romania and especially in Bucharest City. This general observation is a combination of several particular characters of the 4.03.1977 event that might be:

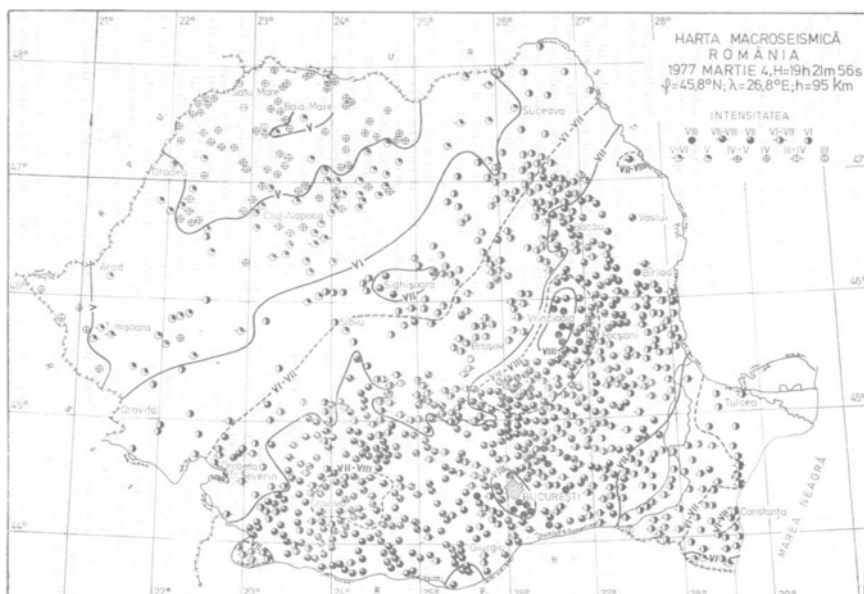


Fig. 5 Macroseismic map of the earthquake of March 4, 1977. Equal intensity lines are in MSK scale. After Radu and Polonic (1982)

1. The multi-shock character of seismic event likely increased the effects because of the multiple interferences of the waves, along their path to surface. In some places along the path an additional effect developed as different seismic waves just arrived in the same moment, increasing in this way the destruction effect of the earthquake.
2. The damaging effect is visibly greater to the SW direction to Muntenia, and farther in the NW part of Bulgaria, due to the rupture developed from one shock to the other, with a general direction towards SW. It is interesting to note that in seismic measurements with controlled source it is a custom to increase the force of explosion toward a certain direction by grouping the explosions, which are fired in a certain manner. It looks like the multiple shocks of the 4.03.1977 event occurred in the same scenario, the observation being made first by Bălan, Cristescu and Cornea (1982).
3. The boom of construction in Bucharest took place in the period 1960–1977, but following a weak standardized seismic hazard map from 1952 (STAS 2923-52). After this year the following codes and associated maps were adopted, which provide seismic hazard values that were inferior to the values within the original macroseismic map of Demetrescu (1941).

4. The main recommendations made by Beleş (1941) were largely ignored by the authorities of the time and because of the war. After that seismic regulations were introduced, but they were not respecting all the observations made in 1941. His predictions about the endangered old blocks with reinforced concrete frames were gradually forgotten, but they come to reality during the 1977 earthquake, with a deadly precision.

Some observations should be made on the macroseismic maps made by the specialists as a consequence of the earthquake of 10.11.1940. The map presented by Demetrescu (1941) with intensities on MCS scale, can be seen in Fig. 2.

The first official seismic zoning of the country was approved by Ministry of Public Constructions at 30.12.1941, published in 19.01.1942 (Georgescu 2003). It contains a map of seismic zonation based on the Demetrescu map, 1941, but very schematic and with a VIII degree in the area in front of Carpathians (Bălan, Cristescu and Cornea 1982; Georgescu 2003). The seismic zonation that followed in 1952 (STAS 2923-52) have also taken the Demetrescu map as a base, but it was reduced with two degrees in the epicentral area and with one degree in the area which surrounded Vrancea.

However, the macroseismic map of Atanasiu (1961) presented the known area in Muntenia and Moldova with a mosaic of zones with local amplifications with degrees 8, 9 and even 10 on MCS scale, based on studies made until 1949 (Georgescu 2003).

Previous seismic design norms prior to the earthquake of 1977 are P13-63 and P13-70 and associated seismic map of STAS 2923-63, which replaced the similar map from STAS 2923-52, introducing major reductions seismic intensity design in several areas. After the map adopted in 1963 a large number of localities were placed in the intensity grade 6 MSK, on the macroseismic map. In spite of the warnings of some of the Romanian seismologists, the intensity was gradually decreased in these maps as the time passed from the 1940 earthquake (Georgescu 2003).

The list of 32 unfortunate buildings that collapsed in Bucharest in 1977 is presented by M. Lupan (1982) in (Bălan et al. 1982). Some of them suffered only a partial collapse, but have been demolished after that on the account that they were beyond repair. Their positions are very familiar as they were presented also by Beleş (1941), as being endangered buildings. Other damaged buildings were in the same category of old buildings constructed in the years 20s and 30s, in which no seismic rules or regulations have been in force and which have suffered the bombardments of the war and the previous earthquake in 1940. It is true that they are concentrated in the Bucharest center, but it seems that their collapse is due mainly to the fact that they belonged to the same category. The buildings made in 1960–1970 had a much better behavior. The collapse was rather exceptions, the cases are different, being a combination of factors, but most often they were mistakes of contractors.

4 Conclusions

Over time, some 2–3 devastating earthquakes per century occurred in Romania in the Vrancea zone at intermediate depth, and hit especially Muntenia and Moldova. In average, every 35–50 years Bucharest is heavily hit, as well as Iasi in Moldova and the epicentral region of Vrancea. With some variations, the earthquake looks the same, but the capital city is changing and developing every day and so is becoming more vulnerable. Vrancea region produce many earthquakes every year, most of them are recorded only by seismographs. The events exceeding 7° magnitude are responsible for considerable damage not only in the epicentral area, but also in other cities in Romania and abroad. Large earthquakes might produce considerable damaging effects especially on an axis NE–SW which crosses Vrancea area in front of Carpathians. Last disastrous event, the 1977 event, made 1,578 dead people and 11,321 injured, with 90 % of the fatalities being in the capital city Bucharest. The reported damages included 32,900 collapsed or heavily damaged dwelling units, 35,000 homeless families, thousands of damaged buildings, as well as many other damages and destructions in industry and infrastructure (Georgescu and Pomonis 2008).

According to World Bank estimates in 1978, the direct damage was over \$2 billion USD, and amortization of long-term effects has absorbed almost as much. More detailed but until recently classified and largely ignored damage data contain information from 19 counties plus Bucharest, with the total damage value reaching Romanian Lei 3.7 billion (Georgescu and Pomonis 2008).

Today costs in case of an earthquake in Romania, similar to 1977 would amount to around 20 billion dollars, according to estimates, up from 2 billion as it was in 1977, this is an estimate of Munich Re group analysis. Damage estimates refer only to the capital, without regard to disasters in other areas because the missing information required to make a solid assessment (Munich Reinsurance Company 1998). The *World Map of Natural Hazards* prepared by the *Münich Re*, 1998 indicates for Bucharest: “Large city with Mexico-city effect”. The map focuses the dangerous phenomenon of long (1.6 s) predominant period of soil vibration in Bucharest during strong Vrancea earthquakes.

The occurring of great seismic events at about 35–50 years it means that it comes but rarely enough to forget it, and so society is unprepared at the next event; but often enough to be sure that people will try the disaster at least once in a lifetime. It is not a high enough frequency, so the phenomenon become an everyday experience, as in Japan, which knows how to live with the danger; but it come at an interval long enough to make from most of us an unexperienced potential victim. The main conclusions about the two great and destructive earthquakes that hit Romania in the XX century are:

1. The earthquake of 1940 had a greater magnitude, but its effects were directed mostly to the NE, having toward Moscow an intensity of V–VI. Bucharest was hit heavily, but the damages, as well as the number of victims were greater in Vrancea

area and to the NW, until Chisinau. The 1977 earthquake had a lower magnitude and a demonstrated multi-shock character. The foreshock and the succession of triggering of the principal shocks directed the energy towards SW and hit especially Bucharest, Zimnicea and NW Bulgaria. The number of victims and the damages increased considerably in Bucharest.

2. There were some preventive measures after the 1940 earthquake, but they were weakened soon and the principal recommendation made by specialists were forgotten as the time passed. Now almost all the seismologists and civil engineers agreed that Beleş (1941) was right and the absolute retrofitting priority in the case of Bucharest, after the experience of Vrancea earthquakes in 1940 and 1977, is for tall buildings before World War II, that do not have structural resources to withstand a major earthquake.

3. Only after 1940 some anti-seismic rules were adopted, there was a concern of legislators and civil engineers. Geologist Atanasiu (1962) has made a scientific study and sketched a seismic map of Romania, stressing that, although there are several seismogenic areas—Transylvania, Banat, Danubian zone, Fagaras Mts., Pontic zone—the most destructive earthquakes are the ones located in Vrancea area. Atanasiu's map alignments are figured two major seismic sensitivity in southeast Romania: first, Lehliu–Urziceni–Calarasi; second, Bucharest. Many years passed and many of the lessons of the 1940 earthquake have been forgotten. Deep cracks in buildings elements disappeared covered with plaster, walls were toppled down and even structural columns to make room on the ground floor premises. Even worse, the upper floors were sometimes overloaded. As a result 25 of the buildings damaged in 1940 earthquake, some of those on the list of Beleş (1941), collapsed totally or partially during the 1977 earthquake.

After 1977 a lot of studies have been made in the seismic hazard assessment and reduction of the seismic risk. Romania is now covered with a dense network of more than 100 real-time seismic stations. Seismologists and civil engineers were trying hard to link the destruction produced by earthquakes to their characteristics as magnitude, frequency, earthquake mechanism as well as the seismic site effects. As a result new Romanian standards appear (P 100–2013) which are successfully applied to the construction of new buildings.

However most of the damages may occur in Bucharest at a specific category of old buildings with reinforced concrete frames, with characteristics described by Beleş (1941). A list of buildings with technical expertise in terms of seismic risk that are endangered in the case of a strong Vrancea earthquake was published on the site of the Bucharest City Hall, most of them being assessed beginning with the years 90s (Fig. 6). The problem is that in the *Class I of seismic risk*, there are now listed 178 buildings which is dangerous for the population. Other more 182 buildings belong to the same list of *Class I of seismic risk*. Only some 57 buildings were retrofitted in the past 20 years (PMB 2015).

Further studies on seismology and seismic site effects will bring no news to the condition of these endangered buildings, but considered “danger to human lives”, without a proper retrofitting. Their position on the map in Figs. 3 and 6 is due to the fact that the location was the best position (in the centre of Bucharest) at the time

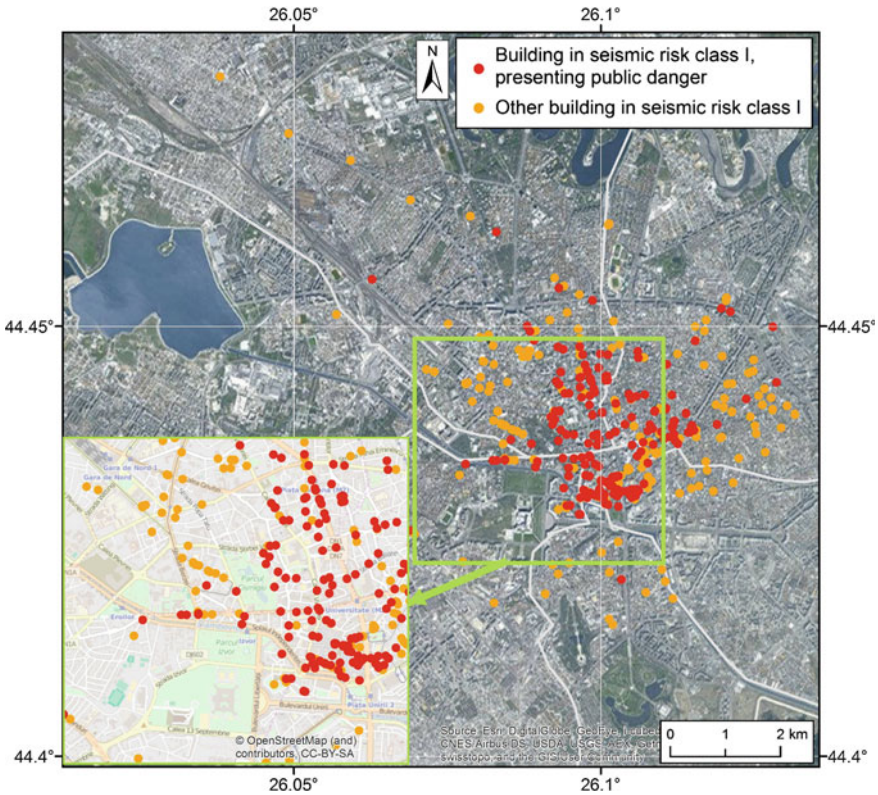


Fig. 6 Position of the buildings in seismic class I in the centre of Bucharest City. *Red dots*—buildings presenting public danger; *orange dots*—other buildings in seismic risk class I. Data from PMB (2015)

when they were built. Studies on local seismic hazard and site effects do not show a certain increase in the spectral amplification in the area occupied by these old buildings. But the position of the endangered buildings in Fig. 6, being almost superimposed on those from Fig. 3, strongly suggest that these buildings, suffering different damages in the past strong earthquakes of 1940 and 1977, will be further damaged in the next strong earthquake.

The risk computed in Bucharest for two Vrancea earthquakes scenarios (one typical for an observed major event, like in 1986, the other for a maximum expected event with $M_w = 7.7$) shows the critical impact of the event magnitude and the higher risk in the central part of the city (Bostenaru et al. 2014). Big quake is inevitable, it is not a question of if it occur, but when it will occur. It is part of the history of our collective experience.

Beleş (1941): In our country the earthquake of 1940 put in front of our generation the problem of the buildings resilience to earthquake, showing the errors of the past and the current shortages. It demonstrated the role of extreme importance that played the

conscientiousness in design, in material choosing and in the execution of a building, in which both the civil engineer and the worker must be imbued. If we can gain the practice of these virtues in the aftermath of an earthquake, we can say that it must be a good thing in a disastrous one.

Acknowledgements This paper was sustained by UEFISCDI Programme Partnerships II, in the frame of the contract 90/2014 in which the author is partner from National Institute of RD for Earth Physics.

References

- Aldea A, Kashima T, Lungu D, Vacareanu R, Koyama S, Arion C (2004) Modern urban seismic network in Bucharest, Romania. In: Proceedings of the first international conference on urban earthquake engineering, 8–9 March, 2004, Tokyo Institute of Technology, Yokohama, Japan, pp 555–563
- Atanasiu I (1961) Earthquakes in Romania. In Romanian. Academy Press R.P.R., Bucharest
- Bălan S, Cristescu V, Cornea I (1982) The 1977 March 4, earthquake in Romania. Academy Press R.S.R., in Romanian, Bucharest
- Bala A, Ritter JRR, Hannich D, Balan SF, Arion C (2007) Local site effects based on in situ measurements in Bucharest City, Romania. In: Proceedings of International symposium on seismic risk reduction, ISSRR-2007, Bucharest, pp 367–374
- Bala A, Grecu B, Arion C, Popescu E, Toma D (2015) Variability of strong ground motion in Bucharest area due to Vrancea earthquakes. In: Proceedings of the 15th international multidisciplinary scientific geoconference SGEM 2015, vol III, pp 1075–1082
- Beleş A (1941) Earthquake and constructions (in Romanian). Politechnic Society Bulletin, LV, Nr. 10–11
- Beleş A, Ifrim MD (1962) Elements of engineering seismology (in Romanian). Technical Publishing, Bucharest
- Bostenaru M, Armas I, Goretti A (eds) (2014) Earthquake hazard impact and urban planning. Environmental Hazards, Springer, Berlin
- Demetrescu G (1941) Remarques sur le tremblement de terre de Roumanie du 10 novembre 1940. Comptes Rendus de Séances de L'Académie des Sciences de Roumanie. 553. Tome V, no. 3, pp 224–241. Cartea Romaneasca, Bucharest
- Enescu D (1980) Contributions to the knowledge of the focal mechanism of the Vrancea strong earthquake of March 4, 1977. Rev Roum Geol, Geophys, Geogr, Geophysique 23:3–17
- Enescu D, Cornea I, Misicu M (eds) (1982) The mechanism of the earthquake on March 4th 1977 and the associated effects of directivity. Mecanismul de producer a cutremurului din 4 martie 1977 si efectele asociate de directivitate. In: Balan S, Cristescu V, Cornea I (eds) The 1977 March 4, earthquake in Romania. In Romanian. Academy Press RSR, Bucharest
- Fuchs K, Bonjer KP, Bock G, Cornea I, Radu C, Enescu D, Jianu D, Nouredine A, Merkle G, Moldoveanu T, Tudorache G (1979) The Romanian earthquake of March 4, 1977. II Aftershocks and migration of seismic activity. Tectonophysics 53:225–247
- Georgescu ES (2003) Earthquake engineering development before and after the March 4, 1977, Vrancea, Romania Earthquake. In: Symposium on 25 years of research in earth physics, 25–27 Sept 2002, Bucharest. St. Cerc. Geofizica, 1:93–107
- Georgescu ES, Pomonis A (2008) The Romanian earthquake of March 4, 1977 revisited: new insights into its territorial, economic and social impacts and their bearing on the preparedness for the future. In: Proceedings of the “World conference on earthquake engineering”, 12–17 Oct 2008, Beijing

- Greco B, Raileanu V, Bala A, Tataru D (2011) Estimation of site effects in the Eastern part of Romania on the basis of H/V ratios of S and coda waves generated by Vrancea intermediate-depth earthquakes. *Rom J Phys* 56(3–4):563–577
- Lupan M (1982) Repairing and retrofitting of the buildings damaged by the earthquake. In: Balan S, Cristescu V, Cornea I (eds) *The 1977 March 4, earthquake in Romania*. In Romanian. Academy Press RSR, Bucharest
- Muller G (1977) *Journées Luxembourgeoises de Geodynamique*, 9–10 May 1977
- Muller G, Bonjer KP, Stökl H, Enescu D (1978) The Romanian earthquake of March 4, 1977, I. Rupture process inferred from fault-plane solution and multiple event analysis. *J Geophys* 44:203–218
- Munich Reinsurance Company (1998) *World map of natural hazards*, 3rd edn, Munich
- Musson R (2012) *The million death quake: the science of predicting earth's deadliest natural disasters*. Macmillan Publishers, London
- Oncescu MC, Mârza VI, Rizescu M, Popa M (1999) The Romanian earthquake catalogue between 984–1996. In: Wenzel F, Lungu D, Novak O (eds) *Vrancea earthquakes: tectonics, hazard and risk mitigation*. Kluwer Academic Publishers, Berlin, pp 43–49
- Pantea A, Constantin AP (2011) Reevaluated macroseismic map of Vrancea (Romania) earthquake occurred on November 10, 1940. *Rom J Phys* 56(3–4):578–589
- Peterschmitt E (1977) Notes sur le seisme de Vrancea, 4 Mars 1977. *CSEM Strasbourg*, 20 Jouillet 1977
- Petrescu Gh (1955) *About earthquakes and seismic regions in our country*. SRSC Collection, no. 108, Technical Publishing, Bucharest
- PMB (2015) List of expertised buildings in Bucharest. http://www.pmb.ro/servicii/alte_informatii/lista_imobilelor_exp/docs/Lista_imobilelor_expertizate.pdf. Accessed 10 Nov 2015
- Radu C, Polonic G (1982) Seismicity in Romania with special reference to the Vrancea region. In: Balan S, Cristescu V, Cornea I (eds) *The 1977 March 4, earthquake in Romania*. In Romanian. Academy Press RSR, Bucharest
- Radulescu F (2009) Romanian seismology—historical, scientific and human landmarks. *Rev Roum Geophys* 52–53:101–121
- Raileanu V, Bala A, Greco B (2007) Local seismic effects in sites located in the south and central part of Transylvania based on spectral ratios. *Rom Reports Phys* 59(1):165–178

Before and After *November 10th, 1940* Earthquake

Ileana Calotescu, Cristian Neagu and Dan Lungu

Abstract The paper focuses on the evolution of seismic design of buildings in Romania with emphasis on Bucharest, “Europe’s capital of earthquakes” (The Guardian, March 25th 2014, online edition). Both seismological data available before and after the November 10th, 1940 event and data related to the damage produced by historic strong Vrancea earthquakes (1802, 1838, 1940) were presented. In the aftermath of the 1940 earthquake, new seismic design codes (1941, 1945) were introduced and macroseismic hazard maps were documented. The most representative macroseismic maps available were compared and discussed.

Keywords Historic earthquakes · Design codes · Macrosesimic hazard maps

The British newspaper *The Guardian* called Bucharest the “European capital of earthquakes” in the article entitled “*Risky cities: red equals danger in Bucharest, Europe’s earthquake capital*” published on the 24th of March 2014 in the online edition.

Throughout its history of more than 500 years, Bucharest has been shaken by numerous strong subcrustal Vrancea earthquakes which have produced damage on approximately 2/3 of the Romania territory as well as in neighboring countries such as Republic of Moldova, Bulgaria, Ukraine, etc.

The largest and the best documented Vrancea earthquakes that occurred in the past 200 years are the earthquakes from 1802, 1838, 1940 and 1977, Table 1. Those events have produced severe losses i.e. more than 2000 casualties and irretrievable building and cultural losses. Historical monuments, churches and important buildings have disappeared for ever.

I. Calotescu (✉) · C. Neagu · D. Lungu
Technical University of Civil Engineering, Bucharest, Romania
e-mail: ileana.calotescu@utcb.ro

C. Neagu
e-mail: cristi.neagu@utcb.ro

D. Lungu
e-mail: lungu@utcb.ro

Table 1 Major historical Vrancea earthquakes, examples

Date	Hour	Maximum macroseismic MSK intensity	Gutenberg–Richter magnitude, M_{GR}	Moment magnitude, M_w	Depth, h km
1802, October 26	10:55	9	7.5–7.6	–	>150
1838, January 23	18:45	8	6.7–6.9	–	...
1940, November 10	01:39	9	7.4	7.7	150
1977, March 4	19:22	8/9	7.2	7.5	94

The effects of Vrancea earthquakes may be defined as major—from macroseismic standpoint—either in the *NE* i.e. Moldova direction or in the *SW* i.e. Bucharest direction. The first category includes the earthquakes from October 26th, 1802 and November 10th, 1940 having epicenters located towards *NE*/Moldova and depths of approx. 150 km. The second category includes the earthquakes from January 23rd 1838 and March 4th 1977 having the epicenters located towards *SW*/Bucharest and depths around 100 km.

Obviously, both human and economic losses produced by an earthquake depend on the location of the exposure, i.e. built environment and number of population. Consequently, the largest number of casualties as well as the most important material losses occurred for almost all strongest earthquakes of Romania in the capital city of the country, Bucharest.

It must be emphasized that local soil conditions in Bucharest are characterized by long predominant periods of ground vibration, $T_p = 1.4 \div 1.6$ s, during strong earthquakes (i.e. moment magnitude $M_w \geq 7.0$). Such periods may induce phenomena of quasi-resonance with ground motion of the high buildings vibration, phenomena that are still insufficiently dealt with by the actual Romanian design codes.

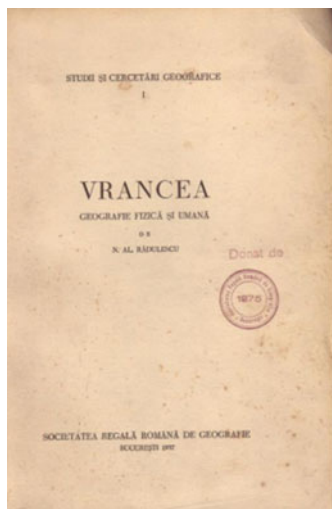
Tall reinforced concrete buildings built before 1940 in the Bucharest city center were proved to be the most vulnerable buildings in Romania, causing most of the losses during the 1940 and the 1977 earthquakes i.e.:

- March 4th 1977, over 1400 casualties and 32 collapsed buildings;
- November 10th 1940, about 200 victims and collapsed *Carlton* building, the tallest reinforced concrete building in Bucharest.

A perfect picture of the “antiseismic” state of mind in Romania before 1940, at about 100 years after the 1838 Vrancea earthquake, is presented in the textbook (Radulescu 1937), Fig. 1:

We can conclude that Vrancea is a region of very low seismicity.

However, two other books, very advanced for their times, written by the Romanian geologist Matei Drăghiceanu (1844–1939), at the end of the XIXth century (1896) and the respectively around the 1940 earthquake, Figs. 2 and 3, must be acknowledged.



În concluzie putem spune că Vrancea e o regiune de foarte mică seismicitate. Puținele cutremure care au avut loc, au fost în medie de gr. III după scara Rossi-Forel. Epicentrele cutremurelor mari nu aparțin depresiunii, ci axei seismice care există de-alungul fracturii Zăbala-Galați-Tulcea. Cutremurele care au avut epicentrul în Vrancea, au avut o intensitate mică și un caracter local.

Reiese deci, că tăsarea Vrancei este astăzi completă și că nu se mai produc dezechilibrări ale stratelor din adânc.

Fig. 1 Vrancea seismic source, as presented in the textbook (Radulescu 1937)

Fig. 2 Draghicienu (1896)

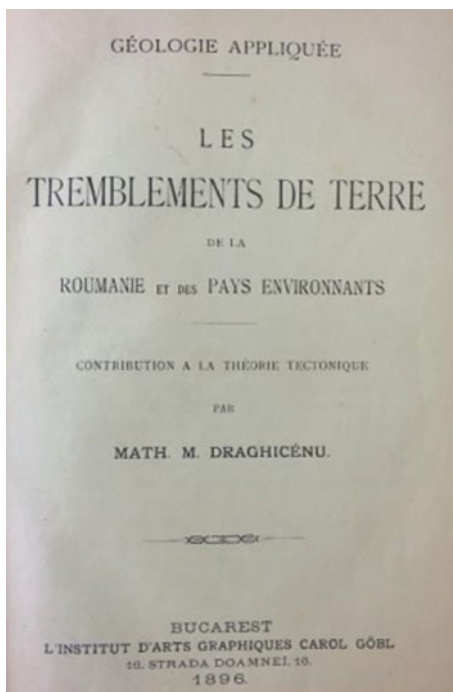
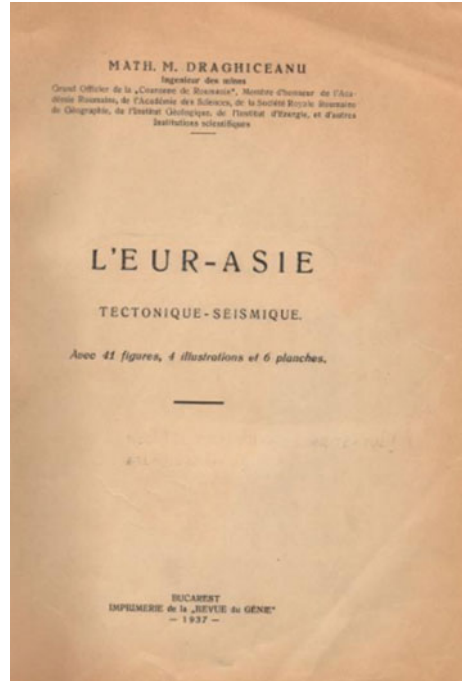


Fig. 3 Draghiceanu (1937)

The 1896 textbook published (in French) by Matei Draghiceanu is a reference book for its time regarding: (i) The causes of earthquakes, (ii) Historic earthquakes 1802 and 1838 “from the East”, (iii) Recent earthquakes (1892–1894), Banat earthquakes, and so on., (iv) Earthquake prediction, etc. However, the name “Vrancea” is missing from the text, since the concept of sub-crustal earthquakes generated by this source was not entirely clarified at that time.

In order to disseminate knowledge about earthquakes, several “pocket-sized” books all entitled “Earthquakes”, published in 1915 at Câmpina (81 p), in 1923 at București (80 p) and in 1926 at Cluj (16 p), may suggest the public’s poor knowledge about earthquakes and seismic building safety, Figs. 4, 5 and 6.

The first significant scientific work regarding the effect on buildings of the November 10th 1940 earthquake on buildings has been produced by Tsoher et al. (1941), at Moscow, only 3 months from the occurrence of the earthquake. The textbook is up until today the richest in information and it is the clearest reference source showing the effects of the 1940 earthquakes on the existing built environment in 1940, Fig. 7.

Another historic photo which illustrates the effects of the 1940 earthquake on the churches in Romania is presented in Fig. 8, from the archives of the *National Institute of Historic Monuments in Bucharest (INMI)* (Fig. 9).

In Romania, the first seismology works dedicated to the November 10th 1940 earthquake are published by the *Romanian Academy of Sciences Journal*, at *Cartea*

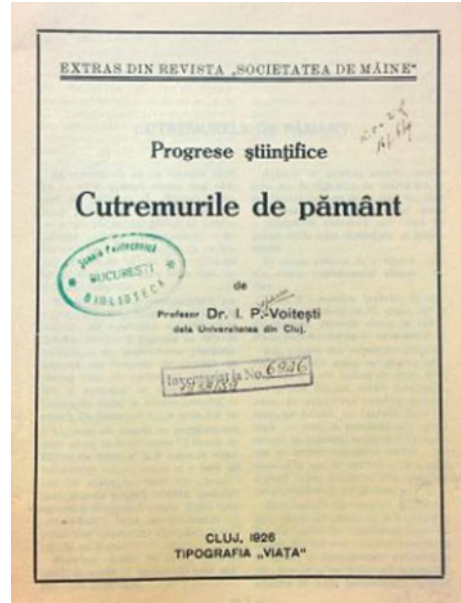
Fig. 4 Anestin (1916)



Fig. 5 Zaharescu (1923)



Fig. 6 Voitești (1926)



Românească, in May–June 1941. Those papers were accompanied by the paper authored by the engineer Aurel Beleş on the earthquakes effects on buildings.

Among important findings of the above seismological works, it may be cited:

- The depth of the November 10th earthquake (prof. G. Demetrescu), Fig. 10:
- Distribution of casualties produced by the November 10th earthquake (N. Al. Rădulescu), Fig. 11.

The first and the most important engineering book dedicated to the November 10th 1940 earthquakes is *Collapse of Carlton building, Causes and Lessons learnt*, Cartea Românească, 1941, by engineer Theodor Achim, 48 p, Fig. 12 (Achim 1941).

It has been completed by the publication *Earthquake and buildings*, 1941, by the engineer Aurel Beleş, Fig. 13.

The exceptional work of Achim summarizes and clarifies the causes which have led to the collapse of the *Carlton* building as follows:

“The *Carlton* building was made up of a tower having dimensions of approximately 18 m by 16 m and the total height, from the foundations to the roof, of 53 m: comprising 2 basements, ground floor and two wings, one towards Brătianu Boulevard having 12 stories and the other towards Regala street, having 4 stories. The tower was located eccentrically in the corner of the building. Behind it, there was a cinema whose balcony, supported by round pillars, was additionally supported by the columns located at the back side of the tall building. We see also that the ratio between the height of the tower and the width at the base is $53/16 = 3.3$.”



Fig. 7 Buildings in Kishinev severely damaged by the November 10th 1940 earthquake
© Institute of Seismology of the Academy of USSR and Institute of Geology and Geophysics Chisinau

Among the “*main*” causes, “the excessive height of the building, especially of the tower” is listed. However, the fixing of the cinema balcony into the columns of the tall building was highlighted the “*fundamental*” cause of collapse.

Some of the lessons learned from the catastrophe of the collapse of the *Carlton* building listed by Achim are:

- Elaborating (as urgently as possible) a Romanian Circular, document focusing the design and the execution of buildings in seismic conditions of Romania;
- To avoid as much as possible, towers exposed eccentrically with respect to the general plan of the structure;
- To be prohibited buildings with setbacks at the top of the building, which involve placing columns on beams;



Fig. 8 Văleni de Munte, The Dormition of the Mother of God church “The Monastery” © INMI

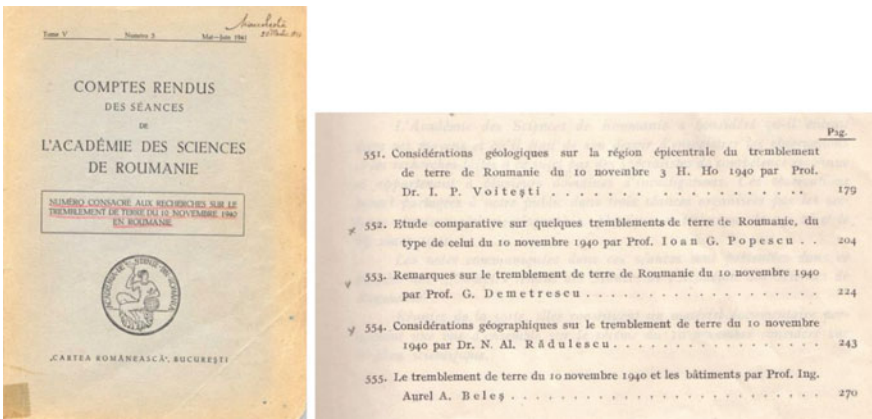


Fig. 9 Comptes Redus des Seanus de L’Academie des Sciences de Roumanie (1941)

- To use regular building shapes, close to cube or parallelepiped;
- To brace tall structures.

It must be emphasized that the set of several hundreds of tall buildings built in the center of Bucharest, mostly in 1930–1940 decade, had the structural system made of reinforced concrete frames infilled with masonry walls. Those buildings often have a flexible/soft/weak ground floor (for shops, restaurants, cinemas, etc.)

Profondeurs de quelques séismes de la région de Vrancea.

Autorités	1929, XI, 1	1938, VII, 13	1940, X, 22	1940, XI,
Jeffreys (2)	184 kms			
Gutenberg et Richter(3)	160	150 kms		
B. C. I. S. (4)			150 kms	150 kms
U. S. C. G. S. (5)			100—150	
J. S. A. (6)				150
Pittsburgh (7)			160	150
Wellington (8)				150
Demetrescu (9), (10)	192	163		

Fig. 10 November 10th 1940 Vrancea earthquake depth

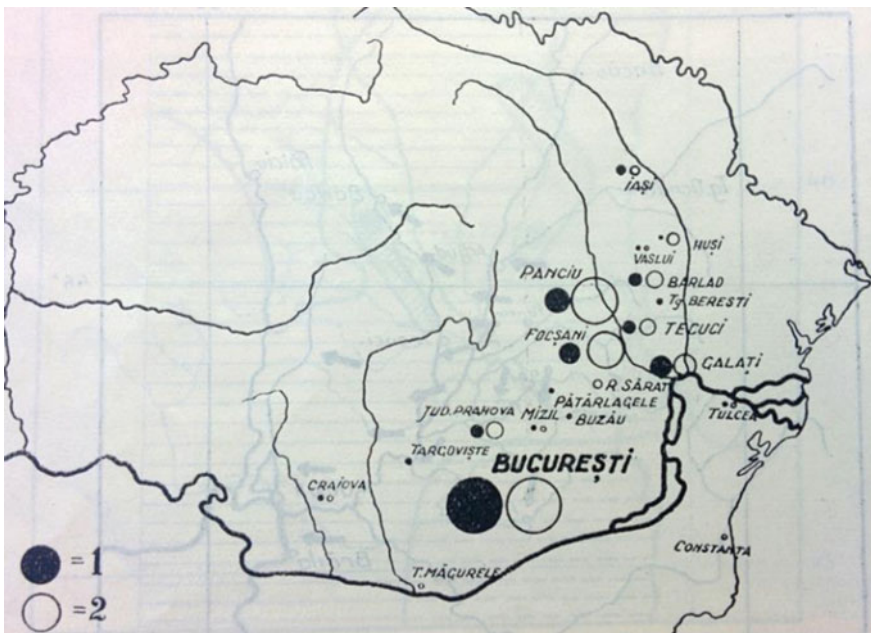


Fig. 11 Distribution of casualties produced by the November 10th earthquake

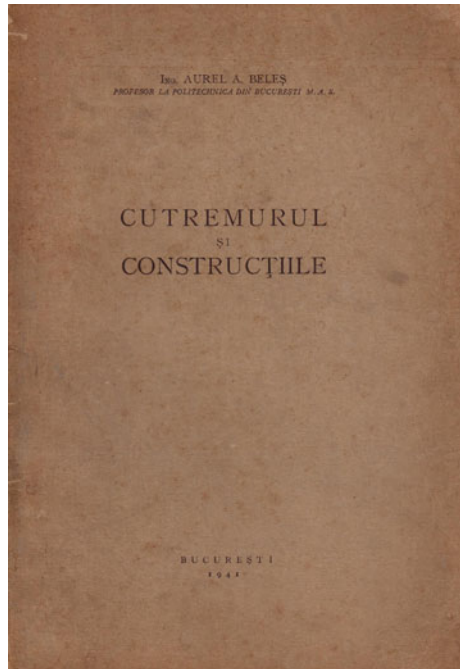
and have been designed without considering, in any way, the possibility of occurrence of an earthquake.

The first *Reinforced concrete* book in Romania (Ionescu 1915) was published in 1915 by the famous professor Ion Ionescu (Fig. 14). However, *The German provisions on reinforced concrete* (1932), Fig. 15 might be considered as the reference code applicable for the design of tall buildings before November 10th, 1940 event in Bucharest.



Fig. 12 *Carlton building*

Fig. 13 Publication of *Earthquake and buildings*, 1941, by the engineer Aurel Beleş



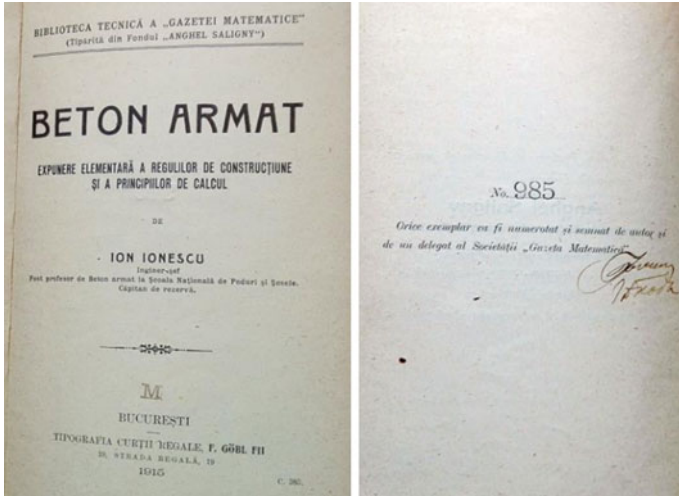
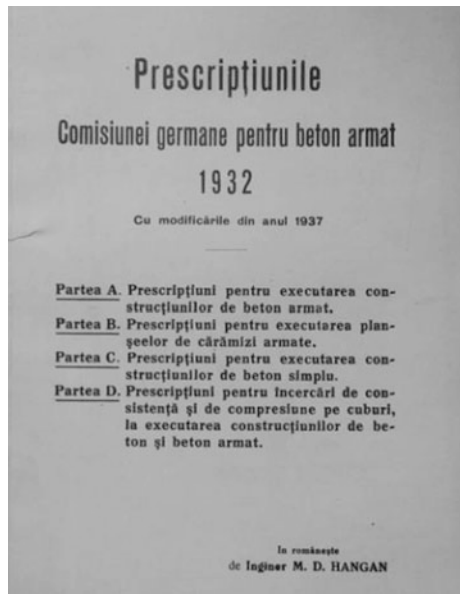


Fig. 14 The first Reinforced concrete book in Romania

Fig. 15 The German provisions on reinforced concrete



The most well known engineering reference text on November 10th 1940 earthquake written by Aurel Beleş and published immediately after the earthquake (Beleş 1941), contains, among others, the following simple rules:

“I believe that it should be required for highly importance buildings to consider a seismic coefficient of 1/20, meaning designing buildings for a horizontal seismic force of 1/20 of their weight”;

- The construction should be as rigid as possible by introducing reinforced concrete stiff walls;
- The structural columns will be designed according to the minimum resistances given by the German circular, having a minimum longitudinal reinforcement percentage of 1 %;
- For the buildings where slabs were made by steel or wood beams it was also recommended to use reinforced concrete beams;
- Finally, in order to achieve the bracing of the building, the masonry walls must be built with perpendicular structural walls placed at not too large distances.

A picture of the effects of the 1940 earthquake on the churches in Bucharest is given in Table 2, after the data excerpted from the *Atlas-guide: History and architecture of the churches in Bucharest*.

Following the disastrous effects of the Nov. 10th 1940 earthquake on constructions and based on the ministry “decisions No. 92525 of December 21st 1940 and No. 3292 of January 15th 1941 which established *The Superior Commission for the study of accidental loadings to which the constructions have been exposed during the November 10th 1940 earthquake*”, the *Ministry of Public Works and Constructions of Romania* approves the following document:

Provisional instructions to prevent damage of constructions from earthquakes and to restore the damaged ones having an Annex comprising a Design example.

The provisions have become mandatory throughout the country, both for the designers as well as for constructors beginning with December 20th 1941.

In Chap. 1 of the *Provisions* the Romanian territory was divided into two seismic regions:

- A. *Region at South and East of the Carpathians*, to which *Braşov County* is added, which are the most exposed to earthquakes;

Table 2 Effects of the November 10th 1940 earthquake on the churches of Bucharest (examples) (Stoica 2000)

Church name	Earthquake effects and countermeasures
Church and cemetery Saint Nicolas-Crângaşi	The big tower and the iconostasis collapse
Cotroceni	Damaged
Saint Elefterie-Old	Repaired
The Hospital-Monastery Saint Pantelimon	Repaired
Oborul-Vechi	Repaired
Precupeţii Noi	Consolidation + washing
Saint Nicolas Tabacu	Big tower collapses
Herastrau, Holy Apostles Peter and Paul	Repaired after earthquake in 1952
Amzei	Damages
Boteanu	The towers collapsed

B. *The rest of the country*, less or not exposed.

The constructions were classified in: (i) Public state buildings, (ii) General interest buildings (theaters, cinemas, restaurants, hotels, apartment buildings and so on), (iii) Private buildings and (iv) Rural buildings.

The “mandatory” provisions refer to all buildings except the rural ones and concern: “Foundations, Masonry brickworks, Slabs, Reinforced concrete structures, Roofing and roof framing”. The “mandatory” provisions state that all public buildings in region A, except the private one story buildings and the rural ones, “will be checked to earthquake loading, considering horizontal forces equal to 5 % of the total corresponding loading (permanent and live loads). Wind loading and earthquake loading are not consider to act simultaneously”.

Four years later, in 1945, the final version of the above seismic code entitled *Instructions for damage prevention on buildings from earthquakes*, has been published by *The Technical Superior Committee of the Ministry of Construction and Public Works* (10 pages), Fig. 16. That work has been completed in 1958 by prof. A. Florinesco’s *Catalogue des tremblements de terre ressentis sur le territoire de la R.P. Romania*, Fig. 17 (Florinesco 1958).

Nine years after the 1941 document, the new seismic *P13-63* code appeared, Fig. 18, which opens a new understanding of seismic problem in Romania.

The document was in fact initiated in 1958 by prof. Al. Cișmigiu and eng. Em. Țițaru which have edited the first proposal in Romania for a seismic design standard for constructions, Fig. 19. That document was subsequently reconfigured to

Fig. 16 The technical superior committee of the ministry of construction and public works

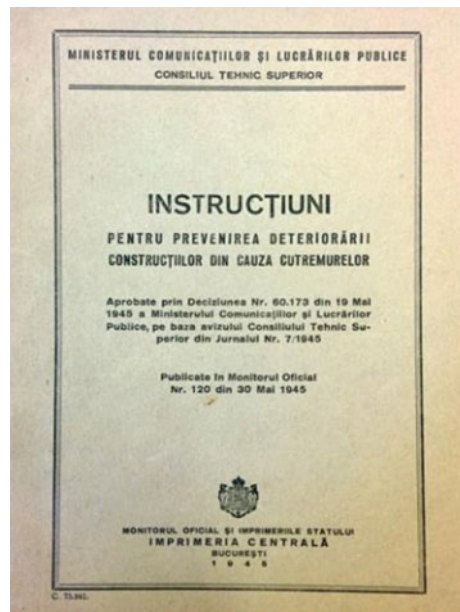


Fig. 17 Professor Al. Cișmigiu and eng. Em. Țițaru which have edited the first proposal in Romania

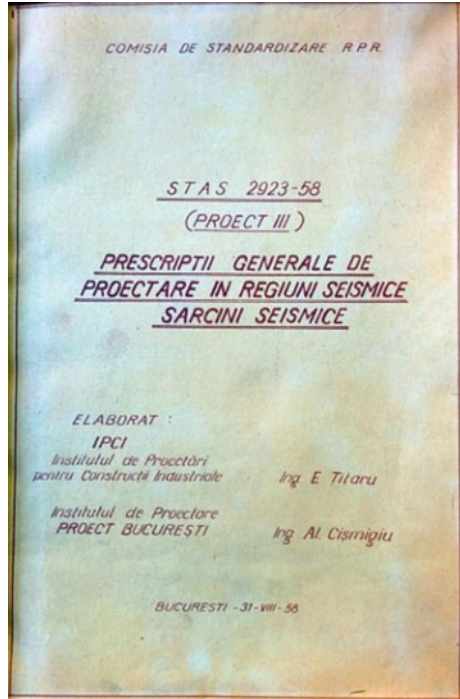


Fig. 18 The new seismic P13-63 code

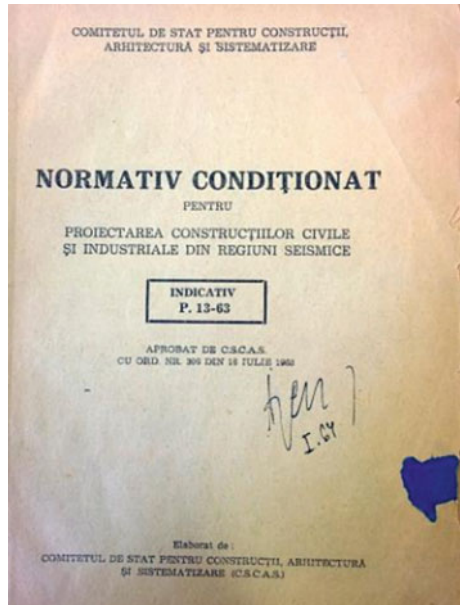
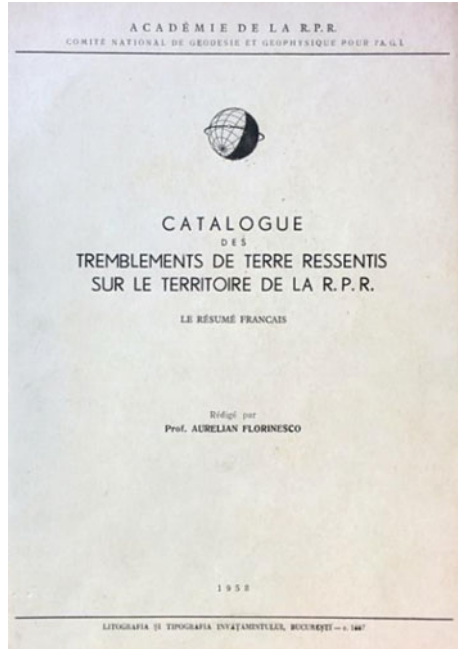


Fig. 19 prof. A. Florinesco's catalogue des tremblements de terre ressentis sur le territoire de la R.P. Romania (1958)



PI3-63, Fig. 19, but without including the names of the two famous and well-known engineers in the list of authors of the code.

It may be underlined that the first textbook in Romania on earthquake engineering has been published in 1961 by professor Aurel Beles, member of *Romanian Academy* and professor Mihail Ifrim from the *Technical University of Civil Engineering (UTCB)*. This textbook becomes the standard course at *UTCB* from the decade of '70.

Finally, it is of utmost importance to search the “effects” of the November 10th 1940 earthquake on the configuration of the macroseismic hazard maps elaborated in the aftermath of that event.

The macroseismic hazard maps for the Vrancea source which have been considered for this study (Figs. 20 and 21) are:

- (i) For the 1940, November 10th earthquake, the map elaborated by Drumea, Moskalenko, Roman and Shebalin;
- (ii) For the 1802, October 26th earthquake, the map elaborated by Radu and Utale;
- (iii) For the 1838, January 23rd earthquake, the map elaborated at the *Institute of Geology and Geophysics, Kishinev*.

All macroseismic maps presented use the *MSK* (Medvedev–Sponheuer–Kárník) intensity scale. The macroseismic hazard regions compared in Figs. 20 and 21 are thus the intensity degrees 7, 8 and 9 *MSK* regions.

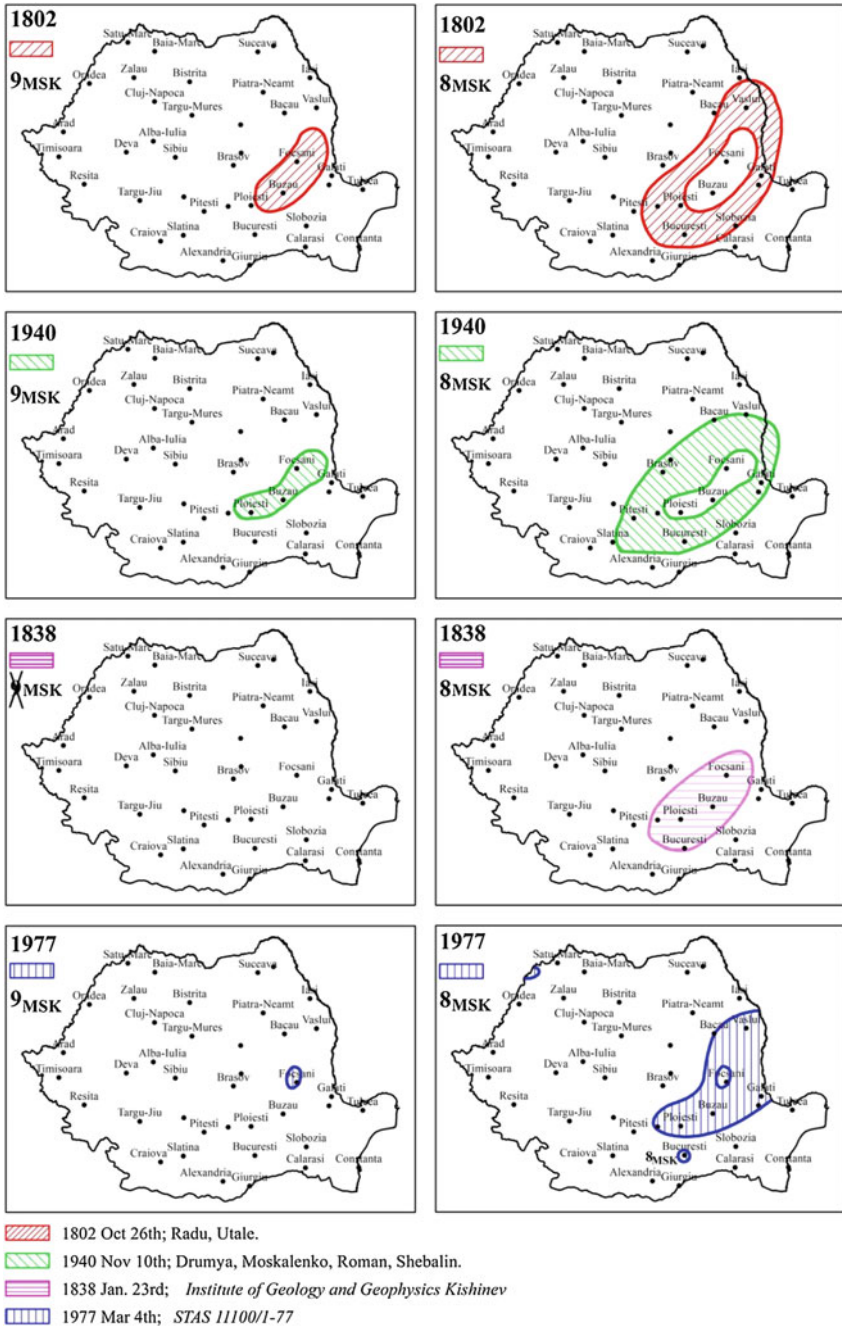


Fig. 20 Hazard macroseismic regions 9 MSK and 8 MSK generated by the subcrustal Vrancea source for the 1802, 1838, 1940 and 1977 earthquakes

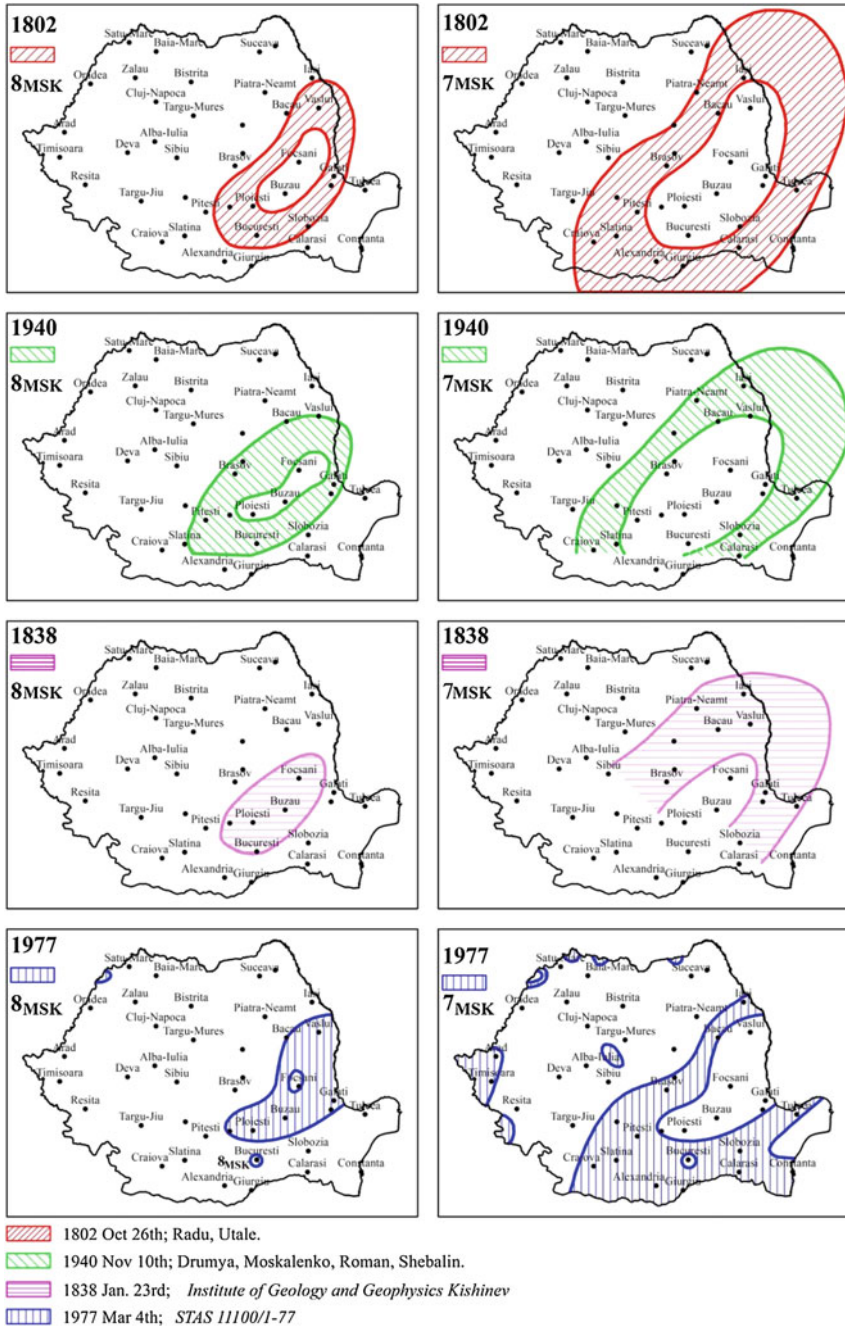


Fig. 21 Hazard macroseismic regions 8 MSK and 7 MSK generated by the subcrustal Vrancea source for the 1802, 1838, 1940 and 1977 earthquakes

It may be noticed from Figs. 20 and 21 the similarity of the macroseismic areas (9 *MSK* and 8 *MSK*) and of the macroseismic areas (8 *MSK* and 7 *MSK*) for all earthquakes.

For Bucharest, in the Romanian standard *STAS 11100/1* which has been published after the 1977 earthquake the intensity 8 *MSK* was considered in an area corresponding to a seismic degree 7 *MSK*! It was a result of the damage that occurred in the capital: 1424 casualties out of a total 1578 in Romania during 1977 event.

The graphical representations in Figs. 17 and 20 are clear and do not need further explanations. However, the similar configurations of the macroseismic boundaries for the 1802 and 1940 earthquakes must be noted, proving that the Vrancea focal mechanisms of the two earthquakes were probably alike. It should also be noted that the differences between the configurations of the macroseismic hazard maps for the 1838 and 1977 earthquakes are largely due to an insufficient macroseismic documentation for the 1838 earthquake.

Another comparison was made between the map recommended by the Romanian standard *STAS 2932-52* (in 1952) and the map from Kárník in the textbook *Seismicity of the European Area, Part 2*, published in 1975 (Kárník 1975). It may be noticed that the macroseismic hazard map for Vrancea source, which has been used by the *STAS 2932-52* in Romania is in fact the macroseismic hazard map accepted by Kárník and vice versa.

*
* *

The advanced earthquake engineering in Romania was born immediately after the March 4th 1977 earthquake as a consequence of (i) the catastrophic number of human losses (over 1500 casualties) and economic losses (over 2 billion US \$ in 1977, meaning probably over 10–12 billion US \$ of today) and of (ii) the possibility of openly importing advanced antiseismic prescriptions from the specialized American standards and codes.

This paper concludes the evolution of the seismic protection in Romania only before the March 4th 1977 earthquake, since it was poorly investigated in Romanian specific references to present date.

References

- Achim T (1941) Cauzele prabusirii Blocului Carlton. Cartea Romaneasca, Bucuresti 36 p
 Al Radulescu N (1937) Geografie fizica si umana, Societatea Regala Romana de Geografie. Bucuresti, 174 p
 Anestin V (1916) Cutremurele de pamant. Editura Tipografiei Gutenberg-Campina, M.S., Gheorghiu 81 p
 Beles A (1941) Cutremurul si Constructiile. Bucuresti

- Comptes Rendus des Seanus de L'Academie des Sciences de Roumanie (1941) Tome V, Numero 3, Mai – Juin. Cartea Romaneasca, Bucuresti, 288 p
- Draghiceanu Math M (1896) Les Tremblements de Terre de la Roumanie et des Pays Environnants. L'Institut d'arts graphiques Carol Gobl, Bucharest 84 p
- Draghiceanu Math M (1937) L'Eur-Asie, Tectonique-Seismique. Imprimerie de la "Revene du Genie", Bucharest, 304 p
- Folrinesco A (1958) Catalogue des tremblements de terre ressentis sur le territoire de la R.P.R. le resume Francais. Litografia si Tipografia Invatamantului, Bucuresti, 168 p
- German Commision for reinforce concrete (1932) Prescriptiile comisiei germane pentru beton armat
- Ionescu I (1915) Beton armat – expunere elementara a regulilor de constructive si a principiilor de calcul. Tipografia Curtii Regale, Bucuresti
- Kárník V (1975) Seismicity of the European Area, Part 2
- Stoica L (2000) Atlas-ghid: istoria și arhitectura lăcașurilor de cult din București din cele mai vechi timpuri până astăzi. Editura Ergorom '79, București, vol 2
- Tszoher VO, Tisenko VG, Popov VV (1941) Carpathian Earthquake of 22 X and 10 XI 1940. Report of the academy commission of this earthquake in Republic of Moldova and Western Ukraine. Institute of Seismology of the Academy of Sciences of USSR, Moscow, 51 p
- Voitesti IP (1926) Cutremurile de pamant. Tipografia "Viata", Cluj, 16 p
- Zaharescu V (1923) Cutremurile de pamant. Tipografia Dim. M, Ionescu 80 p

The Collapse of Carlton Building in Bucharest at November 10, 1940 Earthquake: An Analysis Based on Recovered Images

Emil-Sever Georgescu

Abstract The Bucharest Carlton building collapsed under the Vrancea earthquake of November 10, 1940 (MG-R = 7.4). The building included a high central tower with 2 basements + ground floor + 12 stories, 2 wings without separation joints and a cinema hall in the back side; wings had GF + 5 stories at Bratianu Blvd. and GF + 3 (4?) stories at Regala Street. The collapse of Carlton building deserves a new analysis, because it was the tallest reinforced concrete building in Romania and an avantgarde architectural work in the epoch, it emphasized the extreme vulnerability of tall r.c. structures without seismic design. Although its collapse mechanism was only partially analysed, it has shown the paramount importance of architectural-structural configuration and lead to the first guidelines of earthquake design in Romania. Carlton was the first case of heavy urban Search and Rescue (SAR) in Romania and deployed civil and military Romanian and foreign forces, while the casualty was considerable. The analysis considered the situation before, after collapse and after debris removal, to evaluate collapse pattern and search and rescue operations. We used contemporary images, some of them recently released.

Keywords Vrancea earthquake · Structural configuration · Vulnerability · Casualty · Search and rescue

1 Introduction—the State of the Art of the Domain

The Carlton Building was designed by Arch. G. M. Cantacuzino, Arch. C. Arion and Eng. D. Mavrodin and built by the Enterprise of Schindl Brothers in 1935–1936 (Achim 1941, 1943; Prager 1979). The building included a high central tower with 2 basements + ground floor + 12 stories (18 m × 16 m in plan), 2 wings without separation joints and a cinema hall in the back side; wings had GF + 5

E.-S. Georgescu (✉)

National Institute for Research and Development, URBAN-INCERC,
European Center for Buildings Rehabilitation—ECBR, Bucharest, Romania
e-mail: ssever@incd.ro

stories at Bratianu Blvd. and GF + 3 (4?) stories at Regala Street. The height was of some 52.5 m (45.75 m over ground level) (Figs. 1, 2, 3, 4, 5, 6, 7 and 8). The building collapsed and crushed entirely towards N-E, on the Bratianu Blvd, in the night of November 9–10, 1940 at 3:39:07 AM, under the Vrancea earthquake (MG-R = 7.4).



Fig. 1 Carlton building before collapse, seen from S–E (post-card)

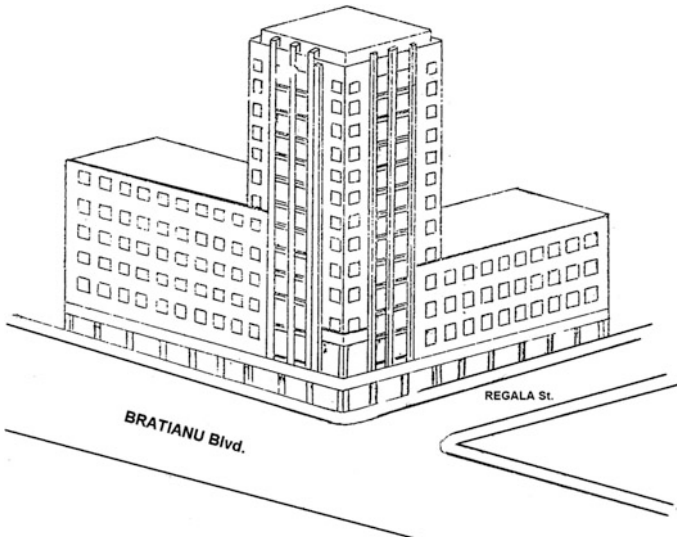


Fig. 2 Sketch of Carlton building, seen from N-E (Hangan 1963)

Fig. 3 Sketch of Carlton building collapse on vertical (Hangan 1963)

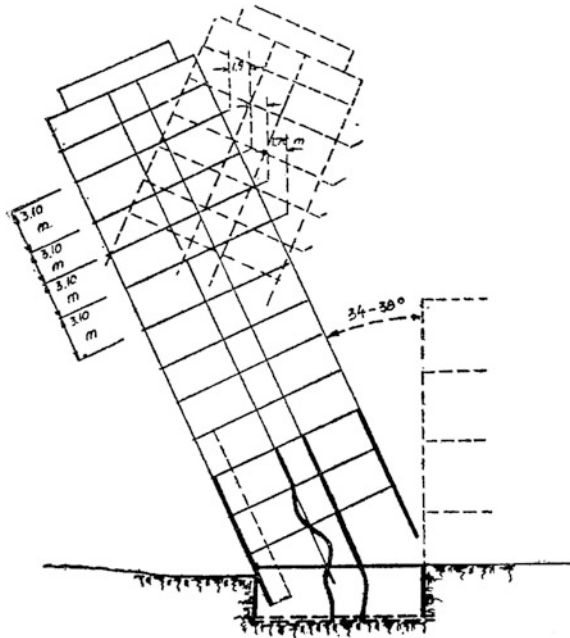
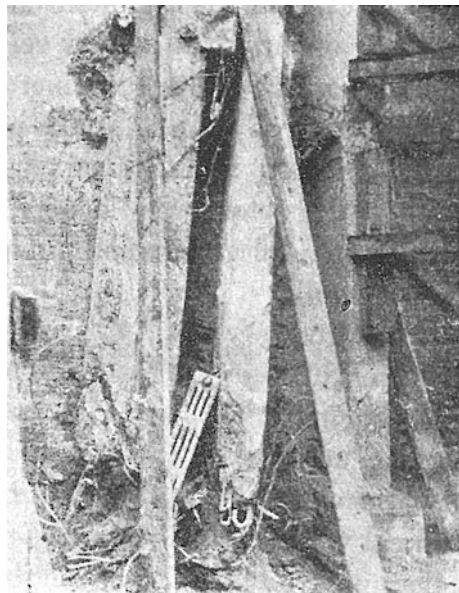


Fig. 4 Carlton building debris—the columns of the ground floor and first floor that were found in basement after punching the slabs (Beles 1941a, b)



The building was a representative work of avantgarde architecture, designed by a famous architect of the new generation and it was the tallest reinforced concrete building in Bucharest and Romania; its collapse was the surprise and the great

Fig. 5 Details of stacked balconies the S-W facade of Carlton building tower having background the Regala Street (Hangan 1963)



Fig. 6 Detail of S-W balconies that are visible in the Fig. 5 and evaluated by Hangan in 1940 (Hangan 1963; Georgescu 2005, 2007)



urban disaster in 1940 earthquake, this building being the first collapse of a r.c. high-rise structure under seismic loading in Europe.

The collapse mechanism was assessed for trial purposes at that time but it cannot be considered entirely understood. As censorship existed at that time, there were only few technical data and photographs in public use. From our evaluation, many wide-angle photographs from press and archives may have been taken by accredited staff from the same building (Creditul Minier) on Bratianu Blvd in front of Carlton and some of them possibly just distributed to foreign guests, institutions or to the press. Few newspapers and magazines were allowed to take their photos (Adevarul–Berman, L’Illustration–Safara).

Main causes of failure were reported elsewhere by Professors Aurel A. Beles and Mihail Hangan, experts of the court in the trial and for some decades there were only a handful number of available papers or books (Beles 1941a, b; Beles and Ifrim 1962; Achim 1941, 1943; Christea Niculescu 1941; Hangan 1963;

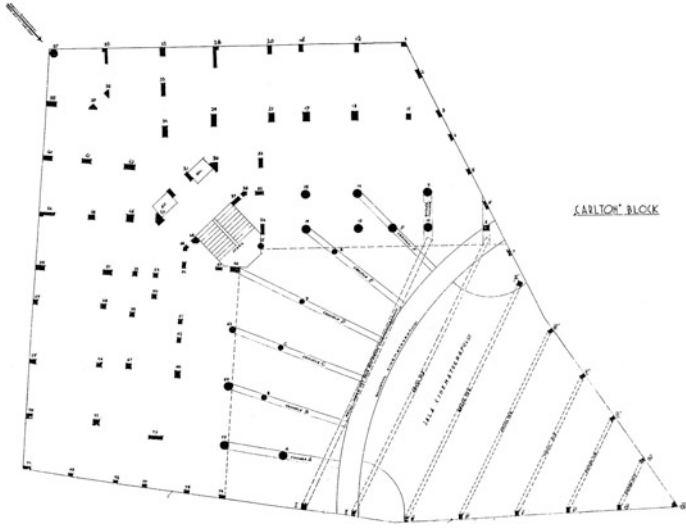


Fig. 7 Sketch of Carlton building layout, featuring the tower, two wings and the cinema hall behind (Achim 1941)

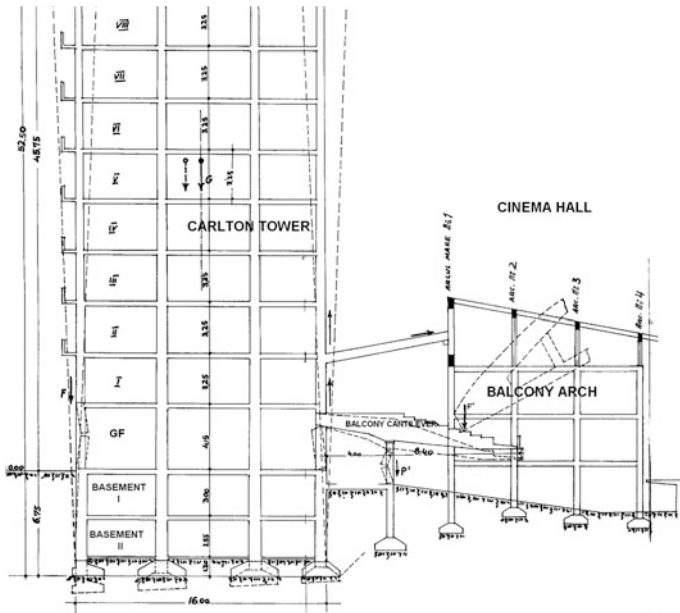


Fig. 8 Sketch of Carlton building structure and cinema with a hypothesis of interaction with the adjacent cinema structure (Achim 1941)

Prager 1979). Although the Second World War was emerging and the period was not proper for detailed analyses, this case was the trigger of first earthquake resistant design codes in Romania, since 1942.

After 1950s the new political situation in Romania contributed to a limited access to archives and less interest for more investigations. However, in 1954 Prof. Radu Voinea wrote a PhD Thesis on this subject under Prof. Hangan guidance (Voinea 1954). The engineering interest was re-open by some papers and books a decade ago (Georgescu 2005, 2007; Georgescu and Pomonis 2010, 2011, 2012). Forensic earthquake engineering was not a current topic in 1940, while issues like the search and rescue and casualties specific were not studied in further detail even afterwards. Since then, new photographs and data became available, thus they invite to revisiting this subject.

2 Objectives of the Paper

2.1 *Revisiting the Damage and Collapse Pattern, as It Was Assessed in 1940s*

The most reliable information about this case was provided by Professors Aurel A. Beles and Mihail Hangan, experts of the court in the trial and some official reports may still exist in Court archives. As technical literature, Prof. Aurel A. Beles (Beles 1941a, b; Beles and Ifrim 1962) and Prof. Mihail Hangan—ICB/UTCB (Hangan 1963) described the possible causes and patterns of structural damage mechanism followed by its collapse, as follows (Figs. 3, 4, 5 and 6)

- the cement content was acceptable, but concrete strength was variable, sometimes under acceptable marks, with casting joints, but this occurred in many other existing buildings; some cracks occurred after the earthquake of October 22, 1940;
- the layout was asymmetrical in plan and on vertical, shape of columns was lamellar (e.g. $b = 0.22$ m; $h = 1.70$ m; unreasonable cross section ratios, e.g. $h/b = 5 \dots 7$), sometimes in L or circular shape, thus the vertical structure was composed of columns of different section shapes, without fitting on the same vertical axes;
- there was not a code to require earthquake design, thus external and corner columns were calculated only for gravitational loads, and not for moments transmitted by beams, although the German standard DIN required it, and this was a term of reference in practice in Romania;
- many columns were indirectly supported, by second, third or fourth order beams;
- transversal beams were thin, some of 14 cm, internal masonry walls of 7 and 14 cm;

- large beams were supported by weak columns or narrow beams, while the reinforcement ratios were under the required ones (e.g. 0.5 vs. 0.8 % in German DIN).

Prof. Beles (1941a, b, 1962) considered as a cause of collapse, besides the improper structural configuration and materials weaknesses, some buckling effects, while some failures occurred in the upper stories beams, the seismic shear forces causing the weak columns failure over the basement level, followed by their punching through the basement slab, (Fig. 4). A general torsion around the vertical axis of tower probably occurred as it was witnessed by some nearby persons.

Prof. Mihail Hangan (Hangan 1963), revisited and detailed the possible damage mechanism evaluated with Prof. Beles in 1940, as follows (Fig. 3):

- the failure could have been started from the weak and lamellar corner columns at the ground floor level; the structure leaned and kneeled towards the Bratianu Blvd (N-E), later on some upper columns failed at seventh story;
- as a general process, the structure rotated in space with some 32° in trigonometric sense, at lower stories, then it was a leaning up to some $34\text{--}38^\circ$ versus vertical, falling on N-E with that upper part almost vertical. In this respect, some S-W balconies were found in a specific position over debris (Figs. 5 and 6).

A photograph that became recently available (Fig. 9) confirm this solution. Also, a widely circulated information claims that a fireman on duty for anti-aircraft surveillance on the top escaped almost unscathed, thus the speed of collapse of the second part of tower was not that high, and the vertical collapse of upper part is credible.

Eng. Theodor Achim (Achim 1941, 1943) considered the N-E to S-W direction of earthquake motion with the line of minimum resistance of the N-E corner column and with the existence of two weaker stories, as well as with the impact and torsion given by the cinema structure from the other side (the cinema balcony was supported on the back columns of the main tower) (Figs. 7 and 8).

Fig. 9 Carlton building after collapse (Ministry of Propaganda Files 1940)



The Romanian earthquake damages and Carlton collapse were of a special interest for the eminent Prof. Sieberg of Germany, and he arrived for the first time, on this purpose, in Romania with his assistant Dr. Wilhelm Sponheuer, on December 8, 1940 and visited shaken areas and Bucharest, giving lectures on December 18 and 20, with slides projections (Cuvantul 1940). In two books published afterwards (Sieberg 1941, 1943), he explained the behaviour of high-rise structures in specific conditions of long-period motions and resonance occurrence (at some 1 s or more) and some possible correlation with the oil extraction impact in seismic zones. His emphasis on the damage pattern of r.c. columns heads, i.e. plastic hinges occurrence, as seen in Carlton case, is outstanding, as well as the warning on corner towers weaknesses, a fact proved again in 1977 Romania earthquake. Some tests on small building models on a shaking table of Jena Institute allowed him to explain the behaviour of different houses, including the soft-story collapse (!), the general response and sandwich type collapse.

Prof. Christea Niculescu (Niculescu 1941) addressed the issue of resonance avoidance in a paper that was quite forgotten for some 30 years in Romania. Voinea (1954) considered the Carlton collapse as being caused by a loss of overall stability and made a theoretical study in this respect, under Prof. Hangan guidance (Voinea 1954).

We may see that the visionary issue of long-periods, firmly stated by Prof. Sieberg, was quite revolutionary for that time and it was not considered at full value until 1977, when long-period record of over 1 s was obtained in INCERC (Fattal et al. 1977; Balan et al. 1982).

2.2 The Collapse Analysis Based on the Newly Available Images

Many images taken in 1940 became available gradually and contributed to fill-up some gaps in understanding the situation after collapse. It should be mentioned that most of photographs and movies before the 1990 have shown some initial site situation (the first day and night) with smoke and less visible structural members, make it difficult to us to check their failure position. Even Beles and Hangan, although they were experts in the case, published details but not publish very clear overall images.

In our present research, we compared initial images and images after failure and cleaning. An important group of images show the place of collapse and their resolution was quite appropriate to see more details. The place of taking of photographs of many pictures seems to be the same, a building that exist and today, over the boulevard.

Later on, after occurrence of photograph seen as Fig. 9, since the place of wreckage was quite empty of people, the pattern of collapse was more visible. To the left, there is a stack of slabs and balconies of Bratianu Blvd. wing, with a

Fig. 10 Carlton building—details of stacked slabs and some parapets or balconies seen from Regala Street (L’Illustration 1940)



height over the first floor of the adjacent building. An arch of the cinema roof is laid down.

The place of failure for tower balconies of the S-W side is visible in the center of photograph and it is fitting with Fig. 5 used by Hangan to argue his collapse model. In the background, on the right side, there are the collapsed and stacked floors and balconies of the Regala Street wing. A large quantity of crushed building materials, concrete, bricks, plaster, timber, heaters etc. are spread around. Recently, we reassessed the photographs of Figs. 9, 10, 11, 12 and others from the same package of Galmeanu/Muzeul de fotografie Galmeanu A (2015). We remarked the balconies along the Regala Street that are now visible in Figs. 11 and 12, hanging on the right side, near the low-rise masonry building which escaped unharmed until today.

Surviving occupants of Carlton declared that those attempting to use elevators died in crash, while those going on stairs were not able to escape and were entrapped under debris.

Fig. 11 Carlton building—the heap of debris and the N–W wing collapsed balconies, on the right of Regala Street, Galmeanu A (2015)



Fig. 12 Carlton building—the details of N–W wing collapsed balconies, on the right, seen from Regala Street (Galmeanu A (2015))



One may say, probably, that when the central tower failed, its front corner column was so brittle and the speed of collapse towards the N-E of the base was very high, thus there was any oscillatory response, but just a fracture. Thus, the structure did not impact the five storied masonry building on Regala Street.

2.3 Search and Rescue Operations

From Figs. 13 and 14, it is visible that SAR operations were started by authorities and some other persons, neighbours etc. without tools, while the rain started soon after earthquake. In the first photographs a crowd covers the site. It is obvious that this collapse was the first urban search and rescue case in the history of Romania, with time-consuming operations and technical difficulties caused by rain and fire during the operations; light projectors allowed the work during the night, and there are some documentary movies proving it (Rumanian Earthquake, (1941)).

Fig. 13 Carlton building debris in the first period of SAR intervention teams (CEGESOMA Archive)



Fig. 14 Carlton building debris in progress of intervention works (Berman 1940)



In 1982, the published memoirs of the vice-premier of Romania in November 1940, indicated 593 killed and 1271 injured in all the country, and in Bucharest 140 killed from the 226 occupants of Carlton block, with another 300 injured in the city (Sima 1982). From the recovered photos it resulted that the percentage of volume loss was very high (>0.70), while the lethality is assessed as 62 % based on new available figures (Sima 1982; Georgescu and Pomonis 2011, 2012). The Cinema was not in use at that hour, thus some rumors about a huge mass loss of lives were denied.

Initially, a large number of trucks were deployed radial around the disaster place, on Bratianu Blvd and a few on Regala Street. As much as the debris was taken away, Figs. 13 and 14 prove that the trucks came gradually closer to the site, along N-E direction. We identified the area covered by debris as being limited by two electricity poles, near the boulevard lanes, and at least one of them survived until 2013!

The visible forces are of Romanian Army, Gendarmery, Firemen and Police, in uniform and some with helmet, mingled with some paramilitary squads of the rightist (“Legionaries”—Iron Guard). In the left side of Figs. 13 and 14 there are the officers and soldiers of the German Army, as reported by L’Illustration 1940 and checked by us in Fig. 14. The troops were under leadership of General Speidel, Head of The German Air Force Mission and General Hansen, Head of the German Army Mission.

Some participation of SAR teams of German Youth Organization (Hitlerjugend) is reported also in L’Illustration (L’Illustration 1940). Members of Italian Fascist Youth Organization, attending some events in Iasi, arrived at site (Sima 1982). The presence of German Army was associated with a possible presence of many German tenants in the building, but there are no data to prove it. On the other hand, on the heap of debris and around the place there is a huge number of usual people in formal dress (Fig. 15), with hat and tail, which indicates a social mobilization and sympathy for victims. However, their contribution was just to give bricks and things in a human chain to release the place, in hope of finding survivors.

Fig. 15 Carlton building—bare hands army members, civilians and paramilitary removing the debris (Galmeanu A (2015))



It is worth of mentioning that after the territorial losses of June and August 1940, followed by the abdication of King Carol II, King Michael I took the throne but the country was governed by the General Antonescu associated with the extreme right party. Romania signed an agreement and the German troops entered in Romania October 7, 1940. This may explain why the German Army offered (!) a camp with 2000 beds for homeless.

Media reported that a number of some 50 persons (?) run in the basement and were entrapped there, and it was confirmed that some called by telephone desperate help (This assertion would imply that there was enough time to run there for so many people just awakened and without knowing what to do; most likely they were the staff of the technical services). First attempts to reach them digging with bare hands were less successful, and the attempt of paramilitary to dig a tunnel to reach the basement failed (Fig. 16).

Fig. 16 Carlton building—digging by unskilled volunteers to reach the basement, while smoke is still present (L'Illustration 1940)



Fig. 17 Carlton building—the site almost cleared of debris (Galmeanu A/Muzeul de fotografie 2015)



It is said that the lack of experience led to a cut of water pipe, a short circuit and a fire to the fuel stored there. Some 60 t of pitch fuel existed in the basement, it ignited on November 10 evening and it took one day to extinguish it. Other sources claim that fire started from the beginning, but the Fig. 9 does not confirm it. Thus, water and fire hampered seriously the rescue operations and survivors lost their lives in the basement.

Until November 15 the debris search and removal teams reached the third floor, while after six days they reached the slab over basement. Eventually, a German Army crane was installed and concrete debris removed with a greater speed. By November 24, 136 bodies were extricated. After two months, the site and basement was cleared (Figs. 17 and 18).

Fig. 18 Carlton building—the site and the crane in the final removal of debris. A part of cinema hall roof is still hanging, damaged (Pragher 1941)



3 Conclusions

The Carlton building collapse was re-evaluated after 75 years and yielded important conclusions:

- the newly available imagery allowed the recovery of many technical details of collapse pattern and the place of various elements after failure was identified;
- Carlton collapse was the first case of gathering wide international media coverage, leading also to geo-political interpretations, joining foreign human forces and logistics in SAR operations and structural analysis of failure reasons;
- the causes of failure were identified by the prominent professor and structural engineers of the time, from Romania and Germany, and it is important that configuration, general dynamic response and detailing importance were considered as causes;
- as a consequence of this disaster, the development of guidelines for earthquake resistant design and codes in Romania started in 1942 and continued in 1945, and an advanced compulsory code was enforced in 1963;
- the Carlton disaster greatly influenced the nature and extent of relationships between architects and engineers, as well as the issues of legal and technical liabilities in earthquake design;
- due to a lack in communication, on long-term, in public perception it was mistakenly considered to be a unique accident, dominated by cumulative errors;
- the Carlton collapse can be considered a forgotten witness of possible resonance effects at long-period motions on tall buildings and of cumulative damage, put into evidence by several Romanian and German scientists;
- in relationship with the next earthquake disaster of 1977, dominated by the collapses of the so many pre-1940 structures in Bucharest, it can be considered as a neglected warning on vulnerability of high-rise buildings;
- the situation of Search and Rescue operations after the 1940 earthquake at Carlton site was assessed for the first time, and a social self-mobilization and volunteerism is obvious, but although the intervention was authoritative, it proved yet to be chaotic and using limited tools;
- some progress in preparedness was remarked in the SAR operations after the 1977 earthquake, as the available logistic was improved, but in many cases army staff and people acted also with bare hands.

Acknowledgements The author express his gratitude to Friedrich-Schiller-Universität Jena, Germany, for assistance and providing excerpts of Prof. Sieberg book, to Mr. Alex Galmeanu and his Website „Muzeul de Fotografie”, to Ceges-Soma Archive, Belgium and to Landesarchiv Baden-Württemberg, Germany for historical photographs with Carlton Building.

References

- Achim T (1941) Cauzele prăbușirii „Blocului Carlton”. În *Învățăminte*. Tiparul „Cartea Românească”, București
- Achim T (1943) Apărarea în Procesul Carlton. Tipografia Ștefan Ionescu-Tămădău, București 1943
- Balan S, Cristescu V, Cornea I (coordinators) (1982) The Romania earthquake of March 1977 (in Romanian, with English abstract). Editura Academiei, Bucharest, Romania
- Beleş AA (1941a) Le tremblement de terre du 10 Novembre 1940 et les bâtiments. In: Tome V (ed) *Comptes Rendus de Séances de L'Académie des Sciences de Roumanie*, no 3, pp 270–288. Cartea Românească, București
- Beleş AA (1941b) Cutremurul și construcțiile. Extras din Buletinul Soc. Politehnice, Anul LV, Nr. 10 și 11, Octomvrie și Noiembrie 1941. București
- Beleş A, Ifrim M (1962) Elemente de seismologie inginerescă. Editura Tehnică, București, pp 16, 203, 223
- Berman I (1940) Blocul Carlton prabusit. https://commons.wikimedia.org/wiki/File:Iosif_Berman_-_Marele_cutremur_din_anul_1940.jpg
- Ceges-Soma Archive (2015) Le tremblement de terre du 10 novembre 1940 en Roumanie. Centre for historical research and documentation on war and contemporary society, Belgium. Archive Photos n° 66670–76. Retrieved 21 Oct 2015 at <http://pallas.cegesoma.be/pls/opac/opac>
- Cuvantul (1940) December 17, 1940. Newspaper clipping. Bucharest
- Earthquake in Romania (1941) https://www.youtube.com/watch?v=J_NIPGAlIMw (INA). Accessed 26 Oct 2015
- Fattal G, Simiu E, Culver, Ch (1977) Observation on the behaviour of buildings in the Romanian earthquake of March 4, 1977. US Department of Commerce, Sept 1977, NBS Special Publication 490
- Galmeanu A (2015) <http://www.muzeuldefotografie.ro/> Imagini noi—Cutremurul din 1940—Blocul Carlton. Accessed 26 Oct 2015
- Georgescu ES (2005) Cutremurul din 10 noiembrie 1940—vector de inițiere a ingineriei seismice moderne în România. Evaluări privind mecanismul prăbușirii blocului Carlton. Cea de a 3-a Conferință Națională de Inginerie Seismică, 9 decembrie 2005, UTCB, București
- Georgescu ES (2007) Bucureștii și seismele. Editura Fundației Culturale Libra, București. ISBN 978-973-7633-50-7
- Georgescu ES, Pomonis A (2010) Human casualties due to the Vrancea, Romania earthquakes of 1940 and 1977: learning from past to prepare for future events. In: Proceedings of mizunami international symposium on earthquake casualties and health consequences, 15–16 November 2010, Mizunami, Gifu, Japan
- Georgescu ES, Pomonis A (2011) Emergency Management in Vrancea (Romania) Earthquakes of 1940 and 1977: Casualty Patterns vs. Search and Rescue Needs. In: Proceedings of TIEMS 2011—the international emergency management society, the 18-th annual conference, Bucharest, Romania, 2011
- Georgescu ES, Pomonis A (2012) Building Damage vs. Territorial Casualty Patterns during the Vrancea (Romania) Earthquakes of 1940 and 1977. In: Proceedings of 15-th WCEE, Lisbon, 24–28 Sept 2012
- Hangan M (1963) Căderea unui bloc de locuințe cu schelet de beton armat la București în timpul cutremurului din anul 1940. Simpozionul Dinamica Construcțiilor și inginerie seismică. ICB, 1962. Buletinul Științific ICB, nr. 19, 1963
- L'illustration (1940) Le tremblement de terre en Roumanie no 5099, pp 309–311, 30 Nov 1940
- Niculescu C (1941) Die Gebäudenschäden des Bukarester Erdbebens vom 10. November 1940. Die Bautechnik, Berlin, July 1941, pp 321–326
- Prager E (1979) Betonul armat în România. Editura Tehnică, București 1979:451–454
- Prager W (1941) Landesarchiv Baden-Württemberg: Staatsarchiv Freiburg; <http://www.landessarchiv-bw.de/staf>. Bukarest: Carlton-Ruine von oben gesehen. Description: Kontext:

- Sammlung Willy Prager I: Rumänienbilder, 1941–44 [Filmnegative, Ordner 290]. DE_ArchLABW_5_169448; W 134 Nr. 031342c. Accessed 26 Oct 2015
- Rumanian Earthquake (1941) <http://www.britishpathe.com/video/rumanian-earthquake>
- Sieberg A (1941) Versuche und Erfahrungen über Entstehung, Verhütung und Beseitigung von Erdbebenschäden. Mit 50 Abbildungen. Veröffentlichungen der Reichsanstalt für Erdbebenforschung in Jena. Herausgegeben von deren Direktor August Sieberg. Heft 39. Reichsverlagsamt. Berlin NW 40
- Sieberg A (1943) Experience and Lessons on the Origin, Prevention and Elimination of Earthquake Damages (Photo-type edition of the Bulgarian language book of 1943. English editing Dilys Grilli, Editorial Board Prof. M. Cara, Prof. G. F. Panza, Assoc. Prof. I. Paskaleva). Publishing House LITSE, Sofia, 2005, ISBN 954–9426-01-7. pp 31 and 71–76
- Sima H (1982) Era Libertatii, Statul National-Legionar, vol. I, Madrid, Accessed on Internet, Oct 2010, chapter II, pp 176–178
- Voinea R (1954) Contribuțiuni la studiul stabilității elastice a construcțiilor static nedeterminate (Teza de doctorat). Extras din Buletinul Științific al Institutului de Construcții București, Nr. 1:1954

Main Characteristics of November 10, 1940 Strong Vrancea Earthquake in Seismological and Physics of Earthquake Terms

Gheorghe Marmureanu, Carmen Ortanza Cioflan,
Alexandru Marmureanu and Elena Florinela Manea

Abstract *Vrancea earthquake on November 10th, 1940* ($M_W = 7.7$; $M_{GR} = 7.5$; $h = 150$ km; $E = 1.122 \times 10^{23}$ ergs, $I_{max} = IX\frac{1}{2}$) represents the first large earthquake in the last century and was preceded by other earthquakes as: October 22, 1940 ($M_W = 6.5$) and November 8, 1940 ($M_W = 5.9$). If recorded, it would be given the opportunity to get basic data for seismic hazard assessment and useful conclusions for seismic design of structures to strong earthquakes. Unfortunately, no seismic ground motion was recorded and, as a consequence, no improvements of the Romanian design building code were made after this earthquake. The earthquake of November 10, 1940 confirms the existence of deep earthquakes in Vrancea area, deeper than Moho discontinuity in the lower lithosphere, and this theory was developed for the first time by H. Jeffreys in 1935. Focșani city and several municipalities (Cotești, Panciu etc.) were almost destroyed and the houses not taller than one floor, were completely damaged. More than 45 churches and monasteries were damaged, destroyed or demolished. New data regarding damages at monasteries have been synthesized and analyzed, the resulting intensities are completing the known macroseismic field and data may be used to construct the isoseismic map of the maximum possible Vrancea earthquake.

Keywords Seismicity · Seismic hazard · Deep earthquakes · Damage

G. Marmureanu (✉) · C.O. Cioflan · A. Marmureanu · E.F. Manea
National Institute for Earth Physics, University of Bucharest, Bucharest, Romania
e-mail: marmur@infp.ro

C.O. Cioflan
e-mail: cioflan@infp.ro

A. Marmureanu
e-mail: marmura@infp.ro

E.F. Manea
e-mail: flory.manea88@gmail.com

1 Introduction

In the confrontation with the risks due to natural hazards, examining earthquakes on the Romanian territory from a historical perspective is an operation that proved to be necessary.

The main objective of this study is to enlarge the knowledge on seismicity in a time span as long as possible to be taken as an advantage for future hazard and risk assessments. In this way, the seismologist can minimize the epistemic uncertainties in the risk assessment due to the hazard part. This operation assumes risks and it must be done carefully, because the information coming from various sources on the so-called “historical” earthquakes are incomplete, approximate, and often subjectively exaggerated, as shown by Mărmureanu (2015). Nevertheless, with regard to the evolution in time of the occurrence of Vrancea earthquakes, after their examination from a historical perspective, there was ascertained the persistence of their Vrancea hypocenters. Ascertaining the persistent character of the Vrancea earthquakes involved a previous localization, at least within wide limits of approximation of their causes.

The intermediary Vrancea earthquakes with focus depths ranging between 70 and 200 km are determinant for the seismicity of the Romanian territory, both in point of occurrence frequency and in point of their magnitudes and their effects on the population and the buildings. There are useful data with important descriptive elements on the historical earthquakes, from which there can sometimes be deduced even certain quantitative parameters, which define their characterization.

The earthquake of November 10, 1940 is characterized by three peculiarities: (i) a great expansion of the macro-seismic area of over 2,000,000 km², from the Danube, at Mohács and Székesfehérvár (Hungary) to Warsaw (Poland); (ii) a quasi-symmetrical disposition of the strongly affected territories, the ones in the Southern Moldova (Bârlad–Focșani–Panciu) and the sub-Carpathian Hills, North of Ploiești; (iii) the existence in several regions of the country (Fig. 1), of some seismic “culminations” which are quite often parallel (Atanasiu 1961).

2 Main Characteristics of November 10, 1940 Strong Vrancea Earthquake

The earthquake occurred on November 10, 1940 has the following characteristics: $M_W = 7.7$; $M_{GR} = 7.5$; $h = 150$ km; $E = 1.122 \times 10^{23}$ ergs (Radu 1979) but was classified with $M_{GR} = 7.4$ in ROMPLUS Catalog (<http://www1.infp.ro/arhiva-in-timp-real>).

At the beginning of the 20th century, Hepites installed in Bucharest (Romania) the first seismographs. Since 1902, the ground motion of the Vrancea earthquakes

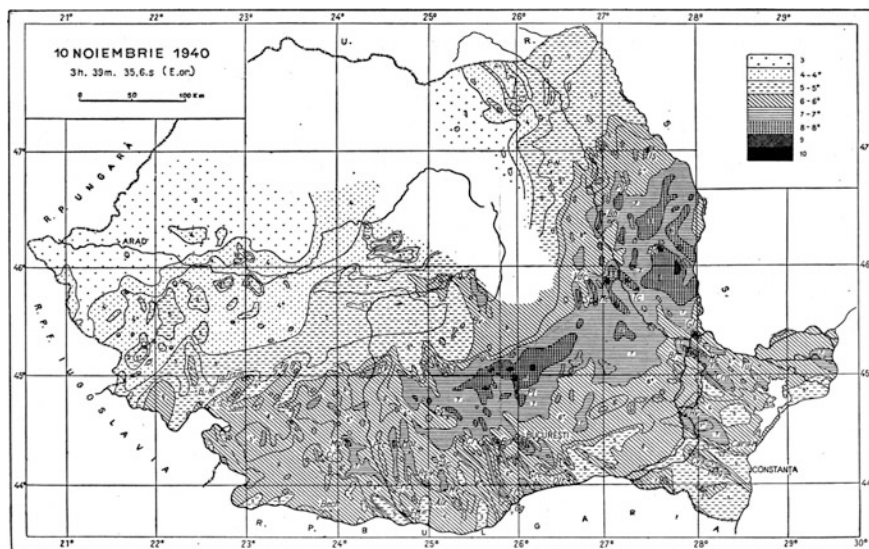


Fig. 1 Isoseismal map of Vrancea strong earthquake on November 10, 1940 (Atanasiu 1961)

started to be recorded (Constantinescu et al. 1985). There were two horizontal mechanical pendulums weighing 10 kg, not damped, with amplification of 10–15 times. These pendulums were kept running by the Meteorological Institute until 1921 and by the Observatory of Bucharest after 1928 (Demetrescu et al. 1942). As Constantinescu et al. (1985) showed, the records obtained here, with these seismographs, although very modest from the quality point of view, contributed to establishing a very important fact—*the existence of intermediate-depth earthquakes in Vrancea*.

Before 1935, the scientific literature over the world did not even mention the existence of intermediate-depth or deep earthquakes. Actually, at that date, geologists did not accept the existence of intermediate-depth and deep earthquakes.

Only in 1935, based on the records made at the “Cuțitul de Argint” Seismological Observatory of Bucharest, for the earthquake occurred on November 1st, 1929 ($M_W = 6.1$; $h = 184$ km; $I_0 = VI-VII$) and on records for other four earthquakes from various parts of the world, Jeffreys (1935) from United Kingdom studied and concluded, for the first time in the world, that there could exist earthquakes deeper than the Mohorovičić (Moho) discontinuity (at more than 40 km depth in Vrancea zone, Fig. 2). Following the study carried out by Jeffreys, the first quantitative result was obtained with regard to the localization of the strong intermediate-depth earthquakes occurring in Vrancea. The coordinates determined for the earthquake of November 1st, 1929 are: $\varphi \approx 45.9^\circ N$; $\lambda \approx 26.5^\circ E$; $h = 184$ km.

The Vrancea earthquake of November 10, 1940 ($M_{GR} = 7.4$ and $I = IX\frac{1}{2}$) occurs at 03:39 in the night, and with the depth of 150 km, preceded by two earthquakes:

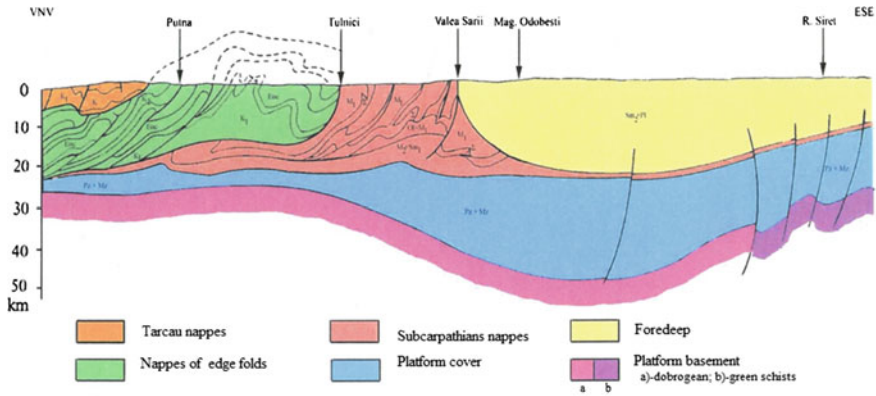


Fig. 2 WNW–ESE geological section through Eastern Carpathians. Mohorovičić (Moho) discontinuity is at 46 km (*source* Mândrescu and Marmureanu 2002)

one in October 22, 1940, at 8:27 h ($M_W = 6.5$; $h = 125$ km and $I = VII$) and another one on November 8, 1940 ($M_W = 5.9$; $h = 145$ km) (Oncescu et al. 1999).

This earthquake is the first great earthquake in the contemporary history of Romania, which would have offered the occasion to collect some useful basic data and conclusions, with regard to the behavior of buildings during strong earthquakes.

But, the November 10, 1940 earthquake found Romania totally unprepared, no ground motion was recorded and, therefore, the engineering seismology and seismic engineering research could not develop in a suitable manner. Demetrescu et al. (1942) affirms that: “the record was done only at the beginning of earthquake. The intensity of the earthquake was so large that it broke all ties, all suspensions and connections of the instruments in Bucharest”. Also, the seismographs from Belgrade (Hungary) and Sofia (Bulgaria) were broken and it was recorded at Kharkov and Poltava (Ukraine) at about 1000 km far away (Atanasiu 1961).

In the same year, another great earthquake was recorded on May 18, 1940, in the USA, at El Centro, California, when the first accelerogram of a great earthquake was recorded. This El Centro–type accelerogram is known throughout the scientific literature, together with its response spectrum (Fig. 3). The response spectrum of this earthquake is totally different from the one of an intermediate depth’s earthquake of Vrancea (e.g. March 4, 1977), and shows that these type of earthquakes have different features from the ones occurred in the terrestrial crust. If an accelerogram had been recorded for the earthquake occurred on November 10, 1940, the anti-seismic design of buildings would have been conceived otherwise until March 4, 1977.

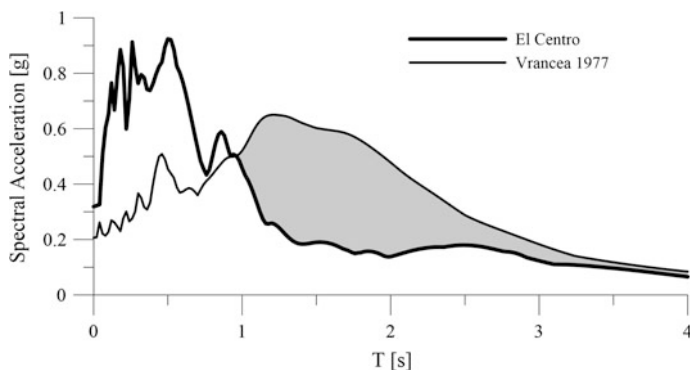


Fig. 3 The comparison of the acceleration response spectra of El Centro, California, and of Vrancea 1977 event ($M_w = 7.4$), recorded in Bucharest, Romania (5 % damping). The grey area represents the unsafe area for mid-rise and high-rise buildings

3 The Effects of the Earthquake Occurred on November 10, 1940

The main effects of this earthquake manifested themselves in the central and Southern parts of Moldova, as well as in the Muntenia. During this earthquake, the Carlton building collapsed in Bucharest. The structure of the building was made from reinforced concrete, it had a two-level basement, cinema theater, ground floor, and 12 floors, and it collapsed entirely after the first vibrations (from the P-waves), burying under the rubble almost all the inhabitants. A famous trial followed, which revealed that there had been serious faults in the design and the construction of the building, but at the end, in 1944, the whole story was forgotten, and the builder and the architect were released from prison. In this city, the earthquake woke the people up, as the buildings “were balancing like toys in the wind”, “in the houses, the furniture was moving, squeaking from their joints, the cupboards were falling, the pendulum clocks stopped, the chimneys were crumbling, pieces of walls were falling, old houses partially crumbled”. In some churches, the plaster fell and the tower crosses broke. (the newspaper *Universul*, November 12, 1940).

The exact number of the victims is not known, as in 1940, during the war, the information in the press was censored. It is estimated that there were 1000 dead, the great majority in Focșani and in Moldova, and approximately 4000 wounded.

In several regions of the country, there was ascertained the existence of some seismic “*culminations*”, rather linear and often parallel. These “*seismic sensitivity lines*” represent areas of wave interference or they would reflect structural lines of the base. This wide macroseismic area, of over 2,000,000 km², was observed by Atanasiu (1961).

Nowadays, it is considered that these lines, as well as the “islands” that mark macroseismic maximums, represent amplifications of the land response to the movements produced by such earthquakes. These amplifications are either effects of

the lithological composition of the land, or of the presence of some superficial or deep faults.

Another fact observed is the almost symmetrical disposition of the territories affected by the earthquake, against the less affected ones (Atanasiu 1961), the latter being situated in an area extended from the Danube to the Carpathian curvature. A part of these strongly affected territories were located in Southern Moldova, in the region Bârlad–Focșani–Panciu, while the other lies on the opposite side of the Sub-Carpathian Hills area, north of Ploiești (Fig. 1).

The earthquake of 1940 strongly affected Moldova, especially the Southern part of Moldova, the Northern Dobrogea, and Odessa. All monasteries in the Northern Dobrogea were affected by that earthquake, especially the monasteries of Saon, Cocoș, and Celic Dere etc. The monastery of Comana, located in the Comana commune, in the Neajlov valley, was not affected by the earthquake of 1940, but the church was affected by the earthquakes of 1977 ($M_W = 7.4$; $h = 109$ km) and 1986 ($M_W = 7.1$; $h = 131.4$ km) and after that consolidated.

Marmureanu et al. (2010) affirm that “In Bârlad city, many houses collapsed down to their foundations, and the remaining buildings were seriously damaged. The city was in ruins. Panciu city was destroyed in a proportion of 90 %, even if most of the houses were made of wood. Everything was demolished, no house resisted only the soldier’s statue was still up, unmoved. In Focșani city all schools were closed down. The firemen’s building was completely destroyed, the boys intern school was closed without any possibility to reopen”. This earthquake caused great damages in Prahova county as well. In Ploiești there collapsed: the building of Piața Unirii (Union Square) over the “Olaru” shop, a building in “Arastra”, on Cavafi street, “Sf. Pantelimon” church collapsed entirely, “Sf. Gheorghe Vechi” church collapsed, “Sf. Ecaterina”, “Sf. Împărați”, and “Sf. Spiridon” churches—each of them had a crumbled tower. The Palace of Commerce Schools had a wall down. “Sf. Petru and Pavel” High School was severely damaged, the Palace of Justice was cracked in several places, the “Carol Palace” and “Băicoi” hotels had each of them a destroyed wall. No building remained untouched, whole city was in ruins. In Prahova county, the communes of Românești, Bărcănești, Crivina, Poienarii Burchii, had a lot to suffer, half of the villagers’ houses being destroyed. In Iași, oscillations were very short in the beginning, followed by strong ones, which lasted for 40–50 s, in total. The direction of propagation was towards North-South (Marmureanu et al. 2010).

Numerous buildings were affected, the most seriously damaged being the Administrative Palace, the former “Bejan” hotel, the main chandelier of Banu Church fell, and so did the crosses of the towers of other churches. “*At the city limits almost all houses collapsed*”. Rogozea (2011) affirms: “In Târgoviște, the earthquake lasted for almost two minutes, causing general panic. Here, serious damages occurred in the buildings of the prefecture, municipality, the school inspectorate, the Pușcaru house, “Gloria” cinema, and the churches of Sf. Gheorghe and Sf. Nicolae–Andronești. Seven houses were completely destroyed, while other hundreds had cracks in the walls. Many of them remained in a danger to collapse. In Buzău, entire buildings were pulled down to their foundations and, in a great

number of buildings, the inner walls cracked. The chimneys of some houses fell onto the roofs. There were damages in the: bishop's palace, gendarme legion, "Zaharescu" and "Haşdeu" high schools, the girls' high school, the boys' pedagogical high school, the palace of justice, and many other buildings. In Constanța, a great number of houses were damaged. Among these, the "Regaș" and "Bistol" hotels were more severely damaged. At Mamaia, the "Rex" hotel was deteriorated. At Curtea de Argeș, the chimneys of the large buildings crumbled down, some of the walls cracked and others fell".

Popescu (in *Universul* newspaper, 15.11.1940) wrote: "There were violent earthquakes in the past, as well, like those that took place in 1802 and 1838, but none of them had the strength of this one, none devastated so many cities and villages and none caused so many human victims".

3.1 The Effects of the Earthquake on November 10, 1940 on Churches and Monasteries

The following churches and monasteries were damaged, destroyed, or demolished by the earthquake of November 10, 1940: *Sihăstria Monastery* (MO/21) located in the Northern part of the Neamț county, on the Secu river valley, 22 km away from the town of Târgu-Neamț; *Biserica Domnească (Prince's Church) of Bârlad* (M/44/2012); *Sfântul Ilie Church of Bârlad* (M/27/2012); *Biserica Domnească of Vaslui* (M/4/2012); *Rafaila Monastery* (M/44/2010) located in Rafaila village, Vaslui county; *Sămurcășești Monastery* (MO/112); *Antim Monastery* (M/50/2012 and MO/73); "Adormirea Maicii Domnului" *Church of Vălenii de Munte* (M/24/2015); Icon Church, a few steps away from Dârvari Schit, Bucharest; *Zlătari Church* (M/33/2012), located downtown Bucharest, on Calea Victoriei; "Precupeții Noi (New)" Church (M/31/2011) in Bucharest, on General Ernest Broșteanu street; *the Patriarchal Cathedral* (MO/120); *Sf. Spiridon Cathedral of Bucharest* (M/5/2014); *Sister Hermitage Church of Bucharest* (J. Național, 18.09.2014); *Zamfira Monastery* (M/13/2011)—North of Ploiești, Zamfira village; *Brâncoveni Monastery* (M/46/2011), Brâncoveni commune, Olt county; *Nucet Monastery* (MO/44); *Hill Monastery* (MO/39); *Căldărușani Monastery* (MO/86); *Glavacioc Monastery* (MO/111), on Pitești-Bucharest highway (70 km); *Pissiota Monastery* (MO/114) Prahova county, 35 km away from Bucharest; "Viforâta" *Monastery* (MO/35) situated in the north of Târgoviște city; *Mamu Monastery* (RO/47), Lungești village, in the south-eastern part of Vâlcea county, 8 km away from Drăgășani and 40 km away from Slatina city; *Snagov Monastery* (MO/81); *the Roman Catholic Church of Câmpina* (M/13/2012); *the Church of Căciulați village* (M/7/2012), Moara Vlășiei commune; *Saint Nicolae Church of Comarnic* (M/26/2012); *Celic Dere Monastery* (MO/77), between Cataloi and Frecăței, beside the Celic Dere brook; *Cocoș Monastery* (MO/83), Northern Dobrogea, nearby Niculițel; *Saon Monastery* (MO/92), between Niculițel village and the Danube;

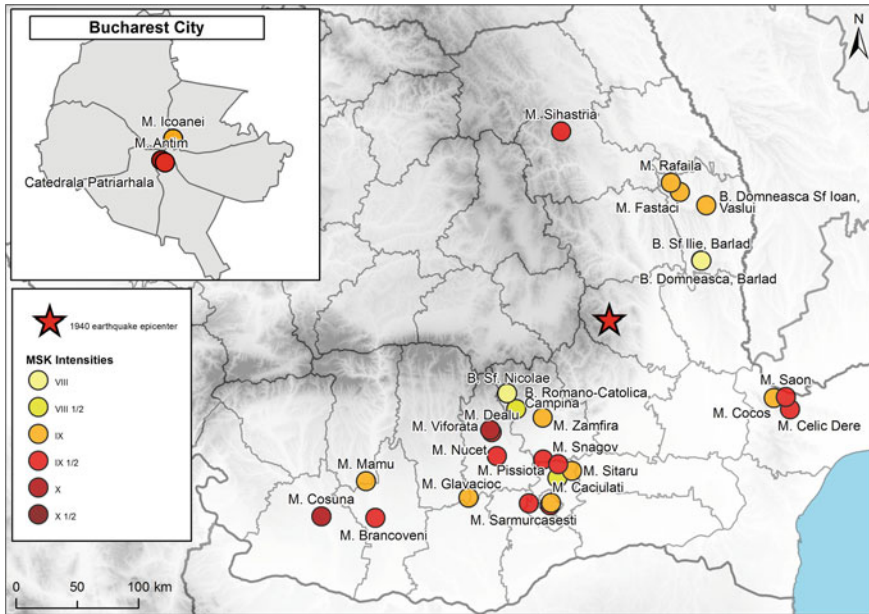


Fig. 4 Seismic intensity values obtained by using data from churches and monasteries after Vrancea strong earthquake on November 10, 1940 ($M_W = 7.7$; $h = 150$ km)

Zimbru Hermitage located in the Bursucani village, Bălăbănești commune, Galați county, was totally transformed into ruins (M/17/2014), etc. (Fig. 4).

Bucharest was much less affected than the south of Moldova. Focșani city was practically destroyed, so were the neighboring towns, such as Cotești, Tâmboiești, Păunești, Golești, Soveja etc. where the inhabitants’ houses were demolished (Fig. 5). Mândrescu and Marmureanu (2002) computed the damage degree in Vrancea region as $d_{mean} = \sum d_i n_i / \sum n_i$; d_i —damage degree of the building “i”; n_i —number of buildings. The damage degree was interpreted as proposed by Shebalin (1975): 1—light damage, 2—moderate damage, 3—severe damage, 4—extensive damage.

In the Address No. 14, 033/November 13th, 1940 sent by Constantin Faur, mayor of Focșani to the Minister of Interior is specified that the Focșani city suffered irremediable damages: (i) 50 % of the dwellings are completely destroyed and part of them deteriorated beyond repair. Maximum 25 % of the buildings in the city will remain standing; (ii) All elementary and secondary schools are seriously damaged, making the teaching process impossible; (iii) The buildings of all public institutions are seriously deteriorated. The City Hall is so damage, that it requires rebuilding, the floor is completely destroyed; (iv) Most churches are demolished, others are seriously damaged (Mândrescu and Marmureanu 2002).

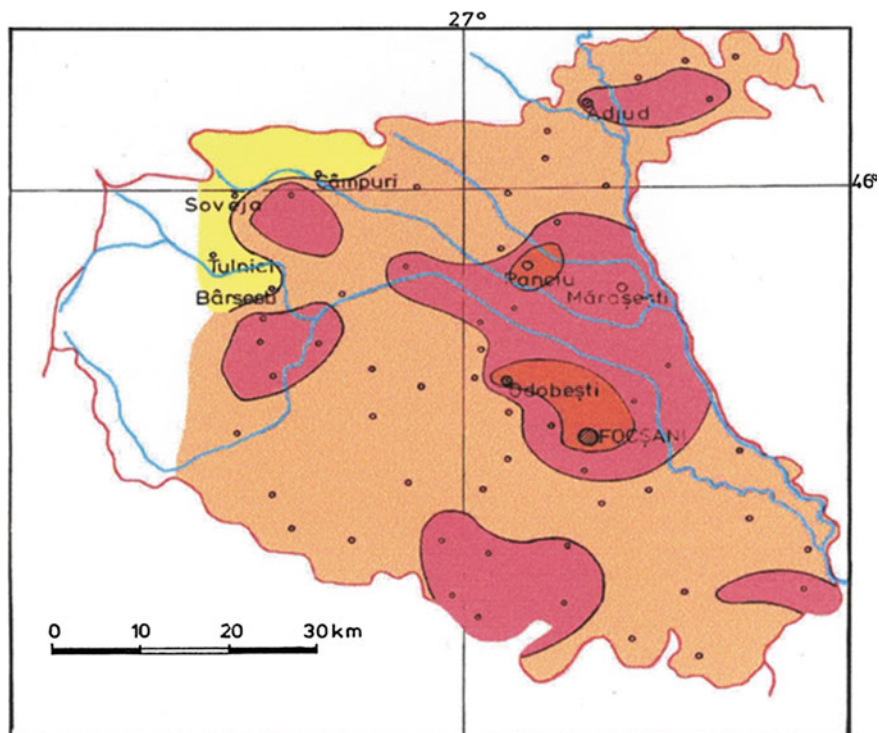


Fig. 5 Distribution of damage degree after large 1940 Vrancea earthquake from Măndrescu et al. (2002). The damage degree factors are: 1 yellow, 2 orange, 3 magenta, 4 red

4 Conclusions

The main objective of this paper is to expand the knowledge on seismicity in a time span as long as possible and in this way to offer an advantage in the analysis of the seismic risk.

The existence of deep earthquakes deeper than Moho discontinuity in the lower lithosphere was concluded by H. Jeffreys in 1935 for the first time in the world.

The earthquake occurred on November 10, 1940 [MW = 7.7; MGR = 7.5; E = 1.122×10^{23} ergs according to Radu (1979)] at 150 km depth demonstrate for the first time the nature of the Vrancea area, with deep earthquakes, since then, the area being classified as an intermediate-depth source. It was seen that these intermediate-depth earthquakes have rather different effects on the tall buildings and free field manifestations from the ones occurring in the crust, everywhere else in Romania and throughout the world.

From historical perspective, the examination of the earthquakes produced in Romania is an operation that proved to be necessary in order to evaluate the risks due to natural hazards.

More than 45 churches and monasteries were damaged, destroyed or demolished in November 10, 1940 earthquake. New data regarding damages at monasteries have been synthesized and analyzed, the resulting intensities are completing the already known macro-seismic field and data will be used to construct the isoseismic map of the maximum possible Vrancea earthquake. Unlike strong earthquakes reported before in the same region the November 10, 1940 event strongly affected Odessa and the northern part of Dobrudja, where most of the monasteries were damaged or destroyed.

The absence of seismic records for the strong earthquake occurred on November 10, 1940 was reflected on the anti-seismic design of buildings, that wasn't conceived until the next large earthquakes struck, on March 4, 1977.

Acknowledgements This work was performed in the frame of the Romanian National Plan for Research, Development and Innovation, PNII, Partnership Program; Project “Bridging the gap between seismology and earthquake engineering. From the seismicity of Romania towards refined implementation of seismic action of European Norm EN 1998-1 in earthquake resistant design of buildings (BIGSEES)”, contract nr. 72/2012–2016. This work was supported also by a grant of the Romanian National Authority for Scientific Research, CNCS—UEFISCDI, project number PN-II-RU-TE-2012-3-0215, and Poseizon project, PN 09-30 03 06.

References

- Atanasiu I (1961) Cutremurele de Pământ din România. Romanian Academy Publishing House, p 194
- Constantinescu L, Enescu D (1985) Cutremurele din Vrancea în cadru științific și tehnologic. Romanian Academy Publishing House, p 230
- Demetrescu G, Iacovshi A (1942) Persistence et isolement du foyer séismique de la région de Vrancea en Roumanie. Observatoire de Bucharest, Station séismique 10 p
- Jeffreys H (1935) Some deep—focus earthquakes. *Geophys Suppl* 3:310–343
- Mândrescu N, Mărmureanu G (2002) Drawing up the seismic hazard map of Vrancea county. Contract nr. 5603/2001 between National Institute of Earth Physics from Bucharest and Vrancea County Council
- Mărmureanu G (2015) Certitudini/incertitudini în evaluarea hazardului și a riscului seismic vrâncean. Romanian Academy Publishing House, 354 p (in press)
- Mărmureanu G, Cioflan CO, Mărmureanu A (2010) Cercetări privind hazardul seismic local (microzonare) a zonei metropolitane București, Tehnopress, 472 p MO (Orodox monasteries): (2010): Nr. 21; 35; 39; 44; 47; 50; 73; 77; 81; 83; 92; 111; 112; 114 and 120. Kapnistos P (ed). D De Agostini Hellas SRL, Atena
- M (Magazin) (from 2010 to 2015): Nr. 44/2010; 13/2011; 31/2011; 46/2011; 4/2012; 7/2012; 13/2012; 27/2012; 31/2012; 26/2012; 17/2014; 31/2012; 33/2012; 44/2012; 24/2015. Stoica I. (ed). Casa Editorială “MAGAZIN”. www.revistamagazin.ro
- MO (Orodox monasteries): (2010) Nr. 21; 35; 39; 44; 47; 50; 73; 77; 81; 83; 92; 111; 112; 114 and 120. Kapnistos P (ed). D De Agostini Hellas SRL, Atena
- Oncescu MC, Marza VI, Rizescu M, Popa M (1999) The Romanian earthquake catalogue between 1984–1997. In: Wenzel F, Lungu D (eds) Contributions from the first international workshop on vrancea earthquakes, Bucharest, Romania, November 1–4, 1997, Kluwer Academic Publishers, pp 43–48

- Radu C (1979) Catalogul cutremurelor puternice produse pe teritoriul României, Partea I—înainte de 1901. Partea II—1901–1979. Cercetări seismologice asupra cutremurului din 4 martie 1977; 723–752, ICEFIZ, București
- Rogozea MM (2011) Caracterizarea seismicității teritoriului românesc în vederea evaluării realiste a hazardului seismic. Ph. D. Thesis, Physics Faculty, University of Bucharest
- Shebalin N (1975) Obotenke seismiceskoi intensivnosti. Seismiceskaia skala I metoda izmerenia seismiceskoi intensivnosti. Izdatelstvo Nauka, pp 87–109

The 10 November 1940—The First Moment of Truth for Modern Constructions in Romania

Radu Petrovici

Abstract The paper presents the technical and legal conditions in which modern constructions in Romania in the decades before the earthquake of 10 November 1940 have built. The expertise of designers and builders and their relations with the legislation, with technical authorities and, not least, with the investors, are shown and commented. The great earthquake by its consequences was the first moment of truth with which has faced Romanian builders, who highlighted the ignorance and negligence in the design and the execution of construction. Based on testimonies and documents of the time recognized specialists, in paper have been identified the main conditions that made the entire building stock built at that time have high seismic vulnerability. Finally, the Paper underline that the consequences of the 10 November 1940 earthquake showed brutally in the earthquake of March 4, 1977, who was the second moment of truth for the world of builders, when materialized, unfortunately, by the collapse of the most 1940 damaged and not rehabilitated buildings.

Keywords Earthquake • Damage • Crash • Technical regulations • Rehabilitation

1 Introduction

The ideas and considerations presented in this paper try to answer of a legitimate question: what are the causes of high seismic vulnerability of buildings built before the 1940 earthquake in Bucharest? The need for an objective response starts from public statements made after the earthquake in 1940 by well-known personalities from the world of builders concerning the absence/lack of information about the seismicity of Romania in the period of rapid development of modern buildings (especially the decade 1930–1940).

R. Petrovici (✉)

“I.Mincu” University of Architecture, and Urbanism, Bucharest, Romania
e-mail: r.petrovici@uauiim.ro

We are primarily quoting the statement of the reputed builder Emil Prager, who writes explicitly in his work (Prager 1979), in the chapter entitled *Reinforced concrete and earthquake*:

Until the earthquake of 1940 that destroyed many lives in 45 seconds, as well as buildings and villages in the Subcarpathian regions, the technical literature lacked sufficient documentation on serious matters of earthquakes in our country.

Equally surprising is the statement of another great builder and professor, Beleş (1941):

Our country was not considered to be a country haunted by earthquakes, the problem of protecting the buildings has not been raised in general and we found ourselves completely surprised before this disaster, lacking not only the remedies, but, we should admit, also the required discernment to assess the gravity and danger of the damages caused and to find technical correction solutions.

Considering the expertness and professional culture of the two leaders of structural engineering in Romania, we have every reason to believe that the allegations regarding the lack of information about earthquakes in our country, invoked after the occurrence of the 1940 earthquake is just a formal excuse addressed especially to the many and uninformed. Moreover, in the booklet (Achim 1941) is mentioned that after the earthquake, to calm the population, “Some people in authority seeks to ensure that it will no longer produce earthquakes with intensity of the last time”. What seems to be still a veiled call to minimize danger and not to invest in seismic protection works.

2 The Well Known Seismic History of the Romania

The seismic history of the Romanian territory is rich in major events. Various means constantly reminded information about the occurrence and manifestations of severe earthquakes. Thus, the chronicler of the fifteenth century Miron Costin (the first to report an earthquake) wrote about the 1471 earthquake occurred in Romania, in Vrancea seismic zone, which caused, among other things, the collapse of the Nebuisei Tower in Suceava. The mention of a severe earthquake, August 1681, is found in “Letopisețul Țării Moldovei” (Chronicle of the Land of Moldova), and many other past earthquakes are recorded in the church chronicles from the Romanian Principalities, from Transylvania and Banat. See, for example, the recent work (Caproșu and Chiaburu 2009).

In the nineteenth century, after the appearance of the print media more descriptions of earthquakes are given. The newspaper “Romania” wrote about the 1838 earthquake “In the evening of 11 January, at a quarter to nine, the earth shaking was preceded by hissing and whizzing, which froze all hearts with fear” The earthquake was also recorded in bilingual newspaper “Albina” which appear in Iași.

Architects, diplomats and foreign travellers recorded the three severe earthquakes (1802, 1829, and 1838). Thus, the effects of the 1838 earthquake on Bucharest were investigated by Arch.-Eng. Achile Thillaye (1807–1874), Romanian official of French origin, who presented a report on the damaged buildings and churches to the authorities and the French consul in Bucharest, Chateaugiron, noted the “disasters caused in this city by this event are huge and cannot be evaluated” (Ștefănescu 1902).

Information about historical earthquakes was published at the beginning of the twentieth century, through the scientific papers by prestigious foreign and Romanian specialists. We mention among these papers the study of Ștefănescu (1902) published in the “Annals of the Romanian Academy” and 2 studies of Hepites (1893, 1908) published in the “Annals of the Romanian Meteorological Institute”. At the same time, in order to make the seismic activity specific to the territory of Romania and neighbouring countries known internationally, Drăghiceanu (1896) published his works at Bucharest in French. Foreign specialists, among which we mention de Martonne (1873–1955) were also aware of the seismicity of Romania and published papers in internationally used languages (Martonne 1902).

In 1901, after the disaster caused by the earthquake in Nobi—Japan (1891) and the preventive measures taken by the Japanese authorities by formation of the Imperial Earthquake Investigation Committee, Hepites (1902) has issued a public warning addressed to builders, recalling the effects of the strong earthquakes that shook our country in the nineteenth century:

In our country, the disasters caused by earthquakes can be avoided, especially if our architects would follow, in constructing buildings and monuments, the advice given by the Seismological Committee of Japan and take into account the earthquakes of 1802, 1829 and 1838 that caused significant damages to the buildings in Romania.

Moreover, at that time, especially at the initiatives and insistences of Șt. Hepites, Romania has obtained significant national achievements and international acknowledgements, such as:

- In 1892, the Romanian Meteorological Institute organized the national observation network of seismic movements. This institute published regularly between 1893–1916 the “Register of earthquakes in Romania”
- In 1900, the Permanent Seismological Committee created at the VII International Congress of Geography, where Romania is member by Șt. Hepites along with representatives of 18 other countries on all continents.
- In 1916, the danger of earthquakes occurring in Romania and potential, disastrous consequences of this phenomenon were the subject of a popularization work (Anestin 1916) written by a nonprofessional, the artist and first SF writer in Romania, Victor Anestin.

The arguments set out above eliminate beyond all doubt the lack of information on seismic hazard as the main cause of the vulnerability of the buildings from that

period. Latter, in the book “Earthquake” (Petrescu 1959) may found the same conclusion:

In our country we do not think there are many people who would say they do not know what an earthquake ... our country is shaken often by earthquakes.

3 Early Worldwide and National Concerns and Achievements in Seismology and Reinforced Concrete

Another cause of building vulnerability in Romania is the ignorance of technical regulations in construction that began to emerge in several countries.

In the early twentieth century, multi-storied buildings began to develop in all European countries, encouraging the widespread use of reinforced concrete as the main building material in place of masonry. In Romania, theoretical studies, teaching and practical applications about the use of this new material appeared virtually simultaneously with the rest of Europe:

- The first mention about concrete (called also molos-ancient spelling of Romanian word “moloz”, “rubble” in English) appeared in 1888 in the work “Architecture and construction practice” (Nițescu 1888)—Fig. 1a, b.
- In 1903, Professor Engineer Ion Ionescu-Bizeț taught the first university course (one lesson!) (Reinforced concrete calculation method after Mathias Koenen).
- In 1904, PhD Prof. Eng. Fritz von Emperger (Vienna) replaced at the Brancovan Hospital the wooden floors with reinforced concrete floors.
- In 1906, Eng. Anghel Saligny—Fig. 1c—built in the seaport of Constanța silos made of precast reinforced concrete, which is a world first in the field.

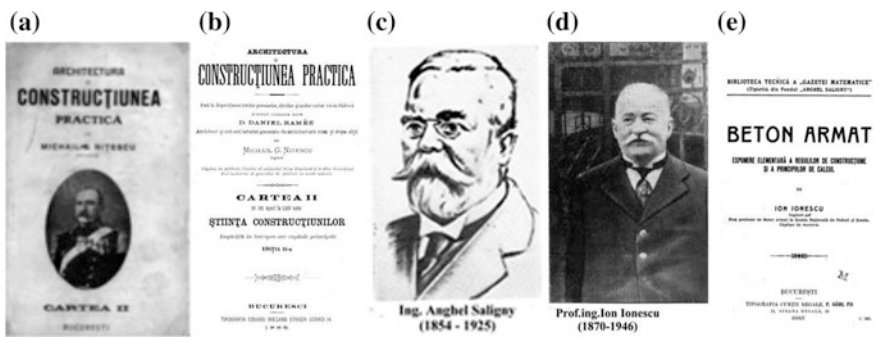


Fig. 1 The beginnings of reinforced concrete in Romania

- In 1915, Prof. Eng. Ion Ionescu-Bizeț—Fig. 1d, e published the first book (Ionescu 1915) about reinforced concrete, 218 pages.

To ensure a coherent approach in order to achieve the required safety, the regulations of the use of reinforced concrete were emerging in Europe, in the first decade of the twentieth century: Switzerland (1903), Germany (1904), France (1906), Russia (1908), Hungary (1909), and Austria (1911). Because these countries are non-seismic, those rules had no provisions for seismic design. Neither subsequent circulars of these countries (1920–1924) presented in Ionescu (1915) did not have references to seismic action.

Almost simultaneously, due to the occurrence of destructive earthquakes in several countries, the first regulations on seismic design appeared:

- After the earthquake in San Francisco—USA (1906) the height of buildings was limited (this regulations remained in force until 1957): Los Angeles: 150 ft \approx 45.0 m (13 stories) and San Francisco: 80 ft \approx 25.0 m or 100 ft \approx 31.0 m.
- In Europe, after the earthquake in Messina—Italy (1908) the first modern regulation of seismic analysis appeared in Europe.
- Later, after the Great Kanto earthquake—Japan (1923)—it was established to limit the building height to 100 ft \approx 31.0 m—which remained in force until 1964.

These regulations also state the obligation of drawing up static calculations with conventional seismic forces and dimensioning the reinforced concrete structures for stresses resulting from calculations.

In the interwar time, in Romania, although the use of reinforced concrete was increasingly widespread, none of the technical regulations adopted in the other countries did receive any official recognition (becoming mandatory). Only in 1927, it was published in Romania, out of private initiative, at the Engineers' (Cotroceni) Print Shop, the translation of the German standards of 1925, drawn up by Chief Engineer Radu M., professor at the Polytechnic School. This one has followed by the translation of the 1932 edition prepared by engineer M.D. Hangan, who was to become the great professor of my generation. The use in the design of the two regulations was not compulsory. Meanwhile, books and magazines for information on and promotion of reinforced concrete appear as soon as 1925, again out of private initiatives—see Fig. 2c, d.

In the *Arhitectura* magazine, since 1926, is mentioned the lack of regulations and control of state authorities in buildings design (Cegăneanu 1926). In the paper “1926”, the author, formulates a number of proposals for improving the efficiency of practical work of architects and designing engineers, among which we mention a clarification of particular significance for this paper:

In the first line, we should ask for the introduction in the common rules of buildings of the obligation to submit for the (building) permit complete execution projects, accompanied by static calculations, prior measurement of quantity and cost estimate. This way protect the builders and those who are unreliable will be forced to seriousness.



Fig. 2 a and b Translations of German reinforced concrete rules; c and d Journals for inform and popularize the use of concrete

This appeal of a leading architect of the time, who was the chairperson of the “Romanian Society of Architects” in 1925, came because of finding a deliberate ignorance, as a rule, of the contribution of structural engineers in designing buildings. This signal that appeared even before the “booming” era of multi-storey buildings largely explains the lack of architectural and structural rigour and under-sizing identified in these buildings at the earthquakes in 1940 and 1977.

As regards the state control in the field of design and execution, also ignored, the Design Standards of the German Committee for Reinforced Concrete (1925)—Fig. 2a, contained essential provisions to ensure construction quality:

The new standards, based on numerous experiences and due to the participation of eminent experts in this specialty, are approved architectural rules in this specialty and are mandatory. The police authority will watch in this regard on the examinations of applications for a building permit... The police authority shall be thoroughly observing the application of these requirements during the execution of works, too.

Because these provisions were not adopted in the national technical legislation in Romania, disorder and numerous private interests continued to dominate the design of buildings of all kinds. We find, for example, that despite the possible negative consequences, the official Specifications for cement strength had requirements (16 MPa at 28 days) far below those of the German standards (35 MPa at 28 days). Corroborating these reduced requirements with the lack of control over execution, particularly in terms of quality of the aggregates and cement dosage, statistics show that in the decade 1930–1940 the concrete strengths reached a “historical” minimum (Fig. 3).

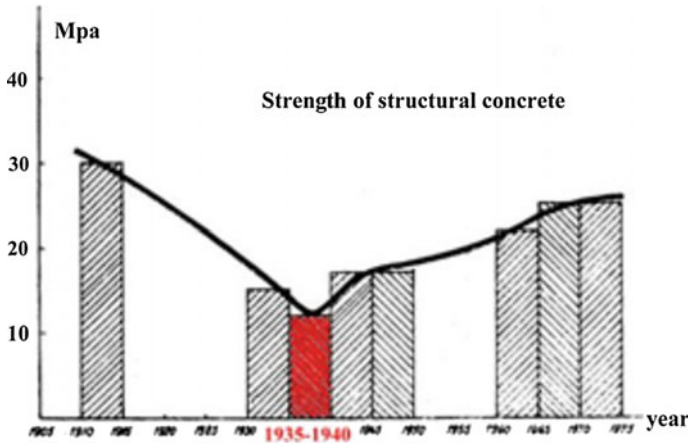


Fig. 3 Evolution of concrete resistance between 1910 and 1975 (Bălan et al. 1982)

4 Main Aspects of Architectural and Structural Building Design in Romania Prior 1940 Earthquake

In the period between the two World War appeared in the community of building designers, increasingly more present and insistent, the idea that the organization of spaces and volumes is justified only by architectural reasons that should prevail over the logical arguments of structural engineering, which were deemed to hinder the creative freedom (Siegel 1968). In their turn, these “architectural reasons” were, in fact, the “architect’s vanity” and “investor’s requests” dominated by the obsessive tendency to reduce investment costs and meeting various outdoor image whims of architects or interior design of future owners.

Due to a questionable requirement of “modernization”, the phenomenon of migration of architectural styles appeared simultaneously. This phenomenon can only be controversial in socio-cultural terms, if the *original* area and the *adoption* area have similar environmental characteristics (particularly close levels of *seismicity*) (Petrovici 1999). However, the migration of styles can have serious consequences, if the seismic effects become “critical” in the adoption area for certain architectural compositions and, especially, for those structures. We recall the serious consequences arising from the takeover of the English architecture (from the Victorian era) in California (Seismic Safety Commission of California 1987) and French architecture (especially the principles of Le Corbusier) in Maghreb (Wang 1981).

In Romania, the same consequences manifested brutally with the most severe damages, due to the takeover without discernment of architectural compositions specific to non-seismic countries. One can easily find in the Bucharest buildings represented in Fig. 4, the random composition of structures depending on the possibilities resulting from the architecture plan and the practical impossibility to

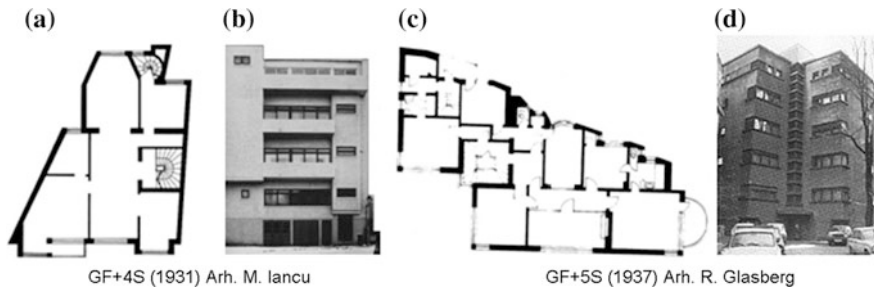


Fig. 4 “Modern” buildings without geometric and structural regularity (Ion and Székely 2003)

implement reasonable interventions for consolidation. In addition, such examples could continue.

We add that the so-called “modernity” consists, in fact, only in visual effects, given by the choice as audacious/unusual volumes and of the facades images. In these conditions have resulted confusing structures, random, with serious technical compromises in terms of resistance to earthquake, solutions accepted by incompetence of the engineers (the team that designed Carlton Building studied engineering in Vienna, where, most likely, the word “*erdbeben* \equiv earthquake” has never been pronounced) or by superficiality.

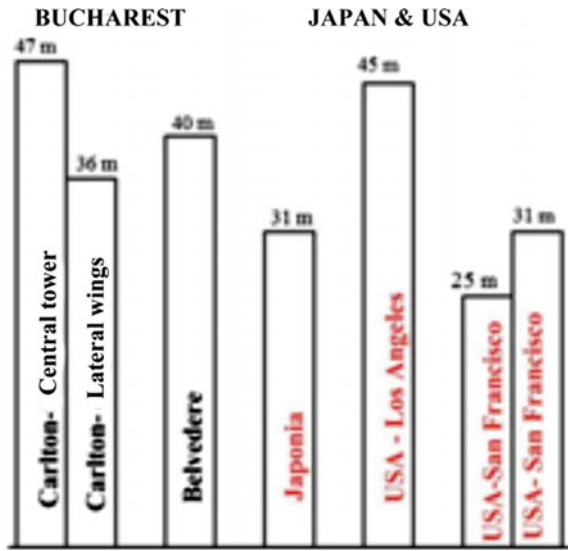
The city witnessed plenty of buildings with facades in console (bowwindow), that have proven to be among the most vulnerable areas of buildings. Masonry exterior walls are mostly designed as “double-walled hollow”—cavity wall) with total thickness of 28 cm. For formal accuracy of the wall, columns have almost in all cases the thickness of 28 cm and resulted elongated or rectangular-shaped corners L. Partition walls, some of them serving as a support floor, are thin and slender (thickness 7.0 or 14.0 cm) and virtually unable to participate at the seismic energy dissipation.

Escalating barriers for height established in the USA and Japan and no obligation for seismic analysis were some of the primary causes that generated the seismic vulnerability of buildings in the capital. In Bucharest, these barriers have been overcome and generous in conjunction with architectural and structural embodiments inadequate for seismic areas have generated spectacular crashes (Fig. 5).

Urban planning that provide high building at intersections and corners favored exceeding the height limits set in other countries. From this provision has resulted implantation of a large number of tall L-shaped buildings in downtown (two perpendicular streets) with a tower at corner. Regarding the observance of Bucharest City Planning, quoting a comment from (Cegăneanu 1926):

Usually the current regulation that sets the height at cornices depending on the street width is bypassed by the approvals of the so-called special committee, which finds reasons for any application addressed to it with sufficient insistences.

Fig. 5 Comparison between heights of Bucharest tallest buildings and the limits permitted in other countries



Regarding the lack of control of the authorities, we bring in the following eloquent information from Bălan et al. (1982): The Belvedere Building built in 1937–1938, it withstood the 1940 earthquake with serious damage and without any consolidation measures, and it collapsed in 1977. The initial project provided for 10 storeys and subsequently obtained authorization for 11 storeys. Finally were executed 13 storeys without obtaining a new permit.

We note also arrests and convictions under existing laws in that period of the project’s chief architect (the well-known architect G.M. Cantacuzino) and of one of the builders. Two booklets written by Achim (1941, 1943) present in detail the causes for the collapse of Carlton building and the arguments of the defence. These booklets contain also more information about the design and execution of structures in the interwar period (Figs. 6b, c and 7).

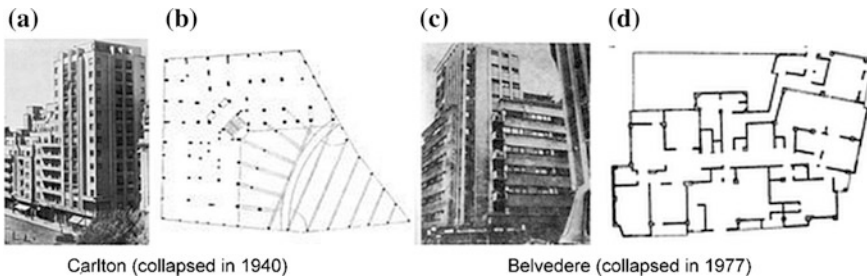


Fig. 6 Two buildings “martyr” together with their tenants

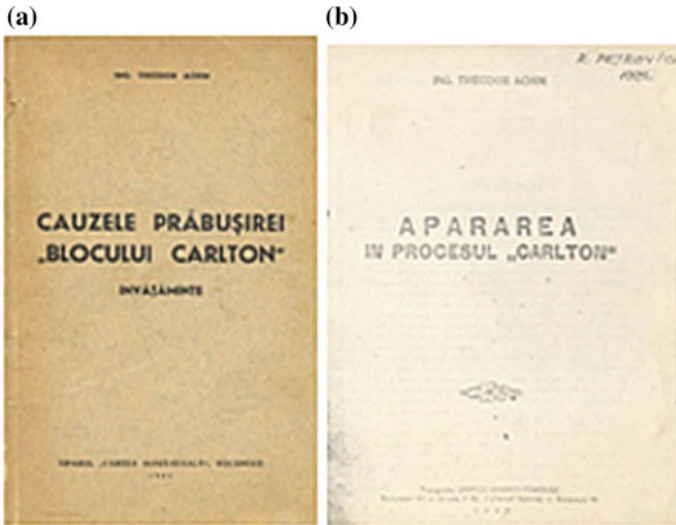


Fig. 7 Two booklets published after the collapse of Carlton building: **a** causes of the Carlton Building collapse; **b** defense in the event of Carlton building collapse

Another cause that favored collapse of Carlton Building and severely damaged other buildings that fell in 1977 is that, in many cases, were not respected neither the limits of design values for gravity load (e.g., the German circulars). The effective compression stresses in columns ($5\text{--}6\text{ N/mm}^2$) greatly exceeded, in some cases even twice, the allowable values for current concrete of those years ($3\text{--}4\text{ N/mm}^2$). We note that the exceedances of allowable values refer to concrete resistance provided for in projects. In reality, the actual exceedances were much higher, if we consider that the actual strength is under specified values in many cases, as shown by tests.

5 The Real Causes of Seismic Vulnerability of “Modern” Buildings in Bucharest (Little Paris)

The earthquake of 1940 was the first confrontation of modern buildings with reinforced concrete skeleton of Romania, with a severe earthquake, confrontation that revealed the hidden weaknesses of the existing building stock, which came from the incompetence and the dishonesty of the builders and investors. This is the reason why we called the date of 10 November 1940 the first moment of truth for modern constructions in Romania.

After the 1940 earthquake, two prominent builders of that time, touched a painful wound: “the architectural and structural design and execution of buildings were inadequate to the seismic areas”.

Thus, trying to identify, immediate and objective, the causes that led to this situation, an architect, Victor Asquini, and an engineer, Aurel A. Beleş, the same who said that Romania is a country without seismic risk, intervened in 1941, each with the arguments of his profession. In paper (Asquini 1941), V Asquini identifies factors that are more responsible:

- First, the investors:

The earthquake of the night of 10 November will make many owners start thinking, who were choosing cheap materials when building, thus making some savings to that what could give more safety in the strength of the building; it will make them think twice before choosing the first builder that appears, just because it was cheaper.

- Then, the builders:

Many builders will be more careful from now on in conducting their works, more cautious in speculating the material they are using.

- And, lastly, the designers (only architects are nominated by the author, but engineers should join them, because they had a significant negative contribution to deficiencies of these buildings):

Architects, in their turn, will be more vigilant and more severe with contractors; they will supervise the different parts of the work more closely. Moreover, they will not trample their conscience and will, giving up to the owner's reasons of savings and thus allowing the later to have a less robust building, that could cost too expensive under unforeseen circumstances due to this monetary restriction.

After listing the main damages found after the earthquake, especially at non-structural construction parts, architect V. Asquini formulates a rough conclusion:

The earthquake has proven to us that we were accustomed to build more quantitatively than qualitatively, that most buildings were erected only in the worship of money, without reliability, unscrupulous; buildings constructed for a short period of years, lasting as long as the fashion. Most buildings constructed in recent years, even the largest, only shows us an era without art, of an elastic morality, and their strength was calculated just for their standing, without the unexpected coefficient arising anytime out of certain events, or caused by mysterious and unpredictable forces of nature; almost all new buildings containing the stigma of "speed drunkenness".

With more precise, but equally rough engineering formulations before the actual effects of the earthquake, A.A. Beleş makes in the work (Beleş 1941) the first post-earthquake field investigation in Romania (Fig. 8).

On this occasion, the author identified with great accuracy the badly damaged buildings whose natural strength resources practically exhausted by the severe stresses for which they not designed. The collapse of most of these buildings in 1977 confirmed the correctness of those assessments. This catastrophe was the second moment of truth showing, without a doubt, the weaknesses of these buildings in the case of repeated earthquakes, especially in the absence of serious rehabilitation works. Maintaining in service of this buildings without works for risk reduction (a situation to which authorities and specialists assists with much

Fig. 8 Book “Cutremurul și construcțiile” (1941)



indifference) can lead us to the next severely earthquake predicted by seismologists to third moment of truth that can be more disastrous than the other two, together.

The main cause of the extensive damage observed, as a first finding, is the effects of the unusual height of buildings:

For the same material and the same execution, the buildings will behave much worse as the height will be higher.

Other serious errors of the concrete skeleton were identified in the work (Beleş 1941), which were found in most of the severely damaged buildings. These systematic mistakes from the incompetence and/or superficiality of some designers, who applied inadequate constructive solutions indiscriminately, but frequently used at that time:

- The use of columns with irrational sections: in “L”-shapes and with thicknesses of 20–24 cm and lengths of 1.20–1.70 m. These columns supported too large loads for the strengths of the concretes available at that time (180–235 tons).
- A bad solution, often encountered, is the lack of vertical continuity of columns. Some columns stopped on a certain level and they continue on the upper floors, in other positions, supported by beams.

In view of this last observation, vertical structures of these buildings are not frames with rigid connections (joints), in the current meaning of the term. They are

only an assembly (skeleton) *of* beams and columns with random connections and cannot be calculated with contemporary programs in the elastic range, and much less in the inelastic range.

With regard to this type of errors, the author intends to specify their origin:

Especially the two fundamental errors that affected the columns, errors due to the mercantile architectural concept affecting so many of our buildings, made this building (author's note: Carlton building) to be very sensitive to earthquake.

Regarding the actual conditions for the design and execution of buildings, this study [Beleş 1941] also provides eloquent considerations:

Nevertheless, the technical solution (author's note: for seismic protection) must be economic and consistent with the financial resources at our disposal, with the available materials and, finally, the workers we can find. Often, these latter three considerations take precedence over the technical one, although the most important is often the most difficult to achieve in practice.

In his conclusion, the author makes a very important clarification (perhaps the most important!) for knowing the actual design conditions:

„...ultimately, we still need to add the difficulty of finding capable and especially honest designers to study and give an adequate solution”

With regard to the foregoing, I propose to recall a conclusion drawn long time ago by a great professional in earthquake engineering, Kiyoshi Muto cited in many works, for example in Beedle (1972) and Petrovici (1975): *“The return period of severe earthquakes in a region is sometimes so long that economic considerations are stronger than the painful lessons of the past and thus disasters repeat themselves”*.

Indifference and lack of involvement of many experts favoured between the two wars the proliferation in designing and executing in Bucharest of a significant number of seismically vulnerable buildings. The decrease of their seismic risk is a material and moral burden, borne entirely by the contemporary generations.

6 Instead of Conclusions

Furthermore, we must insistently highlight another conclusion: the 1977 earthquake demonstrated, if needed (?), the obvious fact that in the absence of efficient consolidation works the buildings with no initial seismic protection or with an insufficient protection collapsed or, if they survived, they have now a high risk of collapse. This earthquake was thus the second moment of truth for Romanian builders. In this context we also emphasize that intervention works executed in interwar buildings, but also in many newer buildings immediately after the earthquake (in order to bring the building to its initial state) provide, in most cases, a deceitful safety (Petrovici 2007).

Table 1 Building sectors with heavy damage (reinforced concrete shear walls structures). Notations for the degrees of damage “D” are: D = 3–4 major damages, D = 4–5 widespread damages (near collapse)

Nr. sectors	Name of project type				Total
	R	OD	M ₁ F ₈	M ₁ F ₄	
	112	167	235	91	605
Σ Damages	24 tr.	23 tr.	25 tr.	21 tr.	93 tr.
D = 3–5	2140 apt.	980 apt.	1150 apt.	920 apt.	5190 apt.
	21.4 %	13.8 %	10.6 %	23.0 %	16.3 %

Currently, obtaining the minimum safety for a large number of buildings, even aiming only at avoiding the collapse and massive loss of human lives, requires time and very high material efforts, which is why it is possible to not be achieved entirely, or at least on a large scale before the next severe earthquake predicted by seismologists. However, learning from the experiences presented in this paper should not forget that many of the buildings constructed before 1977 earthquake are heavily damaged and have not been strengthening. Therefore it is possible that the next earthquake these buildings to produce extensive damage.

To illustrate the effects of the 1977 earthquake on tall buildings (GF + 10S) with structural walls of reinforced concrete, in Bucharest, which had breakdowns Grade D = 3 through 5 (with D = 5 have noted cases of collapse), we reproduce following Table 1 from Petrovici (2007).

The total percentage of about 15 % of total building sections with significant damage, it is alarming and infirm, for the most part, the enthusiasm of those who have counted only three collapsed buildings built after 1945. Without consolidation works, these buildings have a high probability of serious damage/collapse. The existence of the damage in question represent a permanent threat for those residents lives and reducing the vulnerability of these buildings, as those built before 1940, it is a moral duty of the whole society. For this reason, the future severe earthquake may be the third moment of truth.

Acknowledgements The author wishes to emphasize the contribution in the elaboration of this essay of the extensive research conducted by his former students Arch. Ion, P. and Arch. Székely, G. for the final paper at the course of advanced studies “Rehabilitation of buildings” UAUM (“Ion Mincu” University of Architecture and Urbanism of Bucharest), 2003.

References

- Achim T (1941) Cauzele prăbușirii “Blocului Carlton”—învățăminte București, Ed. “Cartea românească”
- Achim T (1943) Defense in the event of Carlton building collapse, Bucharest
- Anestin V (1916) Cutremurele de pământ. Cutremurele din România, Câmpina
- Asquini V (1941) Cutremurul factor de progres, Rev Arhitectura nr.2

- Bălan S, Cristescu V, și Cornea I (coordonatori) (1982) Cutremurul de pământ din România de la 4 martie 1977. Editura Academiei, București
- Beedle L (1972) Introduction. Avant-propos. Congrès International sur les immeubles de grande hauteur, Univ. of Lehigh
- Beleş AA (1941) Cutremurul și construcțiile Buletinul Societății Politehnice, București, Nr.10 și 11, Octombrie și Noiembrie
- Caproșu I, Chiaburu E (2009) Însemnări de pe manuscrise și cărți vechi din Țara Moldovei (vol I, 1429–1750; vol II, 1751–1795; vol III, 1796–1828; vol IV, 1829–1859), editat de Ioan Caproșu și Elena Chiaburu, și la Casa Editorială Demiurg, Iași
- Cegăneanu S (1926) Revista ARHITECTURA, vol V
- Drăghiceanu M (1896) Les tremblements de terre de la Roumanie et des pays environnants, București
- Hepites S (1902) Cutremurele de pământ din România în anul 1901 st.n Analele Academiei Române
- Hepites S (1908–1916) Registrul cutremurelor de pământ din România (1893–1916) Analele Institutului Meteorologic Român. București
- Hepites S (1893) Registrul cutremurelor de pământ din România (1838–1892) Analele Institutului Meteorologic Român. București
- Ion P, Székely G (2003) Reabilitarea clădirilor multietajate încadrate în clasa I de risc seismic din București. Studii aprofundate “Reabilitarea clădirilor” UAUM
- Ionescu I (1915) Reinforced concrete (in Romanian *Beton armat*) București Ed. Tehnică a “Gazetei Matematice”
- Ionescu I (1925) Reinforced concrete (in Romanian *Beton armat*) București Ed. Tehnică a “Gazetei Matematice”
- Martonne E de (1902) Valachie Essai de monographie géographique. Paris
- Nițescu, M (1888) Arhitectura și construcțiunea practică. București
- Petrescu G (1959) Cutremure de pământ. București, Editura Tehnică
- Petrovici R (1975) Théorie des structures pour les Architectes; Alger, Algérie, Editions EPAU
- Petrovici R (1999) *Unele considerații privind relația dintre concepția arhitecturală și răspunsul seismic al clădirilor*. Simpozion Academia Română- UTCB în memoria prof.M.Hangan
- Petrovici R (2007) Protecția localităților împotriva riscurilor naturale și antropice Ed. Universitară “I.Mincu”, București
- Prager E (1979) Betonul armat în România, București, Ed. Tehnică
- Seismic Safety Commission (1987) Guidebook to Identify and Mitigate Seismic Hazards in Buildings. State of California Report No. SSC 87i03, December
- Siegel C (1968) Forme structurale ale arhitecturii moderne. Editura Tehnica București
- Ștefănescu G (1902) Cutremurele de pământ din România în timp de 1391 de ani, de la 455 până la 1874, Analele Academiei Române
- Wang M (1981) Stylistic Dogma vs Seismic Resistance. The contribution of modernist to an Algerian disaster. AIA Journal

Macroseismic Effect of the November 10, 1940 Earthquake in the Territory of Moldova, Ukraine and Russia

Nila Stepanenco and Vladlen Cardanet

Abstract The November 10, 1940 Vrancea earthquake—a remarkable seismic event in the recent history of Eastern Europe. Over the past 200 years, it was the strongest of all that occurred in the Vrancea focal zone. Macroseismic manifestation of the November 10, 1940 earthquake is of great interest, based on the possibility of a repetition of such events in the first half of the 21 century. The collected data about the earthquake November 10, 1940 proved to be very useful in seismic hazard assessment in South-Eastern Europe. This devastating event served also as a pretext to organize systematic seismological observations in the Carpathian region. 75 years have passed since the event happened, but so far, no complete study has been conducted within the East-European Platform. In the present work, we collected and analyzed anew all available macroseismic data to the northeast of the epicenter, up to the limits of the event manifestation. As a result of analysis and generalization of macroseismic information contained in the special literature, the new table with intensity values for the territory of Moldova, Ukraine and Russia was made, and the isoseismal map of this earthquake was drawn. The macroseismic effect for the Eastern Europe was compared with January 23, 1838, March 4, 1977, August 30, 1986 and May 30, 1990 earthquakes. The comparison of the intensity areas for the strongest earthquakes of the Vrancea region was performed.

Keywords Vrancea · Isoseismal map · Focal mechanism · Intensity attenuation

N. Stepanenco (✉) · V. Cardanet
Laboratory of Seismology, Institute of Geology and Seismology of ASM,
Chisinau, Republic of Moldova
e-mail: seismolab@rambler.ru

V. Cardanet
e-mail: seismolab@rambler.ru

1 Introduction

At the present, it is necessary to obtain valid and reliable estimates of seismic manifestations of strongest Carpathian earthquakes in Republic of Moldova and on the territory of neighboring states. That would serve as the basis for solving problems of a quantitative assessment of seismic hazard, updating seismic zoning maps, as well as determining the safety of especially important objects and structures.

Main seismic impact on the territory of the Republic of Moldova is caused by the earthquakes of Vrancea seismic zone. According to the seismic zoning map in the southwestern part of the country intensity reaches 8 of MSK-64 scale.

In this connection, macroseismic manifestation of the November 10, 1940 earthquake is of great interest, based on the possibility of a repetition of such events in the first half of the 21 century.

The work on the macroseismic assessment of earthquake November 10, 1940 was carried out in the research process on the determining of seismic hazard and seismic risk in Republic of Moldova (Drumea et al. 2009; Stepanenco et al. 2006; Stepanenco 2011).

75 years have passed since the event happened, but so far, no complete study has been conducted within the East-European Platform. In the present work, we collected and analyzed anew all macroseismic data available from the papers of previous researches of the November 10, 1940 earthquake. In the end, we have made the new, most complete isoseismal map for the northeast sector from the epicenter up to the limits of the event's manifestation. Main used works are reports, articles, archives, memories of eyewitnesses.

The November 10, 1940 Carpathian subcrustal earthquake—a remarkable seismic event in the recent history of Eastern Europe. Over the past 200 years, it was the strongest of all that occurred in the Vrancea focal zone.

The collected data about the earthquake November 10, 1940 proved to be very useful in seismic hazard assessment in South-Eastern Europe. This devastating event served also as a pretext to organize systematic seismological observations in the Carpathian region. The war of 1941–1945 interfered with plans of organizing the Carpathian seismic stations network proposed by the Commission for the examination of the earthquake effects. Only in 1948, the plan for the development of such a network was launched.

It is known, that during the earthquake of 1940, as with other strong earthquakes of the 20th century: March 4, 1977, August 30, 1986 and May 30, 1990, the seismic waves propagated far along the East European platform (Drumea 1980; Drumea et al. 1990, 1996; Radu et al. 1979).

The earthquake caused severe destructions of many settlements in Romania, significant damage to buildings and structures in Bulgaria. Within the USSR territory, the earthquake with a maximum intensity manifested in Republic of Moldova and southwestern regions of Ukraine.

2 Macroseismic Data and Isoseismal Maps

For the territory of Romania, the vast macroseismic data were collected, used for drawing isoseismal maps. As a result of the population survey there were thousands of written testimonies of the earthquake eyewitnesses received; the intensity in more than 200 settlements defined; dozens of papers published; the isoseismal map of the Romanian territory drawn (Fig. 1) (Atanasiu 1961; Demetrescu and Petrescu 1941; Mandrescu et al. 1988; Pantea and Constantin 2011).

For the territory of Republic of Moldova and neighboring regions of Ukraine, primary materials and photographs made in many settlements were perished, due to the war of 1941–1945. However, after the war a part of information was restored.

November 21, the government of the Moldavian SSR reported the final data of the consequences of the November 10, 1940 earthquake. There were 17 people

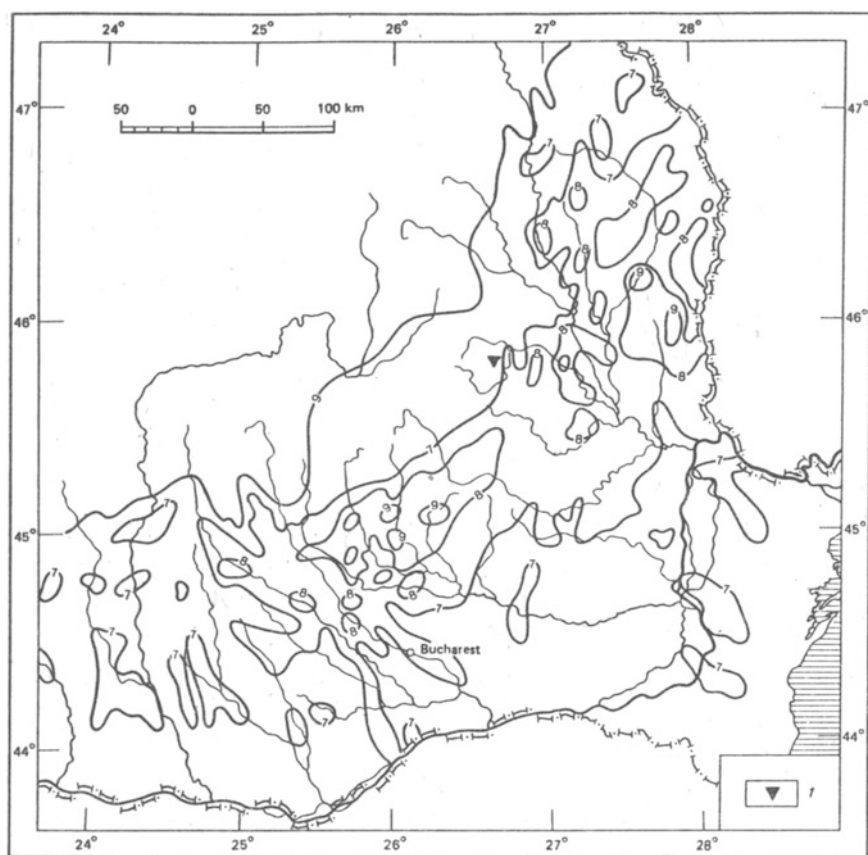


Fig. 1 Intensity distribution of the November 10, 1940 earthquake in Romania (Mandrescu et al. 1988). 1—Earthquake epicenter

killed and died of severe wounds, 66 seriously injured, 546 lightly wounded people. In Republic of Moldova, it turned out to be the most affected Cahul county (207 buildings completely destroyed and 1981 damaged), followed by Chisinau county (136 and 1904 buildings). Even in Tiraspol, there were three totally destroyed and 275 damaged buildings.

In Chisinau, according to research, the number of damaged buildings were 2795. The distribution of the degree of damage was as follows: buildings damaged completely—172, to be completely overhauled—501, to be seriously overhauled—625, to be repaired—1496 (Sukhov 1960).

On the territory of the Moldavian SSR this earthquake was carefully studied and described by the created in 1941, the Special Commission of the Geophysical Institute of the USSR, led by Professor V.O. Tsshokher. The main work carried out in Chisinau. Also the expedition took place along the route Chisinau–Hancesti–Leuseni–Vishnevka–Comrat–Cimislia–Bacioi (Tsshokher et al. 1941).

It had been studied in detail seven localities in the central part of the Republic of Moldova. It should be noted that in the Central Codri visited by the Commission, many peasant houses were built of logs dug into the ground, braided with vines and smeared with clay. In Chisinau, the tsarist government after the devastating earthquake of January 23, 1838 prohibited to build houses higher than two floors. These restrictions existed until 1940.

In Chisinau, it started about 4 h and 40 min (Moscow time) with a very strong tremor, from which all city residents awake. After a brief lull, when some people managed to run outside, the ground under the feet began to move. Many fell down, as it was difficult to stay on the feet. Trees swayed as from a severe storm. The branches up to 4 cm thick broke. Across the city, the flashes of electric light were observed because of the contact of the wire overhead lines. Numerous pillars were knocked down to the ground. The radio mast height of 60 m made huge arcs with red signal lamps against the dark night sky. In the churches bells rang themselves. It was completely destroyed 200 buildings. An even greater number of them were seriously damaged.

Among the damaged buildings should especially mention the Agricultural Institute, the museum of local lore, the Supreme Soviet of the MSSR, distillery, the People's Commissariat, Pedagogical Institute (collapsed pediments, tumbled walls, frustrated furnace, fallen chimneys). No intact factory chimney remained in the city. The churches had quite large cracks. The Dome got very serious damages. Church of the Ascension was so damaged that it was forbidden to serve there, the cross on the dome fell. The services in the Ryshkanovka church were stopped as well. Stone walls overturned; stone gate pillars in many places were destroyed and turned around a vertical axis. At the cemetery, numerous monuments were dumped and overturned. The tank water tower at the corner of Fountain and Kotovsky streets, weighing 952 tons, full of water, was shifted by 3.5 cm.

In the surrounding neighborhood of Chisinau, in Dicescu and near Costiujeni hospital significant portions of the surface of the earth were slumping. In the city, cracks in dry soil up to 5 cm width and 6 m length were marked. The Museum of local lore was damaged (irrevocably lost about 40 % of the most valuable exhibits). It was heard the ringing of bells near almost all the churches of the city (Sukhov 1960).

Under the ruins of houses, crumbled gables and stone fences were killed and mutilated a large number of people.

Fear of the earthquake was so great that people lived on the second and third floors jumped out of the windows and were seriously injured.

Similar damages were observed in other localities of the Moldavian SSR.

Southwestern regions of Ukraine suffered heavy material damage. In Izmail very strong vibrations felt, doors skewed, heavy objects overturned. In the hotel and several other buildings chimneys, ceilings and walls collapsed. The cross fell from the bell tower. The population of Odessa ran outside, the houses were damaged. The main wall of the hotel “Moscow” had a crack. Ceilings and walls of the hotel “Passage” were damaged. At the train station the train moved spontaneously (Evseyev 1961; Sagalova 1969).

In the village of Sarata, Odessa region chimneys tumbled. Some houses were damaged. The church had a crack in a finger-thick (Sukhov 1960).

In Kiev, people woke up. It was marked clatter of dishes, swinging items, crackle of parquet. The tremors were felt particularly in high buildings (Evseyev 1961; Sagalova 1969).

For the territory of Ukraine it was made up a new map of the November 10 earthquake which contains 57 items, in 13 of them the intensity was determined for the first time (Fig. 2) (Korolev et al. 2011).

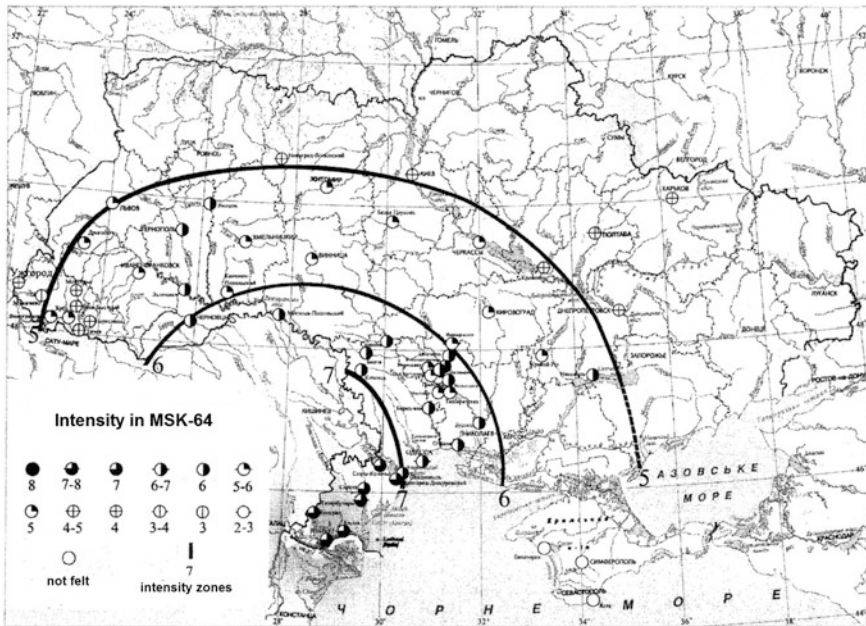


Fig. 2 Intensity distribution of the November 10, 1940 earthquake in Ukraine (Korolev et al. 2011)

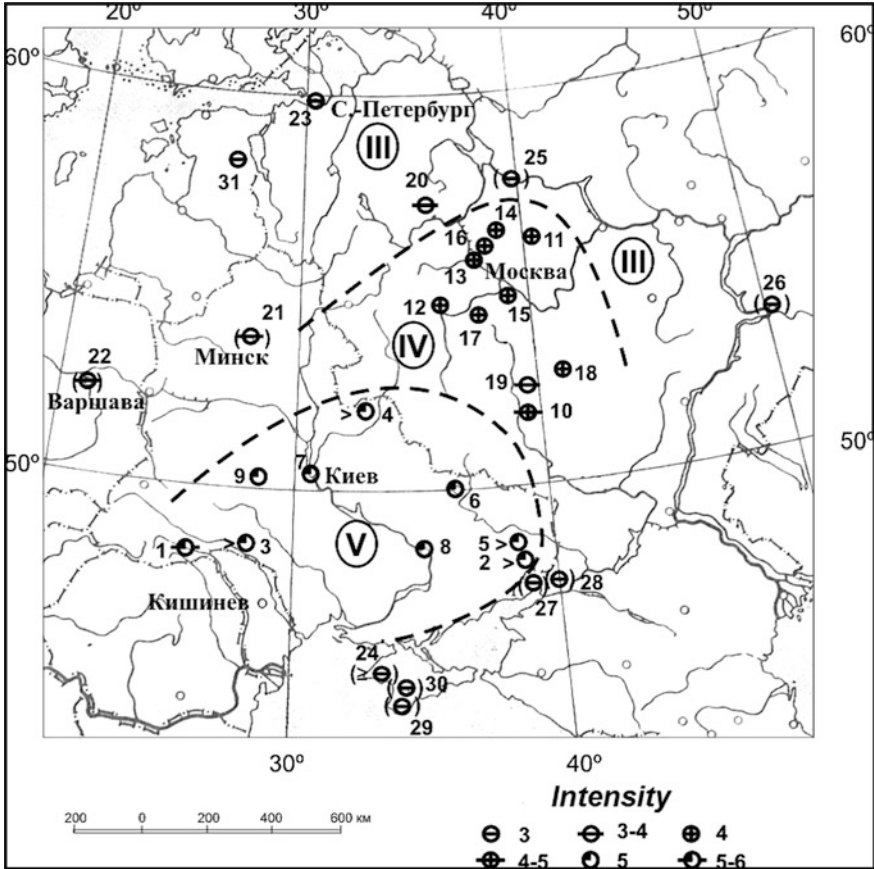


Fig. 3 Intensity distribution of the November 10, 1940 earthquake for the East European platform (Nikonov et al. 2010)

In Moscow, the power of shaking reached intensity 4, that it is a rarity for Moscow. There were swing of hanging lamps, the clatter of dishes, excitement of birds in cages, swing of furniture, stopped the pendulum clock. The Seismological Institute of the USSR, Academy of Sciences received more than three hundred messages about observed signs of the earthquake (Shebalin 1977).

The earthquake was felt in the Crimea (Yalta, Simferopol, Evpatoria and along the coast of the Black Sea).

Weak tremors were observed in Leningrad, Yaroslavl, Vladimir, Rostov-on-Don and Taganrog (Fig. 3) (Nikonov et al. 2010).

Experts from many countries gathered the intensity data of the earthquake and they are available in many sources. In their work Romanian and Russian seismologists Radu, Bune and Polyakova (Bune et al. 1986) summarized the available data and made an isoseismal map in isolines of intensity 5–9 (Fig. 4). Authors

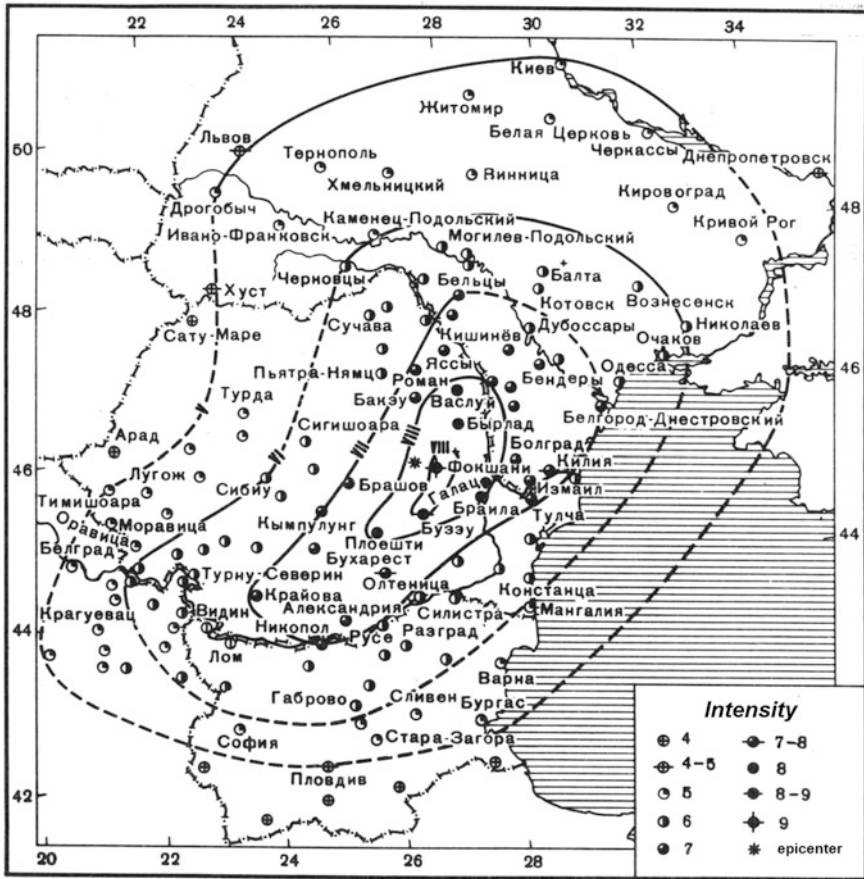


Fig. 4 Intensity distribution of the November 10, 1940 earthquake in the South-East Europe (Bune et al. 1986)

specified data, calculated the predominant macroseismic effect for big cities. We used their map for the territory of Romania.

For creating our general isoseismal map of the November 10, 1940 earthquake we reviewed the available data for the northeastern sector of the region, where the earthquake was felt. Intensity tables were compiled in terms of the MSK-64 scale for the territory of Republic of Moldova (54 points), Ukraine (56 points), Russia and East Europe (23 points). They served as a basis for plotting isoseismal map of Moldova, Ukraine and Russia territories (Fig. 5).

The isoseismal map (Fig. 5) shows that the intensity was 9 at the epicenter; intensity 8 zone includes southwest of Republic of Moldova; intensity 7 zone covers a larger part of Republic of Moldova and southwest of Ukraine; the entire

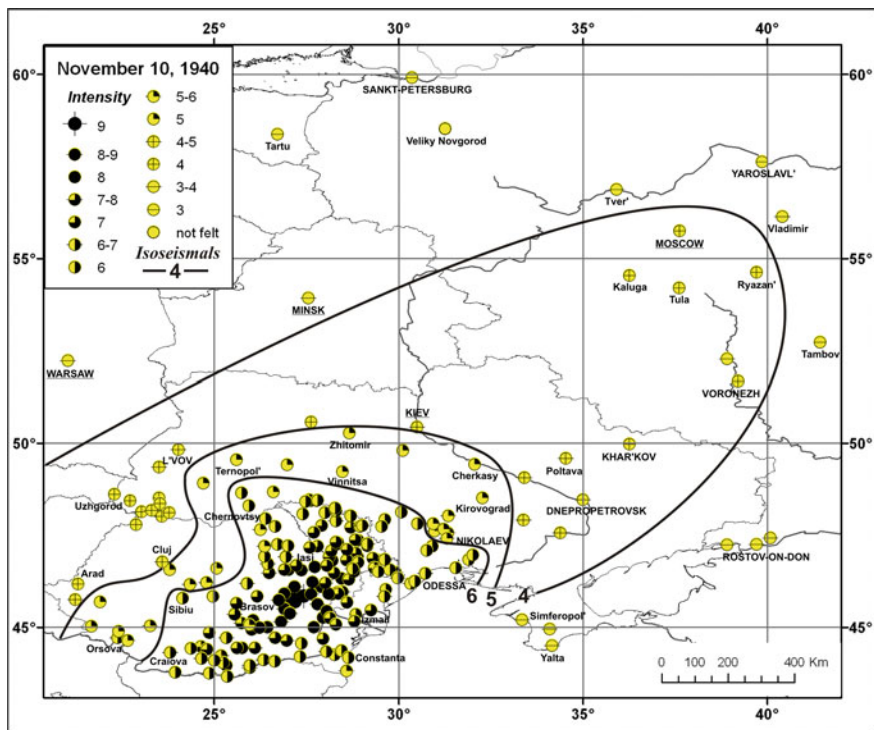


Fig. 5 General isoseismal map of the November 10, 1940 earthquake for the Eastern Europe

central part of Ukraine gets into the intensity 5 zone; the isoseismal of intensity 4 includes Moscow, Ryazan and Voronezh. The end points of the felt zone were St. Petersburg (to the North), Yaroslavl (to the North-East), Tambov and Rostov-on-Don (to the East).

3 Focal Mechanisms

For the November 10, 1940 earthquake, in Iosif and Radu (1962), Ritzema (1974), Vvedenskaya (1969) are given similar focal mechanism solutions according to the first P-wave arriving at 56 seismic stations of the world (Table 1). Two possible fault plane oriented rather steep towards the northeast—southwest, along the curve of the Carpathian arc. The axis of compressive stress is subhorizontal, the deviation angle of the axis from horizon less than 15°. The axis of the tensile stress is almost vertical, the horizontal deflection angle more than 60° (Fig. 6). Northwestern board of the fault is pushed onto the southeastern due to the continuing uplift of the

Table 1 Parameters of the focal mechanisms of the November 10, 1940 earthquake according to different authors

No	Planes						Tensions						Author
	NP1			NP2			P		B		T		
	Stk	Dp	Slip	Stk	Dp	Slip	Az	Pl	Az	Pl	Az	Pl	
1	215	56	94	29	34	85	302	10	33	3	142	80	Iosif and Radu (1962)
2	255	35	134	25	65	64	135	15	37	23	255	60	Vvedenskaya (1969)
3	215	56	95	28	38	84	303	11	34	4	140	78	Ritzema (1974)

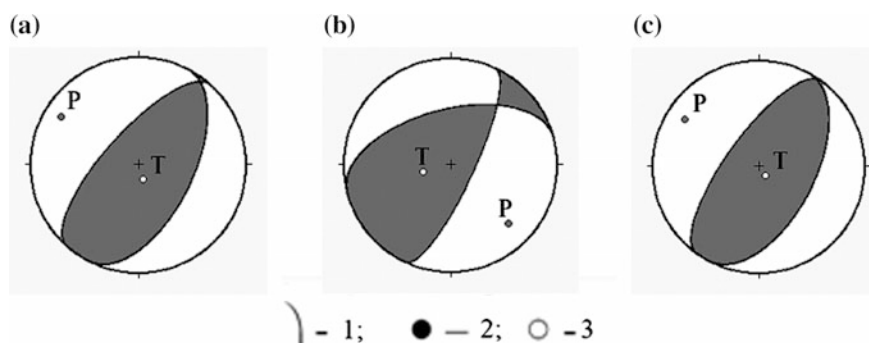


Fig. 6 Stereograms of focal mechanism of the November 10, 1940 earthquake in the projection of the lower hemisphere according to different authors: **a** Iosif and Radu (1962), **b** Vvedenskaya (1969), **c** Ritzema (1974). 1—nodal line; 2 and 3—the major stress axis of compression and extension, respectively; blackened areas of compression waves

Carpathian Mountains. Thus, the earthquake occurred under the influence of compressive stresses, and its mechanism is typical for the Vrancea intermediate earthquakes. Earthquakes with this type of focal mechanism are the most dangerous for entire Carpathian region.

4 The Comparison of Macroseismic Effect in Case of 1940, 1977, 1986 and 1990 Vrancea Earthquakes

We have compared macroseismic effect on the territory of northeastern Europe of the earthquake November 10, 1940, and three other major earthquakes of the twentieth century: March 4, 1977 August 30, 1986 and May 30, 1990. Contours are drawn on base of data from Atlas of Moldavian earthquakes (Drumea et al. 2009).

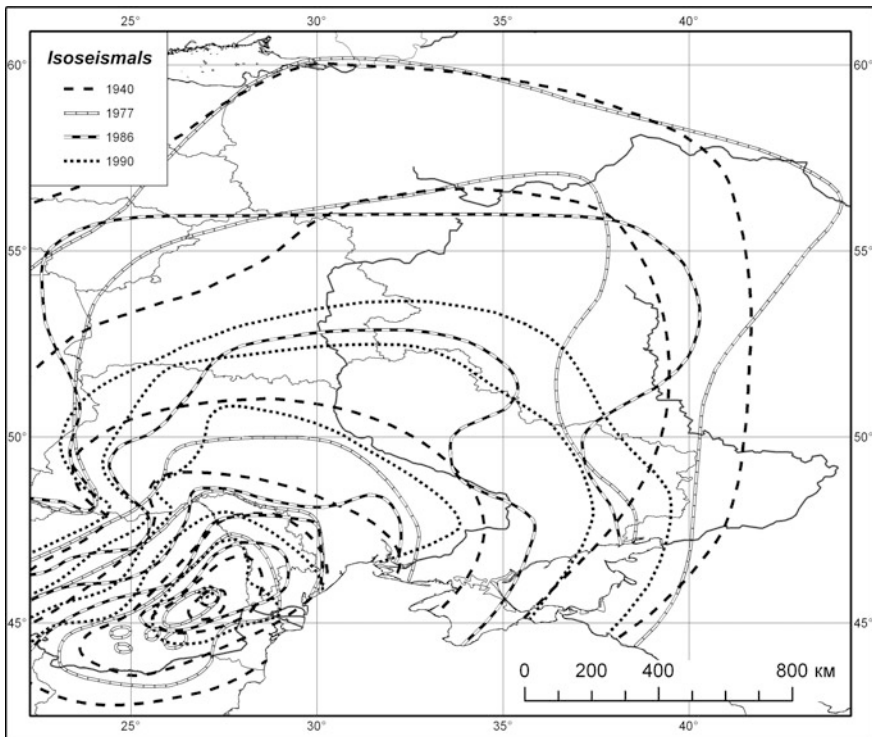


Fig. 7 Isoseismal configurations of the strongest earthquakes in the 20th century

The maximum effect on the territory of Moldova only in 1940 reached intensity 8. In 1977 and 1986 the maximum observed intensity in southwestern Moldova and south-western districts of Odessa region of Ukraine was 7. The isoseismal of intensity 6 for the earthquakes of 1940 and 1977 covers the entire territory of Moldova, and in 1986 in the northern part of its territory tremors achieved intensity 5 (Fig. 7).

During the 1977 earthquake the isoseismals of intensity 3 and 4 are extended in the direction of Moscow, and during deeper the 1986 earthquake in the direction of Kursk and Voronezh. Tremors with intensity 3 reached Leningrad in 1940, 1977. At the same time, in 1986 the boundary of the felt zone reached 56°N.

Strengthening of macroseismic effect to the northeast of the epicenter was observed in 1940 and 1986, with a depth of focus near 130–140 km. The 1977 earthquake with a depth of about 90 km and the epicenter in northeastern part of Vrancea had maximum effect to the south-west of the epicenter. Therefore, despite a smaller magnitude in 1986 ($M = 7.1$), and the greater depth of focus than in 1977 ($M = 7.2$), the earthquake in 1986 caused twice as much damage on the territory of Moldova than in 1977.

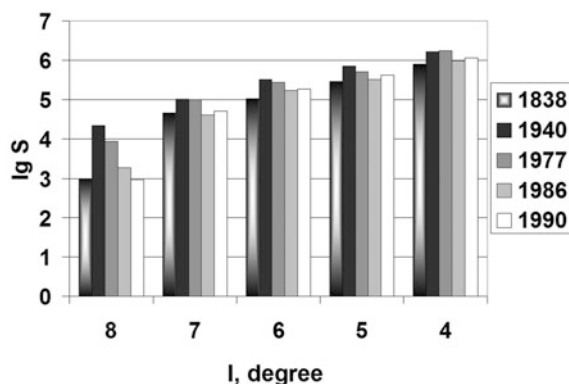


Fig. 8 The comparison of the intensity areas ($\lg S = f(I)$) for the strongest earthquakes of the Vrancea region

The comparative analysis of the intensity areas for the strongest Carpathian earthquakes of the 19–20th centuries shows that the November 10, 1940 earthquake has the largest areas of 4–8 isoseismals (Fig. 8). The March 4, 1977 earthquake has smaller areas and areas of the January 23, 1838, August 31, 1986 and May 30, 1990 are approximately the same (Drumea et al. 2009). However, the earthquakes in 1986 and 1990 differ in the depth of focus (135 and 90 km) and magnitude (7 and 6.7).

5 Conclusions

As a result of the systematic collection and matching of available initial macroseismic data from historical sources and previous publications, their revision and reassessment as well, the intensity in the 130 settlements within the territory of the East European platform was defined. Using the standard seismic intensity scale MSK-64. On the basis of the processed data a new isoseismal map of the November 10, 1940 earthquake was made, which is a good guideline for developing a pattern of the expected impact of future devastating earthquakes in the Carpathian region.

The map of isoseismal configurations showed the most distant spread of seismic waves to the northeast of the epicenter, which is typical for the majority of strong intermediate-depth earthquakes of Vrancea region. However, the overall direction of the waves detects a significant difference for specific areas of maximum radiation of seismic energy for each earthquake.

The comparative analysis of isoseismal areas of strongest earthquakes in the last 200 years revealed that the November 10, 1940 earthquake had the largest territory of manifestation on the Earth's surface.

References

- Atanasiu I (1961) Earthquakes in Romania. Acad. RPR, Bucharest
- Bune V, Radu C, Polyakova T (1986) Analysis of isoseismal maps of Vrancea earthquakes November 10, 1940 and March 4, 1977. Detailed engineering and seismological research. Questions of earthquake engineering. Nauka, Moscow, 27:126–135
- Demetrescu G, Petrescu G (1941) The earthquake of November 10, 1940. Macroseismic map. Bucharest
- Drumea A (1980) Carpathian earthquake of March 4, 1977 and its consequences. Nauka, Moscow
- Drumea A, Knyazeva V, Korolev V (1996) Vrancea earthquakes of May 30 and 31 (macroseismic data). In: Earthquakes in the USSR in 1990. Moscow, pp 12–19
- Drumea A, Shebalin N, Skladnev N, Grafov S, Oyzerman V (1990) Carpathian earthquake of 1986. Stiinta, Chisinau
- Drumea A, Stepanenco N, Simonova N, Alecseev I, Cardanet V (2009) Atlas of the intensity maps of the earthquakes in Moldova (18–21th centuries). Chisinau
- Evseyev S (1961) Earthquakes in Ukraine. AS UkrSSR, Kiev
- Iosif T, Radu C (1962) Mechanisms of strong Carpathian earthquakes in 1940. An Un AI Cuza Iasi 11b(8):171–180
- Korolev V, Knyazeva V, Sklyar A, Safronov O (2011) Macroseismic data of Vrancea earthquake of November 10, 1940 on the territory of Ukraine. Seismol Bull Ukraine 2010. Sevastopol, SPC ECOSI-Hydrophysics, pp 53–57
- Mandrescu N, Anghel M, Smalbergher V (1988) The Vrancea intermediate-depth earthquakes and the peculiarities of the seismic intensity distribution of the Romanian territory. In: Recent seismological investigations in Europe. Nauka, Moscow, pp 59–65
- Nikonov A, Popova E, Fleyfel L (2010) Deep Carpathian earthquakes in 1940, and their manifestation within the East European platform (to the 60th anniversary of the event). In: Proceedings of the XVI international conference structure, properties, dynamics and minerageny of the lithosphere of the East European platform. Voronezh, pp 87–93
- Pantea A, Constantin AP (2011) Reevaluated macroseismic map of Vrancea earthquake occurred on November 10, 1940. Rom J Phys 56(3/4):578–589
- Radu C, Polonic G, Apopei I (1979) Macroseismic field of Vrancea earthquake of March 4, 1977. In: Seismological research on the earthquake of March 4, 1977. Bucharest, pp 345–358
- Ritzema AR (1974) The earthquake mechanisms of the Balkan Region. UNESCO—Survey of the seismicity of the Balkan region, UNDP. Project REM/70/172. De Bilt
- Sagalova E (1969) On the issue of seismic zoning of Bukovina. Seismicity of Ukraine. Naukova Dumka, Kiev, pp 70–80
- Shebalin N (1977) Deep earthquakes. In: New catalog of strong earthquakes on the territory of the USSR. Nauka, Moscow, pp 472–474
- Stepanenco N (2011) Macroseismic field of Vrancea earthquake of November 10, 1940. Bull IGS ASM 1:17–30
- Stepanenco N, Drumea A, Simonova N (2006) The strongest earthquakes of the Carpathian region in 18–20th centuries. Bull IGG ASM 2:37–64
- Sukhov I (1960) Materials to the study of earthquakes of 1940 in Chisinau and Moldavian SSR. The report of the Moldavian branch of the Academy of Sciences of the USSR. Chisinau
- Tsshokher V, Tishchenko V, Popov V (1941) Carpathian earthquakes of October 22 and November 10, 1940. Report of the Commission of the AS of USSR for investigations of the earthquakes' effects in MSSR and regions of Western Ukraine. Funds IPE RAS, Moscow
- Vvedenskaya A (1969) Peculiarities of the stresses acting at the foci of earthquakes near the bend of the Carpathian arc. Nauka, Moscow

Causes and Effects of the November 10, 1940 Earthquake

Ion Vlad

Abstract On November 10th, 1940 a strong earthquake occurred in Romania, being characterized by a seismic magnitude $M_{G-R} = 7.4$ and lasting about 45 s. The seismic motion was felt over an area of 80,000 km² and resulted in significant casualties and property damage. This seismic event aroused particular interest since it was established that its focus was at a depth of about 150 km, in the Vrancea region. Another aspect highlighted by the incidence of the earthquake was that of the existence within the affected area of some “*seismic islands*”, where it was felt more severely compared to how it was perceived in other neighbouring regions, though its instrumental epicenter was located far away both from those “*seismic islands*” and from the areas located in their vicinity. In this respect, the most representative example is that of Bucharest, located nearly 160 km from the instrumental epicentre, and where the macroseismic intensity was set to IX, according to the seismic intensity scale of G. Mercalli and processed by A. Sieberg. The paper contains relevant aspects regarding the design and construction of the building categories that were severely damaged by the destructive 1940 Vrancea earthquake.

Keywords Vrancea • Damage • Collapse • Cotroceni tribune • Carlton

1 Introduction

In 1940, in Romania, five earthquakes of seismic magnitudes M_{G-R} higher than 5.5 occurred: June 24, 1940 ($M_{G-R} = 5.5$), October 22, 1940 ($M_{G-R} = 6.5$), November 8, 1940 ($M_{G-R} = 5.5$), November 10, 1940 ($M_{G-R} = 7.4$) and November 11, 1940 ($M_{G-R} = 5.5$). The November 10, 1940 earthquake severely damaged many

I. Vlad (✉)

Romanian National Centre for Earthquake Engineering and Vibrations,
Technical University of Civil Engineering, Bucharest, Romania
e-mail: vladi@itcnet.ro



Fig. 1 General view of the “Carlton Block” before the November 10, 1940 earthquake (www.muzeuldefotografie.ro)

buildings in Bucharest, including the category of block of flats, also causing the collapse of one of the largest and most modern buildings of that time, known as the “Carlton Block” (Fig. 1).

This major seismic event has highlighted since then the fact that the earthquake “*spectral peaks*” corresponded to the long natural vibration eigenperiods of high-rise blocks of flats in Bucharest. It should be mentioned that at the incidence of the earthquake most buildings had reduced heights, excepting several hundreds of high blocks that were built between 1933 and 1940. In conclusion, the most affected buildings were those that were part of the high-rise buildings category, the least affected being the low-rise ones, with shorter natural eigenperiods of vibration.

The strong seismic events that followed showed that, for the epicentral distance Vrancea—Bucharest, the period of the dominant components of the seismic motions were maintained and will continue to be maintained as long as strong earthquakes will happen in the Vrancea area, with all the consequences that derive from this fact. The major damage that the earthquake caused to many buildings, including the significant number of casualties, especially those resulted after the collapse of the “Carlton” block, put for the first time in Romania the problem of the safety of buildings to seismic actions and of the way to protect them against earthquake effects.

2 Information on the Design Prior to the November 10, 1940 Earthquake

Knowledge in the field of earthquake engineering was absent during the period before 1940 for the Romanian civil engineers. As a result, the seismic action was not taken into account in the design process of constructions. The most reasonable explanation could be that no strong earthquake had occurred in recent past period and, therefore, no official technical requirements together with scientific concerns in seismic design existed. In the period between the two world wars, the most powerful influence over the structural design engineers was held by the German technical legislation. This country had technical regulations in many fields—“DIN” type, including rules for proportioning reinforced concrete structural members. The German rules were translated and published in Romania under the title “*Normele de proiectare ale Comisiunii germane pentru beton armat*” (DIN 1045/1932/1937).

The period between 1920 and 1940 was characterized by an important economic and urban development of large towns in Romania, Bucharest having a prominent place. Thus, an important number of reinforced concrete residential buildings, as well as some of the most representative constructions in Bucharest, were achieved. All these buildings were conceived, analyzed, and designed, by private design entities, which used very “*prompt*” designing methods. The payment, for both entrepreneurs and designers, had a decisive influence on the design process, usually the proportioning of the structural elements being accomplished in order to satisfy their own material interests. A general characteristic of the interbelic period is that the design of buildings was carried out exclusively for “*gravity loads*”. Another significant aspect, which must be considered, is related to the fact that the structural designers had “*rudimentary knowledge*” of structural analysis and “*limited comprehension*” of the reinforced concrete theory and of proportioning of structural elements (Vlad 2007).

The RC structural systems of the buildings (exclusively designed for gravity loads) were conceived as *plane frames* structural systems. In order to correctly understand the way of thinking of the period, it must be mentioned that a plane frame can have two ways of behavior:

- one similar to the behavior of *space frames*, that presumes that the ensemble of plane frames was thus conceived as to resist to actions that generate horizontal forces on any direction in plane;
- a favorable behavior on a preferred direction (transversal or longitudinal), orientating the plane frames on a certain principal direction, the other main one having a weak resistance to horizontal forces, particularly to the ones generated by seismic actions.

An illustrative example, which emphasizes the top of the knowledge and the prototype way of thinking applied in 1937, is represented by the construction of the body building “I” of the Polytechnic School in Polizu St. Bucharest. For this building it was sought to provide a favorable behavior on the transversal direction and, in this

respect, plane frames on this direction were designed. In fact, these frames were the “*principal beams*” of the floor structures, which were sustained by the masonry structural walls disposed on the longitudinal direction. On the other direction (longitudinal), between the columns with transversal orientation (conceived only for gravity loads), secondary floor beams or ribs with small cross-sectional dimensions, were provided (Țițaru 2011).

2.1 “*Professionally Correct*” Engineers’ Category

According to their level of training, engineers pertaining to this category used to calculate separately both beams and columns. The beams were computed as continuous beams with equal spans, based on the 1932 “*Beton Kalender*” tables (admissible resistances). The unequal spans didn’t worry the designer, as he used to make some “*approximations*”, based on his own professional competence. It should be mentioned that engineers pertaining to this category worked honestly, even if they worked for the state, or for private. From this category, engineers as Anton Chiricuță, Mihail Hangan, Aurel Beleş, Ștefan Bălan and Victor Popescu can be given as examples.

When designing buildings for the state, the “*professionally correct*” designers used to make various simplifications and approximations, seeking to obtain a simple covering calculation, so that it did not lead to excessive oversizing (having in mind the “*checking*” which was performed by the state representatives—the famous red-ink checking, both of the calculation notes and of the drawings).

When designing buildings for private, the “*professionally correct*” designers were very careful and watchful not to be accused to have oversized the reinforced concrete structural elements by those who employed them. Engineers, who for various reasons were tempted to oversize, were automatically eliminated from the market. From the category of the ones driven out of business were also included the “*extremely correct*” engineers. In the following, a story lived by the young Eng. Emilian Țițaru, after only one year of professional practice, will be presented. He received from an architect the architectural drawings of a building and was asked to give the dimensions of the reinforced concrete columns. After correctly computing and providing the resulted sizes, the architect considered that these were exaggerated, arguing that another engineer gave him smaller dimensions and, in this “*elegant*” manner, the architect preferred the less professionally correct engineer (Țițaru 2011–2013).

2.2 “*Professionally Incorrect*” Engineers’ Category

In this category engineers working with their own reduced safety coefficients and that used to increase the allowable resistances both for reinforcement and concrete

sections can be included. The designers who formed the “*professionally incorrect*” group realized the undersizing of the reinforced concrete structural elements. This way of working was specific for private enterprises applying this system, which unfortunately has been taken over and has been used afterwards for a long period of time. All these contractors were seeking to earn more and, for this purpose, the only way was “*to squeeze the neck*” of reinforced concrete. In the period that followed, the contractor imposed an unwritten law that had to be applied: regardless of the building height, the average thickness of the concrete must have resulted equal to 20 cm (the entire volume of concrete was divided to the total developed surface of the building, and an average thickness of about 20 cm should have resulted). The amount of steel used in construction should have been equal to 20 kg/m^2 , respectively 100 kg/m^3 , otherwise the designer was eliminated from the market.

The block of flats pertaining to the category built by such contractors and following the above shown manner, are *undersized even for gravity loads*, aspect that has been revealed by all the technical assessments carried out lately.

Another category of “*professionally incorrect*” designers was that of those computing the reinforced concrete elements having the position of “*employees*” of various contractors. They thought as follows: the allowable compressive strength considered in the design of reinforced concrete columns is equal to $1/3$ of the resistance of the RC cubes with sides equal to $20 \text{ cm} \times 20 \text{ cm} \times 20 \text{ cm}$, determined at 28 days, according to the German prescriptions. It is made clear that at that time, in Romania, there were no mandatory technical regulations for constructions. These designers applied a design philosophy based on personal safety coefficients, substantiated by empirical experience and by an incorrect interpretation of the existing “*Circulars*”. How “*perfidious*” was this thinking is apparent from the following arguments: the compressive strength of concrete prescribed by the German “*Circular*” was $1/3$ of the resistance of the RC cube after 28 days from casting.

According to the general theory of concrete, it was known that the concrete strength increases in time. This category of designers, for a concrete of mark B120, instead of considering in computation an allowable compressive strength of 40 daN/cm^2 (that is $1/3$ of the compressive resistance of a concrete cube at 28 days from casting, which they declared to have applied), they considered a compressive strengths equal to 45, 50, or even 60 daN/cm^2 . The motivations of the designer who calculated and proceeded in the previously exposed manner, knowing that the compressive strength increases in time, were: his personal experience accumulated in previous design works and the good behavior in service of the buildings already constructed, in condition of obtaining material savings.

Eng. Emilian Țițaru narrated how, in a personal discussion with Professor Mihail Hangan, the latter spoke about the “*safety coefficients*”: “*Dear, I have my personal safety coefficients*” (the idea to remember is that Professor Hangan used to design in a covering manner, both with regard to the safety coefficients and in relation to the safety requirements set out in the design “*Circulars*”). Professor Mihail Hangan has also been counselor, for a period of time, at the “*Industrial Design Institute*”. The designers of the institute complained that sometimes they could not understand the Professor: “*he came to the drawing board, he looked at the plan that was in*

working process and, not infrequently, he asked us to modify the reinforcement; we replied that we have correctly calculated and then he appealed to one last argument – hard to refuse – please put two extra bars for me". One explanation could be that he wanted to have a certain "cover".

It should be remembered that for a period Professor M. Hangan was the Director of the "Technical Direction" of the Ministry of Public Works. In this quality, he completed projects for the state and, perhaps, this has influenced his thinking in terms of a pronounced caution.

As a result of the findings from buildings damaged by the November 10, 1940 earthquake, a significant amount of technical observations, representative photos and real data, have resulted. Unfortunately, these have remained in the personal archives of various experts, without even having tried an organized collection, in order to achieve a structured material, which thereafter to be at the basis of certain Romanian official prescriptions for the design and construction of buildings in seismic areas.

3 The Cotroceni Tribunes Collapse—The Precursor of the Carlton Block Collapse?

On June 8, 1936, during the celebrations of the "Restoration" day, in front of H.M. King Carol II and of the Heads of State of two friendly countries, Tribune "I", which was filled with public, collapsed. An hour before, a smaller tribune (called Tribune "A") also collapsed, in the immediate vicinity of the Royal Tribune. The collapse of Tribune "I" caused the death of 3 people and injured more than 700 people, of whom 337 were hospitalized. A serious "investigation" and a "merciless punishment for the guilty ones" were asked. The investigation that was done has highlighted an unacceptable state of things and according to one of the most important American engineers J.A.L. Waddell, "there was always something to be learned from the collapse of a building".

On June 24, 1936, at the "Polytechnic Society", a Conference of great interest for the "technical engineering body" of those times was organized. The attraction of the Conference was related not only to the treated subject, but mainly as it had a direct connection with a series of aspects of great interest, much discussed and strongly advocated in the then engineering circles:

- the problem of using the title and of practicing the profession of "engineer";
- the problem of how, by whom, and after what rules must be designed, built and checked the constructions that are achieved in Romania.

The fight and the verticality of professors Ion Ionescu, Cristea Niculescu and Gheorghe Filipescu led to the decision no. 20729/2998A of the Bucharest City Hall, dated June 23, 1936, concerning the "building permits" which stipulated that all "design plans to be calculated and signed by civil engineers". These aspects were

presented with the hope to contribute in some way to eliminate several misconceptions released after the 1940 and 1977 earthquakes, according to which “*the earthquake was guilty*”, or “*the level of knowledge was very low at that time*”. In the analyzed period engineers were substituted by architects, who occupied all the decision positions both in the Ministry of Public Works and in the City Hall, and directed the works in the spheres of their personal interests.

4 The Building Stock in 1940

In order to understand the earthquake effects on the existing building stock on November 10, 1940, the construction features of the earlier periods prior to the incidence of the seismic motion should be emphasized: structural systems, used materials, existing technical regulations, design concepts—in the context of the knowledge available at that time. The aspects that are examined do not refer to the buildings accomplished between 1890 and 1930, having heights of GF + 2F and that are considered unique, being historical and architectural monuments (Vlad and Vlad 2008). Of interest for this scientific communication are the buildings realized in the interbelic period that designates the 21 years period between WW1 and WW2 (1918–1939). The main change that occurred during that period in the overall composition and detailing of the buildings, relatively to the previous period, was the use on an increasingly larger scale of concrete as building material (as reinforced concrete for the completing of the superstructures, respectively as plain concrete for the finishing of the foundations). The reinforced concrete has thus eliminated many of the shortcomings of the structural systems of the buildings built in previous periods and has favored the transition to larger buildings, with heights of up to 10 floors.

In 1921, the civil engineer Emil Prager has founded the first office of studies, surveys and reinforced concrete design projects, so capitalizing the gained experience from the time of his university studies (1907–1912), period when he already started to design RC buildings. The structural systems currently used in the interbelic period form two distinct categories, according to their number of floors:

- *for buildings with reduced number of floors*: structural systems comprising structural masonry walls, which benefited of the advantages offered by the use of reinforced concrete (floors, belts, lintels, local columns), and of plain concrete (foundations);
- *for buildings with high number of floors*: structural systems comprising cast-in-place reinforced concrete beams and columns.

It can be mentioned that the structural systems with beams and columns replaced, depending on the case, the structural masonry wall systems whenever demands for large free space and functional flexibility were present (blocks of flats with ground floor shops, multistory buildings for trade, office buildings a.s.o.).

4.1 *Buildings with Structural Masonry Walls Systems*

The use of cast-in-place reinforced concrete for buildings with a small number of levels (2–3 floors) led to increased performance of their behavior, including to loads generated by seismic actions, even if this aspect was not, in the period we are referring to, a topic of concern for designers. The timber floors and roofs in high-risk seismic zones did not ensure the integrity of these structural elements and their anchorage to the supporting walls.

The main change was that of replacing the timber floors and those with steel beams and brick vaults with reinforced concrete ones. Being perfectly rigid in the horizontal plane (rigid horizontal diaphragms), the RC floor and roof systems assured spatial working together of the brick masonry bearing walls, providing the possibility of redistribution of the horizontal seismic forces between the weaker and the stronger masonry walls, proportionally to their stiffness. For buildings shaped in-plane close to square, floor systems with slabs reinforced on two directions were realized, aspect that favoured a bidirectional transmission of the gravity loads to the bearing walls disposed on the transversal and longitudinal directions, and also a more efficient taking over of the horizontal forces that acted on any direction in plane. By realizing *RC belts* at the upper part of the bearing masonry walls, their proper anchoring with concrete floors was obtained, as well as with timber floors or with the ones with steel beams. The RC belts have created efficient links between the transversal bearing walls and the longitudinal ones as well.

The sizes and positions of wall openings have significant effect on the in-plane resistance of masonry bearing walls. When subjected to seismic loads, stress concentration takes place in the opening zones, causing cracking and deterioration of masonry. For this reason, at the bearing masonry walls with door and window openings, RC lintels were used; their efficient anchoring in the panels allowed the compact masonry between the superposed openings to be able to function as coupling beams under horizontal force actions. The use of reinforced concrete also permitted the completing of “*combined*” structural systems, composed of a structural masonry wall subsystem with walls disposed along the perimeter and in-between the apartments, and a subsystem of RC columns at the interior of the building.

Another aspect that should be mentioned is that concerning the execution of plain or reinforced concrete foundations under masonry walls, which proved to be a satisfactory and economical solution, optimal considered and generally used. The advantages granted by the use of concrete and of reinforced concrete at the construction of this building category were firstly of economical nature, but all the above mentioned aspects have implicitly contributed to the improvement of their behaviour to loads generated by seismic actions (Vlad and Vlad 2008).

4.2 *Multi-storey Buildings (up to 10 Storeys) with Structural Systems Consisting of Beams and Columns*

In the interbelic period the multi-storey buildings (Fig. 2) had structural systems with RC beams and columns with rigid links in joints, but without having the characteristics of RC moment resisting frames with favorable behavior to lateral forces (shaped and reinforced to support both gravity and seismic loads).

For most of the buildings realized in the mentioned period the trend was to consider for the structural RC elements cross sections with very small dimensions, especially in the case of columns, namely for the structural elements with the highest importance in ensuring the resistance, the stiffness and the ductility of buildings to seismic actions. An aspect worth mentioning is the one concerning the poor quality of concrete used for the beams and columns of the structural systems, having marks equivalent to the actual concrete classes Bc7,5...Bc10.

The cumulative effect of the columns insufficient sections with the poor quality of the used concrete led to very high values, sometimes even over unity, of the compression stress level of the columns expressed by means of the coefficient $n = N/b \cdot h \cdot R$, i.e. to flagrant disregard of what we call today “*ductility demands*”. Considering the exposed deficiencies and uncertainties, the multi-storey buildings with RC structural systems, completed in the interbelic period, pertain to the category of “*buildings with structural systems having beams and columns*” and not to the category of “*buildings with reinforced concrete moment resisting frames*”.



Fig. 2 High-rise buildings in the center of Bucharest before the 1940 earthquake (*photo W. Prager*)



Fig. 3 The collapse of the “Carlton Block” (source <http://ro.wikipedia.org>)

At the incidence of the November 10, 1940 earthquake, several such buildings with structural systems having beams and columns (blocks of flats) have been damaged and one of these completely collapsed (Carlton Block, Fig. 3).

As a result of the lack of experience and of the conditions due to the state of war, the buildings that were damaged have been inappropriately strengthened. The natural consequence of this state of facts was the collapse of 28 buildings during the March 4, 1977 Vrancea earthquake. This seismic event emphasized the structural deficiencies of the multi-storey buildings with structural systems consisting of RC beams and columns that were built in the interbelic period. As a comparison, from the thousands of blocks of flats completed after 1950 only two end sections have collapsed (two block staircases). The blocks that collapsed together with the severely damaged ones, showed that the structural systems with beams and columns that were built in the interwar period did not have high capacity to withstand earthquakes with comparable severity as that of March 4, 1977.

Those that survived the 1940, 1977, 1986 and 1990 earthquakes had in their configuration masonry partitioning and exterior walls which, although considered without structural role, had the capacity to resist the horizontal forces generated by the seismic actions. The stiffness of these walls to lateral displacements have been much larger than those provided by the ensemble of beams and columns, that was thus unloaded of most of the horizontal forces. The damage sustained by these walls, 45° cracks type generated by main tension forces, has confirmed the active contribution of these walls to the rescue of the buildings with structural systems with beams and columns. The favourable effect of the exterior walls and of the partitioning ones was random (meaning that they were not foreseen for this purpose), their behaviour being in fact dictated by their number, thickness and their appropriate in-plane arrangement. As a strengthening solution for this building category, the measures that should be considered do not refer mainly to the structural system, composed by beams and columns, but to the brick masonry walls that should be made stronger, transformed or completed, in order to fulfil in the future the “bracing” function associated to structural walls.

5 The November 10, 1940 Earthquake International Echoes

In the publication “*Earthquake Notes*” of the Eastern Section of the “*Seismological Society of America*” the 10.XI.1940 earthquake was notified under the title “*Earthquake in Romania*”, its content being presented in the followings: “*An earthquake, reported to have been the heaviest in Rumanian history, caused a tremendous amount of damage when it occurred about lh 39 m (G.C.T.) on November 10, 1940. According to newspaper accounts over a thousand people were killed and probably several times that many were injured. Bucharest sustained a large part of the damage to houses and buildings, although much destruction occurred throughout the country. The same quake was felt in Kiev and Odessa (Russia) and in Turkey, Bulgaria, and Italy, and some damage is reported from those places. The epicenter is said to have been at or near Focsani, a city of 50,000 in the Eastern Carpathian foothills about 100 miles north of Bucharest, where 70 percent or more of the houses and buildings were destroyed. The cities of Galati (100,000) and Focsani were reported to have suffered the worst damage. Railroads, roads, and bridges, over which extensive military movements had been taking place, were badly damaged...Government seismologists of the Bucharest Geological Institute reported that the shocks originated 100 miles below the earth’s surface and were more intense than the severe Turkish earthquakes last winter. This depth of focus confirms determinations made in this country of 150 km.*”

The publication “*L’Illustration*” printed on November 30, 1940 published the article “*Le tremblement de terre en Roumanie*”, which contained images of damage including the ruins of the “*Carlton Block*”.

6 Scientific Interest Generated by the Earthquake

The way in which the November 10, 1940 earthquake was received in the technical and engineering communities, but especially by the “*Polytechnic Society*”, will be presented in the followings. The source of this information was the booklet entitled “*1941 Report. January 1, 1941 – December 31, 1941*” published by the “*Polytechnic Society*”. Between January 25, and July 5, 1941, 8 conferences were held, and the texts of the last tree ones have been published in the “*Bulletin of the Polytechnic Society*” on October and November 1941 and became the text of a booklet with the same title, also printed in 1941.

On December 8, 1940, the German scientist Professor August Sieberg, accompanied by his assistant Wilhelm Sponheuer, arrived in Bucharest as guests of the Romanian Government, to study the effects of the earthquake. The personality of Professor Sieberg was known at that time both as director of the “*Institute of Seismology*” and, especially, as geophysicist at the University of Jena, quality in which he had many contributions to the study of earthquakes. Among his concerns

at the time may be listed: the study of the geological aspects revealed by strong seismic motions, the mechanical behaviour of the foundation medium during earthquakes, the assessment of the response of buildings to seismic motions—inclusively by using instrumental methods, the introduction in the science of earthquakes of new methods of investigation with practical applications a.s.o. To study of the effects of the November 10, 1940 earthquake, Sieberg and Sponheuer made documentary visits in the most affected by the earthquake areas: Prahova Valley and Southern Moldavia, passing through the towns Focșani, Panciu, Bârlad and Galați. At the end of his visit in Romania, Sieberg presented two conferences, both accompanied by projections. Sieberg launched the idea of the unfavourable behaviour of tall buildings during long period seismic motions, this being confirmed 37 years later by the March 4, 1977 earthquake.

7 The “Carlton Block” Collapse

Since the incidence of October 22, 1940 earthquake, serious cracks have been observed inside the “*Carlton Block*” and the constructor made bungled remedies. No other block of the same type, built by other contractors, collapsed. That’s why it should be pointed out that the collapse of this building can be attributed to the November 10, 1940 earthquake only in a small extent. The causes of the “*Carlton Block*” collapse were presented both by a Commission nominated by the investigative bodies and by Eng. Theodor Achim, who had during the building construction the role of *site-works supervisor*. The essential cause of the complete collapse of the Carlton building was the structural conception on which the design of the reinforced concrete columns has been based, imputable both to the architect and engineers. The columns that should ensure the stability and the resistance of the building were poorly designed. Thus, there were L-shaped columns, followed by rectangular or circular ones, and again continued by other L-shaped columns. Due to these changes there has been a misalignment of the loads transmitted to the columns situated at the lower floors, this fact leading to a disadvantageous behavior. The tower corner columns did not meet even the elementary condition to have the same cross section from the base to their upper extremities. The column axes varied from one floor to the other. They were deployed over five to six floors and rested on beams and consoles. The position of several columns has been modified in respect to their original one, in order to preserve the aesthetics of some apartments. As there were shops at the ground floor, in order to get as big shop-windows as possible, some of the columns were reduced to transversal reinforced concrete walls only 22 cm in width, but 200 cm in length (Beleş and Ifrim 1960). Among other causes that may have contributed to the collapse were the unfavorable position of the 47 m high corner tower with respect to the direction of the earthquake motion, the possible amplification of earthquake effects due to the proximity of the foundation to the water table, the location of the building at the end of a row of tall buildings and the cantilevering of the first floor theater seats from the columns. Professor Cristea Niculescu was the

first one who brought into discussion the *resonance phenomenon* in connection with the total collapse of this building. The collapse of the “*Carlton Block*” and of 28 buildings during the March 4, 1977 earthquake were caused by the “*gravitational collapse*” that occurred due to the breaking of the columns at the bases of the building superstructures. Having low resistance to horizontal motions, the columns broke at their bases, the shear forces and the overturning moments vanished, and the buildings collapsed gravitationally.

8 First Signs of Earthquake Engineering in Romania

From the beginning it should be specified that the expression “*earthquake engineering*” was used for the first time on November 4, 1948, in the name of the then newly born research center “*Earthquake Engineering Research Institute*”. The words “*earthquake engineering*” originally meant the application of engineering to the matters generated by strong seismic motions. The expression in use prior to “*earthquake engineering*” was “*engineering seismology*”. The straight forward original definition of “*earthquake engineering*” could be stated as follows: *the application of civil engineering to the study of strong earthquakes*.

The year of birth of the Romanian interest in studying earthquakes from the engineering point of view is November 10, 1940, date when the first destructive earthquake of the 20th century occurred. Like any beginnings, it was very difficult due to the lack of knowledge and to the existing misconceptions. The strong seismic event that struck Romania in 1940 prompted the “*Ministry of Public Works and Communications*” to direct its “*Department of Public Works and Communications*” to organize a commission referred to as “*The Superior Commission for studying the accidental actions to which the constructions were subjected during the November 10, 1940, earthquake*”. After one-year work, *the first official technical mandatory document in Romania* having the title “*Preliminary Instructions for Preventing the Damage of Constructions Caused by Earthquakes and for Rehabilitating the Damaged Ones*” was published. This document approved by the Ministry Decision No. 84351/December 30, 1941 consisted of four chapters and a calculus example. These instructions were published during the period in which Romania was involved in the World War II, a difficult period for the construction industry. For this reason, their impact in the design process was minor; the instructions have been neither known nor applied. The “*transient*” character of the instructions was eliminated in 1945, when their final draft was published in the “*Official Monitor*” No. 120/May 30, 1945, under the following title: “*Instructions for Preventing the Constructions Damage Caused by Earthquakes*”. The Ministry Decision No. 60173, dated May 19, 1945, has approved the new content of these instructions, based on the technical agreement of the “*Superior Technical Council*”. Although the material remained structured in four chapters, it was reformulated, and the example of calculus was eliminated (Vlad 2007).

9 Final Remarks

- (a) When the seismic event of November 10, 1940 occurred, in Romania scientific knowledge in earthquake engineering were quite limited. However, from the reading of two publications that were printed in 1941 (*“The Earthquake and the Buildings”* by Professor Aurel A. Beleş and *“The Causes of the Carlton Blok Collapse. Learnings.”* by Eng. Theodor Achim), one can see that prominent personalities of the time had access to international publications in this field. There were already known the seismic disasters produced by earthquakes in the US (April 18, 1906, San Francisco, CA; June 29, 1925, Santa Barbara, CA; March 10, 1933, Long Beach, CA; December 31, 1934, Baja, Imperial Valley, CA), in Japan (September 1, 1923, Kanto) and Chile (January 25, 1939, Concepcion), but also in other parts of the world and, therefore, some international experience and development works on the technical regulations existed and were acknowledged in Romania. The strongest argument in this regard was that some of the top personalities of the period, including Professor Aurel A. Beleş, were in possession of the Italian technical regulation (1938) entitled *“Norme tecniche di edilizia con speciali prescrizioni per la localita colpite dai terremoti”* (*Technical Standards for Construction with Special Provisions for Earthquake Exposed Localities*). In Romania no one asked then the question: *“What could produce a strong earthquake in the country?”*, and thus the works carried out by seismologists had shown no interest to civil engineers. In his book *“The Design of the Buildings. My Profession”*, the exceptional design engineer Petru Vernescu stated: *“Seismologists were much better informed than civil engineers on the seismic action in Romania. Data on the occurrence of earthquakes were known and published both in our country and in the world. The moments of the incidence of the destructive seismic motions were known and their magnitudes were estimated. The seismologist experts warned that, basically, these seismic magnitudes could be exceeded.”*

The presented issues reveal an almost total ignorance of the effects of earthquakes on buildings before the incidence of the strong earthquake which occurred on November 10, 1940 (Vlad 2009). In 1941, Gheorghe Demetrescu, the Director of the *“Astronomic Observatory”* stated: *“if the earthquake would have lasted a few seconds more Bucharest would have been a whole heap of debris”* (Achim 1941). During the significant duration of an earthquake there are not cycles of the same intensity, but there are always present cycles of close intensities. In case of the March 4, 1977 earthquake, the cycle with maximum acceleration was practically 1.5 times repeated (and the dynamic amplification ratio for 5 % critical damping approached to 3), while for the September 19, 1985 Mexico City earthquake, the cycle of motion with maximum acceleration was 4–5 times repeated (and the dynamic amplification ratio was approximately equal to 8), as seen in Fig. 4. In relation to the seismic energy quantity released by the 1977 earthquake, the most important aspect

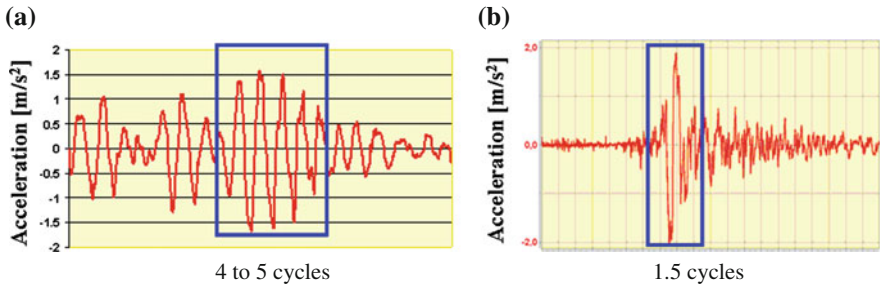


Fig. 4 The 1985 Mexico City (a) and 1977 Vrancea (b) earthquakes accelerograms

that must be taken into account are the followings: *what would have happened if the seismic motion had one, ore more, supplementary cycles and the quantity of seismic energy released would have been greater? Is an accumulation of a bigger quantity of energy possible in the Vrancea seismic zone, the Romanian region where the strongest earthquakes occur?* The same observation could be made in regard to the March 4, 1977 earthquake, but luckily nature favored Romania one more time (Vlad 2012).

- (b) The November 10, 1940 earthquake has demonstrated that RC buildings constructed before the implementation of modern code provisions are among the most vulnerable to serious damage and even to collapse. The damage suffered by many RC buildings during this earthquake led to their collapse in March 4, 1977 earthquake, as Professor Aurel Beleş had predicted even since 1941.
- (c) In densely-resided areas and city centers, neighboring buildings are constructed very close to each other, or even without any clearance between them. In the case of earthquake induced pounding between adjacent buildings two distinct cases are identified during structural assessments carried out: (a) the case of impact between slabs of adjacent stories of equal heights and (b) the case of impact between slabs and the columns of the adjacent buildings. It is true that in some encountered cases *“the effect of a group of buildings”* probably prevented the inevitable collapse, having the support given by the neighboring ones. Unlike the cases of favorable behavior provided by this effect, in the case of the *“Carlton Block”* it didn’t work, as the building was situated on the corner of two streets.
- (d) The representatives of the elite engineers in 1940 took notice of the total collapse of the *“Carlton Block”* and of the severe damage of the high-rise blocks in Bucharest. They did not realize that the damage was due to the long period effect of the seismic motion and have not realized the unfavorable behavior of tall buildings to lateral actions. Living the earthquake of November 10, 1940, the top engineers’ representatives of the period 1940–1941 made some *“empirical”* findings, the most dangerous being the following: *well designed buildings withstood the earthquake action, even if they were designed only for gravity loads.* It is obvious that such way of thinking

was far from taking into account the serious aspects that the strong seismic motions could cause to the existing buildings in Romania. These personalities, including the most vocals and with a role in forming opinions, practically did not realized before this seismic event, and even after its occurrence, that the seismic action caused by earthquakes should be taken seriously in consideration. In this respect, the most illustrative example is the following position of a professor: “*I was not scared of the November 10, 1940 earthquake and there is no need to take action so much*”. This way of thinking has been taken up by many of the personalities of the time and, for a long period after, had produced less desirable effects.

References

- Achim T (1941) Cauzele prăbușirii “Blocului Carlton”. Învățăminte., Tiparul “Cartea Românească”, București
- Beleş AA, Ifrim M (1960) Engineering aspects of earthquakes in Romania in the light of modern investigation. In: 2nd world conference on earthquake engineering, Tokyo
- Țițaru E (2011–2013) Personal communications
- Vlad I (2007) The true history of Romania seismic code development. In: Proceedings of the international symposium “thirty years from the Romania earthquake of March 4, 1977”, Conspress Publishing House, Bucharest, 1–3 Mar 2007
- Vlad I (2009) Acțiunile “Societății Politehnice din România” referitoare la cutremurul de pământ de la 10 noiembrie 1940, A 4-a Conferință Națională de Inginerie Seismică, 18 decembrie 2009, vol 1, Editura Conspress, București, ISBN 978-973-100-096-1, pp 193–213
- Vlad I (2012) Characteristics of seismic wave propagation. Can we accept the “Mexico City Effect” as responsible for the collapse of buildings during strong earthquakes, 15th world conference on earthquake engineering, Lisbon, 24–28 September 2012, ISBN: 9781634396516, Sociedade Portuguesa de Engenharia Sismica (SPES), POD, Curran Associates, Inc.
- Vlad I, Vlad M (2008) Behavior of dwellings during strong earthquakes in Romania. In: 14th world conference on earthquake engineering, Beijing

Part II
Seismicity of Romania. Seismic Hazard
Assessment; Local Soil Conditions Effect

Overview of Part II: Seismicity of Romania. Seismic Hazard Assessment; Local Soil Conditions Effects

Mihaela Popa and Florin Pavel

The papers contained Part II of this volume are devoted to three main subjects, namely: seismicity of Romania, seismic hazard assessment and the evaluation of local soil conditions. A total of 11 papers authored by researchers from several institutions in Romania, as well as from Bulgaria and which cover all the three above-mentioned subjects were accepted for publication and are contained in this chapter. Some very brief abstracts of these papers are given below.

To extract the true information about the occurrence of major earthquakes from historical sources is real challenging for researchers. Information analysis must be done carefully and very critically to be able to correctly interpret the causes and effects of events analyzed. The paper “*Comparison of three major earthquakes with three recent earthquakes*” aims to detect characteristic resemblances and differences in the macroseismic distributions among three big earthquakes recorded in historical time [May 31, 1738 ($M_w = 7.7$), October 26, 1802 ($M_w = 7.9$) and January 23, 1838 ($M_w = 7.5$)] and three major earthquakes produced by the Vrancea subcrustal source in November 10, 1940 ($M_w = 7.7$), March 4, 1977 ($M_w = 7.4$) and August 30, 1986 ($M_w = 7.1$) which were instrumentally recorded. The main goal of the paper was to redefine the parameters of the strongest historical earthquakes produced in Vrancea zone in the last three centuries based on a comparative analysis of the revised macroseismic data for historical events with macroseismic data for instrumentally recorded earthquakes from 1940, 1977 and 1986.

M. Popa (✉)

National Institute for Earth Physics, Măgurele, Romania
e-mail: mihaela@infp.ro

F. Pavel

Technical University of Civil Engineering Bucharest,
Seismic Risk Assessment Research Center, Bucharest, Romania
e-mail: florin.pavel@utcb.ro

The Vrancea seismic source is a distinctive case of unusually clustered seismicity at intermediate depths. To understand and model the tectonic processes responsible for generating earthquakes in a so small confined lithospheric volume is necessary to investigate the source scaling properties. For this purpose, the authors of the paper “*Scaling properties for the Vrancea subcrustal earthquakes: an overview*” applied spectral ratio technique and empirical Green’s function deconvolution to retrieve source parameters. The analysis is carried out over an extended magnitude range from small ($M_w \sim 3$) to large ($M_w \sim 7$) events. The results show that seismic moment-magnitude, seismic moment-source radius and seismic moment-stress drop scaling appear to be self-similar over the entire magnitude range of the considered data set ($3.0 \leq M_w \leq 7.7$). The stress drop values estimated from source radius using spectral ratios and source displacement spectra show a very large dispersion from 0.1 to 1000 MPa. The obtained results lead to an important conclusion with special significance in assessing seismic hazard and strong ground motion characteristics: the rupture process for Vrancea earthquakes is rapid and efficient both for moderate and large shocks implying high dynamic stress drop values and low values of the source dimensions.

The Vrancea zone is known as region with high seismic hazard in the south-eastern part of Europe, generating from small to strong intermediate-depth earthquakes felt not only in Romania but also at great distance. An important component of monitoring the seismic activity of Vrancea source is the detection of precursors anomalies. This is the main task of the paper “*Earthquake precursors assessment in Vrancea region through satellite and in situ monitoring data*”. Precursors like land and air surface temperature and outgoing longwave radiation were studied for seismic hazard analysis. The results revealed the existence of coupling between lithosphere-surfacesphere-atmosphere associated with the seismic events occurrence, but the nature of these precursors anomalies is still unclear and requires more data to be analyzed.

The good azimuthal coverage of the Romania territory with seismic stations of high performance allows the authors of the paper “*Analysis of the seismic activity in the Vrancea intermediate-depth source region during the period 2010–2015*” to analyze the Vrancea intermediate-depth seismicity in terms of space distribution and focal mechanism. The study results highlight the great diversity of the fault plane solutions of the Vrancea intermediate-depth events with magnitude in the range of 3.8–5.5.

The significant development of the Romanian Seismic Network during the last decade allowed the decrease of the detection threshold and location of small magnitude events ($M_L \sim 1.0$). As a consequence, the Romanian earthquake catalogue has been increasingly contaminated with artificial events occurred in different regions. A few discrimination techniques are proposed in the paper “*Use of various discrimination techniques to separate small magnitude events occurred in the northern part of Romania*” to be applied in order to eliminate artificial events. The main goal of the paper was to apply different discriminants like complexity factor, spectral and amplitude ratio techniques and a multi-parameter discriminant on a data set including earthquakes, ground truth events and quarry blasts in the

same magnitude range. The selected data events occurred in the northern part of Romania, in the neighborhood of Bucovina array (BURAR). The study results revealed that complexity factor shows a good capacity to discriminate earthquakes from quarry blasts. When the multi-parameter was used like discriminant, the local geological conditions at the stations influenced the results of study. The technique of amplitude ratios shows also a relative well percentage of events discrimination.

The seismicity of Romania is characterized not only by the events occurred in Vrancea zone at intermediate depths but also by crustal seismicity recorded in different regions of the country. One of these regions is Galati area, where a swarm of 940 events with M_L magnitude between 1.0 and 4.0 occurred during three months in 2013. A first evaluation of seismicity and focal mechanism characteristics of this swarm was done in the paper "***The 2013 earthquake swarm in the Galati area: first results for a seismotectonic interpretation***". The data set used in this study was re-picked in order to increase the location accuracy and to better constrain the fault plane solutions. The analysis of epicenter alignment, focal mechanism and the regional stress was done in correlation with seismotectonic activity of the region. The comparison of swarm events number and the seismicity recorded in the region in a 10-year time interval preceding the swarm highlight that the great number of events occurred during the swarm exceed the normal activity of the region as number and as magnitude. To better understand the mechanism responsible for generating the Galati swarm, the next step will be a model simulation application. Many questions regarding the seismic swarm occurrence remain still open.

An evaluation of the seismic hazard for the territory of Bulgaria is performed in the paper "***A contemporary view to the impact of the strong Vrancea earthquakes on Bulgaria***". The authors discuss the available isoseismal map, and provide photographic evidence of the damage caused by the Vrancea May 30, 1990 earthquake in the north-eastern part of Bulgaria. The analysis of the ground motions recorded in Bulgaria during several Vrancea seismic events reveals a significant impact of the focal mechanism on the frequency content of the recorded ground motions. Response spectra for two scenario earthquakes originating in the Vrancea subcrustal seismic source are computed through neodeterministic seismic hazard assessment. Finally, the authors perform a brief seismic risk analysis using the methodology proposed by the RISK-UE research project.

The paper "***Site dependent seismic hazard assessment for Bucharest based on stochastic simulations***" focuses on the evaluation of the seismic hazard for INCERC site in Bucharest through stochastic finite-fault ground motion simulations. The simulations are performed for a Monte Carlo simulated earthquake catalogue of the Vrancea intermediate-depth seismic source with a time length of 2500 years. The analyses show that the hazard curves obtained through stochastic simulations have similar values as the hazard curves derived from classic PSHA only for short spectral periods. Moreover, the analyses reveal high displacement demands, especially for long period structures. Finally, the study also shows that the most likely candidate earthquakes for generating significant long-period spectral

ordinates are the larger magnitude events which occur at small source-to-site distances (with respect to Bucharest).

The focus of the paper “*Spectral displacement demands for strong ground motions recorded during Vrancea intermediate-depth earthquakes*” aims to derive a relation for the computation of the displacement amplification coefficient which relates the inelastic spectral displacements to the elastic spectral displacements. A database of ground motions recorded during three intermediate-depth Vrancea earthquakes of August 30, 1986, May 30, 1990 and May 31, 1990 is collected. The proposed functional form for the spectral displacement coefficient takes into account the behavior factor (which depends on the structural typology) and the control period as currently defined by the Romanian seismic design code P100-1/2013. The comparison of the results obtained with the ones computed using the relations given by the last two versions of the Romanian seismic design code reveals significant differences and highlights the need for further analyses.

An evaluation of the frequency contents of the recordings from the Vrancea seismic events which occurred in August 1986 and May 1990 shows that for some of the recording seismic stations there are considerable differences from one seismic event to the other while for other seismic stations, the differences are insignificant. Moreover, in the paper entitled “*The Vrancea earthquake of 1940.11.10, in the context of recent strong earthquakes. Use of available accelerographic data*”, the authors evaluate the transfer function of the soil deposits for a site situated in Bucharest. The difference in the spectral content of the ground motions recorded in Bucharest during the Vrancea is attributed by the authors to the source mechanism and not to the local geological conditions. Moreover, a faster attenuation of the Vrancea 1986 earthquake as compared to the event of May 1990 is also noticed by the authors. The study also highlights differences in directivity and radiation patterns between the considered intermediate-depth Vrancea seismic events.

The near-surface site effects in Bucharest are assessed in the study entitled “*Application of engineering tools as guidelines for estimating near-surface seismic effects*”. The shear-waves velocity in the upper 30 m of soil deposits, as well as other dynamic soil parameters are evaluated using both the MASW method, as well as the down-hole PS Logging. The comparison of the results obtained from both methods reveals smaller values derived from MASW method. Moreover, the authors propose a relation for the computation of the shear wave velocities from N-SPT values. Finally, a soil class C, according to Eurocode 8 is inferred from the analysis for all the investigated sites in Bucharest.

Use of Various Discrimination Techniques to Separate Small Magnitude Events Occurred in the Northern Part of Romania

Felix Borleanu, Bogdan Grecu, Mihaela Popa and Mircea Radulian

Abstract During the last decade Romanian Seismic Network has been significantly improved. A total number of 114 3-C seismic stations and the 2 seismic arrays ensure a good coverage of seismically active regions. As a consequence, the detection threshold decreased allowing location with higher accuracy of low magnitude ($M_L \sim 1.0$) seismic events. This led to a contamination of Romanian earthquakes catalog with artificial events occurred in different regions. The goal of the present study is to apply various discrimination methods like: spectral and amplitude ratio techniques, complexity factor evaluation and a multi-parameter discriminant on a data set characterized by lower magnitudes events recorded between 2011 and 2015. The selected data consists of small events occurred in the northern part of Romania in the neighborhood of Bucovina array (BURAR). The analysis was carried out on the waveforms recorded with a high signal to noise ratio using the vertical short period array components. Our results revealed that despite of some overlapping, these techniques show a good capacity to discriminate artificial by natural events for the study region.

Keywords Seismic events · Bucovina array · Signal to noise ratio

F. Borleanu (✉) · B. Grecu · M. Popa · M. Radulian
National Institute for Earth Physics, Măgurele, Romania
e-mail: felix@infp.ro

B. Grecu
e-mail: bgrecu@infp.ro

M. Popa
e-mail: mihaela@infp.ro

M. Radulian
e-mail: mircea@infp.ro

1 Introduction

Study of discrimination techniques to separate artificial by tectonic events is of high interest, as one can see from the various studies dealing with this subject (e.g. Kim et al. 1996; Ursino et al. 2000; Kekovali et al. 2012). One goal of such studies is to refine earthquake catalogs by excluding artificial events and to better define seismicity and tectonics peculiarities for the studied region. Another goal is the discrimination of nuclear tests and comparative analysis with tectonic events in order to calibrate travel times, azimuth and slowness for different seismic waves (Gupta et al. 1992). The goal of the present study is to test and implement powerful discriminant techniques able to differentiate natural by artificial events for a pilot region. The selected area, located in the northern part of the country is characterized by low-magnitude crustal events as well as by artificial events generated by several active quarries in the region (Fig. 1). All these events are detected and located mostly by the seismic stations of the Bucovina array (BURAR), located within 80 km. The peculiarity of this region is that contains various deposits (copper, manganese, iron, hydrocarbons, rocks), therefore numerous quarries blasts being generated due to these explorations. Due to the limitation of the seismic network coverage many of these events are not included in the Romanian earthquakes catalog (Oncescu et al. 1999), their detection and location being possible using only the array stations. On the waveforms recorded by the array stations we applied several discrimination approaches described by Kekovali et al. (2012) which proved a high efficiency for a region located in western part of Turkey.

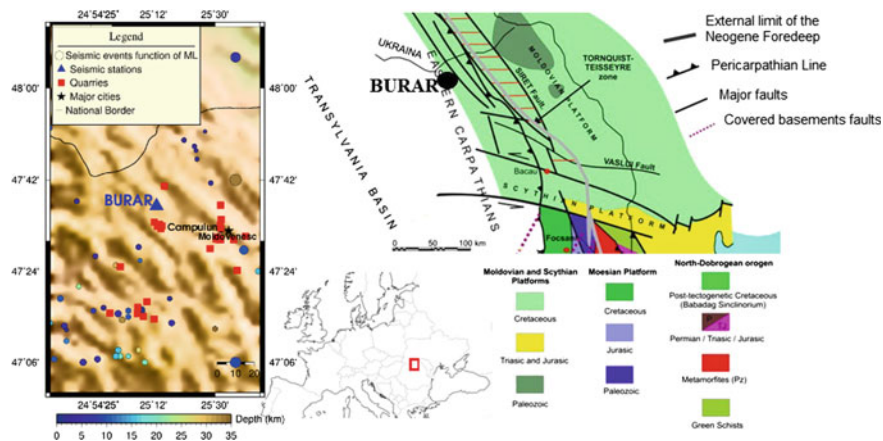


Fig. 1 Background seismicity map with BURAR location (*left side*). Events are plotted with different colors function of depth and different size function of local magnitude. The quarries are plotted with *red squares*. BURAR array is plotted with *blue triangle*. The geology and main tectonics features around BURAR array (*right side*) after Badescu (2005). An overview of the study region (*red square*) is represented on a sketch of European map

The Bucovina seismic array (BURAR) has been operating since 2002 as a result of cooperation between the National Institute for Earth Physics (NIEP), Romania and Air Force Technical Application Center (AFTAC), USA. BURAR array consists of 10 seismic stations equipped with seismic sensors installed in boreholes at depths between 30 and 50 m, spread over an area of 5×5 km. Nine stations (BUR01 ..., BUR09) are equipped with vertical short period sensors, GS21 and one station (BUR31) has a 3 component accelerometer sensor, KS54000. A comprehensive description of the array can be found in Grigore et al. (2004), Ghica (2011) and Borleanu et al. (2011). In the following, we highlight the main seismotectonics and geophysical features of the selected region, briefly describe the applied methods and the selected data set and discuss the obtained results as well as the conclusions drawn from the analysis.

2 Seismotectonics and Geophysical Overview

The Bucovina array is located in a generally aseismic area, which is characterized by sparse seismic events of low to moderate magnitude. A total number of 45 seismic events were recorded and located within a radius of 0.50° around the array in a time interval of 115 years. Most of them were generated in the upper crust, in a depth range between 0 and 35 km with magnitudes M_w below 5 according to Romanian catalog, Romplus (Oncescu et al. 1999). Only three earthquakes with magnitudes greater than 4 have been recorded. The largest earthquakes occurred exclusively before 1971 when the station coverage of the Romanian Seismic Network was poor and therefore the location accuracy and magnitude estimation was modest. A recent earthquake sequence occurred in June 2011 in the south-eastern part relative to BURAR. It consists of two foreshocks, a main shock of 3.5 M_w and aftershocks that lasted for several days. The geology of the site (Fig. 1) consists of epimetamorphic schists from Lower Paleozoic of green schist type and in some regions of limestone that covers the schists. Noise measurements performed revealed a low noise, displacement power spectra (PSD) situated between -8.6 dB at 1 Hz and -38.4 dB to 6 Hz (Grigore et al. 2004). The anomaly gravity map of Nicolescu and Rosca (1991), places the array location in a region of low anomaly while the heat flow map of Demetrescu and Andreescu (1994), highlights the array in a transition region between the Moldavian Platform, characterized by low heat flow levels (50 – 60 mWm^{-2}) and upper part of the Eastern Carpathians where higher values of heat flow predominate (70 – 90 mWm^{-2}). The maps of Moho depth distribution according to Raileanu (2009) and Ioane and Ion (Ioane and Ion 2005), place the discontinuity depth for the studied region at about 40 km.

3 Data and Methods

In order to perform the discrimination analysis, we applied the approaches described by Kekovali et al. (2012) on the recordings of BURAR seismic array components. Several discriminants were applied to investigate the data set: Lg/Pg amplitude and spectral ratios, complexity factor and multi-parameter discriminant (Pe). For this purpose we selected a data set containing 70 events (Fig. 2; Table 1, Appendix 1) with maximum hypocentral distances of 0.72° (25—supposed quarry blasts; 1—experimental blast and 44—supposed earthquakes) in order to test the proposed algorithms. The magnitude range of the selected events is represented in Fig. 2. The supposed earthquakes are within a magnitude range similar with that of the quarry blasts in order to have an appropriate energy release for both types of events. Two short-period stations of the array (BUR01 and BUR04) were randomly selected to exemplify our results.

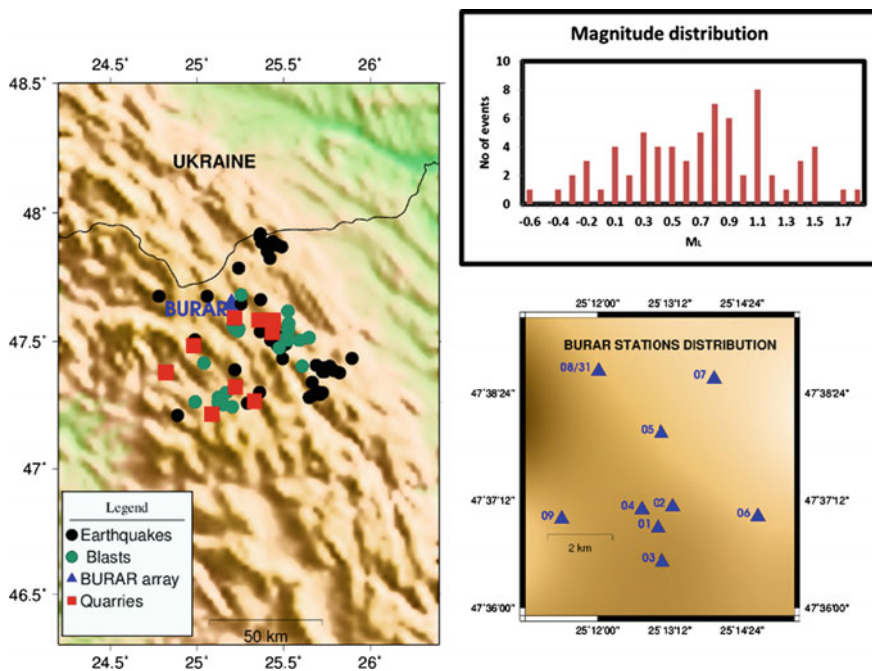


Fig. 2 Distribution of supposed earthquakes (*black dots*), supposed quarry blasts (*green dots*) and quarries (*red squares*) distribution and BURAR seismic array (*blue triangles*) location (*left side*). Local magnitude distribution of the selected events (*upper right corner*). BURAR stations distribution (*bottom right corner*)

4 Results

4.1 Amplitudes Ratio Discrimination

For the selected data set the optimum frequency of Pg and Lg (S)-waves for the vertical component of the velocity seismograms of short period stations of BURAR array. Figure 3 shows the waveforms recorded by BUR01 for a known blast (upper side) occurred on August 31, 2014 at 03:00:20 (UTC) and for an earthquake occurred on December 25, 2013 at 00:32:20. The blast was provided as a ground truth (GT) data from a wide angle refraction and reflection experiment (RomSeis 2014) recently carried out by a consortium of universities and research institutions along a line from the Ukrainian border. It is noteworthy the Pg and Lg (S) amplitudes for both events. Maximum amplitudes of the selected seismic phases were measured using Seismic Analysis Code (SAC, Goldstein and Snook 2005). The maximum amplitude ratios (Lg/Pg) as a function of logarithmic amplitudes of Lg (S) are shown in Fig. 4. The magnitude dependence of Lg/Pg ratios was reduced (Fig. 5) by selecting the same magnitude ranges for both type of events (quarry blasts and earthquakes). The amplitudes ratios dependence on distance for BUR01 station is plotted in the same figure. No tendency for amplitude ratios to change with magnitude or distance is visible. Many studies (Kim et al. 1996; Ursino et al. 2000; Kekovali et al. 2012) revealed a tendency for the earthquakes amplitude ratios to be higher than artificial events generated by the quarry blasts since the S wave amplitude on the (earthquake) seismogram is higher than the P wave amplitude.

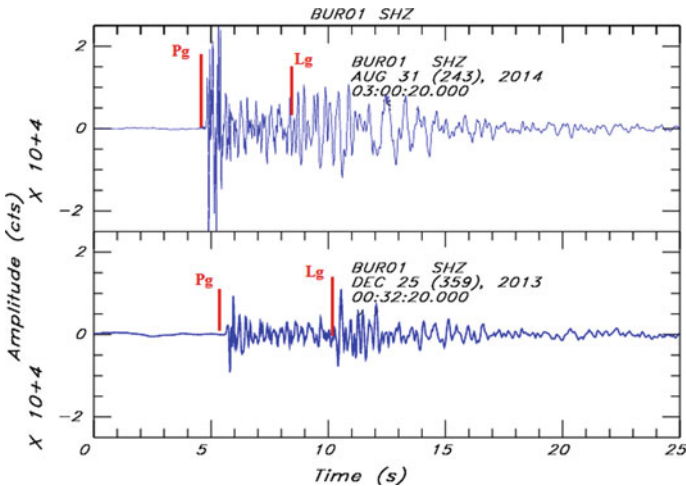


Fig. 3 BUR01 seismograms from a known blast (*upper image*) occurred on August 31, 2014 at 03:00 ($M_L = 1.1$) from an earthquake (*lower image*) occurred on December 25, 2013 at 00:32 ($M_L = 1.4$)

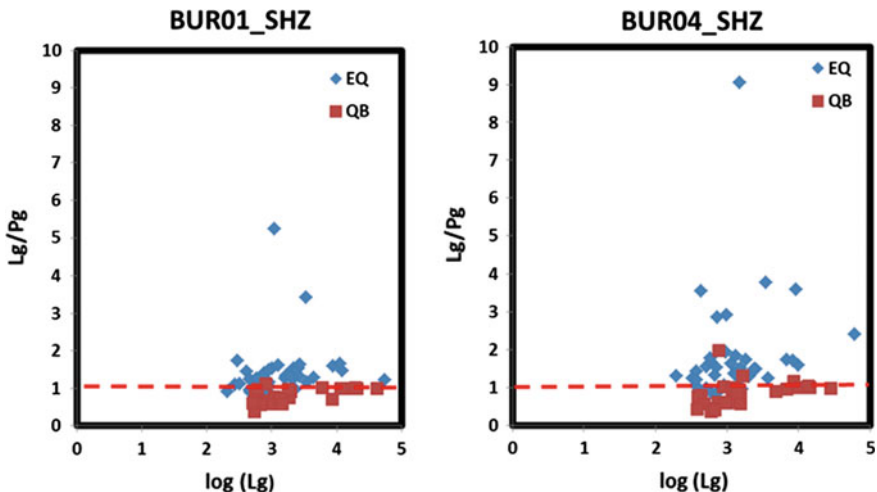


Fig. 4 Maximum amplitude ratios (Lg/Pg) function of logarithm of maximum amplitude of Lg (S)—wave computed for BUR01 and BUR04 velocity seismograms. The red dashed lines represent the separation limits

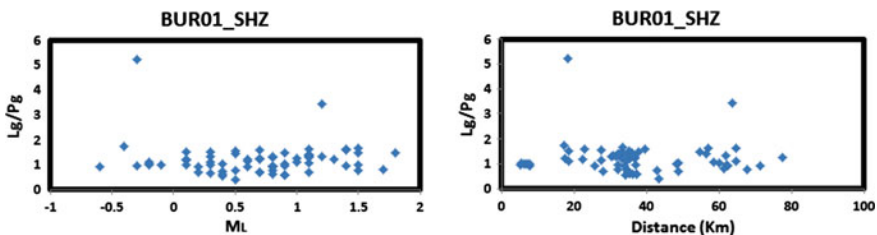


Fig. 5 Amplitude ratios dependence on local magnitude (M_L) and distance for BUR01 velocity seismograms

This usually occurs due to the isotropic character of the explosion sources, which generate mainly compressional P waves with S-waves vanishing or being very weak (Kim et al. 1996; Ursino et al. 2000; Kekovali et al. 2012). The amplitude ratios for the supposed blasts vary from between 0.39–1.11 and 0.78–5.23 for earthquakes (Table 2, Appendix 2). The values overlap for a range situated between 0.77 and 1.11, for both mining events and earthquakes recorded by BUR01 and in the 0.82–1.97 range for both mining events and earthquakes recorded by BUR04. The outcomes highlighted that the discriminant is not able to fully separate the whole set of events. The variability of Pg and Lg (S) amplitudes can be strongly dependent on site geology. The main disadvantage of this discriminant is that it can be easily influenced by signal-to-noise ratio, misidentification of the seismic phases and propagation path (Kekovali et al. 2012).

4.2 Complexity (C) Spectral Amplitudes and Spectral Ratio Amplitude (SR) Analysis

Using the same recordings, we determined complexity and spectral amplitude values with Seismic Analysis Code (SAC) using the Fast Fourier Transform (FFT). The discriminant uses the variation of complexity (C) with the spectral ratio of the seismogram (SR) for the selected events. In order to compute the complexity we used Eq. (1) proposed by Arai and Yosida (2004):

$$C = \frac{\int_{t1}^{t2} S^2(t)dt}{\int_{t0}^{t1} S^2(t)dt} \quad (1)$$

where S(t) represents the signal amplitude as a function of time (t) and C is the ratio of integrated powers of the vertical component of the velocity seismogram $S^2(t)$ in the determined time windows for mining blasts and earthquakes. As a result of previous discriminant we noticed that frequency and amplitude of seismic phases differ from natural earthquakes to artificial events. As a consequence, we used low and high time-frequency ranges to identify the energy distribution as a function of time and frequency. Therefore, we checked different frequency ranges in order to find differences in spectral shapes between these events. The integrals limits of C in Eq. (1) are determined through multiple trials in order to find the best performance of the discriminant. The complexity factor as a function of the maximum Lg/Pg amplitude ratios for the selected events is shown in Fig. 6. The complexity value is generally higher for the supposed earthquakes since the S waveform has a greater degree of complexity for earthquakes than for explosions. Similar results were obtained by Horasan et al. (2009), Oğutcu et al. (2011) and Kekovali et al. (2012). This approximation shows a better separation and better discrimination efficiency than amplitude ratio alone. Further, we tested on BURAR recordings the spectral ratio (SR) discrimination method in order to better separate shallow earthquakes from quarry blast in the array vicinity. The SR was determined using the ratio of integrated spectral amplitudes $a(f)$ of the seismogram in the selected frequency bands for blasts and earthquakes (Kekovali et al. 2012). The spectral ratio (SR) between the high-frequency (h_1, h_2) and the low-frequency bands (l_1, l_2) can be computed using equation of Gitterman and Shapira (1993):

$$Sr = \frac{\int_{h1}^{h2} a(f)df}{\int_{l1}^{l2} a(f)df} \quad (2)$$

The integrals limits were determined comparing the energy levels of earthquakes and blasts spectra. We test for different frequency ranges to find the spectral frequency band where the spectral ratio has a maximum efficiency. Thus, we noticed that for the seismic events occurred within this region the optimum frequency band is between 0.1 and 4 Hz for low frequencies and between 5.0 and 10 for high frequencies. We observed from Fig. 7 that the distribution of the two groups of

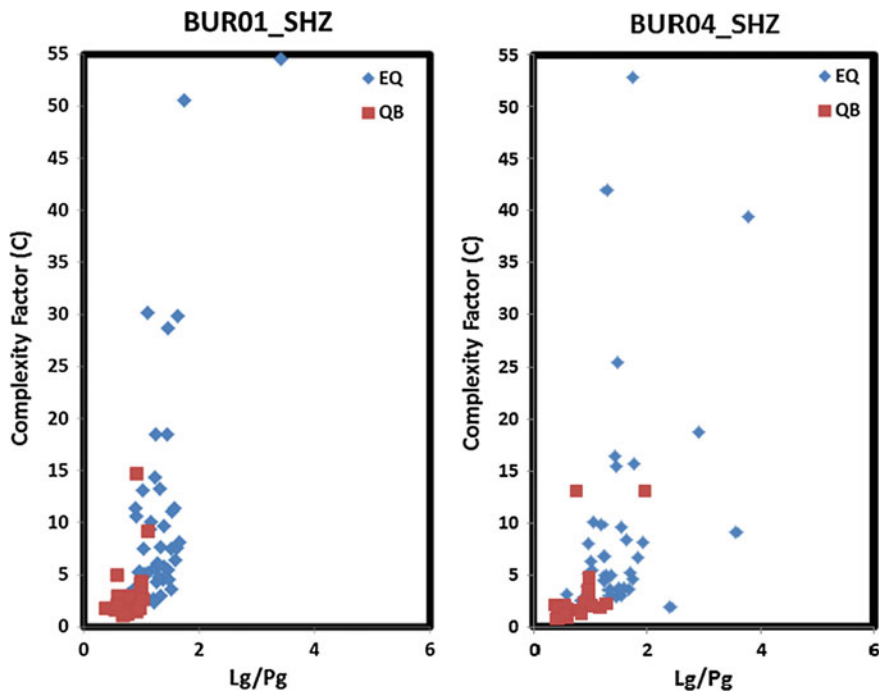


Fig. 6 Maximum amplitude ratio (Lg/Pg) function of complexity (C) factor computed for BUR01 and BUR04 velocity seismograms

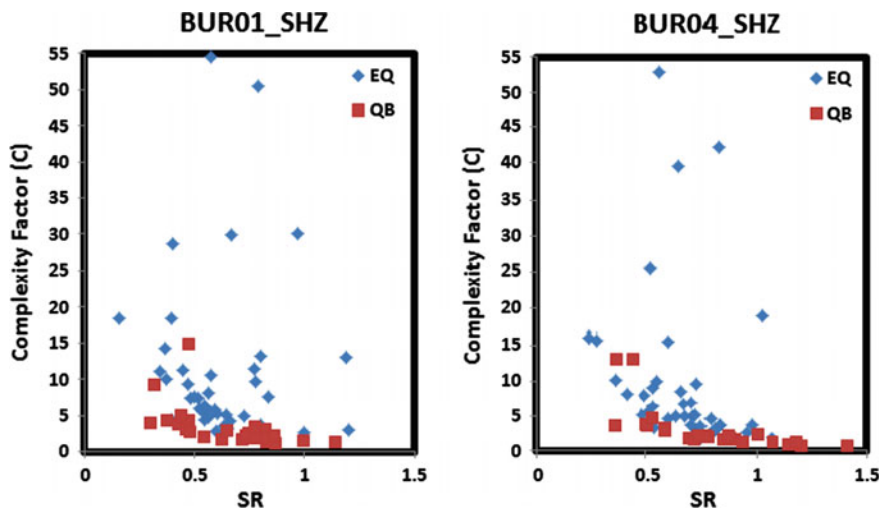


Fig. 7 Complexity (C) factor function of spectral ratio (SR) computed for BUR01 and BUR04 velocity seismograms

events is different. Both measurements (complexity factor and spectral ratios) have higher values for earthquake than for quarry blasts. However, there are still ranges where these values are overlapping, leading to the conclusion that some of the events can be incorrectly associated with the representative group.

4.3 Multi-technique Discrimination Analysis; Power of Event (Pe)

This type of discriminant proved to be very efficient for events with magnitude range between 2.2 and 3.0 occurred in western part of Turkey (Kekovali et al. 2012). It takes into account the amplitude ratios, complexity factor and spectral ratios results as well. In the following we applied this approach in order to improve the discrimination procedure for our study area. As a best compromise for both types of events a multi-parameter discriminant was defined according to Kekovali et al. (2012) as:

$$Pe = (R_{Lg/Pg})^2 \times C \times (SR)^2 \tag{3}$$

This new discriminant Pe, takes the square of amplitude ratio together with spectral ratio multiplied by complexity factor. Figure 8 shows the dependence between logarithmic Pe value and complexity factor (C). The values obtained for Pe considering analysis for earthquakes recorded by BUR01 vary between 0.85 and

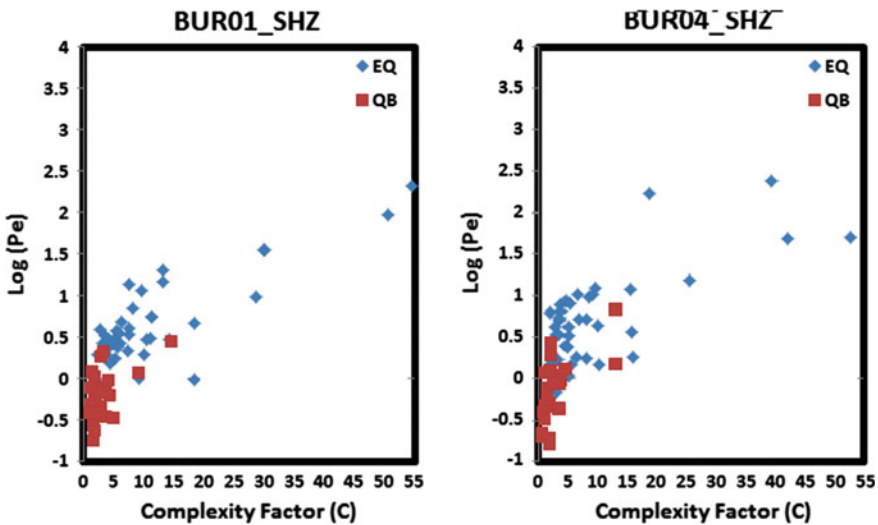


Fig. 8 Log (Pe) function of complexity factor (C) computed for BUR01 and BUR04 velocity seismograms

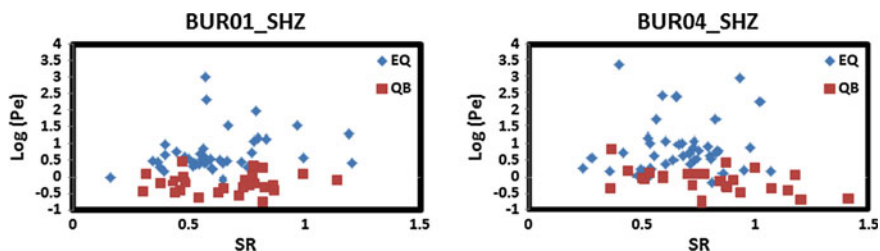


Fig. 9 Log (Pe) function of spectral ratio (SR) computed for BUR01 and BUR04 velocity seismograms

999 while for the quarry blasts, the values are rather close (between 0.177 and 2.79). The threshold given by log (Pe) separates rather well the two types of events (Figs. 8 and 9). The supposed earthquakes are characterized by positive values while the supposed quarry blasts have mostly negative values. For the supposed earthquakes recorded at BUR01 a single value is situated below the threshold (-0.069). For the quarry blasts recorded by the same station, 5 values are above the threshold (the maximum value of log Pe is 0.44). For the events recorded by BUR04, 2 supposed earthquakes have log Pe values below the threshold (-0.02 and -0.165), while for the quarry blasts 4 values were above the threshold (0.112, 0.163, 0.428 and 0.830). The dependence of Pe on spectral ratio, shown in Fig. 9, emphasizes similar results as in previous figure. Both figures reveal a tendency for earthquakes to increase the values of the discriminants taken into account, while for the quarry blasts they tend to be smaller.

5 Conclusions

The present paper represents the first attempt of analysis, where different techniques of discrimination between low magnitude local explosions and earthquakes (in a range of 0.72° relative to array) were applied on the waveforms recorded by vertical short period stations of the BURAR array, located in the northern part of Romania.

To this aim, we followed the approach proposed by Kekovali et al. (2012) for a selected data set spanning an extended time interval from 2011 to 2015 including a ground truth event, supposed earthquakes and quarry blasts in the same magnitude range. The obtained results showed (Table 1) that the proposed techniques are not fully capable to separate natural by artificial events. The Lg/Pg amplitude ratios show a relative well percentage of events discrimination. The amplitude ratios dispersion is slightly larger for supposed earthquakes than for supposed quarry blasts.

If we define a threshold value of Lg/Pg amplitude ratio of 1, the discriminant is overlapping for some events. Similar results were obtained in other studies (e.g. Koch and Fah 2002; Kekovali et al. 2012).

Another discriminant adopted in this study was the complexity factor (computed as the ratio of integral of squared signal for two different time windows) as function of spectral ratio (SR). As expected, the complexity values are larger for earthquakes than for supposed blasts with a threshold value which apparently varies from one station to the other. Despite of some overlapping, this parameter shows a good capacity to discriminate quarry blasts from earthquakes.

Finally, a multi-parameter discriminant (P_e) considered as a function of amplitude ratio, complexity and spectral amplitude ratio was applied on the same data set. The results show a high rate of success mainly for BUR01 station. The differences noticed between BUR01 and BUR04 stations, selected for this analysis, are likely to be influenced by the local geological conditions at stations and ambient noise.

Inherently the adopted methodology is limited as discrimination efficiency mostly because of the 3-D propagation effects and noise perturbation for magnitude below 1. The discrimination approach applied in this paper will be extended for 3-C stations and for other regions. Also, additional discriminants (e.g. cross-correlation) will be tested in order to enhance the efficiency of separate natural from anthropic events in the seismic recordings.

Acknowledgements This study was supported by AFTAC Research Project—FA70211C0015. Data used in the present study were provided by the National Institute for Earth Physics (Romania). The study was partly funded by the projects PN 09—30—0101 and PN 09—30—0102 of the Nucleu programe of the National Authority for Scientific Research and Innovation.

Appendix 1

See Table 1.

Table 1 Selected events for discrimination analysis (with bold are marked supposed blasts)

Crt. no.	Date (yyyymmdd)	Origine time (GMT) {hh:mm}	Latitude (°N)	Longitude (°E)	Depth (km)	Magnitude (M _L)	Discrimination results
1	20110624	13:16	47.38	25.73	4.9	1.7	QB
2	20110624	13:19	47.34	25.67	13.6	1.1	EQ
3	20110624	13:22	47.28	25.65	7.7	1.1	EQ
4	20110624	13:34	47.41	25.69	5.0f	1.1	EQ
5	20110624	13:44	47.29	25.67	5.7	0.9	EQ
6	20110624	14:08	47.4	25.77	5.1	1.4	EQ
7	20110624	14:10	47.38	25.74	9.2	0.8	EQ
8	20110624	14:12	47.4	25.74	10.9	1.2	EQ
9	20110624	14:41	47.43	25.9	5.0f	1.0	EQ
10	20110624	15:30	47.39	25.79	2.6	1.5	EQ
11	20110624	15:42	47.38	25.82	5.0f	0.8	EQ
12	20110625	6:50	47.3	25.7	14.6	1.4	EQ
13	20110625	6:51	47.3	25.73	16.6	1.0	EQ
14	20110701	8:32	47.3	25.36	0.0	0.1	EQ
15	20110701	12:21	47.29	25.71	5.0f	1.2	EQ
16	20131222	18:45	47.89	25.44	0.0	0.7	EQ
17	20131223	7:57	47.92	25.37	0.0	1.1	EQ
18	20131223	9:31	47.88	25.4	6.3	1.5	EQ
19	20131223	10:11	47.82	25.42	11.7	0.8	EQ
20	20131224	3:20	47.88	25.44	0.0	1.1	EQ
21	20131224	10:32	47.88	25.46	0.0	0.9	EQ
22	20131225	0:32	47.87	25.49	0.0	1.4	EQ
23	20131225	7:16	47.89	25.37	9.6	1.1	EQ
24	20131225	13:33	47.85	25.41	2.5	1.1	EQ

(continued)

Table 1 (continued)

Crt. no.	Date (yyymmdd)	Origine time (GMT) {hh:min}	Latitude (°N)	Longitude (°E)	Depth (km)	Magnitude (M_L)	Discrimination results
25	20131227	9:10	47.91	25.36	0.0	1.5	EQ
26	20140312	12:17	47.51	25.51	0.0	0.8	QB
27	20140313	12:13	47.51	25.52	0.0	0.8	QB
28	20140314	12:44	47.5	25.53	0.0	0.9	QB
29	20140412	10:16	47.25	25.15	0.0	0.9	QB
30	20140415	10:17	47.51	25.51	0.0	0.6	Not defined
31	20140423	11:41	47.40	25.61	0.0	1.5	Not defined
32	20140504	10:01	47.3	25.17	0.0	0.9	Not defined
33	20140508	11:02	47.52	25.65	0.0	0.7	QB
34	20140516	12:40	47.24	25.21	0.0	0.9	QB
35	20140522	14:11	47.51	24.99	0.0	0.6	Not defined
36	20140612	10:12	47.56	25.21	0.0	-0.2	QB
37	20140702	9:11	47.5	25.59	0.0	0.4	QB
38	20140702	10:50	47.68	25.25	1.4	-0.6	Not defined
39	20140709	15:40	47.54	25.37	8.1	-0.3	EQ
40	20140709	16:08	47.68	25.06	0.0	-0.2	EQ
41	20140709	16:17	47.68	24.78	0.0	0.4	EQ
42	20140709	16:37	47.79	25.24	0.0	-0.4	EQ
43	20140714	11:24	47.54	25.53	3.2	0.4	QB
44	20140715	10:21	47.55	25.53	11.8	0.3	QB
45	20140719	12:12	47.55	25.22	0.0	0.3	QB
46	20140725	12:17	47.26	25.12	0.0	0.8	Not defined
47	20140726	14:16	47.26	25.29	0.0	0.6	EQ
48	20140728	10:36	47.57	25.53	0.0	0.2	QB

(continued)

Table 1 (continued)

Crt. no.	Date (yyymmdd)	Origine time (GMT) {hh:min}	Latitude (°N)	Longitude (°E)	Depth (km)	Magnitude (M_L)	Discrimination results
49	20140730	11:48	47.62	25.53	13.3	0.3	Not defined
50	20140802	10:36	47.55	25.23	0.0	0.1	QB
51	20140803	9:21	47.48	25.46	13.2	0.8	EQ
52	20140813	9:55	47.47	25.48	7.5	1.5	QB
53	20140820	14:06	47.21	24.89	0.0	1.8	EQ
54	20140826	12:58	47.26	24.99	0.0	0.5	QB
55	20140831	16:54	47.5	25.43	0.0	0.2	EQ
56	20140831	3:00	47.41	25.04	0.0	1.1	GT
57	20140901	10:39	47.51	25.51	0.0	0.4	QB
58	20140902	9:47	47.43	25.5	0.0	0.5	Not defined
59	20140904	11:39	47.39	25.22	0.0	0.7	EQ
60	20140907	21:49	47.65	25.26	3.5	-0.3	EQ
61	20140908	9:33	47.52	25.5	0.0	0.3	EQ
62	20140909	15:18	47.66	25.37	0.0	1.3	EQ
63	20140909	13:01	47.54	25.24	0.0	-0.1	QB
64	20140910	10:37	47.55	25.24	0.0	-0.2	QB
65	20140912	11:15	47.48	25.49	0.0	0.7	EQ
66	20140917	9:35	47.49	25.51	13.2	0.3	EQ
67	20140917	9:30	47.28	25.13	0.0	0.7	QB
68	20140923	11:03	47.56	25.38	0.0	0.1	EQ
69	20140924	9:14	47.54	25.41	0.0	0.1	EQ
70	20140927	10:27	47.53	25.45	4.3	0.5	EQ

Appendix 2

See Table 2.

Table 2 Statistics of the amplitude ratios results

Discrimination technique	BUR01		BUR04	
	Supposed EQ	Supposed QB	Supposed EQ	Supposed QB
Lg/Pg (maximum value)	5.2336	1.1149	9.05015	1.97004
Lg/Pg (minimum value)	0.7705	0.3876	0.57764	0.36881
Standard deviation	0.7142	0.1910	1.34120	0.33946
Arithmetic mean	1.4181	0.7943	1.75720	0.83867

EQ earthquake; *QB* quarry blast; *GT* ground truth

References

- Arai N, Yosida Y (2004) Discrimination by short-period seismograms. International institute of seismology and earthquake engineering, Building Research Institute (IISEE), Lecture Note, Global Course, Tsukuba
- Badescu D (2005) The evolution of the tectono-stratigraphy of the Eastern Carpathians during Mesozoic and Neogene times. Editura Economică, Bucharest (in Romanian)
- Borleanu F, Popa M, Radulian M, Schweitzer J (2011) Slowness and azimuth determination for Bucovina array (BURAR) applying multiple signal techniques. *J Seismolog* 15(3):431–442
- Demetrescu C, Andreescu M (1994) On the thermal regime of some tectonics units in a continental collision environment in Romania. *Tectonophysics* 230:265–271
- Ghica DV (2011) Detection capabilities of the BURAR seismic array—contributions to the monitoring of regional and distant seismicity. *J Seismolog* 15(3):487–506
- Gitterman Y, Shapira A (1993) Spectral discrimination of underwater explosions. *Isr J Earth Sci* 42:37–44
- Goldstein P, Snoke A (2005) SAC availability for the IRIS community. *Incorporated Inst Seismolog Data Manag Center Electron Newslett* 7:1–6
- Grigore A, Grecu B, Rizescu M, Ionescu C, Ghica D, Popa M (2004) A new seismic station in Romania: the Bucovina seismic array. *Rev Roum Géophysique* 48:69–72 (Bucharest)
- Gupta IN, Chart W, Wagner RA (1992) A comparison of regional phases from underground nuclear explosions at East Kazakhand Nevada Test Sites. *Bull Seismol Soc Am* 82:352–382
- Horasan G, Guney AB, Kusmezer A, Bekler F, Oğutcu Z, Musaoğlu N (2009) Contamination of seismicity catalogs by quarry blasts: an example from İstanbul and its vicinity, northwestern Turkey. *J Asian Earth Sci* 34(1):90–99
- Ioane D, Ion D (2005) A 3D crustal gravity modelling of the Romanian territory. *J Balkan Geophys Soc* 8(4):189–198
- Kekovali K, Kalafat D, Deniz P (2012) Spectral discrimination between mining blasts and natural earthquakes: application to the vicinity of Tunçbilek mining area, Western Turkey. *Int J Phys Sci* 7(35):5339–5352
- Kim WY, Aharonian V, Abbers G, Lerner-Lam A, Richards P (1996) Discrimination of earthquakes and explosions in southern Russia using regional high-frequency data from IRIS/JSP Caucasus network. *Bull Seismol Soc Am* 87(3):569–588
- Koch K, Fah D (2002) Identification of earthquakes and explosions using amplitude ratios: the Vogtland area revisited. *Pure appl Geophys* 159:735–757

- Nicolescu A, Rosca V (1991) Romania. The Bouguer anomaly map, scale 1: 1,000,000. Geological Institute of Romania
- Oncescu MC, Marza V, Rizescu M, Popa M (1999) The Romanian earthquakes catalogue between 1984 and 1997. In: Wenzel F, Lungu D (eds) Vrancea earthquakes: tectonics, hazard and risk mitigation. Kluwer Academic Publishers, Kluwer, pp 43–47
- Oğutcu Z, Horasan G, Kalafat D (2011) Investigation of microseismic activity sources in Konya and its vicinity, central Turkey. *Nat Hazards* 58:497–509
- Raileanu V (2009) Caracterizarea geologica si parametrii elastici ai amplasamentelor statiilor seismologice si de accelerometere din retea Institutului National de C-D pentru Fizica Pamantului. In: Marmureanu G (coord.) Cercetari privind managementul dezastrelor generate de cutremurele romanesti, Editura Tehnopress, ISBN:973-702-701-9 (in Romanian)
- Ursino A, Langer H, Scarfè L, Di Grazia G, Gresta S (2000) Discrimination of quarry blasts from tectonic earthquakes in the Iblean Platform (Southeastern Sicily). *Atti del 19° Convegno del Gruppo Nazionale di Geofisica della Terra Solida, Consiglio Nazionale Delle Ricerche, Roma*

Prediction of Site Characterization Based on Field Investigations and Empirical Correlations

Elena-Andreea Călărășu, Cristian Arion and Cristian Neagu

Abstract Significant damages of built environment recorded during past seismic events, closely linked to notable human and financial losses, have led to consideration of Romania's capital city as one of the major earthquake-prone urban area worldwide. Strong historical ground shaking and extensive distribution of seismic networks have outlined that variability and specific parameters of layered unconsolidated sedimentary young deposits represents one of key component in site-response analysis. To predict seismic effects of near-surface soils, comprehensive surveys are needed for a realistic estimation of dynamic behaviour and site characterization. A large number of shallow and deep boreholes, standard penetration tests and non-invasive field techniques as down-hole and SASW measurements have been carried out in Bucharest sites. All the tests reported in the paper were performed at CNRRS (National Center for Seismic Risk Reduction) (now, Seismic Risk Assessment Research Center <https://ccers.utcb.ro>) and UTCB (Technical University of Civil Engineering of Bucharest). Shear wave velocities and penetration resistance have been set as main indicators in quantifying seismic properties. Empirical correlations to predict V_s from N-SPT test values were developed by using statistical methods. A comparative method between soil dynamic indexes determined by in situ investigation and the ones predicted using empirical models have been performed. The end-results can be considered as guidelines to predict the potential effect of site conditions on similar soil types, layer sequences and properties.

Keywords Sedimentary layers · Site characterization · Field measurements

E.-A. Călărășu (✉)
Bucharest INCERC Branch, National Institute for Research and Development in
Construction, Bucharest, Romania
e-mail: andreea.calarasu@gmail.com

C. Arion · C. Neagu
Seismic Risk Assessment Research Center, Technical University of Civil Engineering,
UTCB, Bucharest, Romania
e-mail: arion@utcb.ro

C. Neagu
e-mail: cristi.neagu@utcb.ro

1 Introduction

The consequences of amplification effects induced by near-surface geological site conditions, associated with damage patterns and significant changes in amplitude and variation on certain frequencies of ground shaking, have been documented starting with historical 1891 Mino-Owari earthquake ($M_S = 8.0$), 1906 San Francisco ($M_w = 7.8$) and 1923 Great Kanto earthquake ($M_w = 7.9$). Initial investigations of site effects were primarily concerned on predicting an overall regional seismic response, without special attention of site behaviour estimation. Over the years, worldwide destructive seismic events occurred during 20th century: 1940 El Centro ($M_w = 6.9$), 1964 Niigata ($M_w = 7.6$), 1971 San Fernando ($M_w = 6.7$), 1985 Michoacan ($M_w = 8.0$), 1989 Loma Prieta ($M_w = 6.8$), 1994 Northridge ($M_w = 6.7$), 1995 Hyogoken-nanbu ($M_w = 6.9$), 1999 Kocaeli ($M_w = 7.6$) and 21st century: 2003 Tokachi-Okii ($M_w = 8.3$), 2008 Sichuan ($M_w = 7.9$), 2010 Christchurch ($M_w = 7.1$), 2010 Chile ($M_w = 8.8$), 2011 Tohoku ($M_w = 9.0$) are demonstrated that distribution of severe structural building damages in a specific area is more or less controlled by surface geology and the effect of local soil conditions. A large number of scientific studies for emphasizing the importance of site conditions in characteristics of seismic motion at ground surface have been carried out in the last decades (Borcherdt 1970; Seed et al. 1987; Idriss 1991; Bard 1995). Different effects of shallow layers on ground motion, including impedance contrast of bedrock and overlaid sediments, are linked to topographical terms (Faccioli 1991; Chavez García et al. 1996) and geological and geotechnical setting (Aki 1988; Ansal 1994), which explained the variability of ground accelerations and response spectra values as a result of local site conditions.

Bucharest city is assigned as the most affected area by Vrancea subcrustal earthquakes, with a high concentration of building damages, casualties and economic loss due to its relative proximity to the epicentre and specificity of surface geology structure. Major historical seismic events generated by Vrancea source (1802: $M_w = 7.9$; 1940: $M_w = 7.7$ and 1977: $M_w = 7.4$) have indicated the great influence of particular characteristics and geometrical features of soil layers on seismic motion parameters.

The November 10th, 1940 Vrancea earthquake ($M_w = 7.7$) was largely investigated and represents the starting point of earthquake engineering in Romania. The damage pattern in Bucharest and in Romania was explained by the effect of site geology on ground motion. The earthquake triggered liquefaction at many sites in South Moldavian Plain (Fig. 1) and in Romania Plain including Bucharest, the water blowing out up to 1 m height. The occurrence of mud volcanoes with diameters up to 1.5 m and heights up to 15 cm was reported in the epicentral area. At many sites in Romanian Plain and South of Moldova the earthquake produced ground cracks along river meadows (rivers Prut, Siret, Trotus, Putna, Ialomita, Prahova, Arges and Dambovita). The majority of these cracks were accompanied by liquefaction. Their dimensions reached 250 m length and 2–3 m opening. The earthquake also induced landslides mainly in hilly region in epicentral area. At

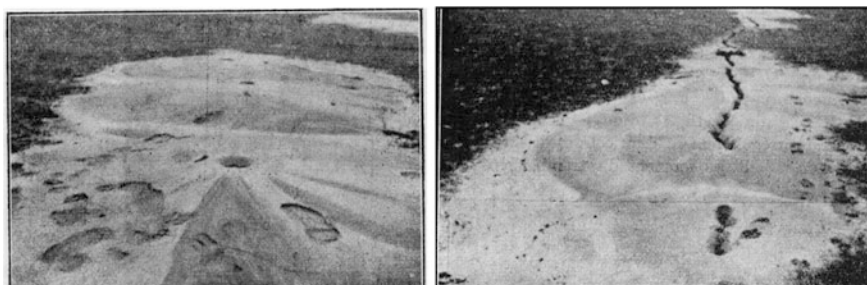


Fig. 1 November 10, 1940 earthquake—liquefaction and ground cracks in Putna river meadow (Moldavia). Reproduced from *Comptes Rendus des Séances de l'Académie des Sciences de Roumanie* (1941)

Galati on Danube border, a church collapsed and the cathedral lost its bell towers due to the sliding of a loess deposit. The vibration of a large loess plateau during the same event caused significant damage to a large number of houses in Braila (also located along Danube River). Landslides were reported even in northern Bulgaria along Danube border. The underground water level was also disturbed by the earthquake, the increase of water table level (up to 7 m) being reported in many places in Moldavian and Romanian Plains.

As a result of paleoclimatic conditions and sedimentary environment during Quaternary period, the surface geological deposits from Bucharest area are composed from unconsolidated alluvial layers with variability in thickness and spatial distribution of cohesive and cohesionless soils. The relative heterogeneity of young formations in an alluvial basin explains the peculiar behaviour during Vrancea strong motions imposed by local geology to seismic response. Concerning the assessment of near-surface site effects during 1977 Vrancea seismic motion, Ishihara and Perlea (1984) provide the first scientific detailed research regarding the liquefaction-associated ground damage of Dambovita river sandy deposits, based on extensive in situ site investigation.

Modern seismic codes (Uniform Building Code, 1997; International Building Code, 2009; Building Standard Law in Japan, 2000 and Romanian P100-1/2013) and other significant regulations and standards (NEHRP 2003, SR EN 1998-1: 2004) include provisions regarding site response. In mentioned codes, site effects are either quantified by seismic response coefficient linked to soil category and seismicity level or through different spectral shapes specific for defined soil types. Generally, ground conditions refers to soil classes differentiated by qualitative criteria as layers sequences in lithological profile and quantitative ones as shear wave velocities and penetration resistance values. Recently, the studies concerning local site effects assessment on Vrancea strong ground motions have substantially increased (Aldea et al. 2003; Arion et al. 2007, 2012; Bala et al. 2013; Lungu et al. 2000), as a result of upgrading and extending of seismic networks, modern equipment used for data recording, storage and real-time transmission, development of specialized software for scenarios and seismic loss estimation and seismic

response modelling, as well as improvement of ground investigation techniques. The present paper will contribute to this research topic by providing data obtained from detailed surveys performed on different Bucharest areas and empirical correlations of specific indicators (V_s and N-SPT) for site characterization of near-surface sedimentary to be further integrated in seismic response studies.

2 Engineering Methods Used for Surface Geology Survey

2.1 Key Parameters Approach and Methodology Description

To assess the seismic effects of near-surface layered structures on ground response, an accurate determination of soil characteristics beneath a target site is required. Usually, site characterization in calculating seismic hazard is governed by shear wave velocities values (V_s), being considered as one of the most important components defining ground motion and soil-structure interaction. The application of V_s has the advantage of being based on an objective measure which affects ground motion in a way that can be modelled. Conventional criteria used for earthquake engineering design purposes (Borcherdt and Glassmoyer 1994) are typically based on the distribution of shear wave velocities with depth in the upper 30 m of surface soil structures ($V_{s,30}$). Considered as reference index of dynamic behaviour at small-strain levels, $V_{s,30}$ is used to classify sites according to the soil class. Although there is a widely application of this basic elastic property, it can be noticed that there is no complete agreement of using $V_{s,30}$ as single parameter in seismic amplification. Recent studies have highlighted additional input factors in ground response assessment, as vibration fundamental period of soil column by referring to thickness, topography and source directivity (i.e., Mucciareli and Gallipoli 2006). Complementary, the number of blow counts gathered from Standard Penetration Test (N-SPT) can be used for seismic classification of soils.

According to global concerns for a more reliable strong motion prediction, comprehensive geophysical and geotechnical investigations have to be conducted in various sites of Bucharest during JICA (Japan International Cooperation Agency) project by the CNRRS team. A large number of shallow and deep boring logs, which covering a significant part on city, have been carried out in order to identify the soil type and thickness of stratified sediments.

Down-hole PS Logging have been used as simple and non-invasive geophysical technique for measurement of seismic waves velocities in more than 20 sites, with a depth investigation ranging from 30 m up to more than 100 m. The impulse source of energy is generated at the ground surface, shear wave records (SH and SV) being obtained by striking a wood plank horizontally and in opposite direction, while compression wave by dropping a wood hammer on the ground. The velocity sensor is composed by three geophones (2 horizontal and 1 vertical). During down-hole measurements, sensor was lowered in borehole up to a predetermined depth



Fig. 2 PS Suspension logging system (down-hole technique)

investigation, being blocked on boring wall for detecting the waves generated by the surface source at 1 m interval of soil column. The equipment system (see Fig. 2) used for velocity measurements is composed from GEODAS acquisition station and PS Logging sensor.

Based on the records collected from down-hole techniques on various sites, measured travel time reflects cumulative travel through layers with different wave velocities. Since P and S wave velocities are calculated from the slope of a depth/travel time curve, wave velocities are obtaining for a velocity layer that has a certain thickness including many measuring points as an average values. Specialized software PsLog has been used for data acquisition and software application PS Start for recorded data processing. The 1D velocity profiles of sites (Fig. 3) are also including a description of soil layer type identified by borehole sampling, which can be considered as a boundary index when dealing with sensitive differences of recorded velocities. It is widely recognized the utility of shear modulus (G_d), Young modulus (E_d) and Poisson's ratio (ν), which represents the key characteristics in predicting soil response and soil-structure system to dynamic load actions. Considering P and S-wave velocity values, elastic soil properties of each soil layer from investigated profile were computed.

An alternative technique to obtain S-wave velocity profile at near-surface soil structure is multi-channel analysis of surface waves (MASW) method, in which the dispersion character of experimental Rayleigh waves is analysed, was also conducted for Bucharest sites. Recently, the method is applied to engineering problems for microzonation and site response studies and geotechnical characterization of shallow sediments (Park et al. 2001). The MASW method developed to estimate Vs profile is considered as a non-intrusive technique, cost effective, easy procedure and less time consuming as compared to other seismic methods used for shallow deposits. The MASW system for measuring short wavelength of surface waves consists in an impact source to generate energy (sledge hammer), 12–48 geophones placed in a linear array at 3 m intervals, with 4.5 Hz frequency and data logger, (Fig. 4).

Additionally to seismic methods, more than 30 applications of standard penetration tests have been performed, with depth investigation ranging from 20 to 50 m

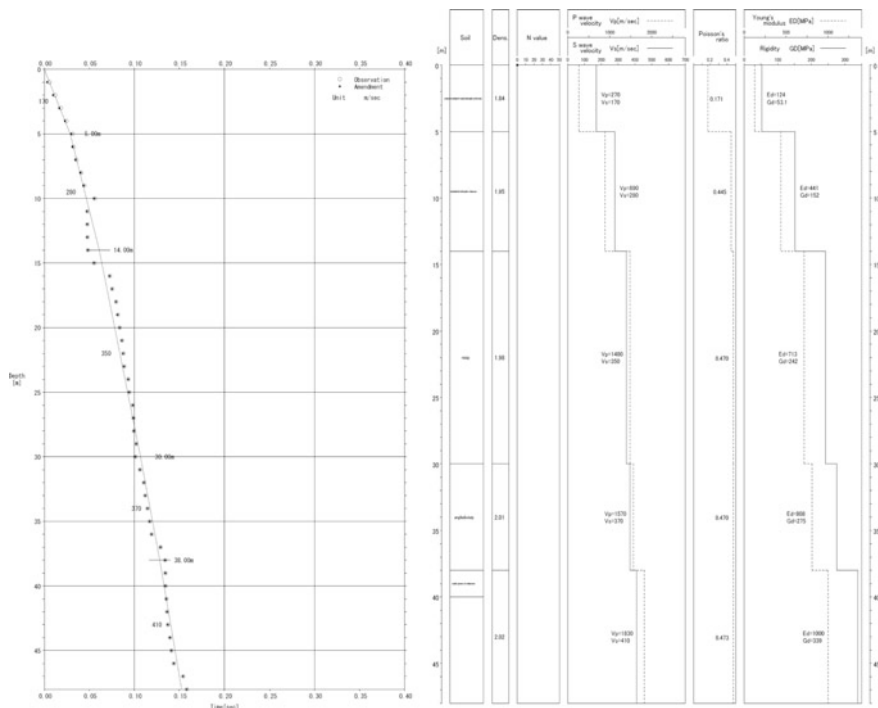


Fig. 3 Velocity profiles and dynamic parameters obtained from down-hole measurements

in order to assess penetration soil resistance of shallow layers. Standard Penetration test (SPT) represents one of the oldest, popular and common geotechnical method for in situ investigation used in geotechnical and earthquake engineering projects because of simplicity of equipment and efficiency of test procedure. Standard Penetration Test is used to determine soil type, strength and deformation characteristics, with special applications in cohesionless soils, being generally recommended for geotechnical investigations of shallow deposits.

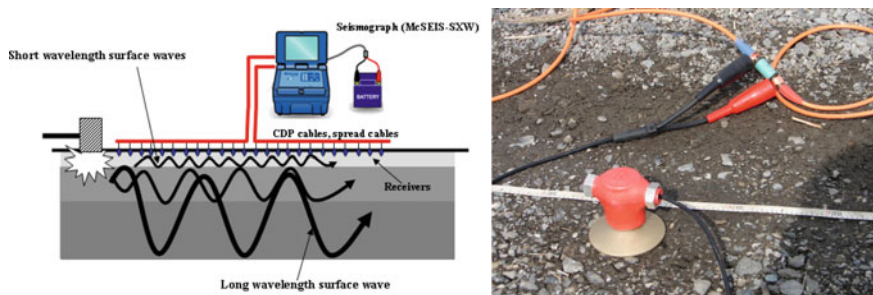


Fig. 4 Data acquisition system and geophone for MASW method



Fig. 5 Standard penetration technique (equipment and sampling)

In particular SPT method are widely used for seismic site characterization, site response and liquefaction studies towards seismic microzonation due to large data availability (Ansal et al. 2004; Dobry et al. 2000; Arion et al. 2015). Penetration resistance values have to be used as a supplementary parameter or combined with V_s for defining soil categories and seismic site characterization. The tests have been carried out by using drilling equipment FRASTE Drilling Rig Type Multidril XL, which has as attachment an automatic device for this test (Fig. 5). The resistance to penetration was obtained by counting the number of blows required to drive a steel tube of specified dimensions into the subsoil to a specified falling height using a hammer with standardized weight. The disadvantage of method consists in limited shallow depth investigation up to 40–50 m and soil disturbance, being considered an invasive geotechnical technique.

2.2 Data Processing and Site Characterization

From geotechnical point of view, based on observational and testing results, investigated sites consists in the following layer sequences from the top to bottom of soil profile: (1) loess-like deposits with clayed and sandy silts, silty and sandy clay, medium to high plasticity and high porosity (40–45 %); (2) poorly-graded fine to medium gravel with fine to coarse sands, loose to medium dense state; (3) clays and intercalation of silty and sandy clays, medium to high plasticity, stiff consistency state with cohesion up to 60 kPa; (4) well-graded medium to coarse sands, with intercalations of sandy clay and silt, medium dense to very dense state;

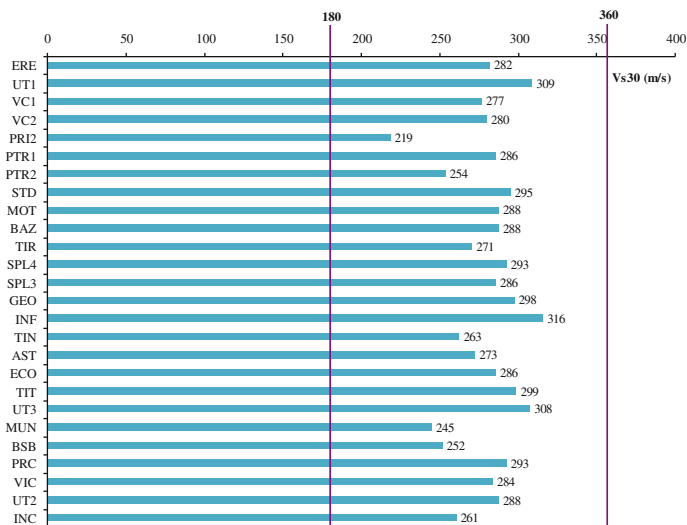


Fig. 6 Distribution of $V_{s,30}$ values on sites

(5) clays and marl clay, very stiff to hard consistency state with cohesion up to 90 kPa, high plasticity. Soil characterization based on specific characteristics in profiles was emphasized lateral and vertical inhomogeneity of soil layers, reflected in thickness variability on sites. Furthermore, for a comprehensive site characterization, results of field investigation are integrated. According to modern seismic code provisions, the average shear wave velocity of the upper 30 m can be calculated with the following eq.:

$$V_{s,30} = 30 / \sum_{i=1}^n (d_i / V_{si}) \tag{1}$$

where: d_i and V_{si} denote the thickness (m) and shear wave velocity of the i th layer from the upper 30 m. By processing field data measurements and developing V_s profiles, $V_{s,30}$ values were calculated in accordance with (Eq. 1) ranging from 219 to 316 m/s, as illustrated in Fig. 6. The sites are classified in soil class S, which correspond to a stiff soil profile ($V_{s,30} = 180\text{--}360$ m/s) according to UBC 97, IBC 2009 and NEHRP 2003 provisions. Compared to these standards, $V_{s,30}$ values belong to class C corresponding to intermediary soil profile according to EC8 and P100-1/2013, consisting in deep deposits, with thick dense and medium dense sand, gravel and clay.

The experimental values of shear-wave velocities gathered from down-hole measurements were grouped and analyzed in several statistical distribution for estimating the factors and relations between parameters for a better understanding of dynamic behaviour of soil conditions from engineering point of view. Using power regression type, it can be observed a strong correlation of V_s values

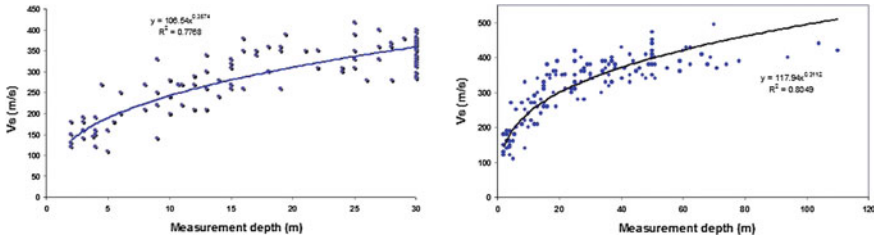


Fig. 7 Distribution of V_s values in the upper 30 m and maximum depth investigation

calculated for each depth interval in the upper 30 m and maximum depth investigation, reflected by coefficient correlation of about 0.78, respectively 0.80, as represented in Fig. 7. V_s values measured down to maximum depth of site investigation are varying from 261 to 361 m/s. Moreover, the comparison of these set of values reveals a relative low increase of S-velocities ranging from 10 up to 15 % for a great part of sites. For deep measurements, the increase of V_s values calculated for total investigation thickness of soil layers can reach 20–30 %, so it can be mentioned that thickness of sedimentary layers intercepted in boreholes can represent an important factor in velocity profiles, especially in case of deep alluvial deposits.

Assessment of soil conditions was also based on the estimation of elastic parameters. In situ measurement of S-wave velocities carried out in different area of Bucharest were indirectly providing data related to shear modulus G , which can be related to low-strain dynamic behaviour. There are several correlations focused on empirical determination of dynamic shear modulus (G_d) based on data collected from standard penetration, grain size distribution and Atterberg limits. The importance of G_d is emphasized by the use of parameter in soil behaviour modelling and dynamic response of soil-structure system. The computed values of G_d were ranging from 27 MPa up to 403 MPa, Young modulus from 68 MPa up to 1227 MPa and Poisson’s ratio from 0.17 to 0.49, covering a large variability of soil and their characteristics which correspond to soft and firm clayey and sandy soil categories.

An important issue in site effects assessments is to estimate characteristic period of site, defined as period of vibration corresponding to the fundamental frequency. The vibration period of soil layers in the upper 30 m ($T_{s,30}$) is calculated using the equation specified in P100-1/2013:

$$T_{s,30} = 4h/V_{s,30} \tag{2}$$

where: h is soil depth (30 m) and $V_{s,30}$ is average S-wave velocities on the first 30 m. The minimum value of $T_{s,30}$ was 0.38 s and the maximum value was 0.55 s for investigated sites. The elastic natural period of a specific site have to be taking into account in relation with vibration period of structure in order to estimate amplification effects on soft soils.

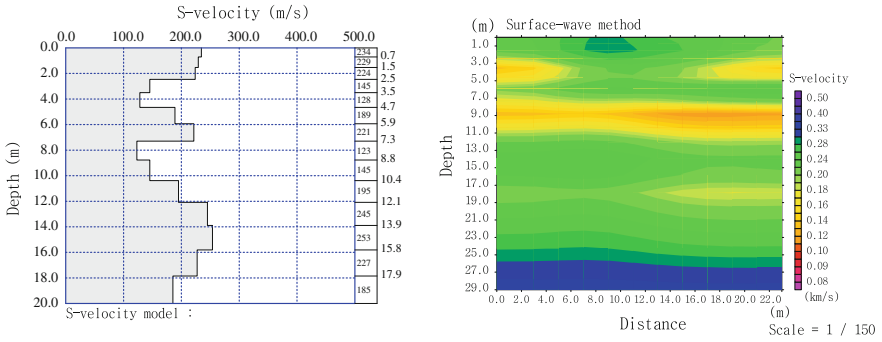


Fig. 8 1D and 2D shear wave velocity profiling

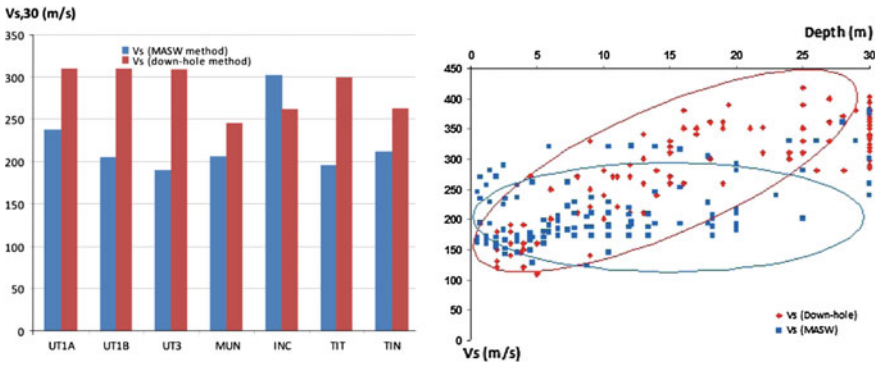


Fig. 9 Differences between down-hole (red) and MASW (blue) shear-wave velocities

By using data recorded during MASW method, measurements of phase velocity of Rayleigh waves of different frequencies have been used to determine V_s profiles. After calculating dispersion curve, it was built an initial V_s model (1D model), followed by inversion algorithms to look up for an optimum V_s profile model that best fits dispersion curve of experimental data (2D model), see Fig. 8.

For several sites where ground survey was conducted by both down-hole and MASW methods, a comparative analysis of V_s values corresponding to each depth interval in soil profile and average $V_{s,30}$ has been performed, as shown in Fig. 9. $V_{s,30}$ data obtained from MASW are ranging from 189 to 302 m/s, which can indicate that sites are included in soil class C, similar to soil type defined through down-hole seismic method. It can be observed that data collected from MASW application are grouped in a constant interval velocity 150–250 m/s comparing to a larger and gradually increase one obtained from down-hole technique. Differences between $V_{s,30}$ values obtained in down-hole and MASW surveys are ranging from 15 to 35 %, probably due to constrain of depth investigation limitation, sensors

sensitivity, procedure and equipment specificity and lateral discontinuities of soil profiles.

In order to complete the site characterization survey, invasive geotechnical methods as standard penetration test have been conducted. The sum of data recorded for 150–300 and 300–450 mm interval of sampler penetration represents the penetration resistance value called N-SPT at a specific depth. During SPT testing procedure, data regarding identification of soil nature, blow counts and layer thickness are recorded. Based on N-SPT values, representative penetration resistance profiles for each investigation site were performed. The results of standard penetration measurements and their empirical correlations with different geotechnical characteristics (shear strength and deformability) can be used in foundation design as bearing capacity and settlement calculations. According to international seismic code provisions (BSSC 2001; IBC 2006; UBC 1997 and EN 1998-1), the soil classes are also accounted by average of N-SPT values in the upper 30 m, recommended as supplementary or indirect investigation needed for seismic site classification and calculated with the following equation:

$$N_{SPT,30} = 30 / \sum_{i=1}^n \frac{d_i}{N_{SPT,i}} \quad (3)$$

where: d_i and $N_{SPT,i}$ denote the thickness (m) and penetration resistance measured on 30 cm of the i th layer from the upper 30 m. Based on penetration resistance measurements and layer thickness, the average values for each site have been computed (Fig. 10). Penetration resistances are varying from 12 to 34 blows/30 cm and it can be observed that are grouped in class C, with corresponding values between 15 and 50 blows/30 cm. In most of geotechnical applications, N-SPT values collected from direct measurements are normalized for various factors related to test procedure and equipment characteristics as N_{60} and $N_{1(60)}$. The normalized N-values were calculated using the equations recommended by NCEER Workshop (Youd and Idriss 1997):

$$N_{60} = N_{SPT} \cdot \frac{ER}{60} = N_{SPT} \cdot C_E \quad (4)$$

where: N_{60} -blow counts corrected for an energy ratio of 60 % from theoretical free fall hammer energy, N_{SPT} -measured blow counts necessary for 30 cm soil penetration, ER -rod energy ratio recommended as 60 % as reference value from standard energy ratio, C_E -energy correction factor.

$$N_{1(60)} = N_{SPT} \cdot C_N \cdot C_E \cdot C_B \cdot C_S \cdot C_R \quad (5)$$

where: $N_{1(60)}$ -blow counts normalized to an effective overburden stress and test equipment factors; N_{SPT} -measured blow counts, C_N -overburden stress correction factor adjusted to 100 kPa overburden pressure, C_E -energy correction factor, C_B -

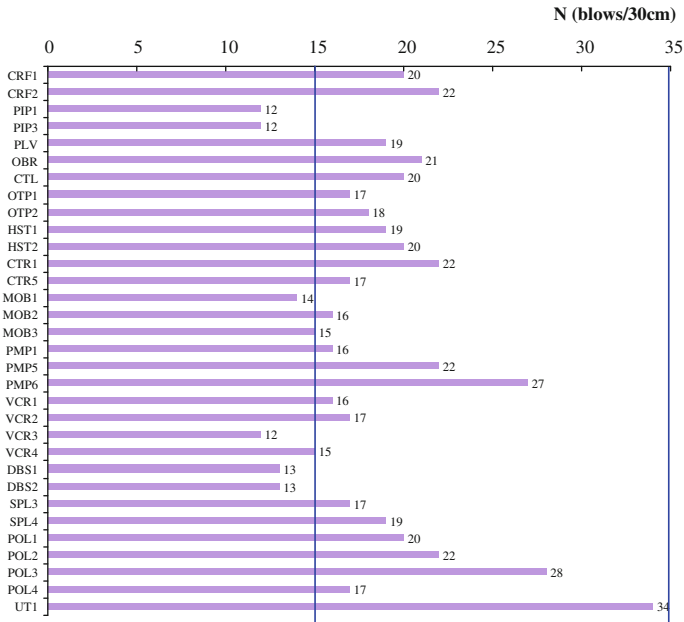
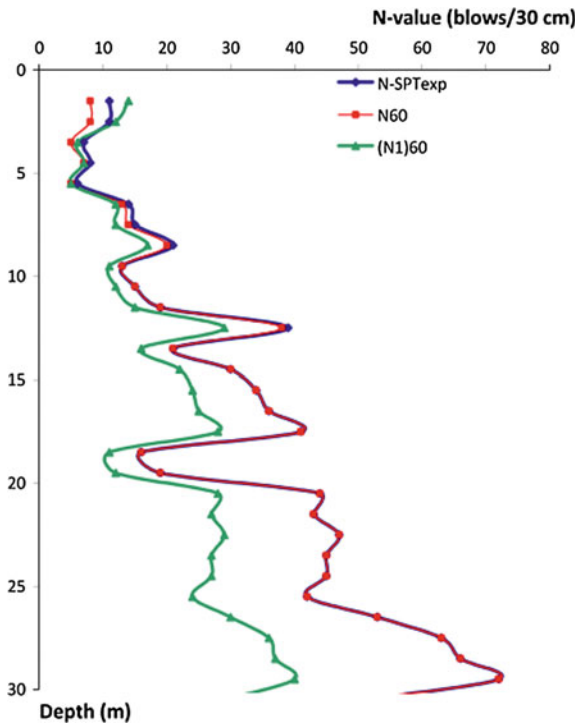


Fig. 10 Average $N_{SPT,30}$ values for investigated sites

Fig. 11 Uncorrected and corrected N-values



correction factor for borehole diameter, C_S -correction for samplers with or without liners, C_R -correction factor for rod length.

N-SPT profiles of recorded data during direct measurements and normalized values (N_{60} and $N_{I(60)}$) are obviously underline the difference between soft and firm layers, besides the thickness of each layer and soil type, as represented in Fig. 11. In terms of relative density, N-SPT values indicate the presence of medium to very dense sands and gravels, with individual values ranging from 15 blows/30 cm to more than 60 blows/30 cm. concerning consistency of cohesive soils, N-SPT values are ranging from soft to hard clay with 8 blows/30 cm up to 30 blows/30 cm.

3 Correlation of Soil Parameters and Comparative Data Analysis

3.1 Overview of Existing Empirical Correlation V_s and N-SPT

Correlations of shear wave measurements are not always feasible due to time consuming, space constrains in urban areas with high level of noise or unstable soil structures, as well as lack of specialized workers. Therefore, it is necessary to determine V_s values through indirect methods such as SPT. In technical studies, as presented in Table 1, the correlations proposed a power law relationship between V_s and N-SPT, expressed as: $V_s = A \cdot N^B$, where A and B are constant parameters determined by statistical regression. Several researchers developed equations for specific soils, depth, geological age or corrected penetration resistance by using data collected from earthquake-prone areas as Japan and Turkey. A significant number of statistical correlations between V_s and N-SPT are based on uncorrected N-SPT values. Recently, various studies have been developed on empirical relationships between corrected N-SPT and V_s data for sand, clay type and for all soils irrespective of soil type. For the present study, there were selected several empirical relations between N-SPT and V_s values from technical literature, presented in Table 1.

Table 1 Empirical correlation between V_s and N-SPT values

Researcher	Proposed correlation	Soil type
Iyisan (1996)	$V_s = 51.5 \cdot N^{0.516}$	All soils
Yokota et al. (1991)	$V_s = 121 \cdot N^{0.27}$	All soils
Hasancebi and Ulusay (2007)	$V_s = 104.79 \cdot N^{0.25}$	All soils
Jinan (1987)	$V_s = 116.1 \cdot (N + 0.3185)^{0.202}$	All soils
Imai and Tonouchi (1982)	$V_s = 96.9 \cdot N^{0.314}$	All soils

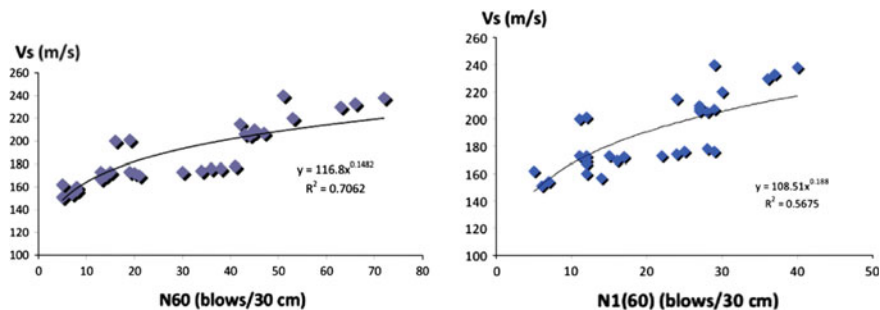


Fig. 12 Correlation of V_s values from MASW and corrected N-values

3.2 Development of Numerical Correlations Based on Field Measurements

One of the aims of present study is focused on development of statistical correlations based on S-wave velocities and N-SPT values corresponding to different sites located in Bucharest area. These soil indicators can be used as input in dynamic site characterization and site response analysis of near-surface deposits. There were selected S-wave velocities values at depth that is nearest to the one where N-SPT value was recorded, being used 78 pairs of data.

Empirical correlation between corrected N-SPT and V_s values resulted from MASW measurements has been obtained using power regression type. We obtained the Eqs. 6 and 7 as representing V_s a function of normalized N_{60} and $N_{1(60)}$ values. Using the data from MASW method, the results highlighted an intermediate correlation of V_s and N_{60} values with correlation coefficient of 0.71, respectively relative intermediate correlations between V_s and $N_{1(60)}$ values with a value of 0.57, as shown in Fig. 12.

$$V_s = 116.8 \cdot N_{60}^{0.148} \quad (6)$$

$$V_s = 108.51 \cdot N_{1(60)}^{0.188} \quad (7)$$

In comparison, V_s values gathered from down-hole measurements linked to corrected N-SPT reveals a better correlation between V_s and N_{60} values with correlation coefficient of 0.81, respectively intermediate correlations between V_s and $N_{1(60)}$ values with a value of 0.66 (see Fig. 13). These correlations were obtained by using data of travel time-distance curves of V_s values in order to obtain corresponding data for each N-SPT measurement, as a result of velocity interval averaging, empirically delimited by impedance contrast of layers, thickness and velocity travel time, comparing to high density of point measurements and detection of thin layers during penetration resistance testing. The equations obtained by

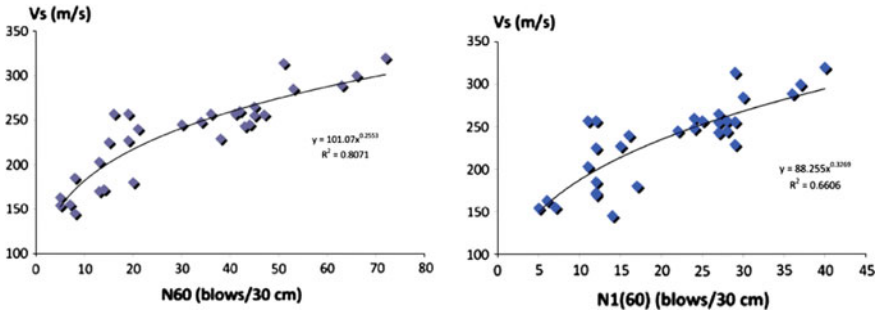


Fig. 13 Correlation of V_s values from down-hole and corrected N-values

power regression type for V_s and normalized N_{60} and $N_{1(60)}$ values were obtained as follows:

$$V_s = 101.07 \cdot N_{60}^{0.255} \tag{8}$$

$$V_s = 88.26 \cdot N_{1(60)}^{0.327} \tag{9}$$

Measured (by DH-downhole and MASW) and estimated S-wave velocities are compared in order to assess the performance of proposed regression models. Considering the higher correlation coefficient obtained in statistical analysis, accuracy of developed formulas based on V_s and N_{60} values (Eqs. 6 and 8) was compared with existing empirical ones (see Table 1) as are represented in Fig. 14. Values of V_s estimated by using equations proposed by Jinan (1987) and Hasancebi

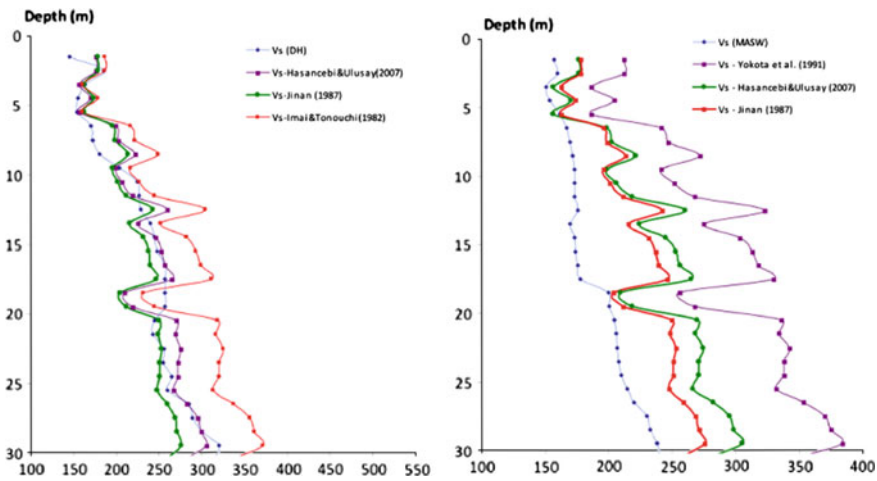


Fig. 14 Distribution of experimental and predicted shear wave velocity, V_s based on N_{60} values with depth

and Ulusay (2007) are considered to be in a better correlation with DH -downhole measured data, with differences that can reach 20 % in both positive and negative trend, comparing to 40–50 % in case of MASW values.

4 Discussion and Conclusions

For the purpose of near-surface site effects assessment during Vrancea strong earthquakes, it is essential to characterize the sites according to seismic classification. In the present paper, the authors have made an attempt to characterize several sites located in Bucharest earthquake-prone area, according to modern seismic codes provisions, using $V_{s,30}$, in order to obtain a comprehensive database to be used in site response analysis. Based on data recorded from boring logs, sampling, geotechnical and geophysical investigation methods, various key parameters for dynamic behaviour analysis have been gathered. Besides soil stratigraphy, layer thickness and other important geotechnical parameters, elastic soil parameters have been obtained by PS Suspension Logging (down-hole technique) and MASW, as well as characteristic period of site related to upper 30 m of soil. Investigated sites located in different part of Bucharest have been grouped, based on $V_{s,30}$ parameter and N-SPT blow count, on seismic class C “intermediary soil profile”. For each investigated site, V_s and N-SPT profiles have been computed for a better structuring of database related to local soil conditions. Geotechnical parameters and elastic properties determined by indirect measurements through correlations from V_s and N-SPT are reflecting the large variability in thickness and surface of stratified alluvial deposits formed by cohesive and cohesionless soils.

A good agreement of down-hole and MASW surveys has been observed for the upper 30 m of ground surface, with small differences due to technical specifications of applied methods. Moreover, it can be concluded that both methodologies used for assessing V_s profiling data can be useful for a more detailed site characterization. Correlations of V_s and N60 values have been proposed using existent empirical equations in simple regression analysis. Correlation coefficients are reflecting a better correlation of V_s data from down-hole method and normalized N-SPT values, comparing with intermediate correlation observed in case of V_s data from MASW. There is generally a relative scatter of measured data due to different resolutions of velocity measurements and natural variability of soil properties, which can introduce uncertainties in data analysis. It may be useful to select the option of V_s values for maximum depth investigation, which includes larger thicknesses. From this point of view, there are several disadvantages related to measurement depth and deep geological structures that directly influence and limit V_s values. The utility of proposed correlations is to estimate a potential range of values for sites where direct measurements are not feasible due to high costs or space constrains. Information provided can contribute to development of mitigation earthquake disaster strategies and continuous improvement of earthquake-resistant design provisions adjusted to specific ground conditions.

Acknowledgements The authors would like to acknowledge the cooperation of Japanese specialists during JICA Project as well as the generous funding provided by Japan International Cooperation Agency (JICA). We kindly acknowledge the support of Building Research Institute (BRI) in Tsukuba and Tokyo Soil Research.

References

- Aki K (1988) Local site effects on strong ground motion. *Earthquake engineering and soil dynamics II—recent advances in ground motion evaluation*, ASCE: 103–155
- Aldea A, Lungu D, Arion C (2003) GIS microzonation of site effects in Bucharest based on existing seismic and geophysical evidence. 6ème Colloque National AFPS 2003, Palaiseau, France, 8p
- Ansal AM (1994) Effects of geotechnical factors and behavior of soil layers during earthquakes, state-of-the-art lecture. In: *Proceedings of 10th European conference on earthquake engineering vol 1*, pp 467–476
- Arion C, Tamura M, Calarasu E, Neagu C (2007) Geotechnical in situ investigation used for seismic design of buildings. In: 4th ICEGE June 25–28, paper no. 1349, Thessaloniki
- Arion C, Neagu C, Văcăreanu R, Calarasu E (2012) In situ investigation for microzonation of Bucharest surface geology. In: *Proceedings of 15th WCEE, Lisbon, Portugal*, paper no. 2034
- Arion C, Calarasu E, Neagu C (2015) Evaluation of Bucharest soil liquefaction potential. *Math Model Civil Eng* 11(1):5–12
- Bard PY (1995) Effects of surface geology on ground motion: recent results and remaining issues. In: *Proceedings of the 10th European conference on earthquake engineering, Rotterdam*, pp 305–323
- Borcherdt RD (1970) Effects of local geology on ground motion near San Francisco Bay. *Bull Seismol Soc Am* 60:29–61
- Borcherdt RD, Glassmoyer G (1994) Influences of local geology on strong and weak ground motions recorded in the San Francisco Bay region and their implications for site-specific building code provisions. *U.S. geological survey professional paper 1551-A, A77–A108*
- Bala A, Arion C, Aldea A (2013) In situ borehole measurements and laboratory measurements as primary tools for the assessment of the seismic site effects. *Rom Rep Phys* 65(1):285–298
- Chavez-Garcia FJ, Cuenca J, Sanchez-Sesma FJ (1996) Site effects in Mexico City urban zone. A complementary stud. *Soil Dyn Earthq Eng* 15:141–146
- Comptes Rendus des Séances de l'Académie des Sciences de Roumanie (1941) Numéro consacré aux recherches sur le tremblement de terre du 10 Novembre 1940 en Roumanie, Tome V (3):177–288
- Dobry R, Borcherdt RD, Crouse CB, Idriss IM, Joyner WB, Martin GR, Power MS, Rinne EE, Seed RB (2000) New site coefficients and site classification system used in recent building seismic code provisions. *Earthq Spectra* 16:41–67
- Faccioli E (1991) Seismic amplification in the presence of geological and topographic irregularities. In: *Proceedings of 2nd ICRAEE, St. Louis, Missouri*, pp 1779–1797
- Hasancebi N, Ulusay R (2007) Empirical correlations between shear wave velocity and penetration resistance for ground shaking assessments. *Bull Eng Geol Environ* 66:203–213
- Idriss IM (1991) Earthquake ground motions at soft soil sites. In: *Proceedings of 2nd ICRAEE, St. Louis, Missouri*, pp 2265–2271
- Iyisan R (1996) Correlations between shear wave velocity and in-situ penetration test results. *Tech J Turk Chamber Civil Eng* 7(2):1187–1199
- Imai T, Tonouchi K (1982) Correlation of N-value with S-wave velocity. In: *Proceedings of 2nd European symposium on penetration testing*, pp 67–72
- Ishihara K, Perlea V (1984) Liquefaction-associated ground damage during the Vrancea earthquake of March 4, 1977. *Soils Found* 24(1):90–112

- Jinan Z (1987) Correlation between seismic wave velocity and the number of blow of SPT and depth. *Chin J Geotech Eng (ASCE)*, pp 92–100
- Lungu D, Aldea A, Arion C, Demetriu S, Cornea T (2000) Microzonage Sismique de la ville de Bucarest—Roumanie. *Cahier Technique de l'Association Française du Génie Parasismique* 20:31–63
- Mucciarelli M, Gallipoli MR (2006) Comparison between V_{s30} and other estimates of site amplification in Italy. In: *Proceedings of 1st ECEES, Geneva, Switzerland*, paper no. 270
- Park CB, Miller RD, Xia J, Ivanov J (2001) Characterization of geotechnical sites by multichannel analysis of surface waves (MASW) method. In: *Proceedings of 10th ICSDEE, Philadelphia, USA*
- Seed HB, Romo MP, Sun JI, Jaime A, Lysmer J (1987) Relationships between soil conditions and earthquake ground motions in Mexico City in the event of 19.09.1985. Report no. UCB/EERC-87/15
- Youd TL, Idriss IM (1997) *Proceedings of NCEER workshop on evaluation of liquefaction resistance of soils*. National Centre for Earthquake Engineering Research, State University of New York at Buffalo
- Yokota K, Imai T, Konno M (1991) Dynamic deformation characteristics of soils determined by laboratory tests. *OYO Tee Rep* 3:13

Spectral Displacement Demands for Strong Ground Motions Recorded During Vrancea Intermediate-Depth Earthquakes

Ionut Craciun, Radu Vacareanu and Florin Pavel

Abstract The main objective of this paper is to obtain an empirical relationship for the displacement amplification coefficient, from strong ground motions recorded in Vrancea intermediate-depth earthquakes. To this end, we collected strong ground motions recorded from the Vrancea earthquakes of August 30, 1986 and May 30 & May 31 1990. The computation of the ratio between the inelastic displacements and the elastic displacements was performed for multiple values of the behavior factor (q). The non-degrading Takeda hysteretic model was used in the analysis, with a damping ratio of 5 %. The analysis results were sorted in several bins as a function of several parameters. Mean and standard deviation values of the ratios of inelastic to elastic spectral displacement demands were calculated for each earthquake and each bin, as well as for the entire database. Through a non-linear regression analysis an empirical relation for the displacement amplification coefficient was obtained.

Keywords Displacement · Elastic · Inelastic · Takeda · Ductility · Vrancea · Earthquakes

1 Introduction

The Equal Displacement Rule (Veletsos and Newmark 1960; Veletsos et al. 1965), which states that the displacements of inelastic and elastic long period structures are approximately the same, has been accepted and used internationally for many decades. Although for long period structures (periods longer than the corner/control

I. Craciun (✉) · R. Vacareanu · F. Pavel

Seismic Risk Assessment Research Center, Technical University of Civil Engineering,
Bucharest, Romania

e-mail: ionut.craciun@utcb.ro

R. Vacareanu

e-mail: radu.vacareanu@utcb.ro

F. Pavel

e-mail: florin.pavel@utcb.ro

period T_c) elastic and inelastic structures have equal displacements, it has been shown by many researchers that the rule does not apply also for short period structures, where the inelastic displacements are larger than their corresponding elastic displacements (e.g. Miranda 2000a, b; Michel et al. 2014).

Several studies investigate the influence of the effect of rupture directivity at near-fault sites (Baez and Miranda 2000), the influence of site conditions on new or existing buildings (Miranda 2000a, b; Ruiz-Garcia and Miranda 2003, 2006) and different approximate methods to estimate the maximum inelastic displacement demand of SDOF systems (Miranda and Ruiz-Garcia 2002; Akkar and Miranda 2005). For Romania, there are numerous studies regarding the elastic and inelastic spectral displacement demands for strong ground motions recorded in Romania (i.e. Lungu and Craifaleanu 2007).

In addition, several studies consider the behavior factor q as a function of the displacement ductility μ and the spectral period T (i.e., Michel et al. 2014; Goda and Atkinson 2009). In the European code EN 1998-1 (CEN 2004) the behavior factor—displacement ductility relations are implemented (as a function of the spectral and corner periods). The displacement amplification coefficient c , defined as the ratio of the inelastic to elastic spectral displacement demands is obtained in the Romanian seismic code P100-1/2013 (MDRAP 2013) as:

$$1 < c = 3 - 2.3 \times \frac{T}{T_c} < \frac{\sqrt{T_c \times q}}{1.7} \quad (1)$$

For the current Romanian earthquake resistant design code P100-1/2013 (MDRAP 2013) the topic has been analyzed in a paper by Gutunoi and Zamfirescu (2014), in which relation (1) for the displacement amplification coefficient was derived using artificial accelerograms.

The main objective of this paper is to propose a relation for the displacement amplification coefficient c using accelerograms recorded during the Vrancea intermediate-depth earthquakes of August 30 1986, May 30, 1990 and May 31, 1990. This issue has also been tackled in the first author dissertation thesis (Craciun 2015).

2 Methodology and Database

The methodology used in this paper consists of performing non-linear time history analyses (NTHAs) of SDOF systems subjected to free-field natural accelerograms recorded during Vrancea intermediate-depth earthquakes. The main parameter observed in the analyses is the behavior factor q . The NTHAs are using the Takeda non-linear hysteretic model. The output data are mainly expressed as displacement amplification coefficient c versus spectral period T for different behavior factor values.

Table 1 Earthquake characteristics (<http://www1.infp.ro/realtime-archive>)

Date	Latitude	Longitude	Moment Magnitude	Depth (km)
August 30 1986	45.52	26.49	7.1	131.4
May 30 1990	45.83	26.89	6.9	90.9
May 31 1990	45.85	26.91	6.4	86.9

Seismic hazard in Romania is generated mainly by the intermediate-depth Vrancea seismic source. In this study, a database consisting of 248 horizontal components of free-field strong ground motions recorded during Vrancea intermediate-depth earthquakes of August 30, 1986, May 30, 1990 and May 31, 1990 is used. The distribution per earthquake of the horizontal components is: 76 for the August 30, 1986 earthquake, 98 for the May 30, 1990 and 74 for the May 31, 1990 earthquake. Table 1 shows some characteristics of the analyzed Vrancea earthquakes (<http://www1.infp.ro/realtime-archive>).

The analogic strong ground motion recordings are initially processed using an Ormsby filter having the low frequency limit of 0.15 Hz and the upper frequency limit of 25 Hz. The computer code named Utility Software for Data Processing (USDP) (<http://web.boun.edu.tr/sinan.akkar/usdp1.html>) was used for computing the elastic and inelastic response spectra. The spectral period range is [0; 4 s], with a step of 0.05 s. The analysis was performed for a damping ratio of 5 %, therefore it can be stated that all the conclusions of this article are valid only for reinforced concrete structures. The NTHAs can be performed with respect to the following parameters: seismic coefficient, the behavior factor or the displacement ductility; in this paper the behavior factor q was chosen because of the current functional relation (1) in the seismic code P100-1/2013 (MDRAP 2013). The Non-Degrading Takeda hysteretic model was used in the analyses.

By using the non-degrading Takeda model, both the effects of the ductility and the over-strength are considered. For the behavior factor, the following constant values were chosen: $q = 1, 1.5, 2.0, 3.0, 4.0, 5.0$ and 6.0 .

3 Evaluation of the Results

In the first step, the output c - T data are sorted for the seven chosen values of the behavior factor q according to the seismic event that generated the recorded strong ground motions: August 30, 1986, May 30, 1990, May 31, 1990, as well as for the entire database. For each of the four data sets, the mean and standard deviation values of the c coefficient were calculated. The mean values of the displacement amplification coefficient c are represented in Figs. 1, 2 and 3.

After analyzing Figs. 1, 2 and 3 the following observations can be made:

- The values of the displacement amplification coefficient c , in the case of short period structures (until the stabilization), increase with the value of the behavior

Fig. 1 Mean values of the c coefficient for the four data sets, for $q = 2$ and $T \in [0; 1 \text{ s}]$

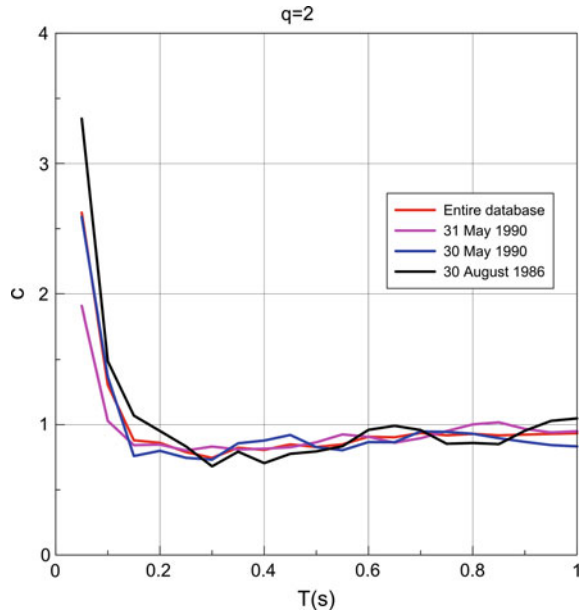
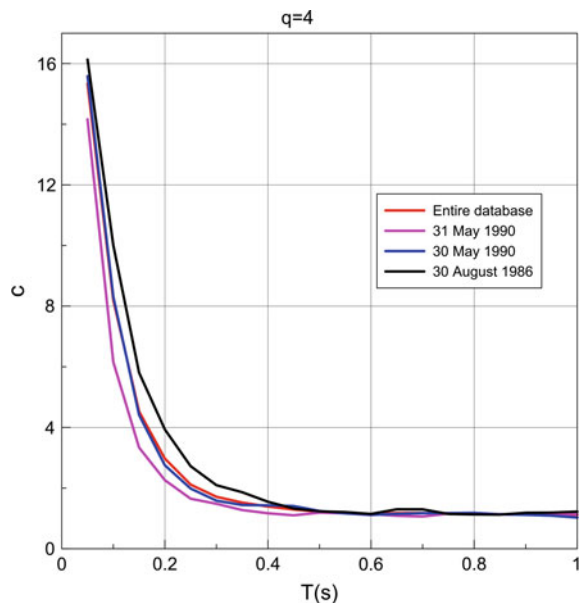
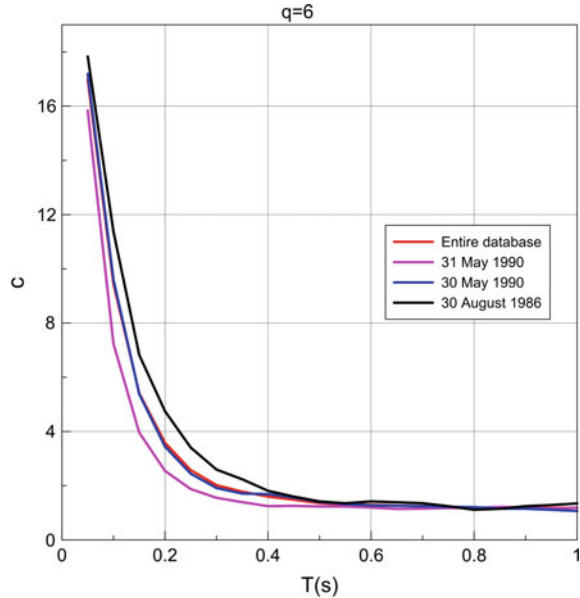


Fig. 2 Mean values of the c coefficient for the four data sets, for $q = 4$ and $T \in [0; 1 \text{ s}]$



factors (for a period of $T = 0.05 \text{ s}$, for the entire database, the displacement amplification coefficient has the following values: for $q = 6 - c = 17$ and for $q = 2 - c = 2.7$, so for a behavior factor equal to 6, the coefficient is up to six times greater than for a behavior factor equal to 2);

Fig. 3 Mean values of the c coefficient for the four data sets, for $q = 6$ and $T \in [0; 1 \text{ s}]$



- A very important aspect shown in Figs. 1, 2 and 3 is the ordering according to the magnitude of the earthquake of the mean values of the c coefficient; in other words, the highest mean values of the c coefficient are for the August 30 1986 (which has the highest magnitude) and the lowest values are for the May 31 1990 earthquake (which has the lowest magnitude);
- Equal Displacement Rule has been noticed for long period structures, whilst for short period structures the coefficient c has higher values; also, the stabilization of the coefficient at $c = 1$, at a value around $T = 0.55 \text{ s}$ is emphasized.

The variability of the results sorted according the seismic events is represented in Figs. 4, 5, 6 and 7 for a behaviour factor $q = 4$. The shaded areas in Figs. 4, 5, 6 and 7 represent the range of the mean ± 1 standard deviation values. The values of the coefficients of variation of c for the entire database ranges from 0.25 to 0.8, the higher values being encountered for short periods of vibration (less than 0.5 s). For vibration periods in excess of 0.5 s the values of the coefficients of variation are almost constant (close to 0.4) with a peak of 0.5 for periods of vibration in-between 1.5 and 2.0 s. Earthquake-wise, the same trend is noticed.

Subsequently, the influence of four parameters (namely, spectral period, behavior factor q , the control period T_c and the peak ground acceleration) on the values of the displacement amplification coefficient was performed.

The corner/corner period T_c is based on the values of *EPA* (Effective Peak Acceleration) and *EPV* (Effective Peak Velocity) initially defined by Applied Technology Council (1978). The procedure used in this paper for obtaining the corner period values is given in Lungu et al. (1997). Depending on the values of the

Fig. 4 Mean values and mean \pm one standard deviation of the c coefficient for August 30, 1986 strong ground motions and for $q = 4$

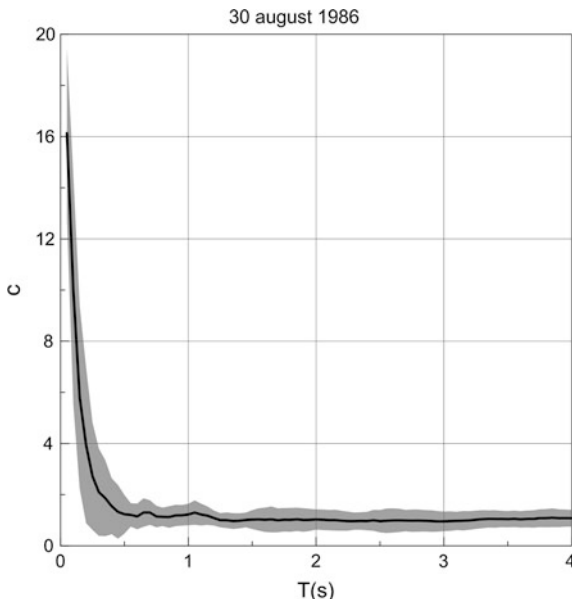
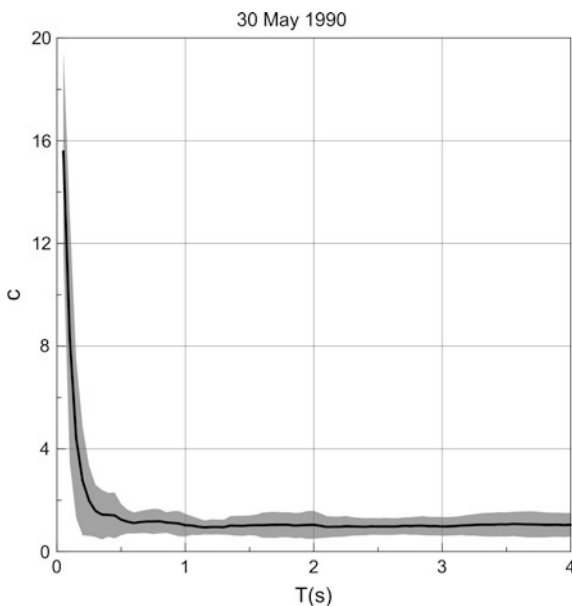


Fig. 5 Mean values and mean \pm one standard deviation of the c coefficient for May 30, 1990 strong ground motions and for $q = 4$



corner period, the values of coefficient c were sorted into the following categories: from recordings with corner period values between (0; 0.7 s], from recordings with corner period values between (0.7; 1.0 s], for recordings with corner period values

Fig. 6 Mean values and mean \pm one standard deviation of the c coefficient for May 31, 1990 strong ground motions and for $q = 4$

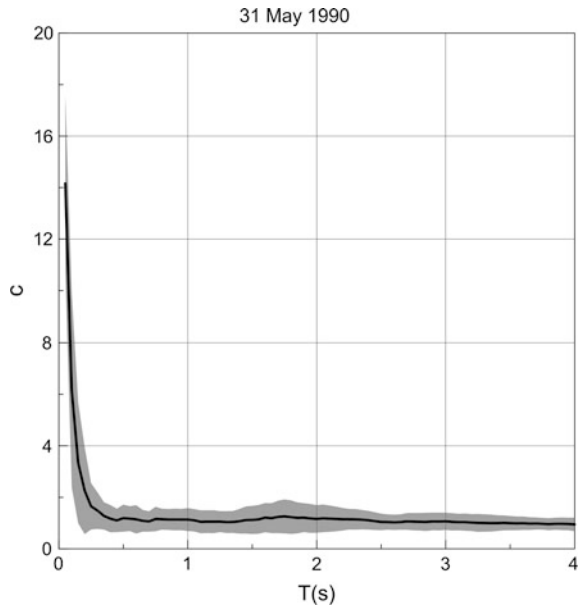
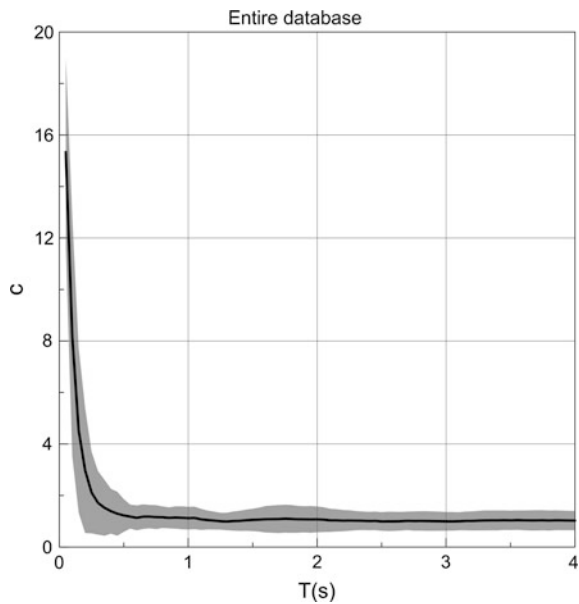


Fig. 7 Mean values and mean \pm one standard deviation of the c coefficient for all strong ground motions in the database and for $q = 4$



above the value of 1.0 s and for all the recordings. For each of the 4 data sets, the mean and standard deviation values of the c coefficient were calculated. The results are plotted in Figs. 8, 9 and 10.

Fig. 8 Mean values of the coefficient c for four data sets sorted after T_c , for $q = 2$ and $T \in [0; 1 \text{ s}]$

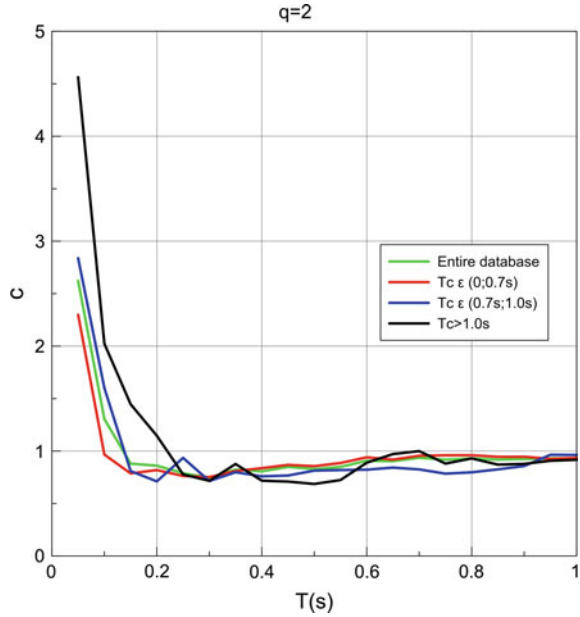
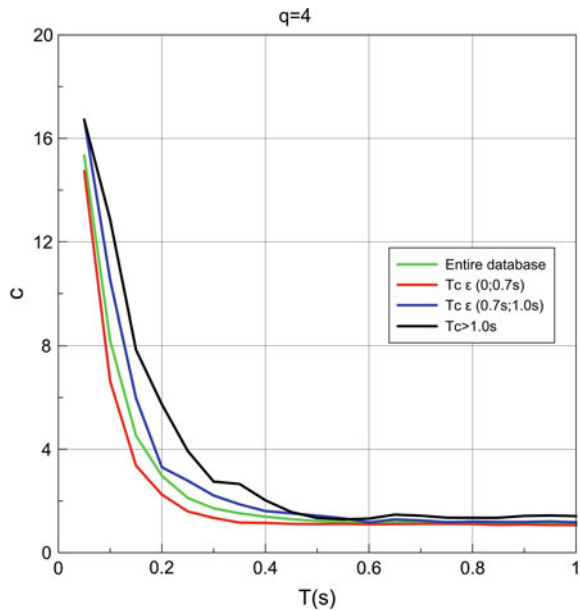
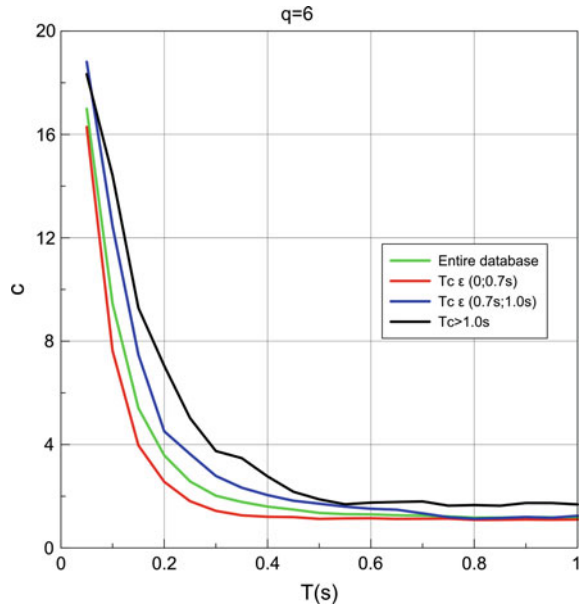


Fig. 9 Mean values of the coefficient c for four data sets sorted after T_c , for $q = 4$ and $T \in [0; 1 \text{ s}]$



From Figs. 8, 9 and 10 one can notice that the mean values of the set with $T_c > 1.0 \text{ s}$ are larger than the ones of the set with $T_c \in (0.7; 1.0 \text{ s}]$, which are also larger than the ones of the set with $T_c > 1.0 \text{ s}$, thus confirming the previously anticipated influence of the corner period over the c coefficient.

Fig. 10 Mean values of the coefficient c for four data sets sorted after T_c , for $q = 6$ and $T \in [0; 1 \text{ s}]$



The variability of the results sorted according to the corner period T_c is represented in Figs. 11, 12 and 13 for a behaviour factor $q = 4$. The shaded areas in Figs. 11, 12 and 13 represent the range of the mean ± 1 standard deviation values. For the strong ground motions with corner period less than 0.7 s there is a peak value of the coefficient of variation at $T = 0.2$ s, then the values decrease to 0.4 at $T = 0.4$ s. Further on, the values of the coefficient of variation are almost constant and close to 0.4 with a peak of 0.5 for periods of vibration in-between 1.5 and 2.0 s. The same remarks are valid for the strong ground motions with corner period in-between 0.7 and 1.0 s, except that for periods of vibration in excess of 2.0 s the constant value of the coefficients of variation is close to 0.3. For the strong-ground motions with control periods higher than 1.0 s the values of the coefficients of variation are much more scattered in the range (0.20; 0.55), but this might be an effect of the more limited sample of strong ground motions.

The values of the coefficient c were finally sorted into the following categories: recordings with $PGA > 0.10$ g, recordings with $PGA \in (0.05; 0.10$ g], recordings with $PGA < 0.05$ g and all the recordings. For each of the 4 data sets, the mean and standard deviation values of the c coefficient were calculated. The results are plotted in Figs. 14, 15 and 16.

After analyzing Figs. 14, 15 and 16, one can notice that the mean values of the set with $PGA > 0.10$ g are larger than the ones of the set with $PGA \in (0.05; 0.10$ g], which are also larger than the ones of the set with $PGA < 0.05$ g; the influence of the PGA is confirmed. Nevertheless, the influence results in low increases of the mean values with the increase of the PGA .

Fig. 11 Mean values and mean \pm one standard deviation of the c coefficient for $T_c < 0.7$ s and $q = 4$

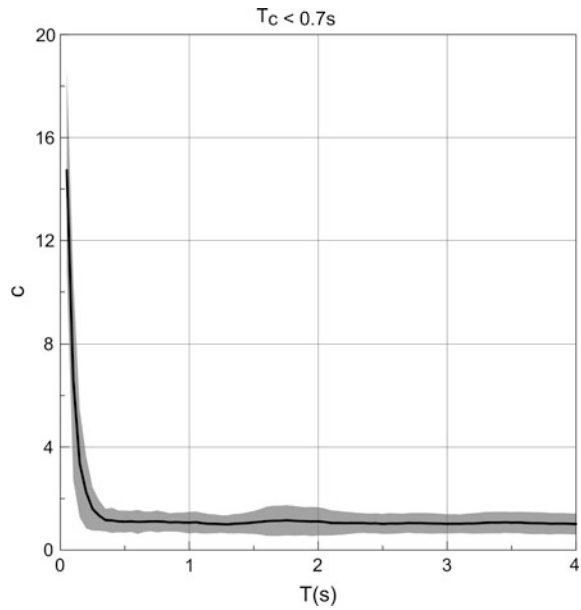


Fig. 12 Mean values and mean \pm one standard deviation of the c coefficient for $0.7 \text{ s} < T_c < 1.0 \text{ s}$ and $q = 4$

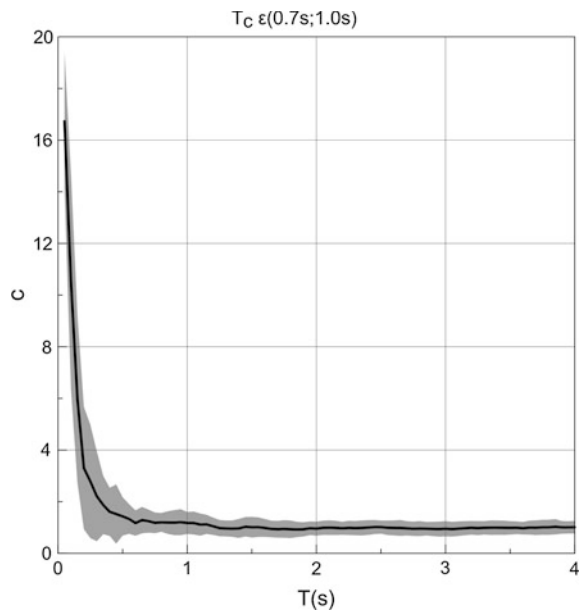


Fig. 13 Mean values and mean \pm one standard deviation of the c coefficient for $T_c > 1.0$ s and $q = 4$

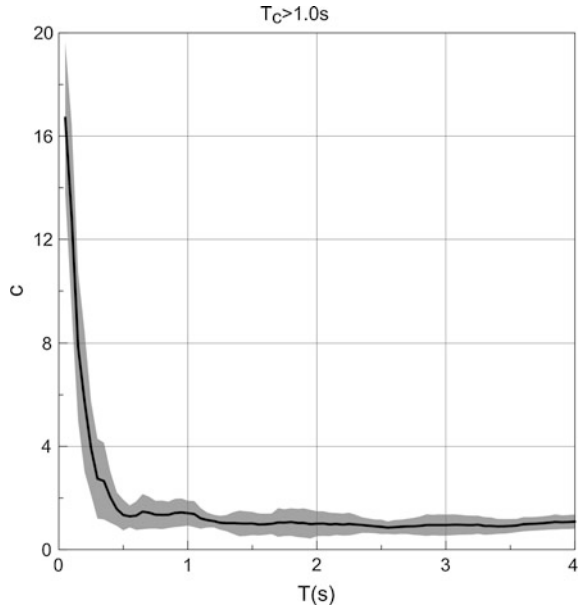


Fig. 14 Mean values of the four coefficient c data sets sorted after PGA , for $q = 2$ and $T \in [0; 1$ s]

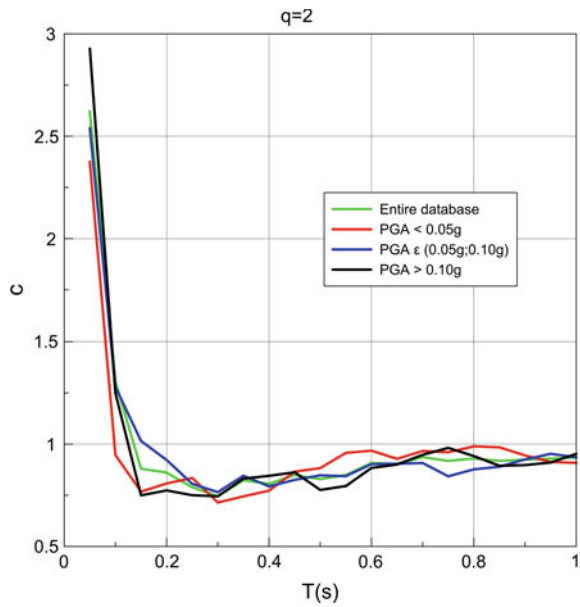


Fig. 15 Mean values of the four coefficient c data sets sorted after PGA , for $q = 4$ and $T \in [0; 1 \text{ s}]$

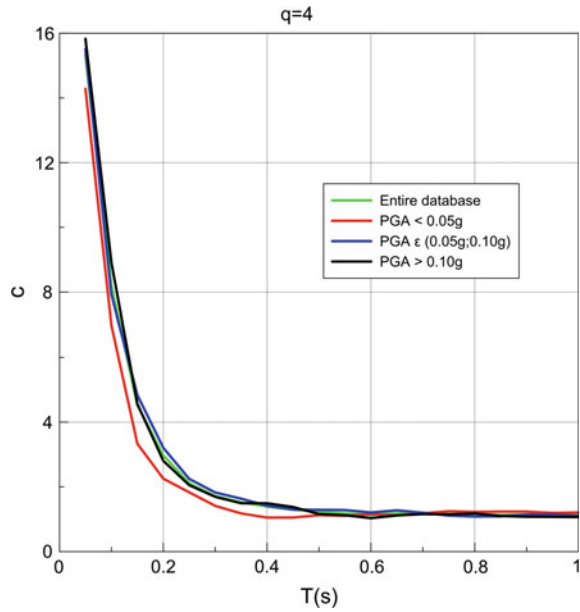
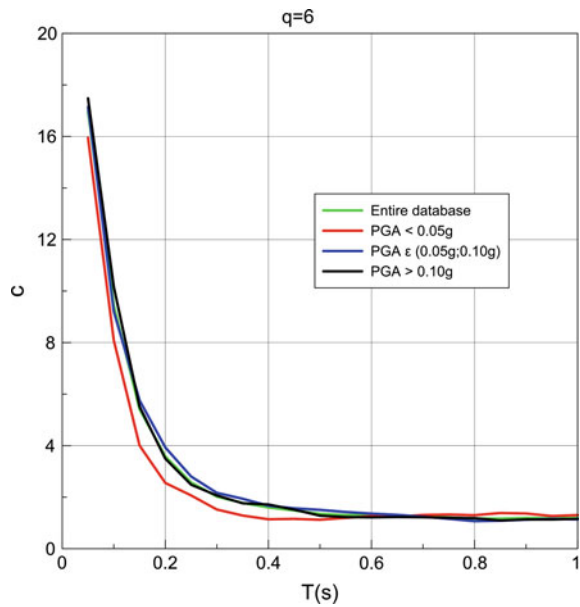


Fig. 16 Mean values of the four coefficient c data sets sorted after PGA , for $q = 6$ and $T \in [0; 1 \text{ s}]$



4 Regression Analysis

So far, the analyses show that the displacement amplification coefficient depends on four parameters: the behavior factor q , the spectral period T , the corner period T_c and the peak ground acceleration PGA . If one considers the ratio of T_c to T , the following functional relation is obtained:

$$c = f\left(q; \frac{T_c}{T}; PGA\right) \quad (2)$$

To conclude over the influence of the three parameters from Eq. (2), the distribution of the values of coefficient c with each parameter must be studied, when the other two are kept constant. To this purpose, three situations were analyzed:

- (a) $c = f(q)$ relations, keeping the parameters T and PGA constant. Statistical analysis is performed, resulting in a correlation coefficient of 0.51;
- (b) $c = f(T_c/T)$ relations keeping the parameters q and PGA constant. Statistical analysis is performed, resulting in a correlation coefficient of 0.67;
- (c) $c = f(PGA)$ relations keeping the parameters T and q constant. Statistical analysis is performed, resulting in a correlation coefficient of 0.0004.

The correlation coefficients for the first two relations have values higher than 0.5, therefore both have been maintained as defining parameters for the displacement amplification coefficient. The correlation coefficient for the third situation, $c = f(PGA)$, is less than 0.05, therefore PGA has been rejected as a parameter in the present study, although a future research study could investigate this issue more in-depth.

For each of the two remaining parameters, the statistic trend is studied further. The final objective is to propose a regression relation of the c coefficient and to find out the regression parameters.

Concerning the behavior factor q , it has been decided that the tendency that best describes the dependence is the logarithmic tendency that is best suited for the more important short period zones ($T < 0.5$ s), also keeping an advantageous shape for the long periods. For the second parameter, the T_c/T ratio, it has been decided that the power trend-line best describes the dependence, both for short and long periods.

A functional form of the displacement amplification coefficient has been proposed as:

$$c = a_0 + a_1 \times \left(\frac{T_c}{T}\right)^{a_2} + a_3 \times \ln q, \quad (3)$$

where a_0 , a_1 , a_2 and a_3 are regression coefficients.

The regression coefficients are: $a_0 = 0.25$, $a_1 = 0.60$, $a_2 = 1.00$ and $a_3 = 0.45$, leading us to a final relation of the displacement amplification coefficient of the form:

$$c = 0.25 + 0.60 \times \frac{T_c}{T} + 0.5 \times \ln q > 1.0 \quad (4)$$

5 Comparison with the Relations of P100-1/2006 and P100-1/2013

In Table 2, the three relations of the displacement amplification coefficient taken into consideration are presented (the relation from the previous Romanian seismic design code, P100-1/2006 (MTCT 2006), the relation from the current Romanian seismic design code, P100-1/2013 (MDRAP 2013) and the relation proposed in this study).

The values of the displacement amplification coefficient obtained with relation (4) are bounded in-between 1.0 and 2.0. The purpose of the upper limit is to avoid unrealistic values of the c coefficient. Nevertheless, a future study should investigate the upper limit of the relation presented in the present study.

In the P100-1/2013 (MDRAP 2013) relation, the only parameter that influences the c coefficient is the T/T_c ratio, the behavior factor being introduced as part of the upper limit, which is an improvement of the relation given by the 2006 version of the Romanian seismic design code. In the proposed relation, the c coefficient depends on two parameters: the T_c/T ratio (the proposed relation uses the inverted period ratio that is being used in the current code) and the behavior factor q , getting closer to the relations presented in the European code EN 1998-1 (CEN 2004).

Amongst the three relations, there are some differences concerning the upper limit. While the proposed relation is limited to the value 2.0, similar to the relation used in P100-1/2006 (MTCT 2006), the upper limit of the relation in P100-1/2013 (MDRAP 2013) is a value that depends on the control period T_c and the behavior factor q .

The values of the displacement amplification coefficient c obtained with the proposed relation and with the other two relations are compared in Figs. 17, 18, 19, 20 and Table 3.

Table 2 Displacement amplification coefficient relations

P100-1/2006 relation	P100-1/2013 relation	Proposed relation
$1 < c = 3 - 2.5 \times \frac{T}{T_c} < 2$	$1 < c = 3 - 2.3 \times \frac{T}{T_c} < \frac{\sqrt{T_c \times q}}{1.7}$	$1 < c = 0.25 + 0.60 \times \frac{T_c}{T} + 0.5 \times \ln q < 2$

Fig. 17 Comparison between the three relations for $T_c = 0.7$ s and $q = 4$

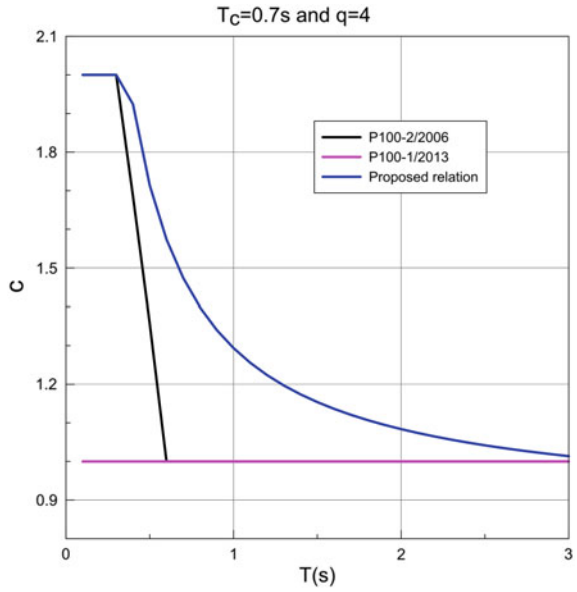


Fig. 18 Comparison between the three relations for $T_c = 0.7$ and $q = 6$

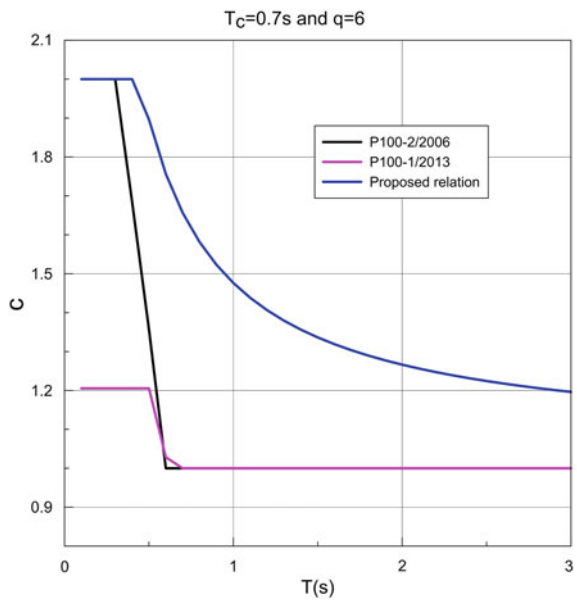


Fig. 19 Comparison between the three relations for $T_c = 1.0$ s and $q = 4$

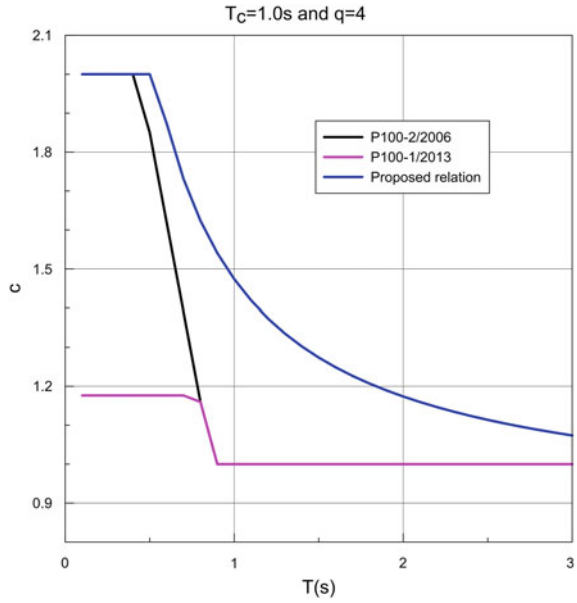


Fig. 20 Comparison between the three relations for $T_c = 1.0$ s and $q = 6$

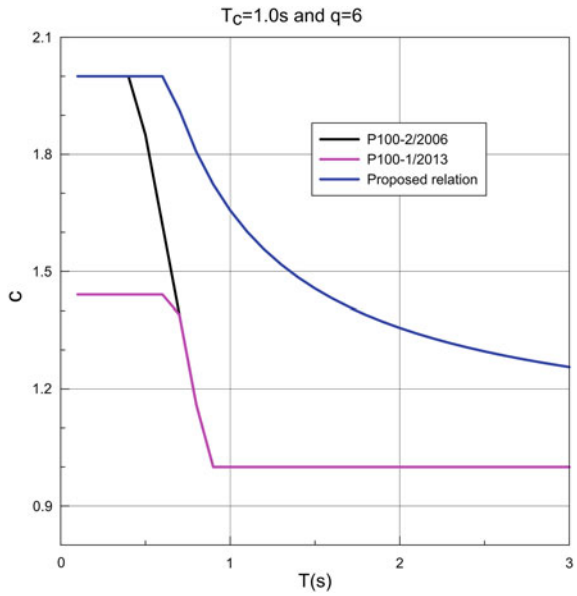


Table 3 Displacement amplification coefficient values obtained with the three relations for $T_c = 0.7$ and $q = 4$; 6

T(s)	T _c (s)		c			T(s)	T _c (s)	q	c			Proposed relation
	q	4	P100-1/2006	P100-1/2013	Proposed relation				P100-1/2006	P100-1/2013	Proposed relation	
0.1	0.7	4	2.00	1.00	2.00	0.1	0.7	6	2.00	1.21	2.00	
0.2	0.7	4	2.00	1.00	2.00	0.2	0.7	6	2.00	1.21	2.00	
0.3	0.7	4	2.00	1.00	2.00	0.3	0.7	6	2.00	1.21	2.00	
0.4	0.7	4	1.69	1.00	1.92	0.4	0.7	6	1.69	1.21	2.00	
0.5	0.7	4	1.36	1.00	1.71	0.5	0.7	6	1.36	1.21	1.90	
0.6	0.7	4	1.00	1.00	1.57	0.6	0.7	6	1.00	1.03	1.76	
0.7	0.7	4	1.00	1.00	1.47	0.7	0.7	6	1.00	1.00	1.66	
0.8	0.7	4	1.00	1.00	1.40	0.8	0.7	6	1.00	1.00	1.58	
0.9	0.7	4	1.00	1.00	1.34	0.9	0.7	6	1.00	1.00	1.52	
1	0.7	4	1.00	1.00	1.29	1	0.7	6	1.00	1.00	1.48	
1.1	0.7	4	1.00	1.00	1.26	1.1	0.7	6	1.00	1.00	1.44	
1.2	0.7	4	1.00	1.00	1.22	1.2	0.7	6	1.00	1.00	1.41	
1.3	0.7	4	1.00	1.00	1.20	1.3	0.7	6	1.00	1.00	1.38	
1.4	0.7	4	1.00	1.00	1.17	1.4	0.7	6	1.00	1.00	1.36	
1.5	0.7	4	1.00	1.00	1.15	1.5	0.7	6	1.00	1.00	1.34	
1.6	0.7	4	1.00	1.00	1.14	1.6	0.7	6	1.00	1.00	1.32	
1.7	0.7	4	1.00	1.00	1.12	1.7	0.7	6	1.00	1.00	1.30	
1.8	0.7	4	1.00	1.00	1.11	1.8	0.7	6	1.00	1.00	1.29	
1.9	0.7	4	1.00	1.00	1.09	1.9	0.7	6	1.00	1.00	1.28	
2	0.7	4	1.00	1.00	1.08	2	0.7	6	1.00	1.00	1.27	
2.1	0.7	4	1.00	1.00	1.07	2.1	0.7	6	1.00	1.00	1.26	
2.2	0.7	4	1.00	1.00	1.06	2.2	0.7	6	1.00	1.00	1.25	
2.3	0.7	4	1.00	1.00	1.06	2.3	0.7	6	1.00	1.00	1.24	

(continued)

Table 3 (continued)

T(s)	T _c (s)	q	c			T(s)	T _c (s)	q	c			Proposed relation
			P100-1/2006	P100-1/2013	Proposed relation				P100-1/2006	P100-1/2013	Proposed relation	
2.4	0.7	4	1.00	1.00	1.05	2.4	0.7	6	1.00	1.00	1.23	
2.5	0.7	4	1.00	1.00	1.04	2.5	0.7	6	1.00	1.00	1.22	
2.6	0.7	4	1.00	1.00	1.04	2.6	0.7	6	1.00	1.00	1.22	
2.7	0.7	4	1.00	1.00	1.03	2.7	0.7	6	1.00	1.00	1.21	
2.8	0.7	4	1.00	1.00	1.02	2.8	0.7	6	1.00	1.00	1.21	
2.9	0.7	4	1.00	1.00	1.02	2.9	0.7	6	1.00	1.00	1.20	
3	0.7	4	1.00	1.00	1.01	3	0.7	6	1.00	1.00	1.20	

6 Conclusions

The present study's objective was to derive a relation for the computation of the displacement amplification coefficient by using ground motions recorded in the Vrancea intermediate-depth earthquakes from August 30, 1986, May 30, 1990 and May 31 1990.

The main findings of this study are summarized as follows:

- (a) A relation for the displacement amplification coefficient c by using the non-degrading Takeda hysteretic model, with a damping ratio of 5 % (applicable for reinforced concrete structures) was obtained.
- (b) Information about the displacement amplification coefficient in Romania based on natural accelerograms, with implications in earthquake resistant building design, has been obtained.
- (c) The aspects shown in recent relevant papers in the literature (Michel et al. 2014; Goda and Atkinson 2009) concerning the dependence of the results on the database used in the study has been confirmed.
- (d) The displacement amplification coefficient values obtained with the proposed relation are higher than the values obtained with the relation from the seismic design code P100-1/2013 (MDRAP 2013). The largest difference between the two relations is in the case of the smallest corner period, $T_c = 0.7$ s, where all the values obtained with the relation from P100-1/2013 (MDRAP 2013) are equal to unity.
- (e) It can be noticed that the relation from the current Romanian code provides the lowest values of the c coefficient; for short corner periods, the relation provides values equal to unity, only because of the lower limit being set at the value 1.

References

- Akkaş S, Miranda E (2005) Statistical evaluation of approximate methods for estimating maximum deformation demands on existing structures. *J Struct Eng* 131:160–172
- Applied Technology Council (1978) Tentative provisions for the development of seismic regulations for buildings (California, United States of America). ATC3-06. Applied Technology Council
- Baez J, Miranda E (2000) Amplification factors to estimate inelastic displacement demands for the design of structures in the near field (New Zealand). In: Proceedings 12th world conference on earthquake engineering, paper no. 1561
- CEN (2004) Eurocode 8: design of structures for earthquake resistance, Part 1: general rules, seismic actions and rules for buildings (Belgium). EN 1998–1:2004
- Craciun I (2015) Spectral displacement demands for strong ground motions recorded in Vrancea intermediate depth earthquakes (Romania). Dissertation thesis. Technical University of Civil Engineering, Bucharest
- Goda K, Atkinson GM (2009) Seismic demand of inelastic SDOF systems for earthquakes in Japan (United States of America). *Bull Seismol Soc Am* 99(6):3284–3299

- Gutunoi A, Zamfirescu D (2014) Study on relation between inelastic and elastic displacement for Vrancea earthquakes (Romania). *Sci J Techn Univ Civil Eng* 4:37–43
- Lungu D, Cornea T, Aldea A, Nedelcu C, Demetriu S (1997) Uncertainties in mapping frequency content of soil response to various magnitude earthquakes (France). *EUROMECH 372 Colloquium of the European Mechanics Society, Reliability in nonlinear structural mechanics. Université Blaise Pascal, Inst. Français de Mécanique Avancée*, pp 39–48
- Lungu D, Craifaleanu I (2007) Shake maps of spectral response ordinates and of other ground motion characteristics for Vrancea earthquakes. In: *Proceedings of the international symposium on strong Vrancea earthquakes and risk mitigation, Oct. 4–6, 2007. Bucharest, Romania*, pp 307–316
- Michel C, Lestuzzi P, Lacave C (2014) Simplified non-linear seismic displacement demand prediction for low period structures (Switzerland). *Bull Earthq Eng* 12(4):1563–1581
- Miranda E (2000a) Inelastic displacement ratios for displacement-based earthquake resistant design (New Zealand). In: *Proceedings 12th world conference on earthquake engineering*, paper no. 1096
- Miranda E (2000b) Inelastic displacement ratios for structures on firm sites. *J Struct Eng* 126(10):1150–1159
- Miranda E, Ruiz-Garcia J (2002) Evaluation of approximate methods to estimate maximum inelastic displacement demands. *Earthq Eng Struct Dynam* 31(3):539–560
- MDRAP (2013) P100-1/2013 Seismic design code. Part 1: Design provisions for buildings. (in Romanian)
- MTCT (2006) P100-1/2006 Seismic design code. Part 1: Design provisions for buildings. (in Romanian)
- Ruiz-Garcia J, Miranda E (2003) Inelastic displacement ratios for evaluation of existing structures. *Earthq Eng Struct Dynam* 32(9):1237–1258
- Ruiz-Garcia J, Miranda E (2006) Inelastic displacement ratios for design of structures on soft soils sites. *Earthq Eng Struct Dynam* 35(6):679–694
- <http://web.boun.edu.tr/sinan.akkur/usdp1.html>
- Veletsos A S, Newmark NM (1960) Effect of inelastic behavior on the response of simple systems to earthquake motions (Japan). In: *Proceedings 2nd world conference on earthquake engineering*, vol 2, pp 895–912
- Veletsos AS, Newmark NM, Chepalati CV (1965) Deformation spectra for elastic and elastoplastic systems subjected to ground shock and earthquake motion (New Zealand). In: *Proceedings 3rd world conference on earthquake engineering*, vol 2, pp 663–682
- <http://www1.infp.ro/realtime-archive>

Analysis of the Seismic Activity in the Vrancea Intermediate-Depth Source Region During the Period 2010–2015

Andreea Craiu, Mihail Diaconescu, Marius Craiu,
Alexandru Marmureanu and Constantin Ionescu

Abstract The goal of this study is to analyze the seismic activity of the Vrancea intermediate depth source zone during the period 2010–2015, time interval when the data provided by the National Seismic Network reached high quantitative and qualitative levels. The Vrancea undercrustal source (60–200 km depth) is located in a small focal volume at the Carpathian Bend, and it dominates the seismicity of Romania. The data set consists of 1603 earthquakes with local magnitudes $1.8 \leq M_L \leq 5.5$, recorded between January 2010 and October 2015. The events were localized using ANTELOPE software for data acquisition and processing. The reliable P-wave polarities were used to estimate the focal mechanism of 80 earthquakes with $M_L \geq 3.8$.

Keywords Vrancea intermediate-depth seismogenic region • Earthquake space distribution • Focal mechanism

A. Craiu (✉) · M. Diaconescu · M. Craiu · A. Marmureanu · C. Ionescu
National Institute for Earth Physics, Magurele, Ilfov, Romania
e-mail: atugui@infp.ro

M. Diaconescu
e-mail: diac@infp.ro

M. Craiu
e-mail: gcraiu@infp.ro

A. Marmureanu
e-mail: marmura@infp.ro

C. Ionescu
e-mail: viorel@infp.ro

1 Introduction

This study aims to analyze the seismic activity in the Vrancea (Romania) intermediate depth source region during the past six years (2010–2015), period when the data provided by the national seismic network have reached high quantitative as well as qualitative levels.

The seismicity in Romania may be characterized as moderate-to-high. It consists in both crustal events—clustered in several source zones: Vrancea, Fagaras-Campulung, Banat, Crisana, Maramures and southernmost Dobrogea—and sub-crustal earthquakes—in Vrancea region.

The strongest seismicity occurs at intermediate depths (between 60 and 200 km), in a small focal volume situated at the Eastern Carpathian Bend (the Vrancea area), where 2–3 major earthquakes with magnitude greater than 7.0 have been reported each century (Radulian et al. 2002).

2 Data Processing

2.1 *The Seismic Network*

The recent upgrade of the seismic network in Romania resulted in 158 stations in operation at present (121 in real time), which cover the entire territory of the country (Fig. 1). The stations are equipped with high quality digital instruments (Quanterra Q330 or Kinemetrics ROCK digitizers). All the real-time seismic stations transmit the data to the National Institute for Earth Physics (NIEP), with a sampling rate of 100 s^{-1} . At most of the sites, the strong motion acceleration sensors (EpiSensor type) are installed together with broadband velocity sensors (Streckeisen STS2 or Guralp CMG40T). NIEP operates also two seismic arrays: BURAR in northeastern Romania and PLOR in the Vrancea region.

An example of waveforms of a subcrustal Vrancea event recorded by the National Seismic Network (velocity sensors, vertical and horizontal components) is displayed in Fig. 2.

2.2 *Event Location*

AntelopeTM program packages (<http://www.brtt.com/software.html>) is used for the real-time data acquisition and earthquake processing. The Antelope real-time system provides automatic event detection, arrival picking, event location, and magnitude estimation. In order to refine the automatic solutions, all the localizations in this paper were obtained by manual processing.

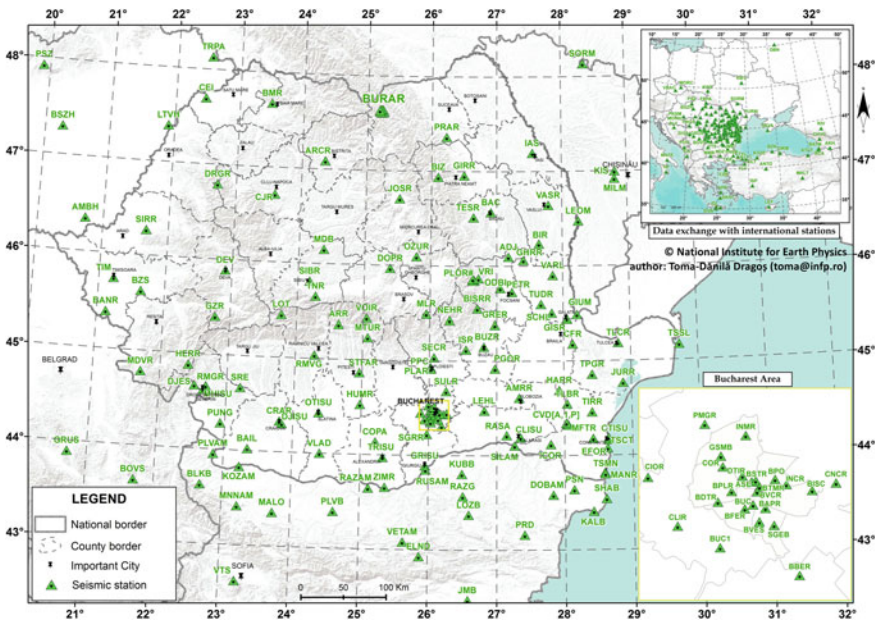


Fig. 1 Romanian seismic network (www.infp.ro)

The relation we used to estimate the earthquake magnitude is (Craiu et al. 2012):

$$M_L = 0.5587 \log_{10}(A) + 1.7218 \log_{10} R + 0.0014 * R - 0.2238 \quad (1)$$

where A—maximum amplitude on the Wood-Anderson seismogram, R—hypocentral distance (in km).

2.3 Fault Plane Solutions

The fault plane solutions of the strongest events ($M_L \geq 3.8$) have been obtained on the basis of the P-wave polarities using FOCMEC code developed by Snoke et al. (1984)—incorporated in SEISAN software (Havskov and Ottemöller 2003). For our estimations, the selected threshold is 10 polarity data; nevertheless, for most of the events, the number of available observations is greater than 25.

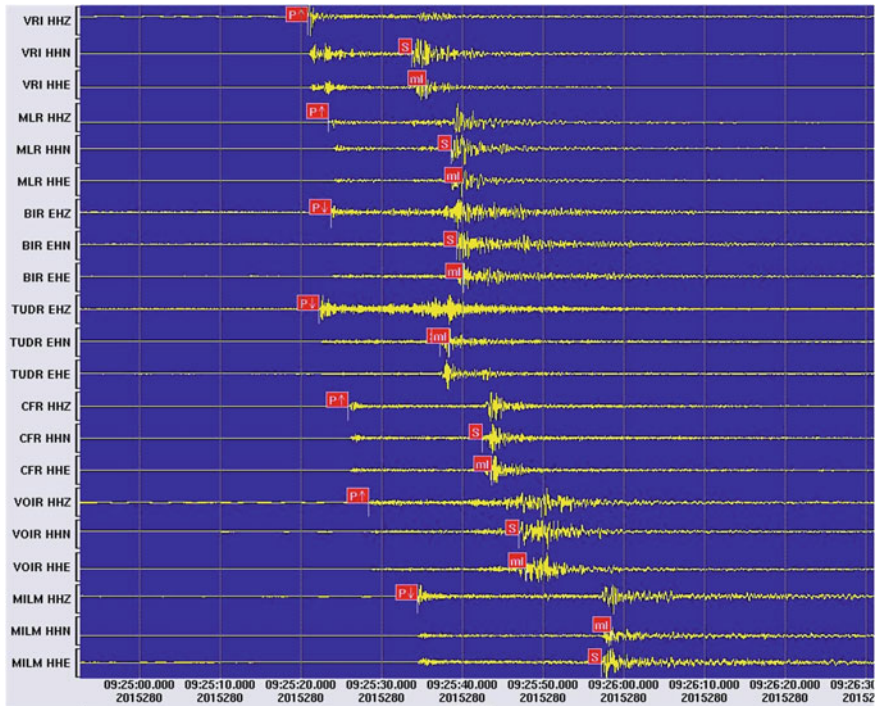


Fig. 2 Example of waveforms of the October 7, 2015 intermediate depth event ($M_L = 4.5$)

3 Results

3.1 Earthquake Distribution

During the study time interval—January 2010–October 2015—1603 earthquakes with M_L magnitudes ≥ 1.8 were recorded in the Vrancea intermediate-depth source zone; the largest one had local magnitude 5.5. Figure 3 displays the space distribution of the epicenters.

The distribution of the hypocenters versus depth points out 2 segments: a shallower one in the range 60–110 km, with a maximum of the activity around 80–90 km, and a deeper one, more active, between 110 and 200 km, with a maximum in the range 120–150 km (Fig. 4). The strongest events—5 earthquakes with $M_L \geq 5.0$ —occurred in the deeper segment (Fig. 5).

The frequency–magnitude distribution of the earthquakes is shown in Fig. 6. The completeness magnitude appears to be around M_L 2.8.

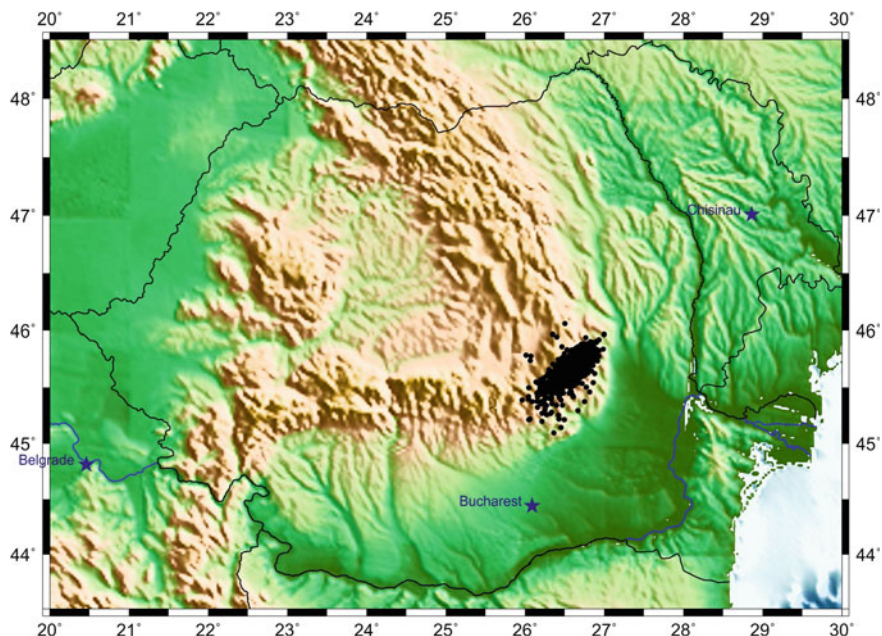
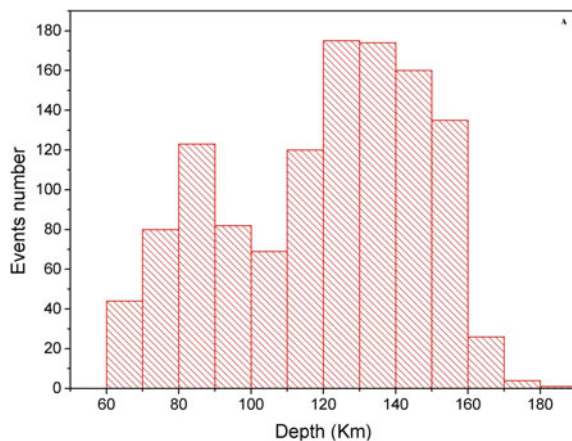


Fig. 3 Distribution of the epicenters of the earthquakes recorded in the Vrancea subcrustal zone, during 2010–2015 ($h \geq 60$ km)

Fig. 4 Depth distribution of the hypocenters



3.2 Focal Mechanisms

We determined the fault plane solutions for 80 events with $M_L \geq 3.8$, for which more than 10 reliable P-wave polarity data have been available (Table 1).

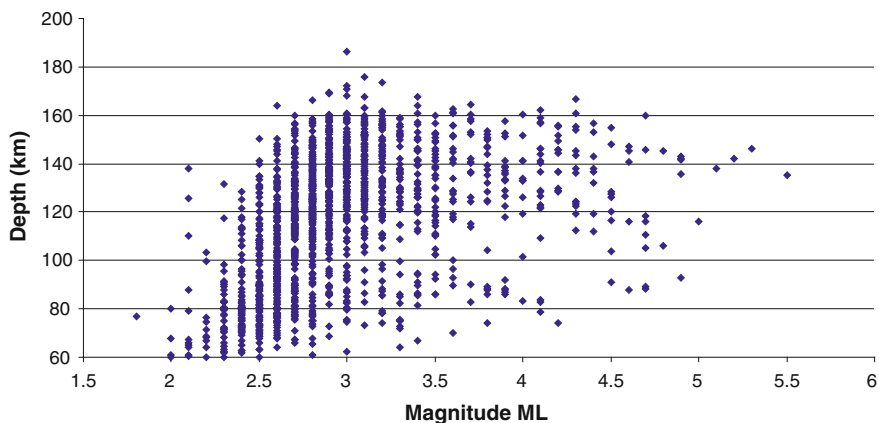
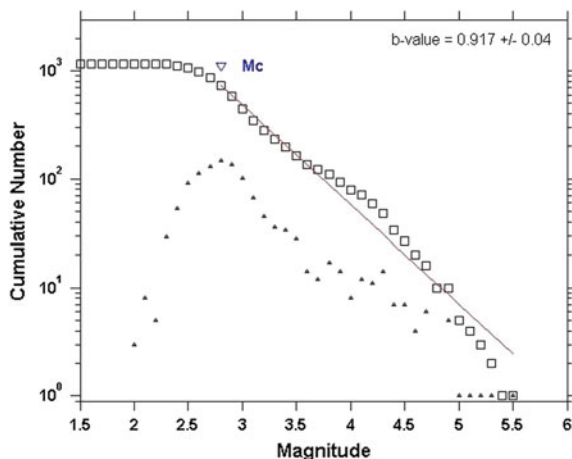


Fig. 5 Earthquake M_L magnitude versus depth

Fig. 6 The frequency—local magnitude (M_L) distribution of the subcrustal earthquakes. *Triangles*—number of events in each magnitude bin, *squares*—cumulative number of events. M_C is the estimated completeness magnitude



Figures 7 and 8 display diagrams of the strike, dip and rake of the nodal planes, and of the azimuth and plunge of the principal axes of the moment tensor, respectively.

The results show that the majority of the estimated focal mechanisms are reverse faultings. Normal faults are observed only for 3 events with magnitudes $M_L \leq 4.2$, located in the deeper part of the seismogenic zone ($h > 135$ km). Several mechanisms exhibit also a strike-slip component, significant only in few cases (7 events).

Regarding the orientation of the nodal planes, they both exhibit a NE–SW direction, parallel to the Carpathian Arc, in the case of almost 40 % of investigated earthquakes (including the strongest one— M_L 5.5). On the other hand, for 25 % of the events, both nodal planes are roughly oriented NW–SE, perpendicular to the

Table 1 The focal mechanisms of the Vrancea intermediate-depth earthquakes occurred during 2010–2015

No.	Date	Origin time hh:mm:ss	Lat. (°N)	Lon. (°E)	h (km)	M _L	Plane 1		
							Strike	Dip	Rake
1	01/01/2010	13:11:45	45.53	26.36	158	4.0	60	54	90
2	04/01/2010	19:55:21	45.54	26.37	126	4.0	52	46	90
3	25/02/2010	15:51:28	45.62	26.53	111	4.7	215	70	66
4	28/02/2010	18:55:11	45.72	26.65	146	4.2	40	20	90
5	13/03/2010	14:20:29	45.68	26.45	149	4.7	214	25	78
6	26/03/2010	18:36:48	45.71	26.53	97	4.2	217	64	74
7	14/04/2010	13:25:52	45.59	26.39	149	4.1	126	34	90
8	06/05/2010	04:50:58	45.53	26.55	126	4.2	143	48	48
9	24/05/2010	08:18:00	45.64	26.49	156	4.3	218	46	49
10	08/06/2010	15:16:10	45.65	26.45	123	5.0	102	58	61
11	25/06/2010	23:14:08	45.67	26.53	151	4.3	102	34	51
12	21/07/2010	22:30:09	45.54	26.36	121	4.5	324	43	72
13	30/08/2010	04:52:46	45.54	26.39	130	4.2	143	48	48
14	30/08/2010	20:51:38	45.71	26.60	147	4.7	210	52	27
15	30/09/2010	05:31:22	45.57	26.41	151	4.9	244	42	84
16	25/11/2010	11:55:01	45.65	26.34	129	4.1	118	56	72
17	02/12/2010	20:59:45	45.69	26.56	114	4.3	86	46	68
18	05/12/2010	02:49:19	45.68	26.53	152	4.5	354	61	78
19	04/02/2011	23:25:16	45.77	26.84	125	4.4	16	43	10
20	05/02/2011	14:28:40	45.64	26.67	126	3.8	205	32	67
21	12/02/2011	14:59:50	45.85	26.67	97	3.8	290	68	44
22	19/02/2011	20:00:49	45.82	26.77	85	3.9	359	45	45
23	17/04/2011	11:41:03	45.65	26.45	126	4.3	288	37	56
24	01/05/2011	02:24:16	45.59	26.43	144	5.3	151	64	79
25	14/06/2011	10:48:49	45.69	26.57	147	3.9	113	16	83
26	10/08/2011	02:37:33	45.75	26.70	139	4.2	290	90	54
27	15/08/2011	19:21:02	45.65	26.41	156	4.4	37	31	74
28	29/08/2011	18:00:40	45.75	26.64	139	4.3	226	62	88
29	05/09/2011	19:58:17	45.82	26.89	95	3.8	76	26	56
30	08/09/2011	13:50:31	45.65	26.53	127	4.5	232	42	69
31	12/09/2011	08:05:24	45.51	26.36	138	4.4	14	46	49
32	16/09/2011	03:02:45	45.65	26.45	153	3.8	98	24	-80
33	04/10/2011	02:40:48	45.57	26.51	141	5.2	11	49	66
34	13/10/2011	20:03:16	45.62	26.44	141	4.2	108	32	35
35	15/10/2011	22:09:02	45.59	26.49	139	3.8	246	43	72
36	24/10/2011	06:19:41	45.63	26.41	148	4.5	145	61	55
37	22/11/2011	04:17:35	45.52	26.35	142	4.2	123	14	45
38	03/12/2011	00:32:24	45.62	26.46	155	4.2	28	36	90

(continued)

Table 1 (continued)

No.	Date	Origin time hh:mm:ss	Lat. (°N)	Lon. (°E)	h (km)	M _L	Plane 1		
							Strike	Dip	Rake
39	10/01/2012	18:25:45	45.52	26.30	148	4.2	38	70	42
40	19/01/2012	18:05:54	45.58	26.46	127	3.8	18	14	82
41	26/04/2012	14:32:40	45.58	26.49	139	4.1	359	83	68
42	05/05/2012	17:07:17	45.69	26.53	125	4.0	311	54	69
43	26/05/2012	02:30:26	45.76	26.7	126	4.0	329	40	87
44	06/07/2012	22:48:00	45.69	26.68	118	4.3	47	30	69
45	12/07/2012	02:20:24	45.71	26.54	119	4.2	185	54	83
46	31/08/2012	20:22:05	45.51	26.32	140	4.0	151	69	58
47	01/12/2012	20:52:07	45.74	26.76	101	4.4	229	51	77
48	06/03/2013	01:10:11	45.49	26.27	132	4.1	199	80	45
49	21/04/2013	08:09:07	45.66	26.58	132	4.1	335	38	80
50	20/06/2013	00:22:54	45.58	26.69	124	4.3	7	54	85
51	12/07/2013	18:02:30	45.52	26.37	137	4.2	311	21	-55
52	28/07/2013	14:25:05	45.68	26.54	96	4.1	159	65	45
53	02/08/2013	04:18:13	45.74	26.54	94	3.8	39	56	53
54	11/08/2013	13:31:08	45.76	26.71	101	4.5	87	64	44
55	06/10/2013	01:37:21	45.66	26.55	139	5.5	35	47	65
56	15/10/2013	19:33:12	45.63	26.53	145	4.9	27	23	69
57	21/11/2013	06:38:52	45.76	26.72	96	4.7	37	69	77
58	12/01/2014	18:26:02	45.54	26.43	142	4.4	169	25	78
59	23/01/2014	06:15:03	45.49	26.29	138	4.9	24	55	52
60	03/02/2014	00:26:30	45.68	26.49	147	4.3	202	31	17
61	24/02/2014	00:22:54	45.78	26.68	112	4.5	54	57	63
62	26/03/2014	19:46:28	45.68	26.54	145	4.6	190	46	73
63	29/03/2014	01:55:16	45.37	26.23	152	4.3	204	36	73
64	29/03/2014	19:18:05	45.63	26.46	145	5.1	162	55	84
65	03/04/2014	12:38:56	45.49	26.38	135	4.9	219	50	69
66	24/08/2014	07:12:49	45.61	26.37	152	4.7	156	25	37
67	29/08/2014	6:24:28	45.53	26.41	129	4.1	174	64	81
68	10/09/2014	19:45:57	45.61	26.47	116	4.8	89	30	66
69	03/11/2014	13:09:59	45.59	26.42	127	4.4	40	47	62
70	03/01/2015	03:39:35	45.79	26.68	89	4.3	39	42	24
71	04/01/2015	00:22:53	45.56	26.42	119	4.3	54	57	63
72	14/01/2015	07:12:49	45.57	26.34	156	4.1	172	13	63
73	24/01/2015	09:55:47	45.73	26.56	100	4.6	42	55	40
74	21/02/2015	21:10:12	45.73	26.61	152	4.2	159	50	-29
75	27/02/2015	06:11:40	45.76	26.69	135	4.2	108	78	90
76	16/03/2015	15:49:47	45.61	26.43	125	4.8	323	44	84
77	29/03/2015	00:44:58	45.65	26.46	154	4.9	111	63	61

(continued)

Table 1 (continued)

No.	Date	Origin time hh:mm:ss	Lat. (°N)	Lon. (°E)	h (km)	M _L	Plane 1		
							Strike	Dip	Rake
78	05/07/2015	14:26:48	45.68	26.61	140	4	102	66	83
79	13/07/2015	23:35:10	45.67	26.51	156	4.2	68	20	90
80	29/09/2015	15:53:49	45.74	26.74	131	4.1	131	62	71
No.	Plane 2			P-axis		T-axis		No. of polarities/no. of inconsistent polarities	
	Strike	Dip	Rake	Azimuth	Plunge	Azimuth	Plunge		
1	240	36	90	150	9	330	81	10/0	
2	232	44	90	142	1	322	89	19/0	
3	87	31	137	322	21	92	59	30/0	
4	219	70	90	310	25	130	65	11/0	
5	47	65	96	133	20	328	69	31/0	
6	70	30	119	319	17	98	67	13/0	
7	306	56	90	36	11	216	79	10/0	
8	17	56	127	82	4	344	60	13/0	
9	89	57	124	155	6	54	61	21/0	
10	327	42	127	212	8	319	64	46/1	
11	327	64	114	40	16	275	63	21/1	
12	167	49	106	246	3	142	78	36/0	
13	17	56	127	82	4	344	60	13/0	
14	103	69	139	160	11	60	43	32/1	
15	72	48	95	158	3	32	85	37/3	
16	329	38	115	221	10	343	72	18/0	
17	297	48	112	11	1	278	74	25/0	
18	197	31	109	93	15	237	72	33/1	
19	279	83	132	337	26	225	37	32/2	
20	51	61	104	131	15	352	71	17/1	
21	181	50	151	52	11	153	46	15/1	
22	234	60	125	300	9	195	59	28/1	
23	149	60	113	222	12	103	66	25/0	
24	356	28	112	250	19	39	69	46/1	
25	301	74	92	29	29	214	61	27/0	
26	200	36	180	50	35	170	35	26/0	
27	235	60	99	318	15	168	73	28/0	
28	50	28	94	317	17	130	73	21/1	
29	293	69	105	11	22	227	63	25/0	
30	79	51	108	156	5	48	75	28/0	
31	245	57	124	312	6	211	61	25/0	
32	267	66	-94	168	69	0	21	22/0	
33	225	47	115	118	1	211	72	45/0	
34	348	72	117	57	22	292	55	17/0	

(continued)

Table 1 (continued)

No.	Plane 2			P-axis		T-axis		No. of polarities/no. of inconsistent polarities
	Strike	Dip	Rake	Azimuth	Plunge	Azimuth	Plunge	
35	90	49	106	168	3	65	78	19/0
36	20	44	136	259	10	5	58	23/0
37	349	80	100	70	39	271	54	32/0
38	208	54	90	298	9	118	81	22/0
39	291	51	154	161	12	262	43	37/0
40	207	76	92	295	31	119	59	31/0
41	256	23	161	108	34	246	48	40/0
42	164	41	116	56	7	166	72	42/0
43	153	50	93	241	5	83	85	42/0
44	250	62	101	332	17	185	70	45/0
45	17	36	100	279	9	65	79	42/1
46	32	38	145	264	18	21	54	33/0
47	69	41	105	328	5	84	79	53/3
48	99	46	166	322	22	70	38	46/0
49	168	52	98	252	7	113	81	42/1
50	196	36	97	101	9	256	80	46/2
51	94	72	-103	346	61	194	26	30/2
52	46	51	146	280	8	19	49	25/0
53	273	48	132	155	4	252	60	22/0
54	334	51	146	208	8	307	49	42/0
55	249	49	114	322	1	229	72	62/1
56	230	68	99	313	23	155	66	61/5
57	262	28	131	141	22	278	61	33/0
58	2	65	96	88	20	283	69	52/2
59	258	50	131	140	3	235	60	60/2
60	98	81	120	164	30	38	45	51/3
61	276	41	125	162	8	271	66	49/2
62	34	46	107	112	0	22	78	47/1
63	45	56	102	126	10	353	76	44/0
64	352	35	99	256	10	49	79	59/2
65	69	44	113	323	3	63	74	47/1
66	32	75	111	105	27	328	55	49/1
67	13	27	108	270	19	65	69	31/1
68	296	63	104	17	17	234	69	68/4
69	258	49	117	239	1	237	70	50/2
70	291	74	130	353	19	241	45	42/1
71	276	41	125	162	8	272	66	45/2
72	20	78	96	105	33	298	57	50/2
73	287	59	137	345	3	252	51	59/1

(continued)

Table 1 (continued)

No.	Plane 2			P-axis		T-axis		No. of polarities/no. of inconsistent polarities
	Strike	Dip	Rake	Azimuth	Plunge	Azimuth	Plunge	
74	269	68	-136	132	46	30	11	52/1
75	288	12	90	198	25	18	65	36/1
76	150	46	95	237	1	133	86	62/0
77	342	39	134	222	13	336	60	78/0
78	298	25	104	197	21	359	68	34/1
79	248	72	90	338	27	158	63	49/1
80	348	33	122	235	15	5	67	40/0

mountain arc; 3 (out of 5) seisms with local magnitude greater than 5.0 belong to this group.

The calculated focal mechanisms are displayed in Fig. 9.

4 Discussion

Using the high quality data provided by the National Seismic Network, 1603 intermediate depth earthquakes with local magnitudes ≥ 1.8 , which occurred during the period January 2010–October 2015 in the Vrancea intermediate-depth seismogenic region, were accurately localized.

The space distribution of the hypocenters comply with the geometry of the source zone, evidenced in several earlier studies (e.g. Martin et al. 2006).

Reliable fault plane solutions for 80 moderate-size subcrustal earthquakes ($M_L \geq 3.8$) were also obtained. The main features of the focal mechanisms of the Vrancea intermediate-depth events, revealed in numerous previous studies (e.g. Enescu 1980; Oncescu and Trifu 1987; Enescu and Zugravescu 1990; Radulian et al. 2000), are emphasized by our results as well. Thus, the reverse faulting with near-vertical tension axis and near-horizontal compression axis—indicating a predominant compressive stress regime in the Vrancea undercrustal source zone—is observed for more than 70 % of the investigated events. Regarding the nodal plane orientation, the two typical solutions evidenced by the earlier studies mentioned above—(i) nodal planes oriented mainly NE–SW and P-axis perpendicular to the Carpathian arc; and (ii) nodal planes oriented mainly NW–SE and P-axis parallel to the Carpathian arc—are also considerably present among our results (type (i)—almost 40 % of the mechanisms, type (ii)—25 % of the mechanisms). Nevertheless, our study points out a larger diversity of the focal mechanisms of the Vrancea intermediate-depth earthquakes within the magnitude range 3.8–5.5.

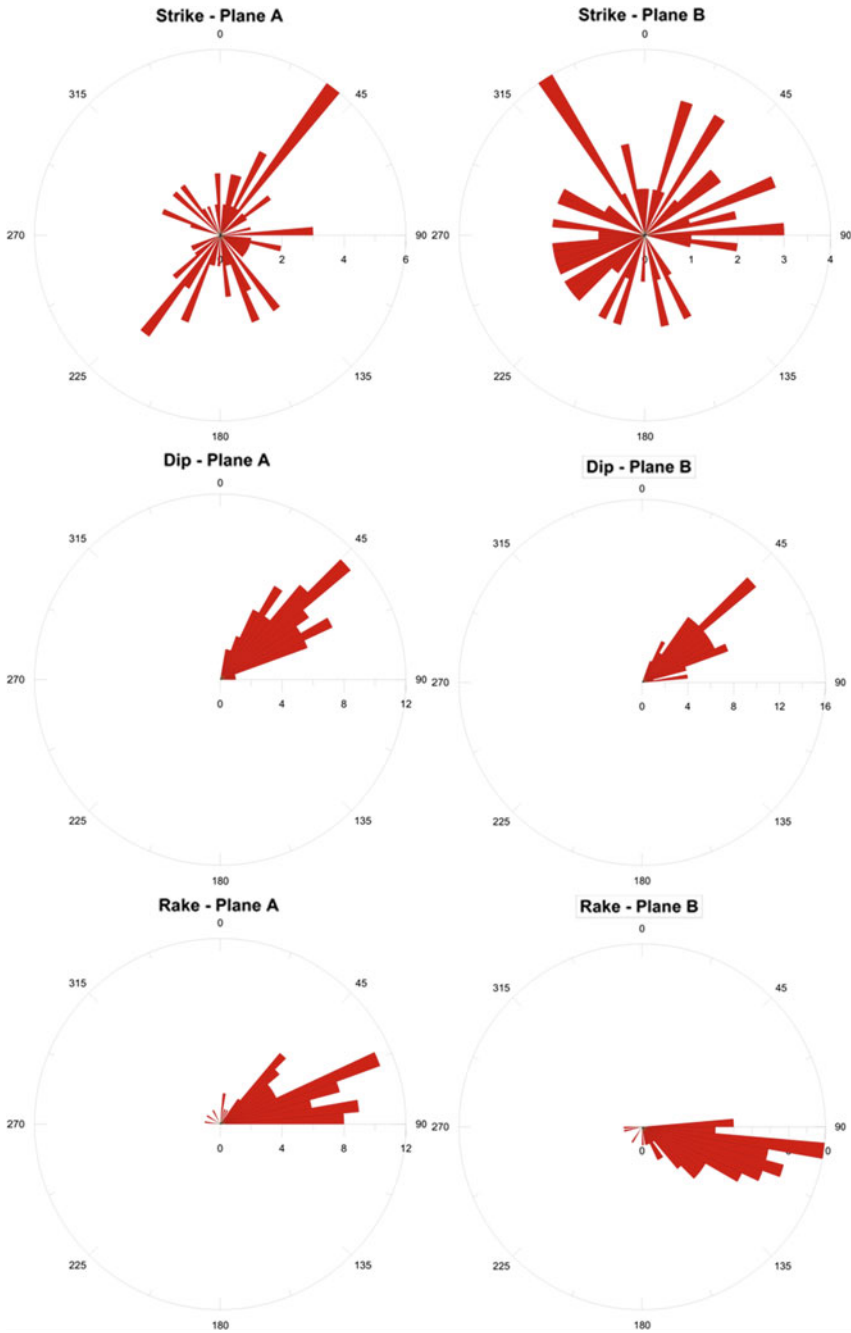


Fig. 7 Diagrams of the strike, dip and rake of the nodal planes of the investigated Vrancea earthquakes

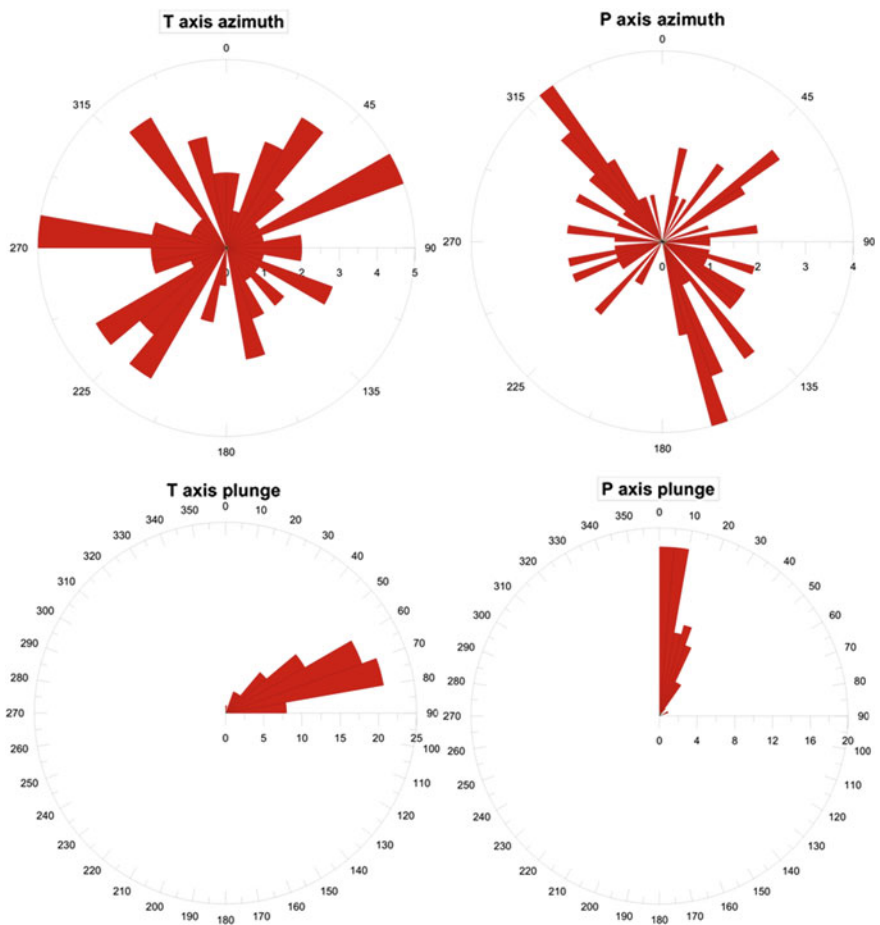
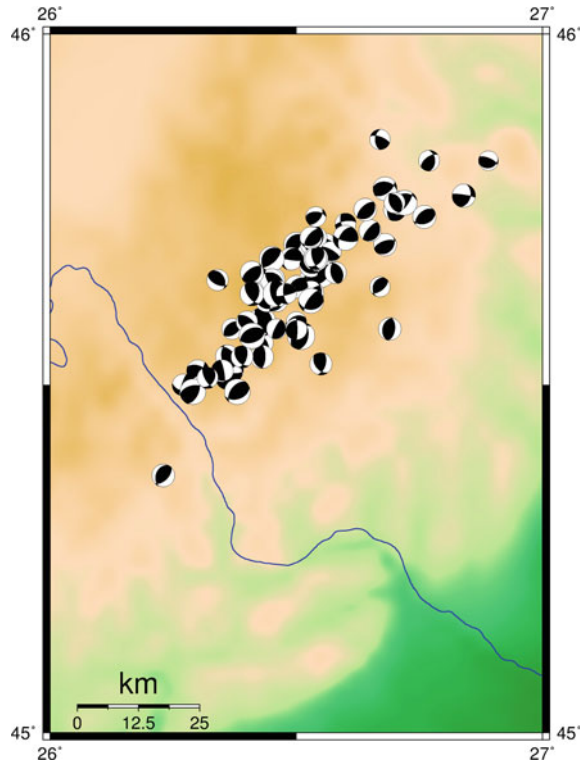


Fig. 8 Diagrams of the azimuth and plunge of the compression (P) and tension (T) axes of the moment tensor of the investigated intermediate depth Vrancea earthquakes

Fig. 9 The focal mechanisms of the subcrustal Vrancea earthquakes with $M_L \geq 3.8$ which occurred during the period 2010–2015



Acknowledgements This work was partially supported by the grant of the Romanian National Authority for Scientific Research, CNCS—UEFISCDI, project number PN-II-RU-TE-2012-3-0215. The authors thank Dr. Luminita Ardeleanu for the constructive discussions, which led to the significant improvement of the manuscript.

References

- Boulder Real Time Technologies—BRTT—<http://www.brtt.com/software.html>
- Craiu M, Craiu A, Ionescu C, Popa M, Radulian M (2012) New local magnitude calibration for Vrancea (Romanian) intermediate-depth earthquake. *Rom R Phys* 64(4):1097–1108
- Enescu D (1980) Contributions to the knowledge of the focal mechanism of the Vrancea strong earthquake of March 4, 1977. *Rev Roum Geol Geophys Geogr Ser Geophys* 24:3–18
- Enescu D, Zogrăvescu D (1990) Geodynamic considerations regarding the Eastern Carpathians arc bend, based on studies on Vrancea earthquakes. *Rev Roum Geophysique* 34:17–34
- Havskov J, Ottemöller L (eds) (2003) SEISAN: the earthquake analysis software for Windows, SOLARIS, LINUX and MACINTOSH Version 8.0. Manual, Institute of Solid Earth Physics, University of Bergen, Norway
- Martin M, Wenzel F, and Calixto Working Group (2006) High-resolution teleseismic body wave tomography beneath SE-Romania—II. Imaging of a slab detachment scenario. *Geophys J Int* 164:579–595

- Oncescu MC, Trifu CI (1987) Depth variation of the moment tensor principal axes in Vrancea (Romania) seismic region. *Ann Geophysicae* 5B:149–154
- Radulian M, Mandrescu N, Panza GF, Popescu E, Utale A (2000) Characterization of seismogenic zones of Romania. *Pure appl Geophys* 157:57–77
- Radulian M, Vaccari F, Mandrescu N, Moldoveanu CL, Panza GF (2002) Realistic modeling of the seismic hazard due to the subcrustal earthquakes beneath Romanian Carpathian, IGCP 430 workshop II, Vietnam, 1–2 Apr
- Snoke JA, Munsey JW, Teague AG, Bollinger GA (1984) A programme for focal mechanism determination by combined use of polarity and SV-P amplitude ratio data. *Earthq Note* 55:15

A Contemporary View to the Impact of the Strong Vrancea Earthquakes on Bulgaria

Mihaela Kouteva-Guentcheva and Krasimir Boshnakov

Abstract State of the art review of recent seismic hazard assessment studies related to the impact of the strong Vrancea earthquakes on the Bulgarian territory is provided. The regional danger due to these quakes requires particular engineers' attention and care, especially with respect to the existing buildings. Some earthquake engineering aspects of these shocks are commented, based on the published analysis of the available macroseismic, instrumental data and first order estimates of the earthquake capacity resistance of typical structural systems exposed to the Vrancea seismic action. Further relevant studies and possible joint activities are set out in brief.

Keywords Vrancea earthquake impact · Bulgaria · Earthquake hazard and earthquake risk

1 Introduction

Earthquakes occurring within the Vrancea seismogenic zone in Romania have been of significant scientific and practical interest because of their social and economic consequences. The total area affected by intermediate-depth Vrancea earthquakes is estimated to comprise 300,000 km² populated by about 25 million people (Zaicenco and Alkaz 2005). This territory encompasses significant part of the territory of the Romanian neighboring countries, including parts of Bulgarian territory that is regularly suffering the long period and far-reaching seismic effects of the Vrancea intermediate-depth earthquakes (damage of severity I–VI MSK). Significant losses were caused in Bulgaria due to the strong Vrancea earthquakes of the last century

M. Kouteva-Guentcheva (✉) · K. Boshnakov
Faculty of Structural Engineering, Computer Aided Design,
University of Architecture, Civil Engineering and Geodesy, Sofia, Bulgaria
e-mail: kouteva_fce@uacg.bg

K. Boshnakov
e-mail: krabosh_fce@uacg.bg

in 1908, 1940, 1977, 1986 and 1990. The wave field radiated by the intermediate-depth (70–170 km) Vrancea earthquakes, mainly at long periods ($T > 1$ s), attenuates less with distance, compared to the wave field generated by the earthquakes located in other seismically active zones in Bulgaria. The quake of March 4, 1977, ($M_w = 7.5$) caused significant damage in Bulgaria and was felt up to Central Europe (Brankov et al. 1983). In fact, the Vrancea intermediate-depth sources represent a regional danger, since large industrial areas can be seriously affected by the strong events originating in this seismogenic area. The changes in the Bulgarian Code for Design and Construction in Seismic Regions'87 were triggered mainly by the losses and damages, caused by the Vrancea 1977 shock. Last strongly felt seismic events were the 1986 and 1990 Vrancea quakes.

This paper aims to commemorate the Vrancea earthquake of November 10th, 1940, being one of the strongest known Vrancea earthquakes stressing once again the necessity of particular attention to the Vrancea subduction zone as regional seismic danger. For this purpose, a state-of-the-art review of the seismic hazard estimates for the Bulgarian territory related to Vrancea strong earthquakes, including some analysis of the available macroseismic and instrumental data are provided, and some ideas for further relevant studies are shared.

2 Available Data—Macroseismic Observation and Instrumental Records

2.1 *Macroseismic Observation*

2.1.1 Overall View to the Available Iseismal Maps

The Vrancea subduction seismogenic zone is a peculiar intermediate-depth source that, in case of large magnitude earthquake, strongly affects significant part of the Bulgarian territory including major cities in NE Bulgaria, among which the biggest Bulgarian port on the Danube river—the town of Russe. The epicenters of the strongest documented Vrancea events occupy an ellipse-like area, with some irregular extensions towards NE, SW and SE. The isoseismal areas are strongly stretched towards NE-EW ($N45^\circ E$ – $N225^\circ E$) for some earthquakes (1940, 1977), but there are also other historical data that show isoseismal ellipses slightly “turned” anti-clockwise (1802) or even oriented perpendicular to the usual direction. The focal depth of the strong events is about 100 km, the increase of magnitude appears to be positively correlated with the increase of depth (Georgescu and Sandi 2000 and references therein; Kronrod et al. 2013). The track record of the Vrancea intermediate depth quakes with magnitude $M \geq 7.0$ shows that these shocks are felt at very large distances, up to 1000 km and NE Bulgaria is affected by intensities $I \geq VI$ (MSK). Sometimes local culminations of intensities can be recorded at epicentral distances of 200–300 km, like the one (above VII intensity) documented at Russe in 1977. Most of the damage due to strong Vrancea earthquakes, so far,

refers to structures constructed before 1970. Observed effects in Bulgaria due to the strong Vrancea earthquakes are well documented. From approximately 9000 shocks ($M > 2.0$, <http://www.infp.ro/catal.php>) with epicenters located in the Vrancea region, we are confident about hundred seismic events, felt in Bulgaria ($M > 5$). Isoseismal maps for 40 of these earthquakes have been elaborated and published, starting with the event of April 6, 1790 and ending by March 4, 1977 (Rigikova 1983). The strongest Vrancea earthquakes according the U.S. Geological Survey Earthquake Hazards Program, 2003, also indicates two strong shocks, $M > 6.5$, occurred in the XIX century (1802, 1838) and five shocks in the XX century (1940, 1977, 1986, 1990). Photos of damages and demolitions due to Vrancea region seismic activity, isoseismal maps and relevant analyses have been subject of numerous scientific publications and books. The review of the overall macroseismic records of strong, intermediate-depth Vrancea quakes indicate that the region of maximum damage lies northeast from Orjahovo to Silistra on the Danube and to the south to the towns of Razgrad and Dulovo. Unfortunately, the Vrancea 1986 impact in Bulgaria is not very well documented by publications record, possibly because the same year two local earthquakes caused significant damages in northern Bulgaria, when 15,000 buildings were damaged by the Feb. 28, 1986—Stragitza, $M \sim 5.1$ and the Dec. 7, 1986, Popovo, $M \sim 5.7$, earthquakes.

2.1.2 Damages in NE Bulgaria Due to the Vrancea 1990 Earthquakes

The recent strong Vrancea shocks causing damages and stress in north-eastern Bulgaria have been the events that occurred in May, 1990 (May 30, $M_w = 6.9$ and May 31, $M_w = 6.2$). Some documented damages in NE Bulgaria due to the Vrancea 1990, May 30–31, earthquakes are shown in.¹ The photos are made during a field trip to the most damaged towns and villages—Chernolik, Alfatar, Dulovo and Silistra. At Russe there were reported very few damages like few old chimneys. As one can see, the age of the damaged building corresponds to lack or low/medium level of earthquake resistant design and construction. Major observation in the small villages/towns was that the damaged buildings represented cases of poor quality of construction, inadequate detailing of reinforcement and absence of capacity design principles. Considering the importance of damage-based assessment of the macroseismic intensity, the proper accounting for the quality of construction directly reflects the realistic estimation of the seismic hazard. It is commonly accepted to define the intensity as measure of the strength of shaking at any place during an earthquake, in terms of its observed effects. Buildings and structures resist different actions by gradually accumulating strains and the corresponding damages. Thus the observed damages encompass the structures response to particular shock combined

¹The photos, shown in Table, are available from Kouteva's personal archive. They were made during a field trip supported by CLSMEE-BAS in collaboration with eng. K. Hadjisky and eng. P. Ranguelov, June 1–3, 1990.

Table 1 Documented damages in NE Bulgaria due to the Vrancea 1990 earthquakes (VR90) according to the EMS-98 scale (Grünthal, 1998)

Type of structure	Vulnerability class	Year of construction	Site	Classification of damage				
				1	2	3	4	5
One storey masonry	B	NA	Alfatar, NE Bulgaria			X		



Type of structure	Vulnerability class	Year of construction	Site	Classification of damage				
				1	2	3	4	5
Frame, moderate ERD* school	D	NA	Alfatar, NE Bulgaria			X		






Type of structure	Vulnerability class	Year of construction	Site	Classification of damage				
				1	2	3	4	5
Frame, moderate ERD * kinder garden	D	NA	Chernolik, NE Bulgaria			X		



(continued)

Table 1 (continued)

Type of structure	Vulnerability class	Year of construction	Site	Classification of damage				
				1	2	3	4	5
Frame, moderate ERD – Post office	D	NA	Chernolik, NE Bulgaria			X		
								
Type of structure	Vulnerability class	Year of construction	Site	Classification of damage				
Walls, masonry - residential	B	1968	NE Bulgaria			X		
								
Chernolik		Silistra→						
Type of structure	Vulnerability class	Year of construction	Site	Classification of damage				
Walls, masonry	B	1910 / 1928	NE Bulgaria			X		
								
Silistra, Residential, 1910			Silistra, Art gallery, 1928-1930			Dulovo, Church, 1928		

with all accumulated visible and invisible strains, damage and relevant weakening up to the considered event. Another logical concern is the unification of macroseismic practices in different countries and local practices for intensity data assessment.

2.2 Instrumental Records

Accelerograms due to Vrancea intermediate-depth earthquakes have been recorded on three seismic networks in Romania as well as on the seismic networks of the Academy of Science in Moldova and the Academy of Science in Bulgaria. Unfortunately, there are only two strong ground motion records of earthquake engineering interest in Bulgaria, recorded during Vrancea earthquakes (Nenov et al. 1990). These are the free field accelerograms recorded at Russe—VR86 (two components) and VR90 (three components). A comparison of the response spectra computed for the available recorded accelerograms in Romania and Bulgaria (Ambraseys et al. 2002; Nenov et al. 1990) with the relevant quantities, considered in the Eurocode 8, is shown in Fig. 1. The Bulgarian data are shown in the last box (bottom, right) in this figure. These comparisons illustrate clearly (i) similar type of response curve for the same event at different recording stations and (ii) some obvious underestimation of the observed values with respect to the structures design code prescribed values. The similarity in the shapes of the response curves, obtained for the considered events, recorded at sites with very different geology, confirms the contribution of the focal mechanism to the frequency content of the recorded ground motions.

A brief engineering analysis of the parameters, related to the damage potential of the strong Vrancea earthquakes was provided by Kouteva (2010). Peak and integral strong ground motion parameters were estimated. The computed values of the chosen parameters for the horizontal components, e.g. $0.06 < PGV/PGA < 0.30$ (0.69) are

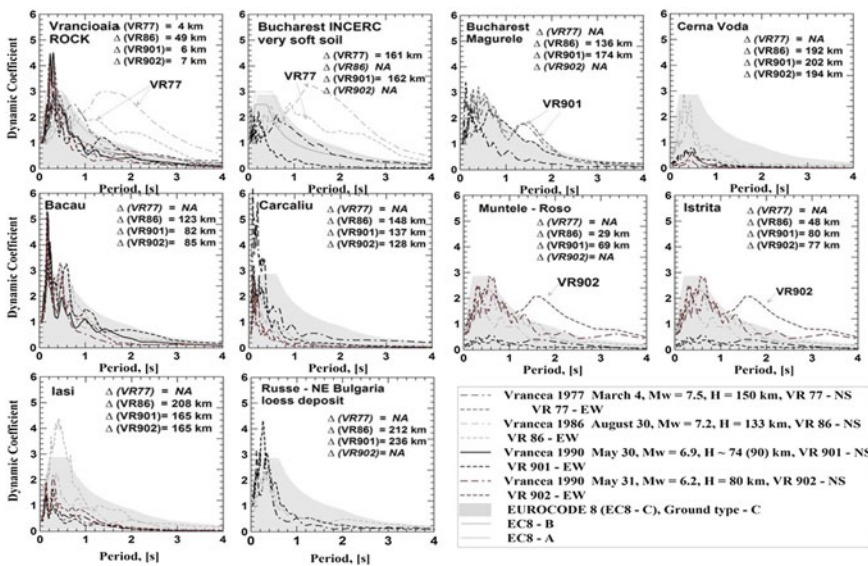


Fig. 1 Comparison of the response spectra computed for the available recorded accelerograms in Romania and Bulgaria (Ambraseys et al. 2002; Nenov et al. 1990) with the relevant EC8 quantities

comparable with relevant values, computed for strong earthquakes, such as Kobe, 1995 ($M_w = 6.9$, $0.06 < PGV/PGA < 0.17$), Chichi, 1999 [$M_w = 7.6$, $0.06 < PGV/PGA < 0.40$ (0.7)] and Wenchuan, 2008 ($M_w = 7.9$, $0.05 < PGV/PGA < 0.16$) (Cosenza and Manfredi 2000).

3 Seismic Hazard Estimates

3.1 *Classical PSHA and DSHA Approaches*

Different seismic hazard assessments related to the Vrancea earthquake danger were performed. Classical probabilistic and deterministic seismic hazard estimates for Russe were performed and published by Todorovska et al. (1994) and by Paskaleva et al. (2001) reproducing the Vrancea events of 1986 (VR86) and 1990 (VR90), respectively. In 2006, a seismic hazard map for Bulgaria was published by Simeonova et al. as a basis for a new building code. The Vrancea earthquake hazard was treated separately for shallow and intermediate-depth zones. Maps obtained for a return period of 475 years show that the seismic hazard at Russe is controlled mainly by the Vrancea intermediate-depth seismic zone (VrIdSZ) with expectations of a macroseismic intensity of I–VIII MSK in both cases analyzed with exposure only to the VrIdSZ and exposure to all source zones considered (Simeonova et al. 2006). Seismic hazard evaluations based on a traditional probabilistic seismic hazard analysis (PSHA) rely on probabilistic analysis of earthquake catalogues, on macroseismic observations and on instrument records. Recently, PSHA's usefulness in providing reliable seismic hazard assessment has been limited possibly due to insufficient information about historical seismicity which can introduce relevant errors in a purely statistical approach based mainly on seismic history (Klügel et al. 2006; Klügel 2007). The standard error of empirical attenuation equations (or the difference between observations and estimates of a physical predictive model) is one of the main sources of errors in traditional PSHA. The macroseismic and instrument data availability is very limited, and the statistical determination of the coefficients of frequency-magnitude relationships (FMR) for the zones controlling the seismic hazard in northeastern Bulgaria is affected by significant uncertainties (Molchan et al. 1997).

3.2 *Neo-Deterministic Seismic Hazard Assessment (NDSHA)*

Regional and national neo-deterministic seismic hazard assessment considering the Vrancea seismogenic zone have been performed and analyzed within the framework of several international research project supported by UNESCO, NATO, EC-INTAS, CEI, DACEA and different bilateral agreements. In 2000, finalizing the

UNESCO-IGCP Project 414 “Seismic Ground Motion in Large Urban Areas” and taking advantage of the existing Central European Initiative (CEI) Network, maps of neo-deterministic seismic hazards including design ground acceleration (DGA) peak ground velocities (PGV) and peak ground displacements (PGD) for some European countries were published by Panza and Vaccari. According to these maps, DGA up to 0.675 g can be expected in that region. The deterministic results of an $M = 7.7$, $H = 150$ km event that occurred in 1940 (Panza and Vaccari 2000), give a DGA in NE Bulgaria, Russe, within the range 0.30–0.60 g maximum displacement of 15–30 cm and maximum velocity of 30–60 cm/s. Theoretical modeling of the seismic loading at Russe due to Vrancea intermediate-depth events considering different frequency intervals (Kouteva et al. 2004; Kouteva 2008, 2010) was performed applying an analytical deterministic procedure (Panza et al. 2001). All ground motion components—transverse, radial and vertical—contribute significantly to the seismic input. It has been shown that the site amplifications at Russe due to different earthquakes show rather different amplification patterns for the various ground motion components. Parametric/sensitivity analysis of the ground motion at Russe, considering different uncertainties regarding the seismic source and the propagation path was also performed (Kouteva et al. 2004; Kouteva 2008, 2010). Various sets of synthetic seismic signals were computed varying the seismic source location, the parameters describing the movement in the source and the V_p/V_s ratio of the superficial layer at the local site. The results showed that all the tensorial properties of the earthquake sources influence the shape and the amplitude of the seismic signal, and among the selected parameters, the focal depth contributes most strongly to these changes. Superficial soil conditions also contribute to both the seismic input and to the damage potential of the ground motion (Kouteva 2008). The lack of enough instrumental strong motion records and the peculiarity of the intermediate-depth Vrancea seismic source results in the necessity of providing, by modelling, reliable seismic input definition that might be used for the purpose of retrofitting and urban planning. Two major Vrancea scenarios have been selected for Bulgaria (Kouteva 2008). The scenario event represents different combinations of parameters, thus the scenario earthquakes can be different in what concerns source location, magnitude and parameters describing the geometry and the kinematics of the seismic source. Considering the specific natural conditions, the various categories of elements and systems of risk and the Vrancea earthquake record, for this area, the suitable scenario earthquakes should correspond to return periods ranging from 50 to 200 years, as far as severe or extreme magnitudes are considered (Georgescu and Sandi 2000). Suitable alternative to Vrancea scenario events quakes in magnitude (Gutenberg-Richter) range from 7.2 (severe earthquakes Sce_1) to 7.8 (extreme earthquakes Sce_2) can be considered. Data on the seismic source mechanisms of the intermediate-depth Vrancea earthquakes are published by Dziewonsky et al. (1991) and Radulian et al. (2000). The scenario earthquakes used to define the seismic input are summarized in Table 2.

Synthetic seismic signals with different frequency content (up to 1, 3 and 5 Hz) were computed taking into account different local sites models following the EC8

Table 2 Scenario Vrancea earthquakes

Quake ^a	Lat. (°N)	Long. (°E)	Magnitude M_w	Focal depth (km)	Strike angle (°)	Dip angle (°)	Rake angle (°)
Scce_1	45.76	26.53	7.2	132.7	240	72	97
Scce_2	45.80	26.7	7.8	150	225	60	80

^aScce_1 seismic source description corresponds to the 1986 Vrancea quake (August 30) (Dzievonsky et al. 1991) and Scce_2 corresponds to the Vrancea 1940, Nov. 10, earthquake (Radulian et al. 2000 and references therein)

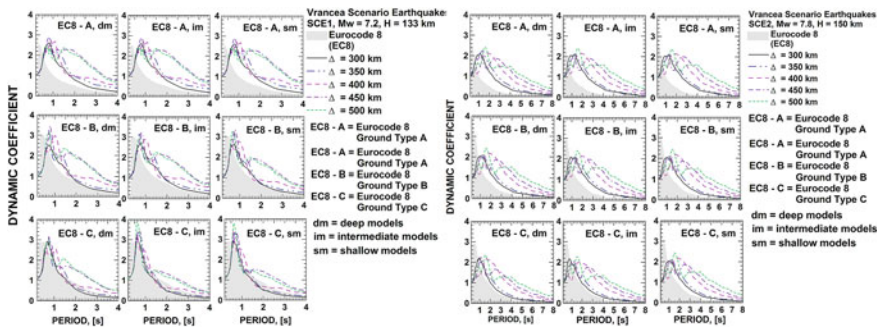


Fig. 2 Vrancea earthquake scenarios—comparison of the computed and the EC8 response curves. *Left* Scce 1, $M_w = 7.2$, $H = 133$ km; *Right* Scce 2, $M_w = 7.8$, $H = 150$ km

soil classification, different depths of the superficial part of the model (Kouteva 2008). The seismic source is considered as a point source. Computed signals, accelerograms and response spectra were successfully validated against the available observations at Russe site, NE Bulgaria (Kouteva et al. 2004; Kouteva 2008). Some response spectral curves, normalized to the corresponding PGA values are shown in Fig. 2. The overlapping of the computed response curves with those, provide by EC8, shows that the synthetics provides conservative decision at larger epicentral distances. These results might be useful, when performing push-over analysis and relevant parametric studies.

4 First Order Seismic Risk Estimates

4.1 The Existing Buildings and Seismic Action

The status of the existing structures related to the impact assessment of the endorsement of the common European legislation for earthquake resistant design in Bulgaria logically raises the question whether the existing buildings meet the new requirements of the Eurocode 8 (BDS EN 1998-1/NA-2010). A brief look at some

statistics of the existing building stock (NSPMWCDB 2011) shows that the predominant part of it in Bulgaria ($\sim 86\%$) was built in the period 1946–1989 and only 7% has been designed and constructed according the contemporary modern standards for design in seismic regions. Most of the buildings are two to four floors of masonry or reinforced concrete structures. Considering that significant part of the existing buildings in both countries, Bulgaria and Romania, is designed and constructed according to low and moderate earthquake resistant requirements, the compatibility of the seismic loading in the cross border areas is very important and useful for the reasonable earthquake risk management. It is curious to take a look at the comparison of the definitions of seismic action in the neighbor regions, e.g. Russe region in NE Bulgaria, according to the current legislation in Bulgaria (BDS EN 1998-1/NA-2010) compared to Romania (SR-EN-1998-1/NA-2008). The definitions of the seismic actions under both legislations are based on different philosophies. The ground type contribution to the seismic action is taken into account in different way. The maps of the reference ground acceleration are prepared for different return periods. Thus direct comparison of the seismic action is not easy. In very general terms, it can be generalized that the EC8 definition of the horizontal component due to Vrancea seismic zone in Bulgaria is consistent with the seismic action definitions, provided in the Romanian documents and the vertical one is higher than the corresponding values prescribed for Romania.

4.2 Brief First-Order Seismic Risk Estimation

Brief preliminary, first-order, seismic risk estimation with regard to the seismic resistance of the building structures with respect to the seismic action is the comparison of the capacity diagrams in Sa-Sd format, that represent the response spectral accelerations versus corresponding spectral displacements. The capacity curves couple basic engineering parameters relevant to the nonlinear structural response during given earthquake. Unfortunately, only few capacity curves for representative building structures in Bulgaria are available. Still, the most comprehensive information source on such data are the reports on the RISK-UE-EVK4-CT-2000-00014 project (www.risk-ue.net), very well elaborated classification of the existing structures and capacity curves for typical buildings in the Mediterranean and the Balkan regions are supplied (Kappos et al. 2002; Milutinovic and Trendafiloski 2003). The RISK-UE typology matrix considers preliminary defined classes of buildings with similar structural characteristics and behaviour. Following the RISK-UE methodology, buildings are additionally grouped according to the availability of Codes for earthquake resistant design and construction and their requirements related to the time of design and construction of these buildings: NC—no code; LC—low level of code; MC—medium and HC—high level of codes (EC8 comparable). Some of these data, listed in Table 3, are compared with the capacity diagrams, corresponding to the BDS EN 1998-1/NA-2010 definition of seismic action as shown in Fig. 3.

Table 3 Data on structures' types, which capacity curves are used in Fig. 3

No	Code	Firs*	Construction		Author—RISK-UE
1	NC	LR	Rubber stone		AUTH, Thessaloniki
2, 3		MR, HR	RC moment frame	RC1 RC	UTCB, Romania
4, 5		MR, HR	Shear walls	RC2 RC	
6		LR, MR	RC moment frame	RC	AUTH, Thessaloniki
7		LC			
8, 9, 10		LC	LR, MR, HR	RC dual system	
11, 12, 13	LR, MR, HR		RC frame, infill masonry	RC	
14	MC		MR	Shear walls	RC2 RC
15, 16, 17	MC	LR, MR, HR	RC frame	RC1 RC	IZIIS-Skopje
18, 19		HC	MR, HR	RC dual system	

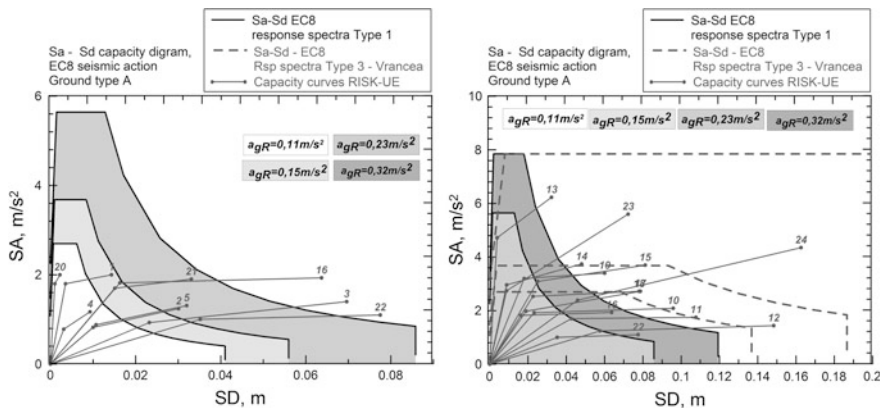


Fig. 3 Comparison of the capacity diagrams (Sa-Sd) of the structures listed in Table 3 with the corresponding BDS EN 1998-1/NA-2010 diagrams

Three typical height classes make further sub-grouping of buildings: LR: low-rise (1–2 stories for masonry and wooden systems; 1–3 for RC and Steel systems); MR: mid-rise (3–5 stories for masonry and wooden systems; 4–7 for RC and Steel systems); HR: high-rise (6+ stories for masonry systems; and, 8+ for RC and Steel systems).

Capacity diagrams in Sa-Sd format for two defined Vrancea scenario earthquakes (Table 2) are overlapped with the capacity curves of some mid-rise reinforced structures, which are representative for the Balkan region for different periods of seismic regulations for design and construction developments are presented in Fig. 4, finally.

The comparison between Sce_1 and Sce_2 shows that residential buildings are most vulnerable to severe (more frequent) events. Figure 4 shifts attention to the

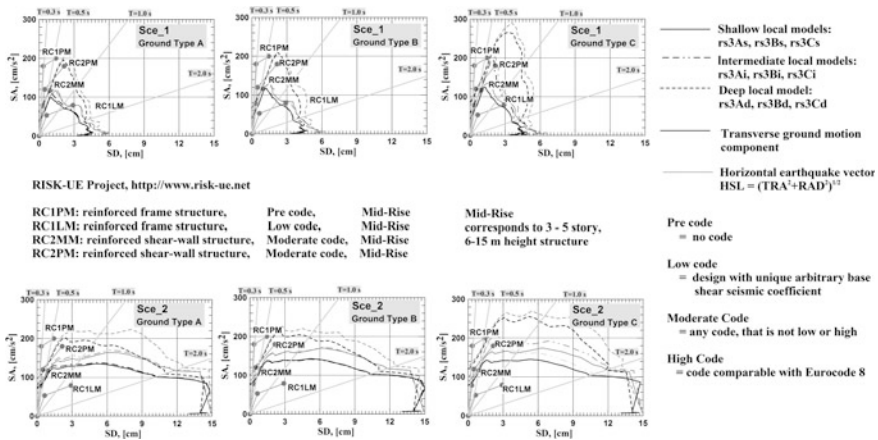


Fig. 4 Comparison of the capacity diagrams of selected structures (Table 3) and Vrancea Scenario earthquakes (Table 2). *Solid line* Shallow local models, *dashed line*—deep local models, *dash-dot line*—intermediate depth local model

fact that the stronger and deeper events Scen_2 ($M_w = 7.8$, $H = 150$ km) keep similar levels of response spectral acceleration for 5 % damping, but create twice larger response spectral displacements, compared to Scen_1 ($M_w = 7.2$, $H = 133$ km). In fact, the Scen_2 results are in agreement with the recently published maps of seismic hazard numerically modelled peak amplitudes of the horizontal ground motion, displacement, velocity and design ground acceleration for some European countries (Panza and Vaccari 2000). The change of the frequency content of the capacity spectra and the low-frequency (long-period) contribution to the seismic input for Scen_2 is obvious. Figure 4 also indicates that Scen_1 is more sensitive to local model changes, as compared to Scen_2. The use of shallow and intermediate local models for ground types A and B does not lead to visibly different results, for Scen_2 these models can be considered identical. Figure 4 clearly illustrates the predominant significance on the seismic input of the influence of the seismic source over that of the local geology at the considered site.

The preliminary estimation, provided here, is based on data that are representative for the neighboring to Bulgaria territories. Adequate vulnerability and earthquake risk assessment might be based only on appropriate particular typology matrix, summarizing the data for the existing buildings in Bulgaria. Further comprehensive estimation of the structural response of buildings requires performing full nonlinear dynamic analysis using acceleration time histories (observed or computed) with particular attention paid to the consecutive damage accumulation due to earthquakes sequence during the lifetime of the building. Damage indices are promising tool for quantitative description of these damages. Thus of crucial importance still remains the choice of appropriately calibrated structural representative models.

5 Challenges, Main Messages and Further Work

- The Vrancea subduction seismogenic zone is a peculiar intermediate-depth source that, in case of large magnitude earthquake, strongly affects significant part of the Bulgarian territory. The impact of a major Vrancea intermediate-depth earthquake may produce strong direct damage, as well as indirect losses in other regions of the country, thus leading to a national disaster. The regional earthquake danger due to the Vrancea intermediate-depth earthquakes dominates the hazard of NE Bulgaria. These quakes have particularly long-period and far-reaching effects, causing damages at large epicentral distances. Urban areas located at rather large distances (>200 km) from earthquake sources may be prone to severe earthquake hazard as well as the near field sites. Therefore, sustainable development of the region, exposed to this danger, depends on the reasonable policy for economic growth coupled with reasonable management of natural risks.
- For areas where very limited or no recordings are available synthetic time series can be used to estimate the expected ground motion, thus leading to a pre-disaster microzonation thus avoiding the necessity to wait for an earthquake to occur. The use of synthetic computations is also useful to cope with the fact that the local site response can be strongly dependent upon the properties of the source of the seismic impact. The use of the scenario-based NDSHA methodology provides synthetic signals that can be used for engineering structural analysis.
- The necessity of preventive action arises from the increasing vulnerability of the society in the processes of running globalization and urbanization due both to the high and underestimated earthquake risk. Prognostic risk estimation is a major prerequisite of the successful disaster risk management. To estimate the accumulated damages in the existing buildings and structures due to the history of the seismic actions, occurred during their life, it is necessary to use advanced earthquake engineering approaches for modelling the structural response to these actions and estimation of the relevant qualities. Full nonlinear analysis taking into account single event or series of earthquakes and the large set of elaborated damage indices are suitable contemporary tools to cope with this responsible task.
- The development of successful risk management strategies for earthquake hazards requires that the benefits from reduced uncertainty provided by improved seismic monitoring are integrated with the factors that influence risk perception and choice. An integrated, dynamic monitoring system for earthquake engineering purposes will contribute in general to (i) site effect assessment, (ii) design parameter assessment, (iii) the dynamic behavior of structures and soil-structure interaction analyses, (iv) calibration of the models used for seismic wave propagation and (v) ground motion modeling. Such an integrated seismic network should contain three types of instrumentation: (i) free-field, (ii) building and infrastructure and (iii) free-field and boreholes.

Acknowledgements Participation to this Symposium was possible due to the kind UTCB invitation and the financial support of the UACG-CNIP Project BH 164/14. The Seismology Group at the Department of Mathematics and Geosciences, University of Trieste, and the ICTP-SAND Group, both led by Prof. Giuliano F. Panza are deeply and sincerely acknowledged for the fruitful long-term collaboration dealing with the Vrancea seismic hazard estimates. Collaborations with NIEP—Romania and MITP-Russia teams are also highly appreciated. The authors would like to express particular gratitude to the team of CLSMEE-NIGGG-BAS led by Prof. Paskaleva, Prof. Miloshev and Prof. Simeonov at the time of performing these studies.

References

- Ambraseys N, Smit P, Sigbjornsson R, Suhadolc P, Margaris B (2002) Internet-site for European strong-motion data, European Commission, RDG, Environment and Climate Programme
- Brankov G et al (eds) (1983) Vrancea earthquake in 1977. Its after-effects in the People's Republic of Bulgaria. BAS, Sofia, 300 p (in Bulgarian)
- BDS EN 1998-1/NA-2010 (2010) Eurocode 8: Design of structures for the earthquake resistance. Part 1: general rules, seismic actions and rules for building, National Annex (in Bulgarian)
- Cosenza E, Manfredi G (2000) Damage indices and damage measures. *Prog Struct Eng Mater* 2:50–59
- Dziewonsky AM, Ekstrom G, Woodhouse JH, Zwart G (1991) Centroid moment tensor solutions for April-June 1990. *Phys Earth Planet Inter* 66:133–143
- Georgescu ES, Sandi H (2000) Towards earthquake scenarios under the conditions of Romania. In: Proceedings of the 12 WCEE, Auckland, New Zealand, Paper no. 1699
- Grünthal G (ed) (1998) European macroseismic scale 1998 (EMS-98). *Cahiers du Centre Européen de Géodynamique et de Séismologie* 15, Centre Européen de Géodynamique et de Séismologie, Luxembourg, 99 p
- Kappos AJ, Chlioumis A, Penelis GG (2002) Quantification of procedure uncertainty in seismic design of R/C buildings. In: Proceedings of 12th European conference on earthquake engineering, London, Paper no. 704
- Klügel JU (2007) Comment on “Why Do Modern Probabilistic Seismic-Hazard Analyses Often Lead to Increased Hazard Estimates” by Julian J. Bommer and Norman A. Abrahamson. *Bull Seismol Soc Am* 97(6):2198–2207
- Klügel JU, Mualchin L, Panza GF (2006) A scenario-based procedure for seismic risk analysis. *Eng Geol* 88:1–22
- Kouteva M (2008) On the damage capacity estimation of the strong intermediate-depth Vrancea earthquakes at Russe site, Visiting Report 2008—junior associated visit at SAND-ESP-ICTP, DST-University of Trieste
- Kouteva M (2010) Estimates of some ground motion parameters, related to the damage potential of strong intermediate-depth Vrancea earthquakes. AGGH, Ref.: Ms. no. AGEOD-D-10-00014R1
- Kouteva M, Panza GF, Romanelli F, Paskaleva I (2004) Modelling of the ground motion at Russe site (NE Bulgaria) due to the Vrancea earthquakes. *J Earthquake Eng* 8(2):209–229
- Kronrod T, Radulian M, Panza G, Popa M, Paskaleva I, Radovanovich S, Gribovszki K, Sandu I, Pekevski L (2013) Integrated transnational macroseismic data set for the strongest earthquakes of Vrancea (Romania). *Tectonophysics* 590:1–23
- Milutinovic Z, Trendafiloski G (2003) RISK-UE, An advanced approach to earthquake risk scenarios with applications to different European towns, contract: EVK4-CT-2000-00014, WP4: Vulnerability of current buildings, 111 p
- Molchan G, Kronrod T, Panza GF (1997) Multi-scale seismicity model for seismic risk. *Bull Seismol Soc Am* 87(5):1220–1229

- Nenov D, Paskaleva I, Georgiev G, Trifunac M (1990) CATALOG of strong earthquake ground motion data in EQINFOS: Accelerograms recorded in Bulgaria between 1981 and 1987. Report No CE 90-02, Southern California University, Sofia, Los Angeles, 55 p
- NSPMWCDB (2011) National Strategic Plan for Management of Wastes due to Construction and Demolishment of Buildings on the Territory of Bulgaria for the period 2011–2020 (in Bulgarian)
- Panza GF, Vaccari F (2000) Introduction in seismic hazard of the Circum-pannonian region. In: Panza GF, Radulian M, Trifu C (eds) Pageoph topical volumes, Birkhauser Verlag, pp 5–10
- Panza GF, Romanelli F, Vaccari F (2001) Seismic wave propagation in laterally heterogeneous anelastic media: theory and applications to the seismic zonation. *Adv Geophys* 43:1–95
- Paskaleva I, Kouteva M, Panza GF, Evlogiev J, Koleva N, Rangelov B (2001) Deterministic approach of seismic hazard assessment in Bulgaria; case study northeast Bulgaria—the town of Russe. *Albanian J Nat Techn Sci* 10:51–71
- Radulian M, Vaccari F, Manderscu N, Panza GF, Moldoveanu C (2000) Seismic hazard of Romania: deterministic approach. *Pure Appl Geophys* 157:221–247
- Rigikova Sn (1983) Macroseismic maps and observations. In: Brankov (BAS, Sofia) G (ed) Vrancea Earthquake in 1977. Its after-effects in the people's republic of Bulgaria. pp 135–150
- Simeonova S, Solakov D, Leydecker G, Busche H, Schmitt T, Kaiser D (2006) Probabilistic seismic hazard map for Bulgaria as a basis for a new building code. *Nat Hazards Earth Syst Sci* 6:881–887
- Todorovska M, Paskaleva I, Glavcheva R (1994) Earthquake source parameters for seismic hazard assessment examples in Bulgaria. In: Proceedings of the 10th European conference on earthquake engineering, Vienna vol 4, pp 2573-25-78
- Zaicenco A, Alkaz V (2005) Design of the Strong-Motion database for Vrancea earthquakes. *Sci Technol Dev Lifeline Syst*, Bratislava, Slovak Repub

Site Dependent Seismic Hazard Assessment for Bucharest Based on Stochastic Simulations

Florin Pavel, Daniel Ciuiu and Radu Vacareanu

Abstract The stochastic method has been and is still one of the most versatile tools for simulating earthquake ground motions. This method has been used in the past for deriving ground motion models or for evaluating seismic hazard. In this study, an attempt is made to evaluate the seismic hazard at INCERC site in Bucharest from Vrancea intermediate-depth earthquake using the stochastic method of simulating ground motions applied in conjunction with a stochastic catalogue. The simulated seismic catalogue which contains only intermediate-depth earthquakes originating in the Vrancea subcrustal seismic source with magnitudes $M_W \geq 5.5$, has a time length of 2500 years and it is based on the seismicity parameters derived from the ROMPLUS catalogue of the National Institute of Earth Physics. For each individual earthquake, the ground motion levels at INCERC station are assessed using stochastic finite-fault simulations. Subsequently, the seismic hazard curves for the INCERC site are obtained and compared with the ones computed through classical Cornell-McGuire probabilistic seismic hazard assessment (*PSHA*). In addition, the influence of the earthquake magnitude and source-to-site distance on the frequency contents of the simulated ground motions is investigated. Finally, the site-dependent displacement response spectrum constructed based on the simulated ground motions puts into evidence large displacement demands for long period structures.

Keywords Soil amplifications · Earthquake catalogue · Hazard curves · Displacement response spectrum

F. Pavel (✉) · R. Vacareanu
Seismic Risk Assessment Research Center,
Technical University of Civil Engineering Bucharest, Bucharest, Romania
e-mail: florin.pavel@utcb.ro

R. Vacareanu
e-mail: radu.vacareanu@utcb.ro

D. Ciuiu
Department of Mathematics and Computer Science,
Technical University of Civil Engineering Bucharest, Bucharest, Romania
e-mail: dciuiu@yahoo.com

1 Introduction

The stochastic method represents one of the most-widely used tools for deriving ground motion recordings. Boore (2003) makes a thorough description of the method and of the parameters involved in the computation process. Basically, the Fourier amplitude spectrum (*FAS*) of the stochastic ground motion is obtained by combining the contribution of the earthquake source, propagation path (taking into account phenomena, such as: geometrical spreading, intrinsic attenuation or ground motion duration increase with distance and local site conditions (both soil amplification and soil attenuation)). Among the best-known and most used computer codes for the stochastic simulation of ground motions are the FINSIM code (Beresnev and Atkinson 1998), SMSIM code developed by Boore (2005) or the EXSIM code (Motazedian and Atkinson 2005) which is also used in this study.

In this research, an attempt is made to evaluate the seismic hazard for the INCERC site in the eastern part of Bucharest using ground motions simulated through the stochastic method (Motazedian and Atkinson 2005). This represents the only site in Romania in which ground motion recordings were obtained during the major Vrancea seismic events of March 1977 ($M_W = 7.4$, $h = 94$ km), August 1986 ($M_W = 7.1$, $h = 131$ km) and May 1990 ($M_W = 6.9$, $h = 91$ km). The stochastic simulations are performed using an earthquake catalogue for the Vrancea subcrustal seismic source generated through the Monte Carlo approach and based on previously computed seismicity parameters (Vacareanu et al. 2016). The Monte Carlo method has been used both for the assessment of the seismic hazard (e.g. Musson 2000; Weatherhill and Burton 2010) and for the testing of the seismic hazard estimates (e.g. Tasan et al. 2014). Consequently, for each seismic event in the generated catalogue, the ground motion level for INCERC site is obtained through stochastic finite-fault simulations. Hazard curves and uniform hazard spectra (*UHS*) are obtained for various mean return periods and the results are compared with the traditional hazard curves and *UHS* (obtained through probabilistic seismic hazard assessment). Finally, an investigation of the resulting spectral accelerations and spectral displacements is performed in order to evaluate the possible influence of the magnitude and/or source-to-site distance on the results.

2 Earthquake Catalogue

The Vrancea subcrustal seismic source is an area of clustered intermediate-depth seismicity concentrated in the depth range 60–170 km (Radulian et al. 2008). This seismic region generated the largest intermediate-depth seismic event in Europe in the XXth century—the November 10, 1940 earthquake ($M_W = 7.7$). Wenzel et al. (1998) noted that the moment release of the Vrancea seismic source in the past century is of the same order of magnitude as that of southern California. Additional computations (Vacareanu et al. 2015) show that the moment release of the Vrancea

intermediate-depth seismic source in the same time span (XXth century) is three times larger than that of all the seismic sources in Italy.

The Monte Carlo based earthquake catalogue (Assatourians and Atkinson 2013) for the Vrancea subcrustal seismic source is based on the seismicity parameters for the Gutenberg-Richter law computed by Vacareanu et al. (2016). The same parameters are employed in the above-mentioned paper for the probabilistic evaluation of the seismic hazard (PSHA) for Romania performed within the BIGSEES national research project. More precisely, the depth-dependent seismicity parameters (a and b parameters of the Gutenberg-Richter law for each of the four layers of depth) were computed for the Vrancea subcrustal seismic source using the updated ROMPLUS earthquake catalogue and by employing the maximum likelihood method (McGuire 2004). The contour of the Vrancea subcrustal seismic source is similar with the one defined in the BIGSEES national research project (Vacareanu et al. 2016).

A time-span of 2500 years was chosen as the duration of the earthquake catalogue, which is a duration sufficient enough to evaluate the ground motion levels for mean return periods of the order $MRP = 200-300$ years (Iervolino 2009). Only seismic events with $M_W \geq 5.5$ are considered in the analysis, since smaller magnitude seismic events have very limited impact on the built environment (albeit they can cause panic for the population), leading thus to a total of 1554 earthquakes generated by the Vrancea subcrustal seismic source in the selected time span. The distribution of the earthquake magnitudes and that of the resulting source-to-site distances is given in Fig. 1.

Figure 2 shows the distribution of the number of earthquakes with $M_W \geq 7.0$ in each century of the simulated earthquake catalogue (a total of 25 centuries). The average number of earthquakes with $M_W \geq 7.0$ is 2.32 per century and the

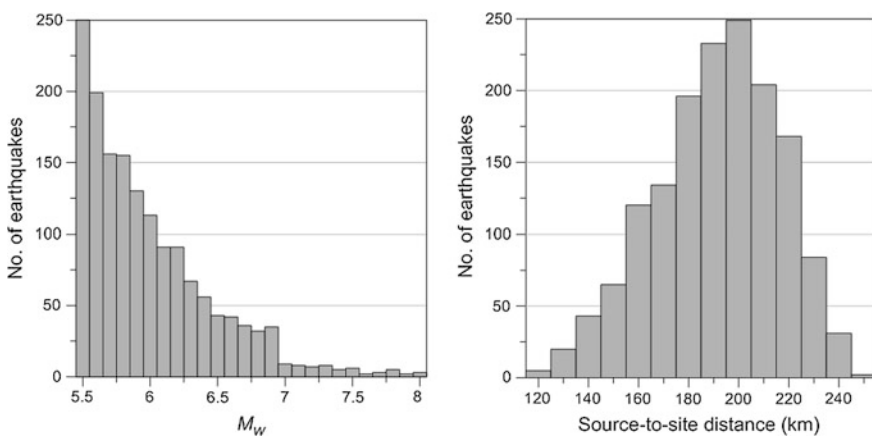
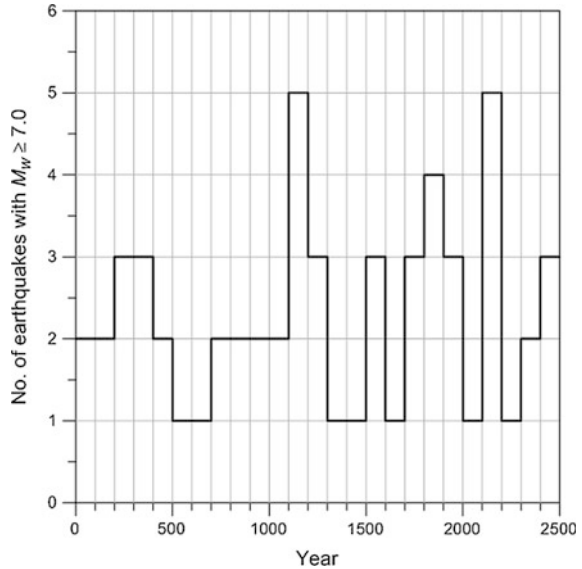


Fig. 1 Histograms of the earthquake magnitudes and source-to-site distances for the considered earthquake catalogue

Fig. 2 Distribution of earthquakes with $M_W \geq 7.0$ in each century of the 2500 years earthquake catalogue



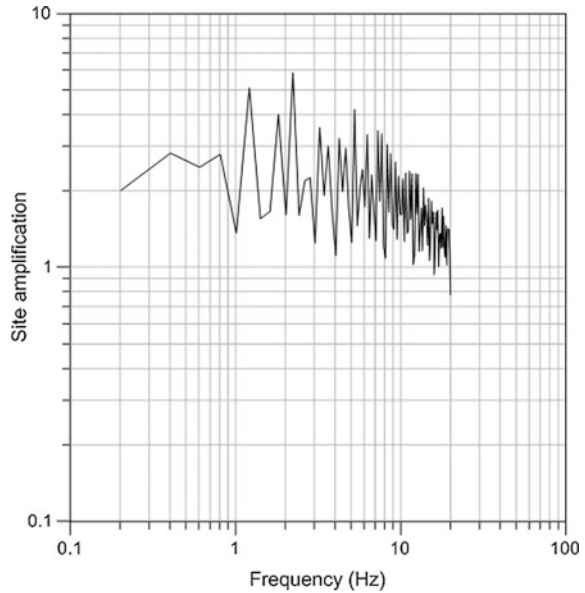
associated coefficient of variation is around 0.50, leading thus to between one and five seismic events with $M_W \geq 7.0$ per century.

3 Simulation of Ground Motions

The INCERC site in the eastern part of Bucharest was chosen for performing the computations due to the availability of soil data from a deep profile (Constantinescu and Enescu 1985) from which the site dependent soil amplification function can be computed. Moreover, this represents the only site in Romania in which ground motion recordings were obtained during the major Vrancea seismic events of March 1977 ($M_W = 7.4$, $h = 94$ km), August 1986 ($M_W = 7.1$, $h = 131$ km) and May 1990 ($M_W = 6.9$, $h = 91$ km). The soil amplification function was computed using the program NRATTLE, which can be found in the SMSIM suite of programs (Boore 2005). This code computes the response of a stack of layers to SH waves. As noted by Thompson et al. (2009), the transfer function computed by NRATTLE is equivalent to the solution computed through equivalent linear site response analysis for linear modulus reduction and damping curves. The resulting site amplifications for INCERC site are shown in Fig. 3.

The simulations were performed using the Q model for the Vrancea subcrustal seismic source from the paper of Pavel and Vacareanu (2015). The selected Q model is derived from the analysis of 247 pairs of horizontal recordings obtained during nine intermediate-depth Vrancea earthquakes which have occurred in the past 30 years. The magnitude-dependent kappa values used in the computations

Fig. 3 Computed site amplification function for INCERC site



were obtained using the relation given in the same study of Pavel and Vacareanu (2015). A reverse faulting mechanism was assigned for all the considered seismic events which is the typical source mechanism for large-magnitude seismic events originating in the Vrancea subcrustal seismic source (Radulian et al. 2000). The density and shear-wave velocity in the vicinity of the source were taken from the work of Oth et al. (2009). The typical values of the strike and dip angles computed for the Vrancea seismic events (Wenzel et al. 2002) were used in the ground motion simulations. The additional simulation parameters were considered as follows:

- constant rupture velocity and equal to 0.8 times the shear wave velocity;
- constant stress drop of 120 bars;
- random slip distribution;
- the rupture area was computed based on the relations given by Wells and Coppersmith (1994).

The comparison of the observed and simulated response spectra at INCERC site in Bucharest during the Vrancea major seismic events of March 1977 ($M_w = 7.4$, $h = 94$ km), August 1986 ($M_w = 7.1$, $h = 131$ km) and May 1990 ($M_w = 6.9$, $h = 91$ km) is shown in Fig. 4. The parameters of the Vrancea earthquakes (strike, dip, rake, stress drop) were taken from the paper of Ganas et al. (2010). The plots show that the simulated strong ground motions are close to the recorded ones, especially for the Vrancea seismic events of March 1977 and May 1990. The similar frequency content in the case of the 1977 seismic event is noteworthy.

The median ground motion obtained through the simulations was corrected subsequently so as to take into account the overall uncertainty. The correction was

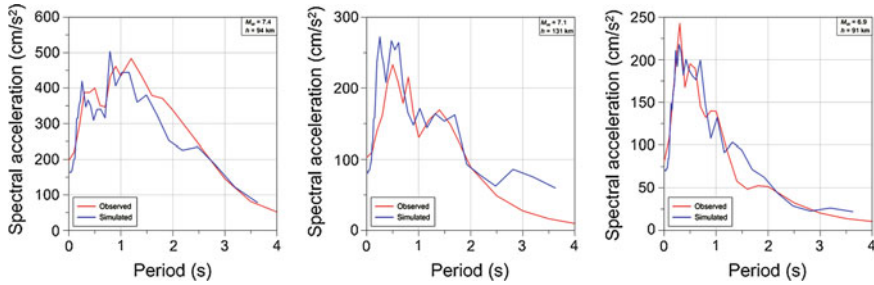


Fig. 4 Comparison of the observed and simulated response spectra for the Vrancea earthquakes of 1977, 1986 and 1990 at INCERC site in Bucharest

performed by adding a random number (drawn from the standard normal distribution) of standard deviations to the already computed median ground motion. The standard deviation was considered equal with the single-station station deviation already computed for INCERC site in the paper of Pavel et al. (2014).

4 Evaluation of Site-Dependent Spectral Accelerations and Displacements

Many seismic hazard assessments were performed for Romania in the past 15 years. The majority of these studies evaluated the seismic hazard in terms of either the peak ground acceleration (*PGA*) or the macroseismic intensity using either a probabilistic or a deterministic approach. A complete list of these studies can be found in the study of Vacareanu et al. (2016). In order to evaluate the results obtained through stochastic finite-fault simulations, the latest *PSHA* results obtained in the above-mentioned study of Vacareanu et al. (2016) are taken as reference. In the study of Vacareanu et al. (2016), performed within the framework of the BIGSEES national research project, the seismic hazard is evaluated by applying the classic Cornell-McGuire probabilistic seismic hazard assessment, both in terms of peak ground accelerations and of spectral accelerations. The comparisons of the simulations with the *PSHA* results are performed only for spectral accelerations.

Figure 5 shows a comparison between the uniform hazard spectra (*UHS*) obtained through classic *PSHA* and taken from Vacareanu et al. (2016) and the *UHS* resulting from the stochastic finite-fault ground motion simulations for two mean return periods (225 years and 475 years), which are similar with the mean return periods from the Romanian seismic code P100-1/2013 and from Eurocode 8 (2004). The mean return periods correspond to an exceedance probability of 20 % in 50 years ($MRP = 225$ years) and 10 % in 50 years ($MRP = 475$ years), respectively. Uniform hazard spectra are characterized by the same exceedance probability of the ground motion level for all the spectral periods (unlike a design response spectrum

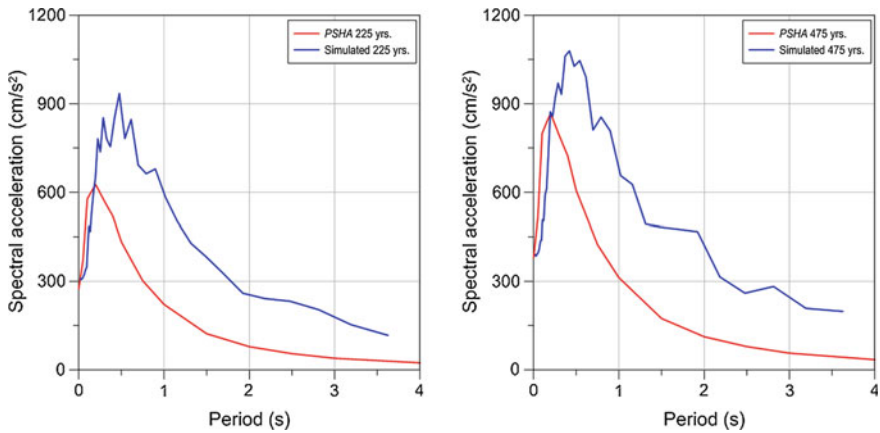


Fig. 5 Comparison of uniform hazard spectra (*UHS*) obtained from classic Cornell-McGuire *PSHA* and from stochastic simulations for a mean return period $MRP = 225$ years (*left*) and $MRP = 475$ years (*right*)

which has different exceedance probabilities for the spectral ordinates). The plots in Fig. 5 show significant differences between the spectral ordinates, especially in the medium and long period range. However, one can notice that the peak ground accelerations for the two mean return periods (225 years and 475 years) are similar in both approaches.

Figure 6 shows a comparison of the hazard curves for spectral accelerations at six different periods ($T = 0.0$ s, $T = 0.2$ s, $T = 0.5$ s, $T = 1.0$ s, $T = 1.5$ s and $T = 2.0$ s). The two hazard curves (from simulations and from classic *PSHA*) resemble the most for $T = 0.0$ s. However, for longer periods the difference between the two curves becomes larger and larger, as the hazard curve from *PSHA* is not able to capture the significant medium- and long-period spectral ordinates observed on INCERC site. It is also interesting to note that the spectral accelerations at $T = 0.0$ s and $T = 0.2$ s coincide in the cases of both hazard curves for the mean return periods $MRP = 225$ years and $MRP = 475$ years. Moreover, the slope of the two seismic hazard curves tends to become similar as the spectral period increases. In addition, one has to consider the fact that the results in Fig. 6 can be considered as reliable only for mean return periods smaller than 300 years (as previously mentioned).

Figure 7 displays the hazard curves for spectral displacements obtained from stochastic finite-fault simulations (Motazedian and Atkinson 2005) for five periods: $T = 0.5$ s, $T = 1.0$ s, $T = 1.5$ s, $T = 2.0$ s and $T = 3.0$ s. One can notice the relatively high displacement demands imposed for long-period structures, especially for mean return periods in excess of 300–400 years. In addition, the results show that the maximum displacement demands (from all the ground motion simulations) can reach 100–150 cm (two or three times larger than the code displacement demand) for structures with natural periods in the region $T = 2–4$ s (Fig. 8).

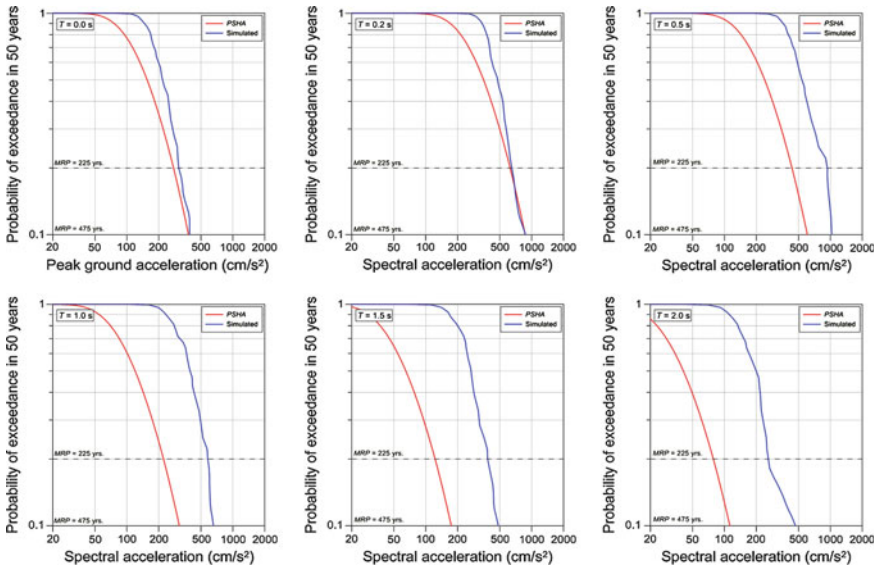
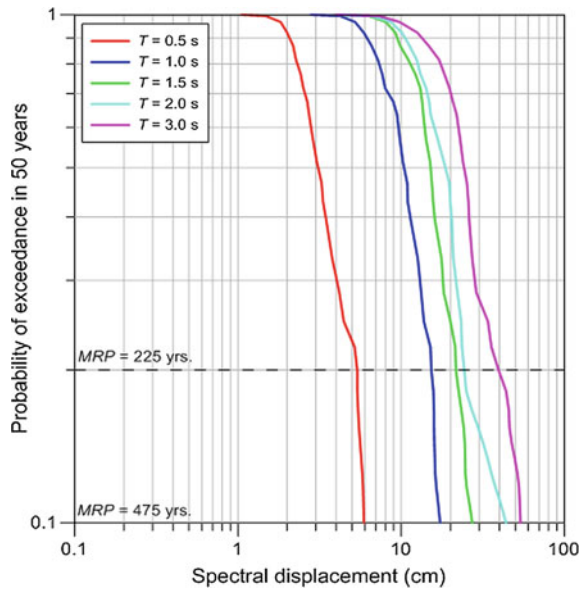


Fig. 6 Comparison of spectral acceleration hazard curves (traditional hazard curve obtained through classic *PSHA* and hazard curve based on simulations) for six different spectral periods

Fig. 7 Comparison of hazard curves for spectral displacement and for different spectral periods



The impact of the earthquake magnitude and of the source-to-site distance is evaluated in the subsequent Figs. 9 and 10. Figure 9 displays the influence of the source-to-site distance on the mean dynamic amplification factor (mean ratio

Fig. 8 Comparison between the displacement response spectra for three mean return periods ($MRP = 100$ years, $MRP = 225$ years and $MRP = 475$ years) and the design displacement response spectrum from the Romanian seismic design code P 100-1/2013 (2013)

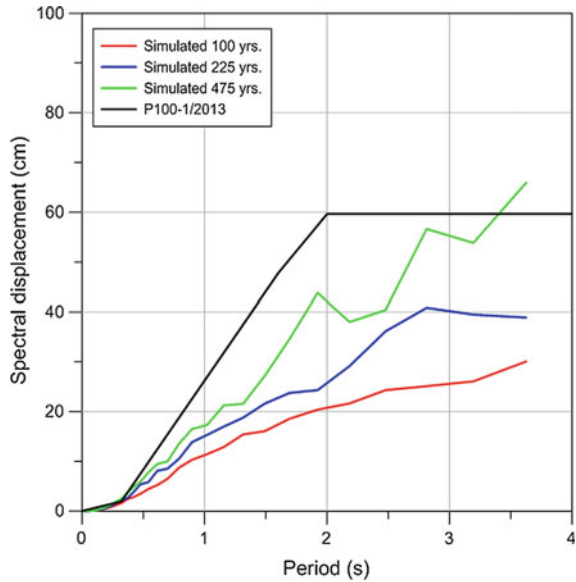
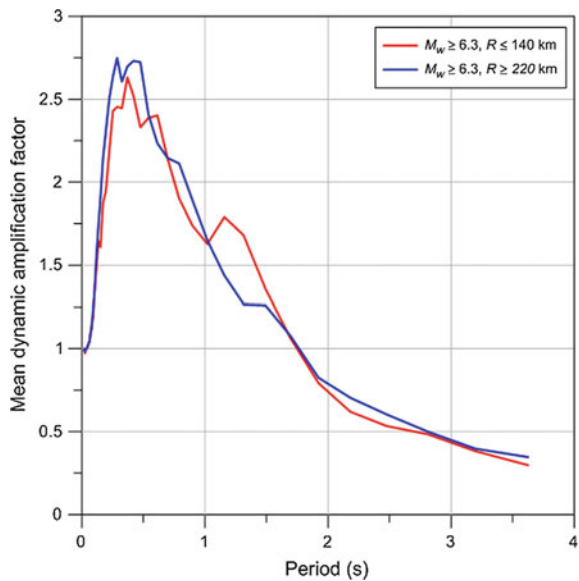
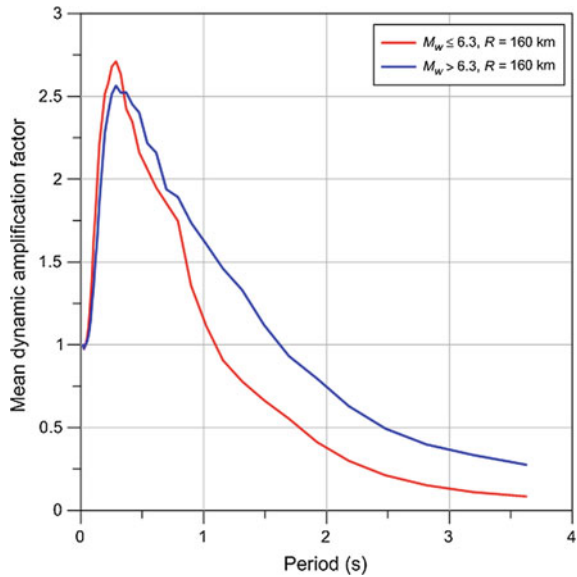


Fig. 9 Comparison of mean dynamic amplification factors for earthquakes with $M_w \geq 6.3$ and source-to-site distances $R \leq 140$ km and $R \geq 220$ km



between spectral acceleration and peak ground acceleration) for earthquakes with earthquakes with $M_w \geq 6.3$. One can notice the higher mean dynamic amplification factors for natural periods T in the range 1.0–1.5 s obtained for short source-to-site distances (similar with the case of the Vrancea earthquake of March 1977). It is also

Fig. 10 Comparison of mean dynamic amplification factors for earthquakes with source-to-site distances $R = 160$ km and $M_W \leq 6.3$ and $M_W > 6.3$



clear that the source-to-site distance has no impact on the maximum value of the mean dynamic amplification factor.

Figure 10 examines the impact of the earthquake magnitude on the mean dynamic amplification factors. One can notice that the earthquake magnitude has a considerable impact, especially for periods $T > 0.5$ s. For spectral periods $T < 0.5$ s, the values of the mean dynamic amplification factor are similar for both categories of seismic events.

Figure 11 shows a comparison between the mean and maximum dynamic amplification factors, computed as a function of the earthquake magnitude and the dynamic amplification factors given in the Romanian seismic design code P100-1/2013 (2013). One can observe that the maximum values of the mean dynamic amplification factors are almost similar with the one given by the Romanian seismic design code P100-1/2013 (2013), albeit the influence of the earthquake magnitude on the spectral shapes is considerable. The earthquake magnitude influence is also clearly visible on the plot which shows the maximum dynamic amplification factors. The decrease in the values of the maximum dynamic amplification factor with the earthquake magnitude, as well as the lengthening of the constant acceleration plateau are clearly visible in the right plot of Fig. 11. It is also noteworthy the fact that the code spectral shape and the envelope of the spectral shapes obtained from stochastic simulations coincide for natural periods T larger than 1.5 s.

In order to check the uncertainty of the results obtained (for spectral accelerations), the method of quantifying the uncertainty proposed by Douglas et al. (2014) was applied. The uncertainty is computed as shown by Douglas et al. (2014) with the relation $100 \cdot \log(PGA_{85}/PGA_{15})$, where PGA_{85} and PGA_{15} are the peak ground

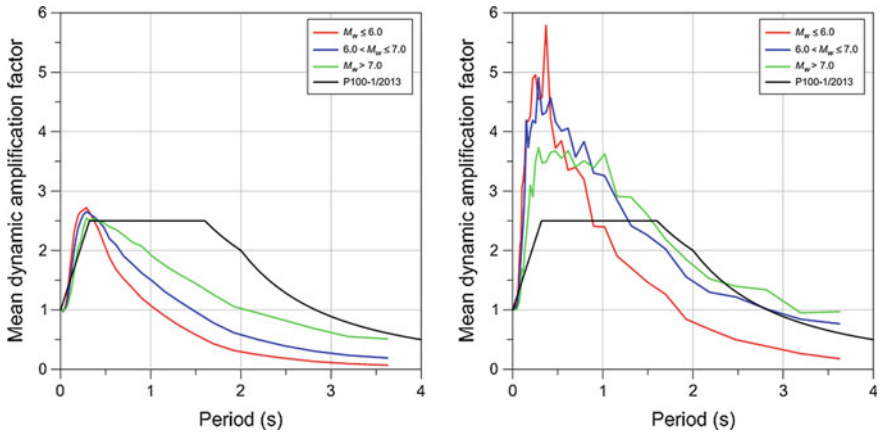
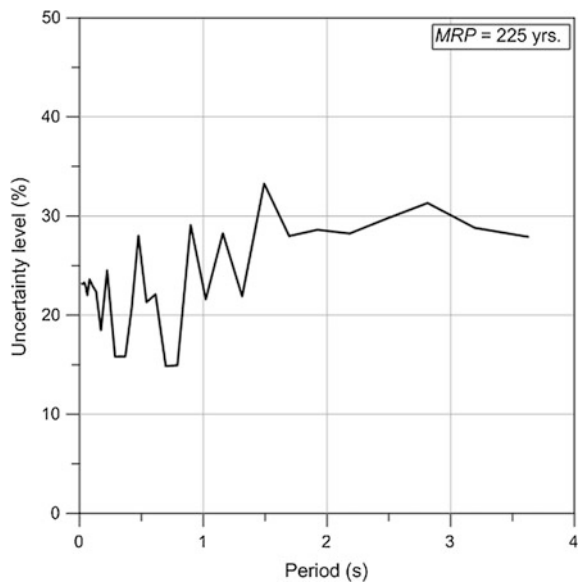


Fig. 11 Mean and maximum dynamic amplification factors as a function of the earthquake magnitude versus design response spectrum from the seismic code P100-1/2013 (2013)

accelerations corresponding to the 15th and 85th percentile. The results are shown in Fig. 12 for a mean return period of 225 years. One can observe that the uncertainty level is generally within the range 0.15–0.30, which is the range for current seismic hazard studies. In addition, one can notice, the increase of the uncertainty with the spectral period.

Fig. 12 Variation of the uncertainty level for the seismic hazard corresponding to a mean return period $MRP = 225$ years



5 Conclusions

In this study, an attempt is made to evaluate the seismic hazard for INCERC site in the eastern part of Bucharest through stochastic simulations. The main conclusions and observations of this study can be summarized as follows:

- The simulated ground motions have a frequency contents similar with that of recordings from the Vrancea earthquakes of March 1977, August 1986 and May 1990;
- The seismic hazard levels obtained from the simulated ground motions and from traditional probabilistic seismic hazard assessment for mean return periods of 225 years and 475 years are similar (only for *PGA*);
- The uniform hazard spectra resulting from the simulated ground motions have much larger medium- and long-period spectral ordinates, as compared with the traditional *UHS*. This can be attributed to the fact that the traditional *UHS* does not account completely for the large site-specific effect at INCERC;
- The displacement demands imposed by the simulated ground motions can be quite high for long-period structures and for mean return periods of the seismic action larger than 400–500 years;
- Larger magnitude seismic events produced at small source-to-site distances are the most likely candidates to generate long-period spectral ordinates;
- The mean dynamic amplification factor has a maximum value similar with the one given in the Romanian seismic design code P100-1/2013 (2013), irrespective of the magnitude bin. In the case of the maximum dynamic amplification factor, the shape obtained for earthquakes with $M_W \geq 7.0$ resembles that given in the code, for periods T larger than 1.5 s;
- The computed uncertainty levels for a mean return period of 225 years is in the range 0.15–0.30, which is the range of values of current seismic hazard studies.

Acknowledgements This work was supported by a grant of the Romanian National Authority for Scientific Research and Innovation, CNCS–UEFISCDI, project number PN-II-RU-TE-2014-4-0697. We thank John Douglas for his very constructive comments on an earlier version of this manuscript.

References

- Assatourians K, Atkinson GM (2013) EqHaz: an open-source probabilistic seismic-hazard code based on the Monte Carlo simulation approach. *Seismol Res Lett* 84:516–524
- Beresnev IA, Atkinson GM (1998) FINSIM—a FORTRAN program for simulating stochastic acceleration time histories from finite faults. *Seismol Res Lett* 69:27–32
- Boore DM (2003) Simulation of ground motions using the stochastic method. *Pure appl Geophys* 160:635–676
- Boore DM (2005) SMSIM—Fortran programs for simulating ground motions from earthquakes: version 2.3—a revision of OFR 96-80-A. U.S. Geological Survey report OFR 00-509

- Contantinescu L, Enescu D (1985) The Vrancea earthquakes from scientific and technologic point of view (in Romanian). Ed Academiei, Bucharest, Romania
- Douglas J, Ulrich T, Bertil D, Rey J (2014) Comparisons of the ranges of uncertainty captured in different seismic-hazard studies. *Seismol Res Lett* 85:977–985
- EN 1998–1:2004 (2004) Eurocode 8: design of structures for earthquake resistance, Part 1: general rules, seismic actions and rules for buildings. CEN, Bruxelles, Belgium
- Ganas A, Grecu B, Batsi E, Radulian M (2010) Vrancea slab earthquakes triggered by static stress transfer. *Nat Hazards Earth Syst Sci* 10:2565–2577
- Iervolino I (2013) Probabilities and fallacies: why hazard maps cannot be validated by individual earthquakes. *Earthquake Spectra* 29:1125–1136
- McGuire R (2004) Seismic hazard and risk analysis. Earthquake Engineering Research Institute MNO-10
- Motazedian D, Atkinson GM (2005) Stochastic finite-fault modeling based on a dynamic corner frequency. *Bull Seismol Soc Am* 95:995–1010
- Musson RMW (2000) The use of Monte Carlo simulations for seismic hazard assessment in the U.K. *Ann Geofis* 43:1–9
- Oth A, Parolai S, Bindi D, Wenzel F (2009) Source spectra and site response from S waves of intermediate-depth Vrancea, Romania, earthquakes. *Bull Seismol Soc Am* 99:235–254
- P100-1/2013 (2013) Code for seismic design—Part I—design prescriptions for buildings. Ministry of Regional Development and Public Administration, Bucharest, Romania
- Pavel F, Vacareanu R (2015) Kappa and regional attenuation for Vrancea (Romania) earthquakes. *J Seismolog* 19:791–799
- Pavel F, Vacareanu R, Ionescu C, Iancovici M, Sercaianu M (2014) Investigation of the variability of strong ground motions from Vrancea earthquakes. *Nat Hazards* 74:1707–1728
- Radulian M, Mandrescu N, Panza GF, Popescu E, Utale A (2000) Characterization of seismogenic zones of Romania. *Pure Appl Geophys* 157:57–77
- Radulian M, Popa M, Carbanar OF, Rogozea M (2008) Seismicity patterns in Vrancea and predictive features. *Acta Geodaet Geophys Hung* 43:163–173
- Tasan H, Beauval C, Helmstetter A, Sandikkaya A, Guéguen P (2014) Testing probabilistic seismic hazard estimates against accelerometric data in two countries: France and Turkey. *Geophys J Int* 198:1554–1571
- Thompson EM, Baise LG, Kayen RE, Guzina BB (2009) Impediments to predicting site response: seismic property estimation and modeling simplifications. *Bull Seismol Soc Am* 99 (5):2927–2949
- Vacareanu R, Pavel F, Aldea A, Arion C, Neagu C (2015) Elements of seismic hazard assessment (in Romanian). Conspress, Bucharest, Romania
- Vacareanu R, Aldea A, Lungu D, Pavel F, Neagu C, Arion C, Demetriu S, Iancovici M (2016). Probabilistic seismic hazard assessment for Romania. In: D’Amico S (eds) *Earthquakes and their impact on society*. Springer Natural Hazards Book Series, pp 137–169. ISBN: 978-3-319-21752-9 (Print) 978-3-319-21753-6 (Online). [10.1007/978-3-319-21753-6](https://doi.org/10.1007/978-3-319-21753-6)
- Weatherhill G, Burton PW (2010) An alternative approach to probabilistic seismic hazard analysis in the Aegean region using Monte Carlo simulation. *Tectonophysics* 492:253–278
- Wells DL, Coppersmith KJ (1994) New empirical relationships among magnitude, rupture length, rupture width, rupture area, and surface displacement. *Bull Seismol Soc Am* 84:974–1002
- Wenzel F, Achauer U, Enescu D, Kissling E, Russo R, Mocanu V, Musacchio G (1998) Detailed look at final stage of plate break-off is target of study in Romania. *EOS Trans AGU* 79:589–600
- Wenzel F, Sperner B, Lorenz F, Mocanu V (2002) Geodynamics, tomographic images and seismicity of the Vrancea region (SE-Carpathians, Romania). EGU Stephan Mueller Special Publication Series 3:95–104

Scaling Properties for the Vrancea Subcrustal Earthquakes: An Overview

Emilia Popescu, Mircea Radulian and Anica Otilia Placinta

Abstract The Vrancea seismic nest is a distinctive case of unusually clustered seismicity at intermediate depths. The source scaling properties are essential elements to understand and model the tectonic processes responsible for generating earthquakes in such a confined lithospheric volume. The purpose of the present paper is to investigate the scaling laws for Vrancea earthquakes on the basis of well-defined source parameters. Spectral ratios technique and empirical Green's function deconvolution are applied to retrieve source parameters. Previous results are combined with new determinations resulting in an enlarged database (298 events), spanning a magnitude interval from $M_w \sim 2.4$ to $M_w \sim 7.7$ (1940 major event). The results show for the most of moderate-magnitude earthquakes a relatively simple source time function and source spectrum, compatible with a circular source model with homogeneous rupture process. The scaling of seismic moment with source radius and stress drop appears to be self-similar over the entire magnitude range of the considered data set ($3.0 \leq M_w \leq 7.7$) and matches well the theoretical scaling for source models generally adopted in source studies. Particular high stress drop values, for moderate and large events, indicate fast and efficient rupture processes at different scales, possibly explained by fast running shear melting processes.

Keywords Spectral ratios · Empirical Green's function · Source parameters

E. Popescu (✉) · M. Radulian · A.O. Placinta
National Institute for Earth Physics, Magurele, Romania
e-mail: popescu@infp.ro

M. Radulian
e-mail: mircea@infp.ro

A.O. Placinta
e-mail: anca@infp.ro

1 Introduction

The Vrancea seismic nest is a distinctive case of unusually clustered seismicity at intermediate depths. Two typical features are highlighted when looking on the seismicity regime of this region: (1) the restriction in space of the hypocenter locations, with a narrow vertical spreading close to a vertical geometrical plane (Cărbunar and Radulian 2011) and (2) the persistent and fairly invariant occurrence rate for the background seismicity (10 ± 5 events of local magnitude above 3 per month). As for the largest events, the seismicity rate estimated since 15th century to the present is 3 ± 1 events of magnitude above 7 per century.

The source scaling properties are essential elements to understand and model the tectonic processes responsible for generating earthquakes in such a confined lithospheric volume. The purpose of the present paper is to investigate the scaling laws for Vrancea earthquakes on the basis of well-defined source parameters. To this aim, we took into account all the information we found available from previous investigations and processed new data recorded for 145 Vrancea earthquakes.

The large amount of waveforms digitally recorded by the National Institute for Earth Physics (NIEP) for the Vrancea intermediate depth earthquakes provides the opportunity to systematically evaluate individual source properties and to investigate collective scaling properties in order to understand the overall seismogenic process in this particular geotectonic area. One intrinsic challenge for this kind of approach is the separation of different factors which intervene and modify the signal recorded at surface: source, propagation path, site and instrument response. This is once more difficult for the Vrancea region, where strong lateral inhomogeneities in the structure are expected both in the crust and in the mantle (see Ismail-Zadeh et al. 2012 and herein references).

The methods that best correct for undesirable propagation and site effects in retrieving source parameters are relative and apply on set of earthquakes that are located as close as possible and are recorded by common stations. For example, in the empirical Green's function (EGF) method the smaller events in a set of co-located earthquakes act as a transfer-medium function that empirically accounts for the path, site, and instrument-response effects on the waveform (Bakun and Bufe 1975; Frankel 1982; Mueller 1985; Mori and Frankel 1990; Hough et al. 1991). In the spectral ratios (SR) method (Lindley 1994; Abercrombie 2015) the requirements are less restrictive as concerns the relative size among the events in a given set.

For the analysis proposed in the present study, we applied relative deconvolution techniques (that implicitly fulfill the required criteria) for a dataset containing waveform recordings for 145 Vrancea intermediate-depth earthquakes (Tables 1 and 2). Additional data were provided from previous studies by Radulian and Popa (1996) and Oth et al. (2007), who applied EGF technique to evaluate source parameters and scaling properties for a limited number of Vrancea events (8 and 9 events, respectively). Finally, we compare the results obtained using relative spectral techniques with similar results using absolute spectral technique by Oncescu (1986) and Gusev et al. (2002). Estimations of the source parameters for the last Vrancea major

Table 1 Hypocentral and source parameters for the main earthquakes

Nr	Data	hh:mm	Lat (°N)	Lon (°E)	H (km)	M _w	f _c (Hz)	f _{sr} [*] (m)	τ _{1/2} (s)	r _{rt} [*] (m)	Δσ _{sr} [*] (MPa)	Δσ _{rt} [*] (MPa)	M ₀ (Nm)
1	1997/10/11	19:00	45.77	26.76	113	4.5	3.35	571	0.110	729	19	9	7.9 x 10 ¹⁵
2	1997/11/18	11:23	45.76	26.71	123	4.7	2.53	742	0.150	952	14	7	1.3 x 10 ¹⁶
3	1997/12/30	04:39	45.54	26.32	139	4.6	3.56	536	0.090	595	26	19	9.3 x 10 ¹⁵
4	1998/01/19	00:53	45.64	26.67	105	4.0	4.25	440	0.086	564	8	4	1.5 x 10 ¹⁵
5	1998/03/13	13:14	45.56	26.33	155	4.7	2.40	795	0.120	793	12	12	1.4 x 10 ¹⁶
6	1998/07/27	15:02	45.63	26.52	134	4.4	2.83	712	0.130	846	6	3	4.5 x 10 ¹⁵
7	1999/03/22	19:25	45.52	26.33	145	4.4	2.79	687	0.120	787	6	4	4.7 x 10 ¹⁵
8	1999/04/28	08:47	45.47	26.28	158	5.3	1.84	1051	0.156	1015	49	54	1.3 x 10 ¹⁷
9	1999/04/29	18:44	45.63	26.40	145	4.0	4.30	443	0.100	653	7	4	1.4 x 10 ¹⁵
10	1999/06/29	20:04	45.60	26.49	133	4.2	3.08	635	0.101	659	5	5	3.0 x 10 ¹⁵
11	1999/11/08	19:22	45.52	26.38	132	4.6	2.91	639	0.117	766	18	11	1.1 x 10 ¹⁶
12	1999/11/14	09:05	45.49	26.29	127	4.6	3.03	658	0.114	745	15	11	1.0 x 10 ¹⁶
13	2000/03/08	22:11	45.87	26.72	71	4.4	2.55	756	0.115	755	2	2	1.8 x 10 ¹⁵
14	2000/04/06	00:10	45.76	26.66	137	5.0	1.88	1044	0.160	1047	15	15	3.9 x 10 ¹⁶
15	2000/05/10	04:27	45.57	26.51	134	4.1	3.32	581	0.080	504	3	5	1.4 x 10 ¹⁵
16	2001/03/04	15:38	45.51	26.27	156	4.8	1.79	1196	0.160	1065	2	3	8.0 x 10 ¹⁵
17	2001/05/24	17:34	45.64	26.46	154	4.9	1.73	1131	0.150	967	28	44	9.1 x 10 ¹⁶
18	2001/07/20	05:09	45.74	26.77	133	4.8	1.87	1063	0.140	918	9	14	2.4 x 10 ¹⁶
19	2001/10/17	13:01	45.62	26.55	92	4.2	2.90	649	0.124	808	11	5	7.0 x 10 ¹⁵
20	2002/05/03	18:31	45.57	26.33	162	4.6	2.45	663	0.112	731	10	8	6.9 x 10 ¹⁵
21	2002/09/06	05:04	45.61	26.45	101	4.1	3.76	501	0.076	498	8	8	2.2 x 10 ¹⁵
22	2002/11/30	08:15	45.62	26.54	166	4.7	1.92	937	0.166	1087	72	55	2.2 x 10 ¹⁷
23	2003/10/05	21:38	45.58	26.45	146	4.6	3.27	552	0.122	795	31	10	1.2 x 10 ¹⁶

(continued)

Table 1 (continued)

Nr	Data	hh:mm	Lat (°N)	Lon (°E)	H (km)	M _w	f _c (Hz)	r _{sr} [*] (m)	τ _{1/2} (s)	r _{rt} [*] (m)	Δσ _{sr} [*] (MPa)	Δσ _{rt} [*] (MPa)	M _o (Nm)
24	2004/02/07	11:58	45.68	26.62	144	4.4	3.17	590	0.140	848	9	3	4.3 x 10 ¹⁵
25	2004/07/10	00:34	45.69	26.57	150	4.3	2.92	661	0.130	878	4	2	2.8 x 10 ¹⁵
26	2004/09/27	09:16	45.65	26.51	152	4.6	2.16	882	0.120	782	26	37	4.0 x 10 ¹⁶
27	2004/10/27	20:34	45.78	26.73	99	6.0	1.60	1222	0.170	1140	130	160	5.4 x 10 ¹⁷
28	2005/05/14	01:53	45.66	26.52	146	5.2	1.72	1190	0.161	1052	20	23	7.7 x 10 ¹⁶
29	2009/04/25	17:18	45.68	26.62	110	5.2	1.70	782	0.168	985	70	35	7.7 x 10 ¹⁶
30	2013/10/06	01:37	45.67	26.58	135	5.3	2.08	528	0.149	845	1180	292	4.0 x 10 ¹⁷
31	2013/10/15	19:33	45.62	26.55	142	4.6	3.34	312	0.122	689	298	28	2.1 x 10 ¹⁶
32	2013/11/21	06:38	45.76	26.71	89	4.2	4.30	240	0.125	680	144	6	4.5 x 10 ¹⁵
33	2014/01/23	06:15	45.47	26.26	143	4.6	4.23	252	0.105	593	470	31	1.5 x 10 ¹⁶
34	2014/03/26	19:46	45.68	26.55	141	4.2	4.91	226	0.113	638	145	6	3.8 x 10 ¹⁵
35	2014/03/29	19:18	45.63	26.47	138	4.8	3.48	311	0.125	706	545	47	3.8 x 10 ¹⁶
36	2014/04/03	12:38	45.48	26.39	136	4.4	3.97	264	0.103	584	230	21	9.7 x 10 ¹⁵

* r_{sr}, Δσ_{sr}—source radius and stress drop from spectral ratios

* r_{rt}, Δσ_{rt}—source radius and stress drop from rise time

Table 2 Hypocentral and source parameters for the empirical Green's functions

Nr	Data	hh:mm	Lat (°N)	Lon (°E)	h (km)	M_W	M_0 (Nm)	f_c (Hz)	r (m)	$\Delta\sigma$ (MPa)
1	1997/03/19	20:51	45.56	26.39	151	3.8	1.1×10^{14}	6.82	290	2
2	1997/07/14	00:37	45.76	26.76	130	4.2	1.3×10^{15}	4.19	443	7
3	1997/11/11	23:06	45.84	26.88	65	3.5	2.43×10^{13}	8.24	224	1
4	1997/12/18	23:21	45.52	26.26	136	3.9	5.9×10^{14}	5.30	350	6
5	1998/01/14	05:01	45.71	26.60	143	4.0	2.3×10^{14}	9.01	234	8
6	1998/01/31	21:14	45.47	26.30	136	3.6	2.3×10^{14}	7.61	258	6
7	1998/02/19	14:34	45.70	26.73	132	3.7	1.3×10^{14}	4.71	397	1
8	1998/03/06	20:28	45.62	26.41	149	3.7	1.8×10^{14}	6.02	308	3
9	1998/06/06	20:34	45.69	26.57	147	3.5	1.9×10^{13}	6.90	269	0.4
10	1998/08/24	23:27	45.57	26.49	141	3.8	4.9×10^{13}	11.60	160	5
11	1998/09/21	13:49	45.73	26.66	141	3.8	1.9×10^{14}	7.47	264	5
12	1998/11/14	11:15	45.70	26.65	140	3.7	2.4×10^{14}	7.53	252	7
13	1998/12/12	10:55	45.40	26.30	147	3.5	5.7×10^{14}	5.65	361	5
14	1998/12/17	19:15	45.72	26.73	127	3.4	3.3×10^{13}	10.45	189	1
15	1998/12/28	21:50	45.64	26.60	141	3.5	7.0×10^{12}	9.65	197	0.4
16	1999/01/06	21:28	45.49	26.30	117	3.5	7.8×10^{13}	11.52	162	8
17	1999/01/09	0:04	45.48	26.41	140	3.5	8.9×10^{13}	9.16	215	4
18	1999/01/23	17:01	45.63	26.55	138	4.1	2.0×10^{14}	7.40	259	5
19	1999/03/09	17:51	45.66	26.56	153	3.6	7.0×10^{13}	7.14	261	2
20	1999/03/17	07:01	45.62	26.48	153	3.8	1.8×10^{14}	6.49	286	3
21	1999/03/23	09:11	45.66	26.55	150	4.0	1.2×10^{15}	3.88	491	4
22	1999/04/04	01:21	45.63	26.55	150	3.7	3.6×10^{14}	8.13	233	13
23	1999/04/15	02:21	45.83	26.84	88	3.7	1.4×10^{14}	9.11	200	8
24	1999/04/30	22:32	45.53	26.24	143	3.7	1.1×10^{14}	5.57	277	2
25	1999/05/05	16:21	45.67	26.56	142	3.5	4.0×10^{13}	6.72	277	1
26	1999/06/06	12:01	45.51	26.32	136	3.4	1.32×10^{13}	11.23	165	1
27	1999/06/22	08:02	45.67	26.46	153	3.7	3.6×10^{14}	6.57	310	5
28	1999/07/15	7:36	45.58	26.46	145	3.7	1.3×10^{14}	5.26	353	1
29	1999/10/12	23:48	45.67	26.41	154	3.7	1.7×10^{14}	7.34	374	1
30	1999/11/24	03:57	45.74	26.78	103	3.5	1.47×10^{14}	10.94	186	10
31	1999/12/17	16:06	45.74	26.72	75	3.5	2.7×10^{14}	8.12	242	8
32	2000/05/13	23:36	45.62	26.79	89	3.8	2.3×10^{14}	7.70	259	6
33	2000/05/28	19:08	45.79	26.64	81	3.2	4.0×10^{13}	10.62	166	4
34	2000/07/01	20:50	45.81	26.80	64	3.4	1.5×10^{15}	6.88	283	29
35	2000/07/27	02:39	45.77	26.74	136	3.7	4.8×10^{13}	7.70	302	1
36	2000/08/06	05:09	45.54	26.36	148	3.9	9.3×10^{13}	6.33	299	2
37	2000/10/12	14:56	45.66	26.59	141	3.9	4.0×10^{14}	7.06	217	2
38	2000/12/19	15:29	45.48	26.36	143	3.8	1.5×10^{14}	3.91	489	0.6
39	2000/12/28	00:17	45.73	26.73	130	3.6	8.0×10^{13}	3.94	466	0.3
40	2001/01/17	19:32	45.70	26.46	158	3.9	2.0×10^{14}	4.74	407	1
41	2001/02/03	20:56	45.74	26.67	143	3.8	8.40×10^{13}	10.22	204	4

(continued)

Table 2 (continued)

Nr	Data	hh:mm	Lat (°N)	Lon (°E)	h (km)	M_w	M_o (Nm)	f_c (Hz)	r (m)	$\Delta\sigma$ (MPa)
42	2001/02/27	19:19	45.67	26.46	164	3.8	6.5×10^{13}	8.14	237	2
43	2001/03/18	06:33	45.51	26.21	157	4.1	8.7×10^{14}	4.64	452	4
44	2001/03/28	22:07	45.77	26.80	136	4.3	5.0×10^{14}	5.91	315	7
45	2001/05/20	03:59	45.59	26.45	154	4.2	1.4×10^{15}	5.10	390	10
46	2001/07/06	15:50	45.53	26.28	160	3.9	1.2×10^{14}	5.91	320	2
47	2001/07/23	19:58	45.82	26.81	145	3.8	6.8×10^{13}	4.74	422	1
48	2001/07/29	00:30	45.58	26.54	137	3.6	6.6×10^{13}	8.34	240	2
49	2001/09/25	18:04	45.48	26.32	151	3.8	1.9×10^{14}	3.56	562	1
50	2001/09/28	07:36	45.70	26.64	89	3.4	1.5×10^{14}	10.40	178	12
51	2001/10/17	15:35	45.69	26.51	160	3.9	5.7×10^{15}	5.90	400	39
52	2001/12/14	11:38	45.79	26.74	69	3.5	1.7×10^{13}	11.27	162	2
53	2002/01/25	10:06	45.62	26.72	129	4.0	2.0×10^{14}	4.81	406	1
54	2002/03/16	22:39	45.55	26.46	143	4.3	2.7×10^{15}	3.50	615	5
55	2002/05/15	04:26	45.55	26.36	153	4.0	2.6×10^{14}	5.83	299	10
56	2002/05/26	00:24	45.73	26.79	118	3.3	2.3×10^{13}	10.31	176	2
57	2002/06/14	23:49	45.64	26.57	133	4.0	2.8×10^{14}	7.10	301	5
58	2002/07/14	20:18	45.52	26.43	126	3.9	1.8 ± 10^{14}	8.21	235	6
59	2002/08/04	06:25	45.66	26.49	158	3.9	1.5×10^{14}	4.61	406	1
60	2002/08/05	21:02	45.53	26.47	139	3.8	2.1×10^{14}	6.42	262	5
61	2002/08/16	08:18	45.53	26.52	129	3.7	2.4×10^{14}	8.61	216	10
62	2002/08/27	06:46	45.60	26.43	149	4.0	1.2×10^{14}	9.04	225	5
63	2002/09/10	15:09	45.73	26.81	129	4.0	1.3×10^{14}	4.27	474	1
64	2002/11/03	20:30	45.74	26.86	90	4.0	9.0×10^{14}	7.77	244	27
65	2002/11/27	18:56	45.55	26.49	146	3.6	2.1×10^{14}	7.33	258	5
66	2002/12/15	13:37	45.74	26.70	109	3.6	1.9×10^{14}	10.33	178	15
67	2002/12/23	19:32	45.56	26.46	114	3.5	3.7×10^{13}	14.72	123	9
68	2002/12/30	15:41	45.69	26.57	153	4.1	2.8×10^{15}	6.31	292	50
69	2003/01/03	03:05	45.48	26.29	139	3.7	1.3×10^{14}	7.08	269	3
70	2003/01/05	04:27	45.80	26.73	95	3.7	3.8×10^{14}	9.30	200	21
71	2003/04/06	06:02	45.59	26.51	142	3.8	8.4×10^{13}	9.50	207	4
72	2003/05/02	20:34	45.63	26.49	152	3.8	1.5×10^{14}	7.27	288	3
73	2003/05/19	08:38	45.64	26.51	148	3.9	2.3×10^{14}	4.62	423	1
74	2003/05/26	12:36	45.73	26.67	138	3.8	1.3×10^{14}	9.76	191	8
75	2003/08/02	01:32	45.59	26.47	149	4.1	5.9×10^{14}	4.15	455	3
76	2003/08/27	13:15	45.61	26.46	151	3.8	2.6×10^{14}	4.94	410	2
77	2004/01/21	05:49	45.52	26.46	118	4.1	7.1×10^{14}	7.21	254	19
78	2004/02/13	17:48	45.68	26.67	134	3.8	2.0×10^{14}	8.24	246	6
79	2004/03/17	23:42	45.63	26.62	146	4.1	9.5×10^{14}	3.80	509	3
80	2004/04/02	03:21	45.68	26.59	147	3.8	3.1×10^{13}	7.77	239	1
81	2004/04/04	06:41	45.68	26.50	150	4.3	6.6×10^{14}	4.39	435	4
82	2004/04/06	22:35	45.64	26.55	141	3.9	6.5×10^{13}	8.93	211	3

(continued)

Table 2 (continued)

Nr	Data	hh:mm	Lat (°N)	Lon (°E)	h (km)	M_w	M_o (Nm)	f_c (Hz)	r (m)	$\Delta\sigma$ (MPa)
83	2004/04/15	00:54	45.60	26.57	101	3.2	1.6×10^{13}	10.66	179	1
84	2004/04/22	16:08	45.44	26.39	124	3.7	8.1×10^{13}	8.73	215	4
85	2004/06/03	21:43	45.79	26.84	62	2.9	2.9×10^{13}	14.50	125	7
86	2004/07/02	01:38	45.68	26.81	108	3.8	$1.6e \times 10^{14}$	9.48	219	7
87	2004/09/12	04:26	45.47	26.33	145	3.2	1.9×10^{14}	6.45	409	1
88	2004/10/24	19:56	45.44	26.39	153	4.4	7.5×10^{14}	2.85	651	1
89	2004/11/17	11:31	45.72	26.73	131	4.4	1.9×10^{15}	7.04	270	42
90	2005/01/10	10:05	45.75	26.79	112	3.5	1.3×10^{14}	10.41	189	8
91	2005/01/10	12:08	45.67	26.60	99	3.7	4.2×10^{14}	8.93	202	22
92	2005/01/29	01:34	45.62	26.38	76	3.4	2.8×10^{14}	14.35	128	58
93	2005/02/17	07:06	45.57	26.59	110	3.7	3.6×10^{14}	8.30	229	13
94	2005/03/06	22:32	45.63	26.52	155	4.3	1.1×10^{15}	3.94	493	4
95	2005/03/07	20:48	45.63	26.50	125	3.5	2.2×10^{14}	12.91	144	32
96	2005/04/15	19:58	45.62	26.52	144	3.7	4.5×10^{13}	5.83	337	0.5
97	2005/05/09	06:53	45.50	26.28	143	4.1	4.2×10^{14}	6.93	286	8
98	2005/05/14	06:36	45.65	26.49	147	4.2	7.2×10^{14}	4.86	405	5
99	2009/04/26	23:19	45.69	26.64	104	3.8	1.6×10^{14}	4.92	270	4
100	2013/04/21	08:09	45.67	26.59	132	3.9	1.45×10^{15}	5.86	181	107
101	2013/04/25	17:12	45.51	26.27	144	3.6	5.63×10^{14}	7.24	146	79
102	2013/06/23	06:16	45.50	26.32	136	3.2	1.24×10^{14}	10.93	96	61
103	2013/07/12	18:02	45.52	26.37	137	3.6	6.38×10^{14}	7.14	156	74
104	2013/10/22	07:16	45.75	26.69	132	3.4	2.21×10^{14}	7.81	140	32
105	2013/11/07	14:34	45.75	26.67	135	3.7	7.37×10^{14}	8.01	133	137
106	2013/12/27	07:58	45.74	26.65	93	3.5	3.87×10^{14}	8.65	122	94
107	2014/03/31	15:48	45.60	26.45	151	3.3	1.73×10^{14}	8.71	131	34
108	2014/04/07	12:59	45.51	26.26	119	3.7	7.61×10^{14}	7.73	155	89
109	2014/06/29	14:38	45.64	26.54	144	3.3	1.38×10^{14}	7.90	133	26

earthquakes (1940, 1977, 1986, 1990) were included as well in order to extend the magnitude range for scaling purposes.

The distribution in space of the events analyzed in this paper is represented in Fig. 1. The two vertical cross-sections represent the projections of the hypocenters on the two perpendicular planes figured in the first diagram. The locations of the major shocks of 1940, 1977, 1986 and 1990 and of the events investigated by Radulian and Popa (1996) are included in the figure. For all the events the locations are those of the Romanian catalogue, performed routinely using Hypoplus software (Onescu et al. 1999). The hypocenters are located in a constraint focal volume situated between 62 and 171 km depth, contracted on NW-SE direction and dipping from NE to SW tangentially to the Carpathians Arc bend. Except the major shocks of 1940, 1977, 1986 and 1990, any event in the input data has at least one associated co-located event. Apparently, the hypocenter of the 1940 major event is

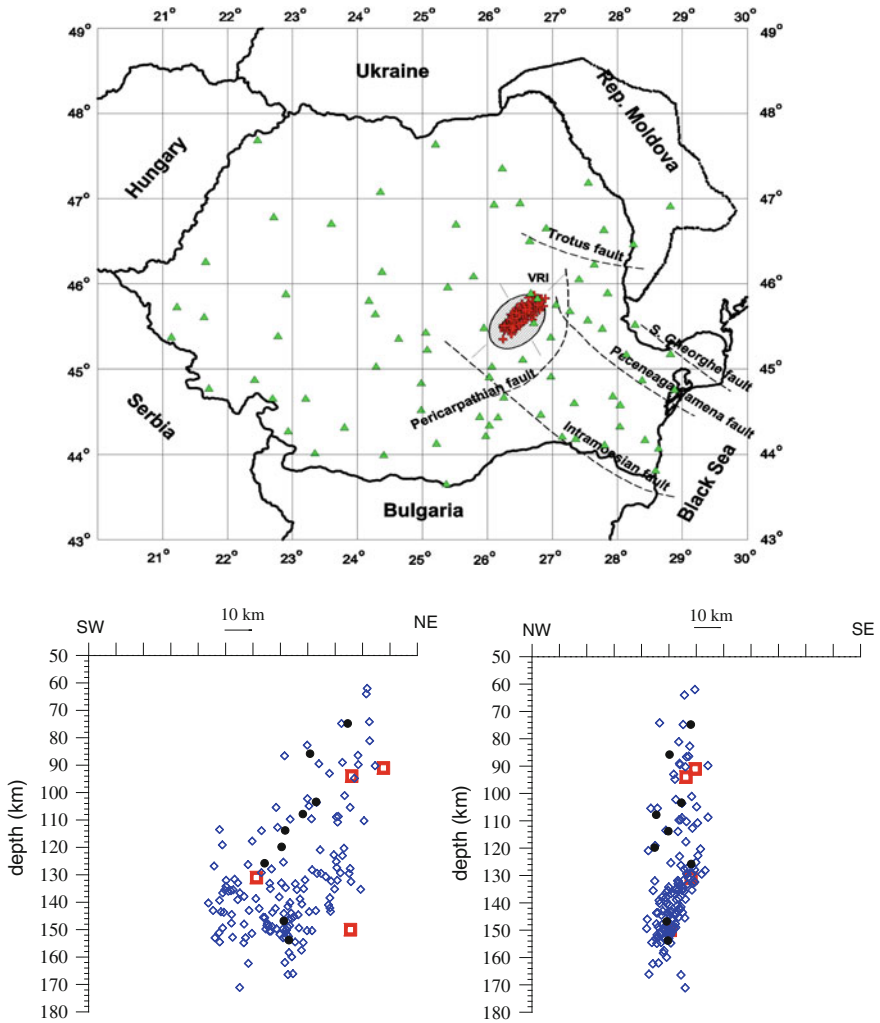
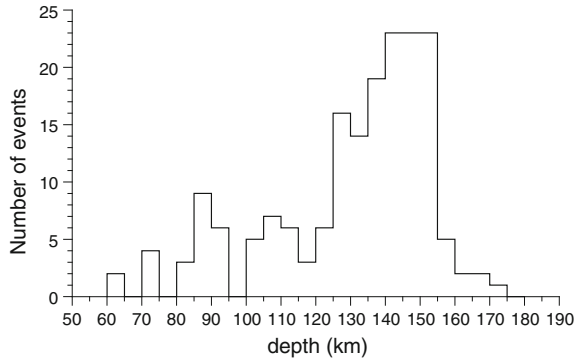
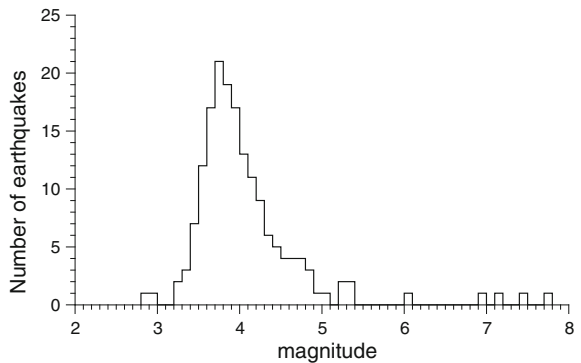


Fig. 1 Distribution of epicenters of the study events and seismic stations of the National Institute for Earth Physics (*upper slide*) and projection of the hypocenters on the two vertical cross sections drawn on the map (*bottom slides*). *Diamonds*—present study events; *solid circles*—events of Radulian and Popa (1996); *squares*—major events

outside the event cluster of the dataset selected in this paper, but there are doubts about the real position of the focus (for example, the depth for this event is 133 km in Oncescu 1987, and 124 km in Hurukawa et al. 2008) (Table 2).

Fig. 2 Distribution of events on depth**Fig. 3** Number of events as a function of magnitude

The distributions of events as function of depth and magnitude are represented in Figs. 2, 3. Note the enhancement in the lower segment of the Vrancea seismic active body. This seems to be a general feature of the seismicity pattern in the Vrancea subcrustal domain (e.g., Radulian et al. 2007).

2 Source Parameters

For the data set investigated in this paper we determine the source parameters applying relative techniques: spectral ratios and empirical Green's function deconvolution. The earthquakes selected as main events are limited to moderate magnitudes (below M_w 5.5 and one single event of magnitude 6.0). We assume in all cases a circular rupture process which is reasonable assumption for small and moderate magnitude earthquakes. Also, we take on a simple rupture process as a general characteristic of the Vrancea small-to-moderate-magnitude earthquakes (see Popescu et al. 2003, 2007).

Application of EGF or SR techniques takes out path, site and instrument effects when the events are co-located, have similar focal mechanism and are recorded by the same instruments at the same sites. The station coverage for Vrancea earthquakes is generally enough to find at least 3 common stations with acceptable signal/noise ratio and less than 230 km away from the epicentre for a given main event—EGF pair. For the more recent earthquakes (occurred after 2009), we can find pairs of events with more than 15 common stations. At the same time, for many of the main events we could select more than one EGF.

The relative deconvolution techniques are applied in the spectral domain using three-component raw-velocity seismograms for both P and S waves. To compute Fourier spectra time windows of 5–10 and 8–15 s, respectively, are extracted starting 0.1–0.2 s before the wave arrival time. A cosine tapering procedure was applied over ten points at both window ends. From the complex spectral division, the spectral ratio is obtained as the amplitude spectral ratio:

$$R(f) = \frac{\Omega_o^M \left[1 + \left(\frac{f}{f_c^G} \right)^{2\gamma} \right]^{1/2}}{\Omega_o^G \left[1 + \left(\frac{f}{f_c^M} \right)^{2\gamma} \right]^{1/2}} \quad (1)$$

where Ω_o^M , Ω_o^G are the low-frequency plateaus and f_c^M , f_c^G are the corner frequencies of the two events in the pair (M —main event, G —EGF event). The source time function is obtained by inverse Fourier transforming the complex spectral ratio back to the time domain. In order to smooth the inherent noise resulting from spectral division at high frequencies, we applied a running window to the spectral ratio and a low-pass filter at 10 Hz, after applying inverse Fourier transform.

A clear source pulse indicates that the EGF earthquake is good in both amplitude and phase. In most cases, rather similar amplitudes and durations are obtained for the source pulses and for the spectral ratios independently of station position. This indicates that source-directivity effects are practically absent and that the EGF earthquake is suitably selected both as location and radiation pattern relative to the main event.

The corner frequencies for the EGF event (f_c^G) and for the main event (f_c^M) are estimated by fitting the observed spectral ratio with a function given by (1) iteratively by a nonlinear regression procedure (Lindley 1994). The free parameters are the ratio of the seismic moments (proportional to the ratio of the low-frequency plateaus of the displacement spectra recorded for the co-located events of the pair) and the corner frequencies. The source duration is estimated from the source time function resulted from the application of the EGF technique. A typical example of spectral ratio and source time function for a pair of Vrancea earthquakes is given in Fig. 4.

The corner frequency is determined by the arithmetic mean of the available corner frequency estimates for different components, different stations and different EGFs (in the last case only for main events). Certainly, the source duration can be

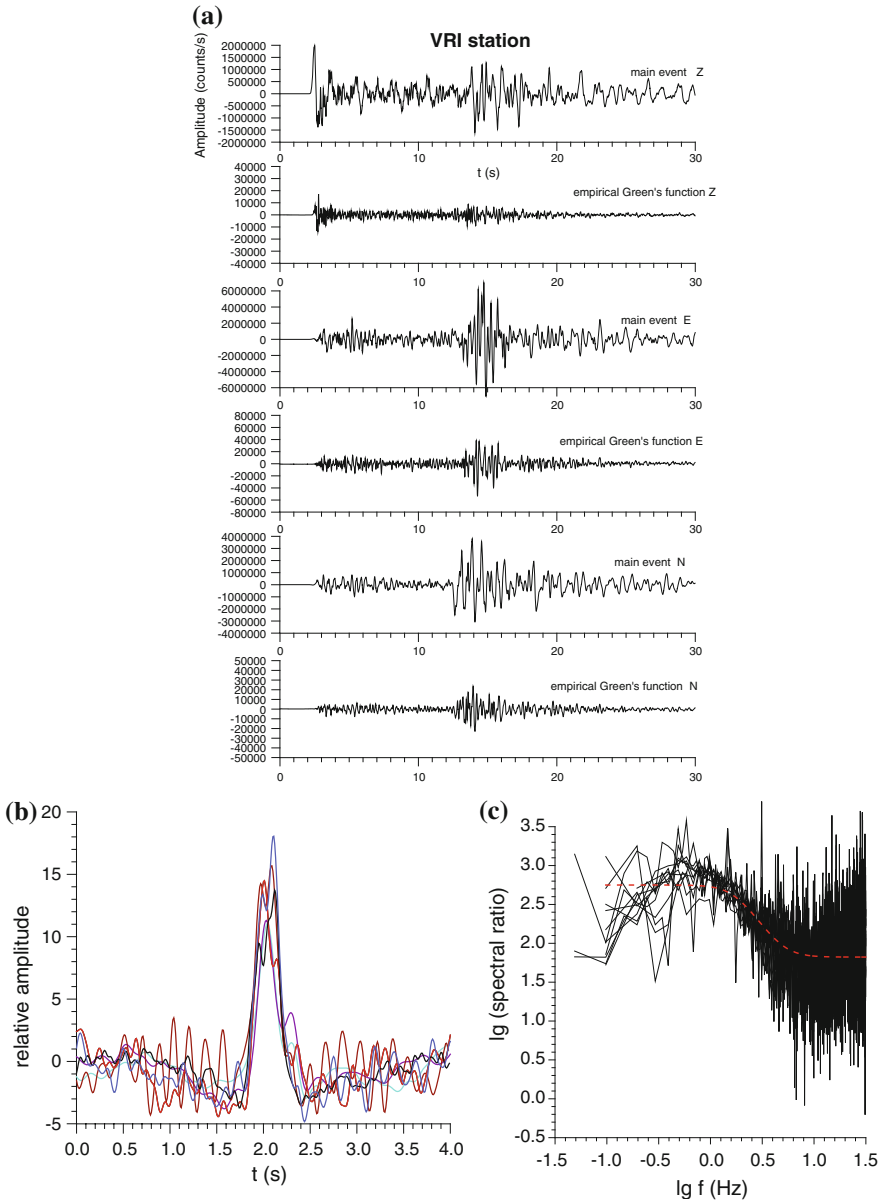


Fig. 4 An example of pair main event—EGF event: **a.** Waveforms recorded at VRI station for event of 25 April 2009, 17:18, $M_w = 5.2$ (main) and of 26 April 2009, 23:19, $M_w = 3.8$ (EGF), **b.** The resulted STFs and **c.** Spectral ratios. *Dashed line*—the theoretical spectral ratio which is best fitting the curves observed for eight stations

obtained only for the main events. It is also determined as arithmetic mean of all the available estimates.

The corner frequency and the source duration both provide equivalent measure of the source size. For a circular source model, in the approximation of a circular simple omega-squared source model, the radius of the rupture area is directly correlated with the corner frequency (Madariaga 1976):

$$r = k v_s / f_c \quad (2)$$

where r is the source equivalent radius, k is a constant ($k = 0.32$ for P waves and $k = 0.21$ for S waves), f_c is the corner frequency and v_s is the velocity of S waves in the focus.

Equivalently, the source radius can be estimated using source time duration (Boatwright 1980):

$$r = (\tau_{1/2} v) / (1 - v / \alpha \sin \theta) \quad (3)$$

where $\tau_{1/2}$ is the rise time in the source (for moderate size earthquakes is roughly half of total source duration τ), v is the rupture velocity in the source (we adopted in the following $v = 0.9\beta$, β —shear wave velocity at focal depth), α —longitudinal wave velocity at source and θ —angle between normal to fault and the emergent angle of the P-wave radiated in the focus.

The relative deconvolution techniques provide only relative measure of the earthquake seismic moment. Thus, the long-period level of the spectral ratio is an estimate of the ratio M_0^M / M_0^G . For evaluation of the absolute value of seismic moment we use (Brune 1970):

$$M_0 = (4\pi\rho\alpha^3\Omega_0R) / (FR_{\theta\phi}) \quad (4)$$

where ρ is the density at source, α is the P-wave velocity at source, Ω_0 is low-frequency plateau of the displacement spectrum, R is the hypocentral distance, F is the free-surface parameter ($F = 2$), $R_{\theta\phi}$ is the source radiation factor [we adopted average values, 0.52 for P waves and 0.63 value for S waves, according to Aki and Richards (1980)]. The structural parameters in Eq. (4) correspond with a velocity model adopted by NIEP in routine locations which includes information from refraction and reflection profiles (Zaharia et al. 2009 and herein references).

The stress drop value for a static crack solution is estimated as a function of seismic moment and source radius (Eshelby 1957):

$$\Delta\sigma = \frac{7M_0}{16r^3} \quad (5)$$

3 Scaling Relationships

The P and S corner frequencies as obtained in our work for the pairs of events are close each other (ratio $f_c^P/f_c^S \sim 1$). Commonly, the P corner frequencies are systematically higher than those estimated for S waves from the same earthquakes (e.g., Molnar et al. 1973; Abercrombie and Leary 1993; Prieto et al. 2004). In the circular model of Madariaga (1976) the f_c^P/f_c^S ratio has an average value of 1.5. A ratio $f_c^P/f_c^S \sim 1$ was obtained by Viegas (2012) and Radulian et al. (2014) for small-to-moderate intra-plate crustal earthquakes. In such cases, we assume that the corner frequency is controlled by the rise time (rupture propagation) which is the same for both P and S waves, rather than the source dimension which causes differences between f_c^P and f_c^S because the fault finiteness interference is different for P and S waves. As expected, for the larger earthquakes the source finiteness effects are more important and the f_c^P/f_c^S ratio comes close to 1.5 as shown by Gusev et al. (2002).

Dependence of inverse of source duration on corner frequency (Fig. 5) shows a linear relation with slope close to 1 ($f_c \sim 1/\tau$) in agreement with the scaling determined by Gusev et al. (2002) from spectral and time-domain analyses on wide-band digital records for 16 Vrancea intermediate-depth earthquakes.

The scaling of the source radius (estimated from spectral ratios because only spectral ratios can provide corner frequencies both for EFGs and main events) with the moment magnitude (Fig. 6) is following the characteristic constant-stress-drop average behavior with the slope close to -3 (Brune 1970). The equation of the regression line in the figure is

$$\lg M_0 = (2.81 \pm 0.13) \lg r + (7.54 \pm 0.34) \tag{6}$$

with correlation coefficient of 0.79 and standard deviation of 0.68. We integrated in our analysis previous results from Oncescu (1986), Radulian and Popa (1996) and the parameters for the four major events. We compared also the corner frequency values obtained in our work with the estimations of Oth et al. (2007) for the events

Fig. 5 Dependence of inverse of source duration on corner frequency for the main events in Table 1. A line of slope 1 is drawn through the points

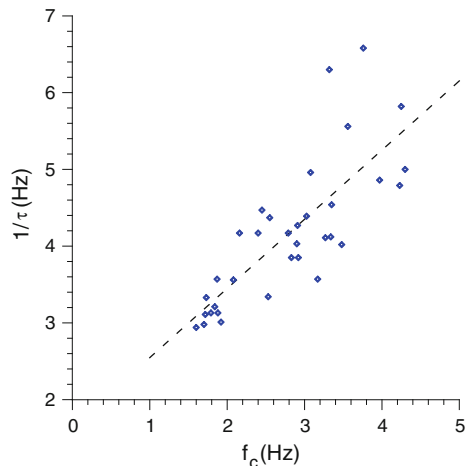
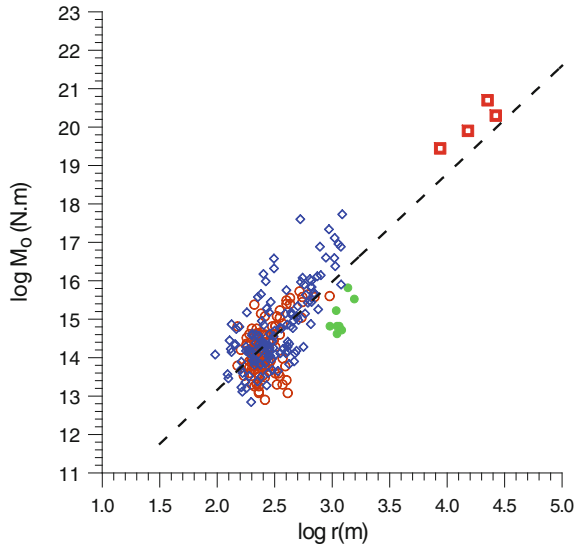


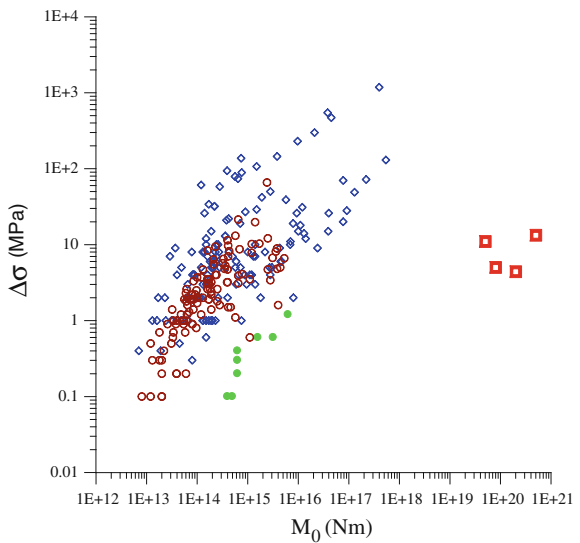
Fig. 6 Scaling of seismic moment with source radius. *Diamonds*—present study events; *solid circles*—events from Radulian and Popa (1996); *squares*—major events; *open circles*—events from Oncescu (1986)



of 1999/11/08 19:22 (M_w 4.6), 1999/11/14 09:05 (M_w 4.6), 2000/04/06 00:10 (M_w 5.0), 2002/09/06 05:04 (M_w 4.1), 2002/11/03 20:30 (M_w 4.0) and 2004/10/27 20:34 (M_w 6.0). While for the 2004 event the corner frequencies are identical, for the other events the estimates of Oth et al. (2007) are roughly by a factor of 1.5 larger than our estimations.

The scaling of the static stress drop versus seismic moment is represented in Fig. 7.

Fig. 7 Scaling of stress drop with seismic moment. *Diamonds*—present study events; *solid circles*—events from Radulian and Popa (1996); *squares*—major events; *open circles*—events from Oncescu (1986)



For the data set investigated in this paper, the radius was estimated from spectral ratios by fitting the observations with a function like that in Eq. (1). Average values for all the available estimates (different components, stations and EGFs) are adopted. The radius in Oncescu (1986) was obtained by simple analysis of the displacement spectra, while for the major shocks we use the estimations inferred from the aftershock distribution in space (Radulian and Popa 1996).

The large variability of the stress drop values follows naturally from the relation (5) having in mind the inherent errors in radius and the variability due to hidden parameters, like rupture velocity or source geometry. In addition, it is important how we define the stress drop: average stress release over the entire source area (static value) or stress release when rupturing a resistant patch inside the source area (dynamic value). The apparent stress drop increasing trend with increasing seismic moment for smaller events (up to magnitude 6) can be due to the limited frequency bandwidth of the instrument (e.g., Hardebeck and Aron 2009; Ide and Beroza 2001; Abercrombie 2015) and low signal/noise ratio at high frequencies leading to an underestimation of the corner frequency for the smaller earthquakes.

4 Discussions and Conclusions

The main goal of the present paper is to set the scaling properties characterizing the Vrancea subcrustal source by integrating an extended data set, practically all the data that authors acknowledged from previous studies and new data processed within this study.

Most of the events in the data set considered in our analysis are of small-to-moderate magnitude. For such events, the circular fault approximation is usually considered to be acceptable.

One crucial issue in investigating source scaling properties in a specified seismogenic zone is the magnitude range for which the scaling laws are properly defined. For example, there were discussions and controversies regarding the change of the seismic scaling laws for small-to-moderate earthquakes and large earthquakes in the crust (see for example Scholz 1982, 1997 and Wang and Ou 1998). One of the significant results of our analysis is extension of the scaling laws over the entire magnitude range, from small-to-moderate earthquakes to the major earthquakes. This is not a trivial outcome if we take into account the class of models for the seismogenic process in the Vrancea source which assume a critical jump between the crack-like and asperity-like rupture processes at small-to-moderate scale to percolation-type processes at large scale (Trifu and Radulian 1991). Thus, seismic moment—magnitude, seismic moment—source radius and seismic moment—stress drop scalings appear to be self-similar over the entire magnitude range of the considered data set ($3.0 \leq M_w \leq 7.7$).

The stress drop values as estimated from source radius using spectral ratios or source displacement spectra show a very large dispersion from 0.1 to 1000 MPa. However, if we take into account the inherent and systematic errors especially at

small earthquakes (underestimation of the corner frequency implying decreasing stress drops) and errors caused by variations in source parameters that were considered similar in our work (rupture velocity or source geometry), we may assume that roughly speaking a constant stress drop model is valid with a mean stress drop value around 10 MPa. This is most probably a value characteristic for a static stress drop. Nevertheless, we cannot exclude that some of the stress drop values are rather dynamic than static for moderate events if we assume that the stress release was caused mainly by rupturing single asperities. Indeed, the parameters obtained by Gusev et al. (2002) using long-range (several hundred to thousands km) and teleseismic data for 12 moderate and large Vrancea earthquakes are systematically lower (corner frequency), respectively greater (source duration) than our determinations. The estimations of source parameters based on source spectral analysis for far-filed waveforms are mainly controlled by the entire source area while EGF procedure is more sensitive to local major asperities acting in the rupture process. This way we can explain also the unusual large stress drop values for the moderate size events in our investigation (reaching hundreds of MPa as can be seen in the Fig. 7).

Oth et al. (2007) estimated the dynamic values of the stress drop for the major Vrancea earthquakes which are about ten times larger than the static values that we use in our paper (Fig. 7). If we sum up all these issues, we come out to an important conclusion with special significance in assessing seismic hazard and strong ground motion characteristics: the rupture process for Vrancea earthquakes is rapid and efficient both for moderate and large shocks leading to high values of the dynamic stress drop and low values of the source dimensions, respectively.

Acknowledgements This work was partially supported by the project “Nucleu” (PN 09 30/PN09-0104) of the National Plan for Research, Development and Innovation of the Romanian Ministry of National Education and by the Partnership in Priority Areas Program—PNII, under MEN-UEFISCDI, DARING Project no. 69/2014.

References

- Abercrombie RE (2015) Investigating uncertainties in empirical green’s function of earthquake source parameters. *J Geophys Res.* doi:[10.1002/2015JB011984](https://doi.org/10.1002/2015JB011984)
- Abercrombie RE, Leary PC (1993) Source parameters of small earthquakes recorded at 2.5 km depth, Cajo Pass, southern California: Implications for earthquake scaling. *Geophys Res Lett* 20:1511–1514
- Aki K, Richards PG (1980) *Quantitative seismology*. Freeman and Co., N.Y
- Bakun WH, Bufe CG (1975) Shear-wave attenuation along the San Andreas fault zone in Central California. *Bull Seismol Soc Am* 65:439–460
- Boatwright J (1980) A spectral theory for circular seismic sources: Simple estimates of source duration, dynamic stress drop, and radiated energy. *Bull Seismol Soc Am* 70:1–28
- Brune JN (1970) Tectonic stress and the spectra of seismic shear waves from earthquakes. *J Geophys Res* 75:4997–5009
- Cărbunar OF, Radulian M (2011) Geometrical constraints for the configuration of the Vrancea (Romania) intermediate-depth seismicity nest. *J Seismolog* 15:579–598

- Eshelby JD (1957) The determination of the elastic field of an ellipsoidal inclusion and related problems. In: Proceedings of the Royal Society of London, A 241. pp. 376–396
- Frankel A (1982) Precursors to a magnitude 4.8 earthquake in the Virgin Islands: Spatial clustering of small earthquakes, anomalous focal mechanisms, and earthquake doublets. *Bull Seismol Soc Am* 72:1277–1294
- Gusev A, Radulian M, Rizescu M, Panza GF (2002) Source scaling for the intermediate-depth Vrancea earthquakes. *Geophys Int J* 151:879–889
- Hardebeck JL, Aron A (2009) Earthquake stress drops and inferred fault strength on the Hayward fault, east San Francisco Bay. *California Bull Seismol Soc Am* 99:1801–1814
- Hough SE, Seeber L, Lerner-Lam A, Armbruster G, Guo H (1991) Empirical green's function analysis of loma prieta aftershocks. *Bull Seismol Soc Am* 81:1737–1753
- Hurukawa N, Popa M, Radulian M (2008) Relocation of large intermediate-depth earthquakes in the Vrancea region, Romania, since 1934 and a seismic gap. *Earth Planets Space* 60:565–572
- Ide S, Beroza GC (2001) Does apparent stress vary with earthquake size? *Geophys Res Lett* 28:3349–3352
- Ismail-Zadeh A, Mațenco L, Radulian M, Cloetingh S, Panza GF (2012) Geodynamics and intermediate-depth seismicity in Vrancea (The South-Eastern Carpathians): Current state-of-the-art. *Tectonophysics* 530:50–79
- Lindley GT (1994) Source parameters of the 23 April 1992 Joshua Tree, California earthquake, its largest foreshock and aftershocks. *Bull Seism Soc Am* 84:1051–1057
- Madariaga R (1976) Dynamics of an expanding circular crack. *Bull Seismol Soc Am* 66:639–666
- Molnar P, Tucker BE, Brune J (1973) Corner frequencies of P and S wave and models of earthquake sources. *Bull Seismol Soc Am* 63:2091–2104
- Mori J, Frankel A (1990) Source parameters for small events associated with the 1986 North Palm Springs, California earthquake determined using empirical green functions. *Bull Seism Soc Am* 80:278–285
- Mueller CS (1985) Source pulse enhancement by deconvolutions with empirical green's function. *Geophys Res Lett* 12:33–36
- Onescu MC (1986) Some source and medium properties of the Vrancea seismic region, Romania. *Tectonophysics* 126:245–258
- Onescu MC (1987) On the stress tensor in Vrancea region. *J Geophys* 62:62–65
- Onescu MC, Marza V, Rizescu M, Popa M (1999) The Romanian earthquakes catalogue between 1984 and 1997. In: Wenzel F, Lungu D (eds) *Vrancea earthquakes: Tectonics, hazard and risk mitigation*, Kluwer Academic Publishers, pp. 43–47
- Oth A, Wenzel F, Radulian M (2007) Source parameters of intermediate-depth Vrancea (Romania) earthquakes from empirical green's functions modeling. *Tectonophysics* 438:33–56
- Popescu E, Popa M, Radulian M (2003) Efficiency of the spectral ratio method to constrain the source scaling properties of the Vrancea (Romania) subcrustal earthquakes. *Rom Rep Phys* 55:149–169
- Popescu E, Radulian M, Popa M, Plăcintă AO, Ghica D, Moldovan IA (2007) Vrancea seismic source calibration using a small-aperture array. *Rom Rep Phys* 59:147–164
- Prieto GA, Shearer PM, Vernon FL, Kilb D (2004) Earthquake source scaling and self-similarity estimation from stacking P and S spectra. *J Geophys Res B Solid Earth Planets* 109: no. B0, 8310. doi: [10.1029/2004JB003084](https://doi.org/10.1029/2004JB003084)
- Radulian M, Popa M (1996) Scaling of source parameters for Vrancea (Romania) intermediate depth. *Tectonophysics* 261:67–81
- Radulian M, Bonjer KP, Popa M, Popescu E (2007) Seismicity patterns in SE Carpathians at crustal and subcrustal domains: Tectonic and geodynamic implications. In: Proceedings of CRC-461 international symposium on strong vrancea earthquakes and risk mitigation, MATRIX ROM, Bucharest, pp. 93–102
- Radulian M, Popescu E, Borleanu F, Diaconescu M (2014) Source parameters of the December 2011–January 2012 earthquake sequence in Southern Carpathians, Romania. *Tectonophysics* 623:23–38

- Scholz CH (1982) Scaling laws for large earthquakes: Consequences for physical models. *Bull Seismol Soc Am* 72:1–14
- Scholz CH (1997) Size distribution for large and small earthquakes. *Bull Seismol Soc Am* 87:1074–1077
- Trifu CI, Radulian M (1991) Frequency—magnitude distribution of earthquakes in Vrancea: Relevance for a discrete model. *J Geophys Res* 96:4301–4311
- Viegas GL (2012) Source parameters of the 16 July 2010 Mw 3.4 Germantown, Maryland, earthquake. *Seism Res Lett* 83:933–944
- Wang JH, Ou SS (1998) On scaling of earthquake faults. *Bull Seism Soc Am* 88:758–766
- Zaharia B, Enescu B, Radulian M, Popa M, Koulakov I, Parolai S (2009) Determination of the lithospheric structure from Carpathians Arc bend using local data. *Rom Rep Phys* 61(4): 748–764

The 2013 Earthquake Swarm in the Galati Area: First Results for a Seismotectonic Interpretation

Mihaela Popa, Eugen Oros, Corneliu Dinu, Mircea Radulian,
Felix Borleanu, Maria Rogozea, Ioan Munteanu and Cristian Neagoe

Abstract An earthquake swarm of 940 events with M_L magnitude between 0.1 and 4.0 and the depth no more than 25 km occurred during three months in the South-Eastern Carpathians foredeep, in an area of around 200 km², at 27 km north-east of the Galati city. JHD relocation highlights a rupture area steeply dipping down to 15 km depth along a NE-SW alignment. Although the area is known as seismically active, it was for the first time that such a massive sequence was recorded. Specific seismicity alignments and stress field patterns are emphasized and interpreted in terms of geotectonical features of the region. The analysis of the stress associated with the seismic swarm shows a predominant EW compression and NS extension which is compatible with the regional stress regime in the Carpathians

M. Popa (✉) · E. Oros · M. Radulian · F. Borleanu · M. Rogozea · C. Neagoe
National Institute for Earth Physics, Măgurele, Romania
e-mail: mihaela@infp.ro

E. Oros
e-mail: eugenoros@gmail.com

M. Radulian
e-mail: mircea@infp.ro

F. Borleanu
e-mail: felix@infp.ro

M. Rogozea
e-mail: mrogozea@infp.ro

C. Neagoe
e-mail: cristian.neagoe@infp.ro

C. Dinu · I. Munteanu
Faculty of Geology and Geophysics, University of Bucharest,
Bucharest, Romania
e-mail: corneliu.dinu@g.unibuc.ro

I. Munteanu
e-mail: ioan.munteanu@gmail.com

I. Munteanu
Repsol E&P, Madrid, Spain

foredeep area. The rather small b -slope value of the frequency-magnitude distribution (0.743) for the swarm events in contrast with the value characterizing the regional seismicity (1.890) suggests a significant increase in the local stress accumulation on relatively larger tectonic structures and is in favor of a major tectonic component of the mechanism responsible for generating the swarm.

Keywords Earthquake sequence · Crustal seismicity · North Dobrogea · Seismicity patterns

1 Introduction

A large seismic swarm was recorded for a three-month time interval in the SE Carpathians foreland, at about 27 km distance north-west of the Galati city (Fig. 1). The earthquakes were generated between two important crustal faults, Sf. Gheorghe and Peceneaga-Camena Faults (SGF and PCF) along a perpendicularly oriented alignment over an area of approximately 200 km². This alignment is situated on a prolongation to the west of the North Dobrogea block and is crossing an inter-fluvial zone rich in underground water and loess-like thick deposits.

The North Dobrogea block with an elongated NW-SE direction is delimited by SGF and PCF from the Scythian Platform to the north and the Moesian Platform to the south-west (Fig. 1). This accretionary unit was displaced in the present-day position by successive strike-slip horizontal movements, dextral relative to the Scythian Platform and sinistral relative to the Moesian Platform. The North Dobrogea block is sinking towards NW under the Carpathian Neozoic foredeep deposits, Badenian-Quaternary in age, as has been proved wells drilling metamorphic rocks (Precambrian to-Ordovician in age), similar with those from the outcropping Măcin area. This prolongation is known in the Romanian literature, as the North Dobrogea Promontory (Paraschiv 1979).

The major strike-slip bounding faults (e.g. PCF and SGF in Fig. 1) are extending toward SE on the Black Sea continental shelf. The progressive opening toward SE correlates with the quasi-continuing decrease of the faults step, in parallel with decreasing of crustal thickness (Pompilian et al. 1991). Towards NW a complex system of active young faults acting as satellites of the two major faults has been identified in the area (Tărăpoancă et al. 2003; Mațenco et al. 2007). These faults are accompanied by an enhancement in the diffuse seismicity spread in front of the Carpathians Arc bend (i.e., Radulian et al. 2000). Only small-to-moderate earthquakes have been recorded here. The largest event was recorded recently in the northern edge of the Mărășești-Galați-Brăila lineament on November 2014, $M_w = 5.7$).

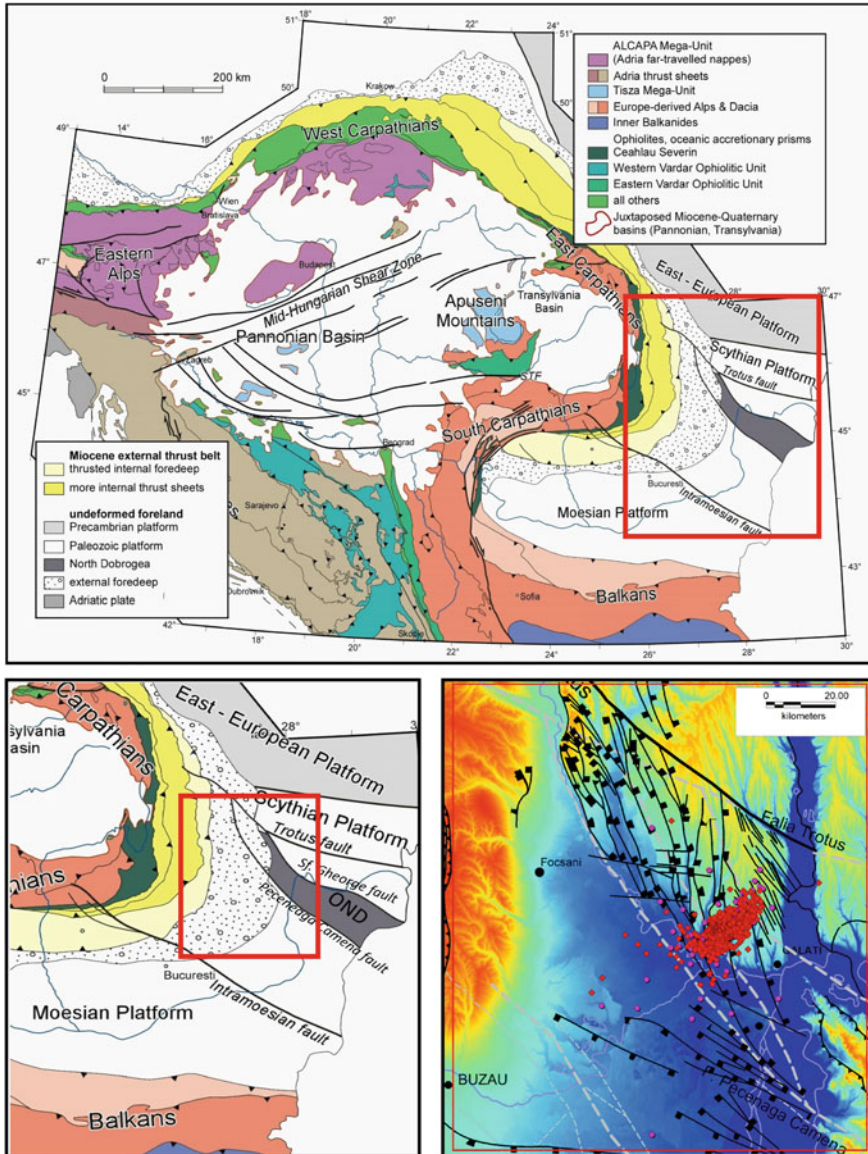


Fig. 1 Upper Carpatho-Pannonian system and the position of the study area (*solid red polygon*); *Bottom* distribution of the epicenters of the seismic swarm in the Galati area. The fault system consists of large crustal faults (*heavy dashed lines*) oriented SE-NW and a complex of normal faults (*black lines*), clustered between the Trotsuș Fault and Peceneaga-Camena Fault (after Matenco et al. 2007)

The geodynamics in this region is rather complex with a predominant post-collisional process which controls both the cluster of seismicity in the mantle, beneath the Vrancea Zone, and the seismicity in the overlying crust. The process of lithosphere decoupling and descending in the mantle is unusually concentrated in space and time. It explains the increased shallow seismicity in front of the arc in contrast with the poor seismicity in the back-arc side. Also the particular tectonic environment which concentrate several major tectonic units (East-European Platform, Scythian Platform, Moesian Platform and North Dobrogea Orogen), deeping towards Eastern Carpathian Orogen and major faults (Peceneaga-Camena, Sf. Gheorghe and Troțuș in Fig. 1) in a narrow zone, as well as significant structural inhomogeneities, such as the development of a deep sedimentary basin in the Focșani Depression, allowed the partial reactivation of some segments of these major faults and to generate a large amounts of local active faults (Fig. 1).

2 Seismic Activity

The seismic sequence started on 15–31 August 2013 with 3 small events. The activity is re-initiated on 23 September and continued with alternate enhanced and reduced intervals until November 2013 (Fig. 2). A total of 940 events were identified and located with local magnitudes from 0.1 to 4.0 in the time interval from 15th August to 5th November. Sporadic activity has been reported after 5th November 2013 until present day which was not be envisaged in our analysis.

The timing of seismicity represented in Fig. 2 shows an alternating more active and less active intervals. Three of the clusters of enhanced seismicity include shocks with magnitude above 3.5: 23–25 September, 28–30 September and 2–5 October. It is interesting to note that the seismic activity diminished suddenly after

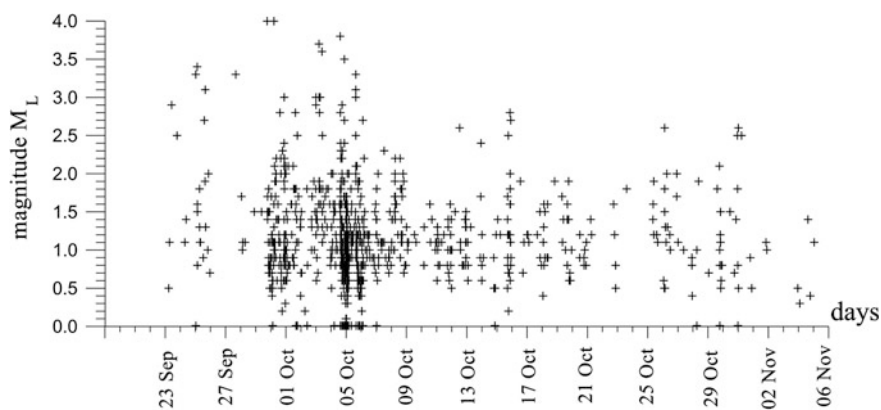


Fig. 2 History of the seismic activity in Galați area for 23rd September–5th November 2013 time interval

the occurrence of a moderate Vrancea earthquake on 6 October 2013 ($M_L = 5.5$). This coincidence would be in favor of the hypothesis of an interdependence between the tectonic regimes in the Vrancea subcrustal domain (predominant) and in the crustal domain of the Carpathians foreland along particular alignments of sensitivity (Mitrofan et al. 2014). Starting with November and somehow continuing in December 2013 the earthquakes generated in the study area decrease in number and size (magnitudes below 2.5).

The National Institute for Earth Physics installed in the epicentral area four temporary stations at Izvoarele village (IZVR and IZVB), Slobozia Conachi (SLCR) and Negrea (NEGR) which started to operate since 28 September 2013. At the same time, an accelerometer together with a system for recording acoustic signals, a magnetometer and an infrasound station were installed at Izvoarele. Although the magnitude of the events did not exceed 4.0, their effects were unusually high in Izvoarele creating a real panic in this village throughout the duration of the sequence.

Distributions of the events in time and on size are specific for a swarm-type sequence. There are no main shocks that distinguish themselves from the rest of earthquakes. In addition, the rate of activity is not decreasing exponentially over time, but rather is quasi-persistent with a sequence of bursts of enhanced activity distributed throughout the entire sequence. The swarm-type seismicity is commonly encountered in areas with particularly heterogeneous structures.

The past activity in the Galați region, as recorded in the Romplus catalog (Oncescu et al. 1999), shows dispersed seismicity of small-to-moderate earthquakes (maximum recorded moment magnitude is 4.5). Generally, the earthquakes are generated in the North Dobrogea Promontory, which is placed between the SGF and PCF. This is nominated as ‘Predobrogean Depression’ by Radulian et al. (2000) and extends to the North-West in the Bârlad Depression. The entire area belongs to the same tectonic unit and is characterized by similar seismicity and focal mechanism reflecting a predominant transcurrent and extensional regime.

The release of the tectonic deformation in sequences is often reported in the Carpathians foreland area in correlation with specific alignments (i.e., Atanasiu 1961; Popescu and Radulian 2001). Swarm-type clusters are observed mainly in the Vrancea epicentral area, close to Vrincioaia (VRI) station, but the swarm investigated in this paper is an unprecedented case for the Galați region, both as regards the time evolution and number of events. Only occasional sporadic swarms were reported over a few days and consisting of a few small events. Taking into account the severe reduction of the event locations in the past because of the insufficient number of available stations, there is an open question if the sequence of 2013 is indeed an exceptional case or it simply appears like this in comparison with previous sequences recorded by much less stations operating that time.

Some earthquakes in the past induced macroseismic effects up to intensity VI (MSK scale). Apparently, the macroseismic effects concentrated along NW-SE direction (Atanasiu 1961). An earthquake occurred on 15.11.1901 ($M_w = 4.5$), located east of Galați, was felt with intensity V+ in Galați, IV+ in Brăila and III in Isaccea. Another earthquake occurred on 13.03.1908 ($M_w = 4.5$) on the Galați—

Pechea line was felt in Galați with intensity V, in Pechea with intensity IV+ and in Brăila with intensity IV. For these two events, historical documents do not mention the occurrence of aftershocks. More recently, an earthquake sequence was triggered on 11.09.1980 between Galați and Brăila. The main shock of magnitude $M_w = 4.6$ (intensity VI in epicentral zone) was followed by 49 aftershocks, the largest of magnitude $M_L = 3.3$ (Radu and Oncescu 1988).

The seismic swarm of September–November 2013 shows notable peculiarities relative to previous local seismicity: an unusually long time evolution, lack of a predominant shock and the alignment oriented perpendicularly to the common NW-SE trend of the major faults (Fig. 3). We represent in Fig. 3 the locations performed with Locsat algorithm within Antelope system and JHD (Joint Hypocenter Determination—Douglas 1967) program, using the P- and S-wave arrival times at the seismic stations of Romania and Republic of Moldova (Fig. 1). We apply JHD computations for a velocity model compiled after Raileanu (2009) who determined local velocity structure at station TUDR (Tudor Vladimirescu).

As visible in the Fig. 3, the clustering of the relocated events is significantly increased. Application of JHD algorithm led to elimination of 86 events from the initial data set (940 events) since the joint procedure was not able to associate these events with any event of the data set. All the eliminated events have low magnitude ($M_L < 1$) and less than 6 recording stations.

The distribution of hypocenters shows an alignment oriented NE-SW, perpendicularly on the trend of principal faults (PCF to the south and SFG to the North). Most of the hypocenters are located above 15 km in depth.

The frequency–magnitude distribution represented in Fig. 4 shows a maximum of activity in the 0.8–1.1 magnitude interval. Local magnitude was estimated using Wood-Anderson amplitude corrected for distance compiled only for stations with acceptable signal/noise ratio and situated close to epicenter (within 120 km distance).

The magnitude of completeness is located around $M_L = 0.8$ value. The slope of the distribution (0.743) is rather low for a seismic swarm behavior having in mind that for swarm activity larger b-values are mostly found (Scholz 1968; Sykes 1970). However, b-values below 1 were observed for swarms in different regions as well (Vogtland/NWBohemia—Hainzl 2003; Ecuador—Legrand et al. 2004).

The a-value of the frequency-magnitude distribution of the swarm events ($a = 3.51$) is smaller than the a-value at regional scale computed for a 10-year time interval preceding the swarm in an enlarged rectangle area around the swarm. The annual a-value scaled for 200 km² area is in the last case $a = 0.097$. The corresponding b-value (1.89) is greater than two times the b-value of the swarm (0.743). The striking difference between the a value and b value of the swarm relative to the background regional seismicity shows significant enhancement in seismicity and stress concentration on larger tectonic structures.

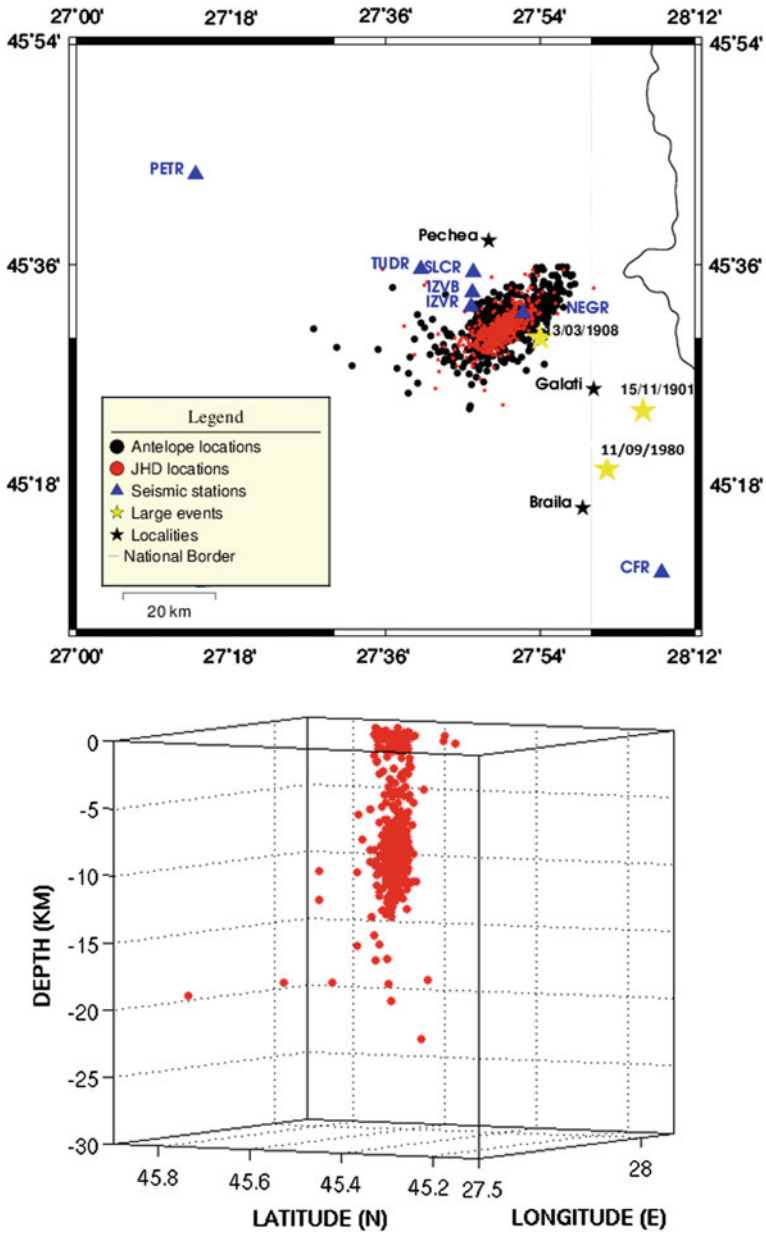
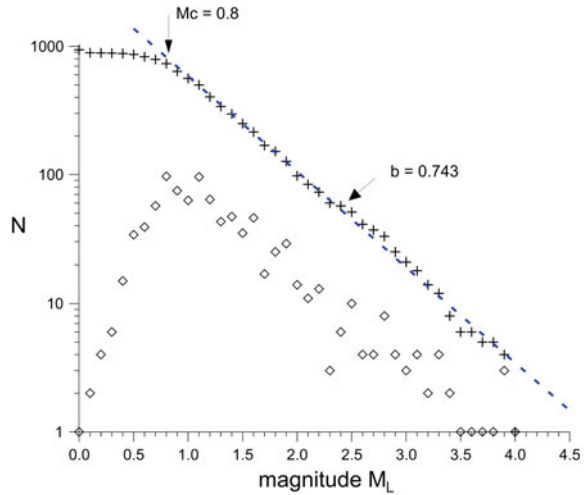


Fig. 3 Upper epicenter distribution for initial locations (black dots) and relocations with JHD (red dots). Yellow stars are the epicenters of the past significant events. Bottom 3D representation (JHD hypocenters) of events location (view from SW)

Fig. 4 Frequency—magnitude distribution (cumulative and non-cumulative) for the seismic swarm in the Galați area



3 Focal Mechanism

The fault plane solutions (Table 1) are determined by two methods incorporated in the SEISAN algorithm (Havskov and Ottemöller 2001). *Focmec* method uses the first P-wave polarities together with the amplitudes measured on all the three components (vertical, transversal and radial). *HASH* method uses only S/P ratios

Table 1 Seismic events for which the fault plane solutions are computed (crt. no. corresponds with the numbers in Fig. 5)

Crt. no.	Date ZZ/MM/YYYY	Origine time HH: MM:SS	Latitude (°N)	Longitude (°E)	Depth (km)	Magnitude (M_L)	Faulting type
1.	04/10/2013	14:29:27	45.548	27.815	3.0	3.8	SS
2.	04/10/2013	21:08:11	45.504	27.831	4.1	3.4	N
3.	05/10/2013	15:20:19	45.505	27.801	5.3	3.3	SS
4.	25/09/2013	00:36:11	45.537	27.833	9.7	3.3	SS-N
5.	27/09/2013	16:11:12	45.533	27.867	3.9	3.3	SS-N
6.	25/09/2013	02:50:41	45.537	27.860	6.8	3.4	SS-N
7.	03/10/2013	09:27:41	45.492	27.830	4.7	3.9	SS
8.	03/10/2013	04:37:39	45.577	27.881	5.8	3.9	SS
9.	29/09/2013	18:10:50	45.533	27.898	5.5	4.0	SS
10.	30/09/2013	05:01:57	45.510	27.810	5.5	3.9	SS
11.	02/10/2013	23:52:37	45.580	27.894	3.2	3.1	SS-N
12.	03/10/2013	05:52:49	45.595	27.959	1.0	3.3	SS
13.	03/10/2013	05:34:43	45.421	28.043	1.0	3.6	SS

measured on the radial component in addition to first P-wave polarities. Only P_g and S_g phases are considered in the spectral amplitudes because the waveforms are generally very noisy, frequently contaminated with coda waves belonging to events generated just before the current event. Since the two methods are different, we performed a comparative analysis in order to test the reliability of the solutions.

Focmec method is drastic since it removes the erroneous polarities and the ratios above an imposed limit (we adopted 0.5 in our case). *HASH* method uses weights for the polarity and amplitude ratios errors and provides averaged values, without eliminating the stations with large errors. For both methods we filtered the seismograms for frequencies below corner frequency and measured the maximum amplitudes on intervals of maximum 2 s starting at P_g , respectively S_g onset. In all cases, the solutions obtained through both methods are comparable what makes us think the solutions are close to reality. We plot in Fig. 5 the fault plane solutions determined by applying first method for 13 events ($M_L > 3.1$).

We can group the solutions into three sets:

- strike-slip faulting—SS (8 events)
- combination strike-slip with normal faulting SS-N (4 events)
- pure normal faulting—N (1 event)

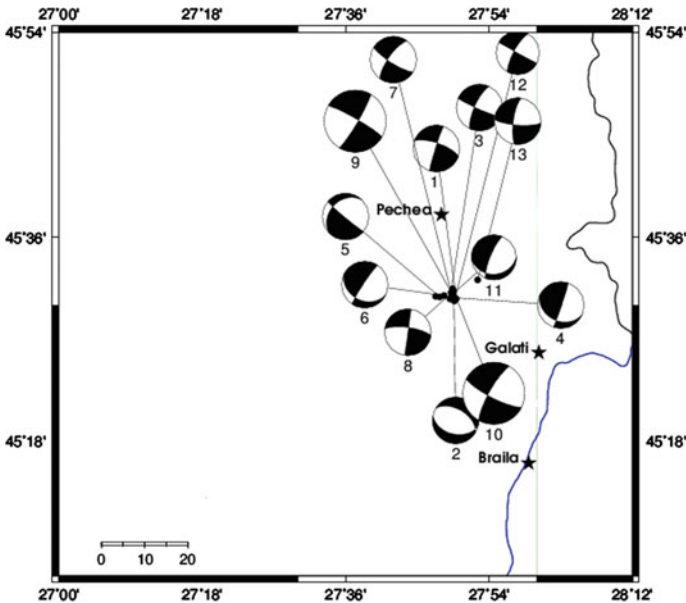


Fig. 5 Fault plane solutions determined for 13 events of the swarm (numbers associated with the fault plane solutions correspond with the crt. no. in Table 1). Beach-ball size is a function of magnitude. *Black dots* are earthquake epicenters

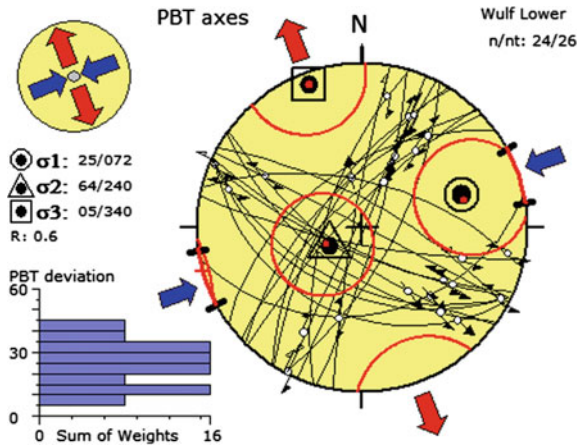


Fig. 6 Stress inversion: Wulf projections on the lower hemisphere for the fault planes (13 events, 26 nodal planes), principal stress axes, maximum horizontal stresses (*blue arrows* compression; *red arrows* dilatation); distribution of the associated errors (*red circles*); 1σ standard deviation for the maximum horizontal stress (*heavy black lines*); n_t Total number of the nodal planes; n Number of the nodal planes compatible with the final stress solutions; R Stress ratio (0.6 value indicates a strike-slip faulting process); histogram of the PBT (focal mechanism axis) deviation from the average (in degrees)—*bottom left corner*

Note the remarkable similarity among the solutions in each group. Apparently, there is no correlation between the faulting type and spatial location of the event.

The analysis of the stress associated with the seismic swarm points out a predominant N72°S compression and N160°S extension (Fig. 6). This is compatible with the regional stress regime in the Carpathians foredeep area (Radulian et al. 1999).

If we look in comparison with the regional tectonic setting (Fig. 1), we assume that the nodal planes oriented NW-SE to be the most probable direction of slip. It is likely that the motion has been driven in this direction by the general NW-SE transcurrent forces. According to this interpretation, the epicenters alignment along a perpendicular direction is explained not by the presence of a physical fault NE-SW oriented, but by the stress transfer among the multitude of faults all striking from SE to NW.

4 Discussion and Conclusions

By scale and specific evolution in space and time, the earthquake swarm occurred in September–November 2013 in the Galați area represents a unique phenomenon on the seismicity map located in front of the South-Eastern Carpathians Arc bend. The sequence had also a strong impact in Romania mass-media through the unexpected effects reported in the epicentral area, mainly in Izvoarele village, where minor

damage and acoustic signals have been reported by the local inhabitants almost continuously during the swarm.

In the present paper we re-picked all the available seismograms recorded in the interval 15th August–5th November 2013 and come out with a total of 940 events detected and located in the Galați area. The distribution of hypocenters shows an alignment NE-SW, somewhat perpendicular to the general NW-SE trend of the faults in the region regardless of fault scale. In depth, the foci are restricted to depths smaller than 15 km.

There is an ambiguity as regards the epicenter alignment, focal mechanism and the predominant NW-SE trending of the regional stress. One can assume that a local fault, NE-SW oriented, has been activated during the swarm (Ioane et al. 2015). However, apparently the seismicity alignment strike (Fig. 3) is too away from the nodal planes oriented NE-SW which are mostly close to a N-S direction (Fig. 5). From other point of view, we can suppose that the faulting planes are oriented in parallel with the NW-SE general trending, and that they are activated sequentially along the seismicity alignment crossing on a perpendicular direction.

The analysis of the stress associated with the seismic swarm points out a predominant N72°S compression and N160°S extension. This is compatible with the regional stress regime in the Carpathians foredeep area (Radulian et al. 1999).

This paper is limited to a first evaluation of seismicity and focal mechanism characteristics of the seismic swarm produced in the Galați area. A lot of open questions remain related to the possible mechanisms underlying this complex seismotectonic activity. While we know that from geodynamical point of view the region is able to generate small-to-moderate earthquakes, there is still to explain the well-defined peculiarities of seismicity distribution in space, time and size and of the associated focal mechanisms as highlighted by the present investigation. We cannot put aside for now the possible role played by diffusion-like increase in pore pressure as a triggering factor. Other mechanisms, such as rate- and state-dependent friction (Dieterich 1994) or stress corrosion cracking (Shaw 1993; Main 2000) would be possible candidates.

The rather small b-slope value of the frequency-magnitude distribution (0.743) suggests a high stress accumulation in the region and is in favor of a major tectonic component of the mechanism responsible for generating the swarm. As it is known, the increase in the pore pressure or the presence of magma (thermal gradient) would lead to high b values (e.g., Mogi 1962; Scholz 1968; Warren and Latham 1970; Wyss 1973; Shaw 1995; Barton et al. 1999; Hill et al. 2003; Neunhöfer and Meier 2004; Maxwell et al. 2008; Paul and Sharma 2011; Wessels et al. 2011). The comparison of the frequency-magnitude parameters of the swarm ($a = 3.510$, $b = 0.743$) with the parameters corresponding to a set of events occurred in a 10-year time interval preceding the swarm in a regional setting ($a = 0.097$, $b = 1.89$) shows striking differences. According to these results, the burst of seismicity generated during the swarm exceeded the regular activity of the area as number of events and appeared as a strong focalization of stress on relative large tectonic structures (able to generate more larger events as in the background activity).

A decisive step to explain the mechanism responsible for generating the seismic swarm in the Galați area will be to apply model simulations. The comparison of observations with model simulation will allow a better understanding of the fundamental underlying mechanisms: stress triggering and/or fluid diffusion, which control the process evolution.

Acknowledgements The results of the paper were partly included in the projects PN 09-30-0101 and PN 09-30-0102 of the Nucleu program of the National Authority for Scientific Research and Innovation. The authors thank the analysts Doina Dumitru and Mioara Pompilian for their patience, attention and skill with which reviewed the Galati earthquake swarm. The authors thank one anonymous reviewer for the constructive remarks and suggestions, which led to the significant improvement of the manuscript.

References

- Atanasiu I (1961) Earthquakes in Romania. Ed. Academiei Republicii Populare Române, Bucharest (in Romanian)
- Barton DJ, Foulger GR, Henderson JR, Julian BR (1999) Frequency–magnitude statistics and spatial correlation dimensions of earthquakes at Long Valley caldera. *California Geophys J Int* 138:563–570
- Dieterich JH (1994) A constitutive law for rate of earthquake production and its application to earthquake clustering. *J Geophys Res* 99:2601–2618
- Douglas A (1967) Joint epicentre determination. *Nature* 215:47–48
- Hainzl S (2003) Self organization of the earthquake swarms. *J Geodyn* 35:157–172
- Havskov J, Ottemöller L (2001) SEISAN: the earthquake analysis software, version 7.2. University of Bergen, Norway, 256p
- Hill D, Langhein J, Perigeon S (2003) Relations between seismicity and deformation during unrest in long valley caldera, California, from 1985 through 1999. *J Volcanol Geoth Res* 127:175–193
- Ioane D, Serban A, Diaconescu M, Chitea F, Caragea I (2015) High seismicity sequence in the Izvoarele area (Galați county)—Romania. In: Proceedings of the 15th international multidisciplinary scientific geoconferences SGEM2015
- Legrand D, Villagomez D, Yepes H, Calahorrano A (2004) Multifractal dimension and b value analysis of the 1998–1999 Quito swarm related to Guagua Pichincha volcano activity. *Ecuador J Geophys Res* 109:B01307
- Main IG (2000) A damage mechanics model for power-law creep and earthquake aftershock and foreshock sequences. *Geophys J Int* 142:151–161
- Mațenco L, Bertotti G, Leever K, Cloetingh S, Schmid SM, Tărăpoancă M, Dinu C (2007) Large-scale deformation in a locked collisional boundary: interplay between subsidence and uplift, intraplate stress and inherited lithospheric structure in the late stage of the SE Carpathian evolution. *Tectonics* 26:1–29
- Maxwell SC, Shemeta J, Campbell E, Quirk D (2008) Microseismic deformation rate monitoring. In: SPE annual technical conference and exhibition (SPE) 21–24 September 2008, Denver, Colorado, USA, paper no. SPE-116596-MS
- Mitrofan H, Chitea F, Anghelache MA, Vișan M (2014) Possible triggered seismicity signatures associated with the Vrancea intermediate-depth strong earthquakes (Southeast Carpathians, Romania). *Seismol Res Lett* 85(2):314–323
- Mogi K (1962) Magnitude-frequency relation for elastic shocks accompanying fractures of various materials and some related problems in earthquakes. *Bull Earthq Res Inst* 40:831–853

- Neunhöfer H, Meier T (2004) Seismicity in the Vogtland/Western Bohemia earthquake region between 1962 and 1998. *Stud Geophys Geod* 48:539–562
- Oncescu MC, Marza V, Rizescu M, Popa M (1999) The Romanian earthquakes catalogue between 984 and 1997. In: Wenzel F, Lungu D (eds) *Vrancea earthquakes: tectonics, hazard and risk mitigation*. Kluwer Academic Publishers, Berlin, pp 43–47
- Paraschiv D (1979) Romanian oil and gas field. *Geol Prospect Explor* 13:382 pp
- Paul A, Sharma ML (2011) Recent earthquake swarms in Garhwal Himalaya: a precursor to moderate to great earthquakes in the region. *J Asian Earth Sci* 42:1179–1186
- Pompilian A, Rădulescu F, Biter M (1991) Seismic studies in Central and Southern Dobruđa. *St.cerc.geol. geofiz. geogr., seria geofiz.* 29:20–29 (in Romanian)
- Popescu E, Radulian M (2001) Source characteristics of the seismic sequences in the eastern Carpathians foredeep region (Romania). *Tectonophysics* 338:325–337
- Raileanu V (2009) Caracterizarea geologica si parametrii elastici ai amplasamentelor statiilor seismologice si de accelerometere din reteaua Institutului National de C-D pentru Fizica Pamantului. In: Marmureanu G (coord.) *Cercetari privind managementul dezastrelor generate de cutremurele romanesti*, Editura Tehnopress. ISBN:973-702-701-9 (in Romanian)
- Radu C, Oncescu MC (1988) The crustal earthquake of September 11, 1980 from Braila-Galati region. *Rev Roum Geol Geophys Geogr Geophysique* 32:19–27
- Radulian M, Măndrescu N, Popescu E, Utale A, Panza GF (1999) Seismic activity and stress field in Romania. *Rom J Phys* 44:1051–1069
- Radulian M, Măndrescu N, Panza GF, Popescu E, Utale A (2000) Characterization of seismogenic zones of Romania. *Pure appl Geophys* 157:57–77
- Scholz CH (1968) The frequency-magnitude relation of microfracturing in rock and its relation to earthquakes. *Bull Seismol Soc Am* 58:399–415
- Shaw BE (1993) Generalized Omori law for aftershocks and foreshocks from a simple dynamics. *Geophys Res Lett* 20:907–910
- Shaw BE (1995) Frictional weakening and slip complexity in earthquake faults. *J Geophys Res* 100:18239–18251
- Sykes LR (1970) Earthquake swarms and sea-floor spreading. *J Geophys Res* 75:6598–6611
- Tărăpoancă M, Bertotti G, Mațenco L, Dinu C, Cloetingh S (2003) Architecture of the Focșani depression: a very deep basin in the Carpathians bend (Romania). *Tectonics* 22(6) 1074:1–17
- Warren NW, Latham GV (1970) An experimental study of thermally induced microfracturing and its relation to volcanic seismicity. *J Geophys Res* 75:4455–4464
- Wessels SA, De La Pena A, Kratz M, Williams-Stroud S, Jbeili T (2011) Identifying faults and fractures in unconventional reservoirs through microseismic monitoring. *First Break* 29(7): 99–104
- Wyss M (1973) Towards a physical understanding of the earthquake frequency distribution. *Geophys J Roy Astron Soc* 31:341–359

Comparison of Three Major Historical Earthquakes with Three Recent Earthquakes

**Maria Rogozea, Mircea Radulian, Mihaela Popa,
Daniel Nistor Paulescu, Eugen Oros and Cristian Neagoe**

Abstract The macroseismic effects of three major events recorded in historical time (1738, 1802, 1838) are re-evaluated and compared with three major events recorded in the 20th century in the Vrancea subcrustal source (1940, 1977, 1986). The purpose of the paper is to detect characteristic resemblances and differences in the macroseismic distributions among the study earthquakes. They provide important clues in assessing focal depth interval and specific directivity effects of the sources produced in historical times. Certainly, extension of such information to historical earthquakes will contribute essentially to improve the reliability of seismic hazard evaluation.

Keywords Historical earthquakes · Vrancea · Macroseismic maps

M. Rogozea (✉) · M. Radulian · M. Popa · D.N. Paulescu · E. Oros · C. Neagoe
National Institute for Earth Physics, Măgurele, Romania
e-mail: mrogozea@infp.ro

M. Radulian
e-mail: mircea@infp.ro

M. Popa
e-mail: mihaela@infp.ro

D.N. Paulescu
e-mail: dpalescu@infp.ro

E. Oros
e-mail: eugeno@infp.ro

C. Neagoe
e-mail: cristian.neagoe@infp.ro

1 Introduction

Romania is characterized by moderate seismicity. There are few seismic areas where the seismicity is located in the crust (less than 60 km depth): East-Vrancea, Fagaras–Campulung, Danubian, Banat, Crisana–Maramures, Barlad Depression, Predobrogean Depression, Intramoesian Fault, and Transylvanian Depression (Radulian et al. 2000), but is sporadic and of magnitude below 6 (except Fagaras–Campulung zone where two events of magnitude ~ 6.5 were reported within six centuries). The main seismic activity is concentrated in the Vrancea area at intermediate depths (60–180 km). This is the most active seismic zone all along the Carpathians arc. Taking into account the concentration of seismicity in a narrow seismogenic volume, the rate of seismic moment release of about 0.8×10^{19} Nm/year is comparable to that of southern California (Wenzel et al. 1998, 2002) (Fig. 1).

The peculiarities of the macroseismic intensity distribution induced by the Vrancea major earthquakes (extreme extension mostly along NE-SW direction) provide arguments to reliably identify the events in Vrancea source several centuries back in time. The knowledge of the historical earthquakes is very important for hazard assessment and the revision of the data in the earthquake catalogues is

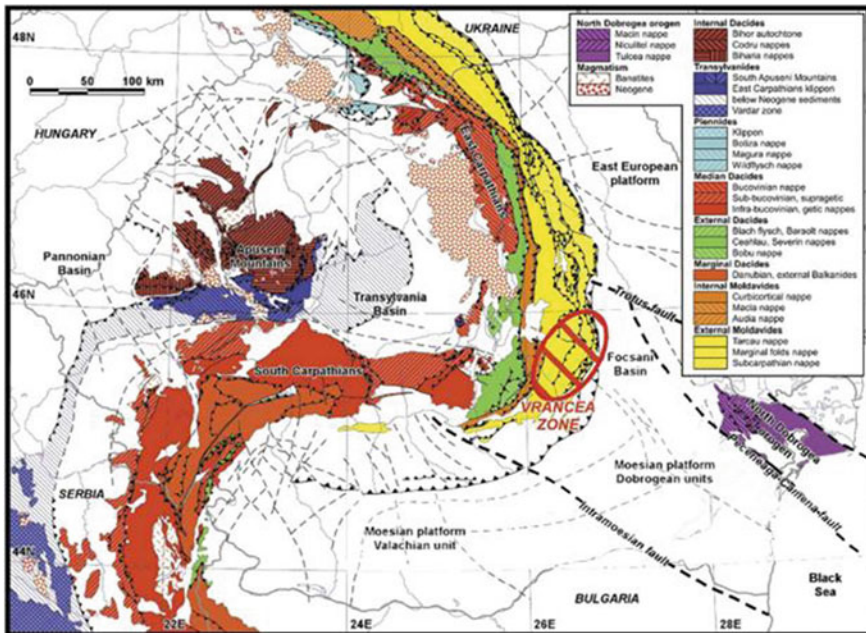


Fig. 1 The position of the Vrancea seismic zone on the geologic map of Romania (modified after Sandulescu et al. 1978). (For interpretation of the references to color in this figure legend, the reader is referred to the web version of this article)

essential. The most damaging earthquakes recorded since 18th century in Vrancea occurred in 11 June 1738 (M_w 7.7), 26 October 1802 (M_w 7.9), 23 January 1838 (M_w 7.5), 1940 (M_w 7.7) and 1977 (M_w 7.4). The goal of this paper is to revise the characteristics of the first three historical earthquakes (1738, 1802, 1838) and make a comparative analysis with the events instrumentally recorded in the 20th century (1940, 1977) to which we added the last earthquake with magnitude above 7 produced in 1986 (M_w 7.1). The earthquake occurred on 10 November 1940 (45.8°N, 26.7°E, 150 km depth) was the largest Vrancea instrumentally ever recorded event. The earthquake occurred on 4 March 1977 (45.77°N, 26.76°E, 94 km depth) was the event that caused the biggest damage ever recorded in Romania. The earthquake of 30 August 1986 (45.52°N, 26.49°E, 131 km depth) was less destructive in Romania, but caused strong damage to the NE (Republic of Moldova) and SW (north of Bulgaria).

Our work continues the efforts over years to integrate historical data in order to improve seismic hazard evaluation in Romania and neighboring countries (Moldovan 2002; Rogozea et al. 2014). Atanasiu (1961) noticed three categories of the major earthquakes in Vrancea: (1) “moldavic earthquakes with symmetrical effects” (symmetrical effects), (2) “moldavic earthquakes with weight center to Moldova” (asymmetric effects, stronger to NE) and (3) “moldavic earthquakes with weight center to Muntenia” (asymmetric effects, stronger to SW). Since the hazard distribution changes significantly from one earthquake category to the other, it is worthwhile to know the parameters that control the generation of earthquake type (focal depth, rupture directivity, stress drop etc.) and if we can define a specific succession in time of these events. The number of well-recorded major events is inherently small (instrumental data are available since one century in the best case). Including historical data from the past could be the one way to prescribe what we expect in the future.

2 Historical Data

Analysis of historical data requires a lot of care and experience. In most of the cases, historical data are not coming from original sources or from contemporary witnesses. They are compiled by someone else and some while after the event. So it is possible that errors arise in copying and interpreting the original data. It is therefore necessary to go back as much as possible to primary historical data.

For the earthquakes investigated in the present study, the historical information was extracted from: chronicles, catalogues of earthquakes in the Carpathian region, drafted in the 19th and 20th century (Perrey 1850; Hoff 1840; Jeitteles 1860; Réthly 1952; Atanasiu 1961, etc.), annals of time, reviews, notes on old religious writings, newspapers, etc. Notes on earthquakes and their effects are found in the work of other historians and literates such as: Mallet and Mallet (1858), Stefanescu (1901), Anestin (1916), Pamfilie (1921, 1936), Popescu (1939, 1941), Montandon (1953), Florinesco (1958), Atanasiu (1961), Corfus (1967), Nussbächer (1987, 2005),

Dudas (1990), Cernovodeanu and Binder (1993), Ambraseys and Finkel (1993), Huica (2000), Georgescu (2007), Caprosu and Chiaburu (2008) and Oprisan (2010), etc.

Previous works were taken into account as well: Medvedev et al. (1964), Shebalin et al. (1974), Tatevossian and Mokrushina (1998), Drumea et al. (2009) and Stucchi et al. (2013). Most of the historical information was systemized and integrated within the SHARE project (www.share-eu.org). The macroseismic data for 1738 earthquake was extracted from Shebalin (1977), (8MDPs, (Macroseismic Data Points), $I_{\max} = \text{VIII}$, MSK scale), for 1802 from Tatevossian and Mokrushina (1998), (81MDPs, $I_{\max} = \text{IX}$, MSK scale), and for 1838 from Shebalin (1977) (40MDPs, $I_{\max} = \text{VIII-IX}$, MSK scale).

Our proposal is to re-evaluate all the available information and results in order to obtain the best possible macroseismic intensity distribution for the historical events and then to analyze comparatively the intensity distributions for historical events versus the modern instrumentally recorded events. In order to facilitate the direct comparison we adopted the scale of intensity of Sponheuer-Medvedev-Kárník (MSK or MSK-64 scale, Medvedev et al. (1964)). Similarities and dissimilarities among these distributions are of great significance if we plan to highlight specific patterns for the effects induced by the Vrancea intermediate-depth earthquakes.

The conversion of historical data into intensities is a complex and delicate process, which may depend largely on the skill of the converting procedure. Since the intensity is based on observations of the effects of earthquakes, it has inherently a subjective component (in terms of how people felt the earthquake). In order to assess intensity in a site, we look for some basic data, such as: date of the event, time of the event, total affected (felt) area, category of damage of property, how many dead and injured people, foreshock and aftershock activities.

2.1 11-06-1738 Earthquake

The great earthquake of 11 June 1738 occurred during the reign of Constantin Mavrocordat, around noon and was felt all over the country and over an extended area beyond borders. Relative high intensity was noticed at more than 200 km distance, both to the NE (Iasi in Moldova) and SW (Nis in Serbia). For example, in Moldova the Golia Monastery and many houses collapsed (Réthly 1952; Corfus 1967). In Muntenia, the towns of Targoviste, Valenii de Munte, Buzau suffered many damages. In Bucharest many houses and churches were cracked and destroyed, (Stefanescu 1901; Corfus 1967; Cernovodeanu and Binder 1993; etc.). In Brasov almost all the houses suffered damage: Catherine Gate, Gymnasium Honerus (Popescu 1939; Atanasiu 1961; Corfus 1967; Cernovodeanu and Binder 1993). The earthquake was followed by several aftershocks which were felt.

The information on damage caused by these earthquakes is compiled and summarized and represented in the macroseismic map of Fig. 2. A total of 32 points

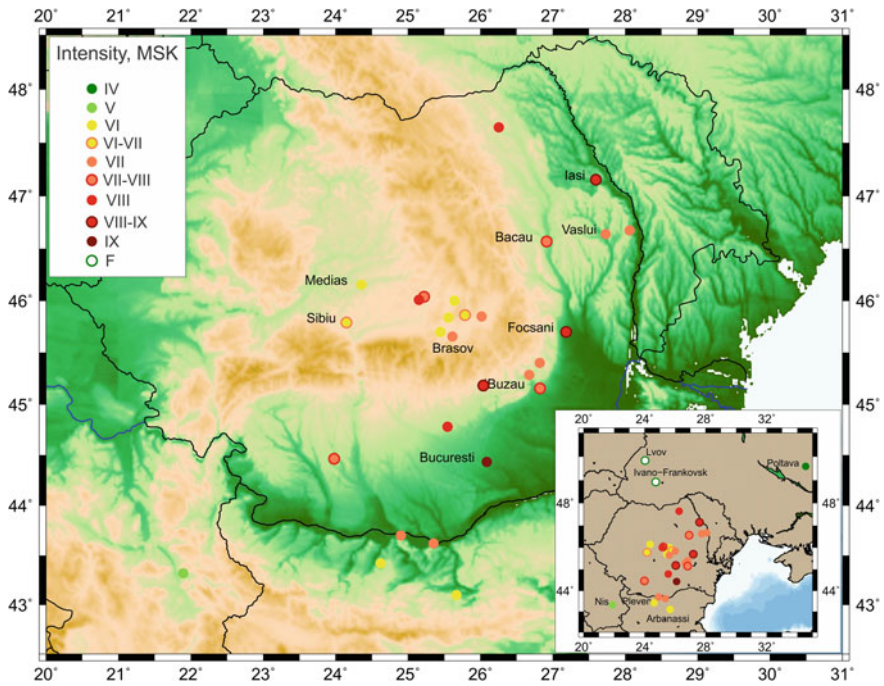


Fig. 2 Intensity data points for the event of June 11, 1738. *Inside panel* is for an area extended beyond borders

with macroseismic information are finally considered. The maximum intensity IX (MSK-64) is assigned to Bucharest city.

The distribution of intensity levels in the database is shown in Fig. 3. The reduced impact of the earthquake effects at low intensity levels (below VI) in written documents or notes could be explained to some extent by the fact that the acknowledgments or comments on the earthquake effects appeared quite a long while after its occurrence. In the databases the highest number of points of intensity was found for the intensities VI and VII and lower for the values IV, V and IX.

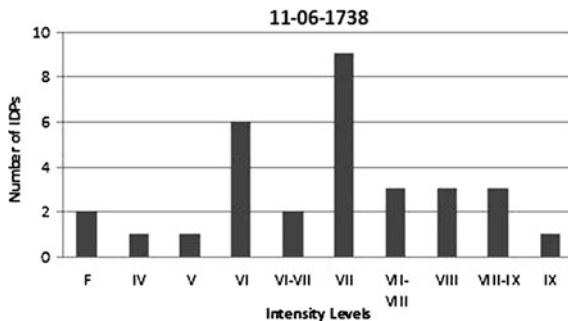


Fig. 3 Number of IDPs (intensity data points) for each intensity level

The comparison with the previous macroseismic mapping as presented in the SHARE project (Stucchi et al. 2013 on the basis of Shebalin et al. 1977 information) shows significantly higher intensity values in our interpretation.

2.2 26-10-1802 Earthquake

This is considered the largest earthquake which took place in the Vrancea zone. The event was called “the great earthquake” being felt from Island Ithaka (Greece) to St. Petersburg. The macroseismic area affected more than 2 million square kilometers.

For 1802 earthquake major damage was reported in Transylvania (Brasov, Rasnov, Bod), Muntenia (Bucharest, Valenii de Munte) and Moldavia (Suceava, Iasi). The most affected city was the capital Bucharest.

During the 1802 earthquake the famous tower of Coltea (Bucharest) built up more than eight decades before, that has endured over time more earthquakes (Stefanescu 1901), broke from the middle and the top of it collapsed on the pavement. Also the tower of Monastery Radu Voda collapsed. Several churches were destroyed: Sf. Spiridon Church and Cotroceni monastery in Bucharest (Cernovodeanu and Binder 1993) and the Monastery in Valenii de Munte (Pamfilie 1921, primary information about the effects are in “Diptych Valeni Monastery”) and Church from Halchiu (Réthly 1952). In Bucharest, after the testimony of contemporaries, all the towers of the churches fell down, in generally all buildings were affected.

In Moldavia the monasteries of Bogdana, Radeanu, and Rachitoasa suffered significant loss (Burlacu 1981). The Brasov city and its surroundings were affected. There were cracked many houses, churches and various walls towers. The Black Church has suffered heavy damage (Réthly 1952; Cernovodeanu and Binder 1993).

Outside Romania, the earthquake was felt in Vidin, Rusciuc, Varna, Istanbul, Kiev, Kagul and Moscow. The earthquake caused damage also in Ukraine, Bulgaria, Turkey, Russia, Serbia and in the Black Sea (The European Magazine, and London Review 1802; “The Gentleman’s magazine” John Nichols 1802; Mallette and Mallet 1858; Draghiceanu 1896; Stefanescu 1901; Atanasiu 1961).

There are several investigations on this event. Popescu (1941) suggests that the ellipse of the intensities is oriented to N-S, stretching to Istanbul, Crimea and Moscow (in the east), Leningrad (in the north) Warsaw and Budapest (in the west) and Athens (in the south). The author makes a parallel with the 1940 earthquake area, and claims that the later differs in south which is limited to Thessaloniki. The studies of Medvedev (1968) and Medvedev et al. (1964), analyzing all the data from Russia and Romania, attributed the intensity IX to Bucharest and Brasov area; VIII for southern Craiova, Russe and Silistra, northeastern Iasi and Chisnau; VII Deva, Sebes, Sighisoara, south of Vidin and Varna.

A new study on the 1802 earthquake was made by Tatevosian and Mokrushina (1998). It was based on primary sources. The authors checked the old names of the sites from sources and associated them with present day names. The highest values

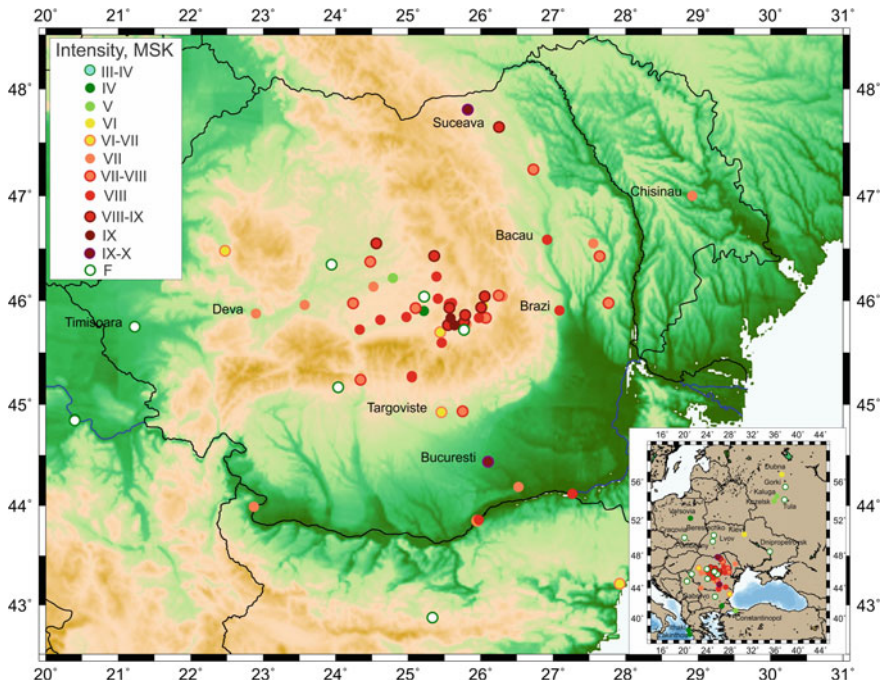


Fig. 4 Intensity data points for October 26, 1802 earthquake. *Inside panel* is for an area extended beyond borders

of intensity were IX in Haghigh, VIII-IX in Brasov, Bod and Bucharest; VIII in Baraolt and Braila, VII-VIII in Galati, Iasi, Ruse and Vidin, VII in Sighisoara, Craiova and Fagaras. In total 81 IDPs (intensity data Points) were considered with I_{max} IX. Shebalin (1977) found only 13 IDPs and the I_{max} VIII-IX MSK.

The macroseismic map compiled in our study for a total of 105 IDPs is represented in the Fig. 4.

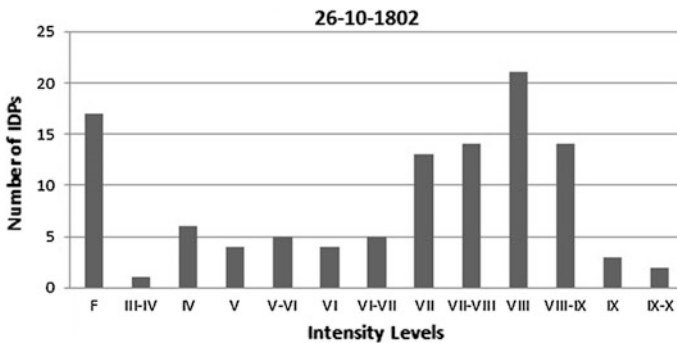


Fig. 5 Number of IDPs for each intensity level

The number of data points distribution in Fig. 5 is best represented at intensities VII to VIII-IX. As expected, only a few points have high intensity values (IX-X). The level of felt effects (F) encompasses all the sites where the reported information referred solely to the fact that the event was felt but gave no information on the specific effects.

2.3 23-01-1838 Earthquake

The earthquake of 1838 caused significant damage in the eastern part of the Romanian Plain, in a number of areas in the counties of Ramnicu Sarat, Buzau, Focsani, in the south of Moldova and Craiova and Slatina, in the western part of the Romanian Plain. The effects of this event are the best documented since a special and detailed report was made up immediately after the event by Gustav Schüller on demand of Romanian authorities.

This event was studied by: Medvedev et al. (1964), Shebalin et al. (1974), Shebalin (1977), Moskalenko (1980) and Drumea et al. (2009) and it appears in the catalog AHEAD (European archive of historical earthquake data) where the information was taken from Shebalin (1977).

Medvedev (1968), presents a comparative map of the events of 1838 and 1940 showing that isoseists of 1940 earthquake are more extended. The highest intensity value is attributed at the confluence of Siret with Barlad rivers. Intensity VIII is observed in Northern Dobrogea, Vaslui, Roman and Bucharest, while intensity VII in the rest of Dobrogea region and Chisinau. After Moskalenko (1980), at Bucharest the intensity was VIII, higher than in 1802 when the intensity was estimated as VII–VIII. Medvedev et al. (1964), Shebalin et al. (1974) and Drumea et al. (2009) have assigned intensities values lower than was estimated in this study. After Shebalin (1977) the VIII intensity was estimated for Vrancea zone, Braila, Ploiesti and Bucharest, VII for Craiova, Sibiu and VI for Soroca (Republic of Moldavia). Drumea et al. (2009) gives estimated much lower intensities for this event: VII for Vrancea area, VI for Bucharest. Georgescu (2007) in his work reviewed all the studies carried out before, about this earthquake.

In a previous paper, Rogozea et al. (2014) reconsidered the macroseismic information and compiled a map containing 127 IDPs (Fig. 6). In the new map the felt area is significantly extended of in the Balkan Peninsula: Trojan, Vastra in Tsaribrod region, Istanbul, Pera and eastern Thrace. The maximum intensity was IX (MSK-64) in Bucharest.

The distribution of intensity levels in the database is shown in Fig. 7. We found more than 10 points of IDPs for intensity V, VII and VIII. The F level has the largest number of points, since it includes all the data points with no information on specific effects.

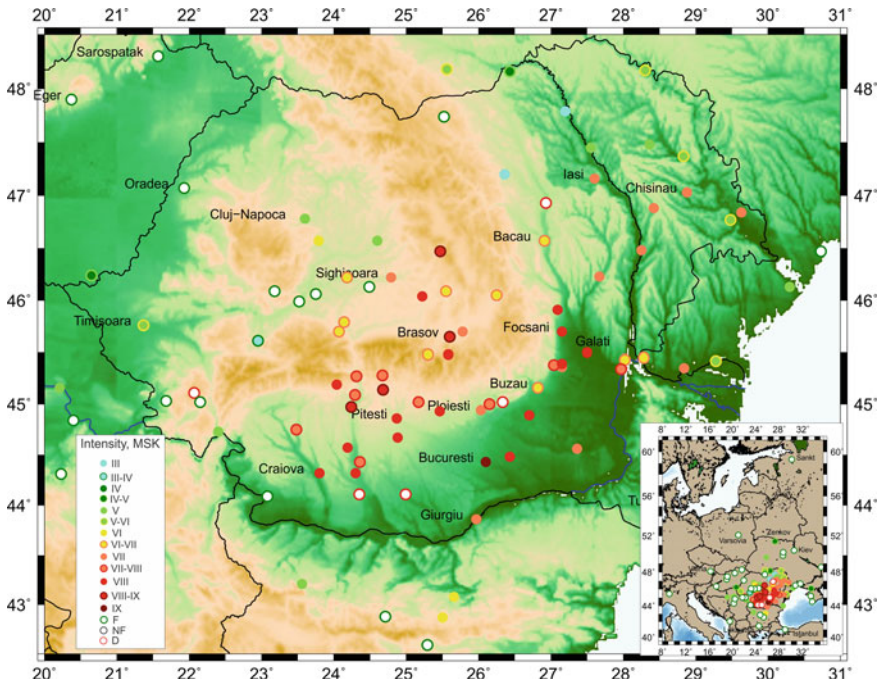


Fig. 6 Intensity data points for January 23, 1838 earthquake. *Inside panel* is for an area extended beyond borders

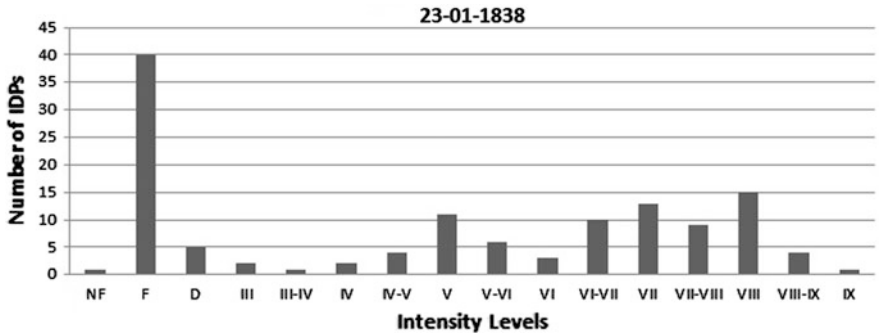


Fig. 7 Number of IDPs for each intensity level

3 Comparison of Historical Earthquakes with Instrumentally Recorded Events

Following Atanasiu (1961) we could divide Vrancea deep earthquakes into three categories: symmetric (the stronger effects are distributed symmetrically to NE and SW), asymmetric with stronger effects toward NE and asymmetric with stronger effects toward SW. We can include in the first category the event of 1738 with strong damage reported both toward SW (Oltenia) and toward NE (Moldova). It looks like that the event of 1986 belongs to the same category as well. We consider the event of 1802 fits the second category, with stronger effects toward Moldova and Transylvania. The event of 1940 falls in the same category. The third category is represented by events of 1838, 1977 and 1990. All of them are characterized by southwest directivity. Some correlation between the focal depth and earthquake category is assumed in agreement with observations (however very scarce for a reliable statistical significance): (1) focal depth in the upper segment of the active descending body—directivity toward SW, (2) focal depth in the lower segment of the active descending body—directivity toward NE, (3) focal depth in between the two segments—symmetric directivity. We shall adopt in the following this assumption.

It is a common observation that the effects of the Vrancea earthquakes strongly depend on azimuth. Hence, in order to compare the distribution of the effects of the most damaging earthquakes occurred in the last three centuries, we use the representation given in Figs. 2, 4 and 6: seismic intensity with respect to epicentral distance (in logarithmic scale), plotted separately in four quadrants. The aim is to test the potential of the historical information in providing support to reliably see if an historical event is falling within a specific category. This is of great significance in assessing seismic hazard. The three categories which are considered as characteristic for the Vrancea earthquakes are exemplified by events of 1940, 1977 and 1986 for which we have well-defined macroseismic maps (Kronrod et al. 2013) and each of the historical events analyzed in this paper (1738, 1802 and 1838) will be compared with these ‘standard’ cases.

3.1 1738 Event

In order to compare the distribution of the effects of major earthquakes from Vrancea area, we use the distribution of the seismic intensity with respect to the epicentral distance, featured separately in four quadrants (Fig. 8). This way, we could characterize a historic event, such as the one from 1738, by comparison with the major earthquakes occurred in the 20th century (1940, 1977, 1986). For the earthquakes generated in the last century, we used the macroseismic data integrated in the paper of Kronrod et al. (2013).

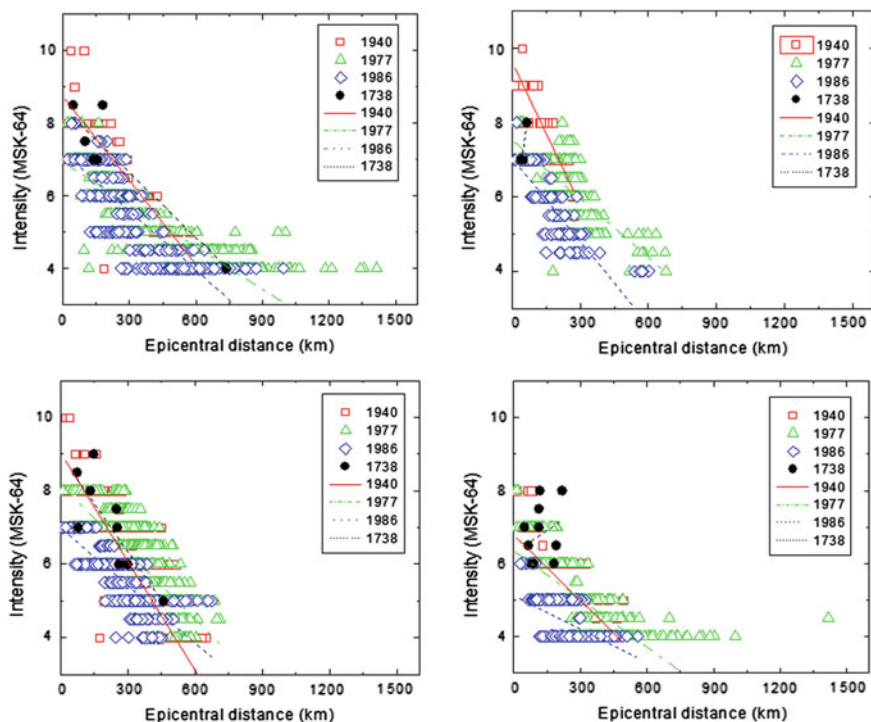


Fig. 8 Comparison of intensity distribution of 1738 event against distribution of intensity for the events of 1940, 1977 and 1986. Representation is made on four quadrants separately: *upper-left* quadrant 0–90°; *upper-right* quadrant 90–180°; *lower-left* quadrant 180–270°; *lower-right* quadrant 270–360°. The regression lines fitting the distributions of 1940, 1977 and 1986 events are plotted as well

The comparative diagrams for 1738 event are represented in Fig. 8. The number of IDPs for this event is small and hence it is a difficult or even impossible task to distinguish with some accuracy the best matching with one of 1940, 1977 or 1986 events. A rough analysis of the effects reported for 1738 event shows as a general feature the symmetry of the effects in relation with epicenter position. Thus, on the NE-SW direction strong damage was reported in Moldova (collapse of Golia monastery in Iasi) as well as in Oltenia (collapse of Horezu monastery). Significant damage was reported also in Transylvania (Braşov and Prejmer) and Muntenia (Bucharest). Although, it is hard to definitely conclude on the category 1738 event belongs, most arguments are in favor of symmetric-type event, such as 1986 event. We reach this conclusion by the comparative inspection of Fig. 8 and by a simple statistical test: we compute the statistical deviation of the epicentral distance for each IDP between 1738 event against 20th century events, for all intensity levels which are common and for all the quadrants. The deviations are: 20.2 km (1738 vs. 1940), 21.5 km (1738 vs. 1977) and 19.0 km (1738 vs. 1986) with the smallest

value for 1738–1986 pair. Therefore, we propose as the most probable focal depth for the 1738 event, a depth within 110–130 km interval.

3.2 1802 Event

Heavy effects were reported for the 1802 earthquake, such as: creation of huge ground cracks (Brasov area) and cavities, a high percentage of severe damage to churches and monasteries, the Coltea tower in Bucharest broke at half and the upper part collapsed. Small damage was reported even up to Moscow. The movements were felt even to the North of St. Petersburg and to the Aegean Sea in the South.

The comparative diagrams for 1802 event are represented in Fig. 9. As observed in figure, the earthquake of 1802 has a higher magnitude than the one of 1940. The main seismic energy propagated toward North-East, which shows a focal depth

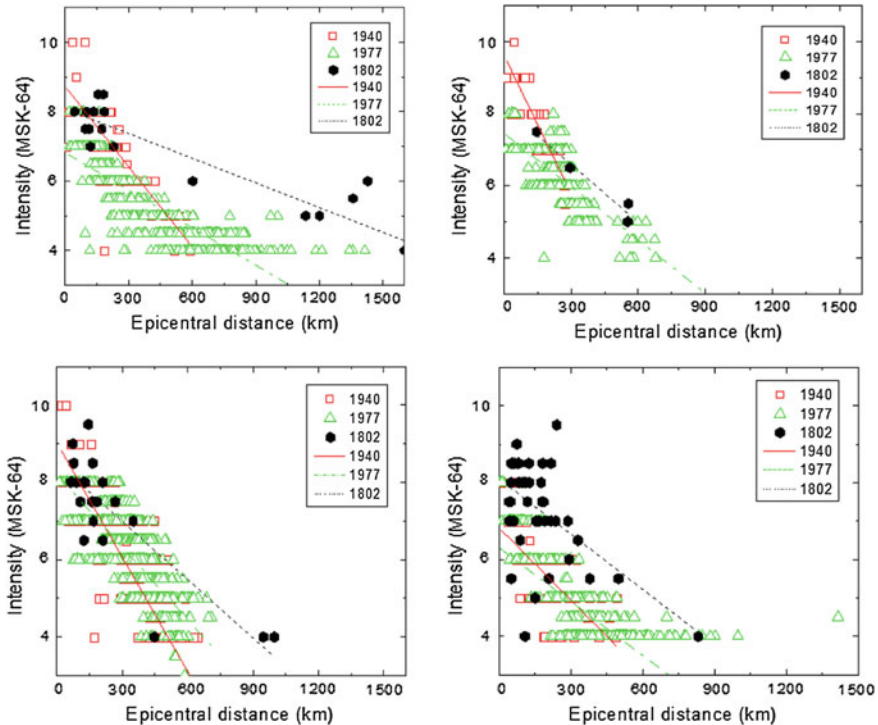


Fig. 9 Comparison of intensity distribution of 1802 event against distribution of intensity for the events of 1940 and 1977. Representation is made on four quadrants separately: *upper-left* quadrant 0–90°; *upper-right* quadrant 90–180°; *lower-left* quadrant 180–270°; *lower-right* quadrant 270–360°. The regression lines fitting the distributions of 1940, 1977 and 1986 events are plotted as well

between 130 and 150 km. It has a similar directivity to the one of event of 10th of November 1940. This is pointed out also by the statistical deviation of the epicentral distance for each IDP computed between 1802 event and the other 20th century events. The estimations are: 71.7 km (1802 vs. 1940), 84.7 km (1802 vs. 1977) and 137.9 km (1802 vs. 1986) with the smallest value for 1802–1940 pair.

3.3 1838 Event

The event of 1838 was extremely destructive as proved by changes in the morphological aspect of the terrain, especially in the outer side of Carpathians Arc bend (Stefanescu 1901; Mandrescu 1979). A lot of information regarding these effects comes from the special report made by the German consul Schuller, immediately after earthquake.

The comparative analysis of the effects of 1838 event against those of 1940 and 1977 events (Fig. 10) shows enhancement of effects toward SW relative to NE.

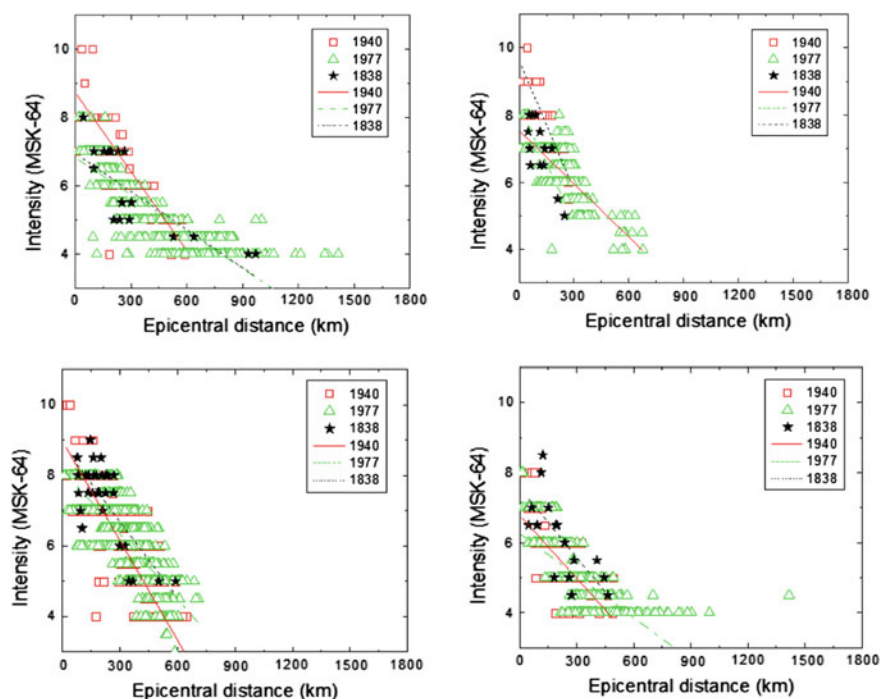


Fig. 10 Comparison of intensity distribution of 1838 event against distribution of intensity for the events of 1940 and 1977. Representation is made on four quadrants separately: *upper-left* quadrant 0–90°; *upper-right* quadrant 90–180°; *lower-left* quadrant 180–270°; *lower-right* quadrant 270–360°. The regression lines fitting the distributions of 1940, 1977 and 1986 events are plotted as well

From this point of view, the 1838 event is similar to the one of 1977. For both events, the intensity was high in Muntenia area (especially in Bucharest) and in Oltenia, and lower in Moldova (Iasi). This is pointed out also by the statistical deviation of the epicentral distance for each IDP computed between 1838 event and the other 20th century events. The estimations are: 25.6 km (1838 vs. 1940), 19.8 km (1838 vs. 1977) and 23.5 km (1838 vs. 1986) with the smallest value for 1838–1977 pair. Based on the similarity as revealed by the comparative analysis on different azimuths, we assume that the focal depth and rupture directivity (more to the SW rather than to NE) should be similar. So, the hypocentral depth proposed for the 1838 event is 90–110 km. On the other hand, macroseismic data suggest a slightly higher value of magnitude for 1838 event as compared with 1977 event.

Field researches accomplished after the earthquake of 1977 revealed permanent soil deformations (landslides, liquefaction, cracks, etc.) generated mostly in the Subcarpathians area, variation of the water level in wells in the Subcarpathians area and in the Danube's river meadow, deep water ejection and the appearance of new springs (Balan et al. 1982). Deep water ejection was observed in the main hydrographic basins—Danube, Prut, Barlad, Milcov, Ialomita and Olt, and also in the areas between Buzau-Prahova and Vlasia-Pociovalistea rivers. Rather similar effects in the same areas were documented after the 1838 earthquake.

4 Conclusions

It is a real challenge to extract from historical sources the true information regarding earthquakes. The documents must be judged very critically, and any correlation between information and potential causes should be done with much care. In the present paper, our goal was to redefine the parameters of the strongest historical earthquakes produced in the Vrancea region in the last three centuries (1738, 1802, 1838) on the basis of comparative analysis of the revised macroseismic data for historical events with macroseismic data for instrumentally recorded earthquakes (1940, 1977, 1986).

We adopted the classification proposed by Atanasiu (1961) as regards the Vrancea strong earthquakes: (1) “moldavic earthquakes with symmetrical effects” (symmetrical effects), (2) “moldavic earthquakes with weight center to Moldova” (asymmetric effects, stronger to NE) and (3) “moldavic earthquakes with weight center to Muntenia” (asymmetric effects, stronger to SW). Each category is associated with specific focal depth and directivity effects.

The 1738 event looks to fit within the category (1), with areas of maximum intensity both to the NE (Moldova) and SW (Muntenia). The earthquake provoked heavy damage in different places over an area extended NE-SW, such as: Moldova (Iasi, Suceava, Ramnicu Sarat, Buzau counties), Muntenia (Bucharest), Oltenia (Horezu), eastern Transylvania (Brasov, Prejmer).

As a consequence of macroseismic data analysis, we consider that a more reliable focal depth for the 1738 event is 110–130 km. The depth specified in Romplus

catalog and taken up in SHEEC catalog (Stucchi et al. 2013) is situated at the bottom end of this interval (130 km). As concerns the size, the macroseismic data points distribution is compatible with a magnitude $M_w = 7.5$, as specified in catalogs.

The comparative analysis for the event of 1802 shows similarities in the macroseismic effects with the event of 1940. First, the extreme extension of the felt area from Russia to the Mediterranean Sea. Then the heavy damage reported in Bucharest and eastern Transylvania. Therefore, the well-suited focal depth for this event is between 140 and 160 km. Also a significant aftershock activity is mentioned in connection with 1802 major shock which appears to match better a deeper rupture process, like that in 1940, than a shallower rupture process, like that in 1977.

The earthquake of 1838 can be assigned in the (3) category of Vrancea earthquakes. This time, the strongest damage was noticed mainly toward SW from the epicenter, starting from the eastern part (Ramnicu Sarat, Buzau, Focsani) to the western part (Craiova, Slatina) of the Wallachian Plain. Once again, the Bucharest city and its surroundings were highly affected. Severe damages to houses and buildings were observed. A total of 36 houses and 5 churches collapsed. Other 50 churches from Bucharest were damaged. There were 8 casualties and 14 wounded people reported.

In agreement with our comparative analysis, the event of 1838 bears resemblance with the event of 1977 and therefore the focal depth is assumed to be between 90 and 110 km, instead of 150 km as specified in Romplus and SHEEC catalogs. As concerns the size, the macroseismic effects pattern indicates a magnitude slightly higher than for the 1977 event. The errors in magnitude estimation are large, the more so as they are resulted from vague macroseismic information. But we have no other choice, and propose as a rough estimation for the magnitude of 1838 earthquake $M_w = 7.5$ (compared with $M_w = 7.4$ for 1977 earthquake). Otherwise, this value coincides with the value in Romplus (SHEEC) catalog (<http://www.emidius.eu/SHEEC/catalogue/>).

Acknowledgements The work was part of the SHARE project (Seismic Hazard Harmonization in Europe, www.share-eu.org). The results of the paper were partly included in the project PN 09 - 30-0102 of the Nucleu Program of the National Authority for Scientific Research and Innovation.

References

- Ambraseys NN, Finkel C (1993) Material for the investigation of the seismicity of the eastern mediterranean region during the period 1690–1710. *Hist Invest Eur Earthquakes* 1(1993):173–194
- Anestin V (1916) *Cutremurele de pamant*. Editura Tipografiei Gutenberg, Campina
- Atanasiu I (1961) *Cutremurele de pamant din Romania*. Ed. Academiei Republicii Populare Romane, Bucharest
- Balan S, Cristescu V, Cornea I (1982) *Cutremurul de Pamant din Romania de la 4 Martie 1977*. Editura Academiei Republicii Socialiste Romania, Bucharest

- Burlacu Gh (1981) Marturii documentare privind contributia locuitorilor judetului Bacau la dobandirea independenței de stat a Romaniei: extras din Carpica XII–1981, Bacau. Muzeul National de Istorie, Bucuresti
- Caprosu C, Chiaburu E (2008) Insemnari de pe manuscrise si carti vechi din Tara Moldovei, Volumul I-IV, Iasi
- Cernovodeanu P, Binder P (1993) Cavalerii Apocalipsului, Calamitățile naturale din trecutul României (până la 1800). Silex, Bucharest
- Corfus I (1967) Insemnari de demult. Junimea, Iasi
- Draghiceanu M (1896) Les tremblements de terre de Roumanie et des pays environnants. Géologie appliquée, Bucharest
- Drumea AB, Stefanenco NA, Simonova NA, Alecsev IV, Carpanez VO (2009) Atlas. Chisinau
- Dudas F (1990) Memoria vechilor carti romanesti, Insemnari de demult. Ed. Episcopiei Ortodoxe Romane a Oradei, Oradea
- Florinesco A (1958) Catalogue des tremblements de terre ressentis sur le territoire de la R.P.R. Le résumé français. Académie de la R.P.R., Comité national de la Geodesie et Geophysique pour l'A.G.I., Bucharest, 167 p
- Georgescu SE (2007) Bucurestiul si seismele. Ed. Fundatiei Culturale Libra, Bucharest
- Hoff KEA (1840) Verzeichniss der Erdbeben seit 1821. Annalen der Physik und Chemi. XXIX. 1833. /b v. Hoff K.E.A. Chronik der Erdbeben und vulkanischer Ausbrüche. Geschichte der durch Ueberlieferung nachgewiesenen natürlichen Veränderungen der Erdoberfläche, Gotha
- Huica I (2000) Cutremurele de pamant, Fenomene geologice natural. Terra, Bucuresti
- Jeitteles LH (1860) A földrengések legnevezetesebb kiindulási vagyis középpontjai Magyar- és Erdélyországban, Természettudományi Közlöny, I. (in Hungarian). (Nature Science Bulletin. I.) Pest
- Kronrod T, Radulian M, Panza G, Popa M, Paskaleva I, Radovanich S, Griboszki K, Sandu I, Pekevski L (2013) Integrated transnational macroseismic data set for the strongest earthquakes of Vrancea (Romania). Tectonophysics 590:1–23
- Mandrescu N (1979) The Vrancea earthquake of March 4, 1977: damage distribution. In: I Cornea, C Radu (eds) Seismological research on March 4, 1977 earthquake, Bucharest, pp 371–388
- Mallet R, Mallet JW (1858) The earthquake catalogue of the British Association with the discussion, curves and maps, etc. Transactions of the British Association for the advancement of Science, third and fourth report, London
- Medvedev SV (1968) Seismic Zoning of the USSR (in Russian)
- Medvedev SV, Sponheuer W, Kárník V (1964) Neue seismische Skala (Intensity scale of earthquakes). 7. Tagung der Europäischen Seismologischen Kommission vom 24.9. bis 0.9.1962 in Jena, Veröff. Institut für Bodendynamik und Erdbebenforschung in Jena 77:69– 6
- Moldovan I (2002) Metode si modele statistice cu aplicatii in studiul complex al cutremurelor de pamant. Teza de doctorat, 430 pag. Con. Șt. Dr. Doc. D. Enescu. Univ. Bucharest (in Romanian)
- Montandon F (1953) Les tremblements de terre destructeurs en Europe. Genève
- Moskalenko TP (1980) Kartî izoseist zemliatriaseniî Karpatskovo regiona. In: Karpatskoe Zemletriasenie 4 Marta 1977 g. i evo posledstvia. Akademia Nauk SSSR, Izdatelstvo Nauka, Moskva, pp. 86–105
- Nussbächer G (1987) Din cronici și hrisoave. Contribuții la istoria Transilvaniei. “Din cronica cutremurelor în Țara Bârsei (secolele XV-XX)”. Ed. Kriterion (in Romanian)
- Nussbächer G (2005) Caietele Coroane, Contributie la istoria Brasovului, caietul 4. Ed. Aldus, Brasov
- Oprisan I (2010) Cutremurele de pamant si semne ceresti, in istoria Romaniei. Ed. Saeculum I.O
- Pamfilie T (1921) Mitologie Romaneasca III, Pamantul, Dupa credintele poporului roman publicatie. postuma, de Tudor Pamfilie 16 Oct. 1921, Academia Romana din viata poporului roman XXXIII, Cultura Nationala, 1924, pp 495–496
- Pamfilie T (1936) Mitologia poporului Roman. ISBN 973-120-011-8 978-973-120-011-8

- Perrey A (1850) Mémoires sur les tremblements de terre ressentis dans la péninsule Turco-ellenique et en Syrie, Mémoires Couronnées et Mémoires des Savant Etrangers. Academie Royale des Sciences, des Lettres et des Beaux Arts de Belgique (Bruxelles), XXIII, pp 363, 366, 389
- Popescu IG (1939) Cutremurele de pamant din Bucovina. Cernauti
- Popescu IG (1941) Etude comparative sur quelques tremblements de terre de Roumanie, du type du celui du 10 novembre 1940. Comptes Rendus des Seances de L'Academie des Sciences de Roumanie, Tome V, Numero 3, Mai-Juin 1941, Ed. Cartea Romaneasca, Bucharest
- Radulian M, Mandrescu N, Panza GF, Popescu E, Utale A (2000) Characterization of seismogenic zones of Romania. *Pure Appl Geophys* 157:57–77
- Réthly A (1952) A Kárpátmedencék földregései (455–1918). Budapest, (in Hungarian)
- Rogozea M, Marmureanu G, Radulian M, Toma D (2014) Reevaluation of macroseismic effects of the 23 January 1838 Vrancea earthquake. *Rom Rep Phys* 66(2):520–538
- Sandulescu M, Kräutner H, Borcos M, Nastaseanu S, Patrulius D, Stefanescu M, Ghenea C, Lupu M, Savu H, Bercia I, Marinescu F (1978) Geological map of Romania 1:1.000.000. Institut de Géologie Roumain, Bucharest
- Shebalin N V, Karnik V, Hadzievski D (eds) (1974) Catalogue of earthquakes of the Balkan Region. Part I, II, UNDP-UNESCO Survey of the seismicity of the Balkan region, Skopje
- Shebalin NV (ed) (1977) Atlas of isoseismal maps for the “new catalogue of strong earthquakes on the USSR territory from ancient times through 1975”. Archive of the Institute of Physics of the Earth, Moscow (unpublished)
- Stefanescu G (1901) Cutremurele de pamant in Romania in timp de 1391 de ani, de la anul 455 pana la 1874. Extras din Analele Academiei Romane, Seria II, vol. XXIV
- Stucchi M, Rovida A, Gomez Capera AA, Alexandre P, Camelbeeck T, Demircioglu MB, Gasperini P, Kouskouna V, Musson RMW, Radulian M, Sesetyan K, Vilanova S, Baumont D, Bungum H, Fäh D, Lenhardt W, Makropoulos K, Martinez Solares JM, Scotti O, Živčić M, Albini P, Batlo J, Papaioannou C, Tatevossian R, Locati M, Meletti C, Viganò D, Giardini D (2013) The share European earthquake catalogue (SHEEC) 1000–1899. *J Seismolog* 17 (2):523–544
- Tatevossian R, Mokrushina N (1998) The 1802, October 26, Vrancea deep earthquake. Internal report for the BEECD project. Institute of Physics of the Earth, Moscow, p 15
- “The European Magazine, and London Review” (1802)
- “The Gentleman’s magazine” John Nichols (1802)
- Wenzel F, Achauer U, Enescu D, Kissling E, Russo R, Mocanu V, Musacchio G (1998) Detailed look at final stage of plate break-off is target of study in Romania. *Eos Trans Am Geophys Union* 79(48):589–594
- Wenzel F, Sperner B, Lorenz F, Mocanu V (2002) Geodynamics, tomographic images and seismicity of the Vrancea region (SE-Carpathians, Romania). *EGU Stephan Mueller Spec Publ Ser* 3:95–104
- <http://www.emidius.eu/SHEEC/catalogue/>

An Attempt to Bridge the Gap Between the Traditional Concept of Seismic Intensity and the Need of Accuracy Required by Engineering Activities

Horea Sandi and Ioan Sorin Borcia

Abstract The concern for the development of more appropriate instrumental criteria to be used in seismic intensity assessment originates in the situation raised by the attempt to assess intensity on the basis of an accelerographic record obtained during the Vrancea earthquake of 1977.03.04. The intolerable gap of about two intensity units between the results of the use of peak acceleration and velocity criteria specified by the MSK scale respectively, required a critical analysis of the assumptions on which these criteria relied. It turned out that the cause of this shortcoming is due to the implicit rigid assumption on the expression of the dynamic factor of response spectra. Two alternative sources for developing appropriate, flexible, criteria relied on one hand on an envelope of response spectra and on the other hand on the integral of the square of acceleration. After defining criteria corresponding to a global intensity, criteria for determining intensity related to some oscillation frequency, as well as to intensity averaged upon a spectral band (leading to the concept of intensity spectrum) were defined. It turned out that the alternative definitions adopted led to strong correlations and that a good correlation with the results of post-earthquake field surveys was obtained too. Analytical developments as well as illustrative applications to the cases of some earthquakes are presented. Some problems concerning the calibration of instrumental criteria developed are revealed too.

Keywords Seismic intensity · Convex spectrum envelope · Arias integral · Intensity spectrum

H. Sandi (✉)

Romanian Academy of Technical Sciences, Bucharest, Romania
e-mail: horeasandi@yahoo.com

I.S. Borcia

URBAN-INCERC, Bucharest, Romania

1 Introduction

The interest in this topic originates in the impact of the 1977.03.04 Vrancea earthquake (when a unique valid accelerographic record at ground level was obtained at the Building Research Institute (INCERC) in Bucharest. The developments presented are aimed to define intensity as a function of instrumental basic data, using some appropriate analytical relations.

A highly placed Government official requested the author to assess seismic intensity on the basis of the quantitative provisions on ground motion characteristics given in Annex I of the Romanian standard STAS 3681-64 (based in its turn on the MSK intensity scale (Medvedev 1962; Medvedev 1977), reproduced in Table 1.

This task proved to fail, due to the fact that a huge gap between the two instrumental criteria on ground motion occurred. According to the *PGA* criterion, the intensity was about VIII, while according to the *PGV* criterion, the intensity was X–XI.

The concern for the development of instrumental criteria of intensity estimate is obviously justified by the fast increase of the number of accelerographic records at hand in numerous countries, as well as by the potential of instrumental data to provide rich and accurate information of engineering interest. Unfortunately, in Grünthal (1998) there is no concern for spectral aspects or for instrumental data, in spite of the explicit recognition (in the comments attached) that instrumental data fully characterize ground motion. It must be stated that developments in this field make it possible to bridge by now the gap between the traditional concept of seismic intensity and the need of more accuracy in dealing with seismic action that characterizes the activities of engineers involved in earthquake protection.

2 Analytical Background for Instrumental Intensity Estimates

2.1 Start Points

Research in this field, on which the paper relies, was started by a search for more appropriate basic criteria. This led gradually to the consideration of improved criteria, organized as IES (intensity estimate system). Two basic sources of ideas for estimating global intensities were adopted:

Table 1 Instrumental criteria according to the MSK-76 scale (average values)

Intensity	PGA (cm/s ²)	PGV (cm/s)	PSD (mm)
VI	50	4	2
VII	100	8	4
VIII	200	16	8
IX	400	32	16

- (a) a product of *EPA* and *EPV* (ATC 1986), which led to a global intensity (Grünthal 1998) denoted I_S ;
- (b) an integral of the square of ground motion acceleration (Arias 1970), which led to a global intensity denoted I_A (the way (b) was further developed into a way (b'), leading to a global intensity I_F , which relies on the use, instead of the acceleration as function of time, on the use of the square of the Fourier transform of acceleration (due to analytical reasons, $I_F \equiv I_A$). Specific details on the way (b') may be found in Sandi and Floricel (1998).

Thinking of the ground motion characteristics that are relevant from the view point of earthquake effects upon various elements at risk (according to knowledge developed in the field of earthquake engineering), a need for more detailed characterization/quantification of ground motion was felt. So, besides definitions concerning the *global intensity*, definitions for topics like the *intensity corresponding to a definite frequency* φ (Hz), $i_s(\varphi)$ or $i_d(\varphi)$, *intensity averaged for a definite spectral band* (φ', φ''), $\tilde{i}_s(\varphi', \varphi'')$ or $\tilde{i}_d(\varphi', \varphi'')$ were adopted. *Averaging of intensities corresponding to the motion along two (horizontal) orthogonal directions* was also introduced.

Two basic ideas and start points were adopted:

- (a) use of a *convex envelope of the response spectrum* for the absolute acceleration (ATC 1986);
- (b) use of an *integral of the square of acceleration* (Arias 1970).

Some basic details on the features of entities used are presented essentially for the ways (a) and (b) referred to. Some details on the way (b') may be found in Sandi and Floricel (1998).

The system IES (intensity estimate system) provides a way to assess: global intensity I_X , intensity related to a definite oscillation frequency φ (Hz), $i_x(\varphi)$, and intensity averaged upon a definite spectral band (φ', φ''), $\tilde{i}_x(\varphi', \varphi'')$. Besides these alternative cases, it may be useful to consider a global intensity $\tilde{i}_x(\varphi', \varphi'')$ averaged upon the reference spectral band (0.25, 16.0 Hz), which might be more appropriate than I_X . The subscripts X, x , which are formal, will be replaced for different definitions of intensity according to Table 2. All these measures of intensity may be considered in relation to a definite (horizontal) direction of motion or to motion in a horizontal plane.

The scheme of the system is presented in Table 2.

2.2 Basic Relations

All variants of intensities referred to, I_X, i_x etc. are to be determined on the basis of homologous kinematic parameters Q_X, q_x etc. that are derived on the basis of instrumental data specific to the kind of intensity of the corresponding row of Table 2. The parameters Q_X, q_x etc. have all the physical dimension $L^2 T^{-3}$.

Table 2 System of instrumental criteria for intensity assessment

Name	Symbols used for intensities: * global; ** related to a frequency φ ; *** averaged upon a frequency interval (φ' , φ'')			Source of definition/comments
	*	**	***	
Spectrum based intensities	I_S	$i_s(\varphi)$	$\tilde{i}_s(\varphi', \varphi'')$	Linear response spectra for absolute accelerations and velocities/use of <i>EPA</i> , <i>EPV</i> , redefined as <i>EPAS</i> , <i>EPVS</i> respectively [see relations (4a, 4b)]; averaging rules specified. (2), (3)
Intensities based on Arias' type integral of acceleration	I_A	$i_d(\varphi)$	$\tilde{i}_d(\varphi', \varphi'')$	Quadratic integrals of acceleration of ground (for I_A), or of pendulum of natural frequency φ (for $i_d(\varphi)$)/both extensible to tensorial definition; averaging rules specified (2), (3)
Intensities based on quadratic integrals of Fourier images	I_F ($\equiv I_A$)	$i_f(\varphi)$	$\tilde{i}_f(\varphi', \varphi'')$	Quadratic integrals of Fourier image of acceleration (for I_F), or quadratic functions of Fourier images [for $i_d(\varphi)$]/also extensible to tensorial definition; averaging rules also specified

The passage from the kinematic parameters Q_x, q_x etc. to the homologous intensities I_x, i_x etc. is to be performed on the basis of relations

$$I_x = \log_b Q_x + I_{x0} = I_{xQ} + I_{x0} \tag{1a}$$

$$i_x(\varphi) = \log_b q_x(\varphi) + i_{x0} = i_{xq} + i_{x0} \tag{1b}$$

where the logarithm basis b was calibrated initially as $b = 4$, in order to provide compatibility with the geometric ratio 2 corresponding to a difference of one intensity unit in the frame of the MSK scale (Table 1). The calibration of b is discussed in Sect. 2.6.

The rule of averaging of parameters $q_x(\varphi)$ upon a frequency band (φ' , φ''), to obtain values $\tilde{q}_x(\varphi', \varphi'')$, is

$$\tilde{q}_x(\varphi', \varphi'') = [1.0 / \ln(\varphi'' / \varphi')] \times \int_{\varphi'}^{\varphi''} q_x(\varphi) \, d\varphi / \varphi \tag{2}$$

The rule of averaging upon two orthogonal horizontal directions is

$$Q_X = (Q_{X1} + Q_{X2})/2 \tag{3a}$$

$$q_x(\varphi) = [q_{x1}(\varphi) + q_{x2}(\varphi)]/2 \tag{3b}$$

The basic expressions corresponding to the rows of Table 2 are respectively

- spectrum based parameter (starting from the ideas of Newmark and Hall from ATC 1986), Q_S ,
- parameter based on Arias' definition (Arias 1970), Q_A , and
- Fourier spectrum based parameter, Q_F (Sandi 1988);

using the notations

$$EPAS = \max_{\varphi} [s_{aa}(\varphi, 0.05)/2.5] \quad (\text{units: m/s}^2) \tag{4a}$$

$$EPVS = \max_{\varphi} [s_{va}(\varphi, 0.05)/2.5] \quad (\text{units: m/s}) \tag{4b}$$

($s_{aa}(\varphi, n)$: response spectrum of absolute accelerations; $s_{va}(\varphi, 0.05)$: response spectrum of absolute velocities), one introduces

$$Q_S = EPAS \times EPVS \tag{5a}$$

then,

$$Q_A = \int [w_g(t)]^2 dt \tag{5b}$$

($w_g(t)$: ground motion acceleration), and

$$Q_F = \int |w_g^{(\varphi)}(\varphi)|^2 d\varphi \tag{5c}$$

($w_g^{(\varphi)}(\varphi)$: Fourier transform of ground motion acceleration); note here that the definitions Q_A and Q_F can be directly extended to tensorial definitions related to the components of ground motion along an orthogonal system of axes, making it possible to account for ground motion directionality and that, due to analytical reasons, one has $Q_A \equiv 2 Q_F$.

The alternative definitions of parameters $q_x(\varphi)$ are:

- spectrum based parameter, $q_s(\varphi)$,
- parameter based on destructiveness characteristic, $q_d(\varphi)$, and
- Fourier spectrum based parameter, $q_f(\varphi)$,

$$q_s(\varphi) = s_{aa}(\varphi, 0.05) \times s_{va}(\varphi, 0.05) \quad (6a)$$

$$q_d(\varphi) = \int [w_a(t; \varphi, 0.05)]^2 dt \quad (6b)$$

$$q_f(\varphi) = \varphi |w_a^{(\varphi)}(\varphi)|^2 \quad (6c)$$

$(w_a(t; \varphi, n)$: absolute acceleration of an SDOF pendulum having an undamped natural frequency φ and a fraction of critical damping n).

$(w_a^{(\varphi)}(\varphi, n)$: Fourier transform of absolute acceleration of an SDOF pendulum having an undamped natural frequency φ and a fraction of critical damping n).

2.3 Correlation Analysis and Calibrations Adopted

The free terms I_{X0} and i_{x0} of expressions (1a) and (1b) were calibrated in Sandi and Floricel (1998) in a way to provide a best correlation between the alternative definitions adopted, after having postulated

- a logarithm basis $b = 4$ and
- a free term value $I_{S0} = 8.0$,

on the basis of comparison of values I_S with macroseismic estimates for several cases of intensity assessment (Sandi and Floricel 1998). Computations were performed accepting at that time the logarithm basis $b = 4$, in order to provide compatibility with the ratios adopted for the instrumental criteria in the frame of the MSK scale (Table 1).

The sample accelerograms used were ground level records, obtained in Romania during the events of 1977.03.04, 1986.08.30, 1990.05.30 and 1990.05.31.

The *primary* processing concerned determination of:

- the global quantities Q_S, Q_A ;
- the frequency dependent quantities $q_s(\varphi), q_d(\varphi), q_f(\varphi)$, determined for 121 φ values each (the values φ represented practically a geometric progression in the frequency interval (0.25, 16.0 Hz));
- the averaged values $\tilde{q}_s(\varphi', \varphi''), \tilde{q}_d(\varphi', \varphi''), \tilde{q}_f(\varphi', \varphi'')$, determined alternatively for the following intervals (φ', φ'') : (0.25, 16.0), (0.5, 8.0), (1.0, 4.0), (0.25, 0.5), (0.5, 1.0), (1.0, 2.0), (2.0, 4.0), (4.0, 8.0), (8.0, 16.0), where the numerical values are expressed in Hz.

The quantities I_{XQ}, i_{xq} and $\tilde{i}_{xq}(\varphi', \varphi'')$, (1a), (1b), were determined thereafter (for $b = 4$). They served as a basis for graphic representations as well as for correlation and regression analysis.

The *secondary processing* was related to correlation and regression analysis. Following combinations were considered:

- (a) $I_S \leftrightarrow I_A, I_S \leftrightarrow \tilde{i}_s(\varphi', \varphi''), I_S \leftrightarrow \tilde{i}_d(\varphi', \varphi''), I_S \leftrightarrow \tilde{i}_f(\varphi', \varphi'')$, where (φ', φ'') was (0.25, 16.0 Hz);
- (b) $I_A \leftrightarrow \tilde{i}_s(\varphi', \varphi''), I_A \leftrightarrow \tilde{i}_d(\varphi', \varphi''), I_A \leftrightarrow \tilde{i}_f(\varphi', \varphi'')$, where (φ', φ'') was the same;
- (c) $\tilde{i}_s(\varphi', \varphi'') \leftrightarrow \tilde{i}_d(\varphi', \varphi''), \tilde{i}_s(\varphi', \varphi'') \leftrightarrow \tilde{i}_f(\varphi', \varphi''), \tilde{i}_d(\varphi', \varphi'') \leftrightarrow \tilde{i}_f(\varphi', \varphi'')$, where (φ', φ'') was the same;
- (d) the same as (c), where (φ', φ'') was alternatively: (0.5, 8.0 Hz), (1.0, 4.0 Hz), (0.25, 0.5 Hz), (0.5, 1.0 Hz), (1.0, 2.0 Hz), (2.0, 4.0 Hz), (4.0, 8.0 Hz), (8.0, 16.0 Hz).

The variants (a), (b), (c) were intended to explore the quantities considered for a global characterization of ground motion, while the variant (d) was intended to go into details for relatively narrow (one—octave, i.e. 6 dB) frequency intervals.

The outcome of correlation and regression analysis is presented in Tables 3, 4 and in the homologous Figs. 1 and 2 respectively. The results obtained were at the basis of data of Tables 5 and 6. Some additional data related to the regression parameters and to the calibration of parameters $I_{S0}, I_{A0}, i_{s0}^*, i_{d0}^*, i_{f0}^*$ are given in Table 5. The values of Table 5 represent differences between the parameter corresponding to a column and the parameter corresponding to a row. The upper triangle represents ranges obtained from computation, while the lower triangle represents a calibration derived from rounding up to the multiple of 0.05 which is the closest to the median value. Accepting the values of the lower triangle referred

Table 3 Correlation coefficients (upper triangle) and rms deviations (lower triangle) for motions as a whole

	I_{SQ}	I_{AQ}	$i_{sq}^*(0.25, 16.0 \text{ Hz})$	$i_{dq}^*(0.25, 16. \text{ Hz})$	$i_{fq}^*(0.25, 16. \text{ Hz})$
I_{SQ}	*	0.94–0.98	0.96–0.98	0.94–0.97	0.93–0.97
I_{AQ}	0.14–0.18	*	0.93–0.98	1.00	0.99–1.00
$i_{sq}^*(0.25, 16.0 \text{ Hz})$	0.12–0.14	0.15–0.23	*	0.93–0.98	0.92–0.97
$i_{dq}^*(0.25, 16.0 \text{ Hz})$	0.14–0.17	0.02–0.03	0.15–0.23	*	0.99–1.00
$i_{fq}^*(0.25, 16.0 \text{ Hz})$	0.15–0.17	0.04–0.05	0.16–0.23	0.04–0.05	*

Table 4 Correlation coefficients for various frequency intervals

$(\varphi', \varphi''), \text{ Hz}$	$i_{sq}^* \leftrightarrow i_{dq}^*$	$i_{sq}^* \leftrightarrow i_{fq}^*$	$i_{dq}^* \leftrightarrow i_{fq}^*$
(0.25, 0.5)	0.96–0.98	0.95–0.98	0.98–1.00
(0.5, 1.0)	0.96–0.98	0.94–0.99	0.99–1.00
(1.0, 2.0)	0.94–0.98	0.92–0.98	0.99–1.00
(2.0, 4.0)	0.92–0.98	0.86–0.96	0.98–0.99
(4.0, 8.0)	0.91–0.96	0.82–0.86	0.95–0.97
(8.0, 16.0)	0.84–0.95	0.52–0.78	0.78–0.88

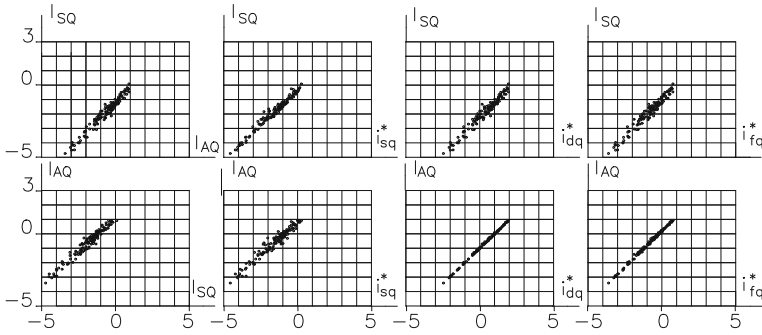


Fig. 1 Correlation of I_{SQ} and I_{AQ} between themselves and with frequency dependent parameters, averaged for the interval (0.25, 16.0 Hz). *Note* In order to shorten the text, the symbols $\tilde{i}_x(\varphi', \varphi'')$ were replaced, when possible, by i_x^*

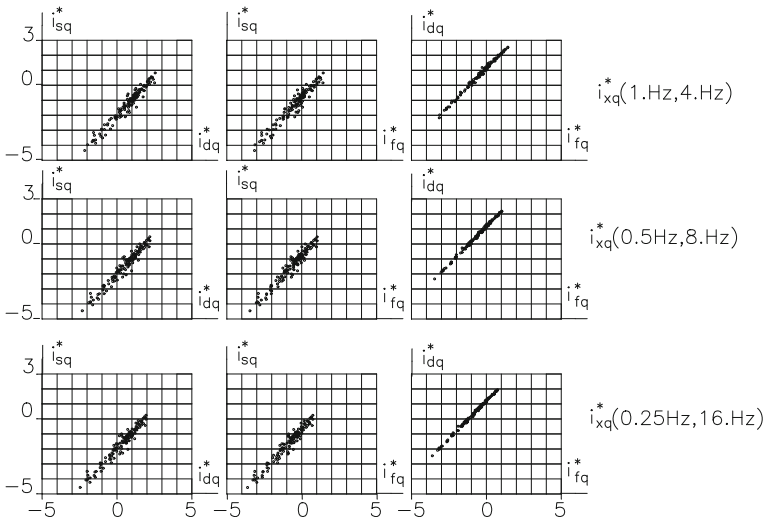


Fig. 2 Correlation between $\tilde{i}_{sq}(\varphi', \varphi'')$, $\tilde{i}_{dq}(\varphi', \varphi'')$ and $\tilde{i}_{fq}(\varphi', \varphi'')$, for various intervals (φ', φ''). *Note* In order to shorten the text, the symbols $\tilde{i}_x(\varphi', \varphi'')$ were replaced, when possible, by i_x^*

Table 5 Differences between conversion constants (intervals of variation—upper triangle and fixed values adopted on this basis—lower triangle)

	I_{SO}	I_{AO}	i_{s0}^*	i_{d0}^*	i_{f0}^*
I_{SO}	*	-1.26 to -1.22	-0.31 to -0.22	-2.27 to -2.20	-1.06 to -1.01
I_{AO}	1.25	*	0.93-1.00	-1.00 to -0.98	0.21-0.22
i_{s0}^*	0.30	-0.95	*	-1.98 to -1.93	-0.79 to -0.72
i_{d0}^*	2.25	1.00	1.95	*	1.19-1.22
i_{f0}^*	1.05	-0.20	0.75	-1.20	*

Table 6 Calibrations proposed for constants I_{XO} and i_{XO} .

Parameter	I_{SO}	I_{AO}	i_{sO}	i_{dO}	i_{fO}
Calibration	8.00	6.75	7.70	5.75	6.95

to, the calibration of Table 6 results, in case one accepts, as in Sandi and Floricel (1998), $I_{SO} = 8$.

Looking at the outcome given in Tables 3 and 4, it turns out that the correlations between the results provided by the various variants of intensity assessment are high, which leads to the conclusion that *the use of different variants leads to practically the same results* (the differences are in most cases less than a quarter of an intensity unit; these differences are in general more important for the results concerning the domain of relatively high frequencies). More details on this subject are provided in Sandi and Floricel (1998).

Looking at Tables 3 and 4, as well as at corresponding Figures, it turns out that:

- the strongest correlations are:
 - for global intensities (with correlation coefficients of 0.99 ... 1.00), the combinations $I_A \leftrightarrow \tilde{i}_d$ (0.25, 16.0 Hz), $I_A \leftrightarrow \tilde{i}_f$ (0.25, 16.0 Hz) and \tilde{i}_d (0.25, 16.0 Hz) $\leftrightarrow \tilde{i}_f$ (0.25, 16.0 Hz);
 - for intensities averaged upon 6 dB bands (with correlation coefficients higher than 0.9), the combinations $i_{sq}^* \leftrightarrow i_{dq}^*$ and $i_{dq}^* \leftrightarrow i_{fq}^*$ for the frequency bands (0.25, 0.5 Hz) up to (4.0, 8.0 Hz) and, also, the combination $i_{sq}^* \leftrightarrow i_{fq}^*$ for the frequency bands (0.25, 0.5 Hz) up to (1.0, 2.0 Hz);
- the lack of smoothness of i_{fq}^* shows its effects in decreasing of correlation coefficients especially for higher frequency bands.

These remarks reveal the domains for which the option for one or another of the alternative definitions of instrumental intensity may be expected to lead to practically equivalent results when applied to concrete case studies, and ergo for which the credibility of the outcome is strongest. They lead also to the conclusion that the variants I_S , I_A (for global intensities), and i_s^* , i_d^* (for various frequency bands) are preferable, while the variant i_{fq}^* is less advantageous (and consequently was no longer used in case studies referred to).

On the basis of data given in previous tables, the calibrations of Table 6 are proposed. Of course, they correspond to the assumption $b = 4$.

Concerning the choice to be recommended for various case studies, the experience of use of the alternative instrumental criteria presented, which is definitely encouraging, shows that:

- the measures I_S , $i_s(\varphi)$ and $\tilde{i}_s(\varphi', \varphi'')$ are easily usable and, after some exercise and experience, even a visual examination of response spectra makes it possible to get a fair estimate of these quantities;

- on the other hand, the measures I_A , $i_d(\varphi)$ and $\tilde{i}_d(\varphi', \varphi'')$ appear to be more stable and to benefit from stronger correlation (not to mention also the advantage of feasibility of an in depth analysis of directionality of motion, based on the possibility of extending their definitions from a scalar to a tensorial one).

Consequently, the option should rely on expert judgement. It may be also stated that the degree of accuracy and certainty of the outcome will be superior to what macroseismic studies can be expected to provide.

The experience available to date has shown that the calibrations derived on the basis of data of Tables 3, 4, 5 and 6 appear to be convenient. On the other hand, an aspect to be revised is represented by the calibration of the parameter b , which is discussed in next subsections. The deviations between the estimates based on the alternative instrumental criteria proposed reach seldom 0.5 intensity degrees and are, usually, lower than 0.25° . So, the definitions adopted lead to a degree of accuracy that exceeds considerably the accuracy that may be provided by the use of macroseismic criteria. Some illustrative examples in this sense are offered by the intensity spectra presented in Sandi and Borcia (2006).

2.4 Possible Recalibrations of Logarithm Basis

The outcome of recent statistical studies referred to subsequently, in Sect. 2.5, shows that the logarithm basis $b = 4$, used to date in relations (1a), (1b), may be not the most appropriate and that using a logarithm basis around $b = 7.5$, derived on the basis of statistical analyses referred to in Sect. 2.5 may be more appropriate. This raises the problem of conversion between intensity estimates corresponding to the use of different logarithm bases. Further relations in this connection are applied starting from the relation (1a), but they are usable also for the relation (1b) and for averaged intensities $\tilde{i}_x(\varphi', \varphi'')$ as well. Given the positive experience acquired to date, the structure of relations (1a), (1b), will be kept further on.

Two alternative logarithm bases, b' and b'' , and two corresponding free terms, I'_{X0} and I''_{X0} respectively, are considered for relation (1a). Their use would lead to different estimated intensities, I'_X and I''_X respectively. In order to make them to coincide for a reference intensity I_{Xc} , the conditions

$$I_{Xc} = \log_{b'} Q_{Xc} + I'_{X0} = I_{XQ'} + I'_{X0} = \log_{b''} Q_{Xc} + I''_{X0} = I_{XQ''} + I''_{X0} \quad (7)$$

are to be fulfilled. This leads to the result

$$I''_{X0} = I_{Xc} - (I_{Xc} - I'_{X0}) \times \lg b' / \lg b'' \quad (\lg: \text{decimal logarithm}) \quad (8)$$

The outcome of an attempt of recalibration is presented in Sect. 2.6.

To end this subsection, some concluding remarks may be presented as follows:

- a comprehensive system of analytical relations, on which in depth intensity estimates can be conducted, was presented;
- the statistical analysis reveals the strong correlation between the alternative criteria proposed;
- the developments presented make it possible to determine discrete intensity spectra (as illustrated in next section), which may represent an attractive tool for case studies;
- basic relations to be used in case of eventual rescaling of the logarithm basis b intervening in the analytical relations presented were developed.

2.5 *Statistical Studies on the Relationships Between Macroseismic Estimates and Motion Parameters*

The wealth of macroseismic and instrumental information which became available more recently made it possible to develop a comprehensive statistical study on the relationships between macroseismic intensity and kinematic parameters (Aptikaev 2005, 2006; Aptikaev et al. 2008). They refer essentially to the outcome of statistical analysis of instrumental data on ground motion, for cases when macroseismic intensity estimates were at hand. Some results obtained in that frame are reproduced here for subsequent discussion. The wealth of data used was considerable, as shown in Table 7.

The results obtained stood at the basis of the specification of instrumental criteria adopted in the frame of the new Russian Macroseismic Scale, RMS-04 (Aptikaev et al. 2008; Shebalin and Aptikaev 2003; НАЦИОНАЛЬНЫЙ 2014).

The empirical relations determined on a statistical basis are [with some updating with respect to (Aptikaev 2005; Aptikaev et al. 2008)] for peak ground accelerations, “ A ”; for peak ground velocities, “ V ”; for peak ground displacements “ D ”; and for peak wave kinematic power, “ P ” respectively:

$$\lg A(\equiv PGA), \text{ cm/s}^2 = -0.755 + 0.4I \pm 0.39(0.25) \quad (9)$$

(correlation coefficient: 0.82)

$$\lg V(\equiv PGV), \text{ cm/s} = -2.23 + 0.47I \pm 0.33(0.20) \quad (\text{correlation coefficient: } 0.84) \quad (10)$$

$$\lg D(\equiv PGD), \text{ cm} = -4.26 + 0.68I \pm 0.65(0.33) \quad (\text{correlation coefficient: } 0.81) \quad (11)$$

Table 7 Number of data used in the statistical studies referred to

Intensities	2	3	4	5	6	7	8	9
Number of cases	75	75	172	391	353	212	178	84

Table 8 Average values of jumps for one intensity unit

Intensities	PGA	PGV	PGD	PGP
Values of jumps	$10^{0.40} \approx 2.51$	$10^{0.47} \approx 2.95$	$10^{0.68} \approx 4.79$	$10^{0.87} \approx 7.41$

$$\lg P(\equiv PGP), \text{cm}^2/\text{s}^3 = -2.22 + 0.87I \pm 0.49(0.41) \quad (12)$$

(correlation coefficient: 0.89)

Quantities under “±” concern standard deviations, related both to intensity and ground motion parameters estimations. Under parentheses are given values for intensities $I > 6$.

It turns out, on the basis of these relations, that the average values obtained for a jump of one intensity unit are those of Table 8.

The facts that the factor 0.47 of relation (10) is higher than the homologous factor 0.40 of relation (9), while the factor 0.68 of relation (11) is higher than the homologous factor 0.47 of relation (10), correspond to a quite well known trend of increase of dominant oscillation periods of ground motion with increasing intensity (this trend was quite systematically observed, on the basis of instrumental data obtained at a same location during different earthquakes). On the other hand, the factor 0.87 of relation (12) is, as it should be, equal to the sum $0.40 + 0.47$ of homologous factors of relations (9) and (10). These results, which correspond to reality, are in direct contradiction with the features of the MSK scale criteria, which relied on the assumption of fixed corner periods, of 0.5 s, irrespective of intensity.

Looking at the values of kinematic parameters derived on the basis of previous relations, it turns out that one obtains reasonable values even for lowest intensities, for which the assumption of a fixed value of 2.0 for a jump of one intensity unit did obviously not work. So, it appears to be reasonable to adopt such values, perhaps with a minor rounding up (e.g.: 2.5 for accelerations, 3.0 for velocities, 4.8 for displacements, 7.5 for peak kinematic power). These results could eventually be combined with the need of revising the logarithm basis $b = 4$, adopted initially in Sandi (1986) and Sandi and Floricel (1998), using the relations (7) and (8). In case the rounded up values suggested are accepted, the result would be a value $b \approx 7.5$, which would make it possible to cover in a satisfactory manner an extensive interval of intensities, going e.g. downwards up to intensity 2. Some first data in connection with the revision of the value of b were presented in Aptikaev et al. (2008). The rather high scatter of results showed that quite numerous basic data should be used in performing a statistical analysis on this subject, in order to obtain conclusive final results.

The new Russian standard on seismic intensity scale (НАЦИОНАЛЬНЫЙ 2014) has adopted, for main instrumental criterion, the product $PGP = PGA$ (cm/s^2) \times PGV (cm/s), which has the physical dimension $\text{L}^2 \text{T}^{-3}$. Its *rms* of variation, $\sigma(I)$, is by far less than that of direct kinematic parameters like PGA or PGV , which means that its credibility is considerably higher than that of other criteria. The values of this product are given in the last row of Table 9.

Table 9 Excerpts from Aptikaev et al. (2008) for intensities $5.5 \leq I \leq 9.5$

Parameters	$\sigma(I)$	Seismic intensity								
		5.5	6.0	6.5	7.0	7.5	8.0	8.5	9.0	9.5
<i>PGA</i> (cm/s ²)	0.60	28.0	44	70	110	180	280	440	700	1100
<i>PGV</i> (cm/s)	0.55	2.2	3.8	6.5	11	19	33	57	98	170
<i>PGD</i> (cm)	0.70	0.30	0.66	1.4	3.2	7	15	33	72	160
<i>PGA d</i> ^{0.5} (cm/s ^{1.5})	0.35	60	95	150	240	380	605	955	1516	2400
Lg (<i>PGA</i> × <i>PGV</i>), (cm ² /s ³)	0.26	2.0	2.4	2.8	3.2	3.5	3.9	4.3	4.7	5.0

The values of *P* of the table correspond to an increase 5.0–2.0, of three intensity units, which means a ratio of 1000 for 4 intensity units, or a ratio of $(1000)^{1/4} \approx 5.62$ for the logarithm basis *b*. This is quite close to the rounded up value of 6, proposed on the basis of results presented in the next section.

2.6 Use of Some Additional Data

The analysis of a new set of data was initiated, in order to acquire additional experience and to explore the possibilities of recalibration of basic relations for intensity assessment. The same set of instrumental and macroseismic data related to some earthquakes of the North American continent and of the Vrancea seismogenic zone (Romania) was used also in view of obtaining the results presented subsequently. The data from the Republic of Moldova, where general investigations of the features and effects of the earthquakes of 1986 and 1990 were presented in Drumea et al. (1990) were determined recently, with a look at the spectral interval for which damage survey data were relevant. The initial macroseismic estimates for Romania were taken from the isoseismal maps developed by INCDFP (National Institute for Research and Development of Earth Physics).

The macroseismic intensities estimated pertained to the interval [VI, VIII. 1/2]. Alternative instrumental intensity estimates, considering on one hand the calibration $b' = 4.0$ of relations (1a, 1b), and on the other hand a recalibration for $b'' = 8.0$ and, alternatively (for the latter one), $I_{Xc} = 7.0$ or $I_{Xc} = 8.0$, were conducted. A summary look to these alternative estimates is provided in Figs. 3 and 4.

The straight lines of the figures correspond alternatively to the different assumptions adopted: the higher slope straight line corresponds to $b = 4$, while the parallel lines correspond to $b = 8$.

These figures show that neither the value $b = 4$, nor the value $b = 8$, appear to be satisfactory. A value $b = 6$, leading to an interpolation between the lines corresponding to the two assumptions considered, would reduce the *rms* of deviations. Note that the developments of the previous subsection led to a value $b \approx 6$, the closest integer to the value $b \approx 5.62$, determined by means of calculations for the data provided by the standard referred to.

Fig. 3 Macroseismic intensities versus global instrumental estimates based on I_A

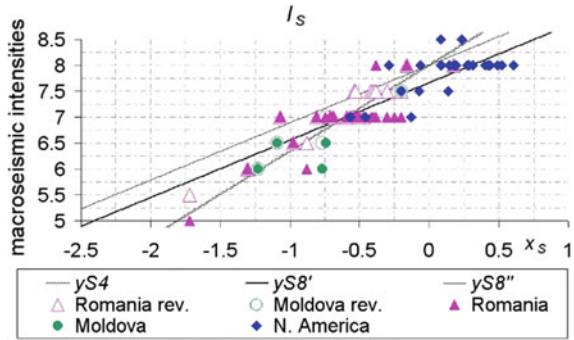
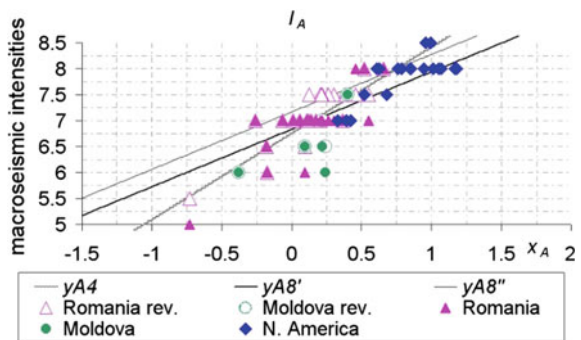


Fig. 4 Macroseismic intensities versus global instrumental estimates based on I_A



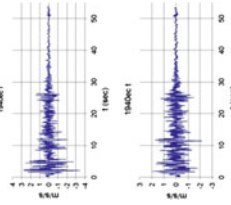
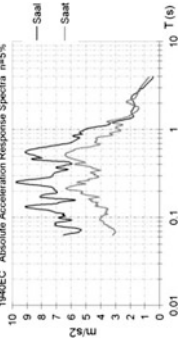
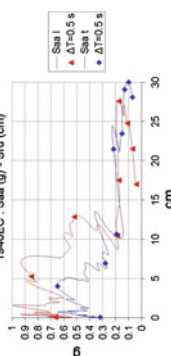
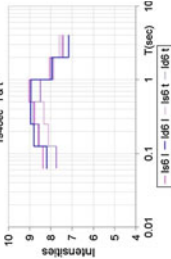
3 Some Illustrative Data

In order to contribute to the readability of the paper, it seemed to be useful to perform some of the calculations corresponding to the analytical developments of the paper. Four earthquakes appeared to be the most suggestive in this connection:

1. The record of El Centro due to the Imperial Valley (USA) event of 1940.05.18, which represents a kind of reference case for strong earthquakes.
2. The record of Mexico City, Segreteria Comunicaciones y Transportes, due to the Guerrero—Michoacán (Mexico) event of 1985.09.19, which is characterized by extremely large dominant periods (exceeding 2.0 s).
3. The record of Bucharest, INCERC (Romania); due to the Vrancea earthquake of 1977.03.04, characterized in its turn by unusually long periods.
4. The record of Cernavodă—Town Hall (Romania), due to the Vrancea earthquake of 1990.05.30, characterized by unusually strong concentration of motion spectral contents.

For each case, the upper row presents general data on the event, two horizontal accelerograms and the response spectra of horizontal components, while the lower

Table 10 Illustrative ground motion characteristics

No	General data on event and on record site/magnitudes and global intensities	Characteristics of ground motion along two orthogonal horizontal directions Accelerograms/displacement—acceleration spectra	Response spectra for absolute accelerations (5 % critical damping) Intensity spectra: $\tilde{i}_s(\varphi t, \varphi'')$, red, and $\tilde{i}_d(\varphi t, \varphi'')$, blue, averaged upon 6 dB intervals
1	<p>Source USA, Ca, Imperial Valley 1940.05.18 φ, λ: 32.73, -115.45 <i>Record site</i>: El Centro Code: 1940ELC φ, λ: 39.72, -115.55</p>		
	<p>M_S: 7.0 I_S: 8.01 (8.18, 7.80) I_{S1}: 8.34 (8.52, 8.09) I_A: 8.43 (8.55, 8.30) I_D: 8.44 (8.56, 8.31)</p>		

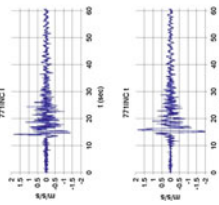
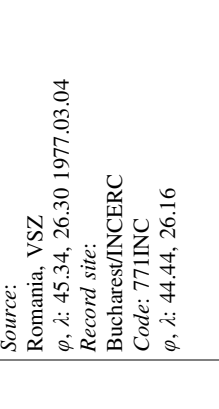
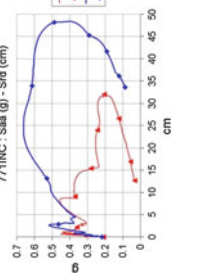
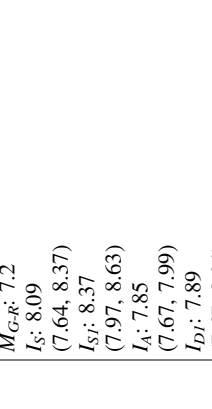
(continued)

Table 10 (continued)

No	General data on event and on record site/magnitudes and global intensities	Characteristics of ground motion along two orthogonal horizontal directions— Accelerograms/displacement— acceleration spectra	Response spectra for absolute accelerations (5 % critical damping)/ Intensity spectra: $\tilde{i}_s(\varphi^t, \varphi'')$, red, and $\tilde{i}_d(\varphi^t, \varphi'')$, blue, averaged upon 6 dB intervals
2	<p><i>Source:</i> N.A./Cocos Plates (Mexico) 1985.09.19 φ, λ: 18.08, -102.94 <i>Record site:</i> Mex. City SCT <i>Code:</i> 1985SCT φ, λ: 19.43, -99.13</p>	<p>1985meioSCT1: Saa (g) - Sdd (cm)</p> <p>1985meioSCT1: Saa (g) - Sdd (cm)</p>	<p>1985meioSCT Absolute Acceleration Response Spectra m/s^2</p> <p>1985meioSCT 1 & 1 Intensity Spectra</p>
	<p>M_S: 8.1 I_S: 8.92 (8.55, 9.16) I_{Sf}: 8.42 (7.90, 8.72) I_A: 8.40 (8.03, 8.64) I_{Df}: 8.47 (8.09, 8.72)</p>	<p>1985meioSCT1: Saa (g) - Sdd (cm)</p>	

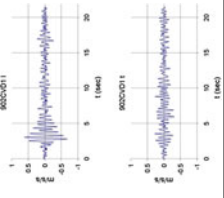
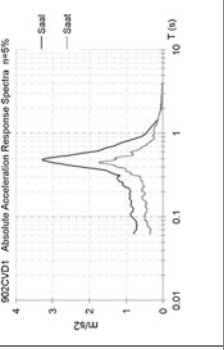
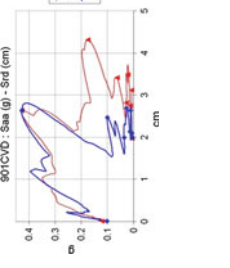
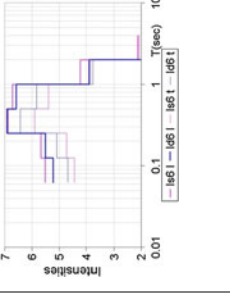
(continued)

Table 10 (continued)

No	General data on event and on record site/magnitudes and global intensities	Characteristics of ground motion along two orthogonal horizontal directions Accelerograms/displacement—acceleration spectra	Response spectra for absolute accelerations (5 % critical damping) Intensity spectra: $\tilde{i}_s(\varphi^t, \varphi'')$, red, and $\tilde{i}_d(\varphi^t, \varphi'')$, blue, averaged upon 6 dB intervals
3	<p><i>Source:</i> Romania, VSZ φ, λ: 45.34, 26.30 1977.03.04 <i>Record site:</i> Buchares/INCERC <i>Code:</i> 77IINC φ, λ: 44.44, 26.16</p>		
	<p>M_G-r: 7.2 I_S: 8.09 (7.64, 8.37) I_{Sf}: 8.37 (7.97, 8.63) I_A: 7.85 (7.67, 7.99) I_D: 7.89 (7.67, 8.04)</p>		

(continued)

Table 10 (continued)

No	General data on event and on record site/magnitudes and global intensities	Characteristics of ground motion along two orthogonal horizontal directions— Accelerograms/displacement— acceleration spectra	Response spectra for absolute accelerations (5 % critical damping)/ Intensity spectra: $\tilde{i}_s(\varphi^t, \varphi'')$, red, and $\tilde{i}_d(\varphi^t, \varphi'')$, blue, averaged upon 6 dB intervals
4	<p><i>Source:</i> Romania, VSZ φ, λ: 45.83, 26.89 1990.05.31</p> <p><i>Record site:</i> Cemavodă/Town Hall <i>Code:</i> 902CVD1 φ, λ: 45.23, 28.03</p>		
	<p>M_{G-R}: 6.1 I_S: 6.21 (6.55, 5.57) I_{Sj}: 5.79 (6.14, 5.07) I_A: 5.84 (6.06, 5.51) I_{Dj}: 5.86 (6.08, 5.53)</p>		

row presents data concerning the recording site, the displacement—acceleration spectra and the intensity spectra.

The colors used in Table 10 are red for I_S and i_s , and blue for I_A and i_d .

The last column of each case makes it possible to examine a relationship between response spectra and intensity spectra.

4 Closing Considerations

The use of concepts and methods specific to structural dynamics appears to be appropriate for bridging the gap between the limits to the concepts of traditional intensity and the needs of accuracy specific to engineering activities (Sandi 2006, Sandi et al. 2006).

Neglecting the spectral characteristic to ground motion may lead to serious mistakes in the assessment of features of ground motion. Among others, this shortcoming led in the past to the partially erroneous zonation in Romania.

In performing post-earthquake surveys, it is necessary to note to what kind of affected elements the field data pertain (assuming thus a corresponding responsibility). This is to be done, of course, for newly undertaken surveys, but also in the frame of attempts of dealing with “historical” earthquakes, in order to get a more comprehensive picture of the characteristics of a seismogenic area of interest.

It is desirable to continue the work presented in this paper in the direction of recalibration of the parameters dealt with. In case the value of the logarithm basis b is modified from 4 to 6, as suggested in Sect. 2.6, the free terms of the relations (1a, 1b) are to be revised, in order to obtain a best possible convergence of criteria presented with the outcome of field surveys.

Acknowledgements The author Horea Sandi is deeply indebted to the memory of Dr. Ioan Sorin Borcia, with whom he cooperated for more than four decades and who played the major role in performing the computer work on which this paper relies.

References

- Aptikaev F (2005) Instrumental seismic intensity scale. Proceedings of the Symposium on the 40-th anniversary of IZIIS, Skopje
- Aptikaev F (ed) (2006) Project of Russian Seismic Intensity Scale RIS-04. Proceedings of the first European conferences on earthquake engineering and seismology. Geneva, Switzerland, paper no. 1291
- Aptikaev FF, Mokrushina NG, Erteleva OO (2008) The Mercalli family of seismic intensity scale. *J Valcanol Seismol* 2(3):210–213
- Arias A (1970) A measure of earthquake intensity. In: Hansen RJ (ed) *Seismic design for nuclear power plants*. MIT Press, Cambridge, MA
- ATC (1986) Tentative provisions for the development of seismic regulations for buildings (ATC-3-06). ATC Publication

- Drumea A, Alcaz V et al (1990) Karpatskoe zemletryasenie 30 Maya 1990 goda. Predvaritelnye rezultaty seismicheskikh i inzhenerno-gheologicheskikh issledovaniy. Izvestiya Akademii Nauk SSR Moldova. Fizika i tehnika, t3
- Grünthal G (ed) (1998) European Macroseismic Scale 1998. Luxembourg: Cahiers du Centre Européen de Géodynamique et Séismologie, 15
- НАЦИОНАЛЬНЫЙ СТАНДАРТ РОССИЙСКОЙ ФЕДЕРАЦИИ (2014) ШКАЛА ИНТЕНСИВНОСТИ ЗЕМЛЕТРЯСЕНИЙ
- Medvedev SV (1962) Inzhenernaya seismologhia. Moscow, Gosstroyizdat
- Medvedev SV (1977) Seismic intensity scale MSK-76. Publ Inst Geophys Pol Acad Sc 117: 95–102
- Sandi H (1986) An engineer's approach to the scaling of ground motion intensity. Proceedings of the 8-th ECEE, Lisbon, Portugal
- Sandi H (1988) Consideration of the spectral content of ground motion in re-evaluation of the seismic intensity. Symp.S5 of the XXI-st General Assembly, European Seismological Commission, Sofia, Bulgaria
- Sandi H (2006) Bridging a gap between seismologists and engineers: possible restructuring of the intensity scale(s). Proceedings of the first European conferences on earthquake engineering and seismology, Geneva, Switzerland, paper no. 571
- Sandi H, Aptikaev FF, Alcaz V, Borcia IS, Drumea A, Erteleva O, Roman A (2006) A NATO project on deriving improved (instrumental) criteria for seismic intensity assessment. Proceedings of the first European conferences on earthquake engineering and seismology, Geneva, Switzerland, paper no. 581
- Sandi H, Borcia IS (2006) Damage spectra and intensity spectra for recent Vrancea earthquakes. Proceedings of the First European Conferences on Earthquake Engineering and Seismology, Geneva, Switzerland, paper no. 574
- Sandi H, Floricel I (1998) Some alternative instrumental measures of ground motion severity. Proceedings of the 11-th European conferences on earthquake engineering, Paris, France
- Shebalin NV, Aptikaev FF (2003) Development of scales MSK type. The earth's magnetic field: mathematical methods for description. Macroseismic Problems. Computational Seismology 34:210–253 (in Russian)

Earthquake Precursors Assessment in Vrancea Region Through Satellite and In Situ Monitoring Data

Maria Zoran, Dan Savastru and Doru Mateciuc

Abstract Vrancea active zone has a high seismic hazard in Romania and in the European-Mediterranean region, generating normal, strong or moderate intermediate depth earthquakes on a confined epicentral area. In this paper, for seismic hazard analysis in Vrancea region have been selected the earthquake precursors anomalies detectable from space as well as in situ monitoring: land surface temperature (LST) and air surface temperature (AT), and outgoing long wave radiation (OLR), provided by time-series satellite MODIS (Terra/Aqua) and AVHRR (NOAA), Landsat TM/ETM, as well as seismicity recorded prior to moderate or strong earthquakes. This study investigated March, 4th 1977, $M_w = 7.4$, $H = 94$ km and October 27th 2004, $M_w = 5.9$, $H = 96$ km earthquakes. The joint analysis of geospatial, geophysical, geochemical, seismological and geological information is revealing new insights in the understanding of the kinematics and dynamics of the complex plate boundary system present in the Eastern Carpathians as support of lithosphere-surfacesphere-atmosphere coupling model.

Keywords Seismic hazard assessment · Time-series geospatial data · Satellite derived geophysical parameters · Earthquake forecasting

M. Zoran (✉) · D. Savastru
National Institute of R&D for Optoelectronics, MG5 Magurele, Romania
e-mail: maria@dnt.ro

D. Savastru
e-mail: dsavas@inoe.ro

D. Mateciuc
National Institute of R&D for Earth Physics, Magurele, Romania
e-mail: dmateciuc@infp.ro

1 Introduction

The mechanical processes of earthquake preparation are always accompanied by deformations associated with complex short or long term precursory phenomena. It seems that Vrancea region in Romania is fitting such a model. Crustal deformation produces a wide variety of landforms at the surface of the Earth and their size depends on the duration of the process involved in their formation. Co- and post-seismic deformations take place over periods of a few seconds to several days, and produce fault scarps and surface displacement ranging from a few centimeters to several meters in magnitude. Along active deformation zones, earthquakes cause short-term and localized topography changes, which may present additional hazards, but at the same time permit to quantify stress and strain accumulation, a key control for seismic hazard assessment (Geller 2011).

Earthquake preparation is a transient dynamic process which can be monitored in real time from geospatial data validated with in situ monitoring. Due to new advanced satellite multispectral sensors and high temporal and spatial resolutions of satellite missions, the data can exhibit processes of spatio-temporal variation of geophysical parameters of seismic active regions.

The study of earthquakes will probably increase due to global urbanization, as millions of people are exposed to earthquakes in geotectonic active areas. Although humans cannot prevent seismic events, we can change the way we respond to them. Satellite remote sensing techniques, both spaceborne and airborne, can bring a very effective contribution. While thermal infrared imagery can be used for earthquake prediction (Ouzounov et al. 2006; Choudhury et al. 2006; Joyce et al. 2009), In-SAR (Interferometric Synthetic Aperture Radar) and GPS networking data are useful for measuring Earth's surface deformation. Optical, SAR, LiDAR (Light Detection And Ranging) data can also be used for building damage assessment after earthquakes, especially in the response and recovery phases (Pan and Tang 2010).

Several studies performed in the last years suggested the existence of anomalous space-time transients, in the thermal infrared (TIR) radiation emitted by the Earth, possibly related to earthquake preparatory phenomena (Tronin et al. 2002; Zoran et al. 2008; Zoran 2010). Among different theories about their origin, the abrupt increase in radon gas (Rn^{222}), greenhouse gases (CO_2 , CH_4 , NO_2 etc.) emission rates has been also proposed to explain the appearance of anomalous TIR precursory signals in some relation with the place and the time of earthquake occurrence in geotectonic active areas. Geospatial data, coupled with ground-based observations where available, enable scientists to survey pre-earthquake signals in areas of strong tectonic activity. Natural radioactivity (in particular, radon Rn^{222}) is considered (Zoran et al. 2012) to be a possible trigger for atmospheric increased ionization and electrical conditions anomalies in the lower atmosphere (atmospheric conductivity and the electric field) and upper atmosphere (ionospheric TEC—Total Electron Content anomalies). The mosaic pattern of the strain field in the epicentral zones creates a specific obstacle to the detection of precursory events and determination of the spatial scale of the earthquake preparation zone. Obviously, the size

of the zone largely depends on the earthquake magnitude. A change in the thermal regime of the epicentral zone and its surroundings is one of the most pronounced changes that can be detected by space-borne sensors such as Advanced Very High Resolution Radiometer (NOAA AVHRR) and the Moderate Resolution Imaging Spectroradiometer (MODIS Terra/Aqua). In spite of some skepticism regarding earthquake prediction (1), early warning signs of earthquakes are diverse, fleeting and often subtle, and they can also be surprisingly strong, even for moderate earthquakes (Freund 2011; Zoran 2012).

2 Seismic Precursors Anomalies

In order to implement an efficient system for earthquake forecasting in the geotectonic active areas it is very important to detect the precise anomaly in a nonlinear time series of several earthquake precursors derived from geospatial or in situ monitoring data. Many approaches have been proposed to improve the seismo-litospheric and atmospheric/ionospheric anomalies detection.

Different criteria can be used to select the remote sensed earthquake precursors for which there is an evidence of geophysical parameters anomalies. Rock microfracturing in the Earth's crust preceding a seismic rupture may cause local surface deformation fields, rock dislocations, charged particle generation and motion, electrical conductivity changes, gas emission, fluid diffusion, electrokinetic, piezomagnetic and piezoelectric effects as well as climate fluctuations. Space-time anomalies of Earth's emitted radiation (thermal infrared radiation linked to air and land surface temperature variations recorded from satellite months to weeks before the occurrence of earthquakes, radon in underground water, soil and near the ground air, etc.), ionospheric and electromagnetic anomalies are considered as earthquake precursors.

This energy transformation may result in enhanced transient thermal infrared (TIR) emission, which can be detected through satellites equipped with thermal sensors like AVHRR (NOAA), MODIS (Terra/Aqua). This paper presents observations made using time series NOAA-AVHRR and MODIS satellite data-derived land surface temperature (LST) and outgoing long-wave radiation (OLR) as well as air temperature anomalies recorded for selected earthquakes to be analyzed in seismic Vrancea region, Romania, using anomalous TIR signals as reflected in LST rise and high OLR values which followed similar growth pattern spatially and temporally. In all analyzed cases, starting with almost one week prior to a moderate or strong earthquake a transient thermal infrared rise in LST of several Celsius degrees (°C) and the increased OLR values higher than the normal have been recorded around epicentral areas, function of the magnitude and focal depth, which disappeared after the main shock. As Vrancea area has a significant regional tectonic activity in Romania and Europe, the joint analysis of geospatial and in situ geophysical information is revealing new insights in the field of hazard assessment.

3 Study Area and Data Used

Vrancea geotectonic zone is one of the most active intracontinental seismic areas in Europe located between latitudes 45.6°N and 46.0°N and longitudes 26.5°E and 27.5°E (Fig. 1).

It has a high potential seismic hazard associated to a few strong intermediate depth earthquakes per century (1940, November 10th, $M_w = 7.7$, $H = 150$ km; 1977, March 4th, $M_w = 7.4$, $H = 94$ km; 1986, August 30th, $M_w = 7.1$, $H = 131$ km; 1990, May 30th, $M_w = 6.9$, $H = 91$ km; 1990, May 31st, $M_w = 6.4$, $H = 87$ km; 2004, October 27th, $M_w = 5.9$, $H = 96$ km). Surrounding Vrancea zone, the several seismic stations belonging to the Romanian Seismic Network are recording seismic and other geophysical, geoelectromagnetic, geodynamic and meteorological parameters. This study investigated: the March 4th, 1977, with moment magnitude $M_w = 7.4$, $H = 94$ km; and October 27th, 2004 earthquake, with moment magnitude $M_w = 5.9$ and epicenter depth of $H = 96$ km. The strength of an earthquake is usually measured on different magnitude scales, but the moment magnitude (M_w) is regarded as the most representative value of the seismic source (Radulian et al. 2004).

This study used time series products of MODIS/Terra land surface temperature/emissivity (LST/E) 8-Day L3 Global 1 km SIN Grid MOD11A2 LST_Day_1 km data over different periods of time provided by Oak Ridge National Laboratory Distributed Active Archive Center (ORNL DAAC) (<http://daac.ornl.gov/MODIS/modis.html>). MODIS/Terra LST/E Daily L3 Global 1 km SIN Grid satellite data were used for comparison of the results.

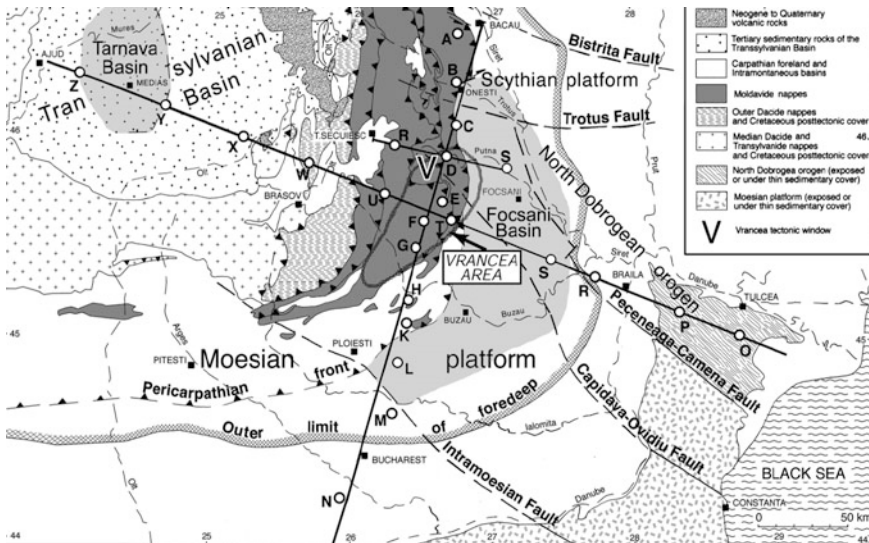


Fig. 1 Vrancea geotectonic active study test site in Romania (after Hauser et al. 2007)

In addition, NOAA-AVHRR data-derived land surface temperature (LST), air temperature and outgoing longwave radiation (OLR) provided by the NOAA/ESRL Physical Sciences Division, Boulder, CO, USA (<http://www.esrl.noaa.gov/psd/>) have been used. Meteorological data around Vrancea region in Romania and anomaly were provided by the National Administration of Meteorology, in addition, in situ meteorological data were compared with satellite data. ENVI 4.7, IDL 6.3 and ORIGIN 8.0 software have been used for satellite images and data processing.

4 Results

Land surface temperature anomalies were obtained by subtracting the multi-year mean from the area-averaged values and dividing by multi-year mean values (Singh et al. 2001). Outgoing Longwave Radiation (OLR), which is the emission to space of terrestrial radiation from the top of the Earth's atmosphere, is controlled by the temperature of the earth and the atmosphere above it, the water vapor content in the atmosphere, and the clouds (Ouzounov and Freund 2004). OLR is a NOAA polar-orbiting satellite derived measurement of the radiative character of energy radiated from the warmer earth surface to cooler space in the 10–12 μm infrared windows. The interpolated OLR data are continuous spatially as well as temporally. The estimates of interpolated OLR values (W/m^2), originally observed by polar orbiting NOAA, are based on dedicated developed algorithms (Tramutoli et al. 2013). Maximum and minimum OLR values ranges, including other parameters, were defined in the analyzed earthquake case.

4.1 Land Surface Temperature

The ability to detect land surface temperatures from space is well developed, and there have been some reports of surface temperature changes prior to earthquakes. These may involve changes in the circulation patterns of groundwater bringing water of different temperature to the surface. This possible precursor is interesting from the remote-sensing viewpoint. TIR (thermal infrared) spectral bands of different satellites like MODIS, NOAA AVHRR, ASTER, Landsat TM/ETM can produce such information. The analysis of the time series LST (Land Surface Temperature) maps for different seismic regions prior strong earthquakes, evidenced building up of thermal anomalies. Based on time-series MODIS/Terra Land Surface Temperature/Emissivity (LST) 8-Day L3 Global 1 km SIN Grid, MOD11A2/LST_Day_1 km was represented land surface temperature variation during 2004 year over Vrancea region (Fig. 2) centered on earthquake of 27th October 2004 epicenter (45.787°N , 26.622°E), $101 \text{ km} \times 101 \text{ km}$ surface area. Time series satellite data analysis revealed increase of land surface temperatures

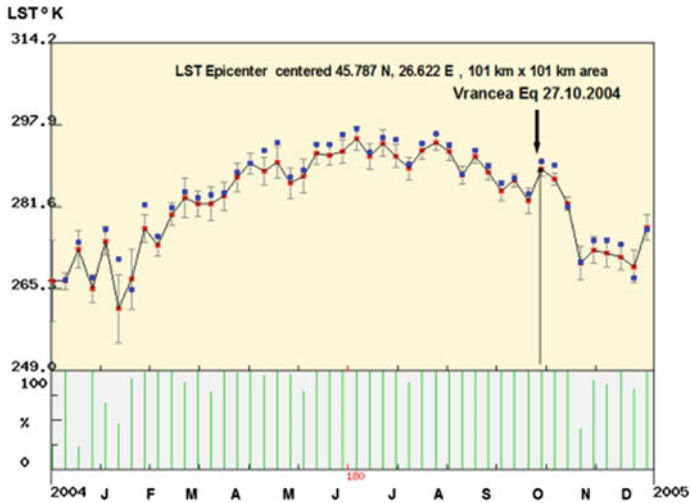


Fig. 2 Land surface temperature (LST) variation during 2004 year over epicentral Vrancea region based on MODIS Terra time series data

LST around epicentral area ranging 5–10 °C. MODIS classification considered Pixel Aggregation Method (PAM) and found that 3559 of 10201 pixels (34.89 %) were belonging to the same class as the center pixel “(5) Mixed Forests”. A clear rise of land surface temperature in epicentral area and surroundings was recorded by MODIS time series satellite data. For October 27th, 2004, $M_w = 5.9$, and epicenter depth of $H = 96$ km in Vrancea area the thermal anomalies of land surface temperature have been developed with about 4–7 days or more prior to the main event depending upon the magnitude and focal depth and disappeared after the main shock.

4.2 Air Temperature

Thermal observations from NOAA AVHRR satellites, NCEP/NCAR Reanalysis, based on climate data 1981–2010 indicate a significant change of the air temperature and near-surface atmosphere layers for strong earthquake March 4th, 1977, $M_w = 7.4$, $H = 94$ km earthquake in Vrancea region. Significant surface air temperature anomaly over Vrancea epicenter region prior to this earthquake was observed with one month before the main shock (Fig. 3).

Immediately after the shock March 4th, 1977 this anomaly continued more several days. Ground observations confirmed satellite data: air and land surface temperature changed simultaneously with thermal anomaly variation.

Ten years of Meteosat TIR observations have been analyzed in order to characterize the TIR signal behavior at each specific observation time and location.

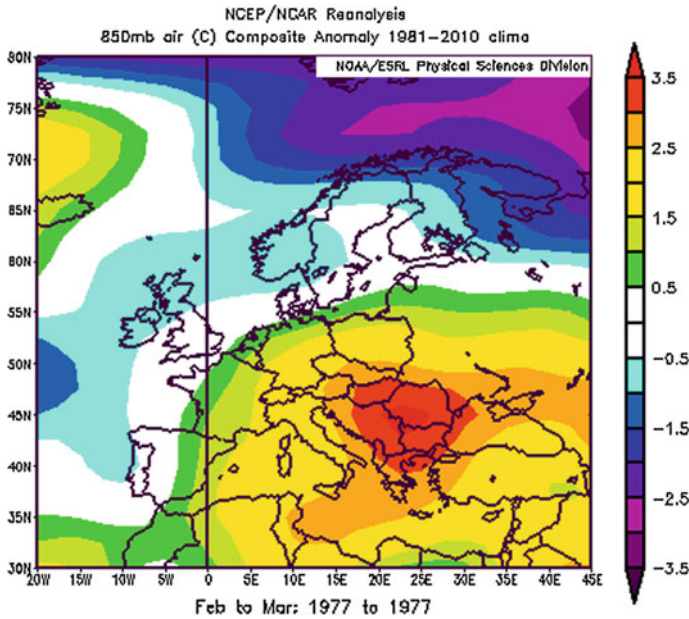


Fig. 3 Air temperature anomaly over Vrancea region one month before March 4th, 1977 Mw = 7.4, H = 94 km, earthquake

Space-time TIR signal transients have then been analyzed, both in the presence (validation) and in the absence of seismic events, looking for possible space-time relationships. In order to study the relationship between the air temperature and 27th October 2004 earthquake, there have been analyzed time-series of mean daily air temperature and anomaly data for period of 15 October–15 November 2004, on the base period of normal 1981–2010 temperatures around Vrancea region provided by NOAA satellites.

The positive air temperature anomaly started developing to North West and South East of the epicentral area, air temperature showing a rise of around 4.8–8 °C during 24–27 October 2004 (Fig. 4), in good correlation with in situ measurements, which revealed a pronounced increase of air temperature over Vrancea region. After the main shock of 27th October, during 27 October–3 November 2004, air temperature recorded a gradual increase with a maximum of 5 °C between 30 October and 3 November.

4.3 Outgoing Longwave Radiation (OLR)

Thermal anomalies before strong earthquakes are observed at different levels, starting from the ground surface up to the top of clouds altitude. The most

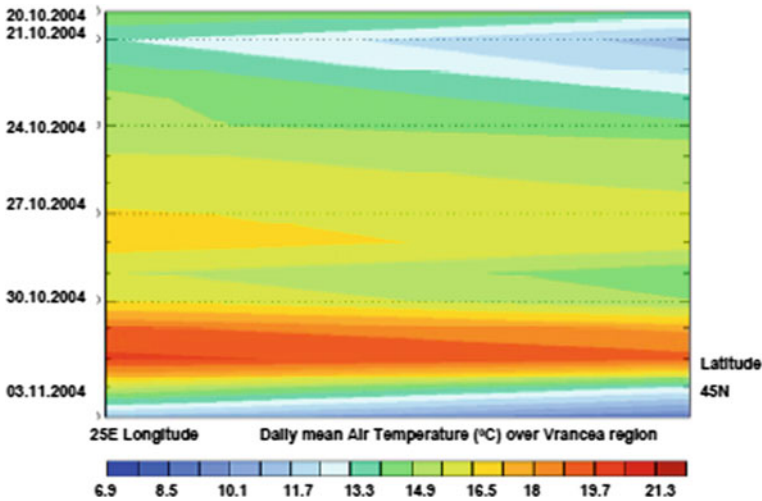


Fig. 4 Daily mean air temperature over Vrancea region before and after Vrancea 2004, October 27th earthquake

promising presignal is the Outgoing Longwave Radiation (OLR) anomaly measured at the top of clouds level. Its advantage is that it is measured within the infrared transparency window of 8–12 μm and does not separate clouds.

For October 27th 2004, $M_w = 5.9$, and epicenter depth of $H = 96$ km in Vrancea area the thermal anomalies of OLR have been developed with about 4–7 days or more prior to the main event function of magnitude and focal depth and disappeared after the main shock. OLR registered anomalies ranged 32–48 W/m^2 higher than the normal values for the same period of time and 10 years of measurements.

Figure 5 presents daily means OLR variation between 20 October 2004 till 3 November 2004, which evidenced gradually increase of the outgoing long-wave radiation OLR emitted by land surface in Vrancea epicentral area before 5.9 M_w earthquake registered on October 27th 2004. The magnitude of the recorded mean OLR anomalies increased firstly starting from 24 October 2004, with a maximum value between 25 and 26 Octobers and then decreased gradually till 27th October in the morning, after that increased again between middle of the day 27th October and 30th October. OLR anomalies covered an extended area described by latitudes 45°N–47°N and longitudes 25°E–27°E and were distributed along the fault zone system in the Vrancea region.

The interpolated OLR data are continuous spatially as well as temporally. The estimates of interpolated OLR values (W/m^2) originally observed by polar orbiting NOAA are based on dedicated developed algorithms. Maximum and minimum OLR values ranges including other parameters were defined in each analyzed earthquake case.

The increase in air and land surface temperature as well as of OLR near epicentral areas can be attributed to enhanced greenhouse gas emission from the

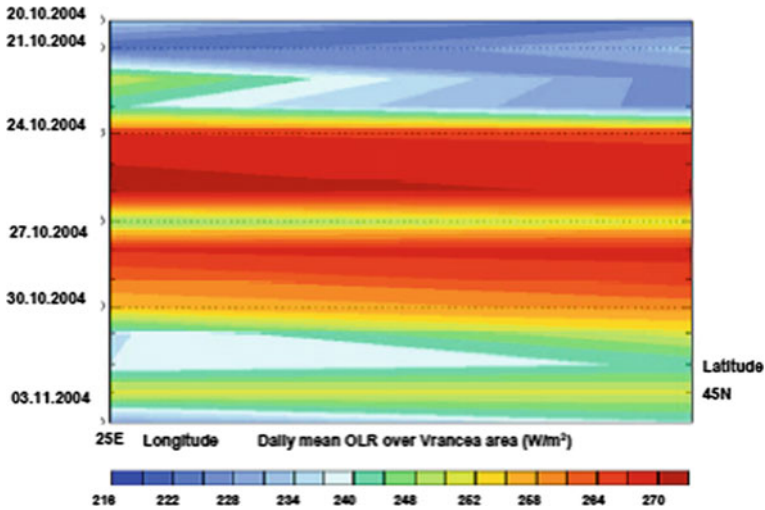


Fig. 5 Daily mean OLR over Vrancea region before and after Vrancea 2004, October 27th earthquake

squeezed rock pore spaces and/or to the activation of p-holes in stressed rock volume and their further recombination at rock-air interface. OLR is dependent of local meteorological parameters temperature and humidity and changes in these variables may be responsible for anomalous OLR values.

5 Conclusions

Earthquake precursors, including thermal anomalies research in Vrancea seismic active area, are developing in the direction of seismic activity monitoring and close integration with ground observations. The anomalies of air and land surface temperatures, as well as of outgoing longwave radiation observed some days to weeks before main seismic shocks, provide early warning signals in all analyzed earthquake test cases. The present results show existence of coupling between lithosphere-surfacesphere-atmosphere associated with preparation and seismic event occurring. Such observations demonstrate promising results, but new data accumulation is required. The nature of air and land surface temperatures, as well as outgoing longwave radiation anomalies, still remain unclear. The joint analysis of geospatial and in situ geophysical information will reveal new insights in the field of earthquake hazard assessment. Due to its theoretical and experimental complexity, the scientific research on earthquake prediction still represents one of the most challenging questions in the scientific community.

Acknowledgements This work was supported by Romanian National Authority for Scientific Research, Program STAR, Contract 73/2013 VRAFORECAST and by grant CNDI– UEFISCDI, project number PN-II-PT-PCCA Contract 86/2014 VRAGEO. We are thankful to Oak Ridge National Laboratory Distributed Active Archive Centre (ORNL DAAC) 2014 MODIS subsetted land products, Collection 5.

References

- Choudhury S, Dasgupta S, Saraf AK, Panda SK (2006) Remote sensing observations of pre-earthquake thermal anomalies in Iran. *Int J Remote Sens* 27(20):4381–4396
- Freund F (2011) Seeking out earth's warning signals. *Nature* 473:452
- Geller R (2011) Shake-up time for Japanese seismology. *Nature* 472:407–409
- Hauser F, Raileanu V, Fielitz W, Dinu C, Landes M, Bala A, Prodehl C (2007) Seismic crustal structure between the Transylvanian Basin and the Black Sea, Romania. *Tectonophysics* 430:1–25
- Joyce KE, Belliss SE, Samsonov SV, McNeill SJ, Glassey PJ (2009) A review of the status of satellite remote sensing and image processing techniques for mapping natural hazards and disasters. *Prog Phys Geogr* 32(2):183–207
- Ouzounov D, Freund F (2004) Mid-infrared emission prior to strong earthquakes analyzed by remote sensing data. *Adv Space Res* 33:268–273
- Ouzounov D, Bryant N, Logan T, Pulinetz S, Taylor P (2006) Satellite thermal IR phenomena associated with some of the major earthquakes in 1999–2003. *Phys Chem Earth* 31 (4–9):154–163
- Pan G, Tang DL (2010) Damage information derived from multi-sensor data of the Wenchuan earthquake of May 2008. *Int J Remote Sens* 31:3509–3519
- Radulian M, Bonjer KP, Popescu E, Popa M, Ionescu C, Grecu B (2004) The October 27th, 2004 Vrancea (Romania) earthquake. *ORFEUS Newslett* 7:1
- Singh RP, Bhoi S, Sahoo AK (2001) Surface manifestations after the Gujarat earthquake. *Curr Sci* 80:1376–1377
- Tramutoli V, Aliano C, Corrado R, Filizzola C, Genzano N, Lisi M, Martinelli G, Pergola N (2013) On the possible origin of thermal infrared radiation (TIR) anomalies in earthquake-prone areas observed using robust satellite techniques (RST). *Chem Geol* 339:157–168
- Tronin AA, Hayakawa M, Molchanov OA (2002) Thermal IR satellite data application for earthquake research in Japan and China. *J Geodyn* 33(4–5):519–534
- Zoran M (2010) Earthquake precursors assessment in Vrancea area, Romania by satellite and geophysical in-situ data. *ESA SP-677*:135–141
- Zoran M (2012) MODIS and NOAA-AVHRR land surface temperature data detect a thermal anomaly preceding the 11 March 2011 Tohoku earthquake. *Int J Remote Sens* 33(21):6805–6817
- Zoran M, Neuner J, Mateciuc D, Ciucu C (2008) Geospatial techniques of seismic zones investigation. *Conspress*, Bucharest
- Zoran M, Savastru R, Savastru D (2012) Radon levels assessment in relation with seismic events in Vrancea region. *J Radioanal Nucl Chem* 293:655–663

Part III
Structural Design in Seismic Areas;
Performance-Based Design

Overview of Part III: Structural Design in Seismic Areas; Performance Based Design

Viorel Popa

The topic of this chapter is related to seismic design of buildings. Included papers refers to the proper selection of seismic action in structural design, structural modelling techniques, advanced algorithms for improving the structural design, earthquake induced interaction between structures and non-structural components, hysteretic behavior of masonry walls.

In the paper entitled “[Selecting and Scaling Strong Ground Motion Records Based on Conditional Mean Spectra. Case Study for Iasi City in Romania](#)” the authors present existing solutions for proper selection of ground motion records in seismic design. The procedure to obtain the conditional mean spectrum, as introduced by Baker in 2011, is applied for Iasi City in N-E Romania, the second largest city in Romania in terms of seismic risk. A ground motion prediction model for intermediate-depth earthquakes and average soil conditions is used for evaluation of the uniform hazard spectrum and the conditional mean spectrum at a vibration period of $T = 1.0$ s which is representative for the new stock of residential and office concrete structures in Romania.

The applicability of time-domain approach for the seismic analysis and design of tall buildings subjected to long predominant period ground motions is discussed in the paper entitled “[A Time-Domain Approach for the Performance-Based Analysis of Tall Buildings in Bucharest](#)”. The use of probabilistic seismic hazard analysis to obtain adequate input ground motions is investigated. Strength-based design criteria related to demand-to-capacity ratios for structural members are used to evaluate the performance of a tall structure.

The feasibility of using advanced genetic algorithms to obtain effective earthquake design solutions for new structures is investigated in the paper entitled “[Viscous Damper Distribution using Genetic Algorithms and Pattern Search](#)”

V. Popa (✉)

Department of Concrete Structures, Technical University of Civil Engineering,
Iasi, Romania
e-mail: vpopa@utcb.ro

Optimization". The aim of this study is to expand existing research regarding the use of genetic algorithms to find the optimal damper distribution in a given structure. This case-study refers to finding of the optimal damper distribution using a genetic algorithm, a pattern search algorithm or a direct descent method. The algorithms are programmed in order to minimize the maximum drift of the structure.

In the paper "**Unidirectional Cyclic Behavior of Old Masonry Walls in Romania**", data regarding the hysteretic behavior of masonry walls as observed from structural testing is presented. Such data is indispensable in evaluation of the seismic vulnerability of existing masonry structures. The structural testing program included six masonry specimens. The masonry walls were designed and built according to the state of practice in Romania. Local materials were used for construction of the specimens. The testing series included two specimens retrofitted by carbon fibre jacketing.

The sensitive issue of earthquake induced interaction between the main structure and the so called "non-structural" components of a building is addressed in the paper "**Influence of the Infill Panels Masonry Type on the Seismic Behaviour of Reinforced Concrete Frame Structures**". This study refers to the structural behaviour of masonry infilled concrete frames subjected to seismic in-plane loading. In the numerical model, infilled masonry walls were modelled as equivalent struts. Nonlinear push-over analyses were carried out for a range of configurations of the outer masonry infills. Bare frame behaviour and masonry infilled frame behaviour were compared. The influence that the ground floor infill absence on the lateral capacity of the concrete frame is analysed as well.

Influence of the Infill Panels Masonry Type on the Seismic Behaviour of Reinforced Concrete Frame Structures

Mircea Bârnaure, Ana Maria Ghiță and Daniel Nicolae Stoica

Abstract A diverse range of masonry infill walls is frequently used for low and medium rise reinforced concrete residential and office buildings. Exterior and interior partitioning walls are usually regarded as non-structural elements, even though masonry infill panels alter the seismic behaviour of buildings. Under earthquake loadings, the influence of infill panels may significantly increase stresses developed in some structural elements of the building. Residential and office buildings that have ground floor commercial or parking spaces develop a particularly dangerous pattern, where soft storey mechanisms might lead to premature failures. This paper examines the structural behaviour of masonry infilled RC frames under in-plane loading. A numerical modelling approach is adopted. Infill masonry walls are modelled as equivalent single diagonal struts. This model depicts the general behaviour of a building adequately enough, even if it cannot accurately reproduce local effects resulting from the interaction between frames and infill panels. Nonlinear push-over analyses are carried out for a range of alternative configurations of an outer wall of a building. Bare frame and masonry infilled frame behaviour are compared and the influence of masonry types is assessed. Subsequently, the influence that the ground floor infill walls absence exerts on the failure pattern is analysed. Conclusions reflect the influence that masonry infills have on the behaviour of RC frames for in-plane lateral loads.

Keywords Masonry infill · Earthquake · Soft storey · Nonlinear modelling

M. Bârnaure (✉) · A.M. Ghiță · D.N. Stoica
Faculty of Civil, Industrial and Agricultural Buildings, Technical University
of Civil Engineering, Bucharest, Romania
e-mail: mircea.barnaure@utcb.ro

A.M. Ghiță
e-mail: ana.ghita@utcb.ro

D.N. Stoica
e-mail: stoica@utcb.ro

1 Introduction

Reinforced concrete frame structures are commonly used in seismic areas for low and medium rise residential and office buildings. For such structures, exterior walls and interior partitions are at times built using masonry introduced as infill between frame members.

In a frame's structural design, the interaction between the frame and the infill is sometimes ignored, the infill being considered to have no influence on the building's structural behaviour, except for its mass. This would be appropriate if the frame and the infill panel were separated by a sufficient gap in-between. Yet this approach is rarely used in common practice due to difficulties related to connecting the walls and the frame together. The infill must withstand out-of plane loads, allow free in-plane deformations and ensure good thermal and sound insulation.

The interaction between infill panels and frames alters a structure's earthquake behaviour through global and local effects. Global effects consist of an increase in lateral stiffness and an increase of the building's plan and/or elevation stiffness irregularity. The latter is due to non-symmetrical geometry and positioning of facade and partition walls. Local effects consist of compression forces and bending moments modifications in frame members, and increased stresses in masonry panels.

Real interaction between the infill panel and the frame results in improved performance of the frame in some cases, and in premature failure in others.

Experimental testing done by Mehrabi et al. (1996) showed that masonry infill is always beneficial on frame behaviour. This observation is confirmed by Kam et al. (2010) and Dhakal (2010) who investigated the behaviour of reinforced concrete buildings with masonry infill walls during the 2010 Canterbury earthquake. According to these reports, the buildings had a very good behaviour, with less than 7 % suffering moderate damage.

Other earthquake reports (i.e., Doğangün 2004; Hermanns et al. 2014; Li et al. 2008) showed that frame structures with masonry partition walls can have an unfavourable seismic response and experience severe damage during earthquakes. This happens in particular when less infill walls are present at the ground floor level as compared to the upper stories. For these buildings, a soft storey mechanism can develop after the deterioration of the ground floor masonry walls. The stiffness of the first story is significantly reduced and the excessive deformation demands for the ground floor columns can lead to serious damage and even to the partial or full collapse of the buildings.

The interaction between the frames and the masonry is taken into consideration by two types of models. The first class of models, generically named macro-models, involve replacing the masonry by equivalent diagonal struts. These models are very easy to implement and offer a good estimation of the overall building behaviour, but cannot accurately represent the local effects of frame-masonry interactions. The second class of models, generically named micro-models, rely on complex analysis using the finite element method. They are much more complex and more difficult to implement, but they allow identifying all modes of failure and all local effects.

Detailed reviews of the most important ways of modelling infilled frames are presented by Crisafulli et al. (2000) and Koutromanos et al. (2011).

The chosen model for this paper involves replacing the masonry by an equivalent single pin-jointed diagonal strut. As shown by Barnaure and Stoica (2015), this modelling assumption does not allow to accurately predict the evolutions of stresses in the frame members, but gives a good estimate of the overall strength and stiffness of the building. The models based on pin-jointed single diagonals were first developed by Polyakov (1960) and later improved by Stafford Smith (1963) and Mainstone (1971). For the paper, the modelling assumptions from the P100-1/2013 Romanian code for seismic design are considered. These are mainly based on the previously mentioned works.

Masonry materials can significantly vary from one country to another and even between regions of the same country. The bricks are made with different local materials and have different shapes. They can be solid or hollow, with various hole sizes and arrangements. The characteristics of the mortars can also vary, as well as the load-bearing bonds geometry. This leads to very different stress-strain characteristics for various masonry types, as shown by Kaushik et al. (2007). The type of masonry strongly influences the response of the frame structure Zovkic et al. (2013). Research done by Celarec et al. (2012) shows that of all the parameters that influence the seismic response of a given RC frame structure, the most important parameter is the characteristics of the masonry infills.

The structural behaviour of masonry infilled RC frames under in-plane loading is examined. Three materials are taken into account for the infills in order to assess the influence of the masonry types. A particular attention is given to the situation where no infill walls are present at ground floor level, which can modify the failure pattern of the building. The assumptions related to the characteristics of the materials correspond to typical configurations used in Romania. The modelling hypothesis are in accordance with the current European and Romanian regulations. The procedure and the results can therefore be of use to the practicing engineers for the design of reinforced concrete frame structures, which is often made without taking into account the interaction between the infill masonry and the frames.

2 Numerical Modelling

Frame structures with reinforced concrete members and masonry infill are analysed for in-plane earthquake loading. The modelling is conducted using the ETABS 2015 software. Several assumptions are made regarding the configuration of the structure, the characteristics of materials as well as the way the structural elements are modelled.

The analysed structure is considered to have 3 floors. Three types of configurations are analysed for 2, 3 and 4 bay frame structures. The first configuration corresponds to the bare frame structure, where the existence of the infill is ignored. In the second configuration, the infill is considered by means of a pin joined

diagonal frame. For the third configuration, full infills are taken into account for the upper storeys while at ground floor level only the bare frame is considered.

The beams' length and storey's height are chosen at 400 and 300 cm respectively.

The reinforced concrete elements (columns and beams) are modelled using frame elements. The infill is also modelled as an equivalent diagonal strut by using frame elements.

The concrete class is C16/20 and the reinforcement type is PC52 ($f_{yd} = 300$ MPa). The beams are 25×45 cm, with bottom reinforcement $A_s = 3d16$ and top reinforcement $A_s' = 4d16$. The columns have a 30×30 cm section with 8d20 reinforcement.

By assumption, the infill is regarded to be 25 cm thick. Three material types are taken into account: solid bricks, vertically perforated HD bricks and autoclaved cellular concrete (ACC) blocks. Materials used as infill are assumed to have the characteristic values shown in Table 1.

Nonlinear hinges are assigned to the beams and frames (M for beams, P-M for columns).

The vertical and horizontal loads are applied as distributed on each beam. The chosen value for the vertical loads at each level is 50 kN/m. The lateral forces have an inverted triangular distribution.

The infills, when present, are considered to be full, without door and window openings. They are modelled by means of an equivalent single pin-jointed diagonal strut. The height of the diagonal is defined as $0.1D$, where D is the length of the diagonal. This value is in accordance with the P100-1/2013 (2013) code. Barnaure and Stoica (2015) analyzed the behaviour of infilled frame structures for various values of the diagonal height from the scientific literature and concluded that the $0.1D$ value leads to the most accurate results of all the considered values.

An idealized bilinear behaviour is considered for the diagonal masonry strut. The strut has constant stiffness until the resistance of the infill panel (F_{Rd}) is reached. For a higher imposed displacement, the diagonal stress is assumed to remain constant. The infill's resistance is calculated by considering three basic failure modes, with the corresponding equivalent failure compressive forces: sliding shear along horizontal joints ($F_{Rd,1}$), diagonal tension ($F_{Rd,2}$) and crushing in the corners that are in contact with the frame ($F_{Rd,3}$). The values of these forces are computed using the equations from P100-1/2013 code for seismic design.

Table 1 Characteristics of the materials that are used as infill

Masonry type	E_z (N/mm ²)	f_b (N/mm ²)	f_{kh} (N/mm ²)	f_m (N/mm ²)	f_d (N/mm ²)	f_{dh} (N/mm ²)	f_{vd0} (N/mm ²)
Solid bricks	5844	15	5	10	3.08	1.78	0.16
Perforated bricks	3302	10	3	7.5	1.74	0.47	0.13
ACC blocks	2200	5	2	6	1.45	0.31	0.08

$$F_{Rd} = \min(F_{Rd,1}, F_{Rd,2}, F_{Rd,3}) \tag{1}$$

$$F_{Rd,1} = f_{vd0} \cdot A_{pan} \cdot k_{1,pan} \tag{2}$$

$$F_{Rd,2} = f_{vd0} \cdot A_{pan} \cdot k_{2,pan} \tag{3}$$

$$F_{Rd,3} = \min(F_{Rd,31}, F_{Rd,32}) \tag{4}$$

$$F_{Rd,31} = f_d \cdot b_{col,eq} \cdot t_p \cdot k_{3,pan} \cdot k_{5,pan} \tag{5}$$

$$F_{Rd,32} = f_{dh} \cdot A_{pan} \cdot k_{4,pan} \tag{6}$$

The values considered for the k_1 to k_5 coefficients are shown in Table 2.

The following notations were made in the previous equations:

- f_d the design compressive strength of masonry perpendicular to the bed joint;
- f_{dh} the design compressive strength of masonry parallel to the bed joint;
- f_{vd0} the design initial shear strength of masonry under zero compressive stress;
- $A_{pan} = h_p \cdot l_p$ the area of masonry panel;
- h_p the height of the masonry panel;
- l_p the length of the masonry panel;
- t_p the thickness of the masonry panel;
- $\lambda_p = h_p/l_p$ the shape factor of the infill panel;
- $b_{col,eq}$ the equivalent width of the column, computed using (Eq. 7);

$$b_{col,eq} = \sqrt[4]{6 \cdot (I_1 + I_2)} \tag{7}$$

where I_1 and I_2 the moments of inertia of the columns in the plane of the infill.

The computed values for the maximum compressive force that can be withstood by the equivalent diagonal, depending on the masonry type, are shown in Table 3.

Table 2 Values of k_1 – k_5 coefficients

$\lambda_p = h_p/l_p$	k_1	k_2	k_3	k_4	k_5
0.75	1.45	2.15	0.512	0.125	1.46

Table 3 Maximum compression force in the equivalent diagonal

Masonry type	$F_{Rd,1}$ (kN)	$F_{Rd,2}$ (kN)	$F_{Rd,31}$ (kN)	$F_{Rd,32}$ (kN)	F_{Rd} (kN)
Solid bricks	229	339	172	222	172
Cored bricks	191	283	113	59	59
ACC blocks	114	170	106	39	39

3 Results and Discussion

Numerical analyses show that the infills have an important influence in terms on stiffness on the building. The ratio between the initial stiffness of a certain configuration and the stiffness of the corresponding bare frame is shown in Fig. 1. For all types of configurations, the masonry infill lead to an important increase. The number of bays has no influence on this increase in stiffness due to the introduction of infills. The only exception appears for full solid bricks infills, where the ratio between the initial stiffness of the infilled frame and the bare frame is 9.60 for the 2 bays, 10.75 for the 3 bays and 13.56 for the 4 bays configurations. Stiffer and stronger masonry leads to higher initial stiffness for the building. The lowest increase in stiffness is obtained for soft-storey configurations with ACC infills, with a value as low as 2.01.

This modification of the building stiffness is very important for the seismic design of the building. The increase in lateral stiffness leads to lower period for the fundamental mode of the building. This could, depending on the design response spectrum, correspond to higher peak acceleration.

This increase in stiffness also leads to lower values for the story drifts. In Fig. 2, the ratios between the maximum story drift for a given configuration and the maximum drift of the same story for the corresponding bare frame are shown for 3 bays structures. The values of the drifts do not decrease with the same value for all the stories. This means that the presence of infills influences the deformed shape of the building, and therefore the value and distribution of stresses between the members.

The characteristics of masonry influence the way the structure deforms under combined vertical and lateral loads. In Fig. 3, the ratios between the maximum story

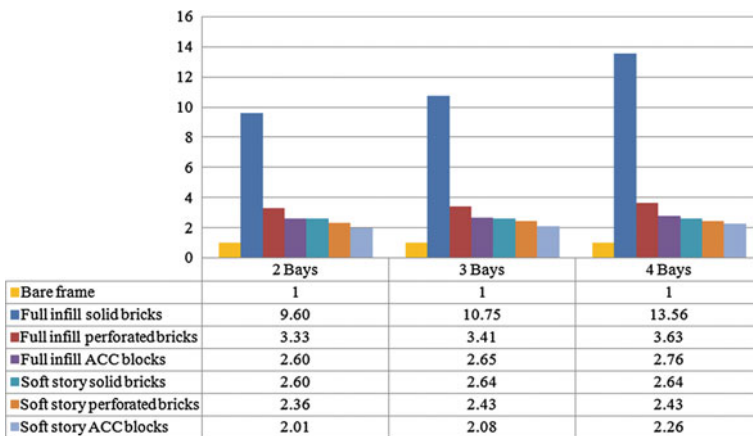


Fig. 1 Ratio between the initial stiffness of a given configuration and the stiffness of the corresponding bare frame

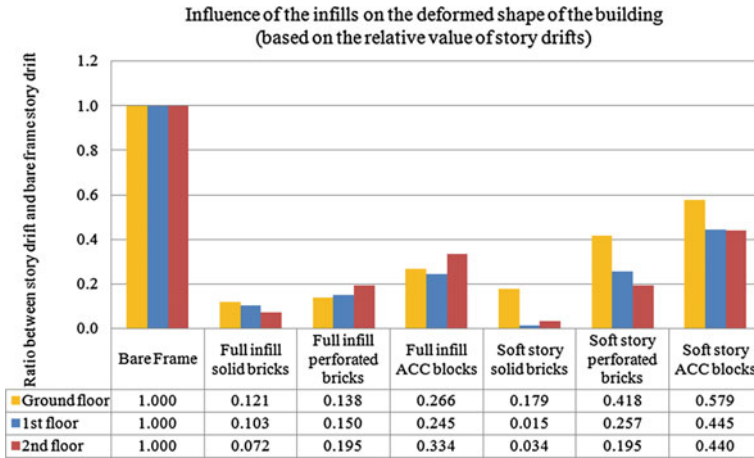


Fig. 2 Ratios between the maximum story drift for a given 3 bays configuration and the maximum drift of the same story for the corresponding bare frame

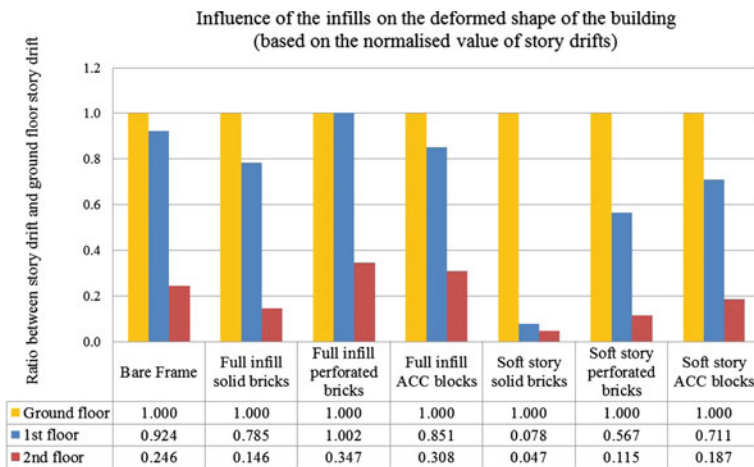


Fig. 3 Ratios between the maximum story drift and the maximum ground floor drift for 3 bays structures

drift and the maximum ground floor drift are shown for 3 bays structures. When compared to the bare frame, introducing full infills made using solid bricks leads to higher drifts occurring at the ground floor level, as compared to the upper stories. On the contrary, introducing full infills made using perforated bricks leads to lower drifts at the ground floor as compared to the upper levels.

A particular case of deformation is seen for soft story configurations. For this particular situation, the deformation occurring at the ground floor level is much higher than the deformation occurring in the upper levels. For soft story

configurations with solid bricks infills, the value of the ground floor drift is 13 times higher than that of the 1st story drift and 21 times higher than that of the 2nd story.

When compared to the bare frame case, solid brick infills influence the structural behaviour the most, while the ACC infills have the lowest influence. The behaviour of structures having perforated bricks is in-between these extremes, closer to those with ACC infills.

The behaviour of the structure with ACC infills is very similar to that of the bare frame structure. This is due to the ACC's low modulus of elasticity and also to the diagonal's compression failure occurring at small stresses. The behaviour can be noticed in both the base shear-displacement curves (Fig. 6) and in the maximum displacement figures that show the plastic hinges' position (Fig. 4). It is to be noted that, while the frame behaviour is not significantly influenced, special measures might be necessary in order to ensure that ACC infill failure does not endanger life safety, as ACC has a low in-plane deformation capacity (Costa et al. 2011).

The behaviour of the structure having solid brick infills strongly differs from that of the bare frame structure. Masonry's modulus of elasticity is high and its equivalent diagonal can withstand forces 4 times greater than those withstood by diagonals which emulate ACC infills. Consequently, very few plastic hinges develop in beams before structural failure is reached (Fig. 2). This structural failure corresponds to ground floor columns reaching their strength capacity under combined bending and axial loads (Fig. 5).

As seen in the force-displacement graphs (Fig. 6), the structures having brick infills are stiffer and can withstand much higher forces before post-elastic deformations start to develop. Yet, these structures show a much less ductile behaviour compared to bare frames, their maximum displacement being significantly lower. As plastic hinges no longer appear at beams' ends, these structures have a much lower capacity to dissipate energy. In the force-displacement graph, the area beneath the graph's curve represents the required energy (work) needed to deform the building until collapse. For the configurations taken into account, this energy is smaller for the infilled structures than for the bare frames.

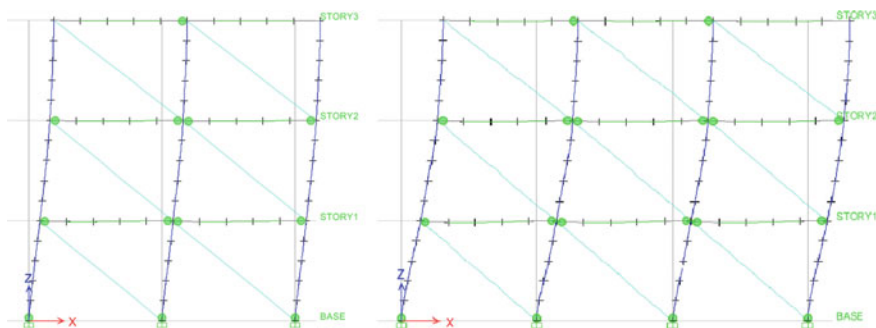


Fig. 4 Plastic hinges at maximum displacement for 2 and 3 bays structures with ACC infills

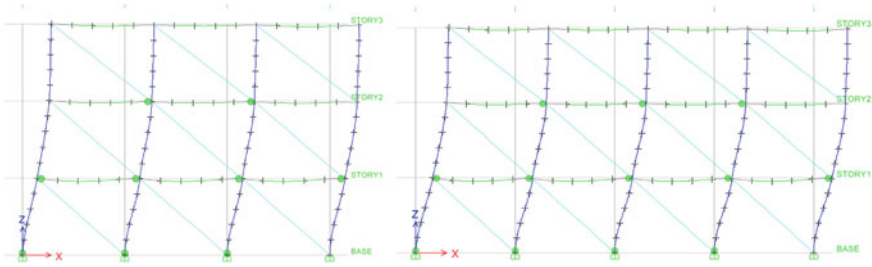
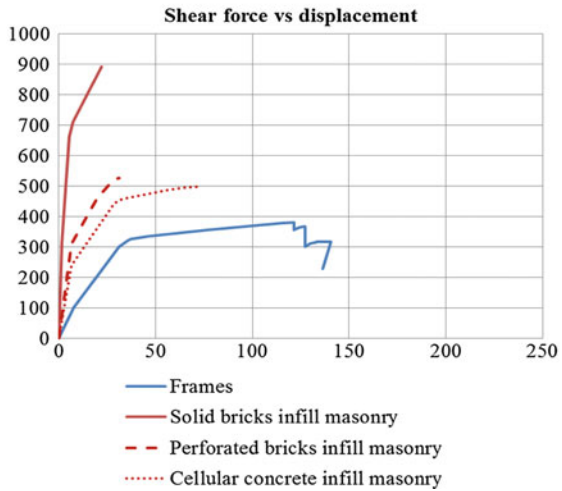
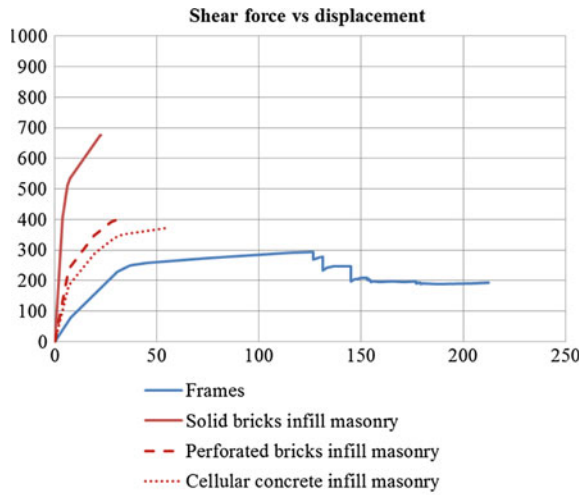


Fig. 5 Plastic hinges at maximum displacement for 3 and 4 bays structures with solid bricks infills

Fig. 6 Base shear (kN) versus displacement (mm) for 3 and 4 bays structures



In the case of soft-storey buildings with solid brick infills, significant horizontal displacement occurs at ground floor level only, while the upper levels remain practically undeformed. For the 3 bays structure, upper levels storey drifts at ultimate displacement are 13 times and 21 times lower than the ground level drift (Fig. 3). Similar values are obtained for the 2 and 4 bay structures. Thus, the fact that plastic hinges only develop at the ground floor level (Fig. 7), before reaching structural failure, is explained.

For the soft-storey buildings with ACC infills, upper levels inter-storey drift values are comparable to the ground floor ones. The value of the drift of the 1st floor is only 1.4 times lower than the drift of the ground floor (Fig. 3). Due to this fact, plastic hinges can develop in a large number of members before structural failure is reached (Fig. 8).

In terms of base shear and displacements (Fig. 9), the plotted curves for soft storey structures with ACC or perforated brick infills are almost identical to the plotted curves corresponding to bare frames. The maximum displacement for these

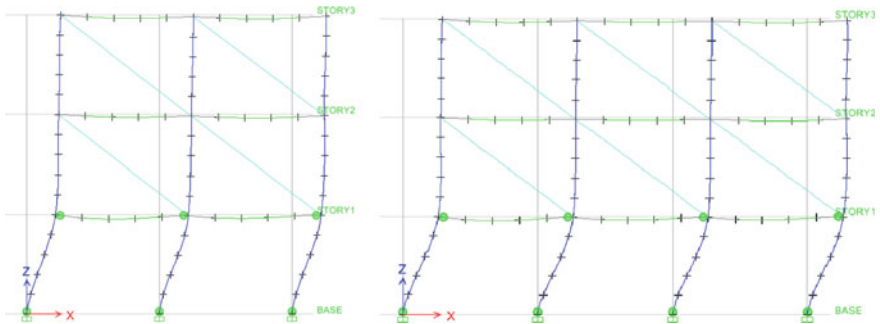


Fig. 7 Plastic hinges at maximum displacement for 2 and 3 bays soft storey structures with solid bricks infills

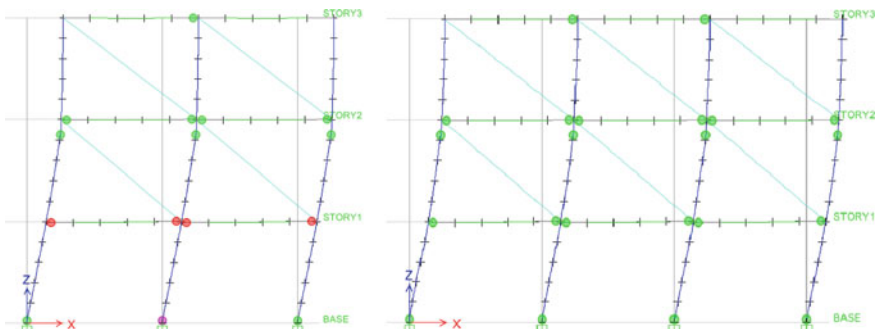


Fig. 8 Plastic hinges at maximum displacement for 2 and 3 bays soft storey structures with ACC infills

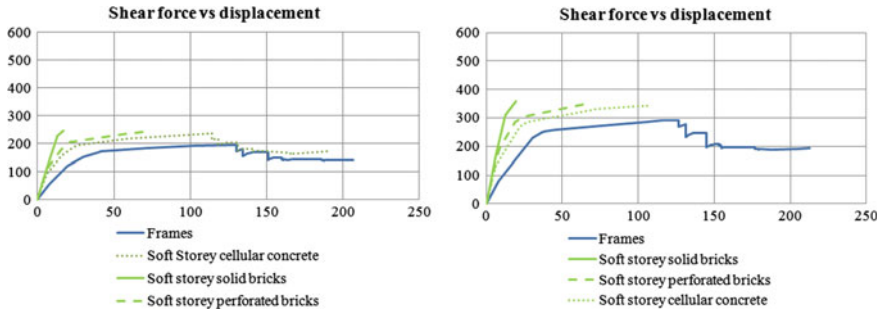


Fig. 9 Base shear (kN) versus displacement (mm) for 2 (*left*) and 3 (*right*) bays soft-storey structures

infilled structures is slightly lower and the base shear is somewhat higher, however they still display high ductility.

On the contrary, soft-storey configurations with solid bricks infills display very low ductility. If we compare, in the force-displacement graph (Fig. 9), the area beneath the curves for the bare frame and the solid brick infill frame we can estimate the energy required in order to deform the building until collapse. This energy is much lower in the case of buildings with solid bricks infills, which means that these types of buildings have a much more unfavourable behaviour and are more likely to show severe damage during earthquakes.

In Fig. 10 (right), the ratios between the input energy for which the building is not damaged and the corresponding energy for the bare frame are shown for 2 and 3 bays configurations. The computed values of the ratio vary from 1.356 for soft story

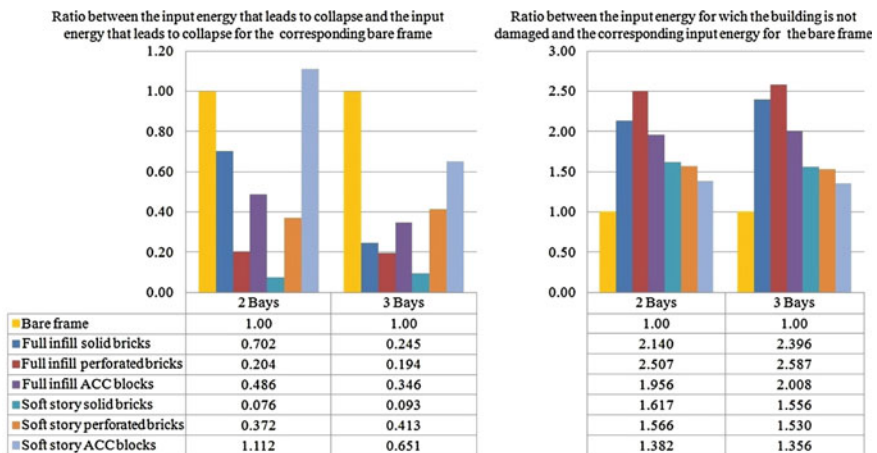


Fig. 10 Ratio between the input energy that leads to collapse for a given configuration and the input energy for the corresponding bare frame (*left*). Ratio between the input energy for which the building is not damaged and the corresponding energy for the bare frame (*right*)

configurations with ACC infills up to 2.587 for full infills with perforated bricks. This means that RC frame structures with brick infills can withstand moderate earthquakes with practically no damage. The statement corresponds to previous earthquake knowledge (Kam et al. 2010).

On the contrary, in the case of more intense earthquakes, the analyzed infilled structures show a less favourable behaviour than the bare frames, with the exception of the 2 bays soft story configuration with ACC infills. In Fig. 10 (left), the ratios between the input energy that leads to collapse and the corresponding energy for the bare frame are shown. For the full infills, the ratio varies from a maximum of 0.702 for 2 bays with solid bricks to a minimum of 0.194 for 3 bays with perforated bricks. For the soft story configurations, the minimum value of the ratio is 0.076 for solid bricks infills.

4 Conclusions

The numerical simulations show that masonry infills can influence the seismic behaviour of reinforced concrete framed structures, and therefore such masonry elements must be taken into account when designing the building.

Infill materials with low stiffness and strength values (such as ACC blocks) do not have a significant influence over a structure's behaviour, especially when compared to the structural behaviour of a bare frame. This can be explained by the fact that a building's stiffness along with frame members stress distribution is not significantly altered by the infill's presence. Yet, particular care must be taken in order to ensure that infill failure does not endanger life safety.

Infill materials with high stiffness and strength (solid or perforated bricks) can significantly modify the structural behaviour of a bare frame. Firstly, the building's stiffness is 2 to 13 times higher and secondly, frame members' stresses distribution is modified such that the building's failure pattern is different. This can be beneficial for low and moderate intensity earthquakes, as the building practically remains in the elastic state and no damage occurs. In the case of high intensity earthquakes, the lack of deformation capacity (ductility) can lead to a much faster collapse of a building. Given the hypothesis considered in this paper, the input energy required for the structure to reach collapse can be 5 times higher for the bare frame structure when compared to the structure having solid brick infills.

A particularly unfavourable structural behaviour is obtained for soft-storey configurations with solid bricks infills. For this situation, significant horizontal displacement occurs at ground floor level only, while the upper levels remain practically undeformed. For the 2 bays structure, the computed story drift at the ground level is 13 times higher than the drift of the 1st level and 21 times higher than that of the 2nd level at ultimate displacement. Because of this, plastic hinges at beams ends only develop at the ground floor level and the building displays very low ductility. The energy required in order to deform the building until collapse is 13 times lower for soft storey configurations with solid bricks infills than for the

bare frames. This means that these configurations are very unfavourable and can lead to serious damage and even to the partial or full collapse of the buildings during earthquakes.

References

- Barnaure M, Stoica DN (2015) Analysis of masonry infilled RC frame structures under lateral loading. *Math Modell Civ Eng* 11(1):13–23
- Celarec D, Ricci P, Dolšek M (2012) The sensitivity of seismic response parameters to the uncertain modelling variables of masonry-infilled reinforced concrete frames. *Eng Struct* 35:165–177
- Costa AA, Penna A, Magenes G (2011) Seismic performance of autoclaved aerated concrete (AAC) masonry: from experimental testing of the in-plane capacity of walls to building response simulation. *J Earthq Eng* 15(1):1–31
- Crisafulli FJ, Carr AJ, Park R (2000) Analytical modelling of infilled frame structures—a general review. *Bull NZ Soc Earthq Eng* 33(1):30–47
- Dhakal RP (2010) Damage to non-structural components and contents in 2010 Darfield earthquake. *Bull NZ Soc Earthq Eng* 43(4):404–411
- Doğangün A (2004) Performance of reinforced concrete buildings during the May 1, 2003 Bingöl earthquake in Turkey. *Eng Struct* 26(6):841–856
- Hermanns L, Fraile A, Alarcón E, Álvarez R (2014) Performance of buildings with masonry infill walls during the 2011 Lorca earthquake. *Bull Earthq Eng* 55(12):1977–1997
- Kam WY, Pampanin S, Dhakal RP, Gavin H, Roeder CW (2010) Seismic performance of reinforced concrete buildings in the september 2010 Darfield (Canterbury) earthquakes. *Bull NZ Soc Earthq Eng* 43(4):340–350
- Kaushik HB, Rai DC, Jain SK (2007) Stress-strain characteristics of clay brick masonry under uniaxial compression. *J Mater Civ Eng* 19(9):728–739
- Koutromanos I, Stavridis A, Shing PB, Willam K (2011) Numerical modeling of masonry-infilled RC frames subjected to seismic loads. *Comput Struct* 89(11):1026–1037
- Li B, Wang Z, Mosalam KM, Xie H (2008) Wenchuan earthquake field reconnaissance on reinforced concrete framed buildings with and without masonry infill walls. In: *The 14th world conference on earthquake engineering*. Beijing, China
- Mainstone RJ (1971) Summary of paper 7360. On the stiffness and strengths of infilled frames. In: *ICE Proceedings*, vol 49, issue no 2, p 230. Thomas Telford
- Mehrabi AB, Shing PB, Schuller MP, Noland JL (1996) Experimental evaluation of masonry-infilled RC frames. *J Struct Eng* 122:228
- P100-1/2013 (2013) Code for seismic design – Part I – Design prescriptions for buildings. Ministry of Regional Development and Public Administration, Bucharest, Romania (in Romanian).
- Polyakov SV (1960) On the interaction between masonry filler walls and enclosing frame when loaded in the plane of the wall. *Earthq Eng* 36–42
- Stafford Smith B (1963) Lateral stiffness of infilled frames. *J Struct Div ASCE* 88(6):183–199
- Zovkic J, Sigmund V, Guljas I (2013) Cyclic testing of a single bay reinforced concrete frames with various types of masonry infill. *Earthq Eng Struct Dyn* 42(8):1131–1149

A Time-Domain Approach for the Performance-Based Analysis of Tall Buildings in Bucharest

Mihail Iancovici and George Vezeanu

Abstract The performance of tall buildings in earthquake-prone regions has been improved due to more accurate representation of seismic action in design regulations and codes. The current design practice addresses two performance levels and appropriate seismic input representation: (i) the *Service Level*—the standard Response Spectrum Approach is allowed and (ii) the *Collapse prevention level*—nonlinear dynamic analysis approach is required (CTBUH 2008). The applicability of time-domain approach for the seismic analysis and design of tall, flexible buildings, subjected to long predominant period ground motions (so called “Mexico-City effects”) is discussed in our paper. The main techniques used by practitioners to obtain ground acceleration time-series are reviewed and discussed. The study mostly focuses on the use of Probabilistic Seismic Hazard Analysis (PSHA) tool and its derivatives (i.e. Uniform Hazard Spectrum and Conditional Mean Spectrum) approach in order to obtain adequate site-dependent input ground motions to be used in the nonlinear dynamic analyses. The evaluation of structural performance of a case-study tall, flexible steel building structure is done by using strength-based design criteria based on demand-to-capacity ratios (DCR) of members. The “peaks-over-threshold” approach is used in conjunction with strength-based principles in order to check the compliance with deformation-based criteria.

Keywords Vrancea seismic source • Probabilistic seismic hazard analysis • Strong ground motion • Nonlinear dynamic analysis

M. Iancovici (✉)

Department of Structural Mechanics, Technical University of Civil Engineering,
Bucharest, Romania

e-mail: mihail.iancovici@utcb.ro

G. Vezeanu

Department of Tunnels and Strength of Materials, Technical University
of Civil Engineering, Bucharest, Romania

e-mail: vezeanu@utcb.ro

1 Introduction

The seismic hazard generated from the Vrancea subcrustal seismic source (hypocentral depths between 60 and 170 km) is the major concern for structural engineers, especially due to medium-soft soil conditions in Bucharest (Lungu et al. 2000; Vacareanu et al. 2013a).

Tall buildings (20–30 stories), newly built in dense urban and historical areas in Bucharest become more and more common for the city. While several mid-rise buildings (6–15 stories) built in the first three decades of the 20th century collapsed in Bucharest during the strong Vrancea earthquakes of November 1940 ($M_w = 7.7$, one building) and March 1977 ($M_w = 7.4$, 32 buildings), so far there is no evidence on the seismic performance of newly built structures (after 1990) on medium-soft soil conditions (Trendafilovski et al. 2009). The soil conditions in Romania are classified according to Romanian Seismic Design Code P100-1 (2013)—an Eurocode 8 (EN 1998-1) (2004) format, in terms of average shear wave velocity on 30 m from the top- $v_{s,30}$ (Borcherdt and Glassmoyer 1992). For design purposes however, soil conditions are introduced through the control period- T_c as defined by Lungu et al. (1997).

These issues drew the attention on: (i) the seismic analysis framework applicable to tall and super-tall buildings and (ii) the need to incorporate appropriate advanced analysis and design tools into the practical design, for higher-reliability structures, making use of more powerful *time*-domain analysis features.

The full capabilities of time-domain approach and associated random vibration theory tools are not of primary importance in the current analysis and design practice. This is due to (i) uncertainties in the input ground motion modeling, (ii) structural modeling issues, and (iii) nonlinear analysis duration and numerical inconveniences. The time-domain framework is not yet available in a standardized format.

Various standards and codes, e.g. Eurocode 8 (EN 1998-1) (2004), ASCE/SEI 7-10 (2010), PEER (2010) and P100-1 (2013) allow the use of appropriate input strong ground motion records to perform nonlinear time-history response analyses. There is little guidance however on the selection, scaling or generating input motions and thus, doors open for consistent research work.

Thus, due to their complexity and associated risk, tall and super-tall buildings design is less suitable for full standardization. Thus, a “pointy” approach looks to be more appropriate for the performance analysis and design of complex building structures. Moreover, the current Romanian Seismic Design Code P100-1 (2013) provisions require adequate local hazard evaluation for the seismic design of tall buildings.

The nonlinear behaviour of tall buildings on soft soil conditions might be significantly influenced by the soil-structure interaction effect (SSI). Naimi and Naimi (2008) concluded that while the SSI influences the overall behaviour of a tall building, for a given soft soil condition this can significantly vary depending on the input ground motion properties, selection and scaling criteria. The SSI effect might

be beneficial or detrimental for the seismic performance corresponding to a particular input ground motion. Therefore complete soil parameters information from geotechnical investigation, local site effects and the geometry of surrounding ground, are necessary information for the final completion of an adequate full structural design taking into account the SSI effects (Stewart and Tileylioglu 2007; Naimi and Naimi 2008).

In the case of tall and super-tall buildings, the Council on Tall Buildings and Urban Habitat (CTBUH) issued specific recommendations (CTBUH 2008), suggesting two performance levels and associated analysis tools to be used: (i) *Service level*, with *no damage* requirement for spectral demands corresponding to a Mean Recurrence Interval (MRI) of about 50 years and use of standard RSA approach and (ii) *Collapse prevention level*, with *no collapse* requirement for spectral demands corresponding to a MRI of 2475 years and dynamic nonlinear analysis procedure. The procedure requires performing a comprehensive Probabilistic Seismic Hazard Analysis (PSHA) followed by the selection/scaling appropriate pairs of input ground motions by either (i) matching the maximum spectrum, (ii) matching the maximum and minimum spectra or (iii) matching the maximum and minimum Conditional Mean Spectrum-CMS (Baker and Cornell 2006). However there is no consensus on the best approach to be used when selecting appropriate input ground motions for analysis.

The current Romanian Seismic Design Code P100-1 (2013) provides the minimum performance level associated to Life Safety Limit State, corresponding to a MRI of 225 years (20 % exceedance probability in 50 years). In the previous version of code (P100-1 2006) MRI was 100 years. Due to its inherent constraints (higher vibration modes contribution and corresponding behavior factors, soil-structure interaction, the effect of incorporated energy dissipation devices etc.), the RSA procedure is thus applicable with limitations to tall buildings.

Earlier studies, conducted in Romania, on tall, flexible building elastic models, suggested a significant discrepancy between the static, code-based, and dynamic approach—using a large number of spectra-compatible representations of input motions (Iancovici et al. 2010, 2011; Wilson 2015).

The Conditional Mean Spectrum (CMS) represents thus a necessary and a straightforward link between the seismic hazard information and the ground motion records selection at a particular site. The procedure to obtain the Conditional Mean Spectrum (CMS) presented by Baker (2011) is applied in this paper, for the City of Bucharest.

Our paper focuses on the analysis of structural seismic performance in relation with the input motion to be used in the analysis of tall, flexible steel building structures. The main techniques, currently used by practitioners to obtain time-series of ground acceleration, are reviewed and discussed based on available artificial time-series of ground acceleration. First, the discrepancy between the current analysis and design approach and the time-domain approach—using code spectrum—compatible representation are discussed. Then, the seismic hazard-consistent representations, i.e. Uniform Hazard Spectrum (UHS) and the Conditional Mean Spectrum (CMS), are used to investigate the applicability of time-domain approach

in a Performance-Based Analysis and Design framework using a large amount of seismic hazard-consistent, site-dependent input ground motions and the full capabilities of nonlinear dynamic analysis tool and random processes theory tools.

2 The Input Ground Motion for Tall Buildings Response Analysis

Alternatively to RSA approach is to develop a site-dependent time-history analysis framework. This approach requires a comprehensive Probabilistic Seismic Hazard Analysis framework that at the end yields a large database of recorded, scaled or artificially generated input motions, associated to different annual probabilities of exceedance/Mean Recurrence Intervals (MRIs).

Although difficult to implement it in a straightforward manner, when compared e.g. with the design for wind loads (Yeo and Simiu 2011), the local seismic hazard modeling associated to different performance levels becomes more important in the design of complex structures as tall buildings.

Currently, site-dependant time-series (at either macro- and micro-level) are obtained by various available accepted techniques: (i) recorded accelerograms, (ii) simulated accelerograms at various subterranean levels, (iii) simulated ground accelerations at free field, compatible with a prescribed time-history envelope, Fourier amplitude spectrum/power spectrum and (iv) artificial accelerograms compatible with a target acceleration response spectrum/design spectrum.

Various papers and reports are comprehensively reviewing and discussing the methodologies used for the selection of the input ground motion records (Katsanos et al. 2010; NIST 2011).

The design code spectrum-compatible accelerograms (Gasparini and Vanmarcke 1976) are used in the worldwide practice, mostly for design checking purposes. For design purposes, comprehensive time- and frequency-domain analyses on artificially generated time-series are to be performed. Unless a validated input database is available, the analyst is requested to perform preliminary, extensive and complete signal processing analyses on a large number of simulated data, in order to check the adequacy of input motions. Thus, the input parameters (peak values, frequency content, duration, energy etc.) variability, with the prescribed hazard level and the target spectrum shape are validated using available observed records.

Using the procedure proposed by Gasparini and Vanmarcke (1976) and a large number of elastic design spectrum-compatible acceleration time-series corresponding to three soil types (described in terms of control period T_c) and two hazard levels-in terms of exceedance probabilities in 50 years (Level 1–39 % and Level 2–20 %, respectively), Iancovici et al. (2010) concluded that the simulation procedure introduces significant higher power content in narrower frequency bandwidths, associated to lower predominant frequencies. While the response spectrum shape mostly influences the predominant period's mobility and the frequency content of

the input, the hazard level influences the input power amount. These are in line with observed tendencies from available real records, obtained in the same site, from seismic events of different intensities in Bucharest (Lungu et al. 2000). This approach was extensively used in our previous studies on flexible elastic models (Iancovici et al. 2010, 2011) and serves for developing credible artificial input motions used in the present case study.

The frequency content-based (i.e. power spectrum) generation of acceleration time-series has the advantage of removing the structural filtering effect when compared to response spectrum-based approach.

Each of technique is obviously questionable. For instance, motions compatible with the code spectrum for soft soil conditions are less realistic ones-especially in the case of long control period target spectral shape. On the other hand the input motions at subterranean foundation level are influenced, in terms of amplitude and frequency content, by the soil-structure interaction effects, difficult to reproduce by current analysis procedures.

Another technique for selecting/scaling/generating time-series of ground acceleration is the Conditional Mean Spectrum (CMS), proposed by Baker and Cornell (2006). It represents an efficient tool to straightforward connect the seismic hazard information with the input motion at a particular site. This is based on a full Probabilistic Seismic Hazard Analysis (PSHA) approach and provides essential information for the Performance-based Seismic Design.

Adequate ground acceleration time-series, using the target spectrum-compatible generation technique (Gasparini and Vanmarcke 1976), are further obtained and used in the case study.

3 Probabilistic Seismic Hazard-Consistent Approach on the Input Motions

3.1 Uniform Hazard Spectrum (UHS) and Hazard Disaggregation Analysis

In our paper, the seismic hazard analysis for Bucharest is performed for the Vrancea intermediate-depth source only. Several authors (Lungu et al. 2000; Sokolov et al. 2008) discussed on the main contribution of Vrancea source to the seismic hazard for Bucharest and over half of the Romanian territory.

The Probabilistic Seismic Hazard Analysis is performed using the procedure presented by McGuire (1999, 2004). Among various ground motion prediction models developed for the subcrustal seismic sources and proposed in the SHARE regional project for Global Earthquake Model (Delavaud et al. 2012), the Youngs et al. (1997) model is selected in this paper based on the results presented in (Vacareanu et al. 2013a).

The annual rate of earthquake occurrence, above a minimum magnitude is (Kramer 1996; McGuire 2004).

$$v_i = e^{(\alpha - \beta m_{min})} \quad (1)$$

where, α and β are seismicity parameters. The seismicity parameters are obtained processing the ROMPLUS earthquake catalogue of National Institute for Earth Physics of Romania (<http://www.infp.ro/catalog-seismic>) for the Vrancea intermediate-depth seismic source and earthquakes having $M_w \geq 5$. The Maximum Likelihood Method yields $\alpha = 10.3164$ and $\beta = 1.9589$ (Vacareanu et al. 2013b).

The Probabilistic Seismic Hazard Analysis (PSHA) is performed for a given site by considering all the ground motions occurring from earthquakes having any possible magnitude (ranging from the lower bound magnitude to the upper bound magnitude, if any) and/or source-to-site distances within the seismic source area, along with their associated uncertainties.

The frequency of exceedance γ of a given ground motion amplitude y is obtained by the following relationship (McGuire 1999):

$$\gamma(y) = \sum_i v_i \iint f_M(m) f_R(r) P[Y > y | m, r] dm dr \quad (2)$$

where, v_i is the activity rate of the seismic source i , m is the magnitude and r is the source-to-site distance.

The epsilon values ε (i.e. the number of standard deviations by which an observed logarithmic spectral acceleration differs from the mean spectral acceleration given by a ground motion prediction equation—GMPE) are bounded in the range of -3.8 to $+3.8$.

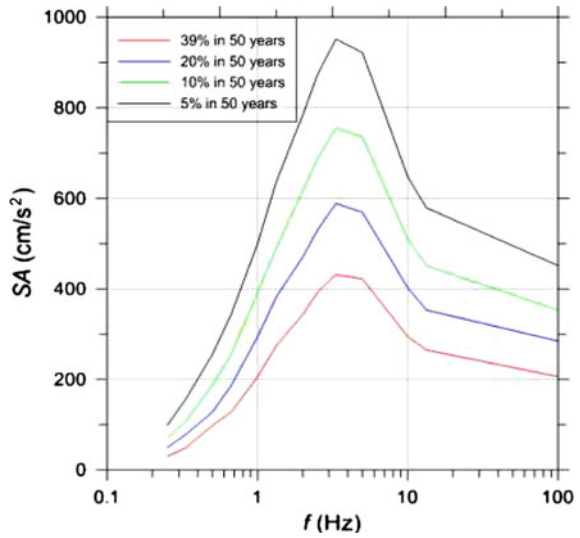
The uniform hazard spectra given in Fig. 1 are computed for four different exceedance probabilities in 50 years, i.e. 39, 20, 10 and 5 %.

The peak ground accelerations having a probability of exceedance of 39 % in 50 years and 20 % in 50 years respectively, are in line with the values given in the previous version of Seismic Design Code in Romania (P100-1 2006) and with the 2013 revised version of code (P100-1 2013), respectively. Of primary study interest is contribution of each earthquake magnitude range corresponding focal depth, on the seismic hazard in Bucharest, using the Youngs et al. (1997) ground motion prediction equation. It has to be noted that the most frequent focal depths are in the range of 90–120 km (1738, 1838, 1977 events) or in the range of 130–150 km (1802, 1940, 1986 events) as given in Marmureanu et al. (2010). The deepest earthquake ever recorded seemed to occurred in 1982 at a 218 km depth ($M_w = 4.1$) as reported by Ismail-Zadeh et al. (2012).

The disaggregation of seismic hazard (McGuire 2004) determines the contribution of each range-magnitude M_w , hypocentral distance R and epsilon ε , to the seismic hazard at a given site.

The disaggregation of magnitude M_w , source-to-site distance R and ε at $T = 2.0$ s (further used in our case study), for the Vrancea intermediate depth seismic source

Fig. 1 Uniform hazard spectra (UHS) for Bucharest



having an exceedance probability of the spectral acceleration in Bucharest of 10 % in 50 years is shown in Fig. 2. The mean causal magnitude yields $M_w = 7.55$, the mean causal source-to-site distance is $R = 214.3$ km and the mean causal epsilon is $\epsilon = 1.84$.

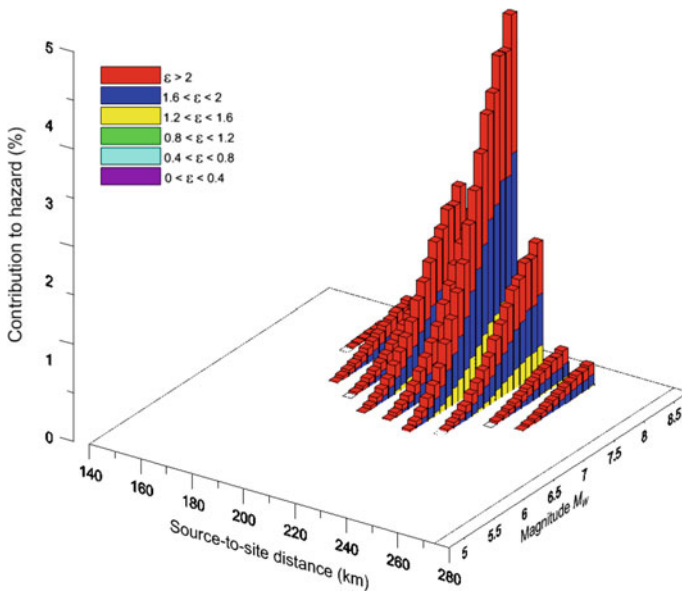


Fig. 2 Disaggregation of magnitude M_w , source-to-site distance R and ϵ for an exceedance probability of 10 % in 50 years of the spectral acceleration in Bucharest at $T = 2.0$ s

The information provided by the disaggregation analysis is further used to develop the Conditional Mean Spectrum (CMS) for Bucharest-city.

3.2 Conditional Mean Spectrum (CMS) for Bucharest

The Conditional Mean Spectrum (CMS) represents a target spectral representation likely caused at a given site by a magnitude (M), hypocentral distance (R) and ε values. The epsilon parameter ε is the number of standard deviations by which an observed logarithmic spectral acceleration differs from the mean spectral acceleration given by a ground motion prediction equation (GMPE), as:

$$\varepsilon(T) = \frac{\ln SA(T) - \mu_{\ln SA}(M, R, T)}{\sigma_{\ln SA}(T)} \quad (3)$$

where, $\mu_{\ln SA}(M, R, T)$ and $\sigma_{\ln SA}(T)$ are the predicted mean and standard deviation of the natural logarithm of spectral acceleration at a certain period T , while $\ln SA(T)$ is the natural logarithm of spectral acceleration.

In Fig. 3 a comparison is given between the (i) median spectrum of the geometric means of absolute acceleration spectral values of horizontal components corresponding to the ground motions recorded in Bucharest area, (ii) the Uniform Hazard Spectrum computed for a probability of exceedance of 10 % in 50 years and (iii) the median spectrum obtained using Youngs et al. (1997) ground motion prediction equation corresponding to mean causal values of $M_w = 7.55$ and $R = 214.3$ km.

Fig. 3 Comparison of (i) median response spectra computed from ground motions recorded in Bucharest area, (ii) UHS (10 % in 50 years) and (iii) median prediction for $M_w = 7.55$ and $R = 214.3$ km

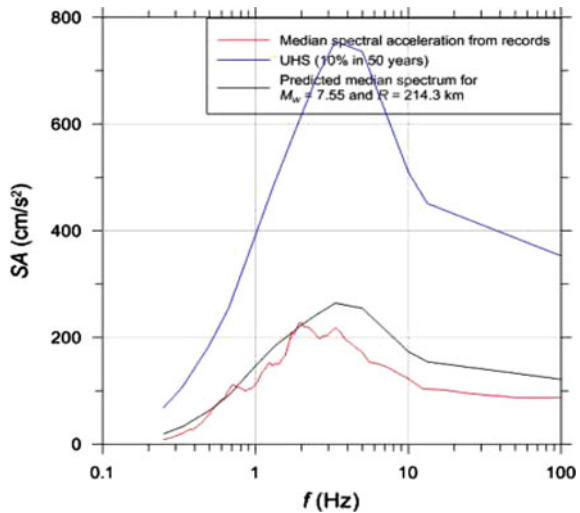
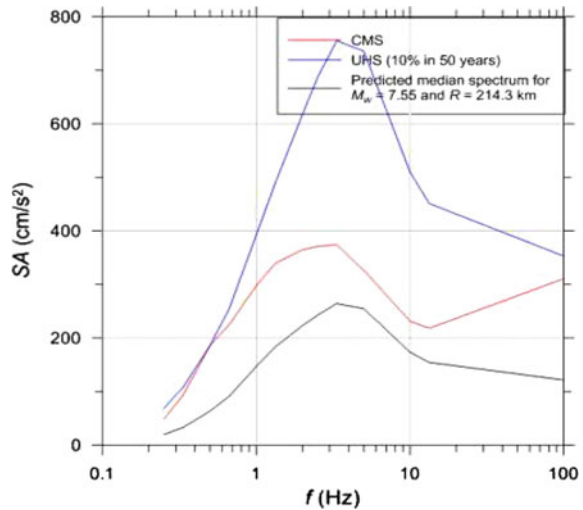


Fig. 4 CMS, UHS (10 % in 50 years) and the median prediction for $M_w = 7.55$ and $R = 214.3$ km



The actual epsilon value for $T = 2.0$ s natural period, obtained for the mean causal value of moment magnitude and source-to-site distance, is 1.35. The CMS for Bucharest-city is plotted in Fig. 4, altogether with the UHS, for a probability of exceedance of 10 % in 50 years and with the mean predicted spectrum, for $M_w = 7.55$ and $R = 214.5$ km.

4 Generation of Input Ground Motions for Seismic Performance Analysis of Tall Buildings

In order to perform the seismic hazard-consistent response analysis, a large set of ground acceleration time-series compatible with the UHS and CMS is generated using the same procedure of code spectrum-compatible generation using SIMQKE I software (Gasparini and Vanmarcke 1976).

A number of 20 accelerograms are selected for the nonlinear dynamic analyses, after performing appropriate signal processing analysis, for each spectral representation—UHS and CMS. Their response spectra and corresponding target spectra are represented in Fig. 5.

The corresponding Power Spectral Density (PSD) functions of artificial input motions are represented in Fig. 6. This indicates that UHS-compatible artificial input motions contain a significant higher power amount, in a larger frequency bandwidth, than the CMS-compatible input motions.

The statistics of input motions parameters is given in Table 1. *Eps* in Table 1 represents the Cartwright and Longuet-Higgins, frequency bandwidth indicator (Kramer 1996; Vanmarcke 2010).

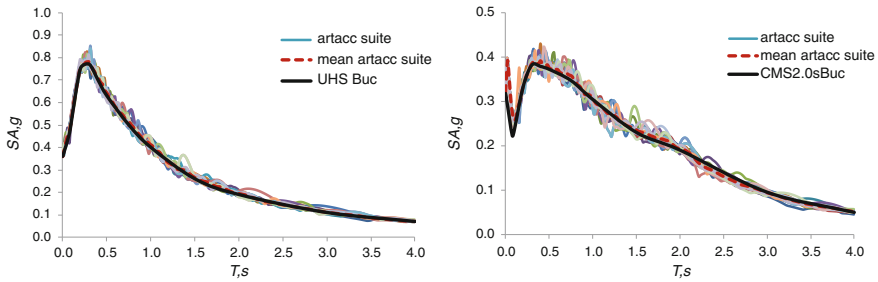


Fig. 5 UHS (left figure) and CMS (right figure) for Bucharest, spectral accelerations and mean spectral acceleration of artificially generated input motions

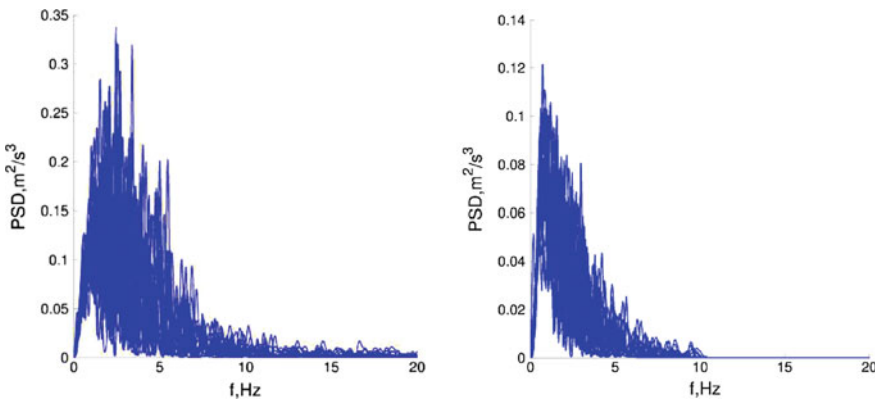


Fig. 6 Power spectral density (PSD) functions of artificial input motions for Bucharest: UHS-based (left figure) and CMS-based (right figure)

Table 1 Statistics of UHS- and CMS-based compatible input ground motions

	PGA, m/s ²	PGV, m/s	PGD, m	T _p , s	Eps
<i>UHS-compatible time-series</i>					
Mean	3.53	0.35	0.24	0.48	0.96
σ	–	0.06	0.12	0.17	0.01
CoV	–	0.16	0.52	0.36	0.01
<i>CMS-compatible time-series</i>					
Mean	3.14	0.25	0.21	1.15	0.99
σ	–	0.04	0.12	0.40	0.00
CoV	–	0.17	0.56	0.35	0.00

It is to be noted that CMS-based time-series are characterized by significant larger predominant periods in conjunction with narrower frequency bandwidth (in the mean sense), when compared to UHS-based ground acceleration time-series.

5 Seismic Response Analysis and Structural Design Issues

For any given input data set and directivity, the structural design should follow the requirement that the capacity exceeds the demand in a reliable manner. From practical design point-of-view, if the internal forces are the interest response parameters, the demand-to-capacity ratio (DCR) would control the structural design through the interaction formula for steel structures given (e.g. EN 1993-1 Eurocode 3 (2005), PEER 2010)

$$DCR_j^{(e)}(t) = \frac{N_{Ed}(t)}{N_{Rd}} + \frac{M_{y,Ed}(t)}{M_{y,Rd}} + \frac{M_{z,Ed}(t)}{M_{z,Rd}} \Big|_{j,e} \leq 1 \tag{4}$$

where, the numerators are the time-instant demand values and the denominators are the associated resistance values of axial force and bending moments respectively, corresponding to a given section (*j*) of an element (*e*). A 14 story steel flexible building (S355 steel grade) with macro-X outer braces, having 58 m height and 21 m by 21 m plan dimensions, is used in our study (Fig. 7). The design was performed according to the Romanian Seismic Design Code (P100-1 2006) for Bucharest-City (*PGA* = 0.24 g and *T_c* = 1.6 s) for medium ductility level (*q* = 4). The full nonlinear SAP2000, 3D model, has the fundamental natural periods of 1.97 and 1.94 s (sways) and 1.36 s (for fundamental torque component). The damping ratio is set to 3 %—for the fundamental sway modes and the Rayleigh damping model is selected for constructing the damping matrix of the superstructure.

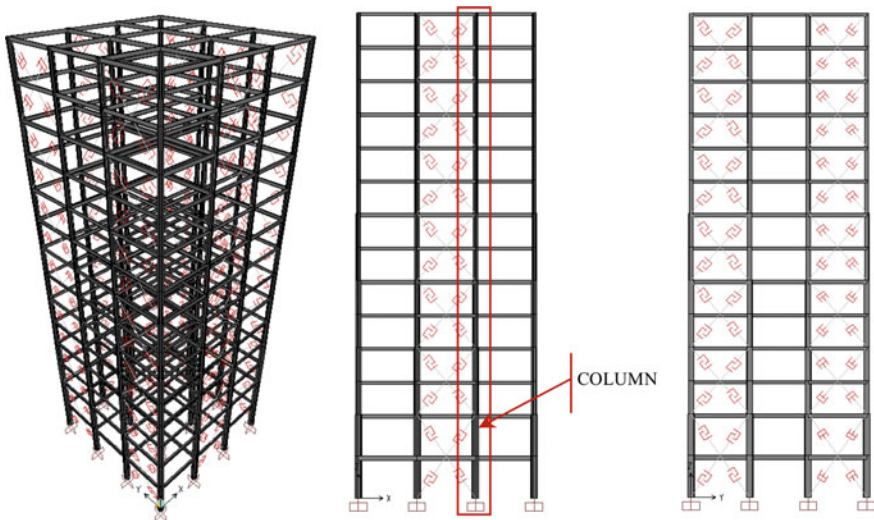


Fig. 7 14 story steel structure model: 3D and elevation views

The columns and beams are modelled as elasto-plastic hysteretic model, while the braces are modelled as Multi-Linear Plastic Hysteretic type—Pivot and treated as critical members—i.e. the failure of one component induces significant changes in the overall behaviour. For the sake of time-history nonlinear procedure duration, in order to compare static-equivalent and time-history results a significant number of synthetic motions of 21 s duration (10 pairs), compatible with the reduced design spectrum (P100-1 2006) were generated. For the first story base column (Fig. 7), the time-history of DCR for a single set of orthogonal input motions only, applied under the x - and y -directions is represented in Fig. 8. The effect of ground motion input directivity is also shown in Fig. 8, in terms of peak DCRs.

For the entire column over the building height, the comparison between static, code-based, and dynamic DCRs is given only for, say 0° directivity of orthogonal input motions in the Fig. 9.

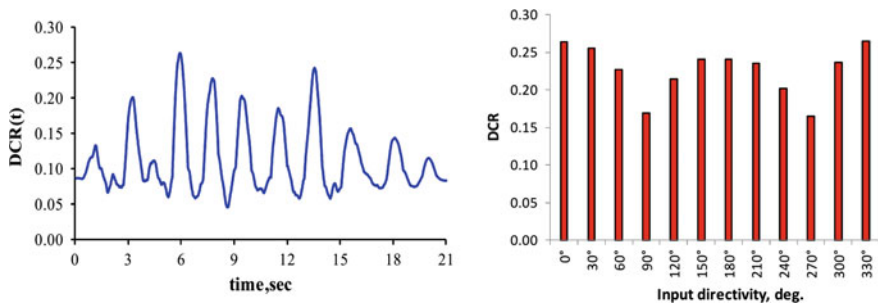
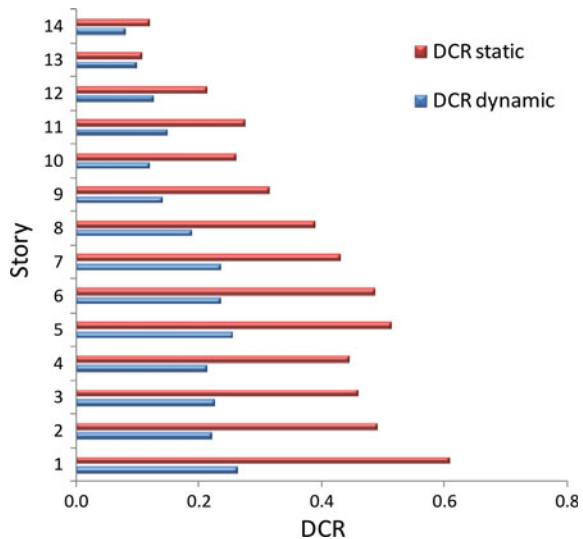


Fig. 8 Time-history of DCR for the base column (0° directivity, *left figure*) and input motions directivity effect on the peak DCR (12 directions, *right figure*)

Fig. 9 Peak DCRs for columns: static versus mean values from dynamic analysis (0° input directivity)



From the point-of-view of deformation-controlled design, if the response parameters are the drift ratios (threshold limit states are given in EN1998-1-Eurocode 8 (2004), Sect. 4.4.3.2), then the analysis and design framework can accommodate a “peaks-over-threshold” approach. Thus, for normally distributed parameters, the mean up-crossings rates with positive slope over a threshold limit u , is given by Rice formula (Vanmarcke 2010):

$$\mu^+(u) = \frac{1}{2\pi} \sqrt{\frac{\lambda_2}{\lambda_0}} \exp\left(-\frac{u^2}{2\lambda_0}\right) \quad (5)$$

where, λ_0 and λ_2 are the 0 and the 2nd order moments respectively, about the mean.

The i th spectral moment given in Eq. (5) is

$$\lambda_i = \int_{-\infty}^{+\infty} \omega^i S_x(\omega) d\omega \quad (6)$$

where $S_x(\omega)$ is the spectral density function and ω is the circular frequency (Vanmarcke 2010).

Focusing on critical members, time-histories of say, the axial deflection of the 7th story brace—ascending to the right (Fig. 8 elevation, center), corresponding to 3 different directivity angles of input motion (e.g. 0° , 30° and 300°) is given in the Fig. 10. The mean up-crossing rates of axial deflections associated to Serviceability limit (say 10^{-4} m) for 12 directions of orthogonal input motions are presented (Fig. 10 down).

This approach additionally emphasizes the most unfavourable loading case and associated directivity (330° directivity, in this example) for any structural member. Any other performance level can be thus explicitly considered and the results stored in a structural performance database.

Using the UHS and CMS 2.0 s, 10 suites of artificial compatible accelerograms, corresponding to a probability of exceedance of 10 % in 50 year. were obtained (Figs. 5, 6 and Table 1) and nonlinear dynamic analyses were performed for the steel structure model (Fig. 8).

The results, in terms of peak DCRs straightforward obtained from time-domain analyses (Eq. 4), are shown in Fig. 11 (for 0° directivity of input motion only).

The DCRs statistics for the base column section, considering those 10 input motion suites, is given in Table 2.

The results are comparable, showing however slightly higher maximum DCRs corresponding to CMS-based approach, and lower value in the mean-sense. The variability is low if compared with the input motions predominant periods variability (Table 1). In most cases however, the deformation-controlled criteria will govern the structural design. Thus, the corresponding peaks of tip drift ratios (%) in x - and y -direction, are presented in Fig. 12.

The statistics of the corresponding tip drift ratios is given in Table 3.

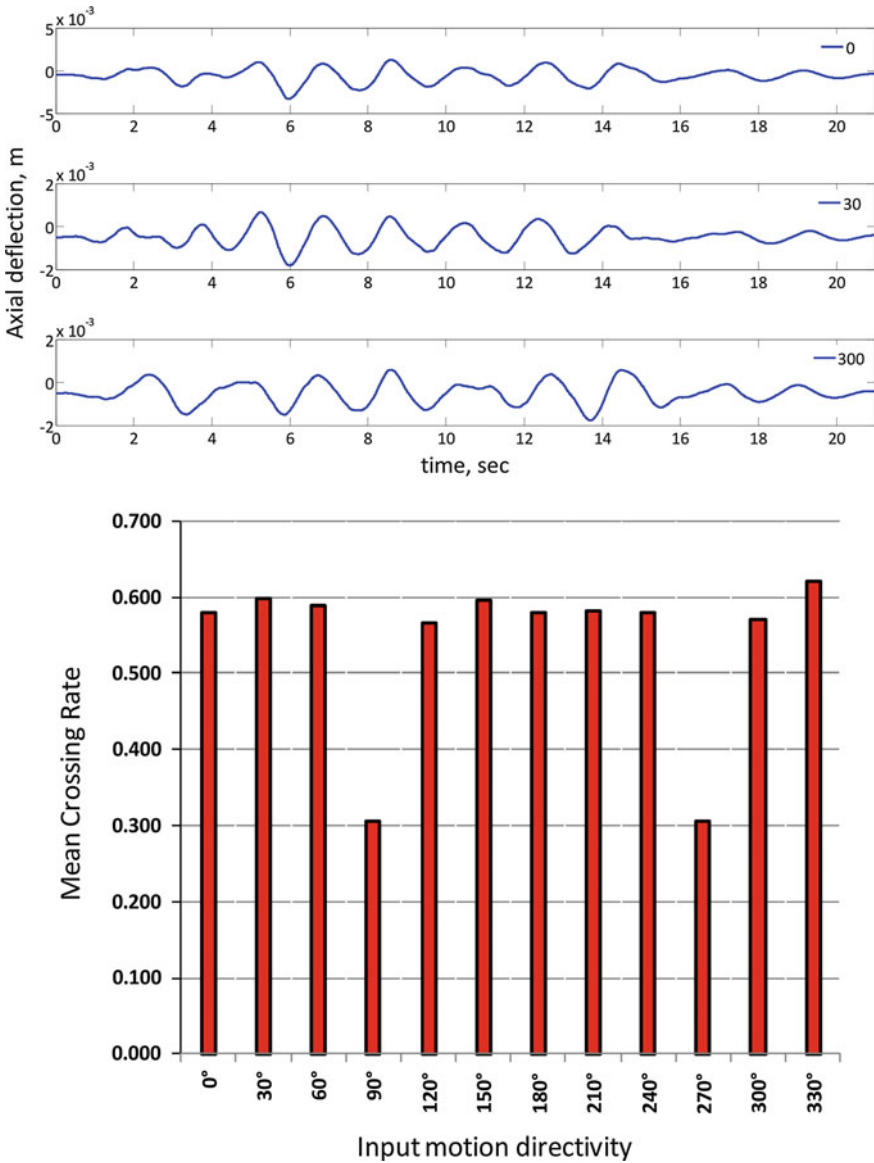


Fig. 10 Time-histories (3 directions, *upper figure*) and mean up-crossing rates of axial deflection in the ascending to the right X-brace at the 7th story (*down figure*)—(12 directions of orthogonal input motions)

In terms of tip drift ratios, the results are in line with the tendency observed for strength-based analysis. However, due to the limited number of analyses, a final conclusion cannot be drawn on the advantages of using neither UHS nor CMS as

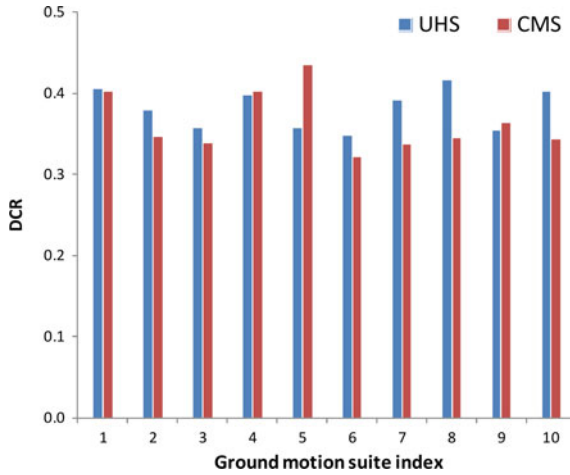


Fig. 11 DCR for columns: UHS and CMS 2.0s, 10 % in 50 year, (0° input directivity)

Table 2 Statistics of DCRs for the base column (0° input directivity)

DCR	UHS	CMS 2.0s
Maximum	0.417	0.435
Mean	0.385	0.365
σ	0.025	0.037
CoV	0.064	0.101

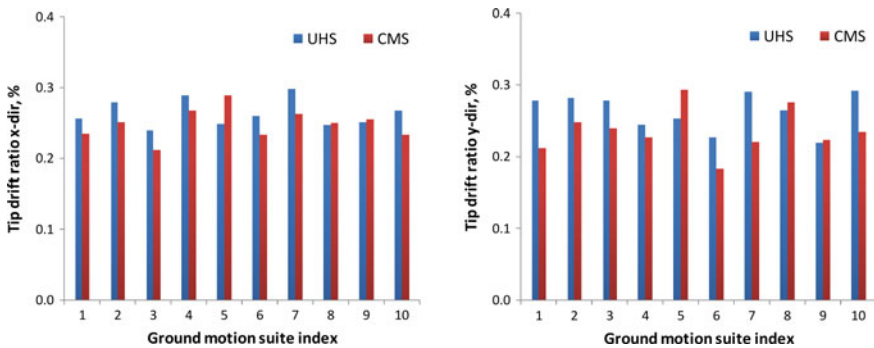


Fig. 12 Tip drift ratios (%) in x- and y-directions: UHS and CMS 2.0 s, 10 % in 50 year (0° input directivity)

Table 3 Statistics of tip drift ratios, % (0° input directivity)

Tip drift ratio	UHS		CMS 2.0 s	
	x-dir	y-dir	x-dir	y-dir
Maximum	0.298	0.292	0.289	0.293
Mean	0.264	0.263	0.249	0.235
σ	0.019	0.026	0.022	0.031
CoV	0.073	0.098	0.087	0.133

target spectrum. While both approaches are hazard-consistent, UHS-based approach has the advantage of the uniform distribution of hazard information over the entire range of natural periods. On the other hand CMS-based approach additionally brings-in the causal hazard information in the mean sense. This looks to be more appropriate from the practical design point-of-view. When a significant number of recorded accelerograms are available to be selected or scaled for a given site, the selection of input ground motions using available criteria can be performed (Baker and Cornell 2006). The GMPE influence on the input motion selection procedure should be also analyzed in conjunction with the structural response.

6 Conclusions

The time-domain approach gives the full range of advantages and is the most appropriate tool for the Performance-Based Design of tall buildings, thanks to current computational capabilities. The lack of available records to be selected or scaled for a given site can be suppressed by using synthetic input motions generated using available techniques after proper signal processing analyses and engineering judgment. A database-assisted analysis and design approach could be thus readily available in a not too distant future. The case studies are emphasizing the tendency for more conservative strength design using the code provisions when compared to the full dynamic analysis approach. A Probabilistic Seismic Hazard Analysis (PSHA) approach based on UHS and CMS representations to obtain a large number of credible input ground motions would allow a more rational and cost-effective design. The global structural model is to be further refined in a next level analysis, able to account for a broad range of SSI-induced effects, discussed in the paper. This requires further extensive analyses and validations using available records, in an undergoing research work using recorded input motions.

Acknowledgements Funding for this research was provided by the Romanian National Authority for Scientific Research (ANCS) under the Grant Number 72/2012. This support is gratefully acknowledged. The earthquakes catalogue of Vrancea subcrustal source was provided by the National Institute for Earth Physics (INFP) within BIGSEES Project. The contribution of Professor Radu Vacareanu (UTCB) and Dr. Florin Pavel (UTCB) to the seismic hazard analyses is highly acknowledged.

References

- ASCE (2010) Minimum design loads for buildings and other structures, ASCE/SEI 7-10. American Society of Civil Engineers, Reston
- Baker J (2011) Conditional mean spectrum: tool for ground motion selection. *J Struct Eng* 137 (3):322–331
- Baker J, Cornell CA (2006) Spectral shape, epsilon and record selection. *Earthquake Eng Struct Dynam* 35:1077–1095

- Borcherdt RD, Glassmoyer G (1992) On the characteristics of local geology and their influence on ground motions generated by the Loma Prieta earthquake in the San Francisco Bay region. *Calif Bull Seismol Soc Am* 82(2):603–641
- Council on Tall Buildings and Urban Habitat (2008) In: Wood A (ed) Recommendations for the seismic design of high-rise buildings. CTBUH, Chicago. ISBN: 978-0-939493-26-5
- Delavaud E, Cotton F, Akkar S, Scherbaum F, Danciu L, Beauval C, Drouet S, Douglas J, Basili J, Sandikkaya A, Segou M, Faccioli E, Theodoulidis N (2012) Toward a ground-motion logic tree for probabilistic seismic hazard assessment in Europe. *J Seismol* 16(3):451–473
- EN1993-1 Eurocode 3 (2005) Design of steel structures—Part 1-1: general rules and rules for buildings. European Committee for Standardization
- EN1998-1 Eurocode 8 (2004) Design of structures for earthquake resistance: Part 1 general rules, seismic actions and rules for buildings. European Committee for Standardization
- Gasparini DA, Vanmarcke EH (1976) Simulated earthquake motions compatible with prescribed response spectra. Department of Civil Engineering, Research Report R76-4 1976, Massachusetts Institute of Technology, Cambridge, Massachusetts
- Iancovici M, Stefanescu B, Bogdan O, Vezeanu G (2010) Tall buildings under long predominant period ground motions: analysis vs. code provisions. In: Paper presented at the 14th European conference on earthquake engineering ECEE 2010, Ohrid, Macedonia, September, (CD-ROM)
- Iancovici M, Bogdan O, Stefanescu B (2011) Seismic response analysis of tall buildings under uncertain conditions. In: Paper presented at the council of tall buildings and urban habitat (CTBUH) 2011 World Conference, Seoul, Korea
- Ismail-Zadeh AT, Matenco L, Radulian M, Cloetingh S, Panza GF (2012) Geodynamics and intermediate-depth seismicity in Vrancea (the south-eastern Carpathians): current state-of-the-art. *Tectonophysics* 530–531:50–79
- Katsanos E, Sextos A, Manolis G (2010) Selection of earthquake ground motion records: a state-of-the-art review from a structural engineering perspective. *Soil Dyn Earthq Eng* 30:157–169
- Kramer S (1996) Geotechnical earthquake engineering. Prentice Hall, Upper Saddle River
- Lungu D, Comea T, Aldea A, Zaicenco A (1997) Basic representation of seismic action. In: Lungu D, Mazzolani F, Savidis S (eds) Design of structures in seismic zones: Eurocode 8-worked examples, TEMPUS PHARE CM Project 01198: implementing of structural eurocodes in Romanian civil engineering standards. Bridgeman Ltd., Timisoara, pp 1–60
- Lungu D, Vacareanu R, Aldea A, Arion C (2000) Advanced structural analysis. Conspress, Bucharest
- Marmureanu G, Cioflan CO, Marmureanu A (2010) Research regarding the local seismic hazard (Microzonation) of the Bucharest metropolitan area (in Romanian). Tehnopress, Iasi
- McGuire R (1999) Probabilistic seismic hazard analysis and design earthquakes: closing the loop. *Bull Seismol Soc Am* 85(5):1275–1284
- McGuire R (2004) Seismic hazard and risk analysis. Earthquake Engineering Research Institute; MNO-10
- Naimi G, Naimi M (2008) Effect of soil conditions on the response of RC tall structures to near-fault Earthquakes. *Struct Design Tall Spec Build* 17(3):541–562
- NIST (2011) Selecting and scaling earthquake ground motions for performing response—history analyses. NIST/GCR 11-917-15, prepared by the NEHRP Consultants Joint Venture for NIST, Gaithersburg, Maryland
- P100-1 (2006, 2013) Code for seismic design—Part I—design prescriptions for buildings, Bucharest
- Pacific Earthquake Engineering Research Center (2010) Guidelines for performance-based seismic design of tall buildings. Report no. 2010/05-TBI
- Sokolov VY, Bonjer KP, Wenzel F, Grecu B, Radulian M (2008) Ground-motion prediction equations for the intermediate depth Vrancea (Romania) earthquakes. *Bull Earthq Eng* 6 (3):367–388
- Stewart J, Tileylioglu S (2007) Input ground motions for tall buildings with subterranean levels. *Struct Design Tall Spec Build* 16(3):543–557

- Trendafilovski G, Wyss M, Rosset P, Marmureanu G (2009) Constructing city models to estimate losses due to earthquakes worldwide: application to Bucharest. *Rom Earthq Spectra* 25(3): 665–685
- Vacareanu R, Pavel F, Aldea A (2013a) On the selection of GMPEs for Vrancea subcrustal seismic source. *Bull Earthq Eng* 11(6):1867–1884
- Vacareanu R, Lungu D, Aldea A, Demetriu S, Arion C, Neagu C, Pavel F, Marmureanu G, Cioflan CO (2013b) Statistics of seismicity for Vrancea subcrustal seismic source. Paper presented at the SE-EEE Conference, Skopje, Macedonia
- Vanmarcke E (2010) *Random fields, Analysis and Synthesis*. World Scientific Publishing Co., Pte. Ltd, Singapore
- Wilson E (2015) Termination of the Response Spectrum Method—RSM. <http://www.edwilson.org>. Accessed 15 Sept 2015
- Yeo D, Simiu E (2011) High-Rise reinforced concrete structures: database-assisted design for wind. *J Struct Eng* 137(11):1340–1349
- Youngs RR, Chiou SJ, Silva WJ, Humphrey JR (1997) Strong ground motion attenuation relationships for subduction zone earthquakes. *Seismol Res Lett* 68(1):58–73

Unidirectional Cyclic Behavior of Old Masonry Walls in Romania

Eugen Lozincă, Viorel Popa, Dragoș Coțofană
and Alexandru Basarab Cheșcă

Abstract Shear failure of masonry walls is the main cause of collapse for masonry buildings. In Romania, during the 1940 and 1977 Vrancea earthquakes, most of the buildings damage was triggered by the masonry shear failure. Retrofitting of existing masonry buildings is the most effective way of reducing earthquake risk related to buildings in Romania. Reliable input data is necessary to improve the accuracy of the seismic risk assessment of the existing masonry buildings. Worldwide available experimental data should be wisely used as it can be misleading because of scattered materials characteristics and construction practice. Local experimental data that take into account the local materials and state of practice is necessary. This paper presents the results of six experimental tests. Squat masonry walls were subjected to cyclic in-plane lateral loading. Two of the specimens represents unreinforced masonry walls, two others concrete confined masonry elements and the other two retrofitted masonry walls using FRP composites.

Keywords URM · Confined · Masonry · Seismic · Retrofitting · FRP

E. Lozincă (✉) · V. Popa · D. Coțofană
Faculty of Civil Engineering, Technical University of Civil Engineering Bucharest,
Bucharest, Romania
e-mail: elozinca@utcb.ro

V. Popa
e-mail: vpopa@utcb.ro

D. Coțofană
e-mail: cotofana@utcb.ro

A.B. Cheșcă
“Ion Mincu” University of Architecture and Urbanism, Bucharest, Romania
e-mail: basarab.chesca@gmail.com

1 Introduction

Unreinforced masonry (URM) buildings performed very poorly in recent earthquakes worldwide. Many authors reported about the extended damage suffered by masonry buildings in Europe after the 2009 L'Aquila earthquake (D'Ayala and Paganoni 2010; Lagomarsino 2012; Penna et al. 2014) or the 1999 Izmit earthquake in Turkey (Bruneau 2002). In Romania, this poor behavior of plain masonry buildings was tragically reminded by the 1940 and 1977 Vrancea earthquakes (Fattal et al. 1977; Georgescu and Pomonis 2012).

URM buildings were constructed in Romania until the late 1940s when they were gradually replaced by confined masonry buildings. Observations made after Vrancea 1977 earthquake showed that this type of buildings had a better response than URM buildings (Fattal et al. 1977; Monografia 1978). There is still a great number of existing vulnerable masonry buildings in Bucharest, Romania.

These masonry buildings that are seismically at risk can either be demolished or retrofitted. Design of the retrofitting work is currently made in accordance with the performance criteria from national technical regulations (P 100-3/2008). Retrofitting system is designed taking into account not only structural requirements but also operational and architectural aspects. In Bucharest, a significant part of the masonry building stock is listed as "heritage architecture" being protected by special laws and regulations (Lungu 2009). These heritage buildings may not be demolished and special techniques are necessary for their retrofitting and preservation. Common reinforced concrete jacketing solution is not allowed for retrofitting of these buildings. Less intrusive retrofitting solutions are required. These commonly relies on coating masonry walls with fiber sheets or straps (Albert et al. 2001) made out of carbon fibres, glass fibers or other types of polymeric fibers.

This paper presents synthetic results of 6 experimental tests aimed to investigate the hysteretic behavior of plain and confined masonry walls and to assess the efficiency of FRP retrofitting. Effectiveness of carbon fiber jacketing on a single or both faces of masonry walls was investigated.

2 Structural Testing Program

Six masonry walls were subjected to cyclic lateral displacement reversals under constant vertical load up to the failure. Two specimens were made of plain old masonry, two were constructed as concrete confined masonry and the other two consisted of plain masonry retrofitted using carbon fiber reinforced polymers (FRP) sheets.

The objective of these series of experimental tests was to compare the seismic behavior of plain and confined masonry walls and to examine the efficiency of FRP retrofitting. The effectiveness of application of the FRP sheets only on one face of a masonry wall was investigated as well. This is usually the case of historical buildings where frequently no intervention on the façades is allowed.

2.1 Test Specimens

The geometry of the tested specimens is presented in Fig. 1. Height to length ratio is less than one so the specimens can be classified as being “squat”. For this type of walls behavior under lateral loads is controlled by shear force, as opposed to the behavior of the regular “tall” walls that is commonly controlled by bending. The conclusions of these experimental work refers to the tested specimens and should be carefully extrapolated to regular walls.

Specimens were made of old solid bricks having an average compression strength of 10 MPa and relatively weak lime mortar with average compression strength of 2.5 MPa [determined according to EN 1015-11 (2007)]. Old solid bricks used for the masonry have the following dimensions: 240 mm × 115 mm × 63 mm.

Specimens PMW1 and PMW2 were made of plain old masonry (Fig. 1a). Specimens RMW5 and RMW6 were constructed in the same way but were retrofitted using epoxy bonded carbon fiber sheets. The overall amount of FRP sheets was the same for both specimens. For RMW5 the amount was equally distributed on both faces of the wall while for RMW6 the entire amount was placed only on one face of the wall.

The other two specimens, CMW3 and CMW4, were made of masonry panels laterally confined by two RC boundary elements with a transversal rectangular section of 150 mm × 250 mm. These elements have been lightly reinforced with 4 D10 mm longitudinal rebars and D6 mm stirrups spaced at 200 mm. These un-ribbed steel bars have an average yielding strength of 285 MPa and 25 % ultimate strain, according to Romanian standard STAS 438/1-89. Only the horizontal masonry joints were filled with mortar. These specimens were detailed according to the state of practice in Romania for old buildings constructed in the Interwar Years. The general layout of the confined masonry specimens can be observed in Fig. 1b.

More information about the tested specimens is presented in Table 1.

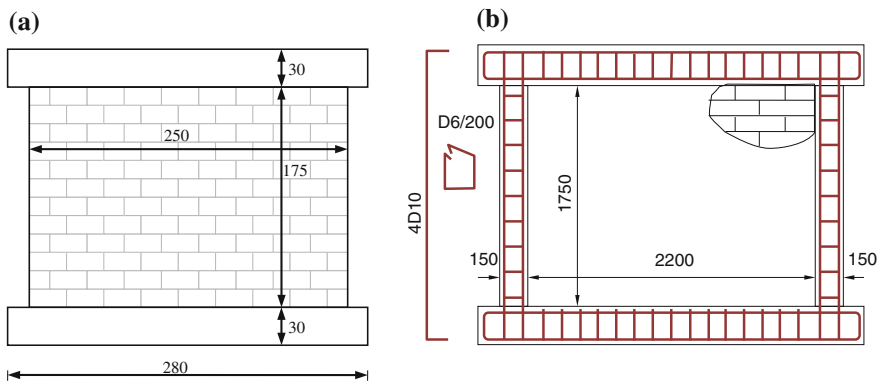


Fig. 1 The layout of the tested specimens

Table 1 Characteristics of tested specimens

Wall	Boundary RC elem.	Carbon fiber sheets	Applied axial force (kN)	σ_0^a (MPa)
PMW1	No	No	750	1.20
PMW2	No	No	375	0.60
CMW3	Yes	No	750	1.20
CMW4	Yes	No	750	1.20
RMW5	No	Yes-on both faces	750	1.20
RMW6	No	Yes-on one face	750	1.20

^aThe axial mean stress (σ_0) corresponds to the average specimen’s sectional dimensions (length = 2500 mm; width = 250 mm)

2.2 Testing Equipment

The testing equipment consists of a steel reaction frame, loading control system and the data acquisition systems. The geometry of the reaction frame and the capacity of the hydraulic jacks are presented in Fig. 2. Vertical load was applied using a vertical jack of 2000 kN. A steel loading beam was installed between the vertical jack and the specimen. The vertical jack could freely slide on horizontal direction to accommodate the in-plane lateral displacement of the loading beam. Vertical load was automatically controlled to maintain a constant oil pressure in the hydraulic

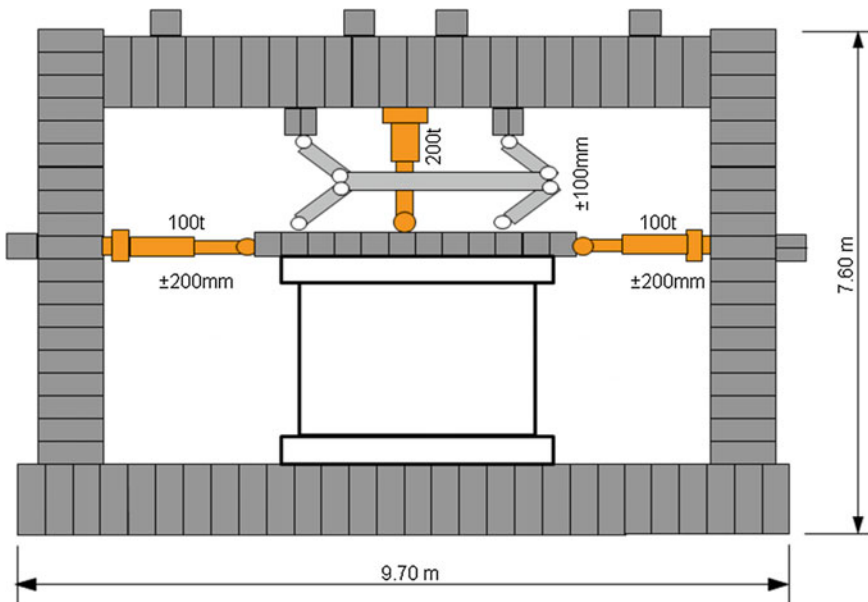


Fig. 2 Structural reaction frame

system. Horizontal load was applied using two horizontal jacks of 1000 kN each. Displacement based control was used for horizontal loading. All jacks were pinned at both ends to allow in-plane rotation of the jacks.

The loading beam was connected to the upper beams of the reaction frame using a pantograph. The pantograph was used to restrain the rotation of the loading beam.

Linear displacement transducers were used to measure the horizontal and vertical displacements of the specimens. In-plane and out of plane displacements were measured. Horizontal and vertical loads were measured using two 1 MN load cells and one 2 MN load cell, respectively. Load cells were located in between the jacks and the loading beam.

2.3 Loading Protocol

All six specimens were subjected to cyclic lateral displacement reversals under a constant axial load. Initially, the vertical compression force was applied.

In the second stage the cyclic lateral force was statically applied using two horizontal 100 t hydraulic jacks. Displacement based control was applied for the cyclic lateral loading. The loading protocol included two cycles at ± 0.025 , ± 0.05 , ± 0.1 , ± 0.2 and ± 0.6 % lateral drifts. This testing protocol follows the Japanese practice (Kaminosono et al. 1993) and is consistent with the recommendations of ACI374.2-R13 (ACI 2013). Figure 3 presents the lateral load protocol, as well as the history of the constant vertical load.

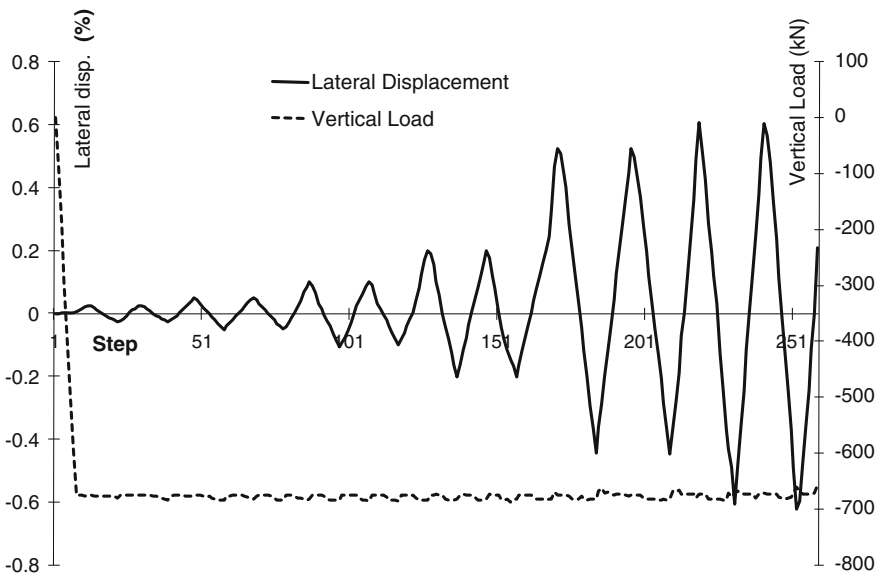


Fig. 3 Loading protocol

Vertical load was maintained constant up to the failure of the specimen. For all specimens, lateral loading was stopped when the loss of the vertical force carrying capacity was observed.

3 Test Results

The recorded lateral force—lateral displacement (drift) curves are presented in the Fig. 4 and the damage state of the specimens at the onset of collapse is presented in Fig. 5.

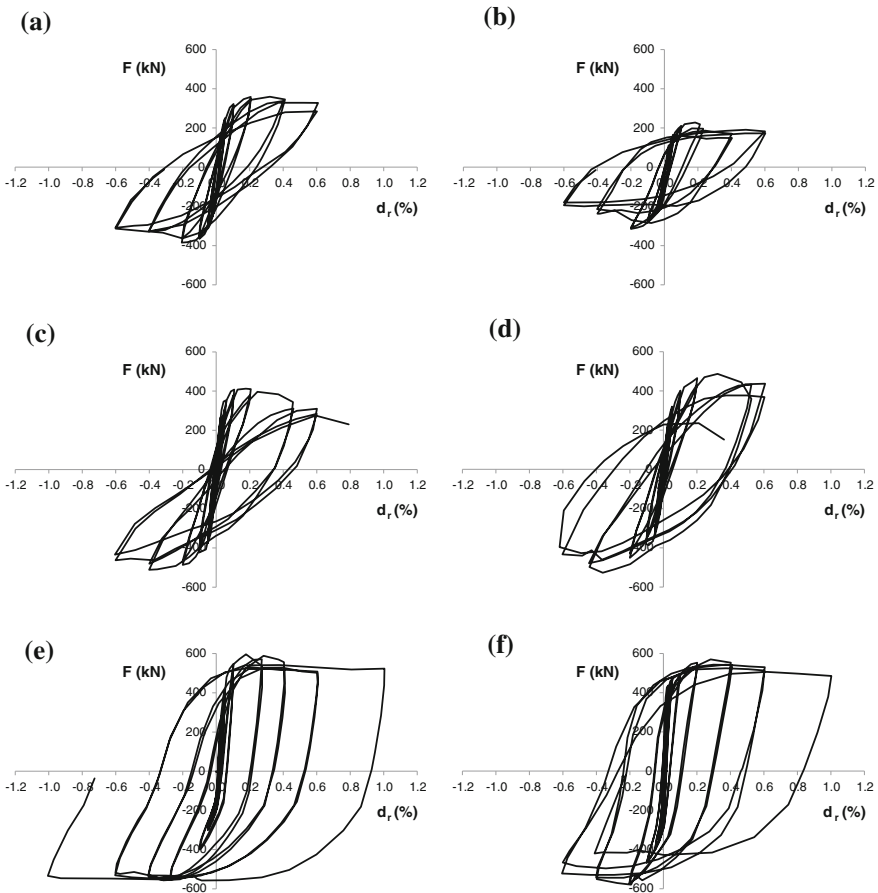


Fig. 4 Recorded lateral force—lateral drift response. **a** PMW1—plain masonry, $\sigma_0 = 1.20$ MPa. **b** PMW2—plain masonry, $\sigma_0 = 0.60$ MPa. **c** CMW3—confined masonry, $\sigma_0 = 1.20$ MPa. **d** CMW4—confined masonry, $\sigma_0 = 1.20$ MPa. **e** RMW5—FRP retrofitted masonry on both faces. **f** RMW6—FRP retrofitted masonry on one face

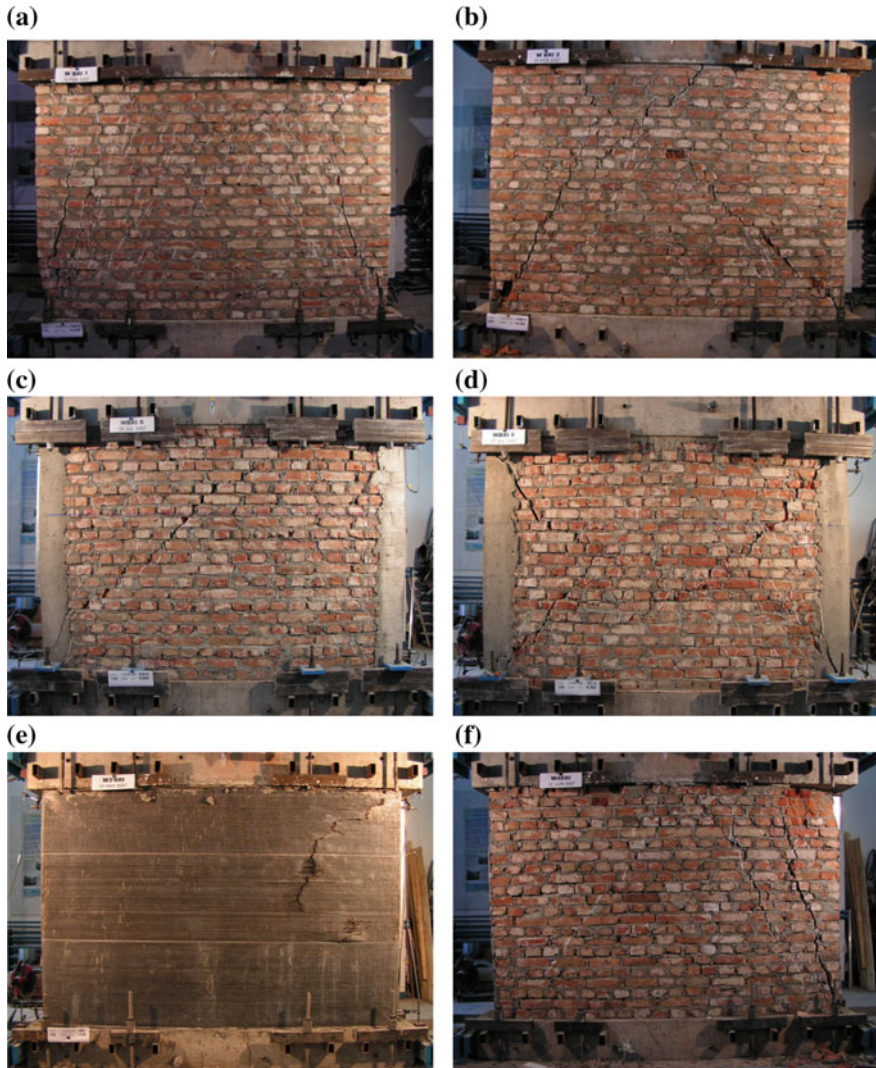


Fig. 5 Damage state of the specimens at the end of test. **a** PMW1—plain masonry, $\sigma_0 = 1.20$ MPa. **b** PMW2—plain masonry, $\sigma_0 = 0.60$ MPa. **c** CMW3—confined masonry, $\sigma_0 = 1.20$ MPa. **d** CMW4—confined masonry, $\sigma_0 = 1.20$ MPa. **e** RMW5—FRP retrofitted masonry on both faces. **f** RMW6—face w/o carbon fiber sheet

In the early loading cycles, a similar response was observed for plain and confined masonry specimens. However, failure patterns presented some differences.

Up to 0.05 % lateral drift response of the specimens was essentially elastic. No cracks were observed up to this point and the residual displacement was around

0.01 %. First diagonal cracks appeared in the masonry in the second cycle at 0.1 % lateral drift.

For the confined masonry walls, first cracks in the RC boundary elements were noticed at 0.2 % lateral drift. These were inclined cracks in the direction of the diagonal cracks already existing in the masonry panel.

No major damages were observed up to 0.2 % lateral drift. No deterioration of lateral strength was recorded in this interval neither for plain or confined masonry walls.

The lateral strength decay began after 0.2 % lateral drift. For the confined masonry walls, the lateral force started to decay when the shear failure was initiated in the RC boundary columns.

Failure of the plain and confined masonry specimens was recorded at about 0.6 % lateral drift when the tests were stopped due to the loss in the axial force carrying capacity.

The small tensile stress recorded in the vertical rebars generated insignificant horizontal cracks in the RC vertical elements of the confined masonry specimens. This shows that these elements were not engaged as vertical ties where severe yielding of the longitudinal reinforcement can be expected due to axial tensile force. In fact, the shear failure indicates that the RC vertical elements responded more like columns than as vertical ties.

Large vertical settlements were recorded for plain masonry walls even after few loading cycles. At the end of the tests after two loading cycles at ± 0.6 % drift, the settlement was almost 9 mm for specimen PMW2. Similar settlement was also observed for the confined masonry specimen CMW4, after the shear failure of the boundary columns.

Hysteretic curves recorded for the FRP retrofitted specimens showed a significant increase of both the lateral strength and deformability capacity of the wall.

The influence of the compressive vertical load in respect with the lateral strength of the plain masonry walls can be observed by comparing the hysteretic curves in Fig. 4. It can be noticed that doubling the vertical load generated a larger horizontal strength, but had little influence on the deformation capacity. Both plain masonry specimens had finally reached the failure point at 0.6 % drift.

The maximum lateral forces recorded for the confined masonry walls were a little larger than the values recorded for the plain masonry specimen. Also fatter hysteretic loops were recorded showing a larger energy dissipation capacity for the confined masonry.

Similar strength and stiffness degradation was recorded for plain and confined masonry specimens and the ultimate lateral displacement did not significantly change due to the presence of the confining elements. However, it should be emphasized that this remark refers only to the tested specimens.

The provision of the same amount of carbon fiber sheets on one face or on two faces did not significantly influence the strength and deformability capacity of the walls. However, the position of the carbon fiber sheets influenced the failure mechanism. For RMW5 the carbon sheets confined and impeded the masonry to move out of plane, while for RMW6 the presence of the carbon fiber on only one

Table 2 The ratio of hysteretic loops area

Wall i/wall j	Hysteretic loops area ratio
PMW1/PMW2	1.57
RMW5/PMW1	2.49
RMW6/PMW1	2.12
RMW5/RMW6	1.18

face allowed wide-opened cracks on the side without FRP sheets that triggered some out of plane deformation of the wall.

The stiffness and the hysteretic behavior stay close for both FRP retrofitted specimens, but the specimen RMW5 (two-side FRP “jacketing”) showed a larger capacity of dissipating seismic energy than for RMW6 (only one-side with FRP “jacketing”).

As the hysteretic energy dissipated within the cycle is proportional to the area of the hysteretic loops, one can notice in Table 2 that the energy dissipation capacity of two-side coated wall is almost 20 % higher than the capacity of one-side coated specimen. This is due to the more stable failure mechanism of the specimen RMW5. Meanwhile, the retrofitting of the masonry walls with carbon fiber sheets increased the energy dissipation capacity of the wall more than two times, thus enabling a much better expected seismic performance of the FRP retrofitted masonry walls.

4 Conclusions

This experimental testing program was aimed at identifying the main parameters that govern the seismic behavior of both unreinforced and confined masonry walls. The study confirmed that FRP composites offer great benefits for the strengthening of masonry walls to resist the cyclic lateral loads induced by big earthquakes.

The tested specimens responded essentially elastic up to 0.05 % lateral drift and limited deterioration of the walls was recorded up to 0.1 %. Therefore, this value can be reasonable considered as an allowable value of the lateral displacement for the damage limitation requirement as defined in EN1998-1 (2004).

The recorded test results showed that the use of boundary concrete elements for squat masonry panel did not significantly improved the lateral strength and displacement capacity. The recorded value of the ultimate drift was roughly 0.6 %, similar to the values recorded for the unreinforced masonry specimens.

For these squat masonry walls subject to medium-to-high vertical loads, no significant tensile forces in the longitudinal reinforcement of the boundary columns were observed. No flexural yielding mechanism could be triggered for this type of confined walls. The concrete boundary elements acted as columns subjected to severe shear forces transmitted in the vicinity of the joints by the compressed diagonal strut in the masonry panel.

The slightly higher horizontal strength recorded for the confined masonry walls can be explained mainly by the higher shear capacity of the reinforced concrete boundary elements. At early loading cycles, prior to their shear failure, the concrete vertical boundary elements prevented the vertical settlement of the wall.

The experimental results showed that the FRP retrofitting solution with carbon fiber sheets is effective irrespective if the same amount of overall coating is placed only on one face or evenly distributed on both faces of the masonry wall. Installing FRP sheets on both sides prevented out-of-plane displacements of the masonry.

Acknowledgements The authors deeply acknowledge the generous, continuous and long-lasting financial support of Japan International Cooperation Agency (JICA) during the implementation of the Technical Project for Seismic Risk Reduction in Romania. The technical and financial support of Building Research Institute (BRI), Tsukuba for the implementation of the test series is gratefully acknowledged.

References

- ACI 374.1 (2013) Guide for testing reinforced concrete structural elements under slowly applied simulated seismic loads. ACI Standard, Reported by ACI Committee 374, Farmington Hills, Michigan
- Albert ML, Elwi AE, Cheng JJR (2001) Strengthening of unreinforced masonry walls using FRPs. *J Comp Constr ASCE* 5(2):76
- Bruneau M (2002) Building damage from the Marmara, Turkey earthquake of August 17. *J Seismolog* 6:357–377. doi:[10.1007/s10518-011-9307-x](https://doi.org/10.1007/s10518-011-9307-x)
- D’Ayala D, Paganoni S (2010) Assessment and analysis of damage in L’Aquila historic city centre after 6th April 2009. *Bull Earthquake Eng* (2011) 9:81–104. doi:[10.1007/s10518-010-9224-4](https://doi.org/10.1007/s10518-010-9224-4)
- EN 1015-11 (2007) Methods of test for mortar for masonry. Part 11—determination of flexural and compressive strength of hardened mortars
- EN 1998-1 (2004) Design of structures for earthquake resistance—Part 1: general rules, seismic actions and rules for buildings
- Fattal G, Simiu E, Culver C (1977) Observations on the behaviour of buildings in the Romania earthquake of March 4, 1977. NBS Special publication 490, US Department of Commerce/National Bureau of Standards, United States
- Georgescu ES, Pomonis A (2012) Building damage vs. territorial casualty patterns during the Vrancea (Romania) earthquakes of 1940 and 1977. In: Proceedings of 15th world conference on earthquake engineering, Lisbon, Sept 24–28 2015
- Institutul Central de Cercetare Proiectare și Directivare în Construcții (1978) Cutremurul din România din 4 martie 1977 și efectele sale asupra construcțiilor – sinteza monografiei
- Kaminosono T et al (1993) Structural testing—training course in seismology and earthquake engineering II—International Institute of Seismology and Earthquake Engineering Lecture Notes
- Lagomarsino S (2012) Damage assessment of churches after L’Aquila earthquake (2009). *Bull Earthqu Eng* 10:73–92. doi:[10.1007/s10518-011-9307-x](https://doi.org/10.1007/s10518-011-9307-x)
- Lungu D (2009) Riscuri natural și antropice pentru patrimonial construit al Bucureștiului. A 4-a Conferință Națională de Inginerie Seismică, București, 18 decembrie 2009, ISBN 978-973-100-098-5

- Penna A, Morandi P, Rota M, Manzini CF, Porto F, Magenes G (2014) Performance of masonry buildings during the Emilia 2012 earthquake. Bull Earthq Eng 12:2255–2273. doi:[10.1007/s10518-013-9496-6](https://doi.org/10.1007/s10518-013-9496-6)
- P 100-3/2008, Cod de proiectare seismică - Partea a III-a - Prevederi pentru evaluarea seismică a clădirilor existente
- STAS 438/1-89, Produse de oțel pentru armarea betonului. Oțel beton laminat la cald. Marci și condiții tehnice de calitate

Viscous Damper Distribution Using Genetic Algorithms and Pattern Search Optimization

Andrei Pricopie and Alin Costache

Abstract The aim of this study is to identify the optimal placement of viscous dampers in existing structures in order to improve their seismic response. A six story steel frame structure, modelled using finite elements and a concentrated plasticity model to represent the nonlinear behavior, was studied. Firstly, a uniform distribution for the viscous dampers, which uses a damper on each storey, is calculated using the principle of equivalent damping and the elastic properties of the structure. Using the results and the same positions for the viscous dampers, as for the uniform distribution, a set of constraints is imposed on the damping constants of the viscous dampers. Secondly, an optimized distribution of the damping constants is calculated using genetic algorithms, pattern search algorithms and a direct descent method. All methods use the drift of the structure as a function to be minimized by introducing viscous dampers. Dynamic time history analysis is used to determine the maximum drift of the structure. The analyses are carried out for three ground motion records which represent the seismic conditions given by the Vrancea source in Bucharest. The article compare the response of the optimization technique in terms of results and computation time.

Keywords Viscous dampers · Genetic algorithm · Pattern search algorithm · Dynamic non linear analysis

1 Introduction

As safety requirements increase for buildings, the amount of energy the structure needs to dissipate during an earthquake also increases. Performance based design assumes that the energy induced by the seismic motion is dissipated through plastic

A. Pricopie (✉) · A. Costache
Faculty of Civil Engineering, Technical University of Civil Engineering, Bucharest, Romania
e-mail: andrei.pricopie@gmail.com

A. Costache
e-mail: costache.alin3@yahoo.com

deformations of the structure. These plastic deformations usually mean damage to the structure which needs to be repaired. Another approach which is becoming more utilized is to control the response of the structure using devices such as viscous dampers. The viscous dampers are passive control devices which are inserted as braces in the structure and are built like a piston with two chambers. When the piston moves the liquid from a chamber to the other a resisting force appears which is proportional to the speed of the displacement. Design using viscous dampers has been implemented in design codes like FEMA 356 (2000).

Although the use of viscous dampers is established as a design solution there are not enough studies on the optimal damper placement in a structure. Takewaki (2000) addressed the problem in a series of studies on optimizing the damper distribution on the height of the structure. The proposed method uses the frequency domain in order to solve the equation of motion. The method takes into account elastic behavior for the structure. Trombetti and Silvestri (2004) use a mass proportional damping system in order to find the optimum distribution. The same authors use genetic algorithms in order to prove their method, Silvestri and Trombetti (2007). In this study the authors conclude that dampers fixed to the ground or dampers spanning more than one story provide greater reductions in the seismic response. Both models account only for the elastic behavior of the structure which is unlikely for a design situation.

A theoretical approach for the nonlinear domain is difficult to develop. Martinez and Romero (2003) rely on a two-step process where the first step consists in determining a cvasi-optimal distribution and the second step aims to further improve the seismic response. In order to optimize the distribution of the viscous dampers in the nonlinear domain heuristic methods need to be used. To that extent there is a study on the optimization of viscous dampers using genetic algorithms published by Pricopie and Pavel (2013). The study presented in this paper aims to:

- expand on studies which use genetic algorithms in order to find an optimal damper distribution;
- asses the potential of pattern search algorithms to determine the optimal damper distribution;
- compare the results of the genetic algorithms and the pattern search algorithms with direct descent optimization method developed by Takewaki (2000);
- compare the results of the two algorithms with a uniform damper distribution.
- compare the amount of time which is required to run the three optimization methods.

2 Problem Definition

For this study a structure has been designed for conditions in Bucharest, Romania, to represent an earthquake intensity with a mean return interval (M.R.I.) of 100 years and a corresponding peak ground acceleration (P.G.A.) of 0.24 g. The

values are consistent with the former Romanian design code. Current design provisions have increased the M.R.I. of the design earthquake to 225 years (Ministry of Regional Development and Tourism (2008) P100/2013) with a corresponding P.G.A. of 0.3 g for Bucharest. To that extent the considered structure does not meet the requirements of the current design code. In order to improve its seismic behavior viscous dampers are added to the structure.

Firstly a uniform distribution of dampers will be determined by imposing a level of equivalent damping $\zeta_d = 0.25$. Then the sum of the damping coefficients from the uniform distribution (C_{tot}) will be imposed as a constraint for the optimization process. The use of constraints reflects a practical design situation, as limiting the sum of values of the damping constants limits the forces developed by the dampers, and thus the cost (Takewaki 2000; Singh and Moreschi 2002; Silvestri and Trombetti 2007).

In order to determine the optimal distribution of the dampers a genetic algorithm, a pattern search algorithm and a direct descent method are used. Both algorithms are programmed in order to minimize the maximum drift of the structure. In order to determine the maximum drift the structure is modeled using finite elements and subjected to nonlinear dynamic analysis. Three ground motion records are used to represent the seismic hazard. The ground motion records used are from Vrancea 1977, 1986 and 1990 subcrustal earthquakes, all recorded at I.N.C.E.R.C station in Bucharest, which have been scaled in order to match the P.G.A. requirements of the current design code.

2.1 Test Structure

The test structure has been studied in a PhD thesis (Pricopie 2012). The test structure is a frame which has 6 storey, each of 3 m and 4 spans of 6 m each (Fig. 1). The structure is made from steel S345. The model includes distributed loads on the beams which accounts for dead loads (30 kN/m) and live loads (12 kN/m). The frame structure has been designed according to the codes and meets strength and displacement requirements for a 100 year M.R.I. Beams have a IPE 300 cross-section while the unbraced columns are HEA 400. For the braced columns HEA 500 has been used for the first two storeys HEA 450 for the third storey and HEA 400 for storeys 4–6. The braces have a pipe cross-section (121 mm \times 6 mm) from the bottom to the 4th storey and a pipe (183 mm \times 4 mm) on storeys 5 and 6.

The inelastic response of the structure is modeled using the finite element analysis software S.A.P. 200 V14. For each beam and column, plastic hinges were defined at both ends. For the braces the plastic behavior given by the axial force is modelled using one hinge, placed in the middle of the length of the brace. All of the properties of the plastic hinges are determined using the mean strength of the materials. The deformation capacities (rotations, elongations) are taken from FEMA 356 (2000). For the nonlinear analysis of the frame the natural damping is considered to be 2 % and represented by a Rayleigh model for damping.

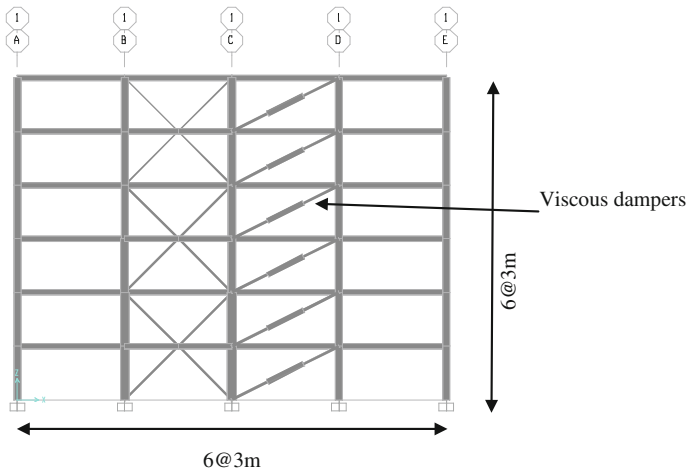


Fig. 1 The test structure

The effect of the shear force on the plastic properties of the elements is neglected and also the joints of the structure are assumed to be detailed in such a manner that plastic deformations do not occur. The model is considered fixed at the base.

The acceptance criteria for plastic rotations and elongations, considered for the design are taken from FEMA 356 (2000) and the structure is compliant for an earthquake corresponding to an M.R.I. of 100 years. For the increased M.R.I. of 225 years the structure does not comply with the design requirements. Both plastic rotations and maximum drifts were checked.

2.2 Design of the Uniform Distribution of Dampers Model

The first method of retrofit is based on a uniform distribution of viscous dampers. In order to determine the damping constants for the uniform distribution the principle of equivalent viscous damping is used (Constantinou et al. 2008). The energy dissipated by the dampers is equated to an increased percentage of critical damping for the structure. Using the characteristics of the structure the uniform damping constants are obtained:

$$C_{wdf} = \frac{4\pi\zeta_d \sum_i m_i \phi_i^2}{T_1 \sum_i m_i \phi_{ri}^2 \cos^2 \theta_i} \tag{1}$$

In this equation ζ_d represents the equivalent viscous damping introduced by the damper distribution and $m_i \phi_i, \phi_{ri}, \theta_i, T_1$ represent the storey mass, normalized displacement in the first mode, relative normalized displacement in the first mode, the angle between the horizontal direction and the direction of the “i” damper and

Table 1 Dynamic characteristics of the structure and damping constant for uniform distribution

Storey	Mass (kN s ² /m)	cos(θ)	T_1	ϕ	ϕ_r	C_{unf} (kN s/m)
6	88.088	0.894	0.77	1	0.145	3284
5	88.090			0.855	0.196	
4	88.165			0.659	0.177	
3	88.256			0.481	0.182	
2	88.350			0.299	0.184	
1	88.351			0.116	0.116	

the first period of the structure. The used values are presented in Table 1 for the studied structure. The damping constant C_{unf} for the uniform distribution was calculated for a value of damping ratio of $\xi_d = 25\%$.

2.3 Optimized Model Using Genetic Algorithms

Genetic algorithms are based on a heuristic search method which determines extreme values of a function. These algorithms have been used in the field of civil engineering in studies like Singh and Moreschi (2002), Silvestri and Trombetti (2007). The genetic algorithm starts with a random set of variables of the objective function which needs to be minimized. Through trial and error, variables which yield the minimum response of the function are selected and then combined in subsequent iterations which are called generations in order to determine the absolute minimum of the function. The general steps followed in this algorithm have been introduced by Holland (1975, 1992) and have been implemented to the current problem. The outline of the steps used by the genetic algorithm are the following:

1. Generate a random initial population of 200 individuals (which represent sets of variables).
2. Evaluate the fitness function for each of the individuals. In the present case the function is the maximum drift of the structure.
3. Create a new population based on the previous one by selecting the best performing individuals which are the variables with the lowest fitness function and subjecting them to crossover and mutation
4. Stop when there is no change in the best individual for a set number of generations.

Furthermore the algorithm has been designed in order to account for two constraints. The first constraint is imposed on each of the damping constants C_i which must not exceed a specified limit. The second constraint is that the sum of damping constants C_i will be for each individual equal to the sum of the damping constants from the uniform distribution. The problem is expressed by the following equations:

$$ff = \max(\delta_i) \quad (2)$$

$$C_{tot}^{unif} = 6C_{unif} = \sum_{i=1}^6 C_i \quad (3)$$

$$0 \leq C_i \leq C_{lim} \quad (4)$$

where Eq. (2) represents the value of the fitness function which needs to be minimized ff , δ_i —represents the maximum drift for each storey of the structure. As a limit for each damper C_{lim} Eq. (4) has a value of 7000 kN/m s a value which is approximately $2C_{unif}$. The limit on the damping constant translates into a limit on the maximum force developed in the damper. A large force in the damper can have a negative impact on the seismic response of the structure. The second constraint is expressed in Eq. (4) and sets a limit on the sum of the damping constants. The genetic algorithm accounts for these constraints when generating individuals. These constraints have been implemented through modifications to the original code by Holland (1975) which generates random individuals. For the current problem the generation, mutation and crossover functions of the genetic algorithm have been modified to generate individuals which fit the constraints. The genetic algorithm uses two point crossover and feasible mutation.

In problems with multiple variables the genetic algorithm can converge on local minimum of the function and not reach the global minimum. To that extent the algorithm was run a number of 5 times until the obtained results stabilized. Similar results were obtained for 4 out of 5 runs. One of the runs converged on a local minimum.

2.4 Optimized Model Using Pattern Search Algorithms

Pattern search techniques are a family of optimization methods that much like the genetic algorithms sample values of the variables in a programmed fashion in order to determine the extreme point of a function (Kolda et al. 2006; Matlab 2012). The algorithm does not require gradients and the objective function to be differentiable being suited for problems where the function cannot be differentiated or is not continuous. The basic idea of the algorithm is to sample the variables by steps of a certain magnitude and when it determines no change in the value of the function, reduce the magnitude of the sampled variables. Once a new minimum is determined the algorithm centers the search on that value and repeats the process until the magnitude of the variables becomes sufficiently small.

The pattern search algorithm uses a pattern of fixed base direction values. For the current example a $2N$ positive basis has been used for the pattern, where N represents the number of variables of the problem in this case 6. The vectors have a length of 6 and have the following form:

$$\begin{aligned}
 v_1 &= [1 \quad 0 \quad 0 \quad 0 \quad 0 \quad 0] \\
 &\quad \dots \\
 v_6 &= [0 \quad 0 \quad 0 \quad 0 \quad 0 \quad 1] \\
 v_7 &= [-1 \quad 0 \quad 0 \quad 0 \quad 0 \quad 0] \\
 &\quad \dots \\
 v_{12} &= [0 \quad 0 \quad 0 \quad 0 \quad 0 \quad -1]
 \end{aligned} \tag{5}$$

This pattern defines a mesh of points around an initial point, by varying each variable by a scalar value Δ^m , which is referred to as mesh size. The initial point for the current problem has been chosen as the point of the uniform distribution of dampers where all dampers have $C = C_{unif}$.

At each step the algorithm polls the points in the mesh by computing the value of the objective function in those points. If the algorithm finds a point with an objective function which is less than the previous the poll is called successful and that point becomes the base for the mesh and a new poll resumes. If the poll does not find a point with a smaller objective function the poll is unsuccessful and the mesh is again modified. The algorithm modifies the mesh by multiplies the mesh size Δ^m by 2 if the polling is successful and by 0.5 if the polling is unsuccessful.

The same constraints which were imposed for the genetic algorithm (Eqs. 3 and 4) are applied to the pattern search algorithm through the use of a penalty factor. Also the objective function is the same as for the genetic algorithm (Eq. 2).

To sum up the pattern search algorithm goes through the following steps:

1. Starts by evaluating the objective function for the uniform distribution.
2. Calculate the mesh size and poll the objective function for the points on the mesh.
3. If the poll is successful a new minimum point is found and the mesh is centered on that point. If the poll is unsuccessful the size of the mesh decreases.
4. The algorithm stops after 100 iterations.

2.5 Optimized Model Using Takewaki (2000) Algorithm

The last optimization model to be used was introduced by Takewaki (2000) and it relies on using a direct descent method. The problem can be formulated using a generalized Lagrange multipliers (λ , μ , η) approach:

$$L(C_i, \lambda, \mu, \eta) = \sum_{i=1}^6 \sigma_{d_i}^2 + \lambda (\sum_{i=1}^6 C_i - C_{tot}) + \sum_{i=1}^6 \mu_i (0 - C_i) + \sum_{i=1}^6 \mu_i (C_i - C_{lim}) \tag{6}$$

A reduced single degree of freedom model is used in order to simplify the problem. Once this model is arrived at the equation of motion can be written in the frequency domain:

$$(K + i\omega C - \omega^2 M)u(\omega) = -Mr\ddot{u}(\omega) \tag{7}$$

where M, C, K are the mass matrix, damping matrix, stiffness matrix of the reduced model, r is a column vector with 1 on every position and $u(\omega)$ is the Fourier transform of the displacement vector. The mean square response of the interstorey displacement $\sigma_{d_i}^2$ can be expressed as:

$$\sigma_{d_i}^2 = \int_{-\infty}^{+\infty} |H_{d_i}(\omega)|^2 P_g(\omega) d\omega \tag{8}$$

where $Hd(\omega) = -TA^{-1}rM$ is the transfer functions for each of the interstorey displacement and $P_g(\omega)$ is the power spectral density of the ground motion in this case the Vrancea 1977 ground motion record, recorded at I.N.C.E.R.C.

Using this formulation the first and second order sensitivities of the structure can be derived and used in order to come up with the optimal distribution of the dampers which minimizes the sum of interstorey drifts. The optimization has been studied in a PhD thesis (Pricopie 2012).

3 Results

Both the genetic algorithm and the pattern search algorithm have been programmed in Matlab. For each evaluation of the objective function in both the genetic algorithm and the pattern search algorithm a nonlinear analysis is run in the SAP 2000 v 14 software. The genetic algorithm converges on the optimal solution in 63 generations of 200 individuals each, which adds up to 12,600 evaluations of the maximum drift. However that number is smaller as similar individuals appear in different generations. On average the routine takes 6 h to solve. The results of the

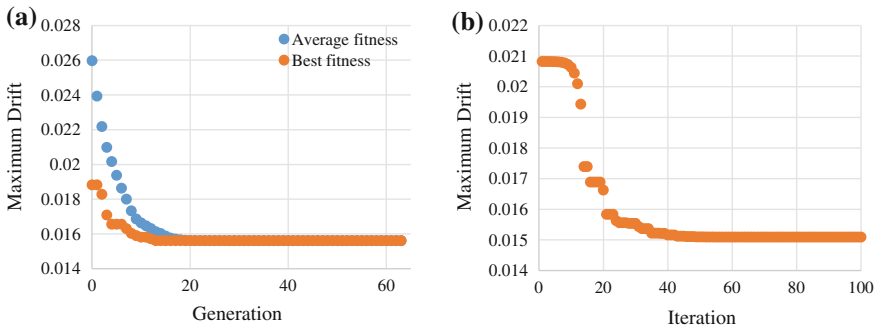


Fig. 2 **a** Best fitness function average fitness function for genetic algorithm; **b** best objective function pattern search optimization

genetic algorithm are presented in Fig. 2a in the form of the evolution of the best fitness function of the generation and the average fitness function of the generation. The conclusion is that the major improvement in the optimization process occurs up to around generation 20, after that the results stabilize.

The pattern search algorithm is programmed to stop after 100 iterations. The best point for the objective function and its variations through the iterations are presented in Fig. 2b. It is evident that the considered number of iterations is enough to obtain a result, as it stabilizes after about 50 iterations. The same is obvious by studying Fig. 3a in which the size of the mesh is presented for the pattern search algorithm. The size of the mesh is very close to 0 after 50 iterations, which means that a new minimum is was not found during the iteration. The run time for the pattern search algorithm is about 4 h and it evaluates the objective function only 309 times, a significantly lower number of runs than the genetic algorithm.

Takewaki's optimization algorithm relies on solving the problem in the frequency domain and relies on the steepest descent algorithm. The most important limitation is that the structure is considered elastic, although as will be shown the structure has high nonlinear response during an earthquake.

The results for the damping constant for the four considered distributions (uniform distribution, optimized using genetic algorithm, optimized using pattern search algorithms (P.S.), optimized using Takewaki's algorithm) are show in Fig. 3b and in Table 2. Analysing the results the dampers on storeys 2, 3 and 4 are the most important to reduce the seismic response. In all of the optimization algorithms these dampers have the highest values for damping constants C_i . The pattern search algorithm is the most efficient from an economic point of view as it only uses 3 dampers on storeys 2, 3 and 4.

The genetic algorithm and the one optimized using Takewaki's method both use 4 dampers and show that the first and last storey damper are not important to

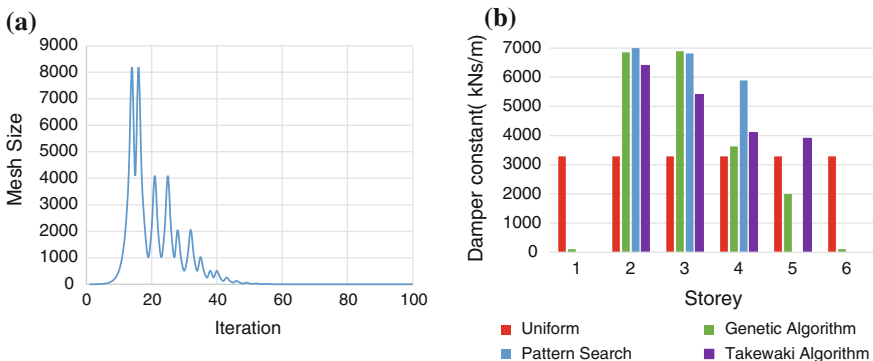


Fig. 3 **a** Mesh size through iterations for the pattern search algorithm; **b** distribution of damping constants

Table 2 Damping constant for each distribution

Storey	Damping constant (kN s ² /m)			
	Uniform	Genetic	P.S.	T.A.
1	3284	101	0	0
2	3284	6850	7000	6400
3	3284	6894	6816	5400
4	3284	3623	5888	4100
5	3284	1996	0	3900
6	3284	101	0	0

controlling the maximum drift. The genetic algorithm instead is closer to the pattern search algorithm concentrating the largest damping constants on stories 2 and 3.

In terms of the maximum storey drift response the profile of the drift is presented in Fig. 4 and the values are given in Table 3 for each of the studied models. The improvement from the model with no dampers to the uniform distribution of dampers is 48 % while the use of the optimized models brings the percentage to

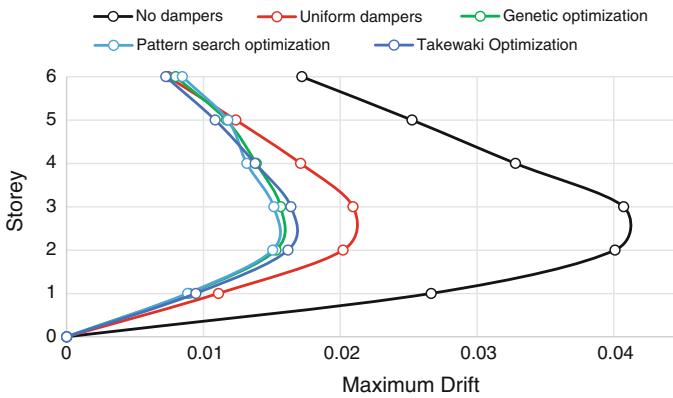


Fig. 4 Maximum drift for each storey and each distribution

Table 3 Maximum drift for each storey and each distribution

Storey	Drift for each type of damper distribution				
	No dampers	Uniform	Genetic	PS	Takewaki
6	0.017193	0.007401	0.007967	0.008458	0.007246
5	0.025245	0.012365	0.011681	0.011782	0.010856
4	0.032807	0.0171	0.013861	0.013167	0.013779
3	0.040713	0.020931	0.015642	0.015146	0.016393
2	0.040084	0.020203	0.015299	0.015061	0.016177
1	0.026646	0.011098	0.008946	0.008841	0.009444

61 % for the genetic algorithm model and to almost 63 % for the pattern search model. Although the reduction in drift from the response given by the genetic algorithm to the pattern search distribution is very small, the results in terms of damping constants are quite different. From a design point of view the pattern search remains the best option as it provides the best drift results while using only 3 dampers to rehabilitate the structure.

In Fig. 5a the number of plastic hinges and the acceptance criteria (immediate occupancy, life safety or collapse prevention) which is reached in each one is presented. If the no damper model has 4 plastic hinges which surpass the collapse prevention level, all of the models which use dampers have plastic hinges which are either in the elastic domain or are below the life safety limit. The pattern search optimized model behaves marginally better than the genetic algorithm having 2 less plastic hinges. The model optimized using the Takewaki method behaves almost as well as the other two optimized models with 5 more plastic hinges forming compared to the pattern search model.

From the point of view of the forces developed in the dampers, Fig. 5b shows the time history force response of the second storey damper, the damper which develops the largest forces on the structure. The force is presented during a sequence of 3 s which includes the maximum acceleration of the ground motion recorded at INCERC site in Bucharest on March 4 1977.

The uniform distribution develops the least force in the damper. The Takewaki optimized distribution provides better results but the largest forces are produced by the genetic algorithm and the pattern search distribution. The differences between the pattern search distribution and the genetic algorithm distribution is very small, suggested also by the close response in drifts. From the point of view of the damper distributions they are more effective when the forces developed in the dampers are largest. However from a retrofit point of view care needs to be given to the capacity of the elements to withstand the forces introduced by the viscous dampers. Generally the maximum forces in the dampers do not occur simultaneously with the maximum forces in the elements resulted from the earthquake load.

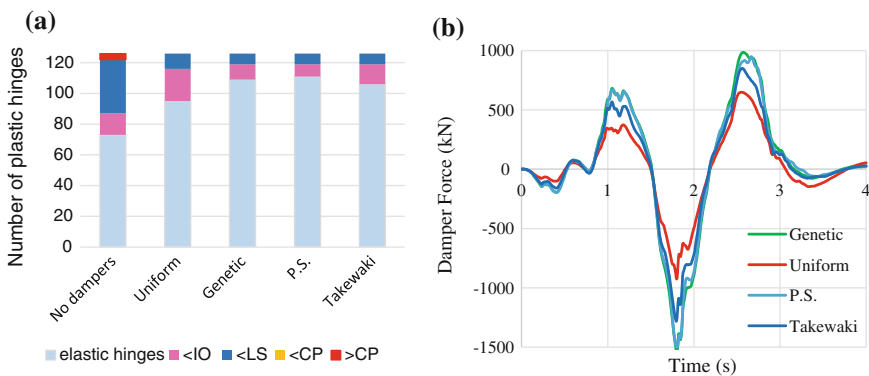


Fig. 5 a Number of plastic hinges and their acceptance criteria; b damper force for each model

4 Conclusions

The current study investigates the use of viscous dampers to improve the seismic response of a 6 storey steel structure. A uniform distribution is proposed and then optimized using 3 optimization methods, genetic algorithms, pattern search algorithms and a method developed by Takewaki (2000). Both the pattern search algorithm and the genetic algorithm use the maximum drift of the structure as the function which needs to be minimized. Takewaki's algorithm uses the sum of the drifts as the function to be minimized. All of the three methods optimize using constraints on the total sum of the damping constants and an upper limit on each damping constant. The following conclusions can be drawn from the study:

1. The use of genetic algorithms in order to determine the optimal distribution has been successful. The reduction in drift is of 61 % from the model without dampers. The advantage over the uniform distribution is that it uses 2 less dampers than the uniform distribution. The disadvantage of the genetic algorithm optimization model is that it is the most time consuming of the methods with 7 h of run time and it also failed to produce the absolute minimum of the function.
2. The pattern search algorithms to determine the optimal distribution was also successful and took only half of the time of the genetic algorithm. It converged to a lower value of the objective function which decreases the drift of the structure by 62 %. Although the difference is minimal with respect to the genetic algorithm (only 1 %) the value is obtained using only 3 dampers, one damper less than the optimized genetic algorithm distribution. Out of the studied methods the pattern search algorithm obtained the largest reduction in both drift and number of dampers which need to be used.
3. The optimization method proposed by Takewaki (2000) is the fastest optimization method with a run time for the current problem of under one hour. The results which it produces are close to both of the other two optimization techniques. The maximum drift of the structure is reduced by 59 % and the number of dampers used is 4 the same as the genetic algorithm results. The improvement in response is better than the uniform distribution but the other two optimization techniques provide marginally better results. This is caused by the fact that the method does not account for the plastic behavior of the structure. However taking into account the time required to run the analysis the method provides a reasonable estimate of the optimum distribution.

The pattern search algorithm was proved to provide the best results in a reasonable run time. For larger structures which have more elements, using genetic algorithms will be unfeasible because of the considerable run time. The Takewaki (2000) algorithm is the fastest method but the reduction in seismic response is better for the genetic algorithm and the pattern search algorithm. The pattern search algorithm has a balance between the run time and reducing the seismic response.

Further developments can be made by studying optimization for nonlinear viscous dampers and also considering other objective functions other than interstorey drift.

References

- A.S.C.E., FEMA 356 (2000) NEHRP guidelines for seismic rehabilitation of buildings, Washington D.C
- Constantinou MC, Kircher CA, Whittaker AS, Johnson MW, Gomez J, Ramirez OM (2008) Development and evaluation of simplified procedures for analysis and design of buildings with passive energy dissipation systems, Buffalo
- Holland JH (1975) Adaptation in natural and artificial systems. University of Michigan Press, Ann Arbor
- Holland JH (1992) Genetic algorithms, scientific American, July 1992, pp 44–50
- Kolda TG, Lewis RM, Torczon V (2006) A generating set direct search augmented Lagrangian algorithm for optimization with a combination of general and linear constraints. Technical report SAND2006-5315, Sandia National Laboratories
- Martinez RM, Romero ML (2003) An optimum retrofit strategy for moment resisting frames with nonlinear viscous dampers for seismic applications. Eng Struct 25:913–925
- MATLAB 8.0 and Statistics Toolbox 8.1 (2012) The MathWorks, Inc., Natick, Massachusetts, United States
- Ministry of Regional Development and Tourism (2008) Seismic design code. Part 1—Design provisions for buildings. P100-1/2013, Bucharest
- Pricopie A (2012) Attenuation of seismic response through the use of viscous dampers. Ph.D. thesis, U.T.C.B., Bucuresti
- Pricopie A, Pavel F (2013) Rehabilitation of structures using optimal viscous damper placement. In: Earthquake engineering conference, Skopje, 29–31 May 2013
- Silvestri S, Trombetti T (2007) Physical and numerical approaches for the optimal insertion of seismic viscous dampers in shear-type structures. J Earthq Eng 11(5):787–828
- Singh MP, Moreschi LM (2002) Optimal placement of dampers for passive response control. Earthq Eng Struct Dyn 31(4):955–976
- Takewaki I (2000) Optimal damper placement for critical excitation. Probab Eng Mech 15: 317–325
- Trombetti T, Silvestri S (2004) Added viscous dampers in shear-type structures: the effectiveness of mass proportional damping. J Earthq Eng 8(2):275–313

Selecting and Scaling Strong Ground Motion Records Based on Conditional Mean Spectra. Case Study for Iasi City in Romania

Radu Vacareanu, Mihail Iancovici and Florin Pavel

Abstract The Conditional Mean Spectrum (CMS) represents one of the versatile tools for selecting and scaling the strong ground motion records for a particular site. The procedure to obtain the Conditional Mean Spectrum (CMS) presented in Baker (2011) is applied for Iasi City in N-E Romania, the second largest Romanian city in terms of seismic risk. The major seismic hazard for most of Romanian territory is dominated by the Vrancea intermediate-depth seismic source. The ground motion prediction model, proposed in Vacareanu et al. (2015) for intermediate-depth earthquakes, is used for the computation of Uniform Hazard Spectrum (UHS) and the Conditional Mean Spectrum (CMS) at a vibration period of $T = 1.0$ s in Iasi City. The spectral period of 1.0 s is considered to be representative for the new stock of residential and office RC buildings in Romania. Disaggregation of seismic hazard is performed in order to determine mean causal values of magnitude, source-to-site-distance and epsilon. Empirical correlations between epsilon values at different vibration periods are calculated using a set of strong ground motions recorded during ten intermediate-depth Vrancea earthquakes. Moreover, based on the empirical values of the correlation coefficients, corresponding predictive relations are developed specifically for strong ground motions generated by Vrancea intermediate-depth earthquakes. Record selection and scaling based on the criteria proposed by Baker and Cornell (2006) and Baker (2011) is performed for Iasi City using a database consisting of strong ground motions recorded during Vrancea intermediate-depth earthquakes with moment magnitude larger than 6.0.

R. Vacareanu (✉) · F. Pavel

Seismic Risk Assessment Research Center, Technical University of Civil Engineering,
Bucharest, Romania

e-mail: radu.vacareanu@utcb.ro

F. Pavel

e-mail: florin.pavel@utcb.ro

M. Iancovici

Department of Structural Mechanics, Technical University of Civil Engineering, Bucharest,
Romania

e-mail: mihail.iancovici@utcb.ro

© Springer International Publishing Switzerland 2016

R. Vacareanu and C. Ionescu (eds.), *The 1940 Vrancea Earthquake.*

Issues, Insights and Lessons Learnt, Springer Natural Hazards,

DOI 10.1007/978-3-319-29844-3_26

Keywords Vrancea seismic source · Ground motions · Uniform hazard spectrum · Conditional mean spectrum · Selection and scaling of ground motions

1 Introduction

EN 1998-1 (CEN 2004), ASCE/SEI 41-06 (ASCE 2007), ASCE/SEI 7-10 (ASCE 2010), P100-1/2013 (MDRAP 2013), just to mention some seismic design technical regulations and codes, require the use of appropriate input strong ground motion records to perform linear and nonlinear time-history analyses. The structural engineer, consequently, is responsible for selecting and scaling seismic records for earthquake-resistant design of buildings and structures. Nevertheless, the information provided to this aim to the structural engineer by the technical regulations is rather scarce and incomplete. To fill in this gap, the research community embarked in a concentrated effort for better defining the target response spectra and for developing criteria and algorithms for selecting and scaling strong ground motion records. In a narrow time-span, valuable results were produced and incorporated in several documents and computer codes.

The conditional mean spectrum (CMS) was introduced by Baker and Cornell (2006) as “*a target spectrum that accounts for the magnitude (M), distance (R) and ε values, likely to cause a given target ground motion intensity at a given site*”.

The use of CMS as target spectrum for strong ground motion selection is analyzed in Baker (2011). A review of current methodologies used in the selection of ground motion records for response time-history analyses is given in Katsanos et al. (2010). A critical analysis on the use of the Uniform Hazard Spectrum (UHS) in the selection of ground motion records is also given in Baker (2011).

NIST (2011) contains guidance for selecting, generating, and scaling strong ground motions records to be used as input for performing linear and non-linear dynamic response analyses. The background information and the relevant application of NIST (2011) are discussed in Haselton et al. (2012).

The issue of amplitude scaling of strong ground motion records is evaluated in Luco and Bazzurro (2007). The paper analyzes whether scaling of records randomly selected from a magnitude-distance bin to a target fundamental-mode spectral acceleration level introduces bias in the expected nonlinear structural response of both single-degree-of-freedom oscillators and multi-degree-of-freedom building. Luco and Bazzurro (2007) showed that scaling can indeed introduce a bias in the expected seismic response that, for the most part, can be explained by differences between the elastic response spectra of the scaled versus unscaled records.

Wang et al. (2015) presents an interactive tool for selecting strong ground motion records—Design Ground Motion Library (DGML)—based on contemporary knowledge and engineering practice. The interactive tool constructs design response spectra (i.e. conditional mean spectra, code spectra and user-specified

spectra) based on the Next Generation Attenuation relationships (<http://peer.berkeley.edu/nga/>).

Iervolino et al. (2010) discussed the difficulties for practitioners to apply the prescriptions of codes and guidelines on the use of real records as input for non-linear time-history analysis. In order to tackle this issue, the REXEL software tool for the selection of real strong ground motion records was developed (freely available at http://www.re Luis.it/index_eng.html). REXEL allows searching for suites of waveforms from the European Strong-motion Database and Italian Database (ITACA) that are compatible with reference spectra (either user-defined or automatically generated according to EN 1998-1 (CEN 2004) and the recently released new Italian seismic code) (Iervolino et al. 2010).

Smerzini et al. (2013) address the selection of displacement-spectrum compatible real strong ground motion records. To this aim, a software tool for computer-aided displacement-based record selection is developed. Examples of application in Italy show that sets of unscaled, or lightly-scaled, strong ground motions with limited record-to-record spectral variability can easily be selected even if a broadband spectral compatibility is required.

The issue of selection of input ground motions for linear and nonlinear time-history analyses based solely on a target mean response spectrum, and thus ignoring the variance of the target response spectrum and likely producing biased structural response estimates, is discussed in Jayaram et al. (2011). In order to obtain unbiased estimates of structural response, Jayaram et al. (2011) proposes a computationally efficient and theoretically consistent algorithm to select ground motions matching the target response spectrum mean and variance; the algorithm is further used to select strong ground motion records for the analysis of sample structures in order to assess the impact of considering ground motion variance on the structural response estimates.

Cimellaro (2013) proposes new prediction models for the correlation coefficients of ε values at different periods using earthquake records from a European ground motion database and highlights the dependence of the predicted values of correlation coefficients to the database and to the ground motion prediction model used for obtaining the ε values.

The scope of the present study is three-folded: (i) to obtain the Uniform Hazard Spectra for Iasi City in Romania based on the ground motion prediction equation (GMPE) developed for Vrancea intermediate-depth seismic source in Vacareanu et al. (2015); (ii) to obtain the correlation coefficients of ε values and their predictive relations based on a database of strong ground motions recorded during several Vrancea intermediate-depth earthquakes and on the GMPE given in Vacareanu et al. (2015); (iii) to obtain the Conditional Mean Spectra (CMS) at the vibration period of $T=1.0$ s for Iasi City in Romania based on the results of (i) and (ii) and to select and/or scale strong ground motion records from Vrancea database that match the CMS for Iasi.

Iasi City, located in N-E part of Romania, is the second largest city in terms of exposure to seismic risk. The influence on the seismic hazard of Iasi of the Vrancea intermediate-depth seismic source is overwhelming if compared to Barlad Basin crustal seismic source (Vacareanu et al. 2016). Consequently, the seismic hazard for

Iasi City is evaluated in this study considering solely Vrancea intermediate-depth seismic source. A detailed description of the seismological features of the Vrancea intermediate-depth seismic source is beyond the scope of this paper and relevant information can be found elsewhere (e.g. Radulian et al. 2000; Ismail-Zadeh et al. 2012; Lungu et al. 2000).

In a previous paper of Vacareanu et al. (2014) the Uniform Hazard Spectrum (UHS) and Conditional Mean Spectrum (CMS) for the city of Bucharest are obtained and a record selection based on the criteria proposed by Baker and Cornell (2006) and Baker (2011) is performed using a database of strong ground motions recorded during four Vrancea intermediate-depth seismic events.

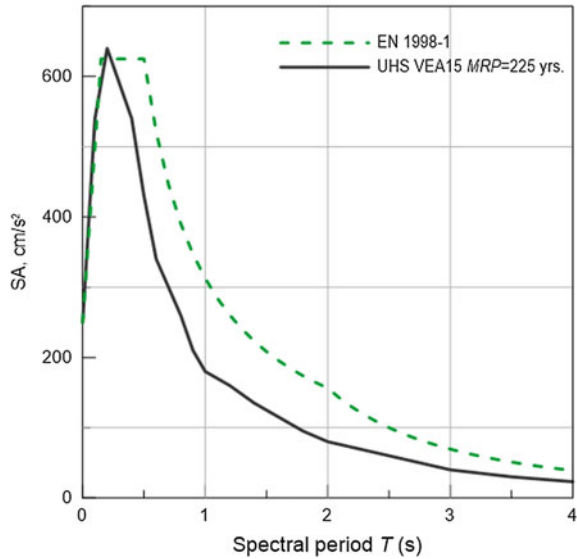
2 Uniform Hazard Spectra (UHS) and Seismic Hazard Disaggregation Analysis for Iasi City

An important step in obtaining the CMS is the development of Uniform Hazard Spectrum (UHS) through probabilistic seismic hazard analysis (PSHA) (Kramer 1996; McGuire 1999, 2004). The spectral ordinates of the UHS have the same annual exceedance rate at each period of vibration.

The information on seismicity of Vrancea intermediate-depth seismic source is obtained from ROMPLUS earthquake catalogue of National Institute for Earth Physics of Romania (<http://www.infp.ro/catalog-seismic>). The minimum magnitude considered in the analysis $M_{W,\min} = 5$ ensures the completeness of catalogue for the 20th century; the maximum magnitude taken into account in the PSHA is $M_{W,\max} = 8.1$. More details on the input data and the results of PSHA can be found in Vacareanu et al. (2016).

For PSHA analysis, the ground motion prediction equation developed for Vrancea intermediate-depth seismic source (Vacareanu et al. 2015) is used (called hereinafter VEA15). VEA15 is applicable on soil classes B and C and on average soil conditions, as well. Moreover, VEA15 provides faster attenuation in the back-arc region (with respect to the Carpathians Mountains) than in the fore-arc region. The uniform hazard spectrum is computed using the seismicity parameters of Vrancea intermediate source given in Vacareanu et al. (2016) and the VEA15 GMPE. The UHS with 20 % exceedance probability in 50 years (mean return period $MRP = 225$ years) is presented in Fig. 1. The mean return period of 225 years selected in the representation is considered for the Life Safety Limit State in the Romanian earthquake-resistant design code P100-1/2013 (MDRAP 2013). According to the soil conditions database assembled in BIGSEES research project (<http://infp.infp.ro/bigsees/default.htm>), soil class B, as it is defined in EN 1998-1 (CEN 2004), can be considered for Iasi. The same soil class is assigned if one uses the methodology of Wald and Allen (2007) implemented on USGS website (<http://earthquake.usgs.gov/hazards/apps/vs30/custom.php>). The UHS in Fig. 1 is compared with the design spectrum of EN 1998-1 (CEN 2004) for soil class B anchored at the peak ground acceleration value with 20 % exceedance probability in 50 years.

Fig. 1 Uniform hazard spectrum with 20 % exceedance probability in 50 years for Iasi. The UHS is compared with the EN 1998-1 type I elastic spectrum for soil class B



The close match between the EN 1998-1 design spectrum for soil class B and the obtained UHS in the short period range is emphasized.

It is noted that the values obtained in this study for the peak ground acceleration in Iasi City with a probability of exceedance of 39 % in 50 years and, respectively 20 % in 50 years, match very closely the values given in the seismic design code of Romania previously in force, P100-1/2006 (MTCT 2006) (design peak ground acceleration of 0.20 g) and currently in force, P100-1/2013 (MDRAP 2013) (design peak ground acceleration of 0.25 g), respectively. The values of the design peak ground acceleration given in P100-1/2006 and P100-1/2013 are obtained with the same methodology described in this chapter but the input data on seismicity and the GMPEs are different. Details on the seismicity parameters for Vrancea intermediate-depth seismic source and on the GMPE used for the seismic hazard map of the previous design code P100-1/2006 (MTCT 2006) can be found in Lungu et al. (2000).

The magnitude M_w of the earthquake and source-to-site (hypocentral) distance R to be used for obtaining the predicted mean of the natural logarithm of spectral acceleration at the period of vibration of interest T_1 are obtained through the disaggregation of the seismic hazard (Bazzurro and Cornell 1999; McGuire 1999). This method allows the identification of the relative contribution magnitudes M_w , distances R and epsilon values ϵ to the conditional exceedance of seismic hazard parameter $SA(T_1)$. The seismic hazard disaggregation analysis, as shown in McGuire (1999), quantifies the contribution of each magnitude M_w , distance R and epsilon ϵ ranges, to the hazard. Epsilon ϵ parameter—the normalized residual—represents the number of standard deviations by which an observed logarithmic spectral acceleration differs from the mean logarithmic spectral acceleration given by a GMPE (Baker and Cornell 2006).

The contributions to the hazard of M_w , R and ε for the parameter of interest in our analyses, $SA(T = 1.0 \text{ s})$ with a probability of exceedance of 10 % in 50 years are shown in Fig. 2. The results are obtained using 0.1 units bins for magnitude, 10 km units for source-to-site distance and 0.2 units for ε , respectively. One can notice from Fig. 2 the overwhelming contribution to the seismic hazard of Iasi City of Vrancea intermediate-depth source, situated at hypocentral distances in excess of 200 km, if compared to the Barlad Basin crustal source situated at much closer source-to-site distances.

The mean causal values of magnitude, source-to-site distance and epsilon for Iasi are given in the Table 1.

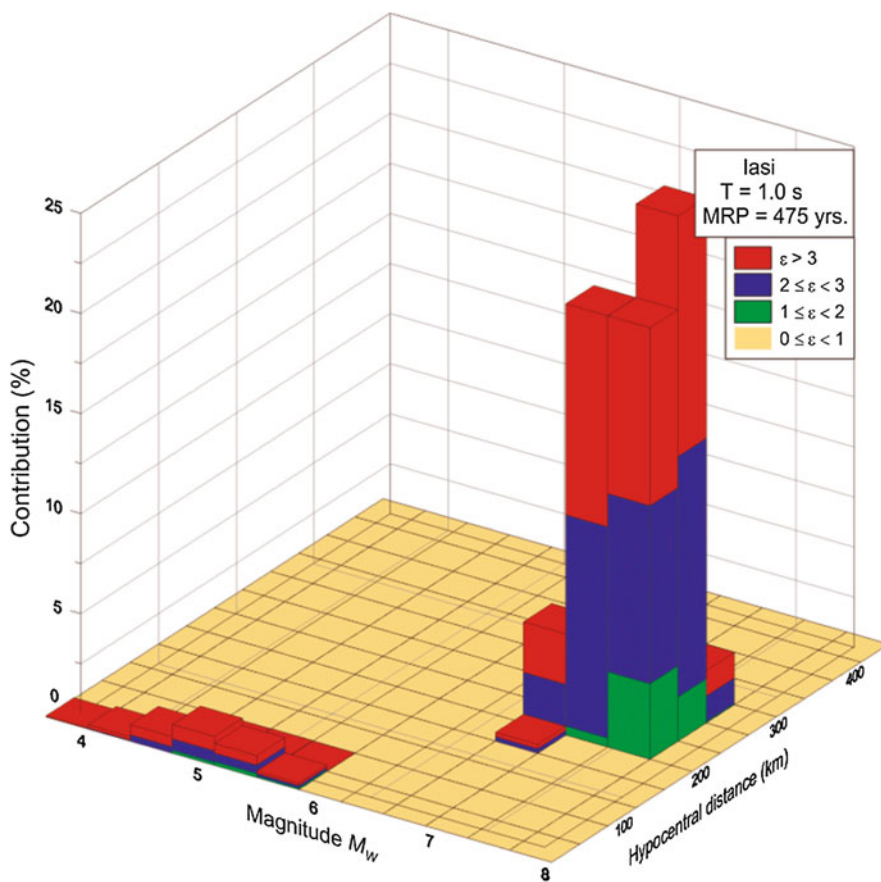


Fig. 2 Seismic hazard disaggregation at Iasi for $SA(T = 1.0 \text{ s})$ with 10 % exceedance probability in 50 years

Table 1 Mean causal values for $SA(T = 1.0 \text{ s})$ at Iasi

M_w	R (km)	ε
7.50	209.8	1.104

3 Correlation Coefficients Between ε Values. CMS for Iasi City

If T_1 is the period of vibration of interest in developing the CMS and the corresponding value of ε is $\varepsilon(T_1)$, then the conditional mean of ε at another period T_2 is (Baker 2011):

$$\mu_{\varepsilon(T_2)|\varepsilon(T_1)} = \rho(T_2, T_1) \cdot \varepsilon(T_1) \quad (1)$$

where $\rho(T_2, T_1)$ is the correlation coefficient between the ε values at the two spectral periods.

The CMS is obtained by adding the predicted mean of the natural logarithm of spectral acceleration at the period of vibration of interest T_1 with the product between the standard deviation of the natural logarithm of spectral acceleration at the period of vibration of interest T_1 and the conditional mean of ε at some other period T_2 (Baker 2011):

$$\mu_{\ln Sa(T_2)|\ln Sa(T_1)} = \mu_{\ln(Sa(T))}(M, R, T_1) + \rho(T_2, T_1) \cdot \varepsilon(T_1) \cdot \sigma_{\ln SA}(T_1) \quad (2)$$

The correlation coefficients $\rho(T_2, T_1)$ between the ε values at two periods T_1 and T_2 are used in Eq. (1) to obtain the conditional mean of ε at another period T_2 given the mean value of ε at period T_1 . Various relations exist in the literature for the prediction of $\rho(T_2, T_1)$ (Baker and Cornell 2006; Chiou and Youngs 2008; Cimellaro 2013). Nevertheless, the values of the parameters of the prediction relations depend on the database and on the GMPE used for the calculation of ε values at different periods of vibration. Cimellaro (2013) showed the differences between the correlation coefficients obtained using European and Californian datasets. Goda and Atkinson (2009) noticed differences between correlation coefficients obtained using Californian and Japanese datasets. The previous remarks point out the need for regional calibration of the predictive relations for correlation coefficients $\rho(T_2, T_1)$.

The Vrancea strong ground motions database used in the present regression analysis for predicting the values of the correlation coefficients was assembled for the BIGSEES research project and consists now (as of November 2015) of more than 400 triaxial accelerograms recorded during ten seismic events of intermediate-depth with moment magnitudes M_W ranging from 5.2 to 7.4. The strong ground motions were recorded by four seismic networks of Romania: INFP (National Institute for Earth Physics), INCERC (Building Research Institute), CNRRS (National Centre for Seismic Risk Reduction) and GEOTEC (Institute for Geotechnical and Geophysical Studies). Details on the structure of the databases used in the analysis can be found in Vacareanu et al. (2015).

The ε values at different vibration periods are obtained using the observed values in the Vrancea strong ground motion database and the predicted mean values obtained using VEA15 GMPE with the mean causal values of magnitude and

source-to-site distance from Table 1. Figure 3 presents some examples for pairs of ε values at vibration periods of 0.2, 1.0 and 2.0 s. It is noted that the observed correlation between $\varepsilon(1s)$ and $\varepsilon(2s)$ is better than the observed correlation between $\varepsilon(1s)$ and $\varepsilon(0.2s)$ and the slope of the trend line is lower for the second case. Both previous remarks are in line with the conclusions drawn in Baker (2011).

The correlation coefficients of ε values at different vibration periods are then obtained. The contours of the empirically obtained correlation coefficients of ε values versus vibration periods T_1 and T_2 are represented in Fig. 4. As it is expected, the correlation coefficients approach unity when the two vibration periods are close together and they decrease as the vibration periods become further apart from each other. Our conclusions are in line with Cimellaro (2013) and Goda and Atkinson (2009). Moreover, the results obtained from Vrancea dataset show no increase of the correlation coefficients for pairs of well-separated vibration periods; the same conclusion is drawn in Cimellaro (2013) for the Italian dataset and it is opposite to the trend observed by Baker and Cornell (2006) for Californian data.

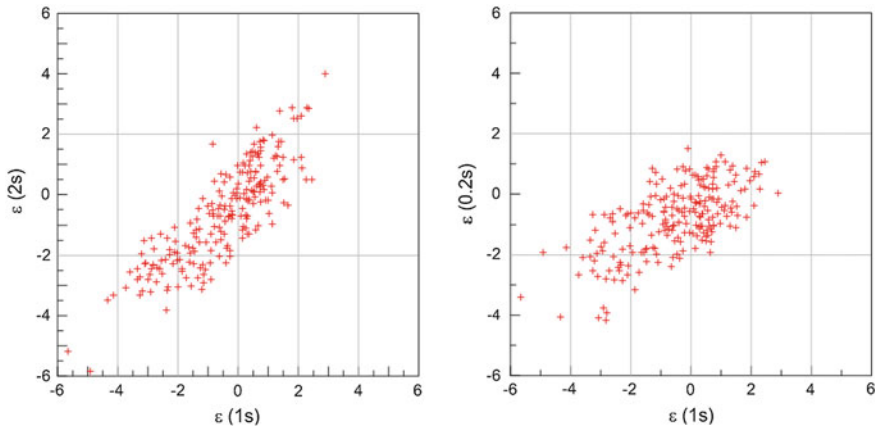
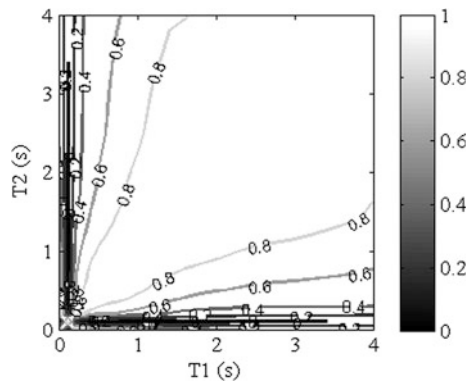


Fig. 3 $\varepsilon(1s)$ versus $\varepsilon(2s)$ (left) and $\varepsilon(1s)$ versus $\varepsilon(0.2s)$ (right)

Fig. 4 Contours of the obtained correlation coefficients of ε values versus vibration periods T_1 and T_2



The predicted values of the correlation coefficients for ε at different vibration periods are determined from regression of empirical observations using the functional form (Cimellaro 2013):

$$\rho(T_2, T_1) = 1 - \left(\frac{A_0 + A_2 \lg(T_{\min}) + A_4 (\lg(T_{\max}))^2}{1 + A_1 \lg(T_{\max}) + A_3 (\lg(T_{\min}))^2} \right) \cdot \ln \left(\frac{T_{\min}}{T_{\max}} \right) \quad (3)$$

where $T_{\min} = \min(T_1, T_2)$ and $T_{\max} = \max(T_1, T_2)$ and $A_0 \dots A_4$ are the parameters of the regression model. The values of the parameters in Eq. (3) corresponding to Vrancea dataset are given in Table 2 for VEA15 GMPE.

The predicted correlation coefficients are compared with the ones empirically obtained in Fig. 5. There is no bias in the predicted values and the ratios of the predicted to observed values have mean values very close to unity. One can notice the close match between the predicted and the observed correlation coefficients, except a region of negative correlation coefficients situated around the vibration period of 0.1 s. The residuals between the observed and the predicted values are in the range of $-0.08 \dots 0.08$. The mean and median values of the residuals are 0.007 and 0.014. The statistical indicators mentioned previously and the plots in Fig. 5 prove the validity of the model proposed by Eq. (3) and of the parameters given in Table 2.

Table 2 Parameters of the regression model (3)

A_0	A_1	A_2	A_3	A_4
-0.3066	0.5073	-0.0683	-0.4939	0.0162

Fig. 5 Observed versus predicted correlation coefficients

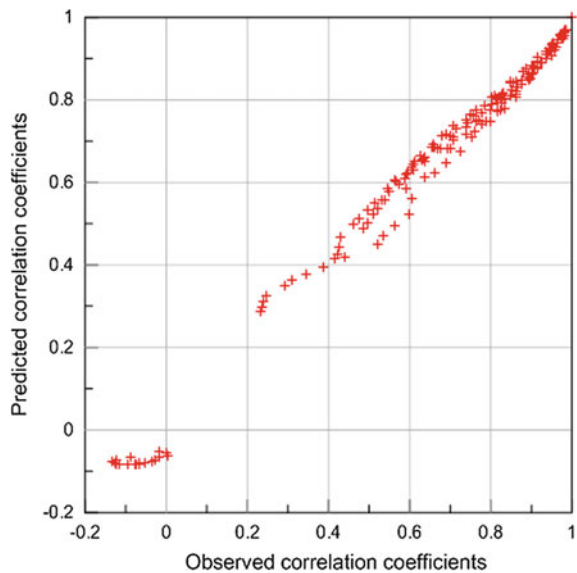
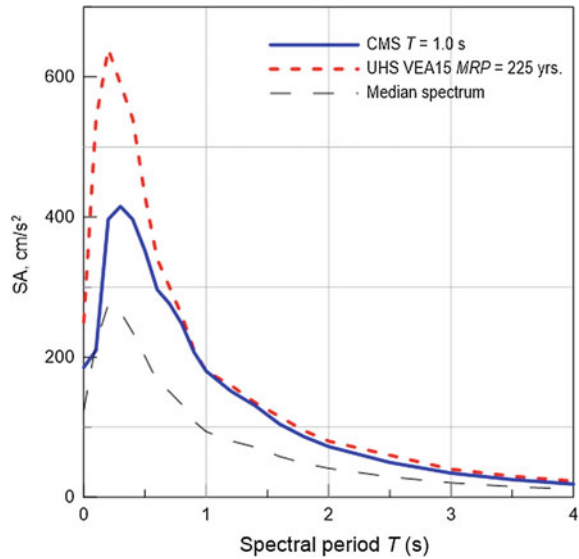


Fig. 6 CMS at $T = 1.0$ s, 20 %/50 years UHS and median spectrum for Iasi



Eventually, the Conditional Mean Spectra at $T = 1.0$ s for Iasi City is determined with Eq. (1). The results obtained are reported in Fig. 6, as follows: (i) the Conditional Mean Spectrum for a vibration period of $T = 1.0$ s, (ii) the Uniform Hazard Spectrum with an exceedance probability of 20 % in 50 years and (iii) the predicted median spectrum corresponding to the mean causal values $M_W = 7.50$ and $R = 209.8$ km. The epsilon value for the vibration period of $T = 1.0$ s is 1.104. As expected, for positive epsilon values, the CMS falls below the UHS for the entire vibration period range, except for $T = 1.0$ s, where the two spectral ordinates are equal.

The spectral period of 1.0 s is considered representative for a large part of the new and future building stock in Iasi; in the decade, residential buildings of 15–20 stories with dual RC structural system (moment resisting frames and shear walls) and office buildings of 8–12 stories with RC moment resisting frames came in large numbers in Romania and the current trend is quite similar; since the fundamental vibration period of these buildings is in the vicinity of 1.0 s, the CMS developed in this study, as well as the selected strong ground motions, will provide a useful tool for linear and nonlinear time-history analyses that are recommended by P100-1/2013 (MDRAP 2013) earthquake resistant design code.

4 Selection and Scaling of Strong Ground Motions

The pool for the selection of strong ground motions for Iasi City is a subset of Vrancea intermediate-depth database consisting of over 250 horizontal components recorded during four intermediate-depth Vrancea earthquakes with moment

magnitudes larger than 6.0: March 4, 1977 ($M_W = 7.4$, $h = 94$ km), August 30, 1986 ($M_W = 7.1$, $h = 131$ km), May 30, 1990 ($M_W = 6.9$, $h = 91$ km) and May 31, 1990 ($M_W = 6.4$, $h = 87$ km). Several criteria for selecting strong ground motions are given in Baker and Cornell (2006) and Baker (2011). In this study, three criteria are used for selection:

- I. ground motions having representative ε values for the site;
- II. unscaled ground motions with the smallest *SSE* (sum of squared errors);
- III. scaled ground motions with the smallest *SSE*; this criterion requires beforehand the computation of the scaling factors *SF* and then of the *SSE*.

Using these three selection criteria, we rank the most appropriate strong ground motions for Iasi on average soil conditions, matching the CMS conditioned upon the spectral absolute acceleration at a vibration period of $T = 1.0$ s with 20 % exceedance probability in 50 years.

The sum of squared errors (*SSE*) is obtained as (Baker 2011):

$$SSE = \sum_{j=1}^n (\ln SA(T_j) - \ln SA_{CMS}(T_j))^2 \quad (4)$$

SSE represents here the sum of the differences between the logarithm of actual spectral acceleration and the logarithm of the spectral acceleration from the target spectrum (in this case, CMS). The sum is considered for a period range $0.2T_1$ to $2T_1$ (Baker 2011), where $T_1 = 1.0$ s.

The ground motion parameter ε has been identified as an indicator of spectral shape; the spectrum shape does not change with scaling (Baker and Cornell 2006). For the previously mentioned arguments, the scaling procedure can be applied for selecting representative strong ground motions.

The scaling factor represents the ratio of target spectral acceleration and actual spectral acceleration of ground motion corresponding to the structural natural period of interest T_1 as (Baker 2011):

$$SF = \frac{SA_{CMS}(T_1)}{SA(T_1)} \quad (5)$$

The most representative seven strong ground motions resulting from the application of criteria I–III are given in Table 3. The response spectra of the top three most representative strong ground motions according to the criteria II and III are compared with the CMS in Fig. 7.

The correlations between *SSE* and $\varepsilon(1s)$ for both unscaled and scaled strong ground motions are shown in Fig. 8. There is a strong negative correlation between the *SSE* of unscaled strong ground motions and the values of $\varepsilon(1s)$ providing thus further evidence that epsilon is indeed a valid spectral shape indicator. On the other hand, this strong correlation vanishes for the case of scaled strong ground motions.

Table 3 Most representative strong ground motion for CMS at $T = 1.0$ s for Iasi

Strong ground motion	Criterion I	Criterion II	Criterion III	SSE
	$\varepsilon(1s)$	SSE	SF	
I.1. BIR NS—record of August 30, 1986	1.112			
I.2. CLS N30E—record of May 30, 1990	1.122			
I.3. BIR EW—record of May 30, 1990	1.128			
I.4. CVD NS—record of May 30, 1990	1.143			
I.5. CVD EW—record of May 30, 1990	1.022			
I.6. INC EW—record of May 30, 1990	1.189			
I.7. BLV N155E—record of May 30, 1990	0.997			
II.1. RMS N55E—record of August 30, 1986		0.716		
II.2. BIR EW—record of August 30, 1986		0.795		
II.3. BIR EW—record of May 30, 1990		1.029		
II.4. BIR NS—record of August 30, 1986		1.040		
II.5. BIR NS—record of May 30, 1990		1.102		
II.6. EREN N162E—record of August 30, 1986		1.139		
II.7. EREN N72E—record of August 30, 1986		1.150		
III.1. BIR EW—record of August 30, 1986			0.796	0.153
III.2. ARM EW—record of May 31, 1990			6.748	0.448
III.3. VAR N162E—record of May 30, 1990			4.670	0.475
III.4. DIMO NS—record of May 30, 1990			3.073	0.539
III.5. RMS N168E—record of May 31, 1990			3.187	0.556
III.6. BOZ EW—record of May 30, 1990			2.493	0.592
III.7. TIT N55W—record of August 30, 1986			2.115	0.597

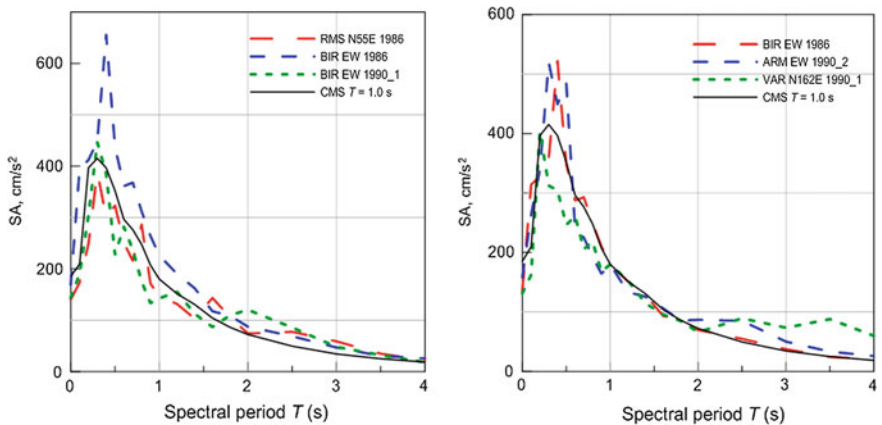


Fig. 7 Conditional mean spectrum and response spectra of the top three records selected using the SSE criterion for unscaled strong ground motions (*left*) and the SSE criterion for scaled strong ground motions (*right*)

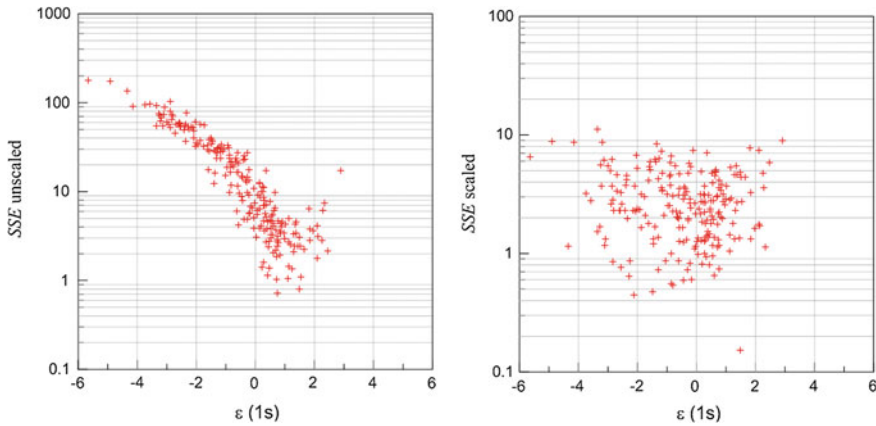


Fig. 8 SSE versus $\varepsilon(1s)$ for unscaled strong ground motions (*left*) and for scaled strong ground motions (*right*)

5 Conclusions

In this paper we obtained the Uniform Hazard Spectrum (UHS) and the Conditional Mean Spectrum (CMS) for the selection of acceleration time-series to be used for the linear and nonlinear time-history analysis of buildings and structures with a vibration period of $T = 1.0$ s located in Iasi, a representative city in Romania in terms of seismic hazard and risk exposure.

The results presented in this paper contributed to (i) developing specific predictive relations for the correlation coefficients of epsilon values at two vibration periods using the GMPE given in Vacareanu et al. (2015) and a set of strong ground motions recorded during ten Vrancea intermediate-depth earthquakes; (ii) obtaining Uniform Hazard Spectrum and Conditional Mean Spectrum at $T = 1.0$ s for Iasi City; (iii) selecting and scaling strong ground motion records compatible with CMS at $T = 1.0$ s for Iasi City.

The main conclusions of our paper are summarized as follows:

- The values obtained in this study for the peak ground acceleration at Iasi having a probability of exceedance of 39 % in 50 years and, respectively 20 % in 50 years, closely match the values given in the seismic design code of Romania previously in force, P100-1/2006 (MTCT 2006) and in the code in force, P100-1/2013 (MDRAP 2013), respectively.
- The EN 1998-1 elastic spectrum for soil class B closely matches the obtained UHS in the short period range.
- The obtained parameters of the predictive relation for the correlation coefficients of epsilon values at different vibration periods valid for strong ground motions recorded during Vrancea intermediate-depth earthquakes are different from the ones reported by Cimellaro (2013), thus showing the rationale for regional calibration.

- There is a strong negative correlation between the SSE of unscaled strong ground motions and the values of $\varepsilon(1s)$, providing thus further evidence that epsilon is indeed a valid spectral shape indicator. On the other hand, this strong correlation vanishes for the case of scaled strong ground motions.

Acknowledgements Funding for this research was provided by the Romanian Ministry of National Education and Scientific Research under the Grant Number 72/2012. This support is gratefully acknowledged. The earthquakes catalogue of Vrancea subcrustal source was provided by the National Institute for Earth Physics INFP within BIGSEES Project.

References

- ASCE (2007) Seismic rehabilitation of existing buildings, ASCE/SEI 41-06. American Society of Civil Engineers, Reston
- ASCE (2010) Minimum design loads for buildings and other structures, ASCE/SEI 7-10. American Society of Civil Engineers, Reston
- Baker J (2011) Conditional mean spectrum: tool for ground motion selection. *J Struct Eng* 137 (3):322–331
- Baker J, Cornell CA (2006) Spectral shape, epsilon and record selection. *Earthq Eng Struct Dyn* 35:1077–1095
- Bazzurro P, Cornell CA (1999) Disaggregation of seismic hazard. *Bull Seism Soc Am* 89(2): 501–520
- CEN (2004) EN 1998-1 Design of structures for earthquake resistance—Part 1: General rules, seismic actions and rules for buildings. European Committee for Standardization, Brussels
- Chiou BS-J, Youngs RR (2008) An NGA model for the average horizontal component of peak ground motion and response spectra. *Earthq Spec* 24(1):173–215
- Cimellaro GP (2013) Correlation in spectral accelerations for earthquakes in Europe. *Earthq Eng Struct Dyn* 42:623–633
- Haselton CB, Whittaker AS, Hortaacsu A, Baker JW, Bray J, Grant DN (2012) Selecting and scaling earthquake ground motions for performing response-history analyses. In: Proceedings of the 15th world conference on earthquake engineering (WCEE), Lisbon, Portugal, (CD-ROM)
- <http://peer.berkeley.edu/nga/>
- <http://www.infp.ro/catalog-seismic>
- http://www.reluis.it/index_eng.html
- <http://infp.infp.ro/bigsees/default.htm>
- <http://earthquake.usgs.gov/hazards/apps/vs30/custom.php>
- Iervolino I, Galasso C, Cosenza E (2010) REXEL: computer aided record selection for code-based seismic structural analysis. *Bull Earthq Eng* 8:339–362
- Ismail-Zadeh AT, Matenco L, Radulian M, Cloetingh S, Panza GF (2012) Geodynamics and intermediate-depth seismicity in Vrancea (the south-eastern Carpathians): current state-of-the-art. *Tectonophysics* 530–531:50–79
- Jayaram N, Lin T, Baker JW (2011) A computationally efficient ground-motion selection algorithm for matching a target response spectrum mean and variance. *Earthq Spec* 27(3): 797–815
- Katsanos E, Sextos A, Manolis G (2010) Selection of earthquake ground motion records: a state-of-the-art review from a structural engineering perspective. *Soil Dyn Earthq Eng* 30: 157–169
- Kramer S (1996) Geotechnical earthquake engineering. Prentice Hall, Upper Saddle River

- Luco N, Bazzurro P (2007) Does amplitude scaling of ground motion records result in biased nonlinear structural drift responses? *Earthq Eng Struct Dyn* 36:1813–1835
- Lungu D, Vacareanu R, Aldea A, Arion C (2000) *Advanced structural analysis*. Conspress, Bucharest
- McGuire R (1999) Probabilistic seismic hazard analysis and design earthquakes: closing the loop. *Bull Seism Soc Am* 85(5):1275–1284
- McGuire R (2004) *Seismic hazard and risk analysis*. Earthquake Engineering Research Institute, MNO-10
- MDRAP (2013) P100-1/2013. Code for seismic design—Part I—Design prescriptions for buildings. Ministry of Regional Development and Public Administration, Bucharest, Romania (in Romanian)
- MTCT (2006) P100-1/2006 Code for seismic design—Part I—Design prescriptions for buildings. Ministry of Transports, Constructions and Tourism, Bucharest, Romania (in Romanian)
- NIST (2011) Selecting and scaling earthquake ground motions for performing response history analysis, NIST/GCR 11-917-15, prepared by the NEHRP consultants joint venture for the National Institute of Standards and Technology. Gaithersburg, Maryland
- Radulian M, Mandrescu N, Popescu E, Utale A, Panza G (2000) Characterization of Romanian seismic zones. *Pure appl Geophys* 157:57–77
- Smerzini C, Galasso C, Iervolino I, Paolucci R (2013) Ground motion record selection based on broadband spectral compatibility. *Earthq Spec* (in press). doi:<http://dx.doi.org/10.1193/052312EQS197M>
- Vacareanu R, Iancovici M, Pavel F (2014) Conditional mean spectrum for Bucharest, earthquakes and structures. *Int J* 7(2):141–157
- Vacareanu R, Radulian M, Iancovici M, Pavel F, Neagu C (2015) Fore-arc and back-arc ground motion prediction model for Vrancea intermediate depth seismic source. *J Earthq Eng* 9 (13):535–562
- Vacareanu R, Aldea A, Lungu D, Pavel F, Neagu C, Arion C, Demetriu S, Iancovici M (2016) Probabilistic seismic hazard assessment for Romania. In: D'Amico S (ed) *Earthquakes and their impact on society*. Springer Natural Hazards Book Series, pp 137–169, ISBN 978-3-319-21752-9 (Print) 978-3-319-21753-6 (Online), <http://dx.doi.org/10.1007/978-3-319-21753-6>
- Wald DJ, Allen TI (2007) Topographic slope as a proxy for seismic site conditions and amplification. *Bull Seismol Soc Am* 97(5):1379–1395
- Wang G, Youngs R, Power M, Li Z (2015) Design ground motion library (DGML): an interactive tool for selecting earthquake ground motions. *Earthq Spectra* 31(2):617–635

Part IV
Seismic Evaluation and Rehabilitation.
Seismic Risk Assessment

Overview of Part IV: Seismic Evaluation and Rehabilitation. Seismic Risk Assessment

Carmen Ortanza Cioflan and Mihail Iancovici

This chapter includes papers that deal with the seismic evaluation and rehabilitation of existing buildings in Romania and neighbouring countries- e.g. Republic of Moldova, using both fundamental and cutting-edge approaches.

The seismic assessment and rehabilitation of existing constructions after the 10th of November 1940 and 4th of March 1977 earthquakes in Romania are investigated in a very practical approach, presenting the main concepts, the analysis methods and the strengthening methods used for existing structures. Two examples of such structures, one from Bucharest, the other from Focsani, are thus discussed in the paper entitled “[Seismic Assessment and Rehabilitation of Existing Constructions After the 10th November 1940 and 4th March 1977 Earthquakes in Romania](#)”. The authors conclude that the original method, based on energy concepts to judge the failure criteria for resistance and deformation, by comparing the surface of member’s capacity, for a single degree of freedom model of various multi-story constructions, to the surface required by the building response to different types of earthquakes, is still valid today. The failure theories, based on the energetic model from strut-tie models, or taking into consideration the areas in which the theories based on the continuous, homogenous and isotropic body hypothesis cannot be applied, for which specific finite element models apply for the potential cracking areas or probabilistic models with the aid of fragility curves, are all analysis methods of medium or greater complexity which are necessary to be applied for the structures or areas of structures of important constructions and which will be developed more in the future.

C.O. Cioflan (✉)

National Institute for Earth Physics, Măgurele, Romania
e-mail: cioflan@infp.ro

M. Iancovici

Seismic Risk Assessment Research Center, Technical University
of Civil Engineering Bucharest, Bucharest, Romania
e-mail: mihail.iancovici@utcb.ro

In the paper entitled “[Some Remarks Regarding Seismic Vulnerability for Orthodox Churches](#)” the sensitive problem of seismic evaluation of historical buildings is treated using cutting-edge approaches. The large number of existing and unique historical monuments in Romania draws the attention over the importance of rehabilitation and conservation works that need to be carried out in order to prevent their damage. The global concern regarding the conservation of world heritage is obvious if the ongoing projects would be considered. Integrated Rehabilitation and Research on Architectural and Archaeological Heritage (IRPP/SAAH) is one of the main projects in this field, in which a priority list was made containing 186 architectural monuments and archaeological sites from nine participating countries, which need to be rehabilitated. In the paper the authors present an analysis of the seismic vulnerability of masonry orthodox churches located in Moldavia region. Old masonry structures were considered and a comparison between the three main types of churches is shown—churches with rectangular, trefoil or Greek cross plan configuration. Structural vulnerability analysis for the considered typologies is done based on nonlinear static analysis (pushover). Vulnerability and fragility curves for the analyzed structures are plotted based on the results and on the well-known methodology. The paper also discusses the way of reducing the risk of casualties caused by the vulnerability in case of a mass gathering of people. In this respect, numerical simulations are performed for the analysis of evacuation time required in relation to a certain level of structural response, for the three types of the considered structures.

The paper entitled “[The Effects of an Analogous to November 10, 1940 EQ Over the Buildings Stock in Republic of Moldova](#)”, presents an estimation of seismic-induced damage in the Republic of Moldova through a comprehensive Damage-Loss Methodology. The territory of the Republic of Moldova has been suffering heavy damages and losses as a result of the activity of the intermediate depth earthquake sources located in the area of Vrancea region, Romania. The severity of these earthquakes, combined with limited resources, has a significant negative impact on the population and infrastructure of the Republic of Moldova. The Vrancea earthquake of November 10, 1940 was selected as the earthquake scenario—the strongest event occurred in the 20th century. The total number of buildings taken into account into analysis is about 1.5 million units. The potential loss was represented in damage terms through the “the average damage grade”. The authors conclude that in Moldova there are areas presenting high probability of large damage caused by future strong earthquakes. Weaknesses concerning seismic safety in the Republic of Moldova as well as the necessary preventive scientific, political, administrative measures have been also listed.

Another work addressed to the nowadays consequences of an earthquake similar to the November 10, 1940 event is “[Seismic Loss Estimates for Scenarios of the 1940 Vrancea Earthquake](#)”. Using the newly implemented System for Estimating the Seismic Damage in Romania operated by NIEP, (SeisDaRo), authors estimate the possible damage caused by scenarios of this earthquake. In order to provide a reasonable dimension of the possible accelerations and their distribution over the territory of Romania, 3 ground motion prediction equations developed especially

for Vrancea intermediate-depth events have been selected. An analytical methodology (Improved Displacement Coefficient Method) implemented in SELENA software has been used to estimate direct seismic losses. Vulnerability data comes from the last available census and consists in number of buildings for 1400 territorial administrative zones/units (cities, communes or sectors of Bucharest) located in the extra-Carpathian area. For each TAZ 48 building types are identified (depending construction materials, height classes and construction periods) with their associated capacity and fragility curves and corresponding number of residents per building type. The damage estimates for each ground motion scenario are presented on relevant maps, discussed and compared with the ones reported after the November 10, 1940 event. Authors conclude that a similar earthquake nowadays will produce greater damage and mitigation actions are much required. Seismic risk analyses in Romania are focused mainly on buildings (which concentrate most of the damage). Also, many studies refer to the action of earthquakes on bridges and/or other individual infrastructure elements that require special design and analysis. Much less (published) work is treating in an applicative manner the impact of earthquakes on transportation network.

The paper entitled “[Conceptual Framework for the Seismic Risk Evaluation of Transportation Networks in Romania](#)” is an attempt to identify viable ways to analyse the seismic risk of transportation networks, considering the availability and characteristics of specific data, the possibilities of adapting external knowledge and new methodologies recently developed. The integrative framework described here incorporates GIS capabilities (ArcGIS Network Analyst Toolbox), fragility functions for critical structures (bridges, tunnels) used for estimations of the damage level and traffic characteristics in order to analyse the connectivity and capacity of the transportation network to accommodate the demand in post-earthquake context. The proposed quantification of risks is based on comparison between performance indicators estimated for the undamaged network and the damaged one in order to identify critical elements and to improve its configuration. Framework’s applicability to Romania is tested for the case of Bucharest by using mostly public information available for road networks. Results are presented in suggestive maps for intervention times (ambulances and for fire trucks) or fastest routes between northern and southern Bucharest for emergency intervention vehicles, considering various scenarios. Further developments/improvements of the traffic modelling are proposed and discussed.

Modern approach in mitigation of seismic risk requires not only the decrease of seismic vulnerability of the build environment but also preparedness measures and planning of the emergency reaction. The paper “[Rapid Earthquake Early Warning \(REWS\) in Romania: Application in Real Time for Governmental Authority and Critical Infrastructures](#)” presents the Romanian Rapid Early Warning System (REWS) operational since 2013. REWS is sending alerts and notifications to the emergency response authorities, emergency centres from ministries and also to critical nuclear infrastructures (nuclear research facilities, power plants and other similar activities). Recent technical upgrades of seismic equipment and rapid communication together with research on methodologies to estimate magnitude

allows a rapid broadcast of alerts. Using only 4 s of data after P wave detection in epicentral area, REWS is rapidly locating and estimating the magnitude; alert is issued only if the magnitude of the seismic event is larger than 4. Taking into account that Vrancea intermediate depth events can produce extensive damages to neighbour countries, the REWS is sending alerts also to the Bulgarian Civil protection and Kozloduy nuclear power plant. Up to now, 19 alerts have been issued by REWS and no false alerts recorded. The performance and present development of the REWS is suitable to send alerts according to the user requirement in order to activate systems that can contribute to risk reduction before the dangerous waves reach the target area.

In the paper “[Analytical Seismic Fragility Functions for Dual RC Structures in Bucharest](#)” the issue of fragility functions is tackled using the analytical approach. To this aim incremental dynamic analyses are performed on two dual RC mid-rise and high-rise building structures designed according to the relevant codes in force in Romania. The buildings have the same horizontal layout with five spans of 8.00 m in both orthogonal directions. The nonlinear time history analyses required by the incremental dynamic analysis method are performed with STERA 3D ver. 5.8. The hysteretic model employed is a trilinear degrading one based on the Takeda model. The input ground motions for the nonlinear time history analyses are 75 horizontal components of site-dependent simulated accelerograms that are randomly selected from a larger set developed for the INCERC site in Bucharest. The selected site is characterized by predominant long-periods of vibration of soil in strong earthquakes and the simulated accelerograms are reproducing this trend. The analytical fragility functions are obtained using the results of NTHAs. The conditional intensity measures of the fragility functions are the peak ground acceleration and the spectral response values at the fundamental period of vibration of the buildings. The fragility functions are developed for both damage states and limit states and are fully defined by the median values and the lognormal standard deviations of the intensity measures.

Estimation of Damage-Loss from Scenario Earthquake Analogous to November 10, 1940 in Republic of Moldova

Vasile Alcaz, Eugen Isicico, Victoria Ghinsari and Sergiu Troian

Abstract The territory of the Republic of Moldova has been suffering heavy damages and losses as a result of the activity of the intermediate depth earthquake sources located in the area of Vrancea Mountains, Romania. The severity of these earthquakes, combined with limited resources, has a significant negative impact on the population and infrastructure of the Republic of Moldova. In order to provide a background of protection strategies, it is of utmost importance to perform the impact assessment of Vrancea earthquakes. In the present study an earthquake damage—loss assessment has been performed, with the aim to control and reduce the seismic risk on the territory of the Republic of Moldova. The Vrancea earthquake of 10.11.1940 was selected as an earthquake scenario—the strongest event of the 20th century with approximately 100 years return period and magnitude $M_{G-R} = 7.4$. The total number of buildings taken into calculation is about 1 million 50 thousand units. The potential loss was represented in damage terms through a parameter—“the average damage grade”. It was noticed that in Moldova there are areas with a high probability of serious damage caused by future earthquakes. Weaknesses concerning seismic safety in the Republic of Moldova as well as the necessary preventive scientific, political, administrative measures have been listed.

Keywords Hazard · Vulnerability · Buildings stock · Preventive measures

V. Alcaz (✉) · E. Isicico · V. Ghinsari · S. Troian
Institute of Geology and Seismology, Moldavian Academy of Sciences,
Academiei str., 3, Chişinău, Republic of Moldova
e-mail: alcazv@gmail.com

E. Isicico
e-mail: eisicico@yandex.ru

V. Ghinsari
e-mail: ginvictoria@yandex.ru

S. Troian
e-mail: troian.sergiu@gmail.com

1 Introduction

Seismic safety is among the most important factors to affect the social welfare and economic progress in a country which territory is within a seismic active region. The whole territory of the Republic of Moldova might be affected by seismic activity. Around 2/3 of the territory, which hosts approximately 3 million inhabitants, is considered to be high seismic hazard area (Alcaz 2004).

During the XX century the territory of Republic of Moldova has experienced several strong earthquakes originating from Vrancea intermediate-depth seismic source. The most significant seismic events were recorded in 1940, 1977, and 1986. These events resulted in numerous victims and economic losses. The severity of these earthquakes, combined with limited resources, has a significant negative impact on the population and infrastructure of the country. The disaster effect of the last strong earthquake (August, 30, 1986, $M = 7.0$) was represented by 2 deaths, 561 injured persons, 1169 completely destroyed buildings, meaning around 800 million \$US direct financial losses (Tshocher et al. 1941). The earthquake of November 10, 1940 caused damage to 2795 buildings in Chisinau, out of which 172 were totally ruined. There were about 78 victims and almost 1000 injured (note that this data is incomplete) (Oizerman et al. 1986).

It is a well-known fact that it is easier, less expensive and more efficient to invest in the prevention of seismic hazards, rather than to remove the damages after one destructive earthquake. The research regarding seismic risk has the aim to provide a new scientific background for the evaluation and prevention of human and material losses caused by seismic activity.

2 Data and Methodology

In Republic of Moldova there is a total number of 1650 localities. Over 50 of these are considered to be urban localities, cities or large villages, with the population from tens to hundreds of thousands people. In 2012–2013 a seismic risk evaluation of the 11 largest cities in Moldova was performed (Alcaz et al. 2012, 2013). However, considering that the urban population in Moldova represents 53 % of the total, it is important to consider evaluating the seismic risk for the whole territory of the country, and not only major urban localities.

The existing urban structure in Moldova was built in 1960–1980. The densest areas were populated with multi-storey buildings, which were constructed according to the typical Soviet designs, considering local seismic conditions. In the rural areas however, the most popular are one storey buildings, which are basically defined by the materials used in the construction process.

In the current study a classification of the buildings constructed in Moldova was performed, considering the degree of seismic resistance according to the MSK-64 scale. The whole building range was divided in three major types—*A*, *B*, *C*. *Type A* represents the low-rise buildings, built of local traditional materials, like air bricks,

adobe bricks, clay bricks or stone aggregates with clay mortar. *Type B* includes buildings built from burnt bricks or cut natural stones. *Type C* includes three stories or taller buildings constructed on individual or serial designs, considering anti-seismic measures, and built of precast concrete elements, cast concrete, brick or natural stone walls.

A total number of 1 million 50 thousand buildings were evaluated in the current research.

The collected information was structured accordingly for each locality, representing the three building categories (*A*, *B*, *C*) and the number of inhabitants. Afterwards, the data was structured for each administrative region of Moldova (districts), and the largest administrative entities: Autonomous Territorial Unit of Gagauzia, Transnistria, cities of Chisinau and Balti.

As known, *risk R* represents the probability of expected losses (deaths, injuries, property, livelihoods, economic activity disrupted or environment damaged) resulting from interactions between hazards *H* and vulnerability *V* and exposure *E*.

$$R = H * V * E \tag{1}$$

The parameter characterizing the *seismic hazard H* is generally used as the maximum seismic actions arising with a certain probability in a given area in a given time interval.

It is well known (Papadopoulos and Arvantides 1996) that the methods of risk assessment are scale-dependent. Short-, Mid- and Long-term may indicate, for example time scales of 1, 50 and 100 years respectively. In the present paper the seismic risk was determined in the long-term sense. According to this, the design seismic action (earthquake scenario) was selected the Vrancea earthquake of 10.11.1940—the strongest event of the 20th century with approximately 100 years return period and magnitude $M_{G-R} = 7.4$ (Constantinescu and Enescu 1963). Another aspect supporting this choice refers to the fact that the rocks rupture in the earthquake foci was directed to northeast to Moldova. As noted in chapter “[Overview of Part 1](#)”, the major earthquakes of 10/11/40 and 08/30/86, have had significant macro-seismic effect on the territory of Moldova in the last century. The data from these earthquakes have formed the basis for determining the equation of the macro-seismic field for the territory of the country, taking into account the direction of the rupture.

The resulting equation, considering the ellipsoidal macro-seismic field, is as follows (Alcaz et al. 2012):

$$I = 1.585 \cdot M - 6.72 \cdot \lg R + 1.5 \cdot \cos \gamma + 10 \tag{2}$$

where:

I is MSK intensity,

M Gutenberg-Richter magnitude,

R hypocentral distance,

γ angle between the azimuth of observation point and the major axis of the ellipse [$\theta_0 = 54 \pm 2^\circ$ (Shumila 1990)].

According to (Shumila 1990) the equation ($\theta_0 = 54 \pm 2^\circ$) was calculated as an average of 28 different earthquakes of Vrancea region with magnitudes $M = 4.2\text{--}7.5$, and is representative for any earthquake of the region.

The correlation coefficient of required parameters is 0.873, dispersion of intensity values for the chosen model of correlation is 0.17.

Unlike some previous investigations (Marza and Pantea 1994; Zaicenco et al. 1999) studying the general laws of intensity attenuation of Vrancea earthquakes, the Eq. (2) is derived for the best approximation in Moldova territory intensity field, with north-east direction of the focal rupture. This provides the estimation of earthquake intensity value anywhere in the Republic of Moldova for events similar to the earthquake of 11/10/40.

Another important part of determining the seismic risk is the *seismic vulnerability* of the objects. Vulnerability is the sensitivity of the elements exposed at risk to seismic hazard. The dependence of the vulnerability of the seismic action is usually represented by vulnerability function. Vulnerability function linking the degree of damage and the level of seismic action (defined in terms of MSK intensity) is determined, as a rule, empirically for different classes of seismic resistance of buildings. For creating vulnerability functions the engineering consequences of strong local earthquakes are studied and worldwide statistical data of damages for various classes of objects are attracted. The functions of vulnerability reflect primarily, the current construction practices in the region. As an example, in Fig. 1 the vulnerability function of limestone (manufactured stone units) buildings type B, widely represented in Republic of Moldova, is given (Alcaz et al. 2010). According to the MSK-64 scale, the degrees of damage ($d1\text{--}d5$) represent the following characteristics: $d1$ —slight damage, $d2$ —moderate damage, $d3$ —heavy damage, $d4$ —complete damage (beyond reparability), $d5$ —building collapse.

Knowing the distribution of seismic intensity, buildings stock and its vulnerability allows to calculate the seismic risk. Probabilistic value of seismic risk represented in the classical form (1), is largely abstract and difficult to be perceived by the majority of users. Rather than using abstract mathematical probabilities, for practical purposes it is more convenient to operate with clearer indicators, such as the expected damage, estimated volume of destructions, the number of affected

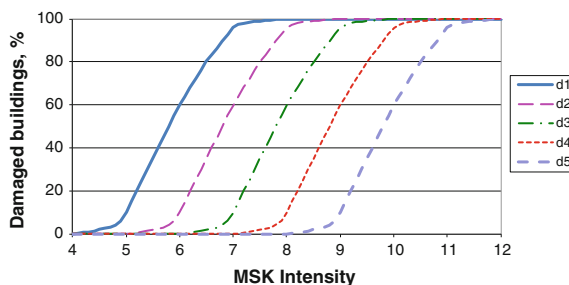


Fig. 1 Vulnerability function of the limestone (manufactured stone units) of buildings

residents, etc. In the present study seismic risk was calculated as (1) the average degree of damage and (2) the number of destroyed buildings within each locality of Moldova.

In the first method, in all localities applying the developed vulnerability matrices, the average degree of damage of the buildings at the selected seismic event (scenario) was determined:

$$\bar{d} = \frac{\sum_i d_i n_i}{\sum_i n_i} \quad (3)$$

where d_i —damage degree of the buildings; n_i —number of similar buildings with damage degree d_i .

In the second case, the indicator of seismic risk was represented by the volume of destruction within each administrative-territorial unit, namely the total number of buildings with damage of the fourth (d4) and the fifth degree (d5)—buildings that usually cannot be restored.

It is important to mention that the results presented are probabilistic. Using the method of a scenario earthquake requires that a series of assumptions are made, such as the magnitude of the earthquake, the position of the focus point, the intensity as a function of distance etc. The vulnerability of structures is considered by damage probability matrices.

3 Results and Discussions

Figure 2 shows diagrams of the distribution of potential building damages in some administrative-territorial units during the scenario earthquake, similar to the 11.10.1940 event. The diagrams show a full range of possible damages, from lowest (Ocnita district) to highest (Cahul and Cantemir districts). For medium damage potential the district of Straseni was selected as representative. The four largest administrative areas are presented in the diagram as well: Gagauzia, Transnistria, Chisinau and Balti.

Statistical overview of the results is presented in Table 1, and contains the results for all districts of Republic of Moldova. Table 1 presents the number of buildings which might be critically affected, having damages of degree 4 and 5. Table 1 also represents the average damage degree \bar{d} for each district. From the results it is observed that the average damage degree varies from 0.93 (Ocnita district) to 2.84 in the district of Cantemir.

Analysing the results presented in Table 1, the credibility of the results can be doubted, especially considering that both seismic hazard H and vulnerability V in Formula 1 are probabilistic values. However, the results impose that it is possible that once in a century, the Republic of Moldova with its current infrastructure and building vulnerability, if being exposed to an earthquake similar to the scenario

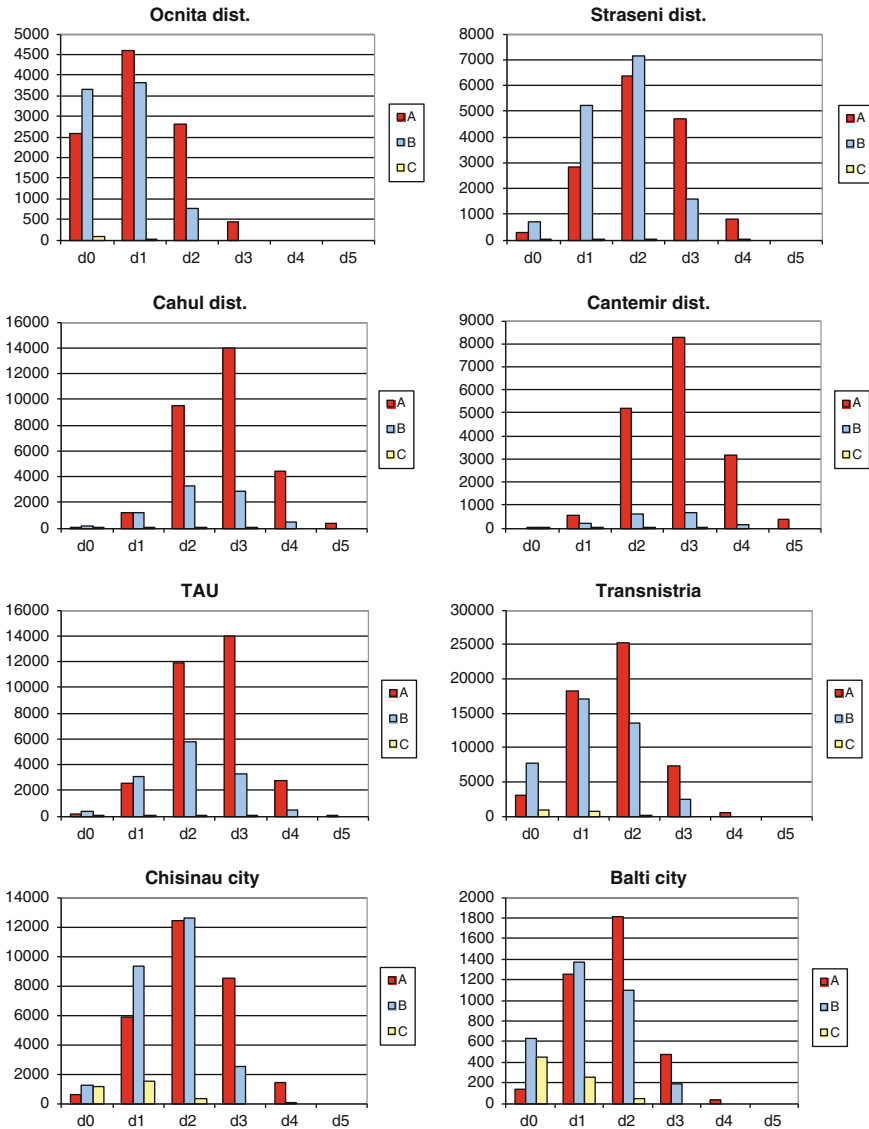


Fig. 2 Distribution of damage degrees of different types of buildings for some districts of Moldova, following the scenario earthquake 10.11.1940

presented in the current research paper, will suffer the likely consequences quantified and presented in Table 1.

Referring to the precision of the values of possible damages, the authors believe that the numbers reflect the true mathematical estimation of the damages and casualties which can occur. In other words, it can be firmly stated that an earthquake

Table 1 Likely damages following the scenario earthquake

N	Administrative-territorial units	Number of destroyed buildings	Average damage degree
1	Edineț	0	1.19
2	Briceni	0	1.03
3	Ocnîța	0	0.93
4	Dondușeni	0	1.16
5	Bălți	26	1.48
6	Fălești	743	1.89
7	Rîșcani	0	1.52
8	Glodeni	107	1.61
9	Sîngerei	342	1.74
10	Soroca	0	1.26
11	Drochia	0	1.33
12	Florești	1	1.43
13	Șoldănești	0	1.38
14	Orhei	430	1.66
15	Rezina	13	1.56
16	Telenești	363	1.71
17	Ungheni	1841	2.19
18	Călărași	969	2.05
19	Nisporeni	1319	2.34
20	Strășeni	837	1.93
21	Criuleni	425	1.74
22	Dubăsari	133	1.62
23	Anenii-Noi	358	1.77
24	Ialoveni	762	1.89
25	Hîncești	2700	2.37
26	Chișinău	1410	1.9
27	Cahul	5347	2.71
28	Cantemir	3657	2.84
29	Taraclia	832	2.48
30	UTA Găgăuzia	3238	2.4
31	Căușeni	767	1.86
32	Ștefan-Vodă	194	1.6
33	Basarabeasca	454	2.21
34	Leova	1888	2.62
35	Cimișlia	1451	2.37
36	Transnistria	565	1.45
	Total	31,172	1.81

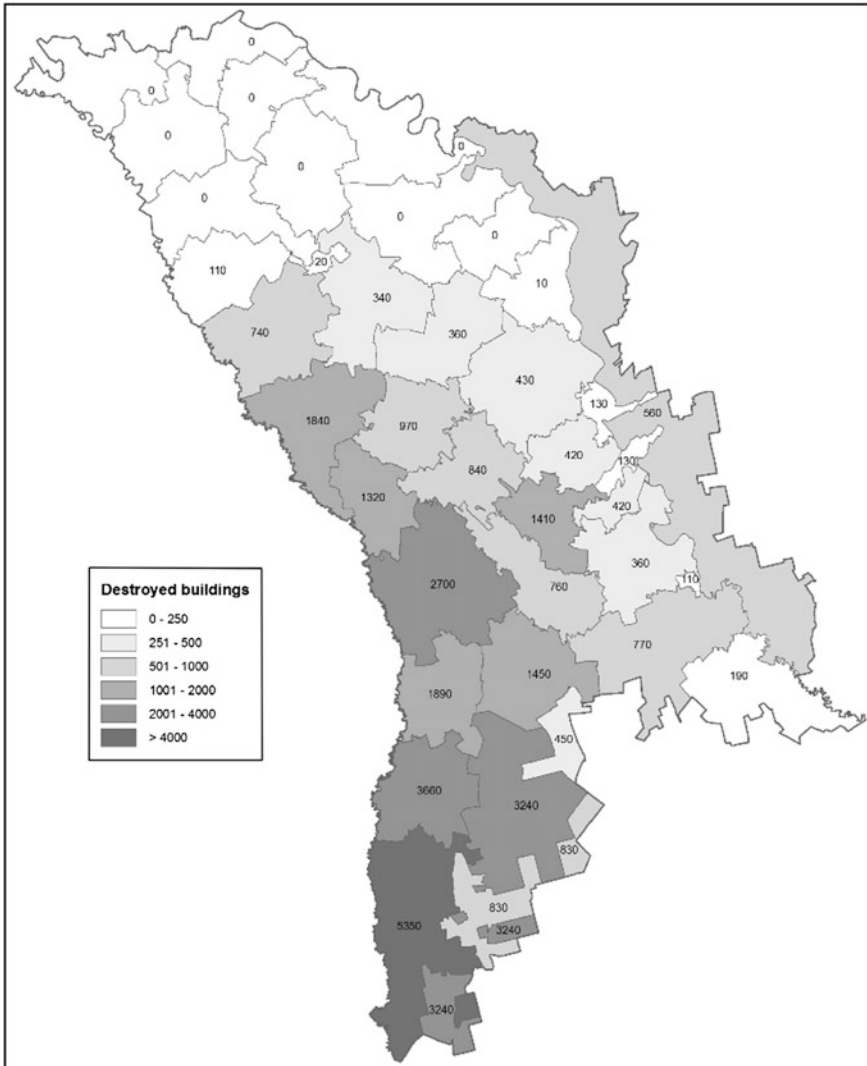


Fig. 4 The number of buildings which might be destroyed as a result of the scenario earthquake 10.11.1940

Analysing the figures it can be stated that the most affected might be the localities placed in the south-western part of the country. The least number of casualties and financial losses will happen in the northern districts of Moldova. The results of this research can be used by the local authorities, insurance organizations, and regional departments of Civil Protection and Emergency Situations Service for casualty prevention.

4 Conclusions and Recommendations

As a result of this research a quantitative map of the damage distribution in Republic of Moldova was developed. Expected losses were estimated in terms of average degree of damage of buildings with different seismic resistance. The results indicate areas with a high probability of heavy damages cause by future earthquakes. Therefore, expected damages from an earthquake analogous to November 1940 one reach levels of concern in the districts of Cahul, Leova and Cantemir.

The results of the current research helped to identify the most vulnerable regions in the country. This information can be used for the development of medium and long term strategic plans to minimize losses and casualties in case of earthquake hazards.

Concluding, it is to be mentioned that in order to ensure citizens safety on the territory of Republic of Moldova it is necessary to consider the following issues:

- Although the seismic risk in Moldova is being forecast, there is a lack of concrete measures to decrease it. Thus there are no projects being developed which would retrofit the important engineering structures of Moldova (buildings, dams, communication infrastructure);
- There is a low level of social awareness regarding earthquake hazard risks;
- Unauthorized reconstruction of flats in multi storey buildings is widely spread;
- Territorial planning and related decision making are often carried out without considering the existing risks and dangers;
- No well-designed strategy for removing damages following earthquake hazards has been developed.

In order to address the earthquake challenges developing and implementing a wide range of scientific, political and administrative measures is necessary.

Among the most urgent are:

- Developing methods for monitoring, warning and quantification of seismic hazard risk;
- Improving the regulatory framework that provides seismic resistant design and construction on the territory of Republic of Moldova in line with European standards;
- Investigation of existing buildings in order to determine the actual degree of seismic resistance, having as main targets the stocks of schools, kindergartens, hospitals, buildings of high importance, especially the ones deteriorated in time;
- Develop seismic micro zoning maps of the territories densely populated and economically important towns and cities;
- Setting up economic bodies which would monitor the seismic risk and would be responsible for increasing the awareness among the population of Moldova.

Implementation of the above mentioned measures would ensure prevention of potential hazard risks caused by earthquakes, enable sustainable development of the territory of Republic of Moldova and ensure social safety.

References

- Alcaz V (2004) Probabilistic seismic hazard assessment for the Republic of Moldova. *Geology* 29:11–14, Kiev
- Alcaz V, Ghinsari V, Isicico E (2010) Methodological aspects and results of seismic risk assessment in Chisinau city (in Russian). *Bull Inst Geol Seismol Moldavian Acad Sci, Elena, Chisinau* 1:17–24
- Alcaz V, Ghinsari V, Isicico E (2012) Seismic risk assessment for largest cities Republic of Moldova (in Russian). *Bull Inst Geol Seismol Moldavian Acad Sci, Elena, Chisinau* 2:69–77
- Alcaz V, Ghinsari V, Isicico E (2013) Probable damages at strong scenario earthquake in Chisinau City (in Russian). *Bull Res Inst Constr INCERCOM, Chisinau* 2:134–144
- Constantinescu L, Enescu D (1963) Energy—magnitude—intensity relation for the Carpathian earthquakes. seismic parameters for Vrancea Region (in Romanian). *Geophysical* 1:239–268
- Marza V, Pantea A (1994) Probabilistic estimation of seismic intensity attenuation for Vrancea subcrustal sources. In: *Proceedings of the XXIV general assembly V.III. Athens, Greece*, pp 1752–1761
- Oizerman VN, Curmaev AM, Onofrash NI (1986) Report: about the investigation results of the consequences of the 31 August 1986 earthquake on the territory of Moldavian SSR (in Russian). *Archive of IGS ASM*, p 335
- Papadopoulos GA, Arvantides, A (1996) Earthquake risk assessment in Greece. In: Schenk V (ed), *Earthquake hazard and risk*, Ser. “Advances in Nat Technol Hazards Res”, vol 6. Editorial Office Kluwer Academic Publishing, The Netherlands, pp 221–229
- Shumila VI (1990) Field models of Carpathian seismic hazards in Vrancea region (in Russian). In: *Carpathian earthquake of 1986, science*, pp 127–133
- Tshocher VO, Tischenko VG, Popov VV (1941) Carpathian Earthquakes of 22.10.1940 and 10.11.1940 (in Russian). Report of the academy of sciences commission of USSR. Moscow, *Archive of IGS ASM*, p 149
- Zaicenco A, Lungu D, Alcaz V, Cornea T (1999) Classification and evaluation of vrancea earthquake records from Republic of Moldova. *Vrancea earthquakes: tectonics hazard and risk mitigation*. Kluwer Academic Publishers, Dordrecht, pp 67–76

Some Remarks Regarding Seismic Vulnerability for Orthodox Churches

Mihai Budescu, Lucian Soveja and Ioana Olteanu

Abstract The high number of historical monuments in our country draws attention over the importance of rehabilitation and conservation works that need to be carried out in order to prevent their damage. The global concern regarding the conservation of world heritage is obvious if the ongoing projects would be considered. Integrated Rehabilitation and Research on Architectural and Archaeological Heritage (IRPP/SAAH) is one of the main projects in this field, in which a priority list was made containing 186 architectural monuments and archaeological sites from nine participating countries, which need to be rehabilitated. The main purpose of this paper is to realize an analysis of the seismic vulnerability of masonry orthodox churches located in Moldavia region. Old masonry structures were considered and a comparison between the three main types of churches was realized—churches with rectangular, trefoil or Greek cross plan configuration. Structural vulnerability for the considered typologies was assessed based on nonlinear static analysis (pushover). Vulnerability and fragility curves for the analyzed structures were plotted based on the results and on the well-known methodology. Due to their particularities, these churches may cause problems regarding human evacuation in case of earthquake, resulted or not in partial collapse of the structure. For this reason the paper discusses the possibility of reducing the risk of casualties caused by the vulnerability in case of a mass gathering of people. In this respect, numerical simulations were performed for the evacuation time required in relation to a certain level of structural response to a seismic action, for the three types of the considered structures.

Keywords Church · Vulnerability · Seismic risk · Crowd density

M. Budescu · L. Soveja · I. Olteanu (✉)

Technical University Gheorghe Asachi of Iași, Faculty of Civil Engineering
and Building Services, Iași, Romania
e-mail: olteanuioa@yahoo.com

M. Budescu
e-mail: mbudescu@ce.tuiasi.ro

L. Soveja
e-mail: luciansoveja@yahoo.com

1 Introduction

The rehabilitation and conservation of religious buildings and those of heritage have become a matter of great importance around the world, especially in developed countries and represent a model for sustainable development and also an act of culture. This is the result of the need to improve existing buildings in order to fulfil the current requirements of use.

Around the world, there are several organizations which focus on the conservation of cultural heritage which are included in UNESCO: International Council on Monuments and Sites (ICOMOS), International Centre for Study of the Preservation and Restoration of Cultural Property (ICCROM), International Council of Museums (ICOM) and the International Institute for Historic Castle (IBI) (Soveja 2015).

In Romania, the Ministry of Culture is responsible with handling a data base with historical monuments. Table 1 shows the distribution of these monuments for each category and their location—Bucharest or around the country from 2004 (Lungu and Arion 2009). The current situation is very similar with the one presented below.

The most common structural system for monuments is represented by masonry, which is constantly exposed to damage and even collapse under seismic loadings. The structural rehabilitation depends on a rigorous assessment of the existing building. In this direction, Romania took part in several international projects focused on assessing the safety of the monuments and proposes adequate rehabilitation solutions: PROHITECH and IRPP/SAAH (Integrated Rehabilitation Project Plan/Survey on the Architectural and Archaeological Heritage) (Soveja 2015).

In this direction, the article's main objective is to compare the seismic vulnerability of three types of orthodox churches, which are specific for the Romania built environment. Beside this, another important aspect analyzed is referring to the necessary time to exit the building. This is considered in order to reduce human losses in case of earthquake occurring in a crowded situation. Taking into consideration the fact that all the analyzed churches have only one relatively small exit door and the collective behaviour in case of disaster, the human losses represents a real concern for these particular structures.

A classification of the stampede incidents based on the event type reveals that 79 % happen during religious mass gatherings, 18 % in miscellaneous gatherings and 3 % from political events (Illiyas et al. 2013).

Table 1 Historical monuments in Bucharest and in Romania

	No. of monuments	I Archaeological	II Architectural	III For public	IV Memorial
Bucharest	2627	190	2089	112	236
Romania	29,425	9585	17,708	678	1464

Soomaroo and Murray (2012) studied incidents of mass gatherings between 1971 and 2011. 215 stampede events were reported in Hsieh et al. (2009) reviews with 7069 deaths and more than 14,000 injuries. The deadliest three human stampedes in the world include: the event from 2005 in Baghdad during a religious procession—965 fatalities, in 2006 at Mina Valley—380 fatalities and in 2010 in Cambodia—347 fatalities (Hsu 2011). The most recent disaster occurred in September 2015 in Mina, Saudi Arabia, where at least 717 pilgrims have been killed and 863 injured.

Few scientific studies have considered the social and religious aspects of pilgrimage. More detailed analysis should be done in order to correlate the seismic vulnerability of a building with the vulnerability of the occupants.

2 Description of the Analyzed Structures

The influences from the neighbouring cultures can be noticed in the particularities of the churches. In Moldavia and Bucharest, most of the churches have a three-lobed plan, with strong Greek and Byzantine accents, meanwhile in Banat and Transylvania most of the churches are of vessel type due to the Austro-Hungarian influences (Purcariu and Ealangi 2012). A general classification of the structural typology of orthodox churches based on the plan view, show three major types: rectangular, trefoil and Greek cross, Fig. 1 (Crişan 2010). Considering the characteristics of the religious dogma, the altar is positioned to the east, the longitudinal direction being east-west. Correlating this with the seismic specificity of Vrancea region leads to an increase vulnerability on the transversal direction of these types of buildings.

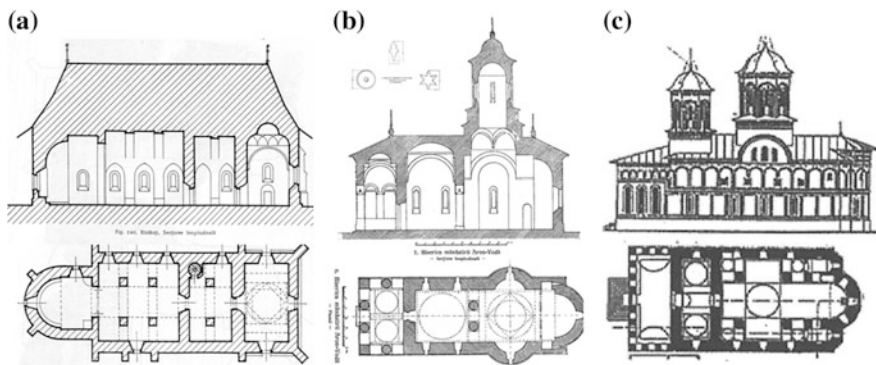


Fig. 1 General classification of orthodox churches: **a** rectangular plan view—Bogdana church from Rădăuți; **b** trefoil plan view—Aroneanu church from Iași; **c** Greek cross—Domnească church from Târgoviște (Crişan 2010)

2.1 *Rectangular Plan View*

The rectangular plan view church is well conformed from structural point of view, without side aisles, with advantageous withdrawals at the altar and longitudinal symmetrical walls connected with transversal walls. Structural strength is increased by transversal walls between the narthex and the nave, as well as the aisle which withdraw the altar from the longitudinal alignment.

Bogdana Church, Fig. 1a, is 32.66 m long and 12.10 m wide, without considering the abutments. Buttresses support the walls of the church in the western corners of the porch, at the transversal walls level between the porch and narthex, nave and narthex and nave and altar and at the level of the two rows of columns in the nave. The height of the church at cornice level is 9.4 m, meanwhile the ridge height is 17.6 m (Soveja 2015).

The church has a basilica shape with a nave. The nave has one higher central opening and two smaller ones on the sides, separated by two rows of columns. At the east end, the altar apse is located, narrower than the width of the church and at the west end is the porch, later added. The porch has a dome, meanwhile the narthex and nave are covered with a system of vaults, supported by arches. The altar is covered by a dome continued by a semi-dome.

2.2 *Trefoil Plan View*

For this type of structure, the transversal stiffness increases due to the curved walls of the lateral apses. A particularity of Moldavian churches is the new room which is introduced between the narthex and the nave, separated by a strong transversal wall from the entrance.

The narthex composition may affect the overall compliance of a church. In Moldavia, it has an approximately square shape, with four relatively small windows and covered by one or two domes supported by simple, slanting or crossed arches (Crişan 2010).

Initially called St. Nicholas, the church was built in 1592 on the site of an older church, being damaged and repaired several times. Today called Aroneanu church (Fig. 1b), the structure respects the classic plan of the churches from that era. To the west, the nave is extended by a porch. The church tower rises above the nave, resting on a star which is supported by a square base. The church measures 22.70 m in length and 7.70 m in width, has the cornice height of 7.80 and 17.60 m at the dome cornice.

The structural system is represented by brick walls with 1.20 m thickness. The base walls are placed on a pedestal from stone blocks bounded with lime mortar, having approximately the same thickness as the walls. The foundations are made of stone and mortar. The foundations exceed the walls with 20–30 cm, raising to 40 cm in the apse area and has a depth between 1.90 and 2.15 m (Soveja and Budescu 2014).



Fig. 2 Greek cross plan view—Barboi church from Iasi

2.3 *Greek Cross Plan View*

In the case of the Greek cross plan churches, the structural sensibilities are concentrated at the roof area, where the towers are located. The towers rest on a system of arches and vaults, which discharge the loads on slender columns. These elements are vulnerable to buckling due to their slenderness. Specific for the old churches are the curved beam and massive walls, which introduce supplementary bending in the structural elements. Often, the degradation of the structural elements is caused by these forces and subsequently by other causes (earthquakes, subsidence, fires).

Barboi church, Fig. 2, has a Greek cross plan with small semicircular apse, shorter than the height of the walls and prismatic pillars support by a pedestal. The church is 28.80 m long and 18.55 m wide. Cornice height of the church walls is 12.16 m (measured from inside floor level) and 18.95 m to the big tower cornice.

The church consists of a rectangular room, divided longitudinally in three naves by two rows of four columns. Transversely, the marginal columns separate the nave and narthex, and the nave from the altar. The entrance is represented by an open porch with one level, situated on the west side. The nave has a square plan, with semicircular apses and semi-domes above. Over the central nave is the central tower resting on a square base, surrounded by four small towers, supported by an octagonal base (Soveja 2015).

3 *Considered Methodology*

In order to assess the seismic vulnerability of the analyzed churches, the methodology used by the authors in previous case studies was considered.

Modal analysis and nonlinear static analysis were performed in ETABS computer software (User's Guide, ETABS 2015). The nonlinear analysis is one of the most utilized techniques for design and seismic performance assessment purposes (Mouzzoun et al. 2013). However, it involves certain approximations which put up for discussion the accuracy in estimating the global and local seismic demands for all types the structures, making mandatory the analysis for different heights, with the consideration of modelling particularities for each structural type (Prabhu 2013).

The result of a pushover analysis is the capacity curve, which represents the relation between total base shear and top displacement. Once calculated, the capacity curve of the structure is transformed in capacity spectrum using ATC-40 procedure (1996). The capacity spectrum is represented in spectral acceleration-spectral displacement coordinates (S_a - S_d) and is often used in the simplified bilinear form, defined by the yielding point (D_y , A_y) and the ultimate capacity point (D_u , A_u) (Barbat et al. 2011).

In order to analyze the expected damage, four non-null damage states are considered: (1) *slight*, (2) *moderate*, (3) *severe* and (4) *extensive-to-collapse*, in order to obtain the damage states thresholds ds and the corresponding fragility curves. These damage state thresholds are defined in the RISK-UE project from the bilinear capacity spectrum in the following simplified way (Barbat et al. 2011, 2012; Olteanu et al. 2015):

$$\begin{aligned} ds_1 &= 0.7 * D_y \\ ds_2 &= D_y \\ ds_3 &= ds_2 + 0.25 * (D_{S4} - D_{S2}) \\ ds_4 &= D_u \end{aligned} \tag{1}$$

Fragility curves define the probability that the expected global damage d of a structure exceeds a given damage state ds_i , as a function of a parameter quantifying the severity of the seismic action and follows a standard lognormal cumulative distribution. Thus, for each damage state, the corresponding fragility curve is completely defined by plotting the probability $P[d \geq ds_i]$ in the ordinate and the spectral displacement, S_d , in the abscissa.

Based on these curves, vulnerability curves are defined from the normalized mean damage grade, DI , and the spectral displacement. Later in the article the vulnerability curves for the considered cases will be compared.

The second part of the analysis refers to the necessary time to exit the three considered churches and the influence of the structural characteristics. The lower the exit time, fewer people risk suffering from structural damages which can occur in case of an earthquake. This analysis was performed in Pathfinder.

Pathfinder is a human movement simulator used to study human evacuation from buildings. The paper uses the steering approach because it is considered to produce more realistic results. Pathfinder approximates the environment as a 3D triangular mesh, which consists of continuous 2D triangulated surfaces—horizontal or inclined. Figure 3 presents the meshes for the three churches considered in the current study.

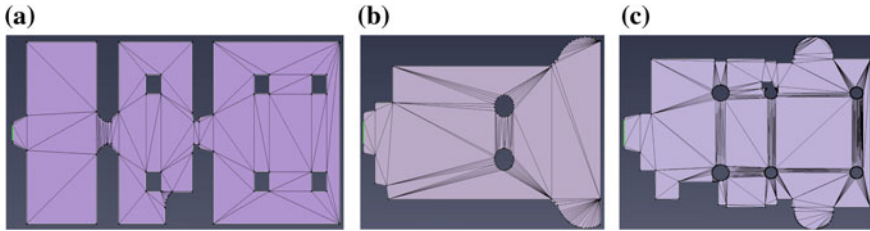


Fig. 3 3D triangular mesh for the studied churches: **a** Bogdana, **b** Aroneanu and **c** Barboi

The 3D triangular mesh is suitable for buildings with complex geometries because it can easily approximate rounded surfaces and ramp/stairs. The obstacles (walls/columns) are represented as gaps (Pathfinder—User manual 2015a, b).

Each occupant is represented by a circle which approximates the shape of the human body. To reach a specific destination a person must follow a path taking into account collision avoidance with others. Pathfinder assumed that an occupant has a global knowledge of the building (distance to the door) and calculate the time to a specific door, a path is then generated to the targeted door and the occupant moves towards. The resulting path is as a series of points on the mesh edge (Grigoraş 2014).

An occupant will evaluate a set of discrete movement direction and choose the direction that minimizes an efficiency function. The efficiency function is evaluated by combining several types of steering behaviour to produce a path. The occupants are selecting an exit by calculating the lowest time to the targeted exit. The criteria used to calculate the efficiency are: current room travel time; current room queue time; global travel time and distance travelled in room (Pathfinder—Technical report 2015a, b).

The following input data were considered: average walking speed—1.19 m/s, one exit and a person shoulder width of 45.58 cm. The following parameters are some of the ones used for the analysis, specific for the steering mode: acceleration time of 1.1 s, persist time of 1 s, collision response time 1.5 s and comfort distance of 0.08 m. The occupants were introduced randomly, considering a concentrated density of 0.65 m²/person.

4 Results

The structures were analyzed in ETABS 2015, considering the same material for all the three structures. The characteristic curve of the material with a compressive strength of 4 N/mm², a tensile strength of 0.05 N/mm² and a specific weight of 18 kN/m³ is presented in Fig. 4.

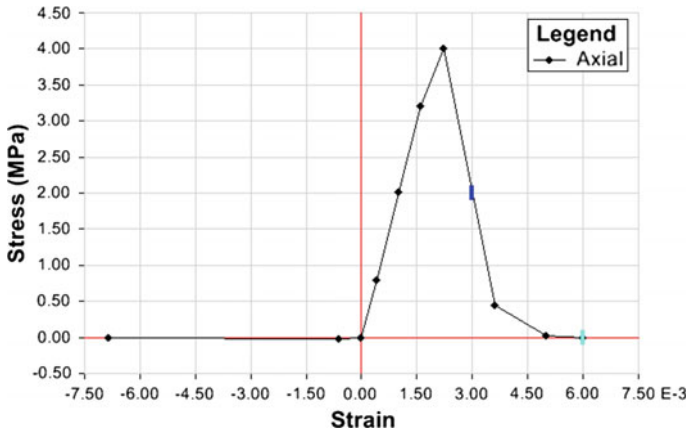


Fig. 4 Characteristic curve of the considered material

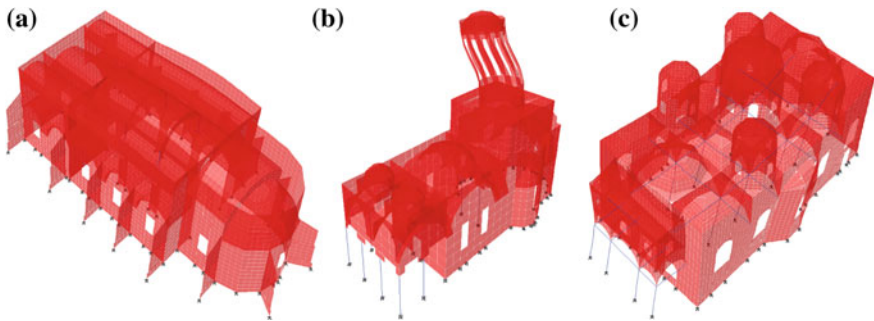


Fig. 5 1st mode of vibration for the analyzed structures: **a** Bogdana church, **b** Aroneanu church, and **c** Barboi church

Considering the modal analysis, the fundamental periods for the Bogdana church is 0.193 s, for the Aroneanu church is 0.391 s and for the Barboi church is 0.392 s. Figure 5 presents the 1st mode of vibration for the analyzed structures. It can be noticed that even though Barboi and Aroneanu have similar fundamental periods, for the second one, the tower bell is extremely flexible in comparison with the rest of the construction. In comparison with these two, the fundamental period for Bogdana church, with rectangular plan, is lower, so this type of church is the stiffest one.

Figure 6 present the displacements for the three considered churches in case of a pushover analysis on X (longitudinal) direction. It is noticed in Fig. 6b, c the flexibility of the tower.

The results for the nonlinear static analysis are represented as capacity curves, which are the relation between the displacement at the top of the structure and the

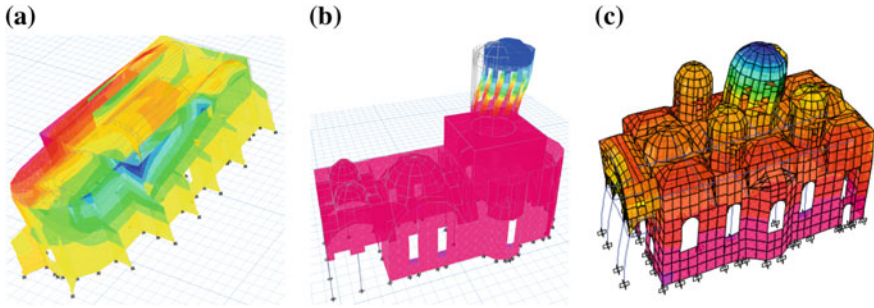


Fig. 6 Displacements due to pushover analysis in X direction: **a** Bogdana church, **b** Aroneanu church, and **c** Barboi church

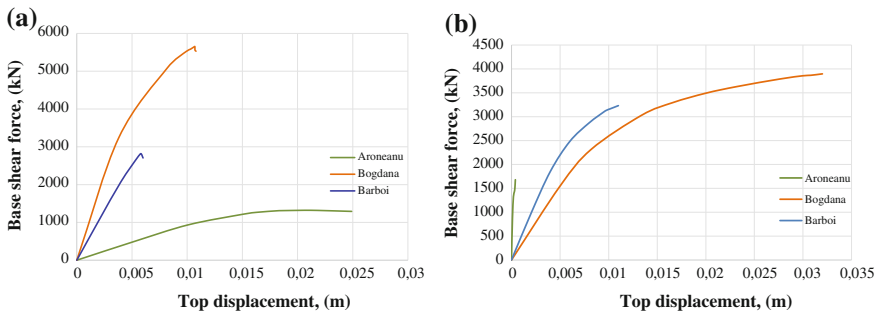


Fig. 7 Capacity curves in case of nonlinear analysis on: **a** X direction; **b** Y direction

base shear force. Figure 7a, b represent the capacity curves for the three analyzed types of churches, on X and Y directions.

Bogdana church has the highest base shear force, 5700 kN, and a displacement of 13 mm, meanwhile Aroneanu church has the maximum allowable displacement—25 mm, but the lowest base shear force—1100 kN. Barboi church has the lowest displacement—6 mm and a base shear force of 2900 kN.

On Y direction, Aroneanu church, is the most sensitive one, having the minimum base shear force and lowest displacement—1.2 mm, meanwhile Bogdana church has the best behaviour with maximum base shear force and maximum displacement.

We can conclude that the rectangular plan church behave better than the other two ones considered in the current case study.

Further more detailed analysis is performed in order to obtain the fragility curves, as in Fig. 8, for all the considered cases. Based on these, vulnerability curves are plotted. Figure 9 presents the relation between the damage index and the spectral displacements for the considered situations.

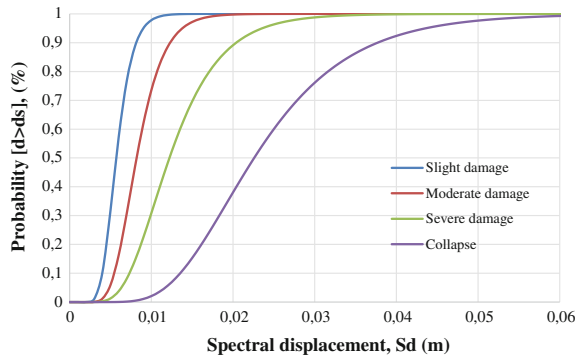


Fig. 8 Fragility curve for Bogdana church

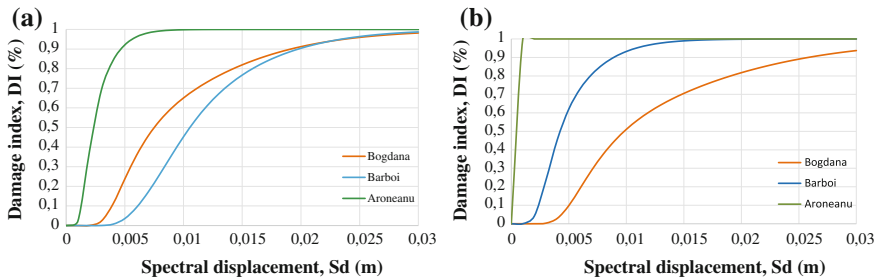


Fig. 9 Vulnerability curves in case of nonlinear analysis on: a X direction; b Y direction

From structural point of view, it can be noticed that Aroneanu church is the most vulnerable one on both X and Y direction. For a spectral displacement of 0.010 m, the damage probability for Bogdana church is 20 % higher than the one for Barboi church, in X direction. Moreover, on Y direction the Barboi church is more vulnerable than Bogdana with almost 40 %, in case of a spectral displacement of 0.010 m.

Comparing the seismic vulnerability of the three considered church types for the two directions, it can be noticed that the vulnerability in case of an action on the transversal direction is greater than the one on the longitudinal one. This conclusion is sustained also by the churches orientation with respect to the seismic particularities of Vrancea region.

The next analysis is performed in Pathfinder, regarding the necessary time to exit the buildings. This analysis is made in order to see if there are any correlations with the structural vulnerability, previously determined. Considering the input data presented earlier, Fig. 10 presents the initial crowd situation and an intermediate one, for all the three analyzed structures. It is noticed that the specific geometry of Bogdana church make the exit of the crowd more difficult. Figure 11 presents a synthesis of the results obtained in Pathfinder. As it can be seen, the longest

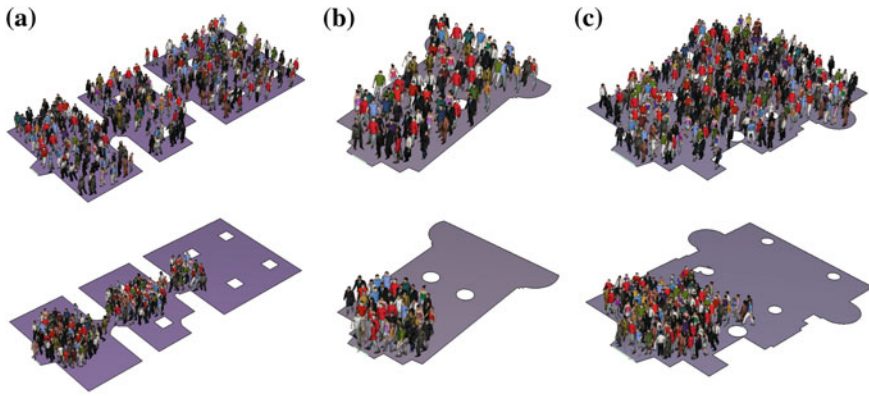


Fig. 10 Evacuation process for the three analyzed orthodox churches: **a** Bogdana church, **b** Aroneanu church, and **c** Barboi church

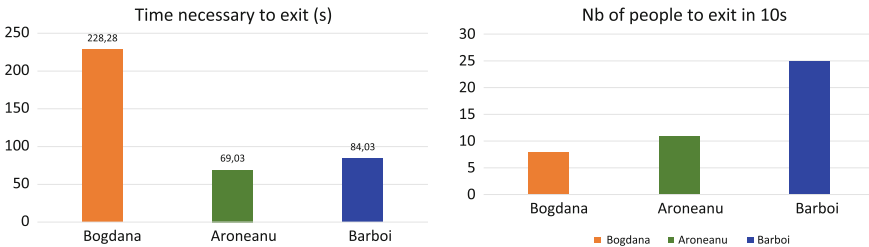


Fig. 11 Synthesis of Pathfinder results

necessary time to exist the building is obtain for Bogdana church, which is consistent with the previously stated idea, that the two narrowing, significantly influence the evacuation process.

The numbers of people considered to be evacuated were: 252 for Bogdana church, 86 for Aroneanu church and 247 for Barboi church. Considering this and the results from Fig. 11, it can be stated that the Greek cross plan churches ensure a more rapid exit of the crowd in case of an earthquake. The time is reduced to more than 50 % comparing with the time needed to exit almost the same number of people from Bogdana church. This conclusion is also sustained by the number of people which exit in 10 s. In this situation, from Bogdana church the maximum number of people who can exit is 8, three times less than for Barboi church—25 people.

Considering the damage index computed in Fig. 9 and the time history analysis performed for the three types of churches the following remarks can be done. In case of a longitudinal action, for a damage index of 0.5 %, with a known spectral displacement for all three cases, the maximum number of people to exit in time is three, for the Barboi church. If a partial or general collapse occurs and the damage

index reaches 1 %, for Barboi church, a displacement of 0.078 m is obtained if a X direction action occurs.

According to the time-history diagram, this displacement is reached at 8 s. Considering the results from Pathfinder, a total number of 20 people can exit safely in this interval. Similar process is performed in order to determine that in case of a X direction action, for the corresponding spectral displacement, from Bogdana church only 3 people can exist safely, meanwhile from Aroneanu 11 people. The results obtained in case on a Y direction action are similar.

The structural particularities of the orthodox churches—one narrow exit, can endanger people lives, especially when crowded situations occur, like on important religious celebration.

The results from the current study emphasize the necessity to further investigate the various causes of stampedes in case of crowded situation and the correlation with the built environment. Solutions regarding crowd management should be developed in order to minimize the number of victims.

5 Conclusions

The results from the modal analysis showed that the rectangular plan structure (Bogdana) is the stiffest one because of the transversal walls and external buttresses. The churches with a trefoil shape plan (Aroneanu) and Greek cross plan (Barboi) have the tower bells extremely flexible in comparison with the rest of the structure, therefore high vibration periods have resulted.

In order to assess the seismic vulnerability of the analyzed types of churches, the capacity curves of the structures were transformed in capacity spectrum using ATC-40 procedure. The considered damage states were established from the bilinear capacity spectrum, based on RISK-UE procedure. From seismic vulnerability point of view, the results concluded that, in general, an action on transversal direction is more dangerous than one on longitudinal direction due to the absence of the transversal walls between the nave and the narthex and between the nave and the aisle. This fact was highlighted by the analysis on the transversal direction, on the rectangular plan church, which resulted with the best structural performance.

Moreover, the positioning of the churches with the transversal direction from north to south, the direction of the seismic action from Vrancea region, negatively influences the seismic vulnerability of these structures.

Analyzing the fragility curves, it can be noticed that the church with a trefoil plan shape is the most vulnerable type on both longitudinal and transversal direction. For a spectral displacement of 10 mm in longitudinal direction, the Greek cross planed church is more vulnerable than the rectangular planed church with almost 40 %.

The next analysis was performed in Pathfinder program, in order to assess the necessary time for the people to exit the churches in case of a seismic event. The analysis revealed that the narrowing in the church structure, the obstacles and one

small exit door significantly influence the time necessary to evacuate such a building. Bogdana church is the most dangerous one from this point of view because of the transversal walls with small doors between the nave and the narthex and between the narthex and the porch.

A more suitable time of evacuation was obtained in the case of Barboi church. The time is reduced to more than 50 % comparing with the time needed to exit almost the same number of people from Bogdana church. This conclusion is also sustained by the number of people which exit in 10 s. In this situation, from Bogdana church, the maximum number of people who can exit is 8, three times less than for Barboi church—25 people.

When the structural results were combined with those from Pathfinder, the conclusion was that the church with the best structural performance (with enough walls on transversal direction) has the longest time to evacuate the indoor people in the case of a seismic event.

For the types of churches considered in the analysis, in case of a partial collapse and a crowded situation, the number of victims will be significantly high. The structural particularities of the orthodox churches—one narrow exit, can endanger people lives, especially when crowded situation occurs, like on important religious celebration.

Considering these conclusions, further studies should be performed to investigate religious buildings regarding the evacuation in case of crowded situation. Various causes for stampede situations should be considered—fire, partial collapse in case of earthquake, external factors, etc. Consolidation processes that are undergoing or will follow should take into consideration also the evacuation process.

Acknowledgements The authors are grateful to Thunderhead Engineering Consultants Inc. USA for providing Pathfinder.

References

- Barbat AH, Carreño ML, Cardona OD, Marulanda MC (2011) Holistic evaluation of seismic risk in urban regions (in Catalan). *Int Paper Numer Methods Comput Design Eng* 27(1):3–27
- Barbat AH, Vargas YF, Pujades LG, Hurtado JE (2012) Probabilistic assessment of the seismic damage in reinforced concrete buildings. *Computational Civil Engineering—CCE2012*. In: International symposium. Societatea Academica, Iasi, Romania, May 25, 2012, ISSN 2285–2735:43–61
- Crîșan M (2010) Structural rehabilitation of orthodox buildings from Wallachia and Moldavia (in Romanian). Bucharest: Editura Universitară “Ion Mincu”
- Grigoraș ZC (2014) Analysing the human behaviour in a fire drill. Comparison between two evacuation software: FDS + EVAC and Pathfinder. *Bulletin of the Transilvania University of Brașov, International Scientific Conference, “CIBv 2014”, 7–8 Nov 2014, vol 7, Series 1, Special issue no. 1:103–110*
- Guide User’s (2015) ETABS 2015. Integrated Building Design Software, USA

- Hsieh YH, Ngai KM, Burkle FM Jr, Hsu EB (2009) Epidemiological characteristics of human stampedes. *Disaster Med Publ Health Preparedness* 3(4):217–223
- Hsu EB (2011) Human stampede: an unexamined threat. *Emer Phys Month*. Available at: <http://www.epmonthly.com/features/current-features/human-stampede-an-unexamined-threat/>
- Illiyas F, Mani SK, Pradeepkumar AP, Mohan K (2013) Human stampedes during religious festivals: a comparative review of mass gathering emergencies in India. *Int J Disaster Risk Reduction* 5:10–18. <http://www.sciencedirect.com/science/article/pii/S2212420913000459>
- Lungu D, Arion C (2009) Seismic risk for monumental buildings in Transylvania (in Romanian). In: International conference rehabilitation of monument-buildings in Transylvania in terms of environmental and climatic influences, Mediaş
- Mouzzoun M, Moustachi O, Taleb A, Jalal S (2013) Seismic performance assessment of reinforced concrete buildings using pushover analysis. *IOSR J Mech Civil Eng (IOSR-JMCE)* 5(1):44–49. ISSN:2278–1684
- Olteanu I, Barbat AH, Budescu M (2015) Vulnerability assessment of reinforced concrete framed structures considering the effect of structural characteristics. *Open Civil Eng J* 9. Available at: <http://benthamopen.com/contents/pdf/TOCIEJ/TOCIEJ-9-321.pdf>
- Prabhu A (2013) Seismic evaluation of 4-story reinforced concrete structure by non-linear static pushover analysis. Bachelor thesis. National Institute of Technology, Rourkela
- Pathfinder (2015a) Technical ref. Available at: http://www.thunderheadeng.com/downloads/pathfinder/tech_ref.pdf
- Pathfinder (2015b) User manual. Available at: http://www.thunderheadeng.com/downloads/pathfinder/users_guide.pdf
- Purcariu M, Ealangi I (2012) Seismic damage process of orthodox churches in Romania (in Romanian). *Sci Bull U.T.C.B.* no. 2/2012
- Soveja L (2015) Evaluation and rehabilitation of historical masonry structures (in Romanian). PhD thesis. Technical University Gheorghe Asachi of Iasi, Iasi
- Soomaroo L, Murray V (2012) Disasters at mass gatherings: lessons from history. *PLOS Curr Disasters*. 2012 Jan 31. Edition1. doi:10.1371/currents.RRN1301
- Soveja L, Budescu M (2014) Failure mechanisms for orthodox churches in Romanian seismic areas. *B.I.P. Iasi, Tomul LX (LXIV), Fasc. 4*:173–183

Seismic Loss Estimates for Scenarios of the 1940 Vrancea Earthquake

Carmen Ortanza Cioflan, Dragos Toma-Danila
and Elena Florinela Manea

Abstract One of the strongest earthquake in Romania was the Vrancea earthquake on 10 November 1940, with moment magnitude 7.7 and depth of 150 km. This event caused significant losses over a wide territory, up to Iasi and Craiova cities. The number of casualties in Romania was around 593 dead and 1271 injured and 65,000 homes were destroyed. A major questions nowadays is: “What could the consequences of a similar earthquake be?”. Through this paper we try to provide insights, by relying on the newly implemented System for Estimating the Seismic Damage in Romania (SeisDaRo), operated by National Institute for Earth Physics (NIEP). This system uses the Improved-Displacement Capacity Analytical Method implemented in the SELENA Software for expressing building loss probabilities. The building database (at city or commune level) is classified into 48 types (depending on construction material, height and age), each with a specific capacity and fragility curve. For this paper we also compute casualty estimates. In the absence of real seismic recordings from the 1940 earthquake we obtained hazard parameters through different ground motion prediction equations (developed by Sokolov, Marmureanu or Vacareanu) specific for the Vrancea intermediate-depth source. Also we test the possibility of using data converted from intensity to acceleration. The damage estimates are represented on relevant maps. Our results show that an earthquake like the one on 1940 could lead to significant damage in our times.

Keywords SELENA · Hazard · Vulnerability · Seismic risk · SeisDaRo

C.O. Cioflan (✉) · D. Toma-Danila · E.F. Manea
National Institute for Earth Physics, Măgurele, Romania
e-mail: cioflan@infp.ro

E.F. Manea
e-mail: flory.manea88@gmail.com

D. Toma-Danila
Faculty of Geography, University of Bucharest, Bucharest, Romania
e-mail: toma@infp.ro

1 Introduction

Vrancea seismogenic zone is controlling the seismic hazard in Romania and in Republic of Moldova. Strong intermediate–depth earthquakes occurring here were felt in the past over a wide area, from the Baltic Republics (Estonia) in the North to Istanbul in the South and from Moscow (NE) to Nice and Marseille (SW). In the rather narrow epicentral area (easily distinguishable in Fig. 1) down to about 200 km depth, about 3 shocks with $M_w > 7$ are produced per century. The updated 1000 years catalog of Vrancea earthquakes (Onicescu et al. 1999) lists 37 such events (with $M_w > 7$) and the maximum reported earthquake occurred in October 26, 1802, and is estimated to have reached a 7.9 magnitude or 8.2, according to Alcaz (2005).

Based on the macroseismic maps of the earthquakes with $M_w > 7$ in the 20th century, Panza et al. (2010) concluded that both source mechanism and focal depth control the parameters of the intensity distribution. The sites with maximum intensities observed in the last century (IX and X MSK) are shifted towards East with respect of the epicentre area, inside or at the edges of the Focsani depression (a foredeep basin formed in front of the East Carpathians, where sediments are reaching even 14 km depth). The shape of isoseismal surfaces is regularly elongated much more towards NE than to the SW.

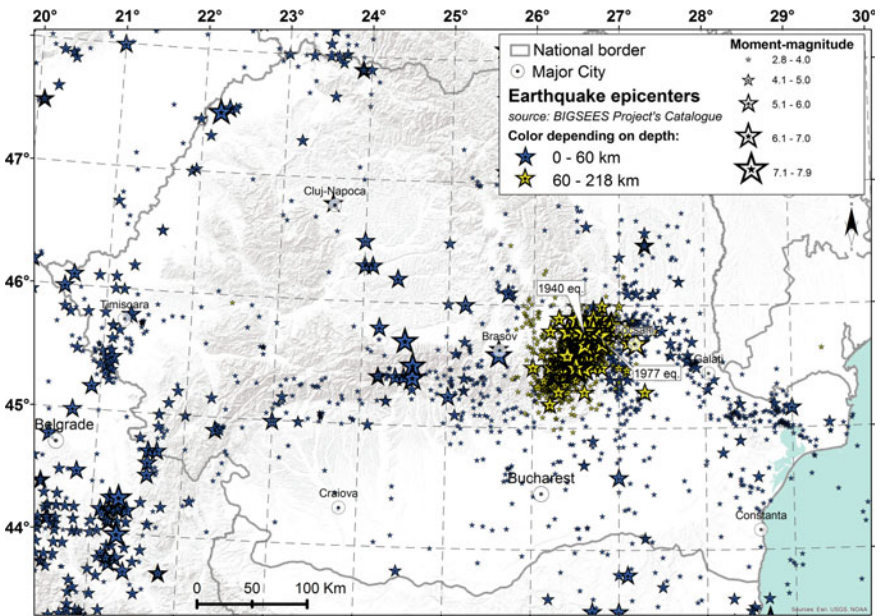


Fig. 1 Seismicity map of Romania, showing also the epicenter of the 1940 earthquake in the Vrancea Source (more than 60 % of the earthquakes in the map occurred here)

The event of November 10, 1940, $M_w = 7.7$ produced extensive damage in Bucharest and in Focsani—Galati area, where intensities up to X (MSK) were reported. Heavy damage was observed in Ploiesti and along the Prahova River, partly due to fires that broke out in the oil refineries. Detailed information regarding the effects of the earthquake can be seen in Table 1 and Fig. 2. Because of the focal depth (150 km), important macroseismic effects up to X (MSK) have been reported in Romania, Republic of Moldova, Northern Bulgaria and South/South-Western

Table 1 Casualties produced by Vrancea earthquakes in the 20th century (modified from Georgescu and Pomonis 2012)

Earthquake	Local hour	Lat	Long	Mw	Depth (km)	Damaged homes	Dead	Dead only in Bucharest
1940.11.10	03:39	45.8	26.7	7.7	150	60,000	593	140
1977.03.04	21:22	45.77	26.76	7.4	94	35,000	1578	1424
1986.08.31	00:28	45.52	26.49	7.1	131	55,000	8	
1990.05.30	12:40	45.83	26.89	6.9	91		9	2

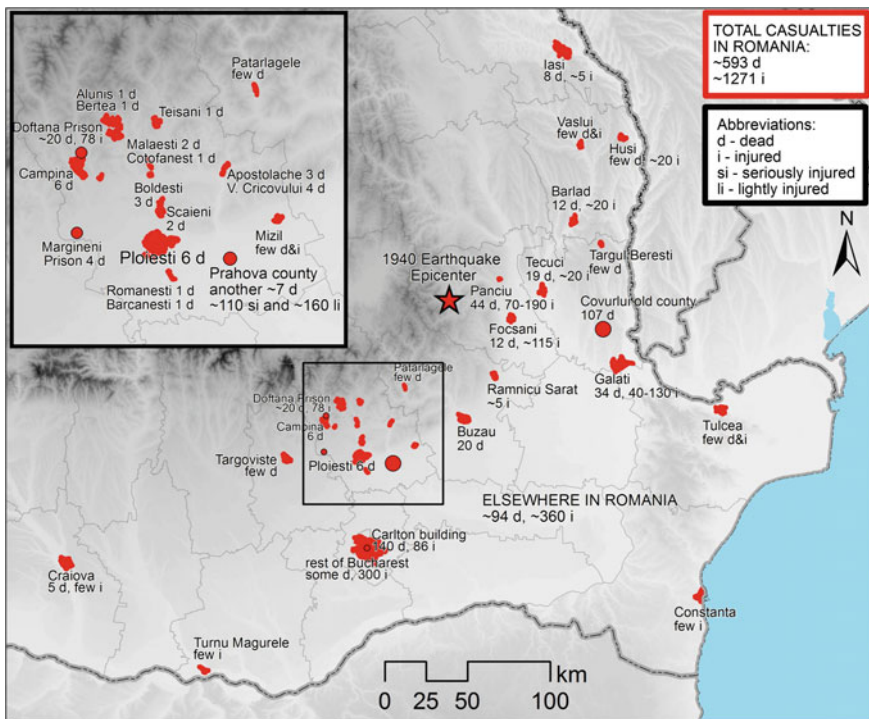


Fig. 2 Map of the distribution and number of casualties from the 1940 earthquake (based on information from Georgescu and Pomonis 2012)

part of Ukraine. Nowadays these areas comprises of densely populated cities (among which 2 capitals), important industrial facilities, railways, bridges, gas and fuel pipelines and 2 Nuclear Power Plants.

As the complexity of our society grows, also the risks become bigger. Our main question in this paper is: how much damage would provoke nowadays an earthquake similar to the one occurred in 1940? This paper tries to provide an insight view of the first attempt to compute the damage caused by scenarios of this earthquake, taking into consideration the limitations of risk estimation and the considerable epistemic and random uncertainties that are introduced in the analysis from the computation or lack of information. Such a sensitive subject has to be treated with care, and we disclaim of the possible consequences of misinterpreting the results.

2 Input Data for the Seismic Loss Scenarios

In order to calculate seismic losses we used the open-source software SELINA (SEismic Loss EstimationN using a logic tree Approach), developed by the NORSAR Institute. This software is one of the state-of-the-art tools in estimating the seismic damage and it is based on the HAZUS software. SELINA has been previously used successfully for Romania (Toma-Danila et al. 2015a; Lang et al. 2012) and it's currently part of the near real-time System for Estimating the Seismic Damage in Romania (SEISDaRo).

2.1 Loss Assessment Methodology

The loss estimates in this paper were calculated in a HAZUS like approach, relying on analytical methods for the analysis of building failure probabilities and empirical relations for determining the correspondent loss of life. This methodology is appreciated (Erdik et al. 2014) and frequently used when assessing the seismic risk for areas with statistics at territorial-administrative zone (TAZ) level, and not at individual building level.

The analytical methods essentially involve the comparison of the capacity of a structure, modelled as a single degree of freedom system (SDOF) that is structurally damaged at different points by displacement rather than acceleration, with the seismic demand represented by an acceleration displacement response spectrum (ADRS) (Mahaney et al. 1993). The “performance point” of a model building type is obtained from the intersection of the capacity spectrum and the demand spectrum (Erdik et al. 2014), and is later used with fragility curves that represent the probability distributions of the damage within the building type to determine a specific damage probability, for a certain damage state (low, medium, extensive, complete damage) (Fig. 3).

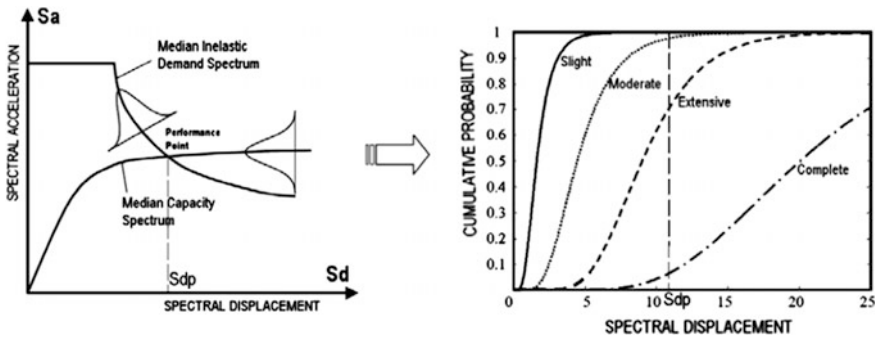


Fig. 3 General scheme of the capacity-spectrum based methodology (source FEMA 2004)

The first analytical method implemented in an earthquake loss estimation software was the Capacity-Spectrum Method (CSM), in HAZUS (FEMA 1999). Since then, new methods were developed, providing improvements. One of them is the Improved Displacement Coefficient Method (IDCM), which modifies the displacement demand of the equivalent SDOF by multiplying it by a series of coefficients in order to generate an estimate of the maximum displacement demand of the nonlinear oscillator (Molina et al. 2010). Although the method selection can influence the results slightly, the most important aspect when using analytical methods is the selection of relevant building typologies that define properly the multitude of buildings within an area. The capacity and fragility functions—obtained from literature or custom modelled (Erdik et al. 2014), have to reflect the mean characteristics of a specific type of building that can be easily defined through generic, non-invasive parameters such as height, age or material, that are collected within censuses, for example.

In order to apply the IDCM method for this study, we used the SELENA open-source software (Molina et al. 2010), obtaining for different hazard scenarios the estimated number of buildings in different damage states.

For further estimating the loss of life or the number of injured people in different injury states (K_{ij}), the following formula is applied, for each type of buildings in a TAZ:

$$K_{ij} = \text{Population per Buildings} * \text{Damage probability for buildings in damage state}_j * \text{Casualty Rate for severity level}_i \text{ and damage state}_j$$

2.2 Hazard Data

For the 1940 earthquake, there was no seismic recording in Romania, therefore we can't tell for certain what was the acceleration or velocity in any location. The next big earthquake in 1977 was recorded at only one station in Bucharest (INC station), revealing a 0.2 g acceleration at surface. Other Vrancea earthquakes with smaller

magnitudes (the biggest in 1986 and 1990) were recorded on multiple stations installed after the 1977 earthquake. The analysis of acceleration values lead to the conclusion that the resulted distribution due to Vrancea intermediate-depth earthquakes can be both special (a directivity pattern was observed, in the direction NE-SW, and a difference between fore-arc and back-arc of Carpathian Mountains values) and unpredictable from an event to another (Pavel et al. 2015). These conclusions are also supported by the observations that the most destructive effects were in Moldavia for the 1940 earthquake and in the opposite direction (Muntenia and Bucharest) for the 1977 event.

In this context, it is clear that hazard is important but unfortunately responsible for high epistemic uncertainties for 1940 earthquake risk scenarios. Nevertheless, the available results obtained by applying the Marmureanu, Vacareanu, Sokolov ground motion prediction equations (GMPE) can provide a reasonable dimension of the possible acceleration values and losses that might occur in today times.

2.2.1 Data Obtained Through GMPEs

The previous studies (Douglas et al. 2011) showed that it is appropriate to use specific GMPEs for the Vrancea Seismic Source. Currently there are available more than 6 variants, from which we selected for this study the ones in Table 2, due to their characteristics (suitability for simulating the 1940 earthquake), actuality and recommendations from other studies (Lang et al. 2012; Vacareanu et al. 2014).

Applied outside the validity domain of the magnitudes, MA06 can be considered more uncertain than SO08 and VA14 GMPEs, also since spectral acceleration values cannot be calculated with this set of equations. Considering the requirements of analytical methods, for MA06, the Eurocode8 spectra (type II, considering soil conditions) was used, while for SO08 and VA14 GMPEs, which incorporate also soil conditions, the IBC-2006 spectrum (for bedrock, in order not to double the amplification) was applied.

In order to check the validity of these GMPE's, a comparison between their results and the real recordings for the same locations is needed. The comparison

Table 2 Characteristics of GMPEs selected for this paper

GMPE	Database	Result values	Magnitude (Mw) range	Depth range (km)	Distance range (km)
Marmureanu et al. (2006)—MA06	Vrancea major earthquakes in 1977, 1986 and 1990	PGA—at baserock	6.4–7.4	60–150	10–310
Sokolov et al. (2008)—SO08	Based on simulations	PGA, SA from 0.1 to 3 s, PGV, II—at surface	5.0–8.0	60–160	1–500
Vacareanu et al. (2014)—VA14	Vrancea + International (344 + 366 strong ground motions)	PGA, SA from 0.1 to 4 s, PGV—at surface	5.1–8.0	60–173	2–399

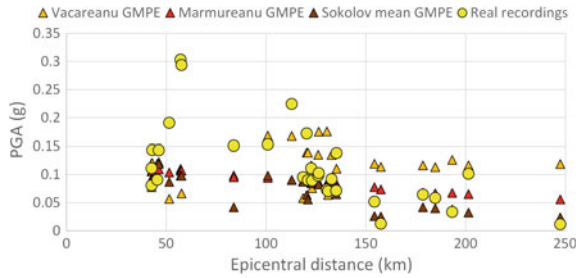


Fig. 4 Comparison between real recordings from the 1986 earthquake and values computed through the GMPEs in Table 2

was made for the 1986 Vrancea earthquake, an event with $M_w = 7.1$, similar mechanism and almost similar hypocentral depth with the 1940 earthquake. The results (Fig. 4) show that although some real values in the 50–100 km range are off the limits of GMPEs (could be greatly influenced by the local soil effects, which the GMPEs fail to consider very particularly), most points are closely equivalent.

2.2.2 Conversion of Intensity Values into Acceleration

One of the difficulties confronted in the seismic damage and loss assessment scenarios is to relate the intensity data to some ground motion parameter—most frequently to PGA. From the comparisons of seismic intensity scales to the PGA presented in the literature (e.g. Reiter 1990; Lliboutry 2000) one can see that for a degree of intensity the average PGA can be found in a wide interval of values (e.g. 0.1–0.2 g for VIII MSK or EMS98; 0.2–0.4 g for IX and so on). The observed/revaluated intensities for the 1940 event are difficult to use “as (it) is” due to their irregular distribution which reflects the population density and the development of the building stock at the time.

In our attempt to use the only available information regarding the force of the earthquake (referring here to intensity values), we applied the conversion equation of Sorensen et al. (2008) to the most recent intensity dataset for the earthquake, published by Kronrod et al. (2013) and illustrated in Fig. 5. This highly empirical equation, determined based on other Vrancea earthquake datasets and for magnitudes from 6.4 to 7.7, has the following form:

$$I_{\text{EMS Scale}} = 6.55 + 4.48 * \log(PGA_{[m/s^2]}) \text{ for average data, or } PGA_{[m/s^2]} = 10^{(I-6.55)/4.48}$$

After the point-to-point conversions, the PGA values were interpolated through the kriging method (in order to smooth the transition between adjacent points and due to the requirements of the vulnerability data level) and extracted for the analysis points. The Eurocode8 spectrum was used in SELENA for computing SA values at 0.3 and 1 s.

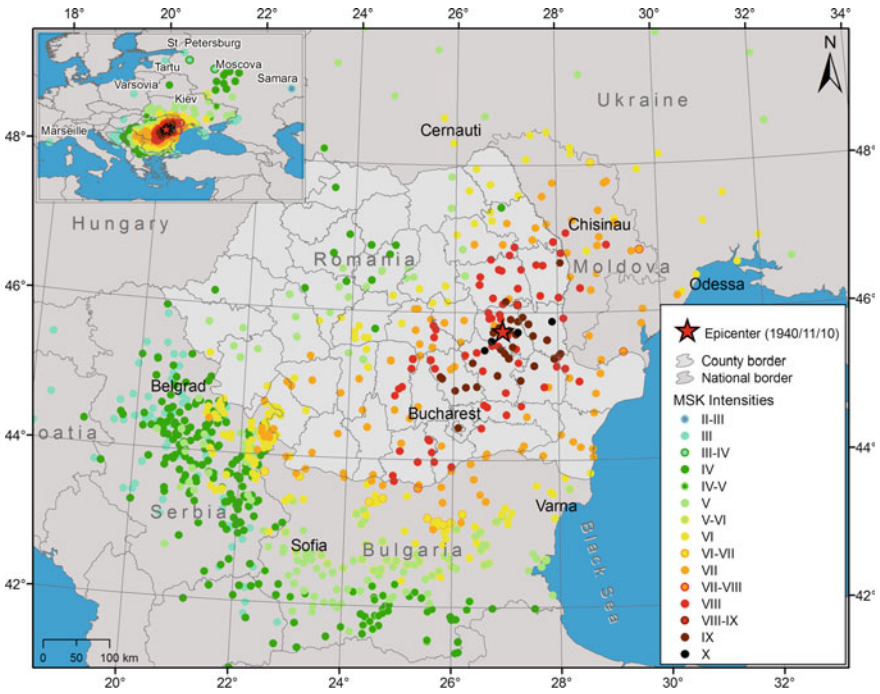


Fig. 5 Intensity values from the 1940 earthquake (data source Kronrod et al. 2013)

As it can be observed in Fig. 6, the converted from intensity PGA values decrease greatly in the 50–100 km epicentral distance. In rest, values are almost always above the values calculated through GMPEs. This can translate into a particular effect of the 1940 earthquake. These can be explained by the local conditions; at 50–100 km of the epicentre, in the extracarpathic area there were small intensities recorded mainly due to low amplification factors or different

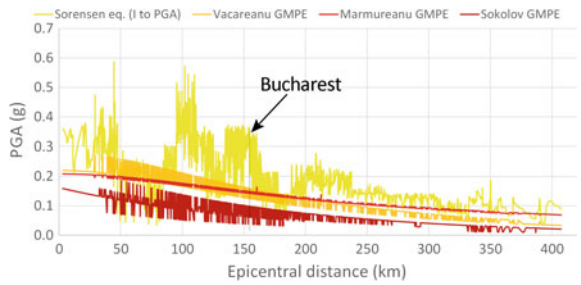


Fig. 6 Comparison between PGA values obtained at surface for the analysis points, using three GMPEs (VA14, MA06 and SO08 in their mean forms) and converted intensities based on the Sorensen equation. For the 1940 earthquake we observed that using sigma + 1 forms of the GMPEs, very unrealistic PGA values are obtained and are irrelevant to the analysis

spectral accelerations that did not caused many building to collapse and increase the observed intensity. In more distant areas, local soil amplifications multiplied the “base” acceleration much greatly, and more significant effects were recorded at surface. Selected GMPEs can’t reflect, by design, this difference.

2.3 Vulnerability Data

As vulnerability data we used the database included within SEISDaRo. A detailed description of this data can be found in Toma-Danila et al. (2015b). The database for half of Romania consists of 1400 TAZs (which represent cities, communes or sectors of Bucharest), each defined by number of buildings according to 48 building types (depending on 8 construction materials, 3 height classes and 4 construction periods) with associated capacity and fragility curves, and corresponding number of residents (per building type). The association of curves (which are partially from

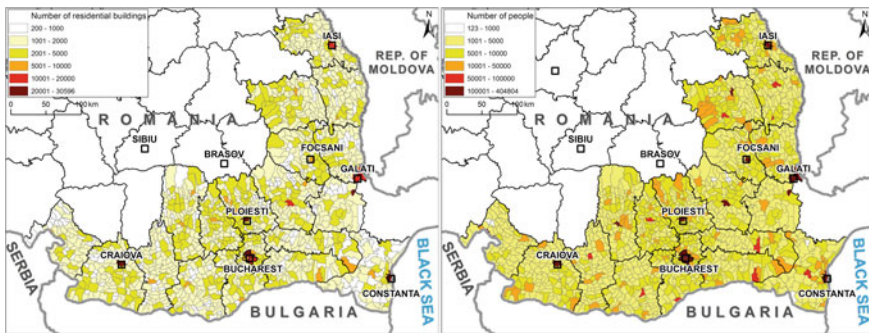


Fig. 7 Total number of residential buildings in the analysed area (left) and number of people (right)

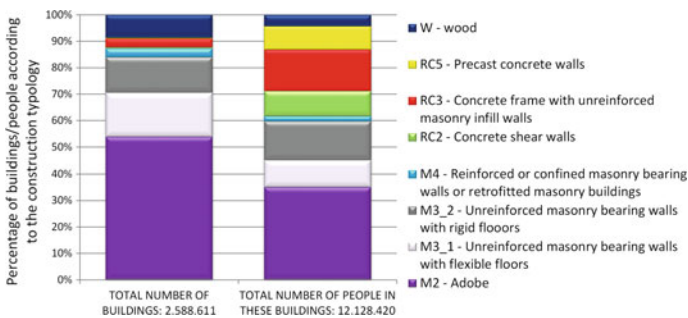


Fig. 8 Charts showing the percentages of the construction typologies from all TAZs and the corresponding specific number of residents within each building typology

literature, from sources like FEMA 2004 and Cattari et al. 2004) was undertaken by NIEP, UTCB and NORSAR, within the DACEA Project. The year of the census used for the data is 2002, however not much has changed since then in terms of risk, since newly built buildings shouldn't have serious failures and not many old buildings were demolished or retrofitted. General characteristics of the vulnerability database can be seen in Figs. 7 and 8.

3 Results

Results obtained with SELENA software consist of estimates for the number of buildings damaged in different states and for the number of people differently injured. For the representations in this paper we selected only the most relevant categories, comparable with real/official reported damage. The computation of economic losses could not be performed due to missing data.

With the purpose of highlighting the difference between results from GMPEs and converted intensities, we created two comparable maps (Figs. 9 and 10). In

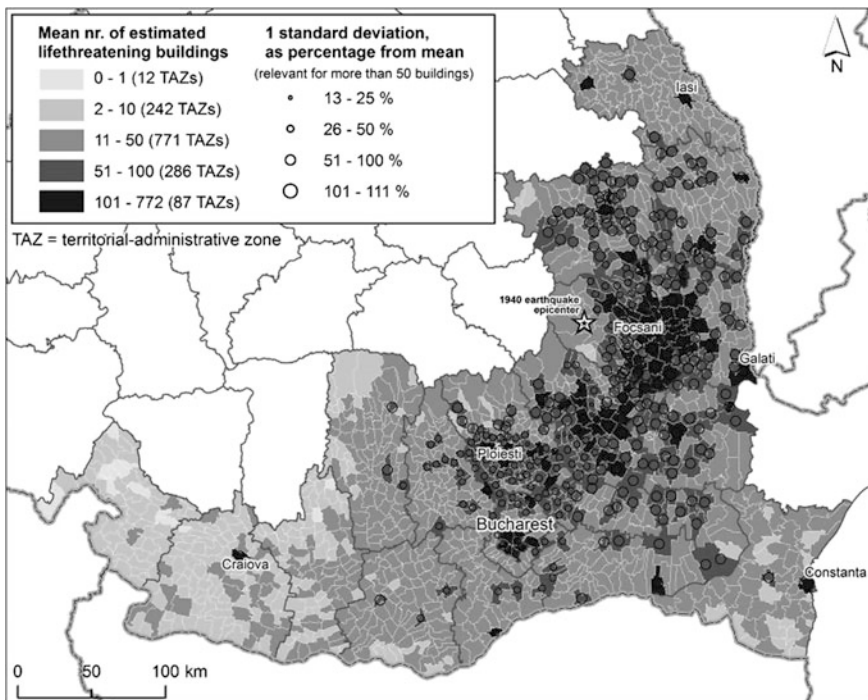


Fig. 9 Estimated number of buildings with life-threatening damage, for three averaged scenarios of the 1940 earthquake, relying on GMPEs (MA06, SO08 and VA14). The map illustrates through circles representing one standard deviation how great the difference between the three results is

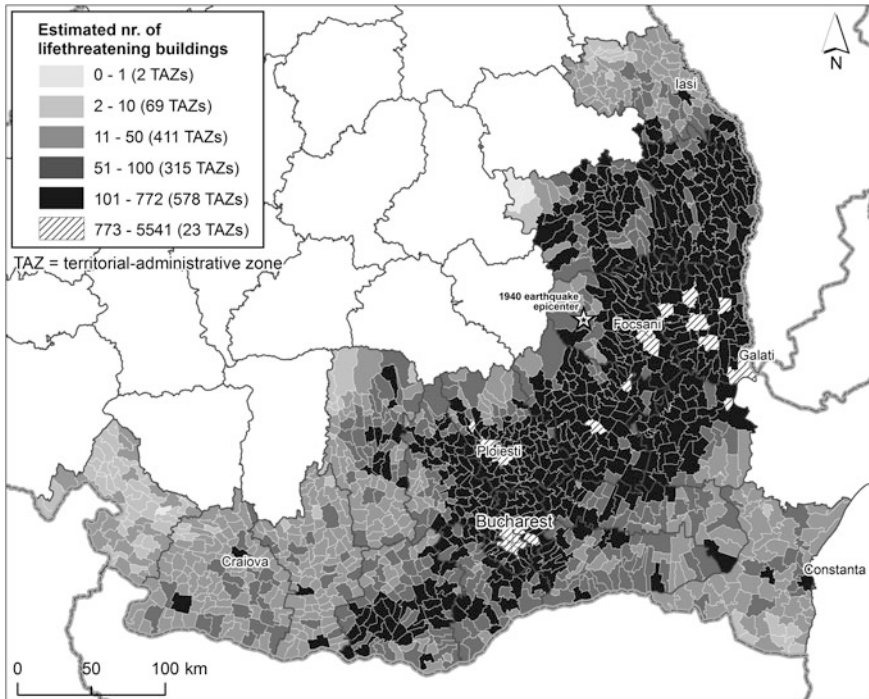


Fig. 10 Estimated number of buildings with life-threatening damage, for a scenario of the 1940 earthquake relying on the conversion of intensities to PGA through the Sorensen equation. Due to this conversion we consider the results both overestimated and highly uncertain

order to show if there are major differences between loss estimates based on the three different GMPEs (in Table 2), we calculated a mean for buildings with probability of presenting life-threatening damage (in complete damage states) and also one standard deviation (std), that we've expressed on maps as percentage from the mean value, in order to show comparable tendencies from a TAZ to another. For less than 50 buildings affected, the std is irrelevant—for seismic risk analysis uncertainties are great, and for such severe scenarios, two results showing a difference of 10 buildings in the epicentral area for example can be considered insignificant. The std percentage is for some TAZs above 100 %, but this result is not wrong; it is explainable by the major fluctuation of loss estimates from a specific GMPE (mostly MA06) compared to approximate values from scenarios with other GMPEs. There are cases, for example, when results from the three GMPEs are 426, 30 and 110; the mean is 189 and the std percentage out of the mean is 111 %. This percentages reflects clear differences between results. In the case of casualty estimates, due to the downscaled values, the std percentage is smaller.

Results represented on Figs. 9 and 10 show the major difference when using GMPEs and converted intensities. First of all, the maximum value for a TAZ is 772

(Braila city) compared to 5541 (sector 5, Bucharest). The total number of buildings that could present life-threatening damage is for Fig. 9: 59460 (comparable with the reported damage) and for Fig. 10: around 200,000 (believed to be overestimated). Due to the high uncertainties behind results plotted in Fig. 10, we consider it misleading and subject to further tuning. Figure 10 shows considerably greater values (except for the distant parts in Craiova area), therefore a new class was added to the legend, in order to show areas with large differences. Both maps show a wide-spread extent of the significant damage, up to 200–250 km away from the epicentre (although for intermediate-depth earthquakes, epicentral distance is not so relevant). As expected, major cities stand out due to the big number of vulnerable buildings.

Going behind the maps we notice that a lot of buildings estimated to collapse are from adobe or unreinforced masonry. Due to the fact that individual buildings of this type don't accommodate a large number of people and don't have a very high casualty rate, they are not expected to generate a comparable number of victims. Figure 11 shows in fact that when estimating the possible number of deaths, the black areas in Figs. 9 and 10 fades. We must say that compared to real casualties in

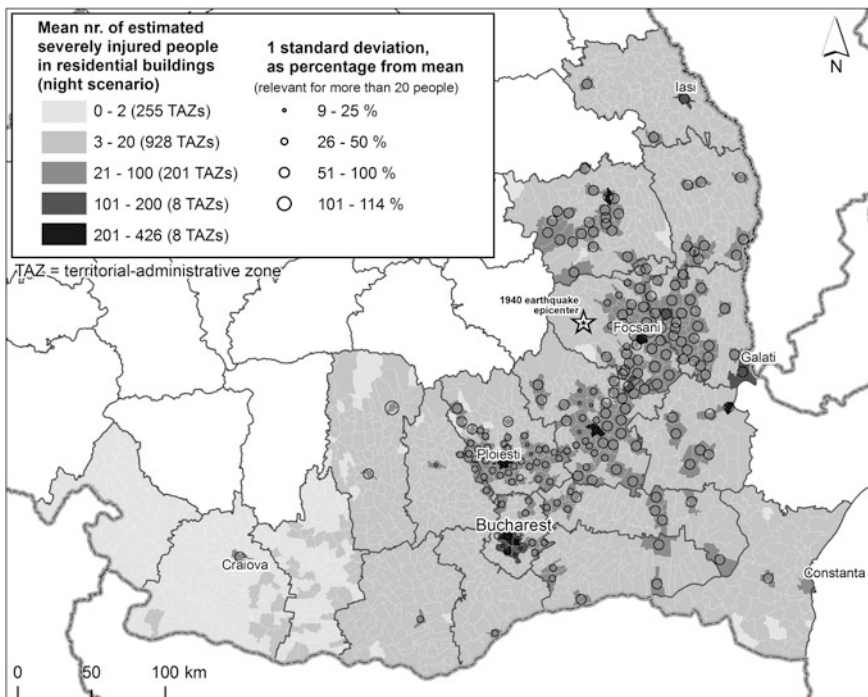


Fig. 11 Estimated number of severely injured people in residential buildings (for a night scenario—all people inside), for three averaged scenarios of the 1940 earthquake, relying on GMPEs (MA06, SO08 and VA14). The map illustrates through circles representing one standard deviation how great the difference between the three results is

1940 (it must be considered that back then Romania had around 13 million people compared to 20 million now), the estimates were significantly bigger, but not ridiculous (less than 10 times greater). In seismic risk estimation such a difference is clearly acceptable. Figure 11, compared with Fig. 2, shows a similar pattern: more severely affected people up to Bucharest, Ploiesti, Galati and Neamt County, and other hotspots like Iasi and Craiova cities.

4 Conclusions

In this paper, seismic loss estimates for different scenarios of the 1940 Vrancea earthquake were obtained, through the use of SELINA software (the Improved-Displacement Coefficient Analytical Method), the SEISDaRo vulnerability database for residential buildings and people and multiple estimates of acceleration values, from sources like MA06, SO08 and VA14 GMPEs or observed intensity values converted.

Based on the results, we can conclude that a major earthquake like the one in 1940 (greatest as magnitude in the recent history of Romania) could nowadays produce greater damage; due to the still remaining vulnerability of buildings, significant losses can be expected, and mitigation actions are much needed. Although after 1940 and especially after the 1977 earthquake, buildings started to be constructed according to ever stricter seismic design codes, there are still so many old buildings inhabited (constructed without any seismic considerations) that are clearly prone to collapse. Not to mention that some of them endured several earthquakes (and were probably already weakened by them).

We can't be happy with the actual state of facts in Romania; everyone seems to notice the risks, but do nothing. We think that, although this paper is as a first attempt to quantify the seismic risk in Romania in case of an earthquake similar to the 1940 event, we obtained useful results that can raise awareness and justify actions.

We are aware that the limitations of the hazard input data used produces significant epistemic uncertainties. One way to minimize them is to compute the PGA and SA from numerical simulation, although this complicated procedure requires velocity profiles and computation of the attenuation factors. The vulnerability dataset also requires further updates, since vulnerability curves are not calculated specifically for Romania, the buildings in the census data are evaluated according to subjective considerations or the spectra used doesn't focus on the 1–2 s interval, which is of interest for intermediate-depth Vrancea earthquakes. In further studies we will extend our research.

Acknowledgements Funding for this research was provided within BIGSEES Project by the Romanian Ministry of National Education under the Grant Number 72/2012 and within DARING Project Grant Number 69/2014. We also acknowledge the contribution of the doctoral scholarship from Faculty of Geography, University of Bucharest of the main author, and the DACEA Project

(Contract no. 52570/05.08.2010). For the association of building vulnerability curves we acknowledge the contribution of UTCB (Prof. Dr. Vacareanu Radu and Prof. Dr. Aldea Alexandru especially).

References

- Alcaz V (2005) Seismic hazard for Republic of Moldova. *Bull Inst Geol Seismolog MAS* 1:5–10
- Cattari S, Curti E, Giovinazzi S et al (2004) Un modello meccanico per l'analisi di vulnerabilità del costruito in muratura a scala urbana. In: 11th conference "L'ingegneria Sismica in Italia". 2004. Genoa, Italy
- Douglas J, Cotton F, Abrahamson N et al (2011) Pre-selection of ground-motion prediction equations. Global GMPEs project deliverable: task 2
- Erdik M, Sesetyan K, Demircioglu MB et al (2014) Rapid earthquake loss assessment after damaging earthquakes. In: Ansal A (ed) *Perspectives on European earthquake engineering and seismology*, vol 1. doi:10.1007/978-3-319-07118-3, pp 53–96
- FEMA (1999) HAZUS technical manual. Washington, DC, USA
- FEMA (2004) HAZUS-MH technical manual. Washington, DC, USA
- Georgescu ES, Pomonis A (2012) Building damage vs. territorial casualty patterns during the Vrancea (Romania) earthquakes of 1940 and 1977. In: *Proceedings of the 15th world conference of earthquake engineering*. Lisboa, Portugal, 2012
- Kronrod T, Radulian M, Panza G et al (2013) Integrated transnational macroseismic data set for the strongest earthquakes of Vrancea (Romania). *Tectonophysics* 590:1–23
- Lang D, Molina-Palacios S, Lindholm C, Balan SF (2012) Deterministic earthquake damage and loss assessment for the city of Bucharest, Romania. *J Seismol* 16:67–88
- Llibouty L (2000) *Quantitative geophysics and geology*. Springer, London
- Mahaney JA, Freeman SA, Paret TF, Kehoe BE (1993) The capacity spectrum method for evaluating structural response during the Loma Prieta earthquake. In: *Proceedings of the 1993 national earthquake conference*, Memphis, 1993
- Marmureanu G, Androne N, Radulian M et al (2006) Attenuation of the peak ground motion for the special case of Vrancea intermediate-depth earthquakes and seismic hazard assessment at NPP Cernavoda. *Acta Geod Geophys Hu* 41:433–440
- Molina S, Lang DH, Lindholm CD, Lingvall F (2010) User manual for the earthquake loss estimation tool: SELENA. <http://selena.sourceforge.net>. Accessed 29 Nov 2015
- Oncescu MC, Marza VI, Rizescu M, Popa M (1999) The Romanian earthquake catalogue between 1984–1997. In: Wenzel F, Lungu D (eds) *Vrancea earthquakes: tectonics: hazard and risk mitigation*. Kluwer Academic Publishers, Berlin, pp 43–47
- Panza GF, Radulian M, Kronrod T et al (2010) Integrated unified mapping of the Vrancea macroseismic data for the CEI region. In: *Proceedings of the 14th WCEE*, Ohrid, Macedonia, 2010
- Pavel F, Vacareanu R, Radulian M, Cioflan C (2015) Investigation on directional effects of Vrancea subcrustal earthquakes. *Earthq Eng Eng Vib* 14(3):399–410
- Reiter L (1990) *Earthquake hazard analysis*. New York. Columbia University Press, USA
- Sokolov V, Bonjer KP, Wenzel F, Grecu B, Radulian M (2008) Ground-motion prediction equations for the intermediate depth Vrancea (Romania) earthquakes. *B Earthq Eng* 6(3):367–388
- Sorensen MB, Stromeyer D, Grunthal G (2008) Estimation of macroseismic intensity—new attenuation and intensity vs. ground motion relations for different parts of Europe. In: *Proceedings of the 14th world conference on earthquake engineering*, Beijing, China, 2008

- Toma-Danila D, Zulfikar C, Manea EF, Cioflan CO (2015a) Improved seismic risk estimation for Bucharest, based on multiple hazard scenarios and analytical methods. *Soil Dyn Earthq Eng* 73:1–16
- Toma-Danila D, Cioflan CO, Balan SF, Manea EF (2015b) Characteristics and results of the near real-time system for estimating the seismic damage in Romania. *Math Model Civil Eng* 11(1):33–41
- Vacareanu R, Radulian M, Iancovici M et al (2014) Fore-arc and back-arc ground motion prediction model for Vrancea intermediate depth seismic source. In: *Proceedings of the 2nd European conference on earthquake engineering and seismology, Istanbul, Turkey, 25–29 Aug 2014*

Rapid Earthquake Early Warning (REWS) in Romania: Application in Real Time for Governmental Authority and Critical Infrastructures

Constantin Ionescu, Alexandru Marmureanu
and Gheorghe Marmureanu

Abstract In Romania, there is an operational early warning system that is able to send earthquake location and magnitude since 2013. Romanian territory, together with the neighbor countries Moldova, Ukraine and Bulgaria, are periodically affected by the intermediate depth earthquakes originating from Vrancea area. In order to rapidly locate and estimate magnitude are used a few seconds of strong motion acceleration data. The alert notification broadcasting to users uses an internal communication network built on redundant links with a very high availability. When an earthquake is detected at the surface by the 24 bits accelerometers and velocity sensors, the digital seismic data is sent in real time to the National Institute for Earth Physics where the first 4 s of data are analyzed and alert is issued. The alert is sent to the users using TCP/IP or UDP communication protocols. At the emergency response units there are computers and dedicated devices that have three levels of warning according to the magnitude of the earthquake. Warning levels are associated to different management systems of strategic facilities than can block or enable automatically chosen activities of those facilities. The REWS is sending alerts also to civil protection and Koslodui power plant, in the northern part of Bulgaria. Since the REWS is able to rapidly locate events and compute magnitude, there were no false alerts recorded and were issued 19 earthquake alerts for earthquakes with $M > 4.0$.

Keywords Early warning systems • Vrancea seismic zone • Seismic risk

C. Ionescu · A. Marmureanu (✉) · G. Marmureanu
National Institute for Earth Physics, Măgurele, Romania
e-mail: marmura@infp.ro

C. Ionescu
e-mail: viorel@infp.ro

G. Marmureanu
e-mail: marmur@infp.ro

1 Introduction

The Romanian territory is exposed to high seismic risk associated to earthquakes occurring in Vrancea area. The historical earthquake catalogue (between 984 and 1900) shows 2–5 intermediate-depth events per century with magnitudes between 7.1 and 7.9. Located at about 140 km epicenter distance from Vrancea, Bucharest—the capital of Romania—experienced at least twice per century heavy damage due to these intermediate depth earthquakes (Böse et al. 2007). A study of the macroseismic maps of the major earthquakes that have occurred in Vrancea area in the last century (November 10, 1940, $M_w = 7.7$, hypocenter depth $h = 150$ km; March 4, 1977, $M_w = 7.4$, $h = 94$ km; August 30, 1986, $M_w = 7.1$, $h = 130$ km and May 30, 1990, $M_w = 6.9$, $h = 90$ km), reveals the fact that macroseismic intensity in Bucharest is just one unit less than the maximum reported (Panza et al. 2008). The observed intensities (in MSK scale) were around IX for the 1940 event and above VIII for the 1977 earthquake.

An earthquake early warning system (EWS) allows rapid detection of an ongoing earthquake and issue rapid alert notifications depending on the potential to cause damage in a target site. There are several such systems all around the world: Japan, Taiwan, Mexico and Romania (Marmureanu et al. 2010) already have operational early warning systems and in other countries they are under testing: Italy, Turkey, California and China (Satriano et al. 2010; Zollo et al. 2006; Alcik et al. 2009; Peng et al. 2011). All the earthquake warning systems are either regional (“network-based”) or “on-site” (standalone).

A “regional” EWS uses the real time data from a dense seismic network that is used to record earthquakes in a seismic area. Usually such systems are able to rapidly locate earthquakes, to estimate the size of the event and to send notifications to a distant target site. This approach is used in situations when the target site is at a distance from the earthquake epicenter zone and allows a significant lead time in order to take the appropriate actions.

An “on-site” earthquake early warning system is based on a single seismic sensor or an array of sensors located at the target site. This approach is used when the target site is close the earthquake epicenter and it is more advantageous to have a rapid estimation of damage as soon as possible.

The recent upgrade of the Romanian Seismic Network with high dynamic accelerometers allows unsaturated recording of moderate-to large earthquake at very small epicentral distances (less than 10 km). This allows an increase of the warning lead-time (the time difference between the moment when the alert notification is issued and the arrival of dangerous destructive waves at a given target site). The current station density together with a rapid communication network allows a rapid real-time detection and location of events. In the last years, the National Institute for Earth Physics (NIEP) increased the number of real-time seismic stations up to 110 (Fig. 1). At each site there are collocated a strong motion acceleration sensor together with a short period or broadband seismometer.

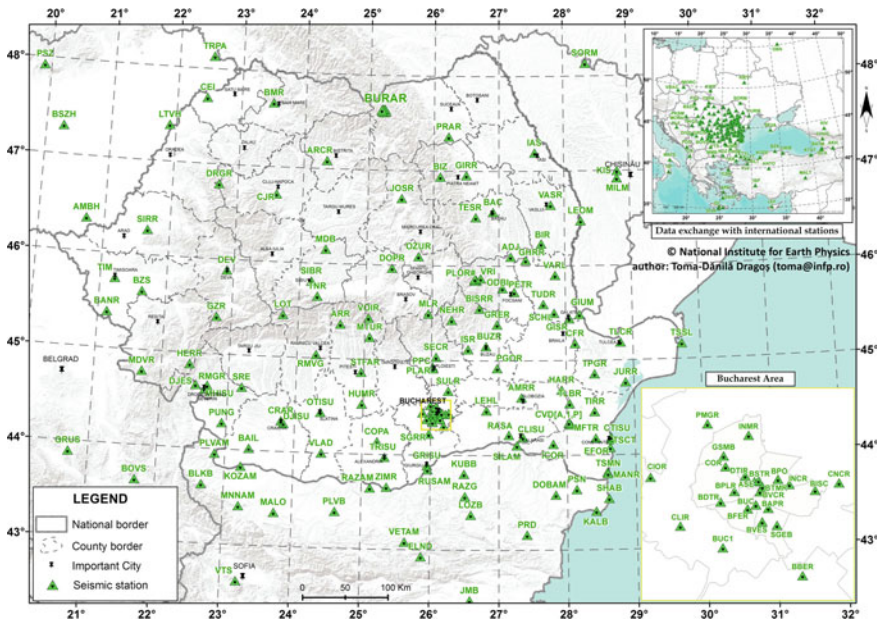


Fig. 1 The Romanian seismic network (February 2015) (modified from Toma-Danila et al. 2012)

Vrancea EWS uses the time interval of 25–30 s between the time when the P wave is detected at the surface, in Vrancea epicentral area, and the arrival time of the dangerous S wave at the site that needs to be protected. It uses four modules: (i) The local seismic network for detecting the P wave, (ii) Two acquisition centers and computing facilities, (iii) a redundant communication network, (iv) a warning distribution network to users.

The development of Vrancea early warning system started in 2002 (Böse et al. 2007). In the beginning were used 3 stations from Vrancea area (MLR-Muntele Roșu, VRI-Vrâncioaia and PLOR-Ploștina) to rapidly estimate magnitude. Since then the seismic equipment was upgraded to ROCK series of digitizers and the communication performance was improved. The system uses now about 35 stations to rapidly estimate earthquake source parameters.

NIEP operates 2 EWS that validates each other in real time. One uses the simultaneous measurement of initial peak displacement (Pd) in the first seconds after the P arrival time at accelerometer stations located at increasing distances from the epicenter. The first EWS uses for real-time implementation the software called PRESTo (Probabilistic and Evolutionary early warning SysTEM) developed by RISSC-Lab, Naples, Italy (Satriano et al. 2010) (Fig. 2).

The second EWS, developed by NIEP uses filtered peak strong motion data to compute only the earthquake magnitude (Mărmureanu et al. 2010). Since it was designed only for Vrancea so it doesn't provide the exact location of the events. This system uses only three stations deployed in the epicenter area (VRI-Vrâncioaia,

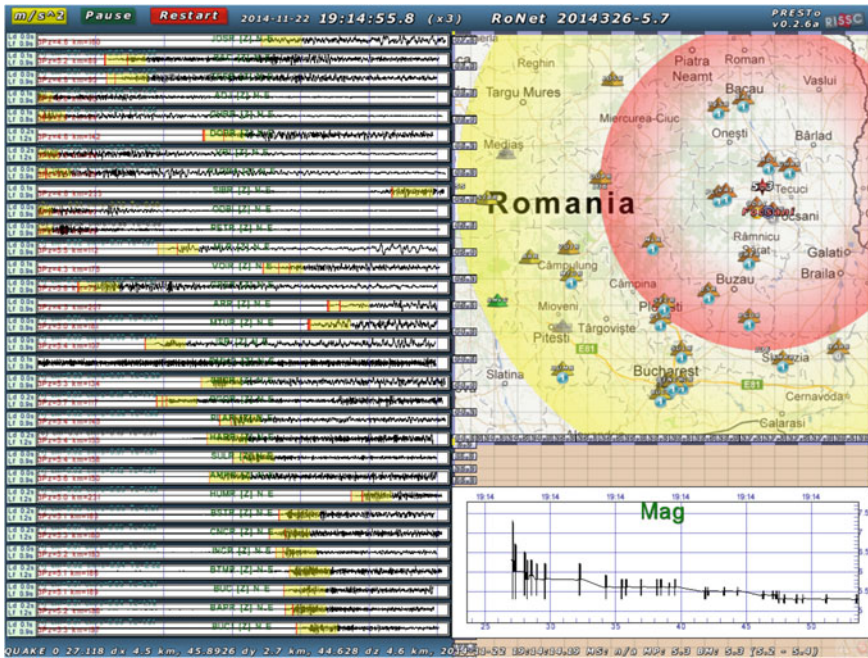


Fig. 2 PRESTO software package

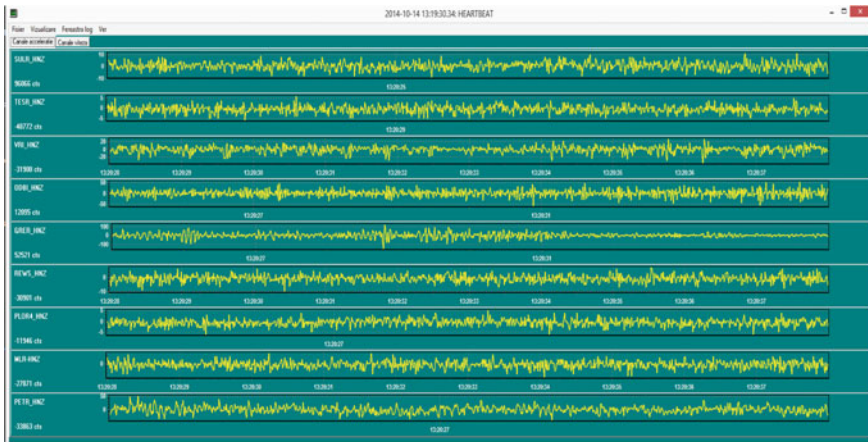


Fig. 3 Secondary EWS used to validate earthquake alerts

PLOR-Ploștina and MLR-Muntele Roșu) (Fig. 3). This EWS is used to validate and avoid false alarms caused by spurious picks.

Depending on the depth of the earthquake there are needed 4 or 6 P picks associated to an event in order to have a first location of an event. As can be seen

from Figs. 4 and 5 the Romanian Seismic Network (RONET) geometry allows a theoretical detection of 4 P/6 P picks in less than 10 s for a 25 km deep events or around 22 s for a 125 km deep events (Marmureanu et al. 2015). For shallow events originating from Vrancea, in order to have a reliable location 4 P arrivals can be used. For intermediate depth events, in order to correctly estimate depth there are necessary 6 P arrivals. It is also necessary to underline the particular case of Vrancea intermediate depth events and the geometry of the network that allows to have 10 P picks associated for a 130 km depth event in less than 25 s after the origin time (Fig. 6).

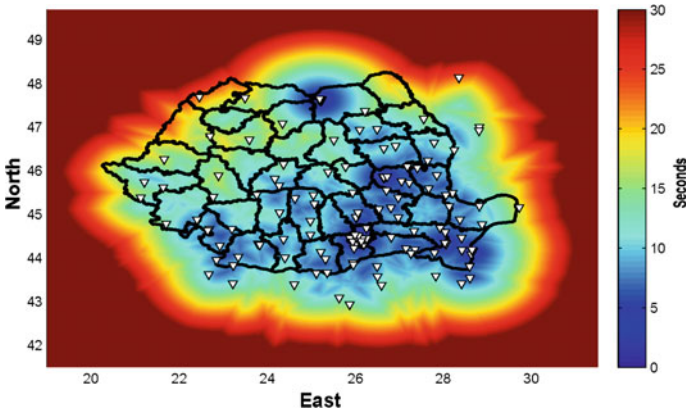


Fig. 4 P wave travel time (seconds) to 4 stations for a 25 km depth event

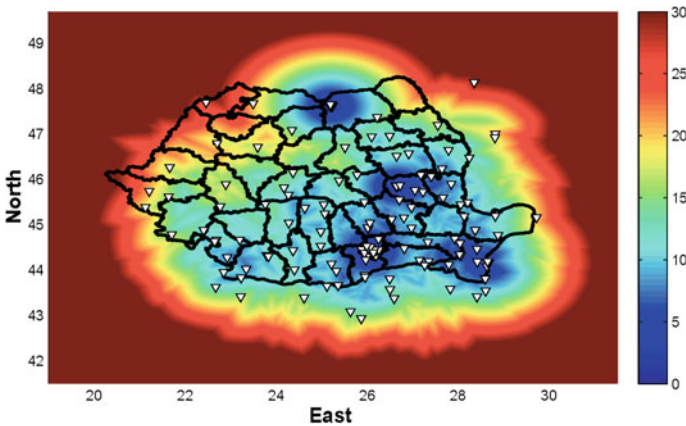


Fig. 5 P wave travel time (seconds) to 6 stations for a 25 km depth event

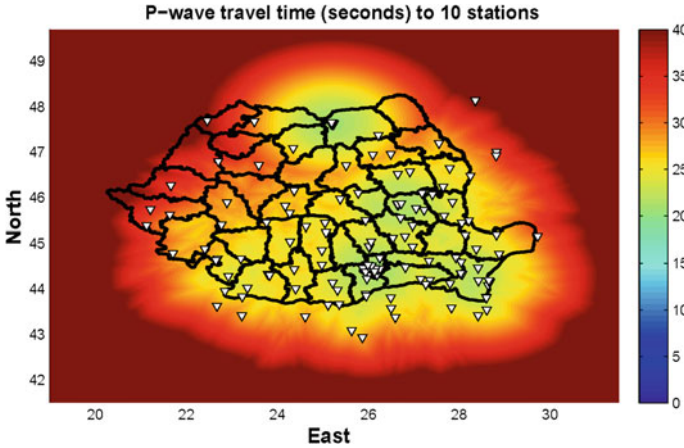


Fig. 6 P wave travel time (seconds) to 10 s for a 130 km depth event

2 Real Time Performance of the Early Warning System

The initial location and magnitude is computed from 6 P-wave detections and the warning notification is sent as fast as possible. Since September 2013 were issued 19 alerts for events with magnitude greater than $M_l = 4.0$. Depending on the depth of the event, a stable solution is generally reached within 10–25 s from the origin time (Figs. 7, 8 and 9).

The earthquake early warning notification alert are sent to a central messaging server that is able to send SMS, emails and is able to control different terminals using TCP/IP communication protocol. At the emergency response units there are computers and dedicated devices that have three levels of warning according to the magnitude of the earthquake (Fig. 10). The first level, corresponds to green light is for earthquakes with magnitude M in the interval $4.0 < M < 5.2$; the second level corresponds to $5.2 < M < 6.5$ and the last level, the red one, correspond to events with magnitude M greater than $M = 6.5$. All these levels are associated to different systems than can block or activate automatically different systems. Taking into account that Vrancea intermediate depth events can produce extensive damages to neighbor countries, EWS is sending alerts to civil protection and Koslodui power plant, in the northern part of Bulgaria. Since the EWS is able to rapidly locate events and compute magnitude, there were no false alerts recorded and were issued 19 earthquake alerts for earthquakes with $M > 4.0$. All these events were detected by EWS and alerts were sent to: 16 early warning receivers at the emergency response units located in Bulgaria and Romania: 7 in Romania at Constanta, Calarasi, Giurgiu, Teleorman, Dolj, Olt and Mehedinti and 9 receivers in Bulgaria, at: Montana, Vidin, Veliko Tarnovo, Ruse, Belene, Dobrich Kozlodui, Kozlodui 2 and Silistra.

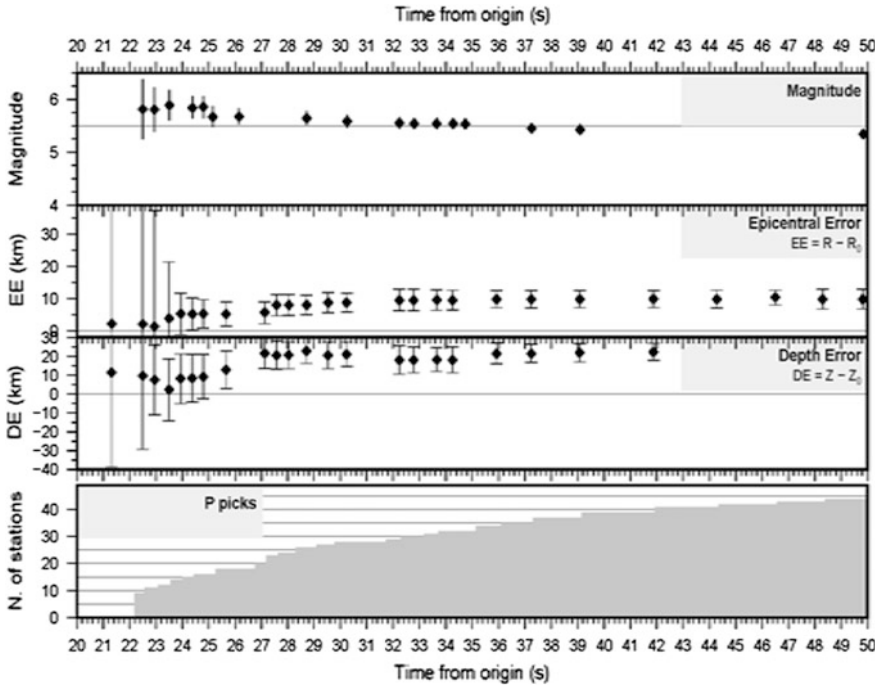


Fig. 7 Timeline for the MI = 5.5 (134 km depth) event from Vrancea 10/10/2013 (biggest recorded event since September 2013) that shows the magnitude error, epicentral error, depth error together with the number of stations that participates to location and magnitude estimation

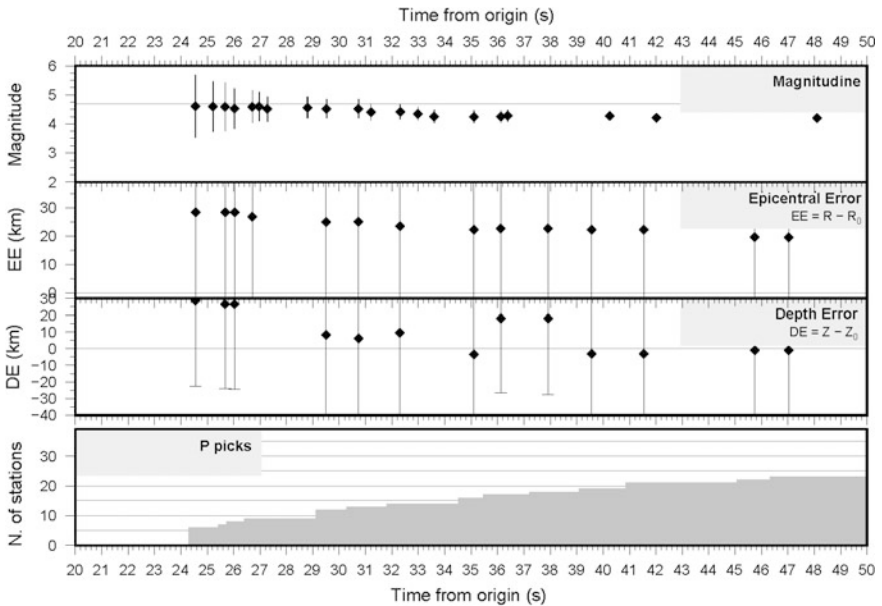


Fig. 8 Timeline for the MI = 4.7 (3 km depth) event from Transylvania, Hunedoara (event that occurred on 08/09/2013) that shows the magnitude error, epicentral error, depth error together with the number of stations that participates to location and magnitude estimation

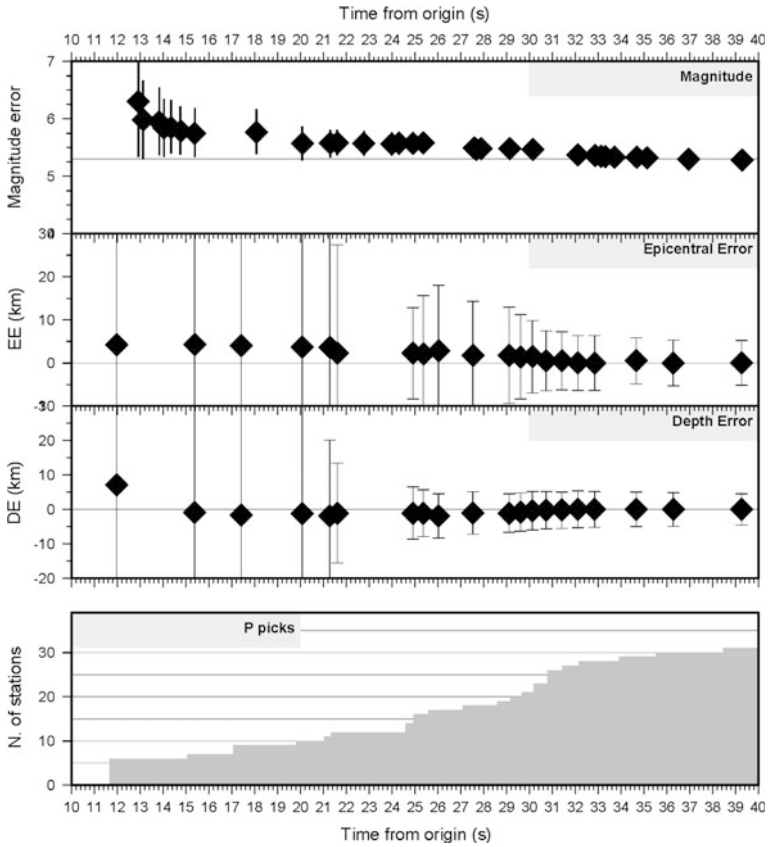


Fig. 9 Timeline for the MI = 5.7 (39 km depth) event from Vrancea 22/11/2014 that shows the magnitude error, epicentral error, depth error together with the number of stations that participates to location and magnitude estimation



Fig. 10 Earthquake early warning system receiver installed at the emergency response agencies

3 Conclusions

Since September 2013, there were recorded 19 events in Vrancea with magnitude $M_l > 4.0$. All these events were detected by EEWS and alerts were sent to: 16 early warning receivers at the emergency response units located in Bulgaria and Romania: 7 in Romania at Constanta, Calarași, Giurgiu, Teleorman, Dolj, Olt and Mehedinti and 9 receivers in Bulgaria, at: Montana, Vidin, Veliko Tarnovo, Ruse, Belene, Dobrich Kozlodui, Kozlodui 2 and Silistra.

The present study shows that the existing EEWS can be upgraded to locate in real time the event source since the offline tests show that a stable solution is generally reached within 25 s from the origin time, depending on the depth of the earthquakes for Vrancea seismic source.

Since rapid location of earthquakes is the first step in issuing early warning notifications, by reducing the time of the first valid location will lead to an increase the lead-time interval. Also rapid location of events will allow a future upgrade of early warning system to cover the entire Romanian territory.

Acknowledgements This work was supported partially by a grant of the Romanian National Authority for Scientific Research, CNCS—UEFISCDI, project number PN-II-RU-TE-2012-3-0215 and partially by NUCLEU PN09 04 01 project.

References

- Alcik H, Ozel O, Apaydın N, Erdik M (2009) A study on warning algorithms for Istanbul earthquake early warning system, *Geophys Res Lett* 36:L00B05
- Böse M, Ionescu C, Wenzel F (2007) Earthquake early warning for Bucharest, Romania: novel and revised scaling relations. *Geophys Res Lett* 34. doi:[10.1029/2007GL029396](https://doi.org/10.1029/2007GL029396)
- Mărmureanu A, Ionescu C, Cioflan CO (2010) Advanced real-time acquisition of the Vrancea earthquake early warning system. *Soil Dyn Earthq Eng.* doi:[10.1016/j.soildyn.2010.10.002](https://doi.org/10.1016/j.soildyn.2010.10.002)
- Marmureanu A, Craiu GM, Craiu A, Radulescu S, Neagoe C, Ionescu C (2015) Vrancea earthquake early warning system: first tests to add location capabilities. *Acta Geodaetica et Geophysica I.* doi:[10.1007/s40328-014-0081-5](https://doi.org/10.1007/s40328-014-0081-5)
- Panza GF, Cioflan CO (2008) Vrancea Earthquakes: a special challenge for seismic base isolation in Bucharest. In: Vlad I, Sandi H, Sannino U, Martelli A (eds) *Modern Systems for Mitigation of Seismic Action*, AGIR Publishing House, Bucharest, pp 339–355
- Peng H, Wu Z, Wu YM, Yu S, Zhang D, Huang W (2011) Developing a prototype earthquake early warning system in the Beijing capital region. *Seismol Res Lett* 82:394–403
- Satriano C, Elia L, Martino C, Lancieri M, Zollo A, Iannaccone G (2010) PRESTo, the earthquake early warning system for Southern Italy: concepts, capabilities and future perspectives. *Soil Dyn Earthq Eng.* doi:[10.1016/j.soildyn.2010.06.008](https://doi.org/10.1016/j.soildyn.2010.06.008)
- Toma-Danila D (2012) Real-time earthquake damage assessment and GIS analysis of two vulnerable counties in the Vrancea seismic area, Romania. *Environ Eng Manage J* 11(12):2265–2274
- Zollo A, Lancieri M, Nielsen S (2006) Earthquake magnitude estimation from peak amplitudes of very early seismic signals on strong motion records. *Geophys Res Lett* 33:L23312. doi:[10.1029/2006GL027795](https://doi.org/10.1029/2006GL027795)

Seismic Assessment and Rehabilitation of Existing Constructions after the 10th November 1940 and 4th March 1977 Earthquakes in Romania

Mircea Mironescu, Adrian Mircea Stănescu, Teodor Brotea,
Radu Florin Comănescu, Daniel Dumitru Purdea
and Mircea V. Stănescu

Abstract The paper mention the context in which the Romanian engineering community has dealt with the aftermath of the 10th Nov. 1940 and 4th March 1977 earthquakes, with regard to seismic rehabilitation of existing constructions at the time of the respective earthquakes. The paper contain the experiences of the authors, both older and younger civil engineers, along with the efforts, emotions, accomplishments and failures inherent in this field. The paper further contain the concepts, the methods used and the influences which have marked this period of time, from outside our country as well as own contributions, for analysis of existing structures and the strengthening methods used. Two examples of such structures, one from Bucharest, the other from Focsani, are discussed in the paper.

M. Mironescu (✉) · A.M. Stănescu · T. Brotea · R.F. Comănescu
D.D. Purdea · M.V. Stănescu
MIRO Grup, Bucharest, Romania
e-mail: office@mirogrup.ro

A.M. Stănescu
e-mail: office@mirogrup.ro

T. Brotea
e-mail: office@mirogrup.ro

R.F. Comănescu
e-mail: office@mirogrup.ro

D.D. Purdea
e-mail: office@mirogrup.ro

M.V. Stănescu
e-mail: office@mirogrup.ro

1 Introduction

The structural repair and strengthening interventions, as approach and achievement methods, for existing constructions were taken into consideration and applied based on historical, technical and economical context specialised knowledge level of the society of the respective country, be it Romania or any other.

In Romania, after the 10th November 1940 earthquake, not many structural interventions were made for damaged constructions, given the economic situation of those times, but also due to the limited existing technical knowledge, both at a national and international level.

The first regulation, which appeared in January 1942 as a provisional regulation for “The Protection of Constructions to Seismic Actions and Necessary Interventions for Damaged Buildings”, showed that the authorities had become aware of the problems related to seismic activities and that, from a technical point of view, a regulation was necessary.

However, due to the lack of necessary knowledge to finalize the provisional instructions of 1942, in May 1945 the mention to “repair damaged constructions” no longer appears. This aspect was then maintained in all following regulations, beginning with P13/63 and continuing with P13-70, P100-78, P100-81, all the way until P100-92, when the idea to regulate the interventions for existing constructions is again introduced, with specific chapters for analyzing existing structures and the necessary interventions.

The current regulation, P100-3/2008, is an already fully established code for the analysis of existing constructions and the necessary strengthening methods.

The period described had a list of well known personalities who contributed directly or indirectly to the structural interventions of damaged constructions after the earthquakes of 10th November 1940 and 4th March 1977, personalities such as: professors A. Beleş, M. Hanganu, V. Popescu, P. Mazilu, A. Caracostea, M. Ifrim, A. Cişmigiu, E. Țițaru, I. Stănculescu, R. Agent, A. Mihu, C. Avram, C. Mateescu, A. Negoită, P. Vernescu.

With regard to modelling the response of constructions to seismic actions, contributions such as that of Cişmigiu and Țițaru (1960), which refers to the participating coefficients of the vibration mode as well as for all the parameters included in the global seismic coefficient show the preoccupation of our personalities in this field to have their own justifications and judgments for protecting constructions against seismic actions.

The analytic modelling and analysis have rapidly and continuously evolved, as have the conformations, detailing and execution methods of these interventions.

At first, static equivalent horizontal forces analysis was used for linear-elastic forces and verifications only from a resistance point of view, and later deformation assessment was applied in elasto-plastic domain. Several problems were exposed, such as that of the failure mechanisms with ductile and fragile properties, limit state analysis, capacity design, and performance criteria.

The examples listed below show two constructions, one in Bucharest, the other in Focșani, with structures where interventions have been necessary, and highlight our contributions regarding the analysis of such works.

2 Conformations, Detailing and Execution Methods of the Interventions

After the earthquake of 10th November 1940, during the 2nd World War, only a few interventions were made to some constructions, such as local repairs, masonry repairs, filling cracks with lime or cement mortars, remaking reinforced concrete sections and even some lime-concrete manual jacketing works.

In some cases vertical and horizontal elements embedded or tied to the masonry walls or metal ties were introduced to prevent the collapse of masonry walls against the seismic component perpendicular to their plane; buttresses were used on the exterior of buildings for this reason, especially in the case of churches.

Professor Beleş (1941) was the first to introduce a mesh of horizontal reinforced concrete elements to sustain masonry steeples, which also had vertical and horizontal reinforced concrete elements embedded within them; the first example of such works is in the case of the Krețulescu church, restored between 1935 and 1938 (see Fig. 1a). Figure 1b, c show the proposal for base isolation of this historical monument.

Concrete or reinforced mortar shotcrete jacketing, fissure or crack injections with pressure pumps, executing the macrostructure at the superior part of churches and infrastructure, with a spatial mesh of reinforced concrete elements embedded in the vertical walls, conceived and sustained through a corresponding analysis model and applied by prof. A. Cișmigiu in many cases, are some of the methods that were introduced with the appearance of new analysis approaches or new technologies and materials.

The introduction of steel rods in drilled holes for the bell tower of the Postolache church in Ploiești was initially done with water cooled drills; later, air cooled drills were used until present day.

Epoxy resin injections for cracks in reinforced concrete elements were applied in Romania after the 4th March 1977 earthquake, as were carbon or glass fiber, polyethylene, carbon bars or plates glued or embedded in epoxy resins or special mortars.

The use of pre-stressed concrete to strengthen existing constructions was not applied in our country due to the low quality of masonry or concrete used in the past.

Great accomplishments which will have many other applications in the future are the use of base isolation method by the engineers Iordăchescu, father and son, for the Academy of Economic Studies situated on Calea Griviței nr. 2-2A, and the use

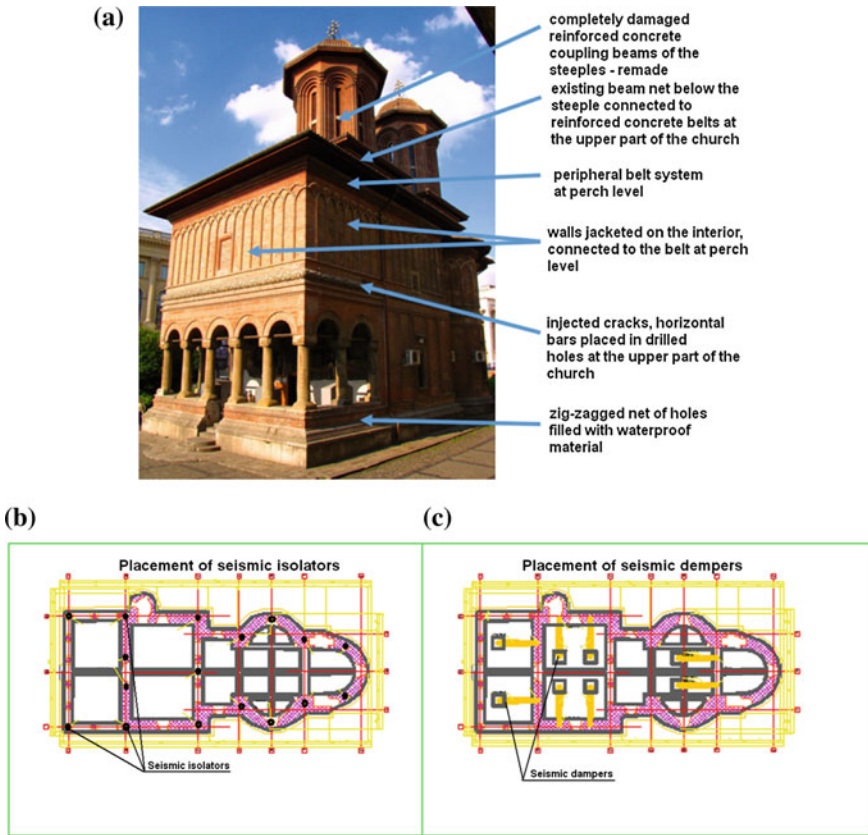


Fig. 1 a Elevation of structural interventions—Krețulescu church. b Placement of seismic isolators for base isolation system—Krețulescu church. c Placement of seismic dampers for base isolation system—Krețulescu church

of TMDS of Popp Traian (controlled system with tuned mass damping) for the construction of the premises of the Government of Romania and the Administrative Palace or the Clock Tower in Arad.

There are already finished projects for base isolation for Krețulescu and Fundenii Doamnei churches in Bucharest in order to provide a suitable protection for these two historical monuments of great value for our country against seismic action and humidity from soil contact, the latter which has yielded poor results with the usual waterproofing methods.

In the examples we show next we will expose the concepts, the detailing and analytic models for two representative constructions for their time, considered for their typology, conformation and composition.

3 Examples of Structural Interventions and Analysis for Existing Constructions

3.1 The Hostel from the Student Campus “Leul”

The first example of a structural intervention after the quake from 4th March 1977 is that of the hostel from the student campus “Leul”, formerly Ștefan Gheorghiu Academy; the construction was built in the late 1970s, it has a basement, ground floor and 11 stories and plan dimensions 15 × 44 m with an above ground height of 33 m (Fig. 2).

The structure has continuous walls as well as walls with openings, perimeter beams and reinforced concrete slabs for the superstructure and reinforced concrete walls and mat for the infrastructure and foundations.

At the COPISE conference of autumn 1978 in Bucharest (Mironescu et al. 1978) we presented the models, original analysis programs and the results for the analysis of this building, these being largely new at the time (see Figs. 3 and 4) (Monograph 1982) (Fig. 5).

The obelisk, located in front of the site, showed very clear direction and intensity of the earthquake (see Fig. 2).

The original content presented consisted of sectional analyses using mean resistances, making a direct envelope through biographic load analysis for the fundamental vibration mode by choosing the correct plastifying and failure mechanisms for reinforced concrete elements, direct dynamic analysis for the

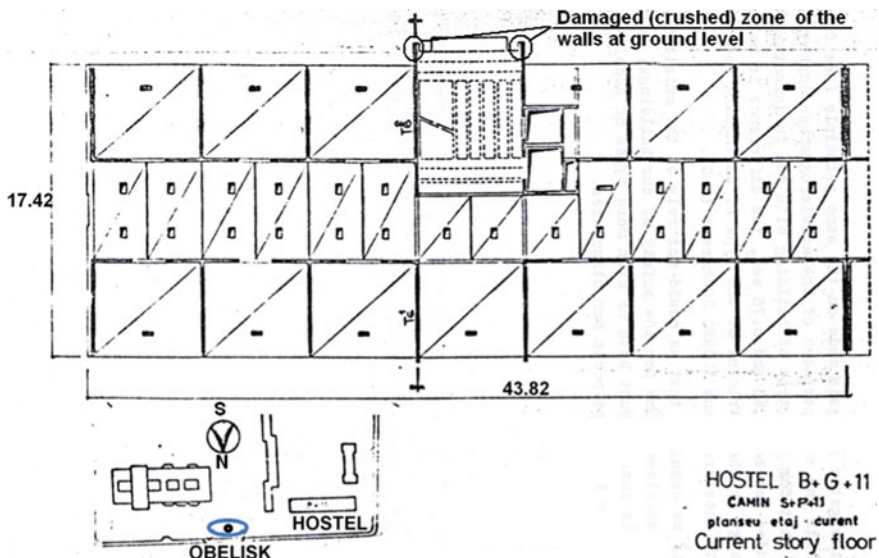


Fig. 2 Plan of the building with placement of obelisk

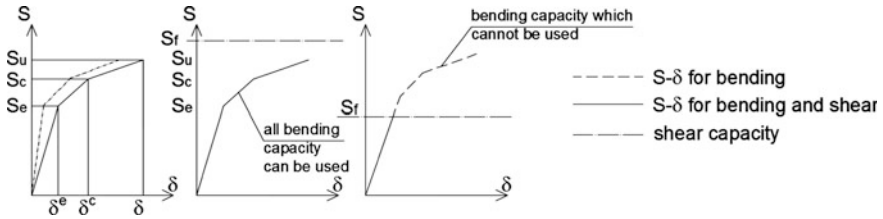


Fig. 3 Main $S-\delta$ relation, force-displacement, taking into consideration the displacement from bending and shear force and the respective breaking criteria

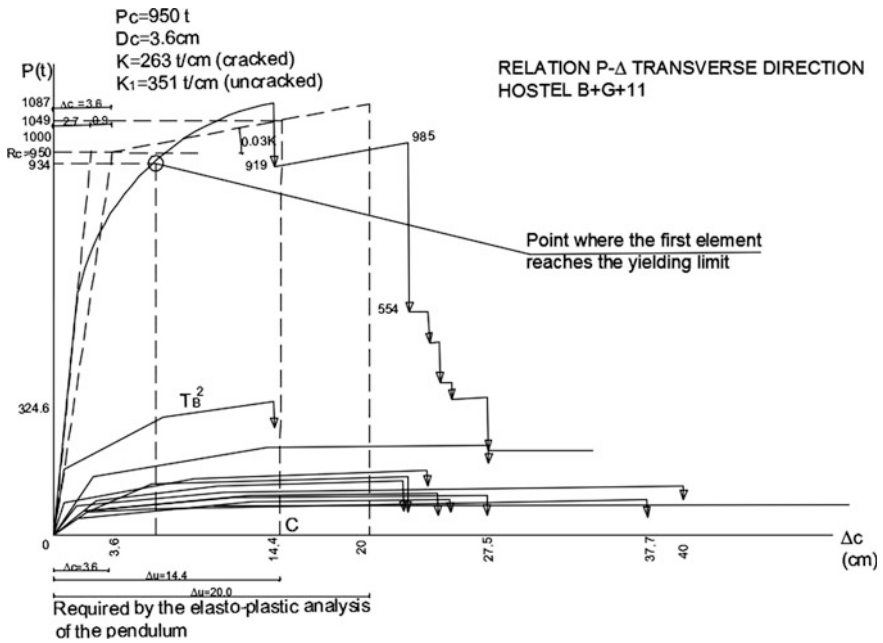


Fig. 4 $S-\delta$ relations and highlights of the displacement requirements for the quake of 4th March 1977 and the transversal direction for the hostel

equivalent system with one degree of freedom in elastic and elasto-plastic domain and taking into consideration the soil interaction with an energetic interpretation of the structure response to seismic actions.

The damages the building sustained consisted of cracks with various openings especially in transversal end walls and those around the stair case, crushed contact areas of the structural walls around the stair case.

The structural interventions consisted of epoxy resin injections for fissures and remaking the crushed areas of the exterior end parts of the structural walls around the stair case, after these areas have been disconnected and completed with stirrups.

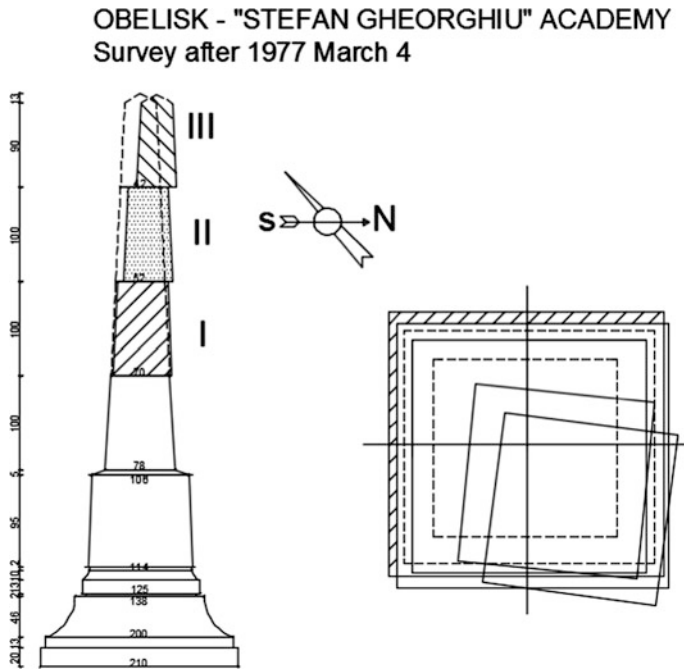


Fig. 5 Obelisk “Stefan Gheorghiu” Academy, survey after 4th March 1977

It must be stated that for our simplified analysis we have used the maximum credible earthquake values by using an amplification factor of 1.75 for determining the equivalent static base shear forces required, and for determining the capable base shear forces in pushover analysis we used the mean values for material characteristics.

3.2 The Former Focșani Courthouse Building

The construction dates back to the beginning of the 20th century. It is rectangular in shape, 36.50×45.0 m, it has a basement, ground floor, first floor and attic, with a tower clock on the main facade. The general height of the building is 14.0 m, reaching a maximum of 19.80 m at the top of the clock tower.

The structure consists of structural masonry walls, 28 or 56 cm in thickness, slabs made of steel beams with small masonry vault over the basement or steel profiles and concrete over the top flange for the slabs over the ground floor and first floor, or wooden structural meshes for the central dome, tower clock and roof (see Figs. 6 and 7).

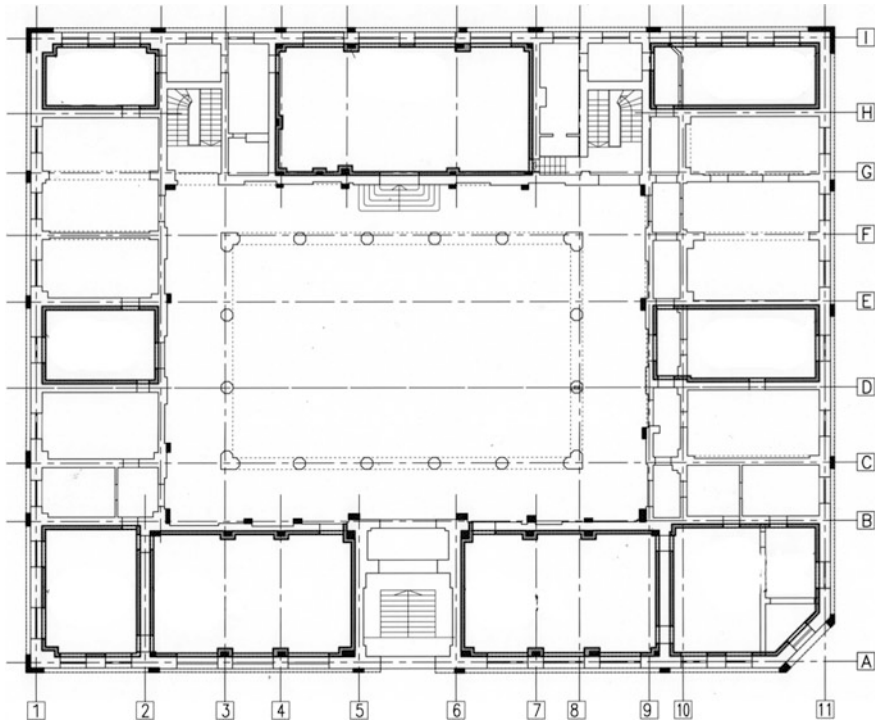


Fig. 6 Floor plan of the former Foçşani courthouse, highlighting the older structural interventions as well as the newer ones proposed in the strengthening project

The successive earthquakes have significantly damaged the building, especially the two large ones of 10th November 1940 and 4th March 1977. Structural repairs took place after the first large earthquake, consisting of adding steel ties where there are wooden slabs, underpinnings in a corner area of the construction and replacement of existing steel beams and masonry vaults slabs or reinforced concrete slabs.

After the 4th March 1977 earthquake another set of structural repairs took place, but also *strengthening works, consisting of an interconnected mesh of vertical and horizontal reinforced concrete elements, inside and outside of the building* (see Figs. 6 and 7). Moreover, a mesh of reinforced concrete beams mesh above the arcs of the “hall of lost steps”, over which steel trusses were placed to support the wooden dome of the roof.

Since the construction has changed functionality, the existing building described above, now a historical monument has been considered for restoration, according to the principles and doctrines thereof.

During the survey made in 2012 it was necessary to take into consideration the necessity to remove the mesh of vertical and horizontal reinforced concrete elements from the facades and recreate the facade as it was originally, according to the

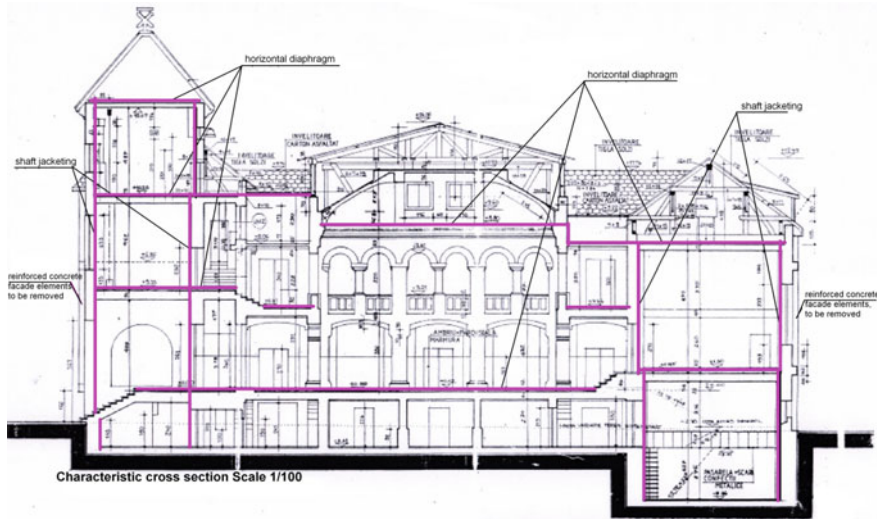


Fig. 7 Elevation of the former Focșani courthouse, highlighting as the newer structural interventions proposed in the strengthening project

restoration principles and doctrines and the strengthening proposals needed to ensure a suitable seismic risk class.

Damage to structural elements was found over the course of the survey investigations, due to the moderate and small quakes that constantly happen in the area.

Because of these findings, both typical structural repairs and strengthening proposals were made, in order to follow the restoration principles, which meant removing the exterior meshes of reinforced concrete elements from the building's facades.

Reinforced concrete jackets were made in areas without existing decorations, horizontal diaphragms were made from steel elements and reinforced concrete, partially at the slab over the first floor and partially over the ground floor around the circulation area, and also a rigid diaphragm with plywood plates for the wooden elements of the clock tower. Special attention was given to connecting the jackets and the slabs with the outside walls in order to compensate for confinement capacity, for the perpendicular action on the plane of the walls, for the mesh of reinforced concrete elements which must be removed from the facade.

The analysis with the original methods mentioned earlier in Chap. 2 (see Fig. 8) (Mironescu et al. 2013) have shown that if in the initial situation, the building had a coefficient, $R_3 \approx 0.35$, which expresses the global actual resistance in comparison to a new building, and the seismic risk class R_s II, after accomplishing the proposed interventions, R_3 will be closer to 1, and the seismic risk class, closer to R_s IV.

Figures 9a–c (Mironescu et al. 2014) show the strut and tie models with reinforced bar or R.C. elements (columns or beams) embedded in masonry.

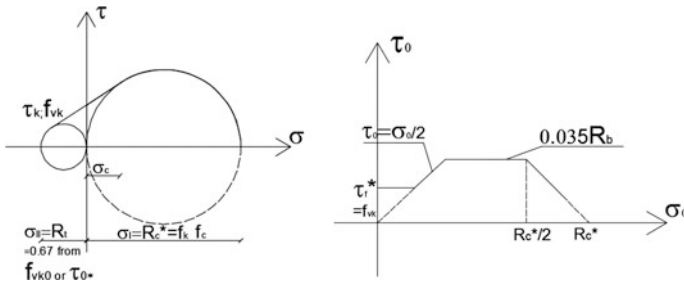


Fig. 8 Compression stress—shear stress simplified relations (intrinsic curve) for masonry elements

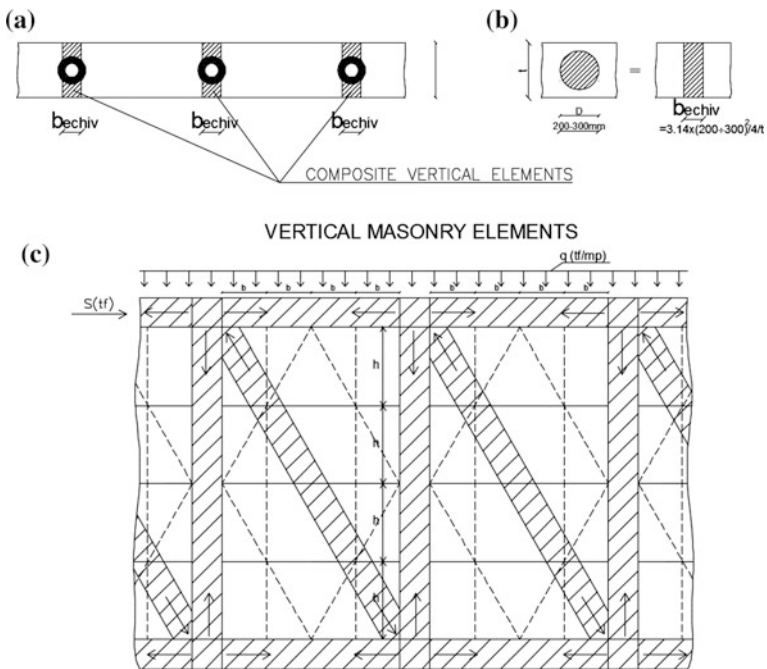


Fig. 9 a Composite vertical elements. b Equivalence between R.C. bars and composite R.C. section. c Layout for vertical, horizontal and diagonal elements for a masonry wall with encased bars or reinforced concrete beams and columns

The original method for strut and tie R.C. elements is shown in Fig. 10a, b (Mironescu et al. 2014).

Both models can be introduced in pushover or incremental dynamic analysis.

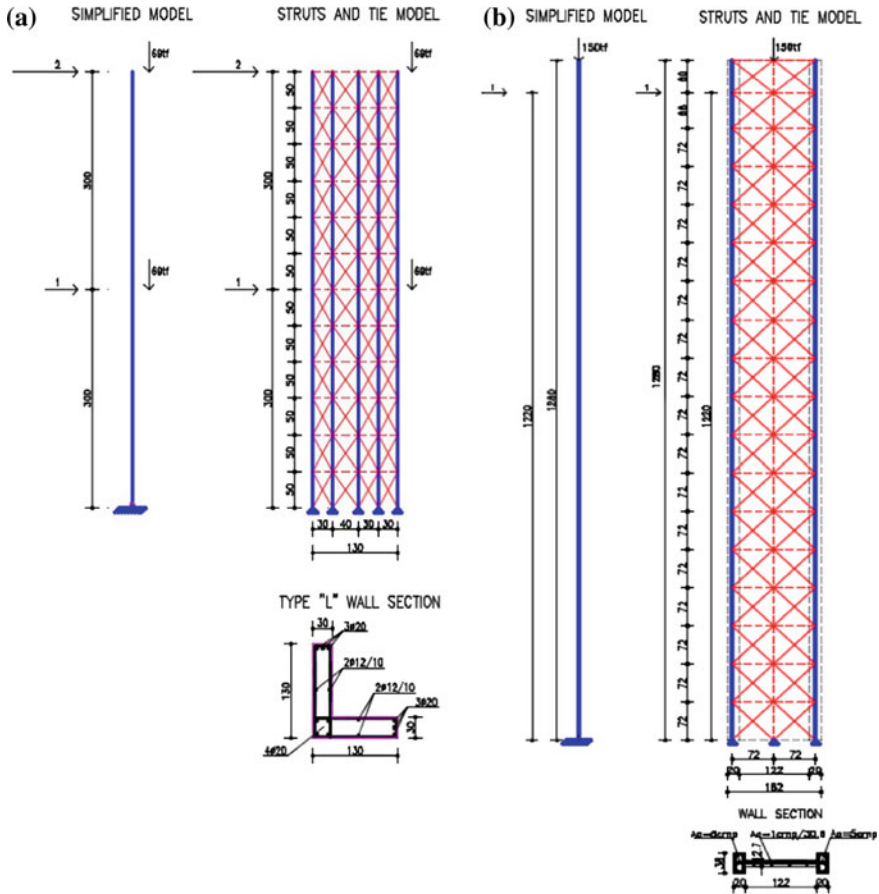


Fig. 10 a and b strut and tie models for R.C. elements

4 Conclusions

The earthquake from 10th November 1940 has become a marker for the importance of protecting constructions against seismic action in the conscience of Romanian builders.

Before this earthquake, we have shown to be in touch with the times as far as building was concerned, as depicted by the many realizations of our great personalities. Sadly, however, the introduction of seismic action protection usually happens after an event with a powerful emotional impact on the whole country.

The 2nd World War was an impediment to realizing the necessary interventions to the buildings damaged in the quake and consequently to the enrichment and perfecting of the knowledge regarding seismic actions and building response to earthquakes.

After the war, in 1960, at the World Seismic Engineering Conference in Tokyo, we were the 5th country in the world to present reports regarding regulations for protecting buildings against earthquakes.

That is what we have shown in Chaps. 2 and 3, the analysis models and the case studies presented.

As such, the original method to make an energy analysis in order to judge the failure criteria for resistances and deformations, by comparing the surface of the capable $S-\delta$ relation, for the model with one degree of freedom realized for the different structures of multi-storey constructions, to the surface required by the building response to different types of earthquakes, is still valid today.

The failure theories, based on the energetic model from strut-tie models, or taking into consideration the areas in which the theories based on the continuous, homogenous and isotropic body hypothesis cannot be applied, for which specific finite element models apply for the potential cracking areas or probabilistic models with the aid of fragility curves, are all analysis methods of medium or greater complexity which are necessary to be applied for the structures or areas of structures of important constructions and which will develop further and further in the future.

References

- Beleş A (1941) Earthquake and constructions (in Romanian) Bucharest
- Cismigiu A, Titaru E (July 1960) On the Romanian general design specifications for civil and industrial buildings in seismic areas. Examples. In: 2nd world conference on earthquakes engineering, Tokyo
- Mironescu M et al (1978) Simplified methods of analysis of the behaviour of constructions to actions of a seismic type. COPISE 1978, Bucharest
- Mironescu M et al (2013) Update of the problems based on the analysis and structural interventions for existing constructions with unreinforced masonry structures (in Romanian). AICPS Rev 4(2013):58
- Mironescu M et al (2014) Repair and strengthening structural interventions based on the restoration principles, reflected in the harmonized regulation of the requirements of ICOMOS and SREN (in Romanian). AICPS Rev 4(2014):20
- Monograph (1982) The Romanian earthquake of 4th March 1977 (in Romanian). Ed. Academie, pp 464–468

Analytical Seismic Fragility Functions for Dual RC Structures in Bucharest

Paul Olteanu, Veronica Coliba, Radu Vacareanu,
Florin Pavel and Daniel Ciuiu

Abstract Incremental dynamic analyses (IDA) of two dual RC structures (six and twelve stories in height), designed according to the provisions of relevant earthquake resistant design codes in force in Romania, are performed in order to derive analytical seismic fragility functions. The horizontal layout of the two structures is similar with five spans of 8.00 m in both orthogonal directions. In order to perform the nonlinear time history analyses (NTHAs) required by IDA method, the two structures are modelled with STERA 3D ver. 5.8. The hysteretic model employed in the NTHAs is a trilinear degrading model based on the Takeda model. The NTHAs are performed using 75 horizontal components of site-dependent simulated accelerograms that are randomly selected from a larger set developed for the INCERC site in Bucharest; the site is characterized by predominant long-periods of vibration of soil in strong earthquakes and the simulated accelerograms are reproducing this trend. The analytical fragility functions are obtained with the procedure given in Porter et al. (Earthquake Spectra 23(2):471–489, 2007) using the results of NTHAs.

P. Olteanu (✉)

Technical University of Civil Engineering & Senior Engineer
at Antiseismic Structural Engineering, Bucharest, Romania
e-mail: p.olteanu@gmail.com

V. Coliba · R. Vacareanu ·
F. Pavel

Seismic Risk Assessment Research Center, Technical University
of Civil Engineering, Bucharest, Romania
e-mail: veronica.coliba@utcb.ro

R. Vacareanu
e-mail: radu.vacareanu@utcb.ro

F. Pavel
e-mail: florin.pavel@utcb.ro

D. Ciuiu
Department of Mathematics and Computer Science,
Technical University of Civil Engineering, Bucharest, Romania

Keywords Vrancea · Intermediate · Earthquake · STERA

1 Introduction

Seismic fragility functions are a compulsory ingredient for the seismic risk assessment. The literature is abundant in seismic fragility functions for reinforced concrete (RC) structures. Full updated collections of fragility functions are provided in relevant report and papers (i.e. FEMA 2009; Kaynia 2013; Pitilakis et al. 2014). Nevertheless, the information is scarce for dual (moment resisting frames and structural walls) RC structures.

In order to fill this gap, the incremental dynamic analyses (IDAs) are performed for two dual RC structures and the results are reported in this paper. To this aim, two dual RC structures designed according to the provisions of relevant earthquake resistant design codes in force in Romania—P100-1/2013 (MDRAP 2013a) and CR2-1-1.1/2013 (MDRAP 2013b)—are subjected to IDAs in order to derive analytical seismic fragility functions. The first structure has a height of 18.0 m (six storeys high), while the second one is double in height (36.0 m) and in number of storeys, as well. According to FEMA (2009) typology, the first building is mid-rise and the second building is high-rise. The horizontal layout of the two structures is similar with five spans of 8.00 m in both orthogonal directions. In order to perform the nonlinear time history analyses (NTHAs) required by IDA method, the two structures are modelled with STERA 3D ver. 5.8 (<http://www.rc.ace.tut.ac.jp/saito/software-e.html>). This software is chosen because of its high speed of computation and because it allows the modelling of RC structures through elements with distributed plasticity. The hysteretic model employed by the software is a trilinear degrading model based on the well-known Takeda model.

The NTHAs are performed using mean values for the mechanical properties of the structural materials (concrete and reinforcing steel) and 75 horizontal components of site-dependent simulated accelerograms that are randomly selected from a larger set developed for the INCERC site in Bucharest; the site is characterized by predominant long-periods of vibration of soil in strong earthquakes and the simulated accelerograms is reproducing this trend. More details regarding the simulated accelerograms can be found in the companion paper of Pavel et al. (2016). The analytical fragility functions are obtained with the procedure given in Porter et al. (2007) using the results of NTHAs.

2 Buildings Description

Two building structures located in Bucharest were modelled, both having the same layout in plan and the same storey height. Both buildings have dual structures, with frames that bear mainly the vertical loads and shear walls that resist a large part of

the lateral loads and their tributary gravitational loads. The frames could provide a second line of defence when the buildings are subjected to very strong earthquakes and provide redundancy to the overall structure.

The floor plan is square so, in both directions there are five spans of 8.00 m. The storey height is 3.00 m. The first structure has six storeys and the second one is twelve storeys high. The location and the length of the walls are the same. The horizontal layout of the structural system of both buildings is shown in Fig. 1.

The structures were designed according to the provisions of earthquake resistant design codes in force in Romania: P100-1/2013 (MDRAP 2013a) and CR2-1-1.1/2013 (MDRAP 2013b). The design values for seismic design are: 0.30g peak ground acceleration with 20 % exceedance probability in 50 years, 1.6 s corner period of the response spectrum, and maximum dynamic amplification factor of 2.5 (MDRAP 2013a). One has to mention that for the higher building the importance factor is 1.2 because its height exceeds 28 m (MDRAP 2013a) while the value of the importance factor is 1.0 for the lower building. The seismic coefficient (ratio of the base shear to building weight in seismic combination) for the two structures is 0.111 for the six storey building and 0.133 for the twelve storey building. ETABS computer software (CSI 2015, <http://www.csiamerica.com/products/etabs>) was used for structural analysis.

The first building is 18.0 m in height. The basic design of the superstructure includes longitudinal and transversal beams of 300 × 700 mm, exterior and interior

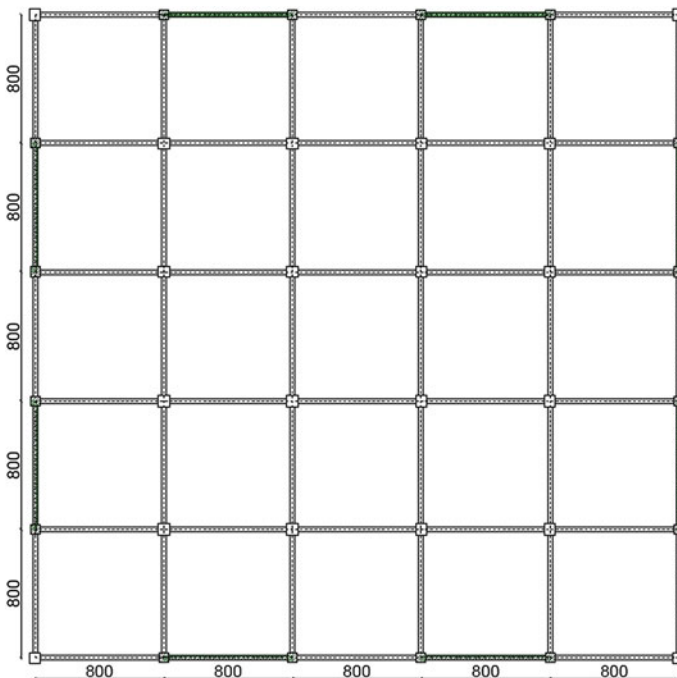


Fig. 1 Horizontal layout of structural system (RC structural walls are highlighted in green)

columns of 700×700 mm. All of the structural RC walls have a thickness of 300 mm. The materials used for this structure are: concrete C25/30 and reinforcing steel S500.

The reinforcement ratios of all structural members are detailed below in Tables 1, 2 and 3.

The total weight of the building is 134,400 kN and it was modelled using ETABS 2015 software, under different loading hypotheses. The eigenperiods of vibration along the two directions of the buildings (translation) are 0.41 and 0.28 s for general torsion.

The twelve-storey building has 700×700 mm columns, 300×700 beams and walls with 400 mm web width. The slab is 180 mm thick. The columns are integrated in the wall at the wall ends, providing enhanced ductility and anchorage for beams framing perpendicular to the wall. The concrete is of class C35/45 and the reinforcing steel is S500.

In Tables 4, 5 and 6 some of the details regarding structural members are given.

Total height of building is 36.00 m, total weight is 224,400 kN and the eigenperiods of vibration are 0.90 s (translation along the two principal directions) and 0.63 s for general torsion.

Table 1 Beams reinforcement

Beam dimensions (mm)	Location	Level	Bottom reinforcement ratio (%)	Top reinforcement ratio (%)	Transverse reinforcement ratio (%)	Stirrups (mm)
300×700	Exterior	3, 4	0.38	0.63	0.52	$2\text{Ø}10/100$
300×700	Exterior	1, 2, 5, 6	0.38	0.47	0.52	$2\text{Ø}10/100$
300×700	Interior	3, 4	0.38	0.63	0.52	$2\text{Ø}10/100$
300×700	Interior	1, 2, 5, 6	0.38	0.47	0.52	$2\text{Ø}10/100$

Table 2 Columns reinforcement

Column dimensions (mm)	Location	Longitudinal reinforcement ratio (%)	Transverse reinforcement ratio (%)	Stirrups (mm)
700×700	Corner and interior	1.72	0.60	$5.41\text{Ø}10/100$

Table 3 Structural walls reinforcement

Web thickness (mm)	Level	Edge reinforcement ratio (%)	Web reinforcement ratio (%)	Transverse reinforcement ratio (%)	Stirrups (mm)
300	1, 2, 3	1.69	0.38	0.75	$2\text{Ø}12/100$
300	4, 5, 6	1.69	0.38	0.52	$2\text{Ø}10/100$

Table 4 Beams reinforcement

Beam dimensions (mm)	Location	Bottom reinforcement ratio (%)	Top reinforcement ratio (%)	Transverse reinforcement ratio (%)	Stirrups (mm)
300 × 700	Edge 1	0.53	1.00	0.67	4Ø8/100
300 × 700	Edge 2	0.82	1.33	0.67	4Ø8/100
300 × 700	Central 1	0.82	1.33	0.67	4Ø8/100
300 × 700	Central 2	0.53	0.83	0.67	4Ø8/100

Table 5 Columns reinforcement

Column dimensions (mm)	Location	Longitudinal reinforcement ratio (%)	Transverse reinforcement ratio (%)	Stirrups (mm)
700 × 700	Interior and corner	1.00	0.60	5.41Ø10/100

Table 6 Structural walls reinforcement

Web thickness (mm)	Level	Edge reinforcement ratio (%)	Web reinforcement ratio (%)	Transverse reinforcement ratio (%)	Stirrups (mm)
400	1, 2, 3	3.14	0.38	0.80	2Ø16/125
400	4	2.78	0.28	0.51	2Ø14/150
400	5	2.49	0.28	0.51	2Ø14/150
400	6	1.60	0.28	0.38	2Ø12/150
400	7–12	1.00	0.28	0.38	2Ø12/150

It is mentioned that for both buildings the eigenmodes and eigenvalues are obtained using cracked stiffness (50 % of the gross section moment of inertia, according to P100-1/2013). Both structures are considered fixed at the bottom of the ground floor.

3 Incremental Dynamic Analysis

Incremental Dynamic Analysis (IDA) is a form of nonlinear parametric analysis which aims to describe the in-depth behaviour of a structure subjected to earthquake loads (Vamvatsikos and Cornell 2001). A suite of strong motion records is used to excite a comprehensive structural model, and for every structure and every ground motion record a nonlinear time history analysis is performed. The selected accelerograms have increasing intensity measures (i.e., peak ground acceleration—

PGA and/or spectral displacement and spectral acceleration at the fundamental period of vibration of the building). Maximum structural response of the model, in terms of inter-storey drift ratio, base shear force and roof displacement, is recorded for every accelerogram.

3.1 *Nonlinear Time History Analyses*

In order to perform the nonlinear analysis, the two structures were modelled in STERA 3D ver. 5.8. This computer program was chosen because of its high speed of computation and because it allows the modelling of RC structures through fibre elements. The hysteretic model used by the program is a trilinear degrading model based on Takeda Model.

In this paper, for analysis purpose we assumed:

- mean values of the properties of the materials ($f_c = 43$ MPa for C35/45 concrete, $f_c = 33$ MPa for C25/30 concrete and $f_y = 575$ MPa for S500 steel);
- the default parameters for beam element—stiffness degradation ratio 0.5, slip stiffness ratio 0.0, strength degrading ratio 0.0;
- P-delta effects were not considered;
- damping is considered proportional to instantaneous stiffness matrix, changing according to the nonlinearity of structural elements;
- numerical integration method is based on average acceleration.

Slip stiffness ratio and strength degrading ratio are available for user editing only for the beam element.

The nonlinear time-history analyses were conducted using 75 horizontal accelerograms, in order to obtain the maximum storey shear force, maximum displacement at the top and the maximum storey drift associated with the ground motion in question.

The horizontal components of the accelerograms were stochastically simulated for the free surface of INCERC site in Bucharest. In the paper of Pavel et al. (2016), the stochastic simulation of 1554 strong ground motions is performed in conjunction with a 2500 years stochastic catalogue for Vrancea intermediate-depth earthquakes with magnitudes $M_W \geq 5.5$. The catalogue is simulated based on the Monte Carlo approach described by Assatourians and Atkinson (2013) and on the seismicity parameters derived from the ROMPLUS catalogue of the National Institute of Earth Physics (<http://www1.infp.ro/realtime-archive>). Out of 1554 horizontal components of simulated accelerograms, 75 were randomly selected as input for the NTHAs. All the selected accelerograms are compatible with the deep soil profile at INCERC site in Bucharest (Constantinescu and Enescu 1985). Details on the Vrancea intermediate-depth seismic source and the seismic hazard from this seismic source can be found elsewhere (i.e. Ismail-Zadeh et al. 2012; Lungu et al. 2000; Radulian et al. 2000; Vacareanu et al. 2016).

Thus, the input for the NTHAs consisted in 75 strong ground motions already mentioned, grouped in eight bins in ascending order of the intensity measure. The intensity measure initially considered is peak ground acceleration with values in between 0.05g and 0.40g; only two values are larger than 0.4g: 0.59g and 0.71g. The dimension of the bin is 0.04g and the last bin comprises accelerograms with peak ground accelerations in excess of 0.33g. Two other intensity measures are also considered in the analyses, namely spectral acceleration and spectral displacement at the fundamental period of vibration of the buildings.

3.2 Incremental Dynamic Analyses Results

For each NTHAs, the maximum values of base shear force, displacement at the top of the building and inter-storey drift are considered and recorded. In Fig. 2 the results of the IDAs are shown synthetically as the plot of the maximum values of the displacement at the top of the building versus base shear force. The IDAs results are compared in Fig. 2 with the pushover curves obtained with a uniform and a modal distribution of the lateral loading.

The evolution of the structural behaviour from cracking to yielding and eventually collapse can be easily seen in Fig. 2. For both buildings it can be seen that most of the IDA cloud of data fits between the two pushover curves, so the static nonlinear analysis provides a reasonable envelope for the response of the building in terms of base shear versus top displacement. One can notice from Fig. 2 that the push-over curve with modal distribution of lateral loading is the lower bound for IDAs results while the push-over curve with uniform distribution of the lateral loading provides the upper bound for the IDAs results.

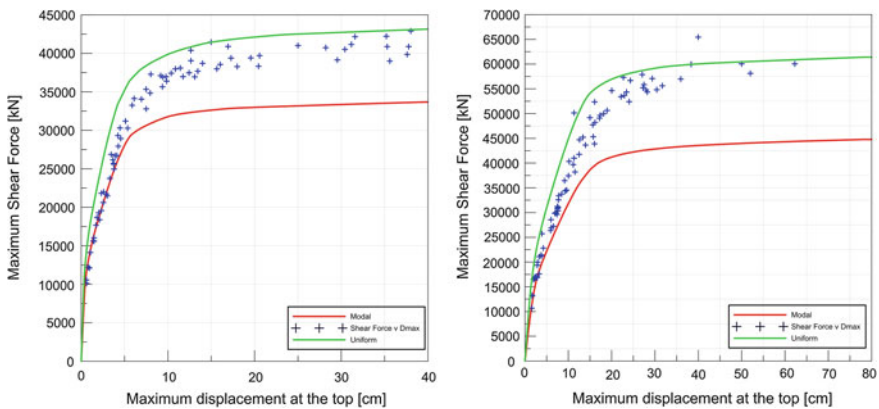


Fig. 2 IDAs results and push-over curves for both structural systems (*left* six storey building; *right* twelve storey building)

4 Seismic Fragility Functions

4.1 Previous Studies

Fragility functions are a powerful tool in assessing the seismic performance of a building structure. In the past decades a great deal of effort was carried out towards improving the defining attributes and quality of such functions. The fragility function relates the probability of reaching or exceeding a certain state of damage to an intensity measure parameter (peak ground acceleration, spectral displacement). Functions parameters usually depend on the structural type, height of structure and material type. There were many attempts to find methodologies suitable for different building types.

One of the first thorough methodologies, which addressed 36 structural categories, was HAZUS (FEMA 2009). These categories were classified according to US practice, and the level of knowledge at the time when design took place was captured through code level approach (i.e. “low code”, “moderate code” etc.). The methodology was integrated with a geographic information system (GIS) in order to obtain exposure and seismic risk maps.

Another important step was the RISK-UE project which took place between 2001 and 2004. The program was meant to assess risk scenarios for European towns located in earthquake prone areas (Mouroux and Le Brun 2006). There were considered 23 building categories and, after building design code and height class was considered, the RISK-UE taxonomy emerged. Some results on the seismic fragility and risk for the RC building stock in Romania can be found in Vacareanu et al. (2004).

SYNER-G is one of the latest European research projects which aim to assess the vulnerability and the seismic risk of buildings, lifelines and infrastructure considering the mutual influence between them (Pitilakis et al. 2014). In order to obtain the fragility functions, one should characterize the analysed structure according to the taxonomy (Hancilar and Taucer 2013). Under the SYNER-G framework the fragility functions can be derived by empirical methods, expert judgement, analytical methods (capacity spectrum method, incremental dynamic analysis) and hybrid methods.

4.2 Results of the Case Studies

In order to assess the probability of exceeding a certain damage state (slight, moderate, extensive or complete) conditioned on the values of peak ground accelerations, spectral displacement and spectral acceleration, the fragility functions are modelled using a log-normal distribution which is described entirely by the

median value of the distribution and the logarithmic standard deviation. Given an intensity measure (IM) of the strong ground motion, the probability of being in or exceeding a damage state, ds , is modelled as:

$$P[ds|IM] = \Phi \left[\frac{1}{\beta_{ds}} \ln \left(\frac{IM}{\overline{IM}_{ds}} \right) \right] \quad (1)$$

where: \overline{IM}_{ds} is the median value of the intensity measure at which the building reaches the threshold of the damage state, ds ;

β_{ds} is the standard deviation of the natural logarithm of the intensity measure of damage state, ds , and

Φ is the standard normal cumulative distribution function.

As described in HAZUS (FEMA 2009), the damage states vary from slight to complete.

Slight structural damage denotes “diagonal hairline cracks on most concrete shear wall surfaces; minor concrete spalling at few locations”, moderate implies that “most shear wall surfaces exhibit diagonal cracks; some shear walls have exceeded yield capacity indicated by larger diagonal cracks and concrete spalling at wall ends”, extensive entails that “most concrete shear walls have exceeded their yield capacities; some walls have exceeded their ultimate capacities indicated by large, through-the-wall diagonal cracks, extensive spalling around the cracks and visibly buckled wall reinforcement or rotation of narrow walls with inadequate foundations” and complete describes the structural collapse or that the structure is in “imminent danger of collapse due to failure of most of the shear walls and failure of some critical beams or columns” (FEMA 2009).

The method employed in this study to obtain the fragility functions parameters is Method B, based on Porter et al. (2007) where different methods for creating fragility functions are presented based on bounding intensity measures (IM). Method B refers to the situation in which a part of the specimens failed (in this study, exceeded the inter-storey or relative drift ratio corresponding to the threshold of the damage state). The damage states are considered as in HAZUS (FEMA 2006), namely Slight, Moderate, Extensive and Complete.

The maximum input values (peak ground acceleration, spectral acceleration and spectral displacement at the fundamental period of vibration of the building) and the corresponding maximum output values (base shear force, top displacement, and inter-storey drift ratio) are organized in bins. Following Porter et al. (2007), each bin must have approximately the same number of parameters and the number of bins is the largest integer less than or equal to the square root of the size of the sample. In this study the size of the sample is 75, thus the number of bins is equal to eight.

For each bin, the number of specimens that failed (number of NTHAs in which the inter-storey drift ratios at the threshold of various damage states are exceeded) is evaluated and the average values of IMs are obtained.

In order to find the number of failed specimens, the inter-storey drift ratios obtained from STERA 3D (calculated at the effective modal height) is compared to the corresponding values at the threshold of the damage states. These thresholds are considered for mid-rise (C2M) and high-rise (C2H) RC structural walls, according to HAZUS (FEMA 2009), and the values are as following:

- C2M: Slight: 0.27 %, Moderate: 0.67 %, Extensive: 2 % and Complete 5.33 %
- C2H: Slight: 0.2 %, Moderate: 0.5 %, Extensive: 1.5 % and Complete 4 %

The parameters of the fragility functions for Slight, Moderate and Extensive damage states, conditioned on peak ground acceleration, are reported in Tables 7 and 8 for six storey building and, respectively, for twelve storey building. Moreover, in Tables 9 and 10, the parameters of the fragility function conditioned on spectral displacement at the fundamental periods of vibration of the buildings are given. The parameters of the fragility functions for Complete damage state are not reported since the authors of the study considered that the values of the logarithmic

Table 7 Parameters of the fragility functions for the six storey building, for $IM = PGA$

Parameters	Slight	Moderate	Extensive	Complete
Median value (cm/s ²), \overline{PGA}_{ds}	120	155	330	827
Logarithmic standard deviation, β_{ds}	0.602	0.527	0.800	1.346

Table 8 Parameters of the fragility functions for the twelve storey building, for $IM = PGA$

Parameters	Slight	Moderate	Extensive
Median value (cm/s ²), \overline{PGA}_{ds}	108	192	704
Logarithmic standard deviation, β_{ds}	0.421	0.546	1.274

Table 9 Parameters of the fragility functions for the six storey building, for $IM = SD(T_1)$

Parameters	Slight	Moderate	Extensive
Median value (cm), $\overline{SD(T_1)}_{ds}$	1.0	1.3	2.9
Logarithmic standard deviation, β_{ds}	0.739	0.649	1.411

Table 10 Parameters of the fragility functions for the twelve storey building, for $IM = SD(T_1)$

Parameters	Slight	Moderate	Extensive
Median value (cm), $\overline{SD(T_1)}_{ds}$	3.0	6.8	55.7
Logarithmic standard deviation, β_{ds}	0.330	0.649	2.049

standard deviation are not well constrained because of the very limited number of cases in which the inter-storey drift ratio at the threshold of the Complete damage state is exceeded.

Some comments on the values of the fragility functions parameters are as follows:

- for the six storey building, the median values of the peak ground acceleration for the Slight and Moderate damage state are closely spaced, showing a very narrow behaviour range within which the structural system might experience quite different types of damage; also, the median value of the peak ground acceleration is only 10 % higher than the design value, revealing that the ultimate limit state given in the P100-1/2013 (MDRAP 2013a) design code is actually exceeded in almost 50 % of the cases for the design acceleration (given that the ultimate limit state must ensure the life safety of the occupants and Complete damage state is far beyond this requirement); the logarithmic standard deviation is increasing as the damage states evolves from Slight to Extensive because of the decreasing number of cases of exceedances of the corresponding inter-storey drift ratio at the thresholds of the damage states;
- for the twelve storey building, the median values of the peak ground acceleration for the Slight and Moderate damage state are widely spaced, showing a large behaviour range within which the structural system might experience quite different types of damage; also, the median value of the peak ground acceleration is more than double than the design value, revealing that the ultimate limit state given in the P100-1/2013 (MDRAP 2013a) design code is actually exceeded in very few cases for the design acceleration (given that the ultimate limit state must ensure the life safety of the occupants and Complete damage state is far beyond this requirement); the logarithmic standard deviation is increasing as the damage states evolves from Slight to Extensive because of the decreasing number of cases of exceedances of the corresponding inter-storey drift ratio at the thresholds of the damage states;
- in the opinion of the authors of this study, the better seismic performance of the twelve storey building (if compared with the six storey building) is due to (i) the 20 % increase in the design seismic force incurred by the importance factor, (ii) its higher redundancy and (iii) the better behaviour of its slenderer RC structural walls if compared with the squatter walls of the six storey building;
- the median values of the spectral displacements (and of the corresponding inter-storey drift ratios) at the thresholds of the damage states obtained in this study are in-between the corresponding values given in HAZUS (FEMA 2009) for RC moment resisting frames and RC structural walls;
- the very high value of the logarithmic standard deviation for the extensive damage state (conditioned upon $IM = PGA$) of the twelve storey building is a consequence of the sampling of PGA values at the high-end of the IM scale; the reason is the very few numbers of runs exceeding the threshold of the extensive damage state (compared to the six storey building) because of the increased

seismic performance brought up by the importance factor of 1.2; nevertheless, very high values of the logarithmic standard deviation, in the same high-end range, are reported in Kaynia (2013);

- the very high values of the logarithmic standard deviation for the extensive damage state [conditioned upon $IM = SD(T_1)$] seems to be a consequence of the change of conditioning IM from PGA (as originally sampled) to $SD(T_1)$ (as formerly transformed), thus losing some accuracy of the sampling and binning since there is no (or poor) correlation between the PGA and $SD(T_1)$ values.

The fragility functions obtained for Slight, Moderate and Extensive damage states for both structures (six-storey building and twelve-storey building) are represented in Fig. 3. The fragility functions for Complete damage state are represented separately in Fig. 4. The intensity measure in Figs. 3 and 4 is the peak ground acceleration.

If one is interested in the probability of a dual RC structural system of being in a given damage state (or undamaged) for a specified value of the intensity measure, the following relations given by Porter et al. (2007) can be applied:

$$\begin{aligned}
 P[DS = ds | IM = im] &= 1 - F_1(im) \rightarrow ds = 0 \\
 &= F_{ds}(im) - F_{ds+1}(im) \rightarrow 1 \leq ds < N \\
 &= F_{ds}(im) \rightarrow ds = N
 \end{aligned}
 \tag{2}$$

where $ds = 0$ for undamaged and $ds = 1 \dots N$ for Slight, Moderate, Extensive and Complete.

Applying relation (2) for $IM = PGA$ and $im = 0.30g$ (the design value of PGA for both buildings), the probabilities are reported in Tables 11 and 12. The values of the

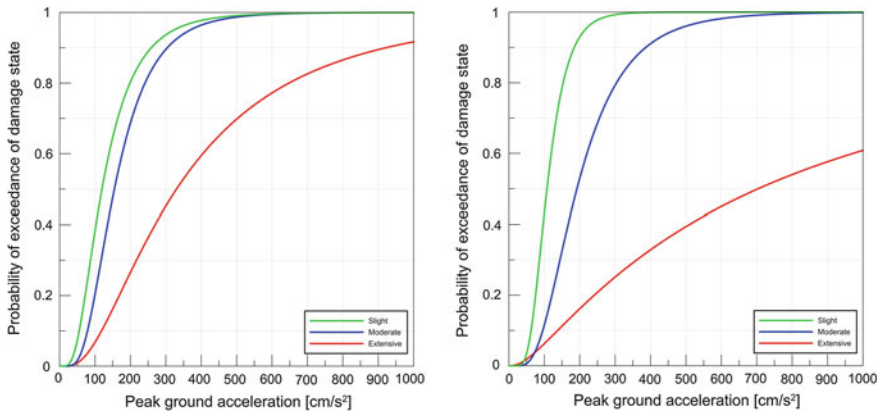


Fig. 3 Fragility functions for slight, moderate and extensive damage states conditioned upon peak ground acceleration (*left* six storey building; *right* twelve storey building)

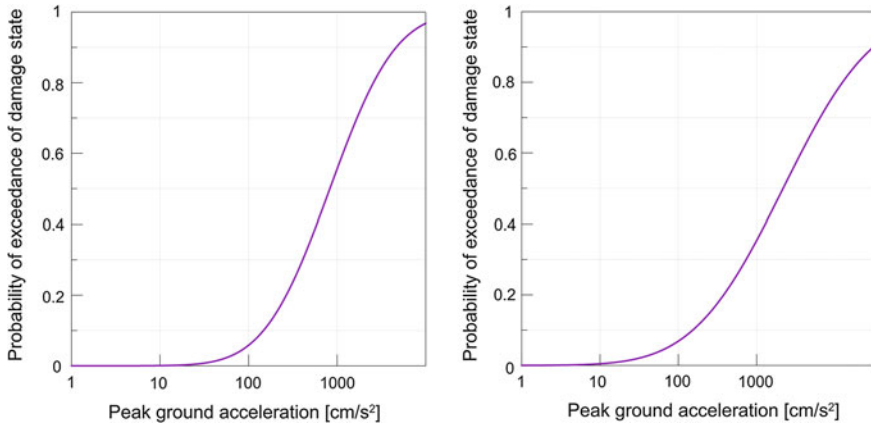


Fig. 4 Fragility functions for Complete damage state conditioned upon peak ground acceleration (*left* six storey building; *right* twelve storey building)

Table 11 Probabilities of being in certain damage states or undamaged for the six storey building, for $PGA = 0.30g$

Undamaged	Slight	Moderate	Extensive	Complete
0.064	0.041	0.443	0.227	0.225

Table 12 Probabilities of being in certain damage states or undamaged for the twelve storey building, for $PGA = 0.30g$

Undamaged	Slight	Moderate	Extensive	Complete
0.007	0.199	0.542	0.082	0.170

probabilities given in Tables 11 and 12 points once again towards a better damage control of the twelve storey building if compared to the six storey building because the probability of being in Extensive or Complete damage states is 0.25 in the first case and 0.45 in the second case.

A set of fragility functions that consider the probability of exceeding serviceability and ultimate limit states conditional upon $IM = PGA$ is also developed using the results of IDAs. The serviceability and ultimate limit states are defined in P100-1/2013 (MDRAP 2013a) in terms of inter-storey drift ratio as 0.5 %, 0.75 % and 1.0 % (depending on the type and connections of the non-structural components) for serviceability and 2.5 % for ultimate limit state, respectively.

Applying the same method as for the previous fragility functions (Method B of Porter et al. (2007), the median values of the IM (in terms of PGA) and logarithmic

standard deviations are obtained and the values are reported in Tables 13 and 14 for the six storey and twelve storey buildings, respectively. The fragility functions for serviceability and ultimate limit states are plotted in Figs. 5 and 6, respectively.

One can notice that for the six storey building the median values of PGA corresponds to one half of the design peak ground acceleration for serviceability limit state and to the design peak ground acceleration for ultimate limit state, matching perfectly the seismic hazard level recommended by the seismic design code in force in Romania for the limit states verifications. On the other hand, the median values are much more scattered for the twelve storey building.

Table 13 Parameters of the fragility functions for the six storey building, for $IM = PGA$

Parameters	SLS (0.5 %)	SLS (0.75 %)	SLS (1.0 %)	ULS (2.5 %)
Median value (cm/s ²), \overline{PGA}_{I_s}	141	143	152	297
Logarithmic standard deviation, β_{I_s}	0.435	0.472	0.455	0.707

Table 14 Parameters of the fragility functions for the twelve storey building, for $IM = PGA$

Parameters	SLS (0.5 %)	SLS (0.75 %)	SLS (1.0 %)	ULS (2.5 %)
Median value (cm/s ²), \overline{PGA}_{I_s}	173	240	330	1251
Logarithmic standard deviation, β_{I_s}	0.483	0.647	0.766	1.653

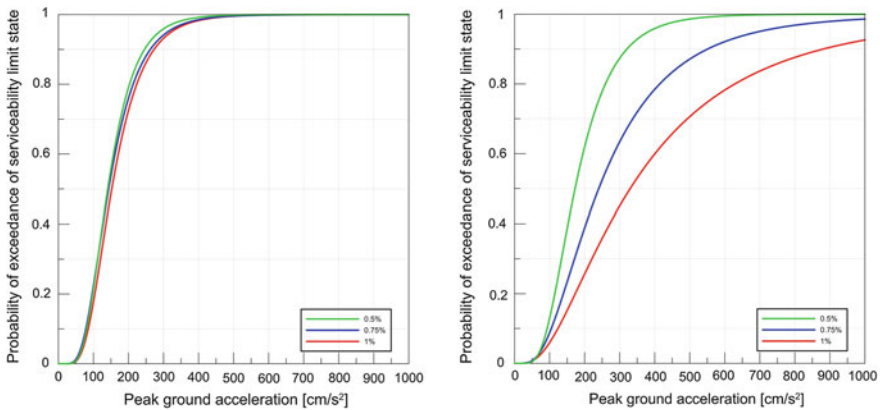


Fig. 5 Fragility functions serviceability limit state conditioned upon PGA (left six storey building; right twelve storey building)

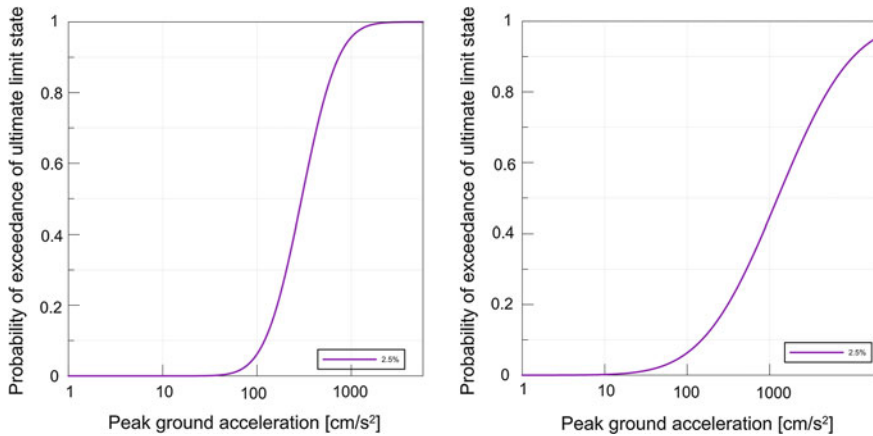


Fig. 6 Fragility functions ultimate limit state conditioned upon PGA (*left* six storey building; *right* twelve storey building)

5 Conclusions

In this study, fragility functions for two model RC dual buildings are obtained. The conditional intensity measures are peak ground acceleration and spectral response values at the fundamental period of vibration of the building.

The fragility functions are developed for damage states and limit states, as well. Although the structural system is the same for the two buildings (moment resisting frames and shear walls), the median values of the fragility functions are different. The higher values of the medians for the twelve storey building (if compared to the six storey building) occur (in the opinion of the authors) because of the:

- importance factor that increase by 20 % the design seismic force for the higher building;
- higher redundancy of the twelve storey structural system;
- better seismic behaviour of the slenderer shear walls of the higher building.

For the twelve storey building, the values of the logarithmic standard deviation are larger than 1.0 for extensive and complete damage states and for the ultimate limit state, as well. Values larger than unity for buildings designed according to high seismic design codes are not reported in HAZUS (FEMA 2009) but are reported in literature and can be found in Kaynia (2013). The reasons for these high values in this study are, in the opinion of the authors, the very limited numbers of accelerograms in the sampling pushing the structural system beyond the thresholds of the extensive and complete damage states and ultimate limit state.

In this paper only the random uncertainties of the seismic excitation are considered. In order to get a full picture of the propagation of the uncertainties into the logarithmic standard deviation of the fragility functions, further studies must

consider other sources of random uncertainties (i.e. mechanical properties of materials, geometrical properties of the structural elements) and of epistemic uncertainties (i.e. alternative structural layouts, softwares to conduct the NTHAs).

Acknowledgements Funding for this research was provided within BIGSEES Project by the Romanian Ministry of National Education and Scientific Research under the Grant Number 72/2012. This support is gratefully acknowledged.

References

- Assatourians K, Atkinson GM (2013) EqHaz: an open-source probabilistic seismic-hazard code based on the Monte Carlo simulation approach. *Seismol Res Lett* 84:516–524
- Contantinescu L, Enescu D (1985) The Vrancea earthquakes from scientific and technologic point of view (in Romanian). Ed Academiei, Bucharest, Romania
- FEMA (2009) Multi-hazard Loss Estimation Methodology. Earthq Model. Hazus[®]-MH 2.1. Technical manual. <http://www.fema.gov/media-library/assets/documents/24609?id=5120>
- Hancilar U, Taucer F (eds) (2013) SYNER-G reference report 2: guidelines for typology definition of European physical assets for earthquake risk assessment. ISBN:978-92-79-28973-6. ISSN:1831-9424. doi:10.2788/68751
- Ismail-Zadeh A, Matenco L, Radulian M, Cloetingh S, Panza G (2012) Geodynamics and intermediate-depth seismicity in Vrancea (the south-eastern Carpathians): current state-of-the art. *Tectonophysics* 530–531:50–79
- Kaynia AM (ed) (2013) SYNER-G reference report 4: guidelines for deriving seismic fragility functions of elements at risk: buildings, lifelines, transportation networks and critical facilities. ISBN:978-92-79-28966-8. ISSN:1831-9424. doi:10.2788/19605
- Lungu D, Vacareanu R, Aldea A, Arion C (2000) Advanced structural analysis. Conspress, Bucharest
- MDRAP (2013a) P100-1/2013. Code for seismic design—part I—design prescriptions for buildings. Ministry of Regional Development and Public Administration. Bucharest, Romania
- MDRAP (2013b) CR2-1-1.1/2013. Design code for RC structural walls buildings. Ministry of Regional Development and Public Administration. Bucharest, Romania
- Mouroux P, Le Brun B (2006) Presentation of RISK-UE project. *Bull Earthq Eng* 4(4):323–339
- Pavel F, Ciuiu D, Vacareanu R (2016) Site dependent seismic hazard assessment for Bucharest based on stochastic simulations. In: Vacareanu R, Ionescu C (eds) The 1940 Vrancea earthquake. Issues, insights and lessons learnt. In: Proceedings of the symposium commemorating 75 years from November 10, 1940 Vrancea Earthquake, Springer Natural Hazards Book Series
- Pitilakis K, Crowley H, Kaynia AM (eds) (2014) SYNER-G: typology definition and fragility functions for physical elements at seismic risk. Springer. ISBN:978-94-007-7871-9 (Print) 978-94-007-7872-6 (Online). doi:10.1007/978-94-007-7872-6
- Porter K, Kennedy R, Bachman R (2007) Creating fragility functions for performance-based earthquake engineering. *Earthq Spectra* 23(2):471–489
- Radulian M, Mandrescu N, Popescu E, Utale A, Panza G (2000) Characterization of Romanian seismic zones. *Pure Appl Geophys* 157:57–77
- Vacareanu R, Lungu D, Aldea A, Arion C (2004) An advanced approach to earthquake risk scenarios with applications to different European towns, Report WP7: seismic risk scenarios handbook. European Commission, Brussels. Available at: ftp://ftp.brgm.fr/pub/RISK-UE/Handbooks_Methodology/WP07_040408.pdf
- Vacareanu R, Aldea A, Lungu D, Pavel F, Neagu C, Arion C, Demetriu S, Iancovici M (2016) Probabilistic seismic hazard assessment for Romania. In: D’Amico S (Ed) Earthquakes and

their impact on society. Springer Natural Hazards Book Series, pp 137–169. ISBN:978-3-319-21752-9 (Print) 978-3-319-21753-6 (Online). <http://dx.doi.org/10.1007/978-3-319-21753-6>

Vamvatsikos D, Cornell CA (2001) Incremental dynamic analysis. *earthquake engineering and structural dynamics* 2002; 31:491–514. doi:[10.1002/eqe.141](https://doi.org/10.1002/eqe.141)

<http://www.rc.ace.tut.ac.jp/saito/software-e.html>

<http://www.csiamerica.com/products/etabs>

<http://www1.infp.ro/realtime-archive>

Conceptual Framework for the Seismic Risk Evaluation of Transportation Networks in Romania

Dragos Toma-Danila, Iuliana Armas and Carmen Ortanza Cioflan

Abstract The assessment of seismic risk for transportation networks is a difficult task, due to its complexity, hard to get detailed data, lack of methods with low uncertainties and difficulty of defining inter-relations. Through this paper we identify viable ways of analysing the seismic risk of transportation networks in Romania, considering the availability and characteristics of specific data, the possibilities of adapting external knowledge and recently developed methodologies. Until now there was no coherent and complex approach in Romania for this task, referring to the bigger picture. Therefore, we propose an integrative framework that incorporates GIS capabilities (like the ones provided by the ArcGIS Network Analyst Toolbox) and test it for Bucharest. This framework can provide answer to important questions, like “which are the critical segments of networks” or “what could the implications of connectivity loss be?” in case of an earthquake. The approach relies on using fragility functions for critical structures like bridges and tunnels, on empirical formulas for estimating damage level, traffic flow characteristics or connectivity analysis. Results are depicted through multiple performance indicators.

Keywords GIS · Infrastructure · Earthquakes · Vulnerability

D. Toma-Danila (✉) · C.O. Cioflan
National Institute for Earth Physics, Măgurele, Romania
e-mail: toma@infp.ro

C.O. Cioflan
e-mail: cioflan@infp.ro

D. Toma-Danila · I. Armas
Faculty of Geography, University of Bucharest, Bucharest, Romania
e-mail: iuliaarmas@yahoo.com

1 Introduction

Each major earthquake has the capability to produce a large amount of damage over a wide extent, in a very short amount of time. The transportation networks play a vital role—both immediately after an earthquake, and also long time before it occurred; they constitute support for the fast intervention and for the recovery efforts. Therefore, their functionality and capability to satisfy traffic demands is a key aspect in reducing human and economic losses.

The impact of large scale natural disasters like earthquakes on infrastructures has two clear dimensions: temporal and spatial. These dimensions have their place in a Geographical Information System (GIS). Beside these there is also the perspective of the actor involved: national institution, citizen, financial system, NGO or others.

Generally, the vulnerability of transportation networks can be analysed at two main levels:

- Structural level—the focus is on the physical (direct) vulnerability of a components
- Functional level—the functional vulnerabilities of the network and the indirect implications are analysed

According to Pinto et al. (2011), a fundamental distinction among the studies related to the seismic performance of road or transportation networks can be made, based on the importance of the role played by the network itself. Therefore, three main categories have been identified:

- Basic: the attention is focused on the functioning of the network in terms of pure connectivity.
- Advanced: the scope of the study is widened to include consideration of the network capacity to accommodate traffic flows.
- Complex: aims at obtaining a realistic estimate of the total loss, whether direct or indirect; economic interdependencies are accounted for.

In general, the simpler the category, the smaller the uncertainties. Simulating the behaviour of transportation networks during an earthquake is a very difficult task and multiple uncertainties and high error thresholds are normal. Still, in the last decades important progress was made into this interdisciplinary field of study, making the models more accurate. Projects like Hazus or Syner-G united resources available at their time (also created new ones) and lead to the development of dedicated tools and methodologies for the analysis of the seismic risk of transportation networks (like roads, railroads, gas pipes or electrical power lines). Theoretical frameworks have been proposed—in the enumerated projects or in papers like Du and Nicholson (1997), Werner et al. (2006), Jansuwan (2013), Miller et al. (2015) and others. These framework's concepts have to be adapted to the national specific of different countries.

Romania is a country that was and will be affected by major earthquakes; the most hazardous seismic source is the Vrancea Area, located in the curvature of the

Carpathian Mountains, approximately 150 km away from Bucharest. Here, in the last century occurred 4 earthquakes with moment-magnitude (M_w) greater than 7 (in 1908, 1940, 1977 and 1986), at depths between 90 and 150 km. Due to this intermediate-depth interval, high intensities and considerable damage to buildings and infrastructure were recorded far from the epicentral area, up to 300 km away. Bucharest was one of the most affected cities, especially during the 1940 and 1977 earthquakes. There are also other crustal seismic sources like Fagaras-Campulung, Banat or Shabla (in the north-eastern Bulgaria), which can produce earthquakes large enough to generate local and regional damage.

As it happens everywhere, when major earthquakes occur, the focus of society is mainly upon the damaged buildings (since most people die due to building collapse, and not solely the seismic waves), the immediate saving of lives and recovery efforts. In an ever more complex system, the role of transportation networks and the need for it to be functional is ever more important; as complexity can be considered directly proportional with vulnerability, we expect that future earthquakes will highlight more and more the tangled dependencies in our societies, all tied through infrastructure.

One of the starting questions of this paper can be: “was the behaviour of transportation networks during earthquakes really an issue in Romania?”. Due to the focus on other aspects, few information is nowadays available regarding how earthquakes affected transportation networks and what the implications were. We certainly know that it wasn't like in California (when the 1989 Loma Prieta and 1994 Northridge earthquakes struck) or Japan (as during the Kobe earthquake on 1995). However, there are still records that some railroads, bridges, road surfaces, pipelines or electrical power lines were affected; in 1977, the railroad employees worked in the very hours after the earthquake to restore the connections. The Otopeni International Airport was also affected and quickly repaired, due to its vital role. In Bucharest, the centre of the city was mostly affected; 32 high-rise buildings collapsed partially or totally, and debris was not an issue in blocking a large number of roads. Although fires were quickly put out, electricity was off for hours. Nowadays we have to be caution and realistic, since many things changed and during future events the rule of the game could be different, because:

- Times have changed. If in the communist era (until 1989) the road traffic was reduced, nowadays it became a major problem; official records (from the Romanian Direction for Driving Licenses and Vehicle Registration Statistics) show that there are more than 1.12 million cars registered in Bucharest (more than 1 car at 2 people) and 6 million cars in total in Romania (which has 22 million people). In case of an earthquake occurs at an unfortunate hour, the traffic jams would greatly increase the intervention times in urban areas—most affected. It is a question of minutes and hours to have a chance of saving people trapped under debris.
- The damage could be much greater; experts included 373 buildings in Bucharest in the seismic risk class I (Bucharest General Municipality 2015), meaning that they could collapse to any major earthquake. And many other buildings still not

evaluated are clearly endangered. There are more than 30,000 buildings constructed without considering seismic effects on buildings.

- Economic activities and recovery efforts are strongly influenced by the disruptions of transportation networks; considering globalisation, the extent of good's circuit and the dependencies on constant flows of materials from distant origins, each delay time can have serious repercussions.

So under this considerations, would the transportation networks be reliable and not risky? We believe that an investigation has to be performed. Especially since in Romania there are so few initiatives that analyse the safety of transportation networks during earthquakes. One of the main legal obligations is the analysis of structures (mainly bridges), according to national normative (such as CD 138-201), but from here to seismic risk there is a long way. The recent research papers that we've found regarding the analysis of not only a singular structure from an engineering point of view (like in Racanel 2015 or Sartori 2012), but a network view, were Ciutea and Atanasiu (2014; with sparse references to road network's seismic risk) and Toma-Danila (2013). We consider that nowadays, with the aid of technology and international scientific knowledge, the few data available for transportation networks in Romania can be put to use, through a specifically designed schema capable of integration within a GIS, which we describe and partially test in the following chapters.

2 Proposed Framework

The conceptual framework that we propose is based on the fundamental idea that the loss of connectivity is the main issue that has to be evaluated (also in terms in implications), since its role is major in the escalating risks. In the framework development we focused on determining logical sequences that link hazard and vulnerability, determining initially the structural and functional behaviour of transportation networks and ultimately the socio-economic influences.

What makes the analysis of the networks special in a seismic context is the fact that the structural damage can have a clear expression for specific targets (link between earthquake engineering and geography); hotspots can be identified and also the modification of the socio-economical patterns (effects on the origin-destination pairs) has a considerable effect right after the event and for a significant period of time.

One of the key input data required is the definition of the network, with its components, subcomponents and attributes that can reflect the vulnerability state (from a seismic point of view, but also seen as capacity to accommodate traffic and new configurations). Some of the elements that can be considered for road networks are presented in Fig. 3. Of course, the spatial dimension has to be specified, and the resulted geodatabase should respect network specifications in order to make it

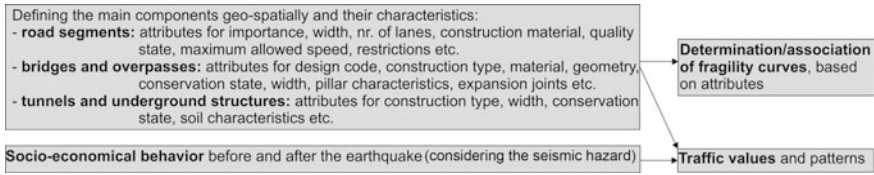


Fig. 1 Proposed definition chart for a road network, applicable to seismic risk assessment

useful. For example, the Network Analyst Module of ArcGIS that we also use in the case study requires beside location (that has to be interconnected) other attributes (such as maximum speed, importance or relative elevation), in order to allow modelling the network behaviour appropriately.

For pipelines (or electrical) networks, the elements can consist of main pipelines (power lines) with attributes like technical state, material, diameter, flow capacity etc., and special buildings (pumping or transformation stations, reservoirs etc.) that can be analysed through fragility curves, for example.

Figure 1 shows some of the main criteria to be considered when defining the components of road networks; by knowing all these aspects, important considerations regarding the behaviour of the network during an earthquake can be emitted. The use of fragility functions is a common practice in seismic risk assessment. These functions (also named fragility curves, from the graphical representation) facilitate the numerical expression of a structure’s probability to be in a vulnerable state (defined more or less subjective), for a certain ground movement parameter or intensity value. A fragility function can be seen as the cumulative distribution function of the capacity of an asset to resist an undesirable limit state (Porter 2015). The research in transportation networks lead to the definition of specific functions for components like bridges, tunnels or even embankments. Many fragility functions are gathered in the HAZUS Software and the SYNER-G project deliverables. There is no warranty that these functions are applicable elsewhere then they were determined or that they are highly reliable, however they can roughly provide the damage probability for a certain type of component. The design of new fragility curves is always an option (for long bridges is generally performed), but the process is quite complicated and hard to validate in natural conditions. Seismic fragility curves for bridges and tunnels usually require values of peak ground acceleration (PGA), intensity or peak ground deformation (PGD_f). Building analysis can also require spectral acceleration values for capacity curves. Embankment, tunnels or pipeline fragility curves require mostly peak ground velocity (PGV). Obtaining seismic damage probabilities is an important step in the analysis, since it reflects the direct damage on transportation networks. Without fragility curves, an empirical assessment can be achieved through formulas like the ones developed by Anbazhagan et al. (2012) or Kaynia et al. (2011). These formulas link intensity or permanent displacement to a certain damage state, based on real observations. In all cases, knowing detailed attributes for the components is important.

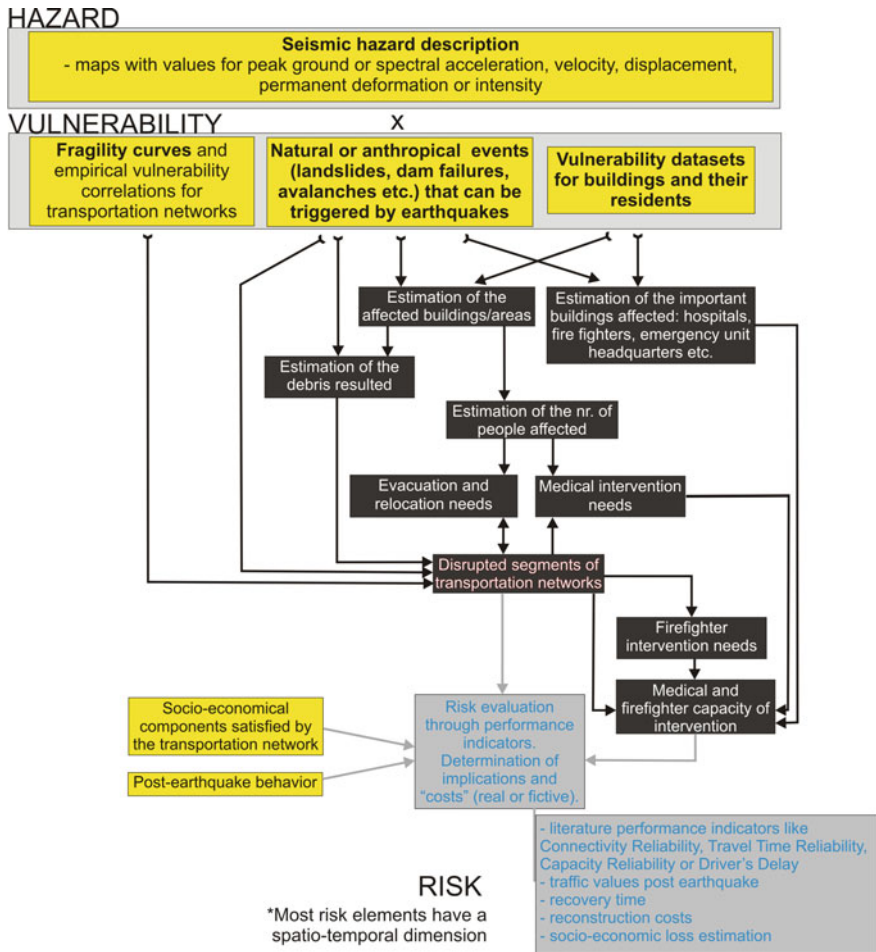


Fig. 2 Conceptual framework for analysing the seismic risk of transportation networks, for a specific seismic event

When an earthquake occurs, the socio-economic behaviour modifies dramatically; for example, people abandon buildings and, due to the failure of communication systems, try to reach home or other safe places; emergency intervention actors fill the streets; some businesses boom and others enter conservation states. Therefore, traffic values and patterns modify. It is best to model these modifications, since they greatly reflect in the computation of fictive costs translatable into risk indicators.

The framework proposed in Fig. 2 leads to trip generation, distribution and traffic assignment (origin-destination pairs) in order to check the capacity of the network to accommodate the demand, in post-earthquake context, and the risks that might occur. The framework focuses on the need for emergency intervention, from

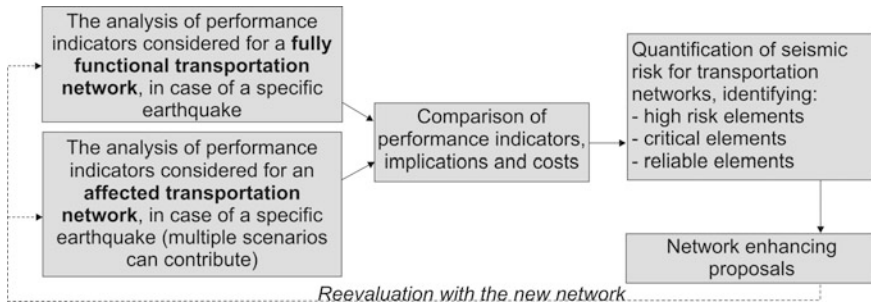


Fig. 3 Conceptual framework for quantifying the overall seismic risk and testing new proposals

fire fighters or ambulances, since the intervention times are vital for saving human lives, and if the road networks affect these times, they pose great risks. Performance indicators regarding connectivity and reliability (expressed in several transportation network papers like Asakura and Kashiwadani 1991; Chen et al. 1999 or Shinozuka et al. 2003) can be used in order to quantify the overall performance of the network and allow direct comparisons with other network configurations. The computation of costs (whether real, like money spent per km or fictive, like minutes of delay) is also important. Although hard to contain, the socio-economic risk can be estimated through different empirical models that express economic losses or life expectancy for people trapped under debris (Coburn and Spence 2002) as a function of time, for example. For network components (bridges, tunnels, km of highway) reconstruction costs can be derived based on building costs, also for different damage states.

Figure 3 presents the quantification of risks, after evaluating individual scenarios with the flowchart in Fig. 2. Basically, a comparison is performed between performance indicators obtained for the undamaged network and the damaged one, desirably at segment level in order to identify specific critical or reliable elements. Through this schema, improved network configurations can also be tested.

3 Framework’s Applicability to Romania

Due to its flexible character, the proposed framework can be applied (although with a lower confidence level) to areas where there is few data regarding the vulnerability of transportation networks, such as Romania. Nowadays, technology has led to a massive increase of datasets (including GIS data) and their public dissemination over internet. Although quality is one of the concerns when dealing with big data or free data, at least road and railway networks can be determined usefully—from a geographic point of view and with basic characteristics. In this chapter we analyse the availability of hazard and vulnerability data for Romania, considering the new capabilities of getting the needed data.

3.1 Data Availability

3.1.1 Seismic Hazard Data

The seismic hazard of the Romanian territory has been the subject of multiple studies that used probabilistic (Ardeleanu 2010; Sokolov et al. 2008; Mantyniemi et al. 2003; Musson 2000), deterministic (Marmureanu et al. 2010) or neo-deterministic methods (Cioflan 2006). The current national seismic design code (P-100/2013) presents maps at national level with design PGA values for 225 years return period and 20 % probability of exceeding in 50 years and response spectrum corner periods (1.6, 1.0 and 0.7 s, each with corresponding elastic response spectrum). Together with other considerations, regulations and recommendations, this code can contribute to expressing the seismic hazard and vulnerability of transportation networks (although its focus is mainly on buildings and individual structures).

Acceleration and intensity maps are of great use in the proposed framework and for Romania they are available, whether from the references presented above or from (near real-time) ShakeMaps and other products of the Romanian Seismic Network, operated by NIEP. Specifically for Vrancea intermediate-depth earthquakes, several ground motion prediction equations have been developed (like Sokolov et al. 2008; Vacareanu et al. 2015), providing PGA, SA, PGV or intensity values (Sokolov et al. 2008) at bedrock or surface. There are also available microzonation maps at city level, for Bucharest (Marmureanu et al. 2010) for example. Therefore, seismic hazard scenarios are obtainable, but their uncertainties are not to be neglected, since major Vrancea earthquakes are far from being understood in detail and can and have shown unpredictability (Cioflan 2006).

3.1.2 Transportation Network Data

In Romania, official GIS data regarding basic transportation networks such as important roads and railroads is not yet public and downloadable. Probably, through the INPIRE directive this is going to change, however until then we investigated other ways of obtaining GIS data with respect to the scheme in Fig. 1.

Knowing the geographical location of the network's subcomponents is one of the basic requirements when analysing the vulnerability or risk of a network. The need of knowing the spatial distribution (considering also the connectivity aspect) is vital for the analysis. Since the seismic hazard is spatially distributed, so the network must be. Romanian roads are viewable on internet websites and services (GoogleMaps, BingMaps, YahooMaps etc.) or in GPS software and actually allow interactivity. However, how can they be used in a custom seismic analysis (without digitisation by hand)? OpenStreetMap data seems to be the top choice nowadays, when requiring data that can be downloaded and manipulated (in a non-commercial purpose). Its advantages lie in the fact that is under an open license, millions of

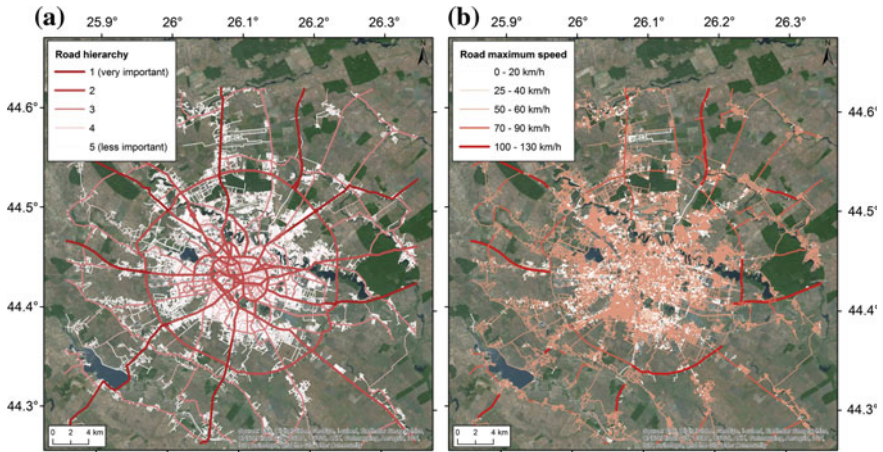


Fig. 4 Maps for different attributes: **a** hierarchy; **b** maximum speed limit, for the Bucharest road network obtained from OpenStreetMap data and processed in ArcGIS according to the Network Analyst Module specifications

collaborators from all over the world update it regularly and respect standardised procedures. We downloaded a dataset for Bucharest and we were not disappointed (as in the case of other webGIS resources that provided to basic information, inaccurate, incomplete or obsolete); the road dataset is complete (up to the smallest streets) and up-to-date, the connectivity of the segments is good and there are also very useful attributes. Also, there are tools that allow shapefile conversion, in order to use the data with the Network Analyst Module of ArcGIS. Among the attributes that enhance the modelling of the road network are relative elevation references (allowing bridges, overpasses, tunnels to not interfere with ground level roads etc.), maximum speed limits, names, importance (hierarchy) or one way and car restrictions (Fig. 4). All these data and attributes contribute to the development of a customisable road network that further requires other attributes that offer the perspective of seismic vulnerability and risk: association of fragility curves, integration of traffic values (before and after the earthquake), origin-destination pair definitions, direct and indirect seismic damage etc.

As mentioned before, fragility curves can be used for the seismic vulnerability definition of individual structures, such as bridges or tunnels. In Romania, no fragility curves were defined until now; however, in the literature there can be found suitable correspondents. Within the Syner-G Project there was compiled a world-wide library of fragility curves for bridges, tunnels or embankments, which can be used if appropriate. For bridges there are for example 6 European alternatives. Many other curves, specific to USA, are available from the Hazus-MH software.

The National Company of Motorways and National Roads (CNADNR) elaborated a normative regarding the criteria of determining the viability state of road bridges (CD 138-201), which particularizes for different construction materials (concrete, reinforced concrete, precompressed concrete, metal or composite) the aspects linked to the seismic action on the structure. A set of instructions for determining the technical state of bridges (AND 522-2002), tied to the normative aforementioned, is also in use. According to it, bridges can be classified into different technical states, requiring different levels of interventions. For the vulnerability evaluation of road network elements and tunnels there are also other regulations (CD 155-2001 and AND 601-2010). These regulations can be very useful in the assessment of transportation network's risk, but until now we haven't been able to receive reports based on these regulations and technical classifications (and we are unsure whether they also exist).

Traffic values for the roads of Romania are the subject of the General Circulation Census, which had its last editions in 2000 and 2010. The public information consists of Daily Annual Mean Traffic Values per category of vehicles (vehicles/24 h), for every national road individually and for all county or communal roads, as mean. Although useful for a wide area analysis (especially for areas outside of cities), these values are irrelevant for big cities like Bucharest, that we analyse further. The national authority that has the task of collecting road traffic values (also in charge of the census) is the Centre for Road Technical Studies and Informatics (CESTRIN), but data has to be paid in order to be used, and the costs are great (partially justified when considering the classical methods of collecting traffic data, with sensors, microwave radars, acoustic and video measurements or others, described in Leduc (2008). Fortunately, new technology—GPS and smartphones offers now a breakthrough and aid greatly in the process of crowdsourcing for traffic values. Services like Google Traffic or BingMaps Traffic allow map generation for live traffic, based on the times spent in traffic by users of the company's apps, transmitted automatically to big data servers. We tested Google Traffic in Bucharest; giving that many Romanians use smartphones (in 2014, 34 % of Romanians had a smartphone according to Initiative Media 2015), almost all roads excepting very local ones had live traffic values. The service can also show mediated values for different times of the day and week. Although GoogleMaps can use these traffic values to predict origin-destination times, due to the fact that no downloadable data is available yet, the processing cannot be easily replicated in other systems. However, for the case study in this article we georeferenced images illustrating the Monday morning traffic, extracted the classes of traffic: slow, medium and fast, and used it as influence on maximum speed limits in our custom road network.

For other transportation networks such as water-supply and waste-water networks, fire-fighting system, electric power network or natural gas system, the framework can also be applied, but the public data is extremely limited in Romania.

A collaboration with companies in charge of these networks, that also possess the data considered restricted, is however achievable, giving also the requirements of the Seveso Directive.

3.1.3 Other Significant Data

As presented in the framework, it is not only necessary to know, for example, if a bridge is affected and that the risk of losing it reflects only in reconstruction costs. If the functionality of the road network is greatly affected by the loss of that bridge, than the losses are far bigger. In order to assess the indirect impact of the damage, most methodologies in transportation networks require origin-destination (O-D) pairs over the network's segments (or traffic flow definition). Right after an earthquake, one of the basic O-D pair formed is between emergency intervention teams and affected areas. Later on, implications in terms of disrupted businesses, delay times, additional costs generated (by detours or more traffic) etc. can be evaluated.

In Romania is hard to anticipate what the affected areas (destinations for the road networks) will be, since right from the beginning, intermediate-depth earthquakes in Vrancea have the tendency of producing wide-spread damage with inconstant directivity (Cioflan 2006); the 1940 earthquake produced more damage in Moldova whether the 1977 earthquake produced more damage in Bucharest and Muntenia. In the recent years, at NIEP it was implemented a near real-time system for Estimating the Seismic Damage in Romania (SEISDaRo). Its results could be used (and were used, in Toma-Danila 2013) as data for different risk scenarios for transportation networks. Also, the Bucharest General Municipality (and other cities) keeps a list of buildings (Bucharest General Municipality 2015) enrolled in different seismic risk classes (I for the most endangered). These buildings were used in the case study of this paper.

Other data that is significant for the proposed framework and can be partially available for Romania is data referring to hospitals, fire stations, Emergency Units or shelters in case of disasters. Socio-economic aspects (commuters, businesses, supply demands etc.) and their links with transportation networks is also desirable, but not easy to find.

3.2 Bucharest Case Study

The risks in an area with collapsed buildings increases significantly, if the place becomes inaccessible. The recent Nepal earthquake (2015) showed exactly this aspect. Beside casualties, earthquakes can easily cause fires (mainly due to gas

leaks). In this demonstrative case study we evaluated for basic scenarios the times for intervention in a possibly affected Bucharest. We applied parts of the conceptual framework defined in this paper to datasets from sources specified above, to evaluate the risk of delays for emergency intervention forces (fire fighters and ambulances) in Bucharest. We considered a Vrancea earthquake with $M_w > 7.4$ that had as effect the collapse of all buildings evaluated by experts as being in the seismic risk class I, and multiple failure situations for road segments, based on traffic values and debris caused by expected to collapse buildings (modelled as 500 m. buffers; if height or volume information for this buildings would be available, specific methods for debris calculation could be employed, such as the ones from RISK Iran or Risk-UE Projects).

The analysis is performed mainly in ArcGis with the aid of the Network Analyst Module, for a complete network of Bucharest's streets, taken from OpenStreetMap and refined based on the attributes specified in Sect. 3.1.2. The analysis procedures consist of applying route, service area and O-D cost matrix procedures. As origin points we used the emergency hospital locations (excluding children hospitals and distinguishing between them based on the Health Ministry's classification) and also fire stations. Since this case study is a proof of concept and we had no data regarding the capacity of each hospital/fire station and also the demand of intervention, we used only indicators reflecting unique/primarily intervention times. In a seismic context it would be of great interest to see what happens in a supersaturated system (that is also influenced and influences the behaviour of transportation networks).

The traffic conditions considered were no traffic and Monday morning traffic (when the city is very crowded). The travel times consider the speed of an ambulance or fire truck with acoustic signals (therefore with priority in traffic and no waiting times at traffic lights).

Figure 5a shows that in no (or very light) traffic conditions, each building should be quickly accessible by ambulances. Also, in Monday morning traffic (Fig. 5b) the times would generally be smaller than 5 min. But if damaged buildings would block the adjacent roads, intervention times for the city centre would exceed 8 min (Fig. 5c). And this times double if victims are to be returned to the closest hospital. In case of a major earthquake, the priority destinations for victims are the top hospitals; we considered the accessibility to these hospitals only, and Fig. 5d shows that in Monday morning traffic conditions and no blocked roads, there are minimum intervention times up to 8 min (to destination). Figure 5 also shows the closest hospitals to buildings, based on travel times.

In Fig. 6a we represented the intervention times for fire trucks, in Monday morning traffic. As it can be seen, the maximum time is of 10 min, mostly for all Bucharest, due to the good spatial distribution of fire stations. Figures 5 and 6 could be combined in a model based on weigh overlay in order to express the risk for each building to be accessed by intervention forces. In this paper we chose not to create

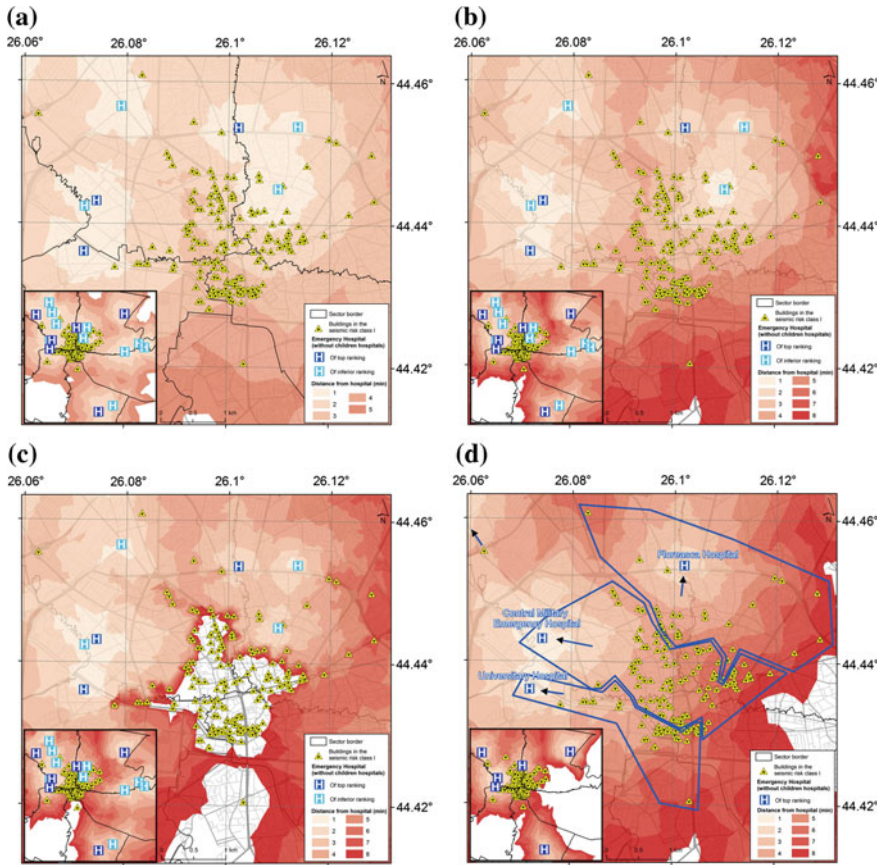


Fig. 5 Intervention time zones for ambulances from hospitals to possibly affected buildings (in seismic risk class I), for different scenarios: **a** no traffic, **b** morning traffic, **c** morning traffic and blocked streets due to buildings collapse (100 m buffer around buildings) and **d** morning traffic, but only top ranked emergency hospitals (according to the Health Ministry classification), showing also the quickest to reach hospitals to buildings with high seismic risk

such a model due to the few scenarios considered. We believe that Monte-Carlo simulations could greatly help in testing the significance of specific road segments in the process of satisfying the traffic demands imposed on it.

Figure 6b answers the question: how affected are the routes that cross the city (N-S) if buildings in the city centre collapse (and block the streets)? As it can be seen, there are plenty of alternatives and the additional time required is not so considerable (as it would probably be in case of non-urban locations).

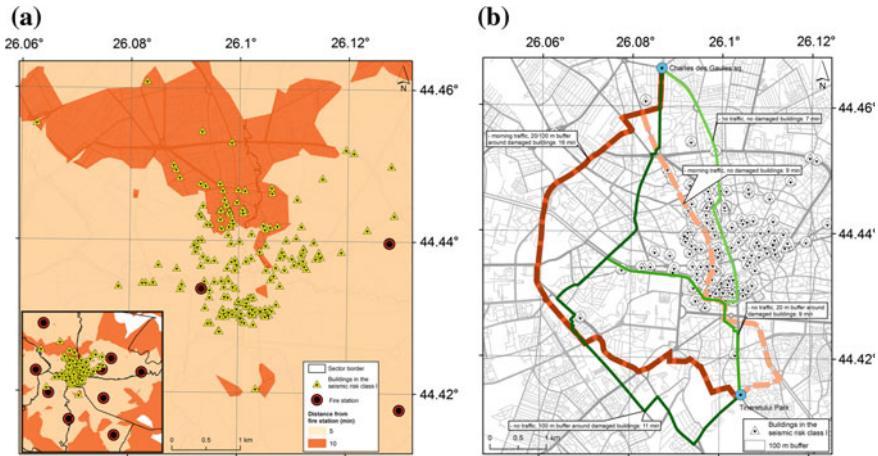


Fig. 6 a 5 and 10 min intervention zones for fire-fighters, considering the fire stations in Bucharest and the morning traffic; it is considered that each station has at least one fire truck, and no other aspects regarding the firefighting capacities are considered; **b** Fastest routes between northern and southern Bucharest for emergency intervention vehicles, considering various scenarios: no traffic or morning traffic, collapsed/not collapsed buildings in seismic risk class I, determining street blockage (computed through 20 and 100 m buffers). Routes show that there are reliable alternatives of crossing the city, with few time differences

4 Conclusions

In this paper we proposed a conceptual framework that allows the analysis of the seismic risk of transportation networks, considering inter/intra dependencies between components and the direct and indirect effects of seismic events. Our goal was to make this framework adaptable to different datasets, more or less complex (as in the case of Romania). GIS proves to be the binder of apparently heterogenic data related to hazard and vulnerability aspects, in an environment that respects the spatio-temporal dimension of the analysis. The framework shows how multiple disciplines can contribute to the characterisation of network risk.

Although without a significant background in Romania, the topic of the paper, as we demonstrated, can be nowadays tackled; by using public information (mostly available for road networks) or other data sources from national authorities, the risks of transportation networks can be quantified (currently in a simplified manner). The availability of useful seismic hazard data for Romania is an important aspect. This study is a first step in trying to understand what the seismic losses in Romania could be, due to network failure and effects.

The case study for Bucharest demonstrates the applicability of the framework to Romania. In case of high traffic and collapse of many buildings in the city centre during a major Vrancea earthquake, it would take more than double to transport injured people to the nearest hospital than normal. The number of trips required

would be considerable, raising the question if hospitals near the city centre can deal with a great amount of casualties. Results also showed that there are good alternatives for detour routes. Although promising, due to the basic inputs of the analysis, results must be treated with care: no post-earthquake traffic, no description of intervention capacities or no assessment of seismic road damage (only empirically, through debris) were considered. We are aware of the limitations, but future studies will add significance to the model. The framework could be of great interest when applied to broader areas (county level), where distance problems, direct and indirect seismic effects and blockage implications like detours are more significant for the analysis of transportation network risks.

Acknowledgements We would like to acknowledge the contribution of the doctoral scholarship from Faculty of Geography, University of Bucharest of the main author, and also the RO-Risk POCA Project.

References

- Anbazhagan P, Srinivas S, Chandran D (2012) Classification of road damage due to earthquakes. *Nat Hazards* 60:425–460
- Ardeleanu LA (2010) Estimări ale hazardului seismic probabilist pentru teritoriul, României edn. Tehnopress, Iași
- Asakura Y, Kashiwadani M (1991) Road network reliability caused by daily fluctuation of traffic flow. In: Proceedings of the 19th PTRC summer annual meeting, University of Sussex, United Kingdom
- Bucharest General Municipality (2015) List of buildings technically expertise, classified into seismic risk classes. Available from: www.pmb.ro/servicii/alte_informatii/lista_imobilelor_exp/docs/Lista_imobilelor_expertizate.pdf. Accessed 30 July 2015
- Chen A, Yang H, Lo HK, Tang WH (1999) A capacity related reliability for transportation networks. *J Adv Trans* 33(2):183–200
- Cioflan CO (2006) Efecte seismice locale. Ed. Universității “Alexandru Ioan Cuza”, Iași
- Ciutea D, Atanasiu GM (2014) Defining seismic resilience within the context of north-eastern region of Romania. *Bull Polytech Inst Iasi—Cons & A, Tome LX(LXIV)* 1:53–62
- Coburn A, Spence E (2002) Earthquake protection. Wiley, Hoboken
- Du ZP, Nicholson A (1997) Degradable transportation systems: sensitivity and reliability analysis. *Transp Res Part B* 31(3):225–237
- Initiative Media (2015) Media FactBook Romania 2015. Available from www.mediafactbook.ro. Accessed 30 July 2015
- Jansuwan S (2013) A quantitative framework for assessing vulnerability and redundancy of freight transportation networks. All Graduate Theses and Dissertations. Paper 2026
- Kaynia AM, Mayoral JM, Johansson J, Argyroudis S, Pitilakis K, Anastasiadis A (2011) Fragility functions for roadway system elements. SYNER-G Project Deliverable 3:7
- Leduc G (2008) Road traffic data: collection methods and applications. Working Papers on Energy, Transport and Climate Change Nr. 1, JRC 47967
- Marmureanu G, Cioflan CO, Marmureanu A (2010) Researches on local seismic hazard (Microzonation) for metropolitan bucharest area. Tehnopress, Bucharest
- Mantyniemi P, Marza VI, Kijko A, Retief P (2003) A new probabilistic seismic hazard analysis for the Vrancea (Romania) seismogenic zone. *Nat Hazards* 29:371–385

- Miller M, Cortes S, Ory D, Baker JW (2015) Estimating impacts of catastrophic network damage from earthquakes using an activity-based travel model. Transportation research board 94th annual meeting compendium of papers, Washington, DC, Paper 15-2366
- Musson RMW (2000) Generalised seismic hazard maps for the Pannonian Basin using probabilistic methods. *Pure Appl Geophys* 157:147–169
- Pinto PE, Cavalieri F, Franchin P, Lupoi A (2011) Definition of system components and the formulation of system functions to evaluate the performance of transportation infrastructures. SYNER-G Project Deliverable 2:6
- Porter K (2015) A beginner's guide to fragility, vulnerability, and risk. University of Colorado Boulder and SPA Risk LLC, Denver, CO
- Racanel IR (2015) Dynamic response of a special bridge in Romania using different types of seismic isolators. In: Proceedings of the 15th international multidisciplinary scientific geoconference SGEM 2015, Book 1(3):807–814
- Sartori M (2012) Seismic protection of the Basarab Overpass in Bucharest. In: Proceedings of the 15th world conference on earthquake engineering (15WCEE), 24–28 Sept 2012, Lisbon
- Shinozuka M, Murachi Y, Dong X, Zhou Y, Orlikowski M (2003) Seismic performance of highway transportation networks. In: Proceedings of China-US Workshop on protection of urban infrastructure and public buildings against earthquakes and man-made disasters, Beijing, China
- Sokolov V, Bonjer KP, Wenzel F, Grecu B, Radulian M (2008) Ground-motion prediction equations for the intermediate depth Vrancea (Romania) earthquakes. *Bull Earthq Eng* 6 (3):367–388
- Toma-Danila D (2013) Transport network vulnerability assessment methodology, based on the cost-distance method and GIS integration. *Intelligent systems for crisis management*. Springer, Berlin, pp 199–213R
- Vacareanu M, Radulian M, Iancovici F Pavel, Neagu C (2015) Fore-arc and back-arc ground motion prediction model for Vrancea intermediate depth seismic source. *J Earthq Eng* 19 (3):535–562
- Werner SD, Taylor CE, Cho S, Lavoie J-P, Huyck C, Eitzel C, Chung H, Eguchi RT (2006) REDARS 2: methodology and software for seismic risk analysis of highway systems MCEER-06-SP08

Appendix A

Members of Scientific and Organizing Committees

Scientific committee	Organizing committee
Alexandru Aldea	Cristian Arion
Luminița Ardeleanu	Dan Bîtcă
Dragoș Badea	Veronica Colibă
Ștefan Florin Bălan	Angela Constantin
Andrei Bălă	Ionuț Crăciun
Virgil Breabăn	Bogdan Grecu
Mihai Budescu	Mihail Iancovici
Sorin Demetriu	Helmuth Kober
Dan Dubină	Elena Florinela Manea
Emil Sever Georgescu	Ancuța Neagu
Paul Ioan	Cristian Neagu
Constantin Ionescu	Vasile Opreșoreanu
Dan Lungu	Andrei Papurcu
Dragoș Marcu	Raluca Partheniu
Mircea Mironescu	Daniel Paulescu
Mircea Petrina	Florin Pavel
Mircea Radulian	Viorel Popa
Horea Sandi	
Radu Văcăreanu	
Ion Vlad	

Appendix B

Program of the *National Symposium* *75 Years from November 10th 1940* *Vrancea Earthquake*

Tuesday November 10, 2015		
8:00–9:00	Registration of participants	Hall I.2, FCCIA/UTCB
9:00–9:15	Opening ceremony	Hall I.2, FCCIA/UTCB
9:15–10:45	<i>Parallel Session 1—Seismicity of Romania. Seismic hazard assessment; local soil conditions effects</i> Chairpersons: M. Popa & A. Aldea	Hall I.1, FCCIA/UTCB
9:15–9:30	Use of crustal local events to map the Vp/Vs ratios variations for the Romanian territory <i>D. Stoicescu, L. Manea, F. Borleanu</i>	
9:30–9:45	Earthquake precursors assessment in Vrancea region through satellite and in-situ monitoring data <i>M. Zoran, D. Savastru, D. Mateciuc</i>	
9:45–10:00	Earthquake precursory signature of Radon (Rn ²²²) <i>M. Zoran</i>	
10:00–10:15	Reconsideration of records obtained on instrumented buildings as an additional source of information on the 1986 and 1990 Vrancea earthquakes <i>I.G. Craifaleanu, I.S. Borcia</i>	
10:15–10:30	Historical Romanian earthquakes research—macroseismic and instrumental methods <i>E. Oros, D. N. Paulescu, M. Rogozea</i>	
10:30–10:45	Comparative analysis of Vrancea major earthquakes in instrumental and historical times <i>M. Rogozea, M. Radulian, M. Popa, D. N. Paulescu, E. Oros, C. Neagoe</i>	
9:15–10:45	<i>Parallel Session 2—Effects and lessons from November 10th, 1940 Vrancea earthquake</i> Chairpersons: D. Lungu & C. Ionescu	Hall I.2, FCCIA/UTCB
9:15–9:30	Main characteristics of November 10, 1940 strong Vrancea earthquake in seismological and physics of earthquake terms <i>G. Marmureanu, C.O. Cioflan, A. Marmureanu, E. Manea</i>	
9:30–9:45	Macroseismic effect of the November 10, 1940 earthquake in the territory of Moldova, Ukraine and Russia <i>N. Stepanenco, V. Cardanef</i>	

(continued)

(continued)

Tuesday November 10, 2015		
9:45–10:00	Before and after November 10th 1940 <i>I. Calotescu, C. Neagu, D. Lungu</i>	
10:00–10:15	10 November 1940 the first moment of truth for modern constructions in Romania <i>R. Petrovici</i>	
10:15–10:30	Causes and effects of the November 10, 1940 earthquake <i>I. Vlad</i>	
10:45–11:15	Coffee break	Room PIB, FCCIA/UTCB
11:15–12:45	Parallel Session 3—Seismic evaluation and rehabilitation. Seismic risk assessment Chairpersons: G. Marmureanu & M. Mironescu	Hall I.1, FCCIA/UTCB
11:15–11:30	Estimation of damage-loss from scenario earthquake analogous to November 10, 1040 in Republic of Moldova <i>V. Alcaz, E. Isicico, V. Ghinsari, S. Troian</i>	
11:30–11:45	Seismic loss estimates for scenarios of the 1940 Vrancea earthquake <i>D. Toma-Danila, C.O. Cioflan, E. Manea</i>	
11:45–12:00	Conceptual framework for the seismic risk evaluation of transportation networks in Romania <i>D. Toma-Danila, I. Armas, C.O. Cioflan</i>	
12:00–12:15	Some remarks regarding seismic vulnerability for orthodox churches <i>M. Budescu, L. Soveja, I. Olteanu</i>	
12:15–12:30	Seismic assessment and rehabilitation of existing constructions after the 10th November 1940 and 4th March 1977 earthquakes in Romania <i>M. Mironescu, A.M. Stanescu, T. Brotea, R. Comanescu, D. Purdea, M. V. Stanescu</i>	
12:30–12:45	Rapid Earthquake Early Warning (REWS) in Romania: Application in real time for governmental authority and critical infrastructures <i>C. Ionescu, A. Marmureanu, G. Marmureanu</i>	
11:15–12:45	Parallel Session 4—Effects and lessons from November 10th, 1940 Vrancea earthquake Chairpersons: S. Demetriu & E.S. Georgescu	Hall I.2, FCCIA/UTCB
11:15–11:30	Buildings behavior during the November 10, 1940, Romanian earthquake <i>S.F. Balan, B.F. Apostol</i>	
11:30–11:45	The strong Romanian earthquakes of 10.11.1940 and 4.03.1977 Lessons learned and forgotten? <i>A. Bălă, D.Toma-Dănilă</i>	
11:45–12:00	The great European 1940 Vrancea earthquake. A bibliographical contribution <i>A. Aldea, R. Enache, C. Neagu</i>	
12:00–12:15	Macroseismic effects and parameters of the strong Vrancea subcrustal earthquake occurred on November 10, 1940 <i>A. P. Constantin, I. A. Moldovan, A. Pantea</i>	
12:15–12:30	The collapse of Carlton building in Bucharest at November 10, 1940 earthquake: an analysis based on recovered images <i>E.S. Georgescu</i>	

(continued)

(continued)

Tuesday November 10, 2015		
12:45–14:00	Lunch break	Room P1B, FCCIA/UTCB
14:00–15:30	Parallel Session 5—Structural design in seismic areas; performance based design Chairpersons: P. Ioan & V. Popa	Hall I.1, FCCIA/UTCB
14:00–14:15	Influence of masonry infill walls on the seismic behaviour of reinforced concrete frame structures <i>M. Bârnaure, A.M. Ghiță, D. Stoica</i>	
14:15–14:30	Undirectional cyclic behavior of old masonry walls in Romania <i>E. Lozinca, V. Popa, D. Cotofana, A.B. Chesca</i>	
14:30–14:45	Considerations for simplifying the capacity design procedure on reinforced concrete frame structures <i>A. Faur, A. Puskas</i>	
14:45–15:00	Modern concrete buildings in Romania: structural design of Bucharest One tower <i>D. Cotofana, M. Dragomir, S. Dima, C. Ursu, V. Oprisoreanu, V. Popa</i>	
15:00–15:15	Seismic resistant eccentrically bracing configurations <i>M. Stoian, H. Köber</i>	
15:15–15:30	Bracing systems in seismic zones <i>H. Köber, B.C. Ștefănescu</i>	
14:00–15:30	Session 6—Seismicity of Romania. Seismic hazard assessment; local soil conditions effects Chairpersons: M. Radulian & R. Vacareanu	Hall I.2, FCCIA/UTCB
14:00–14:15	Strong ground motion spatial patterns generated by the intermediate-depth earthquakes of Vrancea region <i>L. Ardeleanu, B. Grecu, B. Zaharia, C. Neagoe</i>	
14:15–14:30	Discrimination of tectonic and artificial low-magnitude events in the NE part of Romania <i>F. Borleanu, B. Grecu, M. Popa, M. Radulian</i>	
14:30–14:45	Neodeterministic seismic hazard approach applied in Romania and Bulgaria <i>M. Radulian, C.O. Cioflan, M. Kouteva-Guentcheva, A. Magrin, F. Vaccari, G.F. Panza</i>	
14:45–15:00	The 2013 earthquake swarm in the Galati area: seismotectonic interpretation <i>M. Popa, E. Oros, C. Dinu, M. Radulian, F. Borleanu, M. Rogozea, V. Diaconescu, C. Neagoe</i>	
15:00–15:15	Evaluation of seismic hazards on base of probabilistic models of Vrancea zones <i>R. Burtiev</i>	
15:15–15:30	Site-dependent seismic hazard assessment for Bucharest based on stochastic simulations <i>F. Pavel, D. Ciuiu, R. Vacareanu</i>	
15:30–16:00	Coffee break	Room P1B, FCCIA/UTCB

(continued)

(continued)

Tuesday November 10, 2015		
16:00–17:30	Parallel Session 7—Seismic evaluation and rehabilitation. Seismic risk assessment and Structural design in seismic areas; performance based design Chairpersons: R. Petrovici & D. Marcu	Hall I.1, FCCIA/UTCB
16:00–16:15	Analytical seismic fragility functions for dual RC structures in Bucharest <i>R. Vacareanu, F. Pavel, P. Olteanu, V. Coliba, D. Ciuiu</i>	
16:15–16:30	National Museum of Romanian History—seismic evaluation and ambient vibration testing <i>P. Ioan, S. Demetriu, A. Aldea, C. Neagu, C. Robea</i>	
16:30–16:45	Viscous damper distribution using genetic algorithms and pattern search optimization <i>A. Pricopie, A. Costache</i>	
16:45–17:00	A time-domain approach for the performance-based analysis of tall buildings in Bucharest <i>M. Iancovici, G. Vezeanu</i>	
17:00–17:15	Selecting and scaling strong ground motion records based on conditional mean spectra. Case study for Iasi City in Romania <i>R. Vacareanu, M. Iancovici, F. Pavel</i>	
17:15–17:30	Aspects on the performance of buildings with soft and weak storeys <i>D. Stoica</i>	
16:00–17:30	Parallel Session 8—Seismicity of Romania. Seismic hazard assessment; local soil conditions effects Chairpersons: C.O. Cioflan & B. Grecu	Hall I.2, FCCIA/UTCB
16:00–16:15	Source scaling properties for the Vrancea subcrustal earthquakes: an overview <i>M. Radulian, E. Popescu, A.O. Placinta</i>	
16:15–16:30	Spectral displacement demands for strong ground motions recorded in Vrancea intermediate-depth earthquakes <i>I.V. Crăciun, F. Pavel, R. Vacareanu</i>	
16:30–16:45	Seismic activity of Romania and focal mechanisms analysis for Vrancea zone (2010–2015) <i>A. Craiu, M. Diaconescu, M. Craiu, A. Marmureanu, C. Ionescu</i>	
16:45–17:00	Application of engineering tools as guidelines for estimating near-surface seismic effects <i>E. Calarasu, C. Arion, C. Neagu</i>	
17:00–17:15	Some comments on the macroseismic intensity with respect to the Vrancea earthquakes impact in Bulgaria <i>M. Kouteva-Guentcheva, Kr. Boshnakov</i>	
17:30–18:00	Closing Ceremony	Hall I.2, FCCIA/UTCB

Locations FCCIA Building/UTCB, Bd. Lacul Tei nr. 124, Sector 2, Bucharest, Romania
Hall I.1 and Hall I.2 are located at 1st floor; Room PIB is located at ground floor

Appendix C

Testimonies on the Aftermath of November 10th 1940 Vrancea Earthquake in the Putna County

This Appendix represents a summary translation performed by Ph.D. student Ionut Craciun of two publications, The Vrancea Chronicle (“Cronica Vrancei”), Volume 3/2002 and The Vrancea Chronicle (“Cronica Vrancei”), Volume 10/2011, courtesy of The Vrancea Museum (“Muzeul Vrancei”). It is mentioned that Putna County is called nowadays Vrancea County. The information on Vrancea intermediate-depth seismic source and of seismological features of November 10, 1940 earthquake are presented unaltered, as reported 75 years ago. The reader shall differentiate, in the following, between facts (permanently valid) and opinions (subjected to changes according to the advances in knowledge and understanding). The translation of selected excerpts from Vrancea Chronicles is presented hereinafter.

“In the Vrancea Mountains there is one of the most interesting and characteristic seismic points. Here, there is an outbreak of deep and very powerful earthquakes, which in the area of maximum intensity, have greater power in different stray points. Over time, in the Vrancea Mountains occurred numerous earthquakes that had common features, such as wide coverage with maximum intensity or irregularities in the intensity distribution.

Due to its location on the oldest and most significant fault from southern Moldavia, the so called Zăbala fault that starts from Năruja, goes through Focșani, Nămoloașă, Galați, Tulcea and ends in Snake Island and the mobile subsoil consisted of gravels carried by Siret, Putna, Șușița and Milcov rivers, Focșani and its surroundings enjoy the sad reputation of forming this area’s strongest epicentral region.

The November 1st 1940 earthquake, that originated in the Vrancea Mountains, was felt beyond Moscow and Leningrad, in Caucasia, Asia Minor and south-western Bulgaria. In Romania, this earthquake measured different levels on the intensity scale: X in Petrești and Panciu, IX in Bucharest, VIII in Brașov, during which multiple phenomena (such as sparks, globes or light strips) were noticed. In 87 % of the cases, the light manifestations occurred in totally opposite directions to the epicenter (Alexandrescu 1942).

On November 13th 1940, “Timpul” newspaper mentioned the following: *“the catastrophic earthquake on Sunday night is the most powerful in our country for over a century. On the night between November 9th and 10th, at 3:39:36, an*

earthquake of 9 degrees on the intensity scale was felt at the Astronomical Observatory in Bucharest. Most likely, the epicenter is in the Vrancea Mountains. After other observations, the oscillations lasted 45 s and the recordings over an hour” („Timpul”, November 13th 1940, 1).

In the Minister Council meeting of November 16th 1940, the Minister of Internal Affairs, Constantin Petrovicescu presented a preliminary situation of the disaster produced by the earthquake: *“The earthquake was serious in four centers: Bucharest, Prahova Valley, Galați and Focșani. The second area, with less severe effects included: Turnu-Măgurele, Câmpulung, Târgoviște, Mizil, Râmnicu-Sărat, Tecuci, Bârlad, Iași, Brăila. The earthquake manifested with even smaller intensity in: Roman, Piatra Neamț, Bacău, Brașov, Pitești, Craiova, Giurgiu, Ilfov County, Tulcea and Constanța. The rest of the country did not suffer (almost) at all. Until the night of November 10th 1940 the following casualties have been registered: 267 deaths and 476 people injured.” („Timpul”, November 19th 1940, 1).*

The earthquake destroyed a quarter of the Focșani’s buildings, severely damaged another quarter and slightly affected other 25 %. It damaged both the primary and the secondary schools, the courses being suspended. Public institutions were severely damaged, especially the Town Hall. Most churches are destroyed, the rest being seriously damaged. On November 16th, local authorities wrote a statement concerning town’s worship places situation. At that time, there were still five churches with immediate occupancy, 14 that needed retrofitting and five churches were destroyed or seriously damaged, needing to be demolished. In the same situation there were five Jewish temples.

The press dedicated entire pages to the November 10th 1940 earthquake. In the “Timpul” newspaper the shattering testimonies of a Focșani resident were reported: *“From the first shaking, the population broke through the streets with summary outfits. Many, however, were inside buildings when the earthquake reached maximum intensity. Because of that the number of victims is very high. The entire city looks like a mine. The Aro Cinema and dozens of big buildings collapsed in a disturbing noise, trapping under rubble people who were unable to get out in time. The main street is completely destroyed. The buildings that are still standing couldn’t resist another earthquake. In order to help, the Bacău prefect came this afternoon, with six cars of medics and drugs. There were also 1500 kg of flour to be given to the victims. Also from Bacău, help came for the cities of Panciu and Mărășești, where the earthquake was of extreme violence, destroying numerous buildings in Mărășești and almost the entire city of Panciu.” („Timpul”, November 13th 1940, 4). „The population awakened by the shaking, the noise of the buildings that were collapsing and by the screams of the victims trapped under rubble, run frantically through the streets. No building was spared. Immediately, the authorities took the necessary measures. (...) The damages in Focșani are countless.” („Timpul”, November 13th 1940, 4).*

In the “Evenimentul” journal it is said that the city of Focșani *“especially the town’s center gives you the impression of a ruined and deserted city. The outskirts were slightly damaged, many of the buildings staying intact. Buildings on entire streets in the town’s center were destroyed. 70% of homes are unusable. Almost all*

public buildings cannot function properly. The losses are countless. The earthquake was felt much stronger in the city of Panciu. Concerning the other nearby towns, the situation is as follows: Odobești and Adjud had slight damages, and at Mărășești there is almost no damage.” („Evenimentul”, November 12th 1940, 3). Examples of collapsed buildings are shown in Figs. C.1, C.2 and C.3.

On November 13th 1940 Focșani city town hall informed the Ministry of Internal Affairs that the city suffered countless damages “50% of houses are completely destroyed and some are damaged so that any repair is impossible. Only



Fig. C.1 Collapsed house in Focșani, looking from east (Mândrescu 2008)



Fig. C.2 Fallen brick gable wall completely destroyed a next door smaller house in Focșani (Mândrescu 2008)



Fig. C.3 Completely destroyed house in Focșani (on I.G. Duca Street) (Mândrescu 2008)

25% of city buildings are still standing. All primary and secondary schools are severely damaged, all the courses being stopped. All public buildings are severely damaged.” (VNA, file no. 119/1940, f. 46).

Following the chaos caused by the earthquake, the police restricted the traffic through the city, traffic being allowed only on some streets: Carol Boulevard, Cuza-Vodă Street, Mărășești Barrier, Ghergheasa Street and Cotești Barrier. Car access to the railway station was made only through Nicolae Iorga and I.G. Ciurea streets. The drivers were not allowed to exceed 6 km/h. (VNA, file no. 119/1940, f. 40).

Material damage and casualties recorded in urban areas were summarized in a report made by the Focșani Police (Table C.1), at the request of the Galați Police Inspectorate:

Table C.1 Material damage and casualties in urban areas

City	Death toll	Number of injured	Number of destroyed and damaged houses	Damage assessment (lei)
Focșani	22	21	627	110,297.000
Adjud	–	–	18	1,365.000
Mărășești	–	–	51	3,509.000
Panciu	31	141	338	27,801.000
Odobești	–	4	38	7,545.000
Total	53	166	1,072	150,517.000

It is also mentioned that from the well-constructed buildings 10 % were severely damaged, 25 % were partially destroyed, 60 % had minor damages and 5 % were left untouched. Considering old buildings, 45 % were severely damaged, 35 % were partially destroyed and 20 % were left untouched (VNA, file no. 120/1940, f. 152).

On November 11th, local authorities began the reconstruction campaign by submitting to the Ministry of Internal Affairs a list urgently requesting the following: 10,000,000 lei, an Architects' Committee for a new city plan, a team of bricklayers, carpenters, tinsmiths and stove makers, construction materials such as timber, lime and cement. As a consequence, an Architects Committee attached to the Putna County Prefecture was founded. The committee consisted of a delegation sent from Bucharest, their mission being establishing the damage suffered by the town's institutions, places of worship, schools, private homes and to decide the necessary measures.

Also on November 11th, a Support Committee was established, where people affected by the earthquake could register their name, residence and suffered damage. The committee would analyze each request and determine if support is needed. While it functioned, the committee helped 264 people by giving them a financial aid of 600,000 lei.

On November 19th, the Focșani garrison sent 100 soldiers who would, under the surveillance of the architects, start the demolition process.

As immediate measures, through the Order given on November 11th, Focșani's Town Hall informs the public that all water pipes have been broken and that, to prevent a possible epidemic, all water must be boiled before use. Public roads lighting will be functional immediately, movement of pedestrians will be made only in the middle of streets and all schools remain closed (VNA, file no. 119/1940, f. 116–118).

Following the Order no. 19142 given by the Ministry of Internal Affairs, the requisitions of all houses and apartments found in good condition was imposed, which was brought to the knowledge of residents through the December 15th 1940 Notification. By this requisitions, it was found that a number of 98 homes can be occupied by the residents (VNA, file no. 120/1940, f. 147).

From the reports made by the architects in the second part of November emerge the following: Town Hall's first floor is in good condition, with its interior walls cracked. The second floor must be evacuated and eventually demolished. The façade walls bent, almost falling (VNA, file no. 121/1940, f. 25).

In the first apartment house of Focșani's Police Office, the second floor was evacuated, while the first floor is still usable. The second building is in acceptable condition. The desks have been moved. (VNA, file no. 121/1940, f. 52).

The city's prison was severely damaged, being unable to host the convicts. Many parts of the building ensemble must be demolished (VNA, file no. 121/1940, f. 318).

The Fire Department building and the Power Plant are completely damaged and require demolition. The theatre's activity is suspended until the minor damages are solved. The Gendarmerie, the Non-Commissioned Officers School and the Forestry Inspectorate are all partially evacuated. The Popular Athenaeum, the Focșani District Court and the Chamber of Commerce are slightly affected.

On November 18th the report issued by the Architects Committee included the following: the Putna County District Court's activity will be resumed after retrofitting the exterior walls and after checking the central dome.

The most affected bank is the Popular Bank “Unirea”, while the National Bank’s Focșani branch is in good condition and can function normally.

The places of worship situation is very serious. In these difficult times, the town’s population only has five churches that can officiate services. Out of the 14 churches that needed retrofitting, the most affected is the “Domnească” Church from the “Moldovia” Square, where the tower bell and the masonry walls were on the brink of falling, which led to prohibiting pedestrian traffic in the area.

All schools in Focșani were seriously damaged and unfit to continue classes. For repairs, the city needed about 300,000 lei, in order to purchase building materials and to pay workers (VNA, file no. 9/1940, f. 9). In the county, the school situation was as following: 42 schools were completely destroyed, 68 were partially damaged and 70 needed slight repairs (VNA, file no. 9/1940, f. 339). The Architects Committee reports are relevant in this respect.

The Focșani Girls High School needed general retrofitting for the old building and minor repairs for the new one. The Commercial Boys School has its stairs compromised, the roof completely damaged and the ceiling destroyed by fallen chimneys. The only usable classrooms are those with reinforced concrete slabs. At the “Unirea” High school, the old building part is unusable.

The following primary schools are unusable and remain evacuated: the Boys Schools no. 1, 2, 3 and 4 and the Girls Schools no. 2, 3 and 4. No. 1 Girls School is the only one that resumed activity immediately after some minor repairs.

This is briefly the city’s picture in the days following the earthquake. The initiation and progress of the reconstruction campaign, despite the shortcomings and opposition of residents, proved that in difficult times the population and the local and central authorities can mobilize remarkably.

In these two months campaign that took place (it ended on December 21st), the city managed to endure the terrible event and gradually resumed activity. The two months did not mean erasing all the effects, the city keeping a memory of the disaster for a long time.

In the Putna County, the November 10th earthquake left its mark even on the farthest village. The city of Panciu, situated in the middle of the Panciu vineyard, was wiped out from the face of the earth, on the night between 9 and 10 November 1940 (Figs. C.4, C.5 and C.6). The tragedy is amplified by the number of dead and injured people, a number that kept on increasing from day to day.

“All that remains from the city of Panciu is a pile of rubble. In this small city situated in the most dangerous region, the earthquake reached catastrophic proportions. There were only a few houses left standing in the entire city. The number of deaths and injured people is very large.” („Timpul”, November 13th 1940, 1). The earthquake effects on the houses in Panciu can be seen in Figs. C.7, C.8 and C.9.

The report of the 68 Panciu Fortified Infantry Regiment on the situation in the same town, reiterate the idea on an apocalyptic scenario in Panciu: *“Most houses in Panciu collapsed, people are buried under rubble. The city’s appearance is poor because the entire population is now homeless, all clothing and personal things staying under rubble. We took immediate action so that the Panciu control*



Fig. C.4 The northern part of the Carol Street, before the earthquake (Mândrescu 2008)



Fig. C.5 The northern part of the Carol Street, after the earthquake (Mândrescu 2008)

company can restore order and security in the city. Up to 6 AM only a few dead and wounded civilians and only two soldiers have been removed from under the rubble. Because of the ruins that cover the entire city, the rescue operation is very difficult; this is why I brought several platoons from the sector battalions. Telephone and telegraph connections with other towns and battalions are prohibited.” (VNA, file no. 9/1940, f. 79).

In February 1941, traders and victims of Panciu, living now in Focșani, addressed Putna Prefecture the following text: *“all buildings in our city are destroyed, we are homeless, and our furniture and cargo is, in the vast majority, shattered. After the disaster, most of us provisionally established in the village and*



Fig. C.6 General view of the central part of the Carol Street (Mândrescu 2008)



Fig. C.7 Fallen debris on the sidewalk; houses completely damaged (Mândrescu 2008)

some of us have spread in different areas of the country.” (VNA, file no. 8/1941, f. 163). They were requesting authorities for permission to return to their town, to collect the remains of their destroyed houses, hoping to use them in the spring, when they hoped *“we can return to our homes, to rebuild and continue our lives, as we have so far.”* (VNA, file no. 8/1941, f. 163).

In Panciu, from the order of Marshall Ion Antonescu, a detachment of 240 forced workers was founded in order to participate in the rebuild of the earthquake destroyed city. The detachment was staying outside of the village, the food allowance per person being 53.50 lei/day (VNA, file no. 200/1943, f. 3).

Marshall Ion Antonescu issued another decision, Regional Service of Panciu Restoration having the obligation to set up a carpentry workshop, used for the



Fig. C.8 Total collapse of the houses in the central part of the town (Mândrescu 2008)



Fig. C.9 Masonry walls fallen towards north (Mândrescu 2008)

restoration of Panciu, Soveja and all other county areas affected by the earthquake (VNA, file no. 200/1943, f. 40).

A year after the disaster, Panciu city's mayor, Căpățână, a doctor of law and medicine, wrote a history of the city, including the November 10th 1940 moment: „[...] in the morning of November 10th 1940, at 3:40 PM, some horizontal shakings and one vertical made us feel that we had fallen, houses included, in a 10-12 m deep pit, shakings that ended in less than a minute (45 s) and that collapsed the entire city. A few minutes after the shaking we went out in the street. Pitch dark, no screams, no mourning. A horrible silence in full darkness, instead of screaming and

mourning, had paralyzed every one of us. Groans and cries for help started from all sides, followed by shouts and cries as a response. The search for relatives and friends had started. All you can hear is brief and scared questions. [...] All over the city you can't make a tea, coffee or soup, because not even the five houses that were left standing had a usable stove or oven. With dawn we realized the effects of the disaster. Walls and entire floors collapsed, sidewalks and streets filled with huge piles of rubble. [...] The searching ends during the night with 42 people dead and 76 injured.” (Căpățână 1941).

Two neighboring cities to Panciu, Crucea de Sus and Crucea de Jos, were also severely affected by the earthquake, especially concerning the schools and the worship places (Figs. C.10, C.11, C.12 and C.13).

In Mărășești, approximately 80 % of private buildings had cracked walls (VNA, file no. 9/1941, f. 3), the Romanian Railways neighborhood was completely uninhabitable and the railway station building showed severe damage (VNA, file no. 12/1940, f. 230). In Adjud there were no public buildings which had collapsed, but many of them needed small or radical rehabilitation works (Figs. C.14 and C.15) (VNA, file no. 12/1940, f. 6).

In the Putna County, besides the above mentioned cities, the most affected towns were Vidra, Mera, Năruja, Sascut, Nămoloasa, Suraia, Biliești, Ciușlea, Vulturu, Nereju, Reghiu, Câmpuri, Soveja, Tulnici, Nistorești, Diocheți, Mănăstioara, Paltin, Păncești and Vizantea (VNA, file no. 9/1940, f. 90). At the county level, 48 public buildings were proposed by the authorities to be demolished, 24 were in need of extensive repairs and 75 needed slight repairs. The funds for rebuilding the destroyed public buildings in the aforementioned areas amounted to 65,722 million lei with an extra 19,240 million lei representing the cost to repair the public damaged buildings in Focșani (VNA, file no. 9/1940, f. 336).



Fig. C.10 A small church in Crucea de Sus completely destroyed (Mândrescu 2008)



Fig. C.11 The Crucea de Sus steeple roof fallen towards north (Mândrescu 2008)



Fig. C.12 General view of the completely destroyed church in Crucea de Jos (Mândrescu 2008)

In the entire Putna County, teams of firefighters, policemen, soldiers and legionaries were sent in order to rescue the wounded, tearing down walls or freeing access points.

Foçşani Town Hall sent letters to municipalities in Buzău, Bucharest, Râmnicu-Vâlcea, Piatra Neamţ, Roman, with the request to ask the Social Securityes or the workforce placement centers that all available artisans (bricklayers, stove makers, carpenters, tinsmiths etc.) be directed to Foçşani (VNA, file no. 120/1940, f. 150). Following these requests, in the Putna construction sites worked people from different areas of the country, like Hunedoara, Caraş-Severin, Dolj etc. (VNA, file no. 120/1940, f. 224, 227).



Fig. C.13 Close up view of the completely destroyed church in Crucea de Jos (Mândrescu 2008)



Fig. C.14 View of Adjud Main Street: fallen brick gable of the Blănaru house (Mândrescu 2008)

Also, in the Focșani construction sites worked the Polytechnic School students, whose stay was extended by the Ministry of National Education to the entire month of December 1940 (VNA, file no. 120/1940, f. 120).

Since the morning of November 10th 1940, the Putna County Prefecture sent the telegram number 151 to the President of the Council of Ministers with preliminary information about the county's situation: *"Take all the necessary measures to help the residents. The Legionary Movement will report for duty at first hour. We have 45 deaths and 102 people seriously injured. The damages are countless. The city of Panciu is completely destroyed and the city of Focșani is 70% destroyed. Homes are unusable. Almost all public buildings have restricted access. The schools are closed until further notice."* (VNA, file no. 9/1940, f. 30).



Fig. C.15 City front side of the Adjud railway station—fallen brick gable (Mândrescu 2008)

On November 20th 1940, the Ministry of Internal Affairs informed the Putna County authorities that a detachment of 310 workers will be sent, in order to help with the rebuilding of damaged homes and public buildings.

On November 21st 1940, the Ministry of Internal Affairs informed the county's authorities that the General Direction of Romanian Railways already took all the necessary measures to restore the railways affected by the earthquake (VNA, file no. 9/1940, f. 111).

Following the ravages made by the November 10th 1940 earthquake in the cities of Focșani and Panciu, where hospitals were severely affected and where many people were wounded and others needed medical attention, the Labor, Health and Social Welfare Ministry approved the request of the medical team "Horia" to establish in Focșani a new hospital for dermatology. In this purpose, a property on Lascăr Catargiu Street, Number 12, was proposed for requisition (VNA, file no. 9/1940, f. 333).

Because the orphanage „Principesa Elisabeta” suffered major damage, authorities decided to requisite Ion Manea's property, to shelter orphans and the homeless (VNA, file no. 9/1940, f. 347–349).

At the county level, health institutions destroyed by the earthquake and which needed demolition include the Panciu Hospital, the 1st floor of the Focșani and Vidra Hospitals, the dispensaries in Bolotești, Păunești and Străoane and the Focșani nursing home. Other buildings that needed capital repairs include the Năruja, Câmpineasca, Mărășești, Adjud, Odobești hospitals (VNA, file no. 12/1940, f. 347).

The November 10th 1940 earthquake's rage did not forgive the cemeteries and hero monuments. Their situation and the amount of necessary repairs are presented in Table C.2 (VNA, file no. 13/1940, f. 180):

Table C.2 Repairs necessary for cemeteries and hero monuments

Name of cemetery or heroes monument	Damage	Repair cost (lei)
Honorary Cemetery “Sfânta Ana” Focșani	No damage	–
Focșani Mausoleum	No damage	–
Honorary Cemetery “Poiana lui Frunză”	Watchman’s home had small cracks on the joints between walls and the reinforced concrete floors. The entrance reinforced concrete trinity was demolished	30,000
Adjud Crypt	No damage	–
Soveja Mausoleum	Damaged base, fallen stone masonry, cracked brick masonry, fallen masonry chimneys and stoves, damaged stone masonry fence, broken windows	80,000
Sovega German Cemetery	Most of the stone masonry fence was demolished	3,000
Mărășești Mausoleum	Dome cracked, on a 15 m length; damaged plaster in the dome	75,000
Mărăști Mausoleum	No damage	–

Between November 1940 and January 1941, in the Romanian Railways stations in the Putna County, were sent 71 wagons of food and materials for the victims (sugar, flour, cement, potatoes, lime, timber, nails, wire, oat, corn etc.) (VNA, file no. 9/1941, f. 487).

On November 29th 1940 a committee formed by sub-prefect Octavian Vasiliade, Mayor Col. Dr. Constantin Faur, Eliza Luculescu, Red Cross Subsidiary Focșani President and Putna County Prefect’s Office delegates, distributed to the victims money from the 100,000 lei fund received from „Red Cross” Bucharest. The committee members decided that the help should be between 500 and 5,000 lei, depending on financial situation and damages suffered by every victim. In total, 45 people benefited from the “Red Cross” Bucharest help (VNA, file no. 8/1941, f. 28–29).

Panciu city’s Town Hall reserved, from its own budget, 100,000 lei to be distributed especially to people with deceased relatives or to very poor residents (VNA, file no. 8/1942, f. 435, 439).

After the November 10th 1940 moment, Putna County’s victims of the disaster were supported by the Committee of Helping the Victims of the Disaster with money, clothes, food, and building materials, according to the reports found in the National Archives Vrancea residents (VNA, file no. 8/1942, f. 462–472).

On December 1940 the “German Red Cross” donated for Putna County 5 hospitals, each having 10 rooms (VNA, file no. 8/1942, f. 123).

The earthquake harmed 93,816 people in the Putna County, total damage value being up to 176,082,000 lei. Concerning the economic losses, the Putna County Prefecture made a statistic (Table C.3) with the affected professional categories in different geographical regions (VNA, file no. 9/1940, f. 388):

Table C.3 Affected professional categories

Area	Farmers	Artisans	Industrialists	Merchants	Govt. employees	Self employed	Total	Loss (lei)
Focșani	68	186	62	180	94	37	627	110,297.000
Panciu	81	29	4	38	27	41	220	28,800.000
Adjud	7	5	1	2	–	–	15	1,360.000
Odobesti	10	–	–	6	3	–	19	3,200.000
Mărășești	15	10	–	5	5	–	35	1,000.000
Gârlele Region	12,000	500	1,000	1,000	250	250	15,000	6,500.000
Mărășești Region	17,000	1,000	500	700	200	600	20,000	7,800.000
Trotuș Region	18,140	500	300	600	160	300	20,000	5,600.000
Vrancea Region	10,000	150	300	100	150	200	10,900	3,175.000
Zăbala Region	8,000	300	2,000	200	200	300	11,000	4,350.000
Biliești Region	15,500	100	100	100	100	100	16,000	4,000.000

To restore public buildings, local authorities have organized public auctions, in order to designate entrepreneurs; examples of this are numerous: Popular Athenaeum restoration by Ilie Gulie, construction foreman from Craiova (VNA, file no. 135/1940, f. 11), Focșani Court restoration by construction foreman and brick builder Nicolae Dumitrescu (VNA, file no. 135/1940, f. 23), Focșani Town Hall restoration by entrepreneur Dumitru Vasiliu (VNA, file no. 118/1941, f. 23), the “Maior Gherghe Pastia” Monument by the entrepreneur Nicolae Colios (VNA, file no. 118/1942, f. 4, 8, 28, 41), the Primary School in Mărășești by foreman Rudolf Schoverschi (VNA, file no. 12/1940, f. 150) etc.

Following the calamity which bereaved the Putna County, on November 17th 1940 the Putna county was visited by King Michael I, who aided the surviving victims (Fig. C.16).

The powerful November 10th 1940 earthquake did not leave indifferent the rest of the European countries, which supported Romania through donations of money, food, building materials etc.

„[...] Germany helped Romania by donating two hundred thousands german marks (10 million lei), as a personal gift, for increasing fund support of the victims in drugs and materials. The Romanian Government expressed the gratitude of our nation for the gift that Germany has given us in order to help the victims and restore the country.” („Capitala”, November 24th 1940, 1).

The Bulgarian Minister in Bucharest, S.W. Petroff sent to Marshal Ion Antonescu a letter and a two million lei check, representing “*the contribution of the Royal Bulgarian Government to the aid fund of the victims of the recent earthquake.*” („Timpul”, December 16th 1940, 1).



Fig. C.16 Michael I, King of Romania, visiting Panciu after the earthquake of November 10th 1940 (Mândrescu 2008)

The Italian legation in Bucharest offered 100,000 lei. *“In these hard days for our country we had the satisfaction of sympathy manifestations that impressed us. Thus the President of the Minister Council received a letter from the Italian legation in Bucharest, by which it was made known that the officials contributed with 100,000 lei to the aid fund of the Romanians.”* (“Universul”, November 17th 1940, 6).

Another example is the humanitarian of 150,000 lei offered by The United States of America *“Mr. Franklin Mott Gunther, the Minister of the United States of America in Bucharest, sent 150,000 lei to the President of the Minister Council, asking for it to be spend on helping the victims.”* (VNA, file no. 200/1943, f. 85).

After the calamity of late autumn 1940, in the Putna County arrived specialists, in order to study the phenomenon.

Putna County’s prefecture has issued a permit to N.AI. Rădulescu, associative professor at the University of Bucharest, for him to travel *“in the Putna County to research the November 10th earthquake and to photograph the effects.”* (VNA, file no. 9/1940, f. 38).

On December 12th 1940 Putna authorities were informed by the Ministry of National Education that in the period 13–16 December Putna County will receive the visit of German professor and seismologist August Sieberg, accompanied by a nurse and three Romanian seismologists in order to prepare documentation relating to the earthquake (VNA, file no. 9/1940, f. 287).

To gather as much information as possible concerning the subject, on December 7th 1940, the vice director of the Astronomical Observatory in Bucharest, Gheorghe Demetrescu, sent questionnaires to Focșani City Hall, 100 being completed after the poll conducted among the population (VNA, file no. 119/1940, f. 151).

On April 2nd 1943, Marshall Ion Antonescu visited the Putna County, especially the areas affected by the 1940 earthquake, also visiting the village Soveja, destroyed by the 1943 fire.

Since the Marshall's visit and by the summer of 1943, the entire recovery activity in Panciu was synthesized in an Activity Statement made by Panciu Recovery Special Service, led by architect B. Ivanov, aided by architects C. Borcea and Pozzana, engineer Z. Iyszyk, accountant C. Petrescu, secretary V. Borcea, typist M. Mazăre, a driver and a janitor, all employees, plus six other supervisors, temporary employed for release work. The document stipulated that the new civic center market had been marked, on the ground, that the places where they were to build new public buildings once with the arrival of the forced labor detachment (which was equipped with all the work tools, purchased by the General Direction of Recovery) were fixed; on April 16th 1943 they started the collapse of damaged buildings on "Carol I", "Regele Ferdinand" streets and "Apostoleanu" boulevard, all materials were sorted and stored in stacks, by category, on the property of every family, all the debris being loaded into wagons. In the entire city, 1660 m of Decauville lines, with 38 wagons, have been mounted. As far as July 1943, the debris of 80 buildings in the center of Panciu have been removed, the remaining 30 buildings would have followed soon after. The detachment was concerned about cleaning the public garden, the restoration of the Town Hall, repairing wagons of the local authorities, the drainage of wetlands, carrying out repairs at the Vocational School for Girls, discharging parts received from Odessa for the Power Plant, demolishing the Public School "Crucea de Sus", the release of "Sf. Parascheva" Church, in order to make way for constructing a new, timber church, as well as organizing their training camp. In addition to the before-mentioned actions, the Panciu Recovery Special Service drew up plans, sketches and projects for private homes, shops, primary schools in Soveja, Crucea de Sus and Crucea de Jos, for the standard carpentry needed for Soveja, but also for the Power Plant, the "Sf. Parascheva" Church and for other type constructions which were to be allocated to the Panciu residents (VNA, file no. 198/1943, f. 441-443).

According to the data presented by the Panciu Recovery Special Service, during July-August 1944, due to the political events, restoration works stalled, having been resumed after receiving the approval of the Ministry of Public Works and Communications (VNA, file no. 77/1944, f. 279).

This natural phenomenon, unpredictable by its destructive consequences, through the lives taken away, through the caused suffering, gained, with the passage of decades, the features of a historic moment in the life of Vrancea County inhabitants. Forgetfulness, unjust, but natural by life logic, left just a chalk inscription on time."

References

- Alexandrescu AP (1942) Monografia Județului Putna. Tipografia și Legătoria de cărți „Cartea Putnei”, Focșani
- „Capitala” newspaper, Year V, No. 1471, Sunday, November 24th 1940, 1
- Căpățână A (1941) Istoricul Orașului Panciu și a Schiturilor „Brazi” și „Sf. Ion” prăbușite de cutremurul din 10 Noembrie 1940. Tiparul „Cartea Românească”. Bucharest

- „Evenimentul” journal, Year II, No. 551, Tuesday, November 12th 1940, 3
- Mândrescu N (2008) The large Vrancea intermediate-depth earthquakes occurred in the XXth century and their effects on the Romanian territory—Photographic testimonies (In Romanian). Publishing House of the Romanian Academy, Bucharest, 176p
- „Timpul” newspaper, Year IV, No. 1271, Wednesday, November 13th 1940, 1
- „Timpul” newspaper, Year IV, No. 1271, Thursday, November 19th 1940, 1
- „Timpul” newspaper, Year IV, No. 1271, Wednesday, November 13th 1940, 4
- „Timpul” newspaper, Year IV, No. 1304, Monday, December 16th 1940, 1
- „Universul” newspaper, Year 57, No. 317, Sunday, November 17th 1940, 6
- Vrancea National Archives (VNA) Focșani Town Hall fund, file no. 119/1940, f. 40
- Vrancea National Archives (VNA) Focșani Town Hall fund, file no. 119/1940, f. 46
- Vrancea National Archives (VNA) Focșani Town Hall fund, file no. 119/1940, f. 116–118
- Vrancea National Archives (VNA) Focșani Town Hall fund, file no. 119/1940, f. 151
- Vrancea National Archives (VNA) Focșani Town Hall fund, file no. 120/1940, f. 120
- Vrancea National Archives (VNA) Focșani Town Hall fund, file no. 120/1940, f. 147
- Vrancea National Archives (VNA) Focșani Town Hall fund, file no. 120/1940, f. 150
- Vrancea National Archives (VNA) Focșani Town Hall fund, file no. 120/1940, f. 152
- Vrancea National Archives (VNA) Focșani Town Hall fund, file no. 120/1940, f. 224, 227
- Vrancea National Archives (VNA) Focșani Town Hall fund, file no. 121/1940, f. 25
- Vrancea National Archives (VNA) Focșani Town Hall fund, file no. 121/1940, f. 52
- Vrancea National Archives (VNA) Focșani Town Hall fund, file no. 121/1940, f. 318
- Vrancea National Archives (VNA) Focșani Town Hall fund, file no. 135/1940, f. 11
- Vrancea National Archives (VNA) Focșani Town Hall fund, file no. 135/1940, f. 23
- Vrancea National Archives (VNA) Focșani Town Hall fund, file no. 118/1941, f. 23
- Vrancea National Archives (VNA) Focșani Town Hall fund, file no. 118/1942, f. 4, 8, 28, 41
- Vrancea National Archives (VNA) Putna County Prefecture fund, file no. 9/1940, f. 9
- Vrancea National Archives (VNA) Putna County Prefecture fund, file no. 9/1940, f. 30
- Vrancea National Archives (VNA) Putna County Prefecture fund, file no. 9/1940, f. 38
- Vrancea National Archives (VNA) Putna County Prefecture fund, file no. 9/1940, f. 79
- Vrancea National Archives (VNA) Putna County Prefecture fund, file no. 9/1940, f. 90
- Vrancea National Archives (VNA) Putna County Prefecture fund, file no. 9/1940, f. 111
- Vrancea National Archives (VNA) Putna County Prefecture fund, file no. 9/1940, f. 287
- Vrancea National Archives (VNA) Putna County Prefecture fund, file no. 9/1940, f. 333
- Vrancea National Archives (VNA) Putna County Prefecture fund, file no. 9/1940, f. 336
- Vrancea National Archives (VNA) Putna County Prefecture fund, file no. 9/1940, f. 339
- Vrancea National Archives (VNA) Putna County Prefecture fund, file no. 9/1940, f. 347-349
- Vrancea National Archives (VNA) Putna County Prefecture fund, file no. 9/1940, f. 388
- Vrancea National Archives (VNA) Putna County Prefecture fund, file no. 12/1940, f. 150
- Vrancea National Archives (VNA) Putna County Prefecture fund, file no. 8/1941, f. 28–29
- Vrancea National Archives (VNA) Putna County Prefecture fund, file no. 8/1941, f. 163
- Vrancea National Archives (VNA) Putna County Prefecture fund, file no. 9/1941, f. 3
- Vrancea National Archives (VNA) Putna County Prefecture fund, file no. 9/1941, f. 487
- Vrancea National Archives (VNA) Putna County Prefecture fund, file no. 8/1942, f. 123
- Vrancea National Archives (VNA) Putna County Prefecture fund, file no. 8/1942, f. 435, 439
- Vrancea National Archives (VNA) Putna County Prefecture fund, file no. 8/1942, f. 462–472
- Vrancea National Archives (VNA) Putna County Prefecture fund, file no. 198/1943, f. 441–443
- Vrancea National Archives (VNA) Putna County Prefecture fund, file no. 200/1943, f. 3
- Vrancea National Archives (VNA) Putna County Prefecture fund, file no. 200/1943, f. 40
- Vrancea National Archives (VNA) Putna County Prefecture fund, file no. 200/1943, f. 85

- Vrancea National Archives (VNA) Putna County Prefecture fund, file no. 77/1944, f. 279
- Vrancea National Archives (VNA) Putna County Technic Sevice fund, file no. 12/1940, f. 230
- Vrancea National Archives (VNA) Putna County Technic Sevice fund, file no. 12/1940, f. 347
- Vrancea National Archives (VNA) Putna County Technic Sevice fund, file no. 13/1940, f. 6
- Vrancea National Archives (VNA) Putna County Technic Sevice fund, file no. 13/1940, f. 180